GULF DRILLING GUIDES

CASING AND LINERS FOR DRILLING AND COMPLETION

DESIGN AND APPLICATION

SECOND EDITION

TED G. BYROM

G P
P

Casing and Liners for Drilling and Completion

This page intentionally left blank

Casing and Liners for Drilling and Completion

Design and Application

Second Edition

Ted G. Byrom

ELSEVIER

AMSTERDAM • BOSTON • HEIDELBERG • LONDON
NEW YORK • OXFORD • PARIS • SAN DIEGO
SAN FRANCISCO • SINGAPORE • SYDNEY • TOKYO
Gulf Professional Publsihing is an imprint of Elsevier

Gulf Professional Publishing is an imprint of Elsevier
225 Wyman Street, Waltham, MA 02451, USA
The Boulevard, Langford Lane, Kidlington, Oxford, OX5 1GB, UK

Second Edition 2015

First Edition 2007

Notices
Knowledge and best practice in this field are constantly changing. As new research and experience broaden our understanding, changes in research methods, professional practices, or medical treatment may become necessary.

Practitioners and researchers must always rely on their own experience and knowledge in evaluating and using any information, methods, compounds, or experiments described herein. In using such information or methods they should be mindful of their own safety and the safety of others, including parties for whom they have a professional responsibility.

To the fullest extent of the law, neither the Publisher nor the authors, contributors, or editors, assume any liability for any injury and/or damage to persons or property as a matter of products liability, negligence or otherwise, or from any use or operation of any methods, products, instructions, or ideas contained in the material herein.

Library of Congress Cataloging-in-Publication Data
A catalog record for this book is available from the Library of Congress

British Library Cataloguing in Publication Data
Byrom, Ted G.
Casing and liners for drilling and completion : design and application / by Ted G. Byrom. – Second edition.
pages cm
Includes bibliographical references and index.
ISBN 978-0-12-800570-5
1. Oil well casing–Design and construction. I. Title.
TN871.22.B97 2014
622′.3381–dc23

2014014250

For information on all Gulf Professional publications
visit our web site at store.elsevier.com

This book has been manufactured using Print On Demand technology. Each copy is produced to order and is limited to black ink. The online version of this book will show color figures where appropriate.

ISBN: 978-0-12-800570-5

Dedication

To Anne

This page intentionally left blank

Contents

Acknowledgments

I owe very special thanks to Leon Robinson who encouraged the first edition of this textbook as the first in a series of textbooks that he envisioned as an encyclopedia of drilling technology. Simply put, his goal was to publish a record of current drilling technology before the "old timers" all retired and faded away. He recognized that a trend in more frequent personnel turnover was resulting in an industry cycle of having to continually reinvent drilling practices and technology that have been well known by earlier generations of engineers. His encouragement was invaluable to the first edition, and he continues to be an inspiration for this second edition.

Thanks also to Marc Summers for his valuable suggestions on additional load cases and their systematic organization, and so too, the many helpful suggestions of others who used the first edition in teaching casing design.

Finally, and especially, I extend my grateful appreciation to my editors, Katie Hammon, Kattie Washington, and Anusha Sambamoorthy whose enthusiasm and tireless efforts made this the smoothest publishing experience of my career.

This page intentionally left blank

Preface

This second edition represents a significantly revised and improved version of the first edition, and in many respects it is a new book. I have taught various aspects of casing design over more than twenty years, and for the past six I taught a 5-day basic casing design course from the first edition of this book. I felt that some changes in organization and approach would greatly enhance its value for engineers learning casing design. Hence, the present focus is on a clear and logical progression through the design/selection sequence and related practices followed by material on more advanced topics of casing performance mechanics and casing in directional and horizontal wells.

I have added some new material on loading cases and some additional perspective on approaches to design. Especially topical is the addition of a section on casing performance in hydraulic fracturing of horizontal wells, a relatively new application and one in which I have been consulting in the past few years. Along these lines, I have also added a brief overview of some aspects of rock mechanics as it relates to fracturing and horizontal wells in a separate appendix.

While the first edition contained much foundational matter such as units of measure, hydrostatics, and so forth, it was all interspersed throughout the main body of text. That order of presentation works well for an introduction to casing design, but once an engineer is past the fundamentals it makes for an amount of clutter for someone wanting to refer back specifically to the design/selection process. Consequently, I have moved most of the foundational material from the body of the text into appendices for easy study and reference. One might question the necessity for including such foundational material in a text like this, but having taught specific industry training courses for engineers over the past eighteen years, I can assure you that most of this material is essential. Engineers who approach casing design for the first time typically come from various disciplines and may or may not have any previous exposure to solid mechanics, but more importantly, it is an inescapable fact that we forget what we were taught if we are not using it on a regular basis. Those new to the topic of casing design should devote serious study to these appendices, and I highly encourage all to at least review them. In the appendices I have gone into greater depth and detail on some of the peripheral issues of casing than might seem necessary for those whose only interest is in basic level casing design, but I did so to enhance the value of the book as a fairly complete reference on the topic.

I have included scant material on pipe standards and specifications, especially in regard to connections, only what is essential to understand the process of casing design. The reasons for this are twofold, one is that standards and specifications change periodically and a book based heavily on them is out of date as soon as a new specification or standard is published, and the other is that most of the meager published data on oilfield tubulars is of a nominal or minimal performance nature and readily available elsewhere. My focus in this book is on the fundamental mechanics that will not change over time.

Finally and importantly, as with the first edition, I have tried to maintain a conversational style so that it may be easily read and understood by those seeking self education without the necessity of an instructor. There are many precautions and opinions sprinkled throughout, sometime homiletic in tone, but all based in real case histories, most of which could never find their way into print. I hope these add to the content. Overall, the reader should find this edition to be a much improved and more useful textbook.

Ted G. Byrom
Mount Vernon, Indiana
January, 2014

Preface to the First Edition

Hardly anyone reads a Preface. Please read this one, because this book is a bit different and what is written here is the actual introduction to the book. I never read a textbook that I really liked when I was a student. The main reason is that most authors seemed more interested in presenting the information with the goal of impressing colleagues rather than instructing the reader as a student of the subject. For a long time, I thought they were so smart that they could not relate to the ordinary student. I now know that is rarely true. You should know that I have reached a point in my career where no one is important enough that I need to impress, and certainly no money is to be made writing a textbook. My reason for accepting the task of writing this text is that I truly wanted to attempt to explain this subject in an understandable manner to the many petroleum engineers who need or want to understand it but at best received a couple of classroom lectures and a homework assignment on the subject from someone who never designed or ran a real string of casing in his life. I was in that same position some 44 years ago. This book is also intended for those coming into the oilfield from other disciplines and needing to understand casing design.

This book is not written in the style of most textbooks. That is because it its main purpose is to teach you, the reader, about casing and casing design without need of an instructor to "explain" it to you. I would like you to read this as if you and I were sitting down together as I explain the material to you. While some of the material requires a little formality, I have tried to put it on a readable level that progresses through the various processes in a logical manner. I have also tried to anticipate, pose, and answer some of the questions you might ask in the process of our discussion.

The first five chapters of this book lay a foundation in basic casing design. It is, if you will, a recipe book for basic casing design. It does go into some detail at times, but overall its purpose is to actually teach an understanding of basic casing design. If you are not an engineer, and many casing strings are designed by nonengineers, do not be discouraged by the many equations you see. The information in this part should be sufficient to design adequate casing strings for the vast majority of the wells drilled in the world, and although the chapter on hydrostatics contains some calculus, none of it is beyond the capabilities of a second-year engineering student. The sixth chapter is about running and landing casing. Most of it is common sense, but there are some practical insights that are worth the time it takes to read.

Chapter 6 begins the discussion of slightly more advanced material. Some of this material is not covered in universities, except on a graduate level, but I have tried to present it so that any undergraduate engineering student should be able to understand it. The remaining chapters continue in the same vein.

I have not tried to cover everything about casing or casing design in this book. I have never had any aspirations of writing the definitive text on casing or any other subject, mostly because some aspects hold no interest at all for me. I have personally run and cemented close to a couple of hundred casing strings as a field drilling engineer, designed several hundred more, and been involved with several thousand

casing strings over my career. These have ranged from very shallow strings to a few over 23,000 ft. Never have I designed a string for a geothermal well, and my corrosion and sour gas experience is limited. Consequently, little is said about those subjects in this book. There are much better sources for that than what I could write on those particular topics.

Ted G. Byrom
Mount Vernon, Indiana
September, 2006

Acronyms

AEUB	Alberta Energy and Utilities Board
API	American Petroleum Institute
IADC	International Association of Drilling Contractors
ISO	International Organization for Standardization
SPE	Society of Petroleum Engineers

See Glossary for technical acronyms.

This page intentionally left blank

Introduction to casing design

1

Chapter outline head

1.1 Introduction

In this textbook, we will explore the fundamentals and practices of basic casing design with some introduction to more advanced ideas and techniques. We will use a simple process that involves manual calculations and graphical plots. This is the historical method of learning casing design and will instill a depth of understanding. For the vast majority of casing strings run in the world this is still the method

Casing and Liners for Drilling and Completion. http://dx.doi.org/10.1016/B978-0-12-800570-5.00001-2

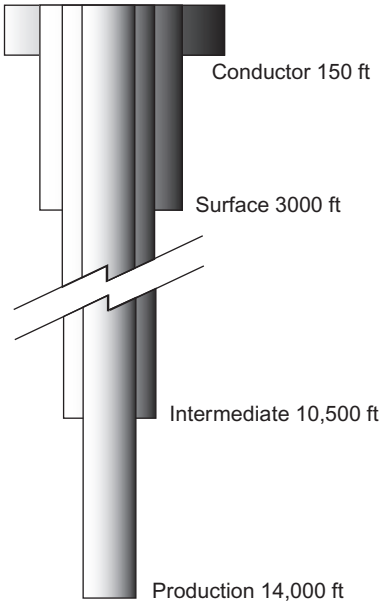

Figure 1.1 Casing string design for a typical well.

employed. Those engineers already well founded in the process may use more advanced techniques and specific software. While there is some excellent software on the market that does casing design, one cannot really learn the process using software. This is not by any means a harangue about casing design software; some of it is excellent and quite sophisticated especially compared to the crude first attempts that hit the market. But the unwelcome fact is that many who are using it are overwhelmed by multipage, detailed printouts, half of which they do not even pretend to understand. And truth be told, many of the "support" personnel experience the same problem. Information is not knowledge if you do not understand it.

1.2 Design basics

Casing design is a bit different from most structural design processes in engineering because the "structure" being designed is a single tubular monolith of given outside diameter primarily supported from the top end. There is nothing to actually "design" in the conventional sense of structural engineering. Geometrically speaking, our structure is already designed. The available tubular sizes and strengths are standardized, so the design process maybe thought of as a two-step process:

1. Calculate the anticipated loads.
2. Selecting from the available standard tubes those with adequate strength to safely sustain those loads.

As simple as that may sound, casing design is still not a linear process. It is not a matter of calculating the anticipated loads and then selecting the casing. The selected casing itself is part of the load. Hence, the process must be iterated to account for that fact. Still, it is quite an easy process in the vast majority of cases.

The basic design/selection sequence in its iterative form might be listed in steps:

1. Determine depths and sizes of casing.
2. Determine pressure loads.
3. Apply design factors and make preliminary selection.
4. Determine axial loads and apply design factors.
5. Adjust preliminary selection for axial design loads.
6. Adjust for combined tension/collapse loading.

Some might not consider Step 1 a part of casing design, and technically that is true. That step might be done by someone other than the casing designer and not in conjunction with the actual design process. However, we are going to include it in our treatment because it is essential for us to understand how it is done and how the results affect our design process.

The actual design process starts with Step 2, where we calculate the pressure loads for various scenarios using basic hydrostatics. We do this for all the strings in the well.

In Step 3 we select the worst case pressure loading from the previous step and apply a design factor which gives us a margin to account for uncertainty in the loads and pipe strengths. The results of that are design pressure-load plots for each string of casing in the well. From these plots, we make preliminary selections of casing, which will safely sustain those design loads.

Because the axial load (weight) of the string is a function of the casing itself, we must then calculate it from the preliminary pressure-load selection. We then apply a design factor to the axial load and check to see if our preliminary selection has sufficient axial strength. If it does, Step 4 is complete and we skip Step 5. If it does not, then in Step 5, we must modify the preliminary selection so that it also satisfies the axial design load. When we modify the preliminary selection, we must recalculate the axial load for the modified string and apply our axial design factor again. We must also check to ascertain that the modified string still meets our pressure-load design requirements. So in this step, the process becomes iterative. It is not difficult though, because in the manual process, it is easy to visually see the values and minimize the iterations. Seldom are more than two iterations required.

Finally, in Step 6, we check for the effects of combined axial tension and collapse loading, often referred to as *biaxial loading*. This is a critical step even in basic casing design, because tension in a string reduces the collapse resistance of the casing. This step too may require several iterations because any change or adjustment in the casing selection always requires that all the loads be rechecked.

For your early reference, Step 1 is covered in Chapter 2, Step 2 in Chapter 3, and Steps 3-6 in Chapter 4. Chapter 5 covers the casing installation process, and the remainder of the chapters covers more advanced topics.

1.3 Conventions used here

There is in the petroleum literature a virtual plethora of odd terminology, incoherent physical units, mathematical inconsistencies, and so forth. I have tried to adhere to several principles in this book:

- A readable text
- A progressive sequence for learning and self education
- Sufficient background material in appendices
- Adherence to ISO mathematics [1] and mechanics [2] standards
- Avoidance of acronyms except for organizational names (5) and those appearing in API/ISO standards (8) that you must necessarily understand plus only one other that is too common to not know (BOP)

Readability is essential for self-education, and I think, one of the most important features I have aimed for in this textbook. Perhaps I have oversimplified some concepts, but I prefer that to pedantic gibberish and superfluous acronyms that are more confusing than educational. And if the copy editor is successful at ironing out my convoluted sentence structure, you should find this book fairly readable.

1.3.1 Organization of book

The book is organized in a logical sequence that a beginner would follow to learn casing design, starting with the basics and proceeding to the more advanced topics. Chapters 2–4 illustrate basic casing design and Chapter 5 covers installation in the well. Having learned that material, the reader will have acquired the skills necessary for a fundamental level of casing design. That is the level of most who actually design the majority of casing strings in the world. Chapter 6 covers the details of casing strengths and performance, and Chapter 7 covers casing in deviated and horizontal wells. That latter chapter also contains materials on casing for hydraulic fracturing in horizontal wells.

Most of the referential and foundational materials on mechanics, hydrostatics, rock behavior, and so forth, have been moved to separate appendices so as not to clutter the logical progression of the design process and casing specific topics. Most of that material has been expanded in these appendices and should serve as handy reference or refresher for those needing it. I have also added an appendix with the most commonly used equations for easy access, rather than requiring a search through the text to locate them. Those equations that are boxed in the text are listed in this appendix along with their respective equation numbers from the text to facilitate locating the qualifications and discussions.

You will notice a number of redundancies in this text, and I can already imagine the number of times a reader may say, "He already said this!" While partly the result of my writing process, I have intentionally left some of these in place and added some. The reason is that it is seldom that anyone would read a text like this from beginning to end. More commonly one reads selectively those topics of concern or need, thus some of the pertinent precautions and qualifications mentioned elsewhere may be missed. I beg your patience when you encounter these.

1.3.2 Units and math

The problem with units in oilfield technology is that there are too many systems and hybrid systems in play, none of which use consistent units in oilfield applications. Here, I adhere to a simple underlying principle: *all physical phenomena are independent of any units used to measure them*. If we use consistent units from a coherent system, no conversion factors are necessary in properly stated physical formulas and equations. Importantly, *none of the formulas or equations in this book require conversion factors if you use consistent units*. There are no conversion factors included in any of the formulas, and it is left to you as a properly educated engineer to know when you need them. All that said, most of the global drilling and completion operations use the USC system (US Customary) of oilfield units, and we will bow to that custom here because it is the system of the vast majority of readers. The fundamental formulas will not require conversion factors, but our calculations will, and we will show them in the examples. Units of measure, physical constants, and material properties used in this text are covered in detail in Appendix B.

As in the first edition [3], I use specific gravity (specific density), $\hat{\rho}$, (SG) for liquid density, where specific gravity is defined as $\hat{\rho} \equiv \rho/\rho_{\text{wtr}}$, rather than the cumbersome lb/gal (ppg) of the USC system. This is done for ease of use in any unit system, where early in their education, every engineer committed

to memory that water density, ρ_{wtr}, is 62.34 lb/ft^3, 8.33 ppg, and 1000 kg/m^3. (We avoid the niceties of temperature variation as we seldom have that data anyway.)

Throughout the petroleum literature (SPE, API, IADC, etc.), there is a virtual hodgepodge of variable names, symbols, multiletter computer variables, mixed mode math, and grade school arithmetic, all of which are inconsistent and quite confusing. All math here will be in strict algebraic form with single-kernel, italicized letter/symbol variables. Nonitalicized subscripts will be used for further identification and clarification. Italicized subscripts will denote variable descriptors rather than names. Further, I will use mostly standard variable names from mechanics rather than from the petroleum literature as per ISO 80000-4 [2] to make this more universal for all readers. At first encounter, this may be a bit confusing to some, but Appendix A defines all the notation and variables used, so you should not have to search through the text to find a variable's definition where first used. A glossary of petroleum related terms and acronyms is also included. There are a few instances where the same symbols are necessarily used to represent different quantities, but those are quite local and should be obvious from the context. Where applicable to terms and abbreviations, I have adhered closely to the SPE Style Guide [4].

For those who have used the first edition of this text, I should call attention to two significant changes in usage. As before all of our pressure loads are defined in terms of a differential pressure across the casing wall. But in this edition, we will define that differential pressure in a single, consistent manner:

$$\Delta p \equiv p_i - p_o \qquad \begin{cases} < 0 \;\rightarrow\; \text{collapse loading} \\ = 0 \;\rightarrow\; \text{no differential loading} \\ > 0 \;\rightarrow\; \text{burst loading} \end{cases} \tag{1.1}$$

where p_i and p_o are inside and outside pressure, respectively. This should avoid some confusion inherent in the previous edition. The second change is in the definition of the conversion factor, g_c, that converts pounds (mass) to slugs (mass). In this edition, I use $g_c = 1/32.174049$ slug/lb, which is the more conventional form (though there is no standard). This is the reciprocal of the value used in the earlier edition. More discussion on this is found in Appendix B.

Roundoff

The API rounds off pressure ratings to the nearest 10 psi, and we will follow that convention in most of our pressure load calculations. We will use the $\approx$ symbol to denote where we roundoff. However, there are a few places where we will not roundoff because intermediate results may have significance in further calculations, and where we want to illustrate something more clearly.

1.3.3 Casing used in examples

All of the design process and calculations will be illustrated with examples. Most are based on real wells. For the sake of simplicity and avoidance of commercialism, I limit all of the casing used in the designs to API threaded and coupled pipe (ST&C, LT&C, and Buttress). This does not constitute a recommendation, but utilizes the most widely used and standardized casing in the world. This book primarily addresses the design process and the mechanics employed, so I have purposely limited the amount of API/ISO standards covered because they can and do change periodically whereas the fundamental mechanics do not. Furthermore, I make scant mention of proprietary casing and connections because those standards are set by the individual manufacturer, not always readily available, and subject to change for marketing and business-related reasons.

1.4 Oilfield casing

Anyone reading this book is assuredlyalready familiar with the oilfield tubes (casing, tubing, drill pipe, and line pipe) referred to as Oil Country Tubular Goods or OCTG, the standardized tubes used in drilling, completion, and production applications. But for a refresher and consistency in our discussions, we include this brief and basic section on oilfield casing.

The steel tubes that become a permanent part of an oil or gas well are called *casing*, and the tubes that are removable, at least in theory, are referred to collectively as *tubing*, which are not covered in this book. Oilfield casing is manufactured in various diameters, wall thicknesses, lengths, strengths, and with various connections. The purpose of this text is to examine the process of selecting the type and amount we need for specific wells. But first, a question: What purpose does casing serve in a well? There are three:

- Maintain the structural integrity of the borehole.
- Keep formation fluids out of the borehole.
- Keep borehole fluids out of the formations.

It is as simple as that, though we could list many subcategories under each of those. Most are self-evident. Additionally, there are some cases where the casing also serves a structural function to support or partially support some production structure, as in water locations.

1.4.1 Setting the standards

By necessity, oilfield tubulars are standardized. Until recent times, the standards were set by the American Petroleum Institute (API) through various committees and work groups formed from personnel in the industry. Now, the International Organization for Standardization (ISO) is seen as taking on that role. Currently, most of the applicable ISO standards are merely the API standards, but that role may expand in the future. In this text, we refer primarily to the API standards, but it should be understood that there are generally identical standards, and in some cases, more advanced standards, under the ISO name.

It is important that some degree of uniformity and standardization is in force and that manufacturers be held to those standards through some type of approval or licensing procedure. In times of casing supply shortages, a number of manufacturers have entered the oilfield tubular market with substandard products. Some of these have resulted in casing failures where no failure should have occurred. Any casing purchased for use in oil or gas wells should meet or exceed the current standards as set for oilfield tubulars by the API or ISO.

Some casing on the market is not covered by API or ISO standards. Some of this non-API casing is for typical applications, some for high-pressure applications, high-temperature applications, low-temperature applications, and some for applications in corrosive environments. Many of these types of casing meet or exceed API standards, but one must be aware that the standards and quality control for these types of casing are set by the manufacturer. It probably should not be mentioned in the same paragraph with the high-quality pipe just referred to, but it should also be remembered that there are some low-quality imitations of API products on the market as well, including some with fraudulent API markings.

1.4.2 Manufacture of oilfield casing

There are two types of oilfield casing manufactured today: seamless and welded. Each has specific advantages and disadvantages.

Seamless casing

Seamless casing accounts for the greatest amount of oilfield casing in use today. Each joint is manufactured in a pipe mill from a solid cylindrical piece of steel, called a *billet*. The billet is sized so that its volume is equal to that of the joint of pipe that will be made from it. The manufacturing process involves:

- Heating the billet to a high temperature
- Penetrating the solid billet through its length with a mandrel such that it forms a hollow cylinder
- Sizing the hollow billet with rollers and internal mandrels
- Heat treating the resulting tube
- Final sizing and straightening

The threads may be cut on the joints by the manufacturer or the plain-end tubes may be sent or sold to other companies for threading. The most difficult aspect of the manufacture of seamless casing is that of obtaining a uniform wall thickness. For obvious reasons, it is important that the inside of the pipe is concentric with the outside. Most steel companies today are very good at this. A small few are not, and which is one reason that API and ISO standards of quality were adopted. Current standards allow a 12.5% variation in wall thickness for seamless casing. The straightening process at the mill affects the strength of the casing. In some cases, it is done with rollers when the pipe is cool and other cases when the pipe is still hot. Seamless casing has its advantages and also a few disadvantages.

Advantages of seamless casing

- No seams to fail
- No circumferential variation of physical properties

Disadvantages of seamless casing

- Variations in wall thickness
- More expensive and difficult manufacturing process

Welded casing

The manufacturing process for welded casing is quite different from that of seamless casing. The process also starts with a heated steel slab that is rectangular in shape rather than cylindrical. One process uses a relatively small slab that is rolled into a flat plate and trimmed to size for a single joint of pipe. It is then rolled into the shape of a tube, and the two edges are electrically flash welded together to form a single tube. Another process uses electric resistance welding (ERW) as a continuous process on a long ribbon of steel from a large coil. The first stage in this process is a milling line in the steel mill:

- A large heated slab is rolled into a long flat plate or ribbon of uniform thickness.
- Plate is rolled into a coil at the end of the milling line.

The large coils of steel "ribbon" are then sent to the second stage of the process, called a *forming line*.

- Steel is rolled off the coil and the thickness is sized.
- Width is sized to give the proper diameter tube.
- Sized steel ribbon is formed into a tubular shape with rollers.

- Seam is fused using electric induction current.
- Welding flash is removed.
- Weld is given an ultrasonic inspection.
- Seam is heat treated to normalize.
- Tube is cooled.
- Tube is externally sized with rollers.
- Full body of pipe is ultrasonically inspected.
- Tube is cut into desired lengths.
- Individual tubes are straightened with rollers.

This is the same process by which coiled tubing is manufactured, except coiled tubing is rolled onto coils at the end of the process instead of being cut into joints. Note that, in the welding process, no filler material is used; it is solely a matter of heat and fusion of the edges.

Welded casing has been available for many years, but there was an initial reluctance by many to use it because of the welding process. Welding has always been a matter of quality control in all applications, and a poor-quality weld can lead to serious failure. Today, it is both widely accepted and widely used for almost all applications except high-pressure and/or high-temperature applications. It is not used in the higher yield strength grades of casing.

Advantages of welded casing

- Uniform wall thickness
- Less expensive than seamless
- Easier manufacturing process
- Inspected during manufacturing process (ERW) and defective sections removed

Uniform wall thickness is very important in some applications, such as the newer expandable casing.

Disadvantages of welded casing

- High temperatures of welding process
- Possible variation of material properties caused by welding
- Possible faulty welds
- Possible susceptibility to failure in weld

Welded casing has been used for many years now. Many of the so-called disadvantages are perhaps more a matter of perception than actuality.

Strength treatment of casing

When a cast billet or slab is formed into a tube it is done at quite high temperature. The deformation that takes place in the forming process is in a plastic or viscoplastic regime of behavior for the steel. As it cools, its crystalline structure begins to form. Once the crystalline structure forms or begins to form, any additional plastic deformation to which we subject the tube will change its properties. The change may be minor or significant, depending on the constituents of the steel, the amount of deformation, and the temperature. Heating a tube above certain temperatures and cooling slowly allow the crystals to form more uniformly with fewer structural imperfections, called *dislocations*, in the lattice structure. The properties of the steel can be modified by the addition of certain constituents to the alloy and, to some extent, by controlling the cooling rate. One common process for enhancing the performance properties

of casing is to heat the tube above a certain temperature then quickly cool it by spraying it with water or some other cool fluid to strengthen and harden it (quenching), especially near the surface. The casing is then heated again, but to a lower temperature, and allowed to remain at that temperature for a period of time to allow "relaxation" of the steel to some specific lower hardness and strength (tempering). This process is called *quench and temper*, or QT for short, and is an inexpensive alternative to adding more expensive alloying constituents.

Some steels are said to get "stronger" when they are deformed plastically at ambient temperatures. This is part of the manufacturing process in some steels and is called *cold working*. Cold working typically increases the steel's yield strength; however, it does not, in general, increase the ultimate strength. Straightening casing joints in the latter stages of the manufacturing process can also have an effect on the properties of the tube depending on whether it is done at "cool" temperatures or "warm" temperatures. It should be noted that any steel that is cold worked is no longer isotropic. Its yield strength will vary depending on the direction of the loading. For example, if a tube is cold worked by axially stretching, it may see an increase in tensile yield strength, but it will suffer a reduction in compressive yield strength. This elastic-plastic behavior will be discussed more fully in Appendix C.

1.4.3 Casing dimensions

Casing comes in an odd assortment of diameters ranging from 4-1/2 in. to 20 in. that may seem quite puzzling at first encounter, e.g., 5-1/2, 7, 7-5/8, 9-5/8 and 10-3/4 in. Why such odd sizes? All we can really say about that is that they stem from historical sizes from so far back that no one knows the reasons for the particular sizes any longer. Some sizes became standard and some vanished. Within the different sizes, there are also different wall thicknesses. These different diameters and wall thicknesses were eventually standardized by the API (and now ISO). The standard sizes as well as dimensional tolerances are set out in API Specification 5CT [5] and ISO 11960 [6].

Outside diameter

The size of casing is expressed as a *nominal diameter*, meaning that is the designated or theoretical outside diameter of the pipe. API and ISO allow for some tolerance in that measurement, and the specific tolerance differs for different size pipe. The tolerances for nonupset casing 4-1/2 in. and larger are given as fractions of the outside diameter in Table 1.1. Note that the amount of minimum tolerance for the outside diameter is much less than for the maximum tolerance. This is necessary to assure that standard threads cut on the joint will be of adequate depth and height.

For upset casing, Table 1.2 shows the current API and ISO tolerances measured 5 in. or 127 mm behind the upset.

Table 1.1 Tolerance for *Non-upset* Casing Outside Diameter [5, 6]

Nominal Outside Diameter, d_o (in.)	Tolerances	
	Maximum	Minimum
$\geq$ 4-1/2	$+0.01d_o$	$-0.005d_o$

Table 1.2 Tolerance for *Upset* Casing Outside Diameter [5, 6]

Nominal Outside Diameter, d_o (in.)	Tolerances (in.)		Tolerances (mm)	
	+	−	+	−
> 3-1/2 to 5	7/64	$0.0075d_o$	2.78	$0.0075d_o$
> 5 to 8-5/8	1/8	$0.0075d_o$	3.18	$0.0075d_o$
>8-5/8	5/32	$0.0075d_o$	3.97	$0.0075d_o$

Table 1.3 Minimum Drift Mandrel Dimensions [5, 6]

Nominal Outside Diameter (in.)	Mandrel Length		Mandrel Diameter	
	(in.)	(mm)	(in.)	(mm)
< 9-5/8	6	152	$d_i - 1/8$	$d_i - 3.18$
9-5/8 to 13-3/8	12	305	$d_i - 5/32$	$d_i - 3.97$
>13-3/8	12	305	$d_i - 3/16$	$d_i - 4.76$

Inside diameter and wall thickness

The inside diameter of the casing determines the wall thickness or vice versa. Rather than a specific tolerance for the amount at which the internal diameter might exceed a nominal value, the tolerance specified by API and ISO is given in terms of minimum wall thickness. The minimum wall thickness is 87.5% of the nominal wall thickness. The maximum wall thickness is given in terms of the nominal internal diameter, however. It specifies the smallest diameter and length of a cylindrical drift mandrel that must pass through the casing (Table 1.3).

The internal diameter of casing is a critical dimension. It determines what tools and so forth may be run through the casing. It is not uncommon to have to select a casing for a particular application such that the drift diameter is less than the diameter of the bit normally used with that size casing, even though the bit diameter is less than the nominal internal diameter of the pipe. In cases like this, it is a practice to drift the casing for the actual bit diameter rather than the standard drift mandrel diameter. This may be done with existing pipe in inventory, and those joints that will not pass the bit are culled from the proposed string. Or it may be done at special request at the steel mill, in which case there will be an extra cost. This procedure applies only to casing where the desired bit diameter falls between the nominal internal diameter and the drift diameter of the casing.

Joint length

The lengths of casing joints vary. In the manufacture of seamless casing, it all depends on the size of the billet used in the process. Usually, there is some difference in weight of the billets, and this results in some variation in the length of the final joints. One could cut all the joints to the same length, but that would be a needless expense and, in fact, would not be desirable. (Wire line depth correlation for perforating and other operations in wells usually depends on an electric device to correlate the couplings with a radioactive formation log; so if all the joints are the same length, it can cause errors in perforating or packer setting depths.) For ERW casing, it is much easier to make all of the joints the same length,

Table 1.4 Length Range of Casing [7]

Range 1		Range 2		Range 3	
(ft)	(m)	(ft)	(m)	(ft)	(m)
16-25	4.88-7.62	25-34	7.62-10.36	34-48	10.36-14.63

but there may still be some waste if that is done. Even if the joints vary in length, they need to be sorted into some reasonable ranges of lengths for ease of handling and running in the well. Three ranges of length are specified by API Recommended Practices 5B1 [7], Ranges 1, 2, and 3 (Table 1.4).

Most casing used today is in either Range 2 or 3, with most of that being Range 3. Range 1 is still seen in some areas where wells are very shallow, and the small rigs that drill those wells cannot handle longer pipe.

Weights of casing

The term *casing weight* refers to the linear "weight" of casing expressed as mass per unit length, such as kg/m or lb/ft. The use of the term *weight* is so common that we are going to use that term for now, but it should be understood that we are not talking about weight but linear density (mass per unit length), and we will use the symbol ρ_ℓ to so designate. One might logically assume that the published casing weight is determined by the density of the steel and the dimensions of the casing body. For instance, we may have a joint of 7 in. 26 lb/ft casing and reasonably assume from that our joint actually weighs 26 lb/ft. Our assumption would be wrong. The published value is the *nominal weight* of the casing, not the actual weight. For outdated reasons, the nominal weight of casing is based on a joint that is 20 ft in length (including coupling). It includes the total weight of the plain-end pipe plus the weight of a coupling, minus the weight of the metal cut away to make the threads on each end, and divided by 20 ft to give the nominal weight in terms of pounds per foot (or kg/m). And the threads used in that calculation are an obsolete thread that is no longer manufactured. In other words, casing almost never weighs the same as its nominal weight. Fortunately, the difference is small enough that in most cases of casing design, it is relatively insignificant. API Spec 5CT [5] has formulas for calculating the actual weight of a joint, but it requires specification of the thread dimensions, and so forth, and we are not going to concern ourselves with that here. One particular formula in API Spec 5CT and ISO 11960 sometimes is useful though, and that is a formula for calculating the nominal casing weight of plain pipe without threads or couplings:

$$\rho_\ell = \rho_s A_t \tag{1.2}$$

or more in the form used by the API

$$\rho_\ell = \rho_s \pi (d_o - t_w) t_w \quad \text{or} \quad \rho_\ell = \rho_s \frac{\pi}{4} \left(d_o^2 - d_i^2 \right) \tag{1.3}$$

where

ρ_ℓ = linear density (mass per unit length), plain-end "casing weight"
ρ_s = density of API carbon steel, 7850 kg/m^3 or 490 lb/ft^3
A_t = cross-sectional area of the tube
d_o = outside diameter
d_i = inside diameter
t_w = wall thickness

This formula (in various forms) appears in several API/ISO publications accompanied by a statement that martensitic chromium steels (L-80, Types 9Cr and 13Cr) have densities different from carbon steels and a correction factor of 0.989 should be applied. Interestingly though, the density of carbon steel is nowhere to be found in those publications. The API/ISO version of the formulas contain an appropriate factor, C, that combines the steel density, π, and a conversion factor for the dimensional units. From these formulas, one can back out the values of steel density used, 490 lb/ft^3 or 7850 kg/m^3. I have cast the formula here as to make sense of the mechanics it is supposed to portray. Here, we must use consistent units as already mentioned. In other words, we must use the diameters and wall thickness in feet or meters with the appropriate density value rather than inches or millimeters. We discuss consistent units in more detail in Appendix B.

1.4.4 Casing grades

Casing is manufactured in several different grades. *Grade* is a term for classifying casing by strength and metallurgical properties. Most of the grades are standardized and manufacture is licensed by the API; a few are specific to the particular manufacturer.

API grades

The API grades of casing are manufactured under a license granted by the API. These grades must meet the specifications listed in API Spec 5CT [5] or ISO 11960 [6]. These grades have yield strengths ranging from 40,000 to 125,000 psi. These grades are listed in Table 1.5.

The letter designations are essentially arbitrary, although there may be some historical connotation. The numbers following the letters are the minimum yield strengths of the metal in ksi (10^3 psi). The minimum yield strength is the point at which the metal goes from elastic behavior to plastic behavior. And it is specified as a "minimum," meaning that all joints designated as that particular grade should meet that minimum strength requirement, although it is allowed to be higher. We use the minimum yield

Table 1.5 API Casing Properties [5]

Grade	Yield Strength (ksi)		Minimum Tensile	Hardness	
	Min.	*Max.*	Strength (ksi)[a]	*HRC*	*HBW/HBS*
H-40	40	80	60		
J-55	55	80	75		
K-55	55	80	95		
N-80	80	110	100		
M-65	65	85	85	22	235
L-80	80	95	95	23	241
C-90	90	105	100	25.4	255
C-95	95	110	105		
T-95	95	110	105	25.4	255
P-110	110	140	125		
Q-125	125	150	135		

[a] A tube property, not a material property.

strength as the design limit in most casing design. The yield strength may be higher than the minimum, and a maximum allowable value is also listed in the table. The reason for the maximum value is to assure that the casing sold in one particular grade category does not have tensile and hardness properties that may be undesirable in a particular application. Some years back, it was common practice to downgrade pipe that did not meet the minimum specifications for which it was manufactured. In other words, if a batch of casing did not meet the minimum specifications for the grade it was intended, it could be downgraded and sold as the next lower grade. There also were cases where one grade was sold as the next lower grade to move it out of inventory. Some of the consequences of this practice were disastrous. One typical example was the use of N-80 casing for tie-back strings and production strings in high-pressure gas wells in the Gulf Coast area of the United States. Many of these wells drilled in the 1960s used lignosulfonate drilling fluids and packer fluids, which over time degraded to form hydrogen sulfide (H_2S). As it turned out, some wells that were thought to have N-80 grade casing, actually had P-110, and there were a number a serious casing failures caused by hydrogen embrittlement. Some of these "N-80" casing strings had P-110 grade couplings on them, and in some wells almost every coupling in the entire string cracked and leaked. It became standard practice (and continues) to add a biocide to the weighted packer fluid to prevent bacterial formation of H_2S, before the manufacture of controlled hardness casing such as L-80 grade.

You will also notice in the chart that some different grades have the same minimum yield strength. Again, this is a case where the metallurgy is different. For instance both N-80 and L-80 have a minimum yield strength of 80,000 psi, but their other properties are different. L-80 has a maximum Rockwell hardness value of 22 but N-80 does not. N-80 actually might be a down-rated P-110 but L-80 cannot be. The grades with the letter designation L and C have maximum hardness limitations and are for specific applications where H_2S is present. Those hardness limits are also shown in the table.

The ultimate strength value listed is the peak strength of the casing in a uniaxial test. In other words, the pipe body should not fail prior to that point. This value is based on tensile test samples and does not account for things like variations in wall thickness, pitting, and so forth. It is not really possible to predict actual failure strength, because there are too many variables, but this value essentially means that the casing should fail at some tensile value higher than the minimum. You should clearly understand that ultimate strength is not a material property, but is the point at which a uniaxial tensile test of a prismatic sample exhibits its highest value. You might say it is the ultimate strength of a structural member, not the material itself.

Also shown in the table are values for minimum elongation. This is specified as the minimum percent a flat sample will stretch before ultimate failure. When you consider that K-55, for instance, yields at an elongation of 0.18%, then you can imagine that nearly 20% elongation is considerable. But one should not be misled into thinking that, if we design casing with the yield strength as a design limit, there is necessarily a considerable additional "strength" remaining before the casing actually fails. Once the material is loaded beyond the elastic limit (yield), the incremental stress required to stretch it to failure is often be quite small. We discuss more on plastic material behavior in Appendix C.

Non-API grades

Non-API grades of casing are not licensed by the API and consequently do not necessarily adhere to API or ISO specifications. This is not to imply that they are inferior, in fact, the opposite is true in many cases. Most non-API grades are for specialized applications to meet requirements not covered in the API or ISO specifications. Examples are high-temperature and/or high-corrosive environments and high-collapse and high-tensile strength requirements. In these cases, one must rely on the specifications, quality control, and reputation of the manufacturer. A particular case in point is V-150 casing with

a minimum yield strength of 150 ksi. It sees frequent use by some companies in some high-pressure applications but has never been adopted as an API standard. For extremely critical wells, many operators elect to do a number of qualification tests and inspections on the specific casing that will be used in a particular application. For instance, one operating company has invested a large amount of money and research into qualifying connections for use in high-pressure wells [8].

It should also be mentioned again that a number of manufacturers make casing that supposedly meets API/ISO specifications but are not licensed as such. Typically, this casing is sold below the market price as so-called "equivalent" to API/ISO casing. While some of this pipe has been found to be acceptable, much of it is not. This was a particular problem in the late 1970s, when the demand for casing far exceeded the supply, and similar situations have re-occurred from time to time and likely will continue. It is a case of "buyer beware."

1.4.5 Connections

Many types of connections are used for casing. These are threaded connections, and there are three basic types: coupling, integral, and weld-on.

The most common type is a threaded pipe with couplings. A plain joint of pipe is threaded externally on both ends and an internally threaded coupling, or collar as it is sometimes called, joins the joints together. A coupling usually is installed on one of the threaded ends of each joint after the threads are cut. The end of the coupling that is installed at the threading facility (usually at the steel mill) is called the *mill end*. The other end of the coupling typically is called the *field end*, since it is connected in the field as the casing is run into the well. An integral connection is one in which one end of the pipe is threaded externally (called the *pin end*) and the other end is threaded internally (called the *box end*). The joints are connected by screwing the pin end of one joint into the box end of another. In most cases, an integral connection requires that the pipe body be thicker at the ends to accommodate both internal and external threads and still have a tensile strength reasonably close to that of the pipe body. The increased wall thickness in this case is called an *upset*, and it may be an increase of the external diameter, *external upset* (EU), a reduction in the internal diameter, *internal upset* (IU), or a combination of both (IEU). Most integral joint casing is externally upset, so as to have a uniform internal diameter to accommodate drilling and completion tools. Finally, the weld-on connection is one in which the threaded ends are welded onto the pipe instead of being cut into the pipe body itself. This type of connection typically is used for large-diameter casing (20 in. and more), where the difficulty of cutting threads on the pipe body becomes more pronounced due to the large size and variations in uniformity of diameter and roundness.

Of the three types of connections mentioned, there are also different ways in which threaded connections bring about a seal. These primary sealing methods are interference and metal-to-metal seals or combinations of both.

Interference sealing relies on the compression of the individual threads against one another to cause a seal. Typically, this is the sealing mechanism of "V" or wedge-shaped threads that are forced tight against one another as the connection is made. The threaded area is tapered so that the more it is made up the greater the contact force between the threads from the circumferential stress in the pin and box. Despite all the force though, interference alone does not cause a total seal, because there has to be some tolerance in the thread dimensions for the connections to be made up. There is always some small gap in the cross-sectional profile of a connection. In the case of wedge-shaped threads, there is a small gap between the crest of one thread and the valley of the other. These connections require a thread lubricant to fill this small gap and effect a true seal. For that reason, it is necessary to use a good quality thread

lubricant. Another aspect of this type of seal is that the contact force must be great enough to resist any pressure force tending to press fluids into the contact area.

Metal-to-metal seals rely on the contact of metal surfaces other than the threads to effect a seal. This may be a tapered surface on the pin and box that contact each other in compression, a shoulder contact, or a combination of the two. These types of seals are strictly metal-to-metal contact and do not rely on thread lubricant to bring about the seal. For this reason, it is extremely important that the connections are protected during handling and running to avoid damaging the seal surfaces. And, since these seals are also dependent on the compression of the metal surfaces, the type of thread lubricant is important to achieve the desired makeup torque.

There is a secondary type of sealing mechanism, called *resilient seals* or *rings*. Resilient seals typically are polymer rings inserted into a special recess in the threaded area to provide additional seals to keep gas or corrosive fluids out of the thread gaps. They usually are not considered a primary seal but only an additional seal to improve the quality of an interference seal and a corrosion barrier for some metal-to-metal seals.

API 8-rd connections

The most common type of casing connection in use is the API 8-rd connection, where 8-rd means 8-round or eight threads per inch and a slightly rounded profile. The profile is a V or wedge shape but slightly rounded at the crest and valleys of the threads. There is also an API 11.5-V thread, which has 11-1/2 threads per inch and a sharp V-profile. This typically is a *line pipe thread* and is seldom used in down-hole applications today. The API 8-rd connection is made in either ST&C (short thread and coupling) or LT&C (long thread and coupling). These two threads are the workhorses of the industry and sufficient for most normal applications. Like most connections, these are not as strong in tension as the pipe body itself because of the reduced net cross-sectional area of the tube, resulting from the threads being cut into the pipe body wall in the absence of an upset. These are interference-seal type connections. The threads are wedge shaped, cut on a tapered profile, and made up until a prescribed torque is attained. At full makeup torque, the threads do not achieve a pressure seal, because the threads do not meet in the base of the groove, leaving two small channels at the base of the thread in both pipe and the coupling. How then do they seal and prevent pressure leaks? They form a pressure seal with the use of thread lubricant that fills the voids between the thread roots. The gap is very small and its length is quite long because of the number of turns at a pitch of eight per inch, so the lubricant forms a good seal in most cases. However, one must always use an approved thread lubricant, because an inferior one that ages and shrinks in time and temperature eventually will leak. Although these connections often are used in gas well applications, they generally are not recommended, because they rely on the thread lubricant for a seal. Another precaution is, that since the threads are wedge shaped, they tend to override each other when subjected to high tension or compression. This override mechanism is referred to as *jump-out*. Because of this jump-out tendency, ST&C and LT&C connections generally are not recommended for wells that have high bending stress caused by wellbore curvature or applications where temperature fluctuations cause high axial tensile and compressive loads.

Other threaded and coupled connections

A number of types of threaded and coupled connections have different profiles from the API 8-rd. Instead of wedge-shaped threads, many have a more square profile or something similar to give them greater tensile and bending strengths. Examples of this type of thread is the Buttress (now an API

thread), 8-Acme, and the like. These threads typically are used where higher tensile strengths are needed in the joints. In general, they also rely on thread lubricant to form a seal and are prone to leak in high-pressure gas applications. Most of these connections require less makeup torque than API 8-rd connections. This is an advantage but also can be a disadvantage, because the maximum makeup torque usually is less than that required to rotate the casing in the hole. Where rotation is planned for cementing or orienting precut windows for multilateral wells, these types of connections are to be avoided. Also, because the makeup torque is relatively low, most of these joints have a "makeup mark" on the pipe. When the pipe is made up properly, the coupling edge is aligned with the makeup mark. If the maximum torque is attained before the coupling reaches the makeup mark, it is an indication that the thread lubricant is the wrong type, the connections have not been properly cleaned, the pipe is not round, or the connection has been damaged. If the makeup mark is reached before the optimum torque is achieved, that is an indication the connections are either worn or the threads were not properly cut. Although not as common, some threaded and coupled pipe also has metal-to-metal seals.

Integral connections

Another type of connection used for casing is one in which a metal-to-metal seal is achieved that is independent of the threaded area. These usually are integral-type connections cut into both ends of the pipe with no separate coupling. Some have a smooth tapered seal that seats very tightly when the proper makeup torque is achieved, others have a shoulder type seal, and as mentioned previously, still others have a combination of both. These types of connections give both high tensile strengths (some greater than the pipe body itself), greater bending strengths for curved wellbores, and greater pressure sealing for high-pressure gas wells. Some of these threads may be cut in nonupset pipe for use as liners, typically called *flush-joint* connections because both the inner and outer diameters are the same in both the tube and connection. Most integral and metal-to-metal sealing connections often are referred to as *premium connections*, but this often is a misnomer. With the exception of API X-line, these should be referred to as *proprietary threads*. They are patented, and their dimensions and properties are strictly those specified by the manufacturer, even though they usually cut are on API specific tubes.

Many of the proprietary connections are designed for special applications, where the loading exceeds typical casing design loads. High tensile loads and high pressures come to mind, but there are other types of loading we often do not consider. One of these is high torsion. If a casing string is to be rotated (for cementing or drilling), the frictional torque often is much higher than the recommended maximum makeup torque of most connections. Additionally, in some wells, where temperatures cycle significantly between flowing and shut-in times, severe compressive loading can take place. That a particular connection may be strong in tension does not necessarily mean that it is as strong in compression. For these applications, special connections have been designed. One proprietary thread is of an interlocking design, so that it may used in high-torque situations, curved wellbores where bending from borehole curvature is a possible cause of connection failure, and situations where axial compressive loading is significant. The interlocking-type thread is somewhat unique in that it is wider at the crest than at the base, and its width also is tapered along its length.

One should always consult the individual manufacturer for properties such as strengths and makeup torque. Another important point is that one should follow the manufacturer's recommendation as to thread lubricant, as some lubricants commonly used with API 8-rd connections can result in loss of pressure seal in some of the proprietary connections. And, on the subject of thread lubricants, it should be mentioned that some connections are coated with special coatings at the mill to avoid the need for

field lubrication. This is not a labor-saving process but one of avoiding possible environmental and formation damage from conventional lubricants.

1.4.6 Strengths of casing

The strengths of the many sizes, weights, and grades of casing are given in various sources. API casing strengths and dimensions are given in API Bulletin 5C2 [9], and formulas used for calculating those values are given in API Bulletin 5C3 [10] or ISO 10400 [11]. These values are also published in many other sources. We discuss in detail the formulas used to calculate casing design strengths in Chapter 6.

1.4.7 Expandable casing

Before leaving our general discussion on casing, we should mention an alternative to traditional casing that falls outside the API and ISO notions of standardized casing. In the last decade or so, reformable metal technology has given rise to a number of applications in the oilfield. The most significant of these is the advent of expandable casing. Expandable casing is an ERW casing that is run into a well, and then the diameter is expanded by a combination mechanical/hydraulic process to a larger diameter before cementing. This gives rise to a number of options where multiple casing strings are required by reducing hole sizes necessary and in some cases reducing the number of strings required. Expandable casing has also been used successfully to patch areas of damaged or corroded casing. The advantages are clearly obvious but there are some drawbacks, specifically in strengths as compared to standard API casing. Expandable casing will be discussed in more detail in Chapter 6.

1.5 Closure

In this chapter, we described an outline of the basic casing design procedure and why it is not a linear procedure. We also commented briefly on the organization of this text and on a few of the conventions employed, all of which will be discussed more fully later.

While we assume a basic knowledge of casing and its usages, we covered a few of the basics of oilfield casing. This section was not intended to be a comprehensive description of the manufacturing, metallurgy, and specifications of casing. The interested reader should refer to other publications for those types of information, such as the API and ISO publications mentioned in the references cited in this chapter as well as the published information of several casing manufacturers and the manufacturers of proprietary connections.

In Chapter 2, we will begin our casing design process where we will learn how to choose casing depths and sizes. Then we will determine the depths and sizes of casing for an example well. That example selection will be carried forward through the remainder of the design process in Chapters 3 and 4.

This page intentionally left blank

Casing depth and size determination

2

Chapter outline head

2.1 Introduction

Arguably the most critical step in well construction is determining the setting depths for the various casing strings. Selecting the casing setting depths is not a part of the actual casing design process, but setting the wrong size casing at the wrong depth can preclude the well ever reaching its objective. Although the engineer who designs the casing strings may not be the same one who selects the depth and sizes, we must cover the fundamental aspects of this critical process in order to fully appreciate the actual design process. Figure 2.1 illustrates a schematic of a typical well showing four strings of casing: conductor casing, surface casing, intermediate casing, and production casing. Why does this well require four strings of casing? How is that determination made? How are the setting depths determined? How are the casing sizes determined? This chapter addresses those questions.

Casing and Liners for Drilling and Completion. http://dx.doi.org/10.1016/B978-0-12-800570-5.00002-4

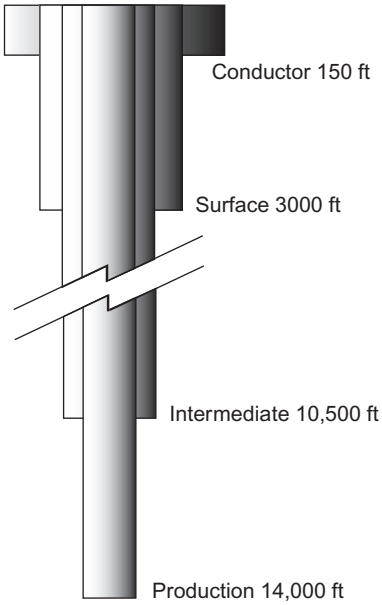

Figure 2.1 A typical casing installation.

2.2 Casing depth determination

While the depths to which the various casing strings are set are critical, those depths are determined by a number of parameters most of which we cannot control. What are those parameters?

2.2.1 Depth selection parameters

When we make a determination of the setting depths for the various casing strings in our well, there are several parameters that we must consider.

- Experience in an area
- Pore pressure (formation fluid pressure)
- Fracture pressure
- Borehole stability problems
- Corrosive zones
- Environmental considerations
- Regulations
- Company policy

Some of these criteria may overlap in practice. For instance, many regulations for the protection of fresh water sources near the surface might also be considered to be environmental parameters. While this is a text primarily about casing, two of these criteria, pore pressures and fracture pressures, are so important that we will discuss them in a little more detail than the others in order to understand their importance and what they represent.

2.2.2 The experience parameter

Of all the depth selection criteria listed in the preceding text, successful experience in an area with previous wells is unquestionably the most reliable of all. It should never be discounted out of hand in order to try something else thought to be more "technologically advanced" or more "cost effective." But the risk, if any, in relying heavily on such experience is often a lack of understanding as to why it has been so successful. Too often, blind use of such experience without understanding, can result in something going wrong when least expected. There are always exceptions, so one should understand *why* the current method has proven successful.

2.2.3 Pore pressure

All sedimentary formations contain pore spaces (voids) that are filled with fluids (gas or liquids). Since the rock is buried, that fluid is under pressure that may vary from a simple hydrostatic column to something near the stress caused by the weight of the overlying rock. The pore pressure dictates our minimum mud density which must be adjusted continually in the drilling process to prevent the formation fluids from entering the borehole. You should already be quite familiar with this topic, but a more detailed discussion and refresher is found in Appendix E.

There are various methods for determining or estimating the magnitude of pore pressures in boreholes, and while we cannot go into those methods, here is a brief list of some methods and sources.

- Before drilling
  - Production data in area
  - Direct measurements in other wells
  - Log correlations
  - Paleontology correlations
  - Seismic correlations
- While drilling
  - Shale density measurements
  - Drilling rate monitoring
  - Gas monitoring
  - Full mud logging
  - Logging while drilling (MWD)

For this text, we will assume that we already have access to reasonable pore pressure estimates for our borehole, and after reading the above we have some fundamental understanding of what it means. Further in-depth reading may be found in the book by Fertl [12].

2.2.4 Fracture pressure

The subject of fracture pressures for drilling mud programs and casing design can be complicated—a lot more so than many realize. Considerable confusion as to what is actually meant by fracture pressure adds to the complexity. A true definition of fracture pressure is the pressure at which a formation matrix opens (fractures) to admit whole liquids through an actual crack in the matrix of the rock as opposed to invasion through the natural porosity of the rock. This sounds straight forward, but some of the things we often hear called fracture pressures are not true fracture pressures by that definition. In order to better grasp the intricacies of the topic, it would serve to understand a little of the fundamentals of

rock mechanics. These are covered in Appendix E, and it is advisable to review that material if you are unclear about any of the following.

Sources of fracture data

There five sources commonly used for obtaining fracture data are as follows:

- Lost circulation caused inadvertent fracture in nearby wells
- Intentional fracturing during stimulation of nearby wells
- Minifracture tests
- Fracture gradient curves and correlations
- Leakoff tests
- Pressure integrity tests
- Some acoustic logging correlations

The first two of these are self-explanatory. The first may be invaluable because it typically singles out the weakest zone in an open hole section. We also refer to this type of fracture as a drilling induced fracture and usually it is inadvertent. The second sometimes has value for correlation purposes but is limited in that it only applies to producing zones, and they are not usually the trouble zones unless they are being depleted by production in nearby wells.

The third method, the minifracture test, is by far the most reliable of all the methods. It is a purposeful and accurate test but is time consuming and expensive. Figure 2.2 illustrates an actual test using less than 5 bbl of fluid. In that test, a packer is set in the hole, usually an open hole drill stem test packer containing a pressure recorder. Circulation fluid, usually drilling fluid, is pumped slowly into the well at a constant rate. Point B on the chart is the maximum pressure and is the fracture pressure of the formation. The pressure immediately drops a bit and levels off as pumping continues at the same rate. This is the fracture propagation pressure. The fracture propagates at a lower pressure than the initial fracture pressure because the fluid entering the fracture now acts as a wedge with a distinct mechanical advantage in opening the fracture to allow growth at the tip. At point C on the chart, the pump is stopped and the pressure drops sharply at first to point D then more gradually as the pressure dissipates until it reaches the hydrostatic pressure of the fluid column where it began (slightly above the formation pore pressure). The pressure at point D is the fracture closure pressure, and at the instant, it closes that pressure is equal to the minimum horizontal stress component (at the borehole wall), σ_h, which is acting perpendicular to the fracture walls and providing the closing force. Several points are important to mention here. First is that the shape of the curve, especially past point C, is dependent on the permeability of the formation and the properties of the borehole fluid. In this particular case, this test was carried out in a shale (for a stability analysis) and with a filter-cake building drilling mud. In a permeable zone with a clear fluid, the curve beyond point C would look identical to this picture because the pressure would dissipate into the formation naturally through the pores. That was not the case in this test though,

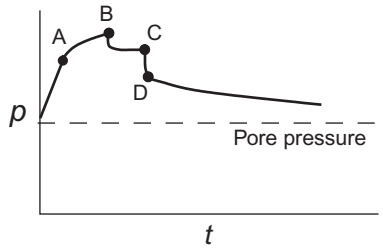

Figure 2.2 A minifracture test for borehole stability analysis.

and the observed "dissipation" behavior was achieved by opening a valve at the surface to affect a bleed-off. Some knowledge and experience is necessary to conduct such a test. Even a poorly done test should give an accurate fracture pressure even if the closure pressure is botched. Fortunately the fracture closer pressure, if missed, can be easily determined by slowly reapplying pressure. The formation, once fractured, will always reopen and take mud at the closure pressure so this can be repeated as many times as necessary to assure success.[1] Notice that I have not yet mentioned point A in this test. That is because I am saving it for later, but for now we will say it is the point at which the pressure-volume relationship becomes nonlinear.

In consolidated rocks with significant tensile strength, a minifracture test has the disadvantage of being a destructive test in that once the rock is fractured it cannot sustain that pressure again in that borehole—only the lesser fracture closure pressure. In unconsolidated or naturally fractured formations (either macrofractures or microfractures), there are no further disadvantages because the rock had no initial tensile strength.

The third method, fracture gradient curves and similar correlations, are most valuable and generally reliable enough to use in casing depth determination. They are used quite successfully in many areas and are most often the most reliable source available. However, you should be aware of something important. These correlations are not to be used in borehole stability analyses because they are based on a plane-strain model that assumes transverse isotropy in the horizontal stress field. Such a condition is extremely rare in real boreholes. In other words, the foundational assumption is not correct. They often suffice for our purposes because a correlation is built into an "effective Poisson's ratio" rather than an actual Poisson ratio of the rock. This is discussed in more detail in Appendix E.

Next on the list is the often used "fracture pressure" called the *leakoff pressure*. Generally speaking, a leakoff pressure test as practiced is not related to actual fracture pressure except in unconsolidated formations or those already containing natural fractures, microscopic or macroscopic. In other words, the validity is limited to formations with no tensile strength. On the positive side, a formation with no tensile strength is not damaged by such a test and will always open at the same pressure, so this is an almost risk-free method to determine the maximum mud density that can be used in a borehole. The downside is, what about a formation that does have tensile strength like that shown in Figure 2.2? Many perform such a test and call point A the "leaf-off point" and stop the test before reaching point B. That is okay in most cases because it is a safe point below the actual fracture pressure. Unfortunately, an appalling amount of nonsense has been written about this point that needs debunking. Some say this is the point at which "whole mud begins to enter the formation." Whole mud particles cannot enter most formations because the permeability is too low. The permeability necessary for most filter-cake building muds to enter the formation is on the order of darcies and not millidarcies. The formation must actually fracture for whole mud to enter. Even if the permeability is very high, most filter-cake building muds will bridge these pores in an instant. Another popular misconception is that such a point represents the beginning of fracture growth down the borehole wall before the fracture opens enough for mud to enter. The reality is that a surface fracture propagating under constant applied pressure (as in this test) propagates at the speed of a Rayleigh wave, or about 1/4 the speed of sound in the rock. So a surface fracture in a 60-ft long borehole (the length of the test hole below the test packer in Figure 2.2) would traverse its length in about 0.02 s. So that notion too is bunk. The only thing we can truthfully say about point A is that *it is the point at which the pressure-volume relationship becomes nonlinear*. That can be caused by a number of things, not the least of which is the all too common error of assuming that rock behaves in a linear elastic mode all the way to failure.

[1] Fracture closure pressure, as used here, means the natural pressure at which the fracture closes. This is not the same pressure as the "fracture closure pressure" after a massive hydraulic fracture treatment in which the near borehole stress field has been significantly affected by the treatment itself.

Our next consideration is the pressure integrity test. This is a test performed to test a casing seat for cement and formation integrity. It is performed after a casing string has been set and cemented in place. Once the cement has adequately cured, the float collar, shoe track, and float shoe plus some small amount of new formation, 30 ft±. The well then is pressured to the equivalent pressure of the maximum mud density to be used in drilling to the next casing point. If there is a cement failure, remedial cementing is performed. If the test fails because of formation weakness at the shoe, then that is a serious problem. The casing string was set too high. The chances of cementing a fractured formation in an open borehole successfully are almost nonexistent. An additional casing string will most certainly be required to reach the objective, and unless this contingency has been planned for, then the well may have to be abandoned because this weak zone must be isolated before achieving the higher mud densities required. All that said, the point is that a successful integrity test does not give us a fracture pressure, and we should not refer to it as such. It merely tells us that the formation can support a given pressure, and often that information is sufficiently adequate for well planning. One further point might be worth mentioning here about integrity tests. Most setting depths are adjusted to place the shoe in a stable, low-permeability zone where possible. This is as it should be, but it calls into question many integrity tests. A casing string set in a shale for instance, should not be integrity tested in the shale except where the permeable formation below it is over pressured. All things being equal a permeable formation will fracture at a lower pressure than an adjacent shale whose permeability is measured in nanodarcies. Typically, a shale has higher values of horizontal stress than an adjacent sandstone because it tends to be more plastic in its deformations.

Finally, relatively new to our tool box is the use of acoustic logs in determining mechanical rock properties. Some of these techniques have unfortunately been sold beyond their actual capabilities, but the technology is good and continues to improve. Like seismology, the technical difficulty is in translating dynamically measured rock properties into quasistatic properties (Young's modulus for instance). It also requires a focused acoustic tool, rather than one that gives averaged readings. The status is that with a given known measurement in close proximity, the ability to correlate using these techniques is very good.

2.2.5 Other setting depth parameters

The other parameters listed previously are self-explanatory and need little elaboration. However, a few comments may be in order.

- Experience in an area should never be casually tossed aside in favor of pore pressure and fracture pressure data. There are usually good reasons that casing setting depths have become standardized in a particular area. Before making any changes one should investigate those reasons thoroughly.
- Borehole stability problems exist in many areas. Casing is not the only solution in but a few cases, so all possibilities should be evaluated.
- Regulations should never be violated. That should not have to be said, but many would be surprised to learn how frequently violations actually occur.

Casing setting depth is determined by the requirements to maintain the integrity of the borehole and protect the environment. Yes, it is that simple. Or perhaps we should say it is that complicated.

2.2.6 Conductor casing depth

The conductor casing is the largest diameter casing run in the well. It often serves to support the weight of the subsequent tubes in the wellbore and also to maintain some minimal amount of borehole integrity while drilling the surface hole for the surface casing. Individual wells may require two conductors, one a

structural conductor to support the well head and casing and another to provide borehole integrity while drilling the surface hole.

Conductor casing may require the drilling of a hole in the ground and cementing in place or it may be driven into the ground with a diesel pile-driving hammer. The criteria for selecting the depth of the conductor can be very simple or very complicated. On the simple side, we want the conductor deep enough to prevent washing out under the rig or platform while drilling the surface hole. In most of these cases, the first casing head is attached to the surface casing once it is in place and cemented so the conductor serves no further purpose. For many shallow wells with hard surface soils the conductor may be set at depths of 50 ft or so, sometimes 100 ft. On the other hand, in areas where the surface soils (or ocean bottom) are extremely soft it may be necessary to set the conductor 200-500 ft below the surface (or ocean bottom) just to drill the hole for the surface casing. There are some situations where the surface formations are so incompetent or problematic that two strings of conductor casing may be required. In other cases, the conductor casing is also a support structure for the well and must additionally support a small platform attached to the wellhead and some minimal amount of production equipment—not as uncommon as many might think, thousands of these type wells exist in shallow waters. While conductor pipe is usually considered the simplest of the casing strings we will run in our well, it is often more complicated in terms of both setting depth and design. The setting depth of conductor in many cases must be determined by soil bearing tests and coring. This gets more into the realm of the civil engineer than it does into the petroleum engineer's domain. Most companies have their own specifications or they rely on the standard practice in the area that has already proved successful.

There are unfortunately no handy formulas for determining the setting depth of conductor casing. There are just too many variables and complexities to consider here. That probably sounds like an avoidance of the issue, and it is. About the only guide, we can offer in the absence of soil bearing tests similar to those performed for foundations of bridges, tall buildings, and similar structures, is to use what has proven successful in the area. And as much as we hate to say it that brings us to a rule of thumb.

In the absence of soil mechanics data and analysis, the only way to reliably select the depth of conductor casing is to use the depth already proved successful in the area. In other words do what everyone else does. The main thing is that if you do not have data to support your choice, do not attempt to set your conductor casing at a lesser depth than is standard in an area. If it is a critical well and there is nothing in the area, then get soil data.

2.2.7 Surface casing depth

There are a number of factors affecting the setting depth of surface casing:

- Pore pressures
- Fracture pressures
- Depth of fresh water bearing zones
- Legal regulations and requirements

Which of those do we choose? Which are the most important? The answer is almost always the one that requires the deepest casing string. Strictly speaking from a design point of view, the first two are the most important—they are related and are our basis for maintaining borehole integrity. We intend that to include well safety. The last two may also be related. Protecting surface fresh water sands is of extreme importance in populated areas and in truth it should be everywhere. Regulations require protecting freshwater in most areas now. However, it is sometimes possible to obtain a variance from

the regulations if the fresh water sands will be protected by the next string of casing. *Damaging a fresh water aquifer is not acceptable and carries stiff penalties in most parts of the world.*

The question of regulations as already mentioned is usually a matter of protecting freshwater aquifers, but in many cases regulations also address safety aspects of setting sufficient surface casing. Unfortunately, regulations do not always take specific situations into account, and they may require more casing than is really needed and sometimes less than what is needed. In those cases, it is best to consult with regulatory agencies, as to what exceptions and variations from the regulations might be possible.

Aside from the regulations, the surface casing must allow us to drill to the next (or final) casing point with the mud density required to contain the formation pressures encountered and not cause fracture failure of the exposed formations near the upper part of the hole. If more than one additional string of casing (an intermediate casing string) is required, then the two become interdependent as to setting depths.

2.2.8 Intermediate casing depth

The most common cause for needing intermediate casing is that the borehole below the surface string may require a mud density too high (or sometimes too low) for the formations between the final drilling depth and the surface casing depth. A high mud density may fracture exposed weak zones or a mud density too low may allow higher pressured zones to flow into the borehole. Additional reasons for running intermediate casing include the presence of unstable zones and corrosive zones. Instability in some zones, usually shales, may make it impossible to drill to total depth without isolating these zones. The presence of corrosive zones may require isolation to protect the production string.

2.2.9 Setting depths using pore and fracture pressure

Aside from regulations and known problem zones, casing depths are typically selected using formation pore pressure and formation fracture pressure, and that is what we will address now. The best way to understand how these two parameters are used is to make a plot of pore pressure and fracture pressure versus depth. Figure 2.3 is a plot of the two parameters for a simple well.

It shows a plot of the formation pore pressure versus depth on the left and the fracture pressure on the right. Notice that the pressure is given in terms of equivalent mud density (specific gravity here) to make the plot more easily used by drilling personnel. Drillers use plots like this to determine mud densities required at various depths for drilling the well. The mud density must be slightly higher than the formation pressure to prevent formation fluids from entering the borehole, and at the same time the density must be less than the fracture pressure so that the drilling fluid does not fracture and enter the formations. These two lines shown in the chart do not include any safety margins. Drillers typically drill with the density slightly higher than that required to balance the formation pressures. This allows some safety margin, especially when making trips because the action of pulling the pipe tends to cause a negative pressure surge or a reduction in the hydrostatic pressure while the pipe is in motion.

Likewise drillers like to keep the maximum density slightly lower than the fracture pressure because running the drill string into the hole causes positive surge pressures. We will refer to this as a *fracture margin*, but in many contexts, it is referred to as a "kick margin" so that during a well-control event, the formation is not fractured in the process of killing the well. Different companies have their own specific policies on the values of these design margins, and it may vary with type and location of individual wells. In Figure 2.3, we arbitrarily used a margin of 0.06 specific gravity ($\sim$ 0.5 lb/gal or 60 kg/m^3) for both the pore pressure and fracture pressure. This is *not a recommendation*, but just a simplification for illustration purposes, and we will use the same values in all our examples to avoid confusion.

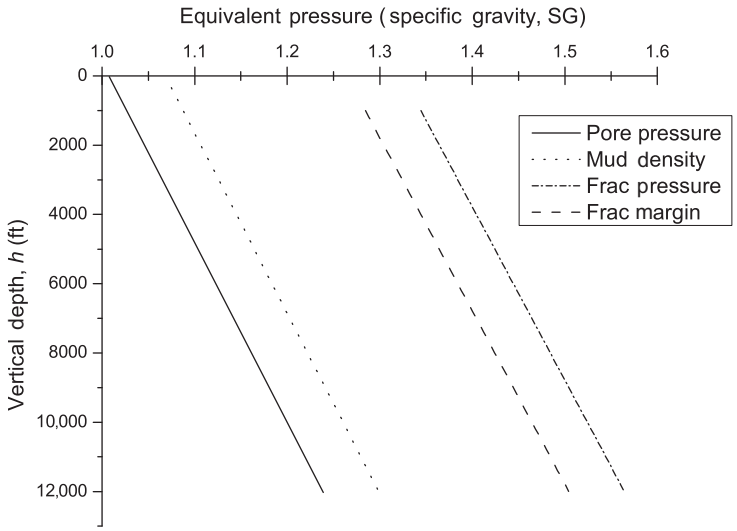

Figure 2.3 Pore and fracture pressures with margins.

We added these two safety margins to the figure, and we can see that the mud density required to contain the pore pressure plus the safety margin at 12,000 ft is 1.4 SG, but above 1700 ft that mud density begins to exceed the fracture margin. In other words, we cannot drill safely to 12,000 ft in the well unless the hole is cased down to 1700 ft or more because the mud density required to contain the pore pressure at bottom is greater than the fracture pressures at the surface (including the safety margins). That is exactly how we determine the setting depth of the surface casing for this well.

In Figure 2.4, we start with the mud density at 12,000 ft (point *a*) and draw a line vertically until it intersects the fracture margin line (point *b*) then horizontally to the vertical axis (point *c*); we can read the setting depth of the surface casing which in this case is about 1700 ft.

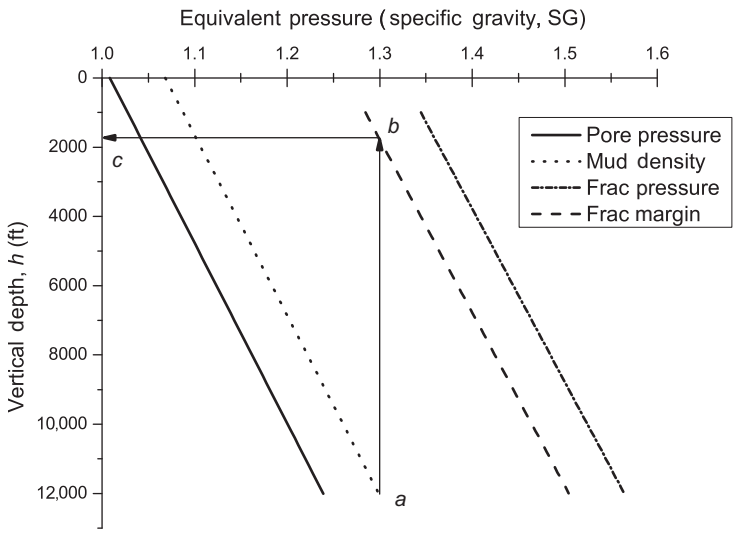

Figure 2.4 Selection of casing setting depths.

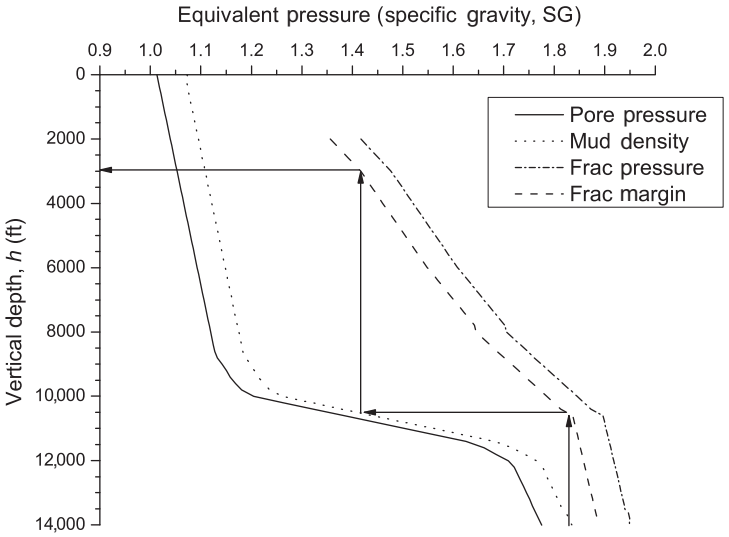

Figure 2.5 Casing selection for example well.

That particular well requires only a surface casing string at 1700 ft and a production string at 12,000 ft. If the surface casing depth of 1700 ft meets the regulatory requirements for this well then, our setting depth selection is complete. If the regulations require more casing, say 2500 ft, we will simply move our surface casing depth to 2500 ft, and it will give us more safety margin in our mud densities as far as a kick is concerned.

That is a relatively simple well. But before we dismiss it as trivial, that is exactly the circumstance for the vast majority of all wells that have been drilled in the world. That said, we will now look at an example in which an intermediate string is required.

EXAMPLE 2.1 Casing Depths

Using the pore pressure and fracture plot in Figure 2.5 and the same margins of 0.06 specific gravity ($\sim$ 0.5 ppg or 60 kg/m^3), we see that the mud density of 1.83 SG required at 14,000 ft will exceed the fracture margin at all depths above 10,500 ft. So we must set a string of casing at that depth. Moving horizontally to the left, we see that the mud density required at 10,500 ft is 1.42 SG. This mud density will exceed the fracture margin at all depths above 3000 ft. So 3000 ft becomes the surface casing depth.

This is a straight forward procedure, but sometimes it can be complicated by depleted zones that have lowered pore pressure and fracture pressure but are located among normally pressured zones. In some cases, we may have situations that require more than one intermediate casing string in which case we typically would install a liner (usually called a drilling liner) before reaching total depth rather than a second, full intermediate string. There are many possibilities, but that is the basic procedure.

2.3 Casing size selection

After determining the number of casing strings required and the setting depths the next step in the design procedure is to select the sizes of casing required. What size casing and what size bits do we require?

2.3.1 Size selection

Once the setting depths have been determined, the next step is obviously to select the sizes of the casing strings to be set. The sizes will depend on a number of criteria, but two important things to know about selection of casing size are as follows:

- Hole size determines casing size
- Hole size at any point in the well except the surface is determined by the previous string of casing

This means that in selecting casing size, we usually start with the casing size at the bottom of the hole and work to the top.

The size of the last string of casing run in a well is generally determined by the type of completion that will be employed. That decision is usually the function of an interdisciplinary team of reservoir, production, and drilling personnel. There are numerous criteria on which this decision is based, so we will assume for our purposes that the size of the final string is predetermined, and we will proceed from that point. From the standpoint of drilling operations, our input into that process is to assess the risks and allow for alternatives. For example, if we know there are serious hole stability problems in an area and our drilling experience in the area is limited, we may be well advised to recommend a final size that is still large enough for us to set an extra string of casing or liner and still reach the objective with a usable size of hole for a good completion. This is a point that is unfortunately too often overlooked in the desire to keep well costs low.

Once we know the diameter of the final string of casing or liner, the process proceeds like this:

- Determine the hole size (bit size) for the final string of casing.
- Determine what diameter casing will allow that size bit to pass through it. That is the size of the next string of casing.
- Repeat the procedure until all of the hole sizes and casing sizes have been determined.

Many times in actual practice, casing sizes are often determined by what is readily available in some inventory (the company's, partner's, or vendor's) and the delivery times. The cost of leaving surplus pipe in inventory or excessive delivery times often supersede any "optimum design" based strictly on engineering calculations.

Precaution: After the casing strings have been designed be sure to check the drift diameters to be certain that all the desired bit sizes can be accommodated.

2.3.2 Borehole size selection

What is the proper borehole size for various sizes of casing? What do we require of the borehole size?

- A borehole must be large enough for the casing to pass freely with little chance of getting stuck.
- There should be enough clearance around the casing to allow for a good cement job.
- In general, the bigger the borehole the more costly it is to drill.

There are no formulas for determining the ideal borehole size.

Selecting the borehole size is primarily based on current practices in the area or areas with similar lithology. There are a number of charts and tables in the literature, some good for some areas, but greatly lacking for other areas. The best advice we can offer is to use what is common practice in the area unless

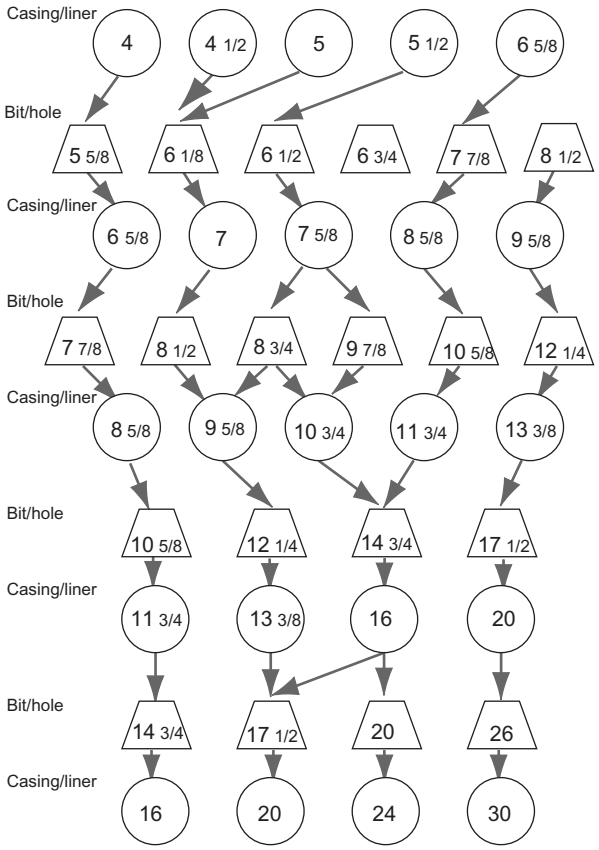

Figure 2.6 Typical bit and casing sizes for hard rock environments.

there is good reason to do otherwise. No matter what specific charts we suggest here, they going to be wrong for some particular locale or application. That notwithstanding, here are two charts that show some typical choices. One chart is for hard rock (Figure 2.6), and the other is for unconsolidated rock (Figure 2.7).

These charts start with the last string of casing or liner and work downward to the first casing string of the well. You can see on these charts that there are many options even for those situations where the same size liner or casing is to be run. In general, hard rock offers us more choices, and clearance between the casing and borehole wall can be less than for unconsolidated formations.

You will note in the chart for unconsolidated rock that there are still some options, but not as many. A few may not be available even though shown on the chart. For instance on the fourth row from the top it shows that either an 8-1/2 in. or an 8-3/4 in. bit may be used from 9-5/8 in. casing. That may be true in some cases, but if the 9-5/8 in. casing string contains any 40 lb/ft or heavier pipe then the 8-3/4 in. bit cannot be used. What is common practice in one area may not work in another because formation pressures may require a heavier pipe.

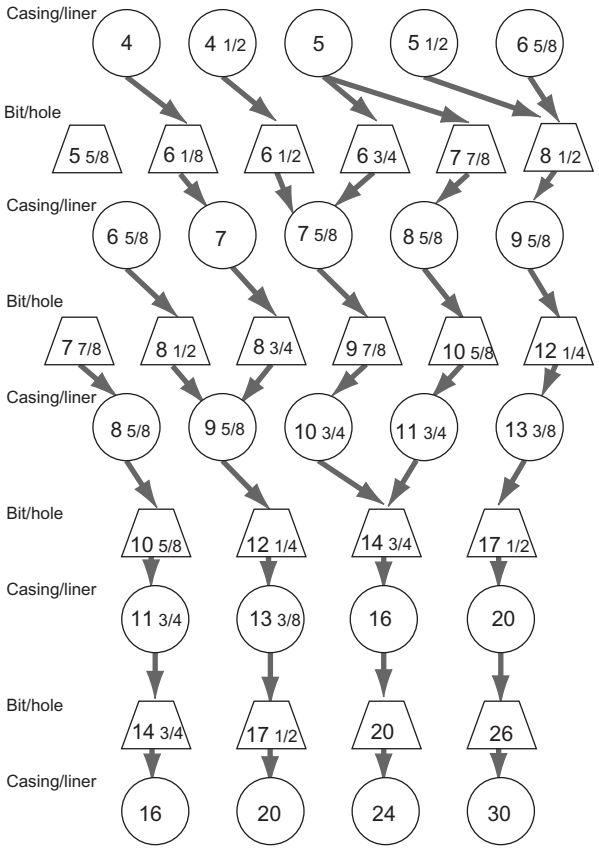

Figure 2.7 Typical bit and casing sizes for unconsolidated rock environments.

EXAMPLE 2.2 Casing Size Selection

Continuing with the same example, we looked at previously in this chapter; assume that we have determined the following casing depths:

- Surface casing: 3000 ft
- Intermediate casing: 10,500 ft
- Production casing: 14,000 ft

The production engineers tell us they will require a production casing diameter of 7 in., so the production casing size is determined. Assume that the well is in an area of *unconsolidated* formations. Use the soft formation chart (Figure 2.7) to determine the intermediate casing size, the surface casing size, and the conductor casing size.

- Intermediate casing: 9-5/8 in.
- Surface casing: 13-3/8 in.
- Conductor casing: 20 in.

Although not shown in the chart as a possible path, some operators in areas where borehole stability is a serious problem elect an alternative for 7 in. casing as follows:

- Intermediate casing: 10-3/4 in.
- Surface casing: 16 in.
- Conductor casing: 24 in.

That choice would be a case where experience in a particular area might influence the decision in order to allow more margin for the effects of anticipated problems.

A precaution

You may note in the two charts above that more casing-borehole clearance is specified in unconsolidated formations than in hard rock formations. Why? Most unconsolidated formations occur in newer geological marine environments where swelling shales and high permeability zones are commonplace. These environments are known for reduced clearance caused by the swelling shales, accumulation of break-out and sloughing debris, as well as differential sticking tendencies in the more permeable formations. There is sometimes a tendency for those inexperienced in these environments to assume that these unconsolidated zones will be washed out and actually have greater clearance instead of less. While that is definitely true through some intervals, it is not true of the entire exposed borehole. The consequences of such an assumption is almost always disastrous.

2.3.3 Bit choices

Obviously from the above charts, we select the hole size for our particular casing and that automatically sets our bit size too. While that is true, there is another aspect to the bit sizes that should be mentioned. Those charts are based on the most commonly available bit sizes. There are special cases where it will be necessary to use an unusually thick wall casing, and you find that the common bit used in that casing will not work—the bit is too large. There are other diameters of bits available for special applications that are not shown in these charts. In general, they tend to cost more, but the biggest problem is that often there is a limited choice of bit types when it comes to uncommon bit sizes. For instance for one common size, we may have a choice of 25 different tooth and hardness characteristics just from a single manufacturer, and maybe 50-100 choices if we include all manufacturers. However, with some odd size bit, we may be limited to a small range of tooth and hardness choices and possibly only one manufacturer. That may be acceptable for some special cases, but it should always be considered.

Bit clearance

To determine the bit clearance, we look at the casing tables for the internal diameter and see if it is larger than the diameter of the bit. But in the tables, we see two diameters listed. One is the nominal internal diameter and the other is the internal drift diameter which is slightly smaller than the internal diameter. The internal diameter is the diameter to which the tube is supposedly manufactured. Once it has gone through the milling process, it is inspected for final diameter by passing a mandrel through it of the diameter listed as the internal drift diameter. So its internal diameter might be the same as the nominal internal diameter or it might be slightly smaller (or larger), but we know that it is at least as large as the drift diameter (assuming the manufacturer does its job). We normally assume that the drift diameter is the maximum bit diameter, we can be assured will pass through the casing. But in many cases, bits greater than the drift diameter have been used. In that case, you must drift the casing with a

mandrel the size of the bit first and cull out those joints that are undersized. Some steel mills will do this for customers (usually at extra cost).

2.4 Casing string configuration

Once we determine the depths of the casing strings, we may still have several alternatives.

Figure 2.8 shows three possible configurations for our example well. The first shows a conventional production casing string. The second shows a production liner where the intermediate string also serves as part of the production string. The third one shows a tieback string inside the intermediate string and connected to a liner at the bottom of the intermediate string. One can see that the second option might save the operator money by eliminating a full production string, but why would an operator elect to choose the third option as opposed to the first or the second? One reason might be to reduce the weight of the final string and save money using a lower tensile strength casing. Of course that has to be more saving than the additional cementing and equipment cost and additional rig time required. However, here is a typical situation for choosing the third option. We are drilling a high pressure, well and the intermediate casing is required to contain the high density mud while drilling the lower part of the hole. In this case, suppose it takes a few weeks to drill the hole below the intermediate casing so there may be considerable wear from the drill string on the intermediate string. This means we have to rule out option number two because the intermediate casing may not be able to contain the pressures required of a production string that has loss of wall thickness from the wear. In this case the first option is usually cheaper than the third option which requires more time, more cement, and more equipment, so we still see no reason for selecting the third option. Consider two more things though. Remember that we said that it was a high pressure well. The operator wants to be assured that the casing above the cement does not leak, and the best way to assure this is a hydrostatic test of the casing connections as the casing is being run in the hole. This cannot be done with a full string of pipe because the static time required to test each connection will probably allow the casing to become stuck before it gets to bottom. That would then be an extremely costly situation which would require another liner of a smaller diameter

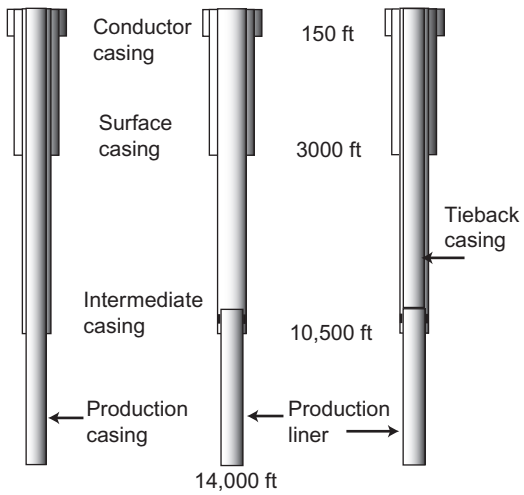

Figure 2.8 Three possible casing configurations.

than the production casing. So, while the third option is not common there are often very good reasons for doing it. And further, there are many wells that require two liners instead of one, and the tieback string is always a preferred option in that case. There are many possibilities. Well conditions and costs dictate the actual choices. We will discuss those choices in more detail later.

2.4.1 Alternative approaches and contingencies

There are additional approaches to allow for more clearance for the casing. One method is to under ream the open hole below the current casing string. This allows additional clearance and is a proven method where the expense of the extra time and reaming can be justified. A similar result can be obtained with a bicentered bit for drilling below the current string of casing. Such a bit will drill a larger diameter hole than its nominal diameter. This technique can eliminate the extra expense of under reaming and accomplish the same result.

Another option is the use of expandable casing. This is a relatively new technology and has proven successful in a number of applications. The hole is typically drilled with a bicenter bit or under-reamed to give more clearance. The casing itself is run just like a conventional liner and is expanded after it is in place. Expandable casing will be discussed in more detail in Chapter 6.

2.5 Closure

In this chapter we have examined the procedures for selecting casing setting depths and casing sizes. We used a plot of formation pore pressures and fracture pressures to select the setting depths. This is a straightforward method that may appear deceptively simple. The truth is that it is not the procedure that is complex, but the data itself for use in the plot. Often, it is not readily available nor is it totally reliable. When this type of procedure first came into use many operators looked at it as a way to save money by reducing the number of casing strings traditionally run in some areas. It appeared that in many cases, it was possible to run surface casing a bit deeper and eliminate an intermediate casing string altogether. When it worked it did save costs, but when it did not work it not only added the string that was "eliminated" but often an additional string as well, and resulted in a very small hole size at bottom and significant additional costs. The problem in these situations was that the data proved unreliable in some cases and that the margins were too close for operating personnel to adhere to in others. So in all cases, the data used in the depth selection process must be scrutinized with care. A prudent philosophy might be stated like this:

- *Exploratory wells or critical wells*. Data are possibly scarce or unreliable, so allow for the unexpected with contingencies in casing size and depths. Usually this means allowing for the possibility of running one more casing string or liner than the plan calls for. These are not the wells where we try to save money on casing.
- *Development wells*. Data reliability and risks are well known. These are the wells where casing costs can be minimized and smaller margins can be used.

No matter what method you use to determine the casing setting depth, always keep in mind that it is one of the most critical steps in assuring a well's success. Do not be caught in the trap of compromising the chances of success by trying to save money by unnecessarily minimizing casing depths and sizes.

Pressure load determination

3

Chapter outline head

Casing and Liners for Drilling and Completion. http://dx.doi.org/10.1016/B978-0-12-800570-5.00003-6

3.1 Introduction

In this chapter, we discuss the pressure loads, collapse and burst, used in the design of casing strings. To illustrate the process, we continue with the example selection from the previous chapter, where we determined the setting depths and casing sizes. Here we will discuss the various types of pressure loads and some particulars as they apply to the different types of casing strings. The actual calculations are merely hydrostatic calculations with various combinations of fluids inside the casing and in the annulus outside the casing. After a discussion of the pressure loads and their application to the different casing strings, we present examples using the casing program we selected in the previous chapter.

To determine the strength of the casing needed, we must now consider the types and magnitudes of the loads the casing must safely bear. A number of different considerations and possibilities accompany each string of casing run in a well. Some simple load situations suffice for most casing strings, but often special conditions may apply to a specific well or type of well. We will discuss the types of loads commonly used as design criteria for each type of casing string. Three basic types of loads commonly are considered:

1. *Collapse loads* are differential pressure loads in which the outside pressure exceeds the inside pressure, tending to cause the casing to collapse, $\Delta p = p_{\mathrm{i}} - p_{\mathrm{o}} < 0$.
2. *Burst loads* are differential pressure loads in which the inside pressure exceeds the outside pressure, tending to cause the casing to rupture or burst, $\Delta p = p_{\mathrm{i}} - p_{\mathrm{o}} > 0$.
3. *Axial loads* are tension or compression loads mostly caused by gravitational and frictional forces on the pipe, but they can also be caused by pressure and temperature changes as well as bending in curved wellbores.

The first two of those load types are dictated by well conditions and anticipated operations in the well. They are functions of formation pore pressures, fracture pressures, drilling fluid pressures, and cement pressures. Those are the two we cover in this chapter. For the most part, we will be working with differential pressure loads across the casing wall, defined as the inside pressure minus the outside pressure, $\Delta p \equiv p_{\mathrm{i}} - p_{\mathrm{o}}$. The third type of load, axial load, is a function of the casing selection process itself; in other words, the axial load is a function of the weight of the casing selected. Axial loads are covered in the next chapter.

We have used the terms, *collapse* and *burst*, rather loosely as if their meanings were obvious, but we should clarify that now because they are somewhat misleading. Collapse is a form of radial instability that results in radial buckling. The actual deformation referred to as collapse of the pipe is a postbuckling event. From that, one would assume that the collapse rating of a casing is the minimum pressure at which the instability occurs and that any small perturbation in the load, could then cause buckling followed by actual postbuckling collapse. That is not quite the case, however. The API collapse rating is defined for two extremes: (1) elastic stability for pipe with a relatively large diameter to wall thickness ratio, $d_{\mathrm{o}}/t_{\mathrm{w}}$, and (2) for thicker wall pipe with smaller $d_{\mathrm{o}}/t_{\mathrm{w}}$ ratios, the formula defines the collapse rating to the minimum collapse pressure that will cause yield in the pipe. The burst rating is a bit easier to define; it is the internal pressure at which the inner wall of the pipe initially yields. It is not the pressure at which the pipe would actually rupture as one might expect from the word "burst." We will delve into these ratings in Chapter 6, but for now we are satisfied with knowing what the two terms mean, and that we can look up the values in available tables.

One more clarification about pressure: We will always work in gauge pressure rather than absolute pressure since the difference is insignificant at the magnitudes and applications we are using. When we specify 0 psi, we mean atmospheric pressure. Further, we will not use any atmospheric gradient when working with empty or partially empty casing.

3.2 Pressure loads

The magnitude of the pressure loads that a particular casing string actually experiences in service for the most part are unknown. Certainly, we can calculate the loads we are likely to encounter if all operations are perfectly successful, but the problem is that often there are imperfections in our cementing results or problems in our drilling operations. We almost always are able to determine loads if all is perfect, and we can almost always determine the type of loading that would take place if things go totally awry. But between those two situations is a great unknown. Hence, our most logical approach is to assume the worst case that can happen, within reason, and that is the one we typically use for our casing design. We assume that we can reasonably predict the nature of the worst case loading and calculate its values. For now, we do not concern ourselves with the probability of such loading occurring. The thing that we have to always keep in mind is that we cannot change our designed casing string once it is in the ground and cemented. If that "unlikely" worst case should occur, it is too late to change our design.

The process we now address consists of determining the types of pressure loads and the sources of those loads. These are listed below:

Types of pressure loads

- Collapse loading
  - Minimum internal pressures
  - Maximum external pressures
- Burst loading
  - Maximum internal pressures
  - Minimum external pressures

Sources of pressure loads

- Formation fluids
  - Water (fresh or salty)
  - Oil
  - Gas
- Drilling fluids
- Whole mud
- Mud filtrate
- Un-set cement
  - Whole cement
  - Cement filtrate
- Stimulation fluids
- Ocean or surface water
- Atmosphere

These are the pressure sources that contribute in various combinations to the pressure loading of casing in wells. It is relatively easy to ascertain the internal pressures for design purposes because we almost always know the internal fluids, at least in the design stages. The difficulty is that we seldom know the external fluids and pressures once the casing is in the ground and cemented. It is the single biggest problem in the pressure loading phase of casing design. All we can do is make some reasonable assumptions, and what is reasonable to one engineer may not be reasonable to another. It can become a

bit too subjective. The most common approach is to consider the worst case, not the most likely case. That may seem like a case of avoidance or oversimplification. It is both, but I will repeat time and again in this textbook: *You cannot change your design once the casing is in the ground*.

3.3 Gas pressure loads

Gas pressure is one of the most common loads in casing design, and we need to make a few comments. It is often the case that we know the gas pressure at a source depth but need the value of the pressure in a gas column at another depth. This is not the same simple hydrostatic calculation we use for incompressible liquids because gas is compressible, and hence, its gradient is not a constant. There are a number of approaches for calculating natural gas pressures using the ideal gas law and compressibility factors. The compressibility factor is itself a function of temperature, pressure, and gas composition. Where the data are available, such methods are employed. However, for our basic casing design, we are going to use the common practice of assuming any gas encountered is pure methane whose molecular mass is 16 g (or 16 lb when using a lb-mol) and whose compressibility factor, $Z = 1$ for a fairly large range. Since methane is the least dense of the natural gas components, it gives us the most conservative results in casing design. Many companies use it as a standard in casing design.

Fortunately, the assumption regarding the compressibility leads to a simple equation that we will use in our basic design work:

$$p = p_0 \exp \frac{M\, g\, (h - h_0)}{ZRT_{\text{avg}}} \tag{3.1}$$

where

p, p_0 = pressures, pressure at h and pressure at h_0, respectively
h, h_0 = vertical depths, depth of interest and reference depth, respectively
M = molecular mass, 16 for methane
g = gravitational acceleration
Z = gas compressibility factor, $Z \approx 1$ for methane
R = ideal gas constant, see Appendix B for appropriate values
T_{avg} = average *absolute* temperature, $T_{\text{avg}} = (T + T_0)/2$

This equation is derived in Appendix D as Equation (D.16). In this equation, $R = 1545$ in USC units and $R = 8314$ in SI units.

3.4 Collapse loading

In the case of collapse loading, our task is to determine the least amount of pressure the casing will have inside and the maximum amount of pressure the casing will have on the outside (*simultaneously* at any given stage in the operations).

Internal loads, collapse

- Evacuated casing (fully or partially)
- Gas
- Oil
- Freshwater
- Field saltwater or stimulation fluids
- Drilling or workover fluids
- Combinations and partial columns of these

To these we might add some applied pressure in various situations.

External loads, collapse

- Freshwater
- Saltwater
- Formation pressure
- Drilling fluid
- Cement (un-set)

3.4.1 Collapse load cases

We categorize collapse loading by operational stage such as installation, drilling, and production. We further breakdown the operations into different events and possible occurrences that may take place within those three operational stages.

Installation stage—collapse loads

The installation stage is the running and cementing of the casing string. It also includes postcementing operations such as pressure testing.

Installation—running

There is only one collapse scenario in running casing and that is running an empty or partially empty casing string. Neither is almost ever done intentionally and few designs account for it.

Installation—conventional cementing

The density of cement is almost always greater than the displacement fluid. Once the cement is in place and the displacement and plug-bump pressure is released, this differential should not cause casing collapse. It is imperative that this calculation be included in the design, especially when the difference in densities is significant.

Installation—inner string cementing

Inner string cementing is a process wherein the casing is not cemented with conventional top and bottom wiper plugs but by running a smaller diameter string (usually drill pipe) inside the casing with a seal assembly that connects to a special float shoe on the casing. The cement is then pumped through the inner string rather than the casing. This is especially effective in cementing large diameter pipe. It reduces pumping time as well as reducing contamination of the cement slurry as it is pumped in the

large diameter pipe. Inner string cementing is usually restricted to conductor and some large diameter surface strings. The collapse situation occurs because the cement is more dense than the fluid inside the casing which may be even less dense than the displacement fluid used in the inner string.

Drilling stage—collapse loads

Collapse during drilling is almost always caused by loss of internal pressure from lost circulation. In some cases it can be severe enough to completely evacuate the casing.

Drilling—lost circulation, evacuated

Complete evacuation occurs when a very weak zone below the casing fractures and allows the drilling mud to enter. The hydrostatic head is reduced and the mud level in the well drops. Continued pumping only pumps more mud into the fractured zone and does nothing to keep the mud level above a static equilibrium with the fractured zone. In some severe cases, the casing string may be completely evacuated. This usually happens when drilling below surface casing, but is not unknown with depleted zones below some intermediate strings. This is the most common case used in surface casing design.

Drilling—lost circulation, partial evacuation

In most cases of lost circulation, the casing is not fully evacuated. With very accurate fracture data and formation pressure data, we could calculate the level to which the drilling fluid would be in equilibrium with a fractured formation. This is mostly wishful thinking since such accurate and reliable data are seldom available during the design process. For surface casing, we usually design for a fully evacuated string, but for intermediate casing, we seldom see a fully evacuated string and to design for such, might seem a bit too conservative. In most cases of lost circulation while drilling below intermediate casing, the most immediate concern is a kick caused by the loss of hydrostatic head. Allowing the well to remain static is not an option, the hole should be kept full if at all possible to avoid gas from reaching the surface. Filling with drilling mud will not work because the level will continue to fall and the mud supply on hand will be quickly exhausted. The common procedure is to try to keep the hole full with fresh water, or if offshore, seawater. That is what we will use in our examples.

Production stage—collapse loads

This case applies primarily to the production casing. One may not think of collapse as a possibility during the producing life of a well. But to the contrary, it is a very real possibility, perhaps not in the early stages but definitely in the later life of the well.

Production—evacuation

How can a production string be evacuated? More easily than many might suspect. For example, a packer in a gas well develops a slow leak, and the packer fluid is “produced” along with the gas until it is exhausted. Or, the perforations sand up below the packer and the flowing gas well bleeds to atmospheric pressure. Or another, a well is stimulated and coiled tubing is run to jet the well with nitrogen. The jetting removes all the fluid but the perforations are plugged. The nitrogen flow is stopped and bled to zero. The casing collapses below the packer. And there are many more. These are things that are almost never planned, but they happen frequently. A production string should always be designed for evacuation if possible.

Table 3.1 Summary Collapse Loading Cases

Collapse Loading	*C*	*S*	*I*	*P*
Installation				
Running, empty	S	S	S	
Cementing, post plug bump	A	A	A	A
Drilling				
Lost circulation	A	A	A	
Cuttings injection		S	S	S
Production				
Evacuation		S	S	A
Artificial lift			S	S
Stimulation, squeeze			S	A

C, conductor; *S*, surface; *I*, intermediate; *P*, production; A, always applicable; S, sometimes applicable.

Production—artificial lift

Artificial lift poses similar hazards as evacuation. It is not at all uncommon to bleed off the gas pressure from casing prior to a workover in a gas-lift well. Depending on the liquid level in the casing a collapse situation might arise. A submersible pump could pump a well "dry" if the perforations should plug.

Production—stimulation, squeeze

It is possible that production casing can collapse during a stimulation or squeeze cementing operation. When a well is stimulated or squeeze cemented through perforations using a retrievable squeeze tool or cement retainer, often times the formation must be fractured to initiate pump in. The collapse problem arises from the fact that whenever we fracture a formation through perforations we have no idea where the fluid is going in the annulus. We like to assume that there is good cement and the fracture takes place in the perforations, but that is not always the case. If there is a channel such that the casing above the packer experiences the fracture pressure it is possible that the casing could collapse above the treatment packer or retainer. It is prudent practice to always assure that the work string annulus above the packer is full and that some amount of pressure is applied to the annulus at the surface. This helps to prevent collapse but also is needed to monitor the casing for work string and packer leaks, especially when squeezing with cement. In all cases, the fluid density in the casing should be equivalent to the formation pressure or slightly higher, so it is a matter of the maximum differential pressure between the formation pressure and the formation fracture pressure.

A summary of collapse loading cases for the three stages of well construction is given in Table 3.1.

3.5 Burst loading

For burst loading, we seek to find the maximum internal pressure and the minimum external pressure occurring simultaneously at any given stage of operations. In low pressure wells or wells that will not flow, burst is seldom considered. However, one should keep in mind the possibility of a future fracture job or high-rate stimulation that might be pumped down the production casing. In burst loading, the

external pressure is the resisting load, and the external loading in a burst situation normally is taken to be the lowest possible pressure externally. At the surface of the string, that pressure is taken to be zero or atmospheric pressure. In a subsea casing string, it would be the seawater pressure at the wellhead. The external pressures other than at the surface could be from a number of sources.

External loads, burst

- Atmospheric pressure (at surface of string)
- Seawater pressure (at surface of string)
- Freshwater
- Saltwater
- Formation pressure
- Drilling fluid

It is never acceptable to assume that hardened cement will give us support in burst, even though it will. The problem with cement is that we have to design our string before the well is cemented. If our cement job is near perfect, then we have additional support in those sections covered by cement. However, if there is even a small interval where the cement is poor, then we have no support at that interval, and there is nothing we can reasonably do to change that. Hence, we can never safely assume that the hardened cement gives us any benefit when we are in the design stage.

Internal loads, burst

- Gas
- Oil
- Water
- Combinations of gas and liquids
- Cement (liquid)
- Pump pressure (plug bump, test pressure, stimulations)

3.5.1 Burst load cases

Burst loading can occur in all stages of well construction and production. The various cases are described here, and they will all be illustrated in the examples later in the chapter.

Installation stage—burst loads

The installation stage is the running and cementing of the casing string. It also includes postcementing operations such as pressure testing.

Installation—plugged float or annular bridge

During cementing, there is always the possibility that a float could plug or the annulus could bridge while displacing the cement. Such an unanticipated event would likely be accompanied by a significant increase in pump pressure before the cementer could become aware and shut off the pump. While this is unlikely, it should be included in the burst cases. The worst case depends on a number of things like the cement volumes and densities compared the annular fluid and displacement fluids. This is one of the more complicated hydrostatic calculations and is better understood by example; hence, we will examine this case later in this chapter in the example cases.

Installation—plug bump

When the top wiper plug (on top of the cement) contacts the top float, it stops the displacement circulation and an increase in pressure occurs. This is an anticipated event and the cementer applies a predetermined *additional pressure above the displacement pressure* before stopping the pump. This is referred to as the *plug-bump pressure*. Its purpose is to assure that the plug is indeed seated on top of the float. Because the cement is almost always more dense than the displacement fluid, the maximum differential pressure occurs when all the cement is displaced. Added to that differential then is the plug-bump pressure. The magnitude of this pressure is a matter of preference, company policy, and so forth, but it is generally on the order of 500-1500 psi depending on the casing and well conditions. And to be candid, its actual magnitude sometimes is a result of careless monitoring of the displacement progress and may exceed the predetermined amount. In any case, the differential burst pressure in the upper portion of the casing can be quite significant, and this should always be a design consideration for all conventionally cemented casing strings.

Installation—pressure test

Everyone should agree that all casing should be pressure tested once it is in place. In many areas, it is required by regulations. Where the controversy arises pertains to when it is tested. Many operators legitimately claim that the plug-bump pressure is the best test. If the casing holds pressure then there is no reason for it to leak later. That is valid, but unfortunately, many regulations require a pressure test be performed later before drilling out the floats and proceeding to drill deeper (or after 24 h or so for production strings). Most who favor the former argue that premature pressure testing after the cement has supposedly set can damage the cement sheath around the casing, and this is a valid point. It is especially valid for surface casing where lower temperatures slow the cement curing process and the curing time while installing and testing the BOP stack on the surface casing is relatively short. Waiting additional time for cement to strengthen is expensive and too often ignored. It is not so critical on intermediate strings where temperatures are higher, more time is required to change out the BOP stack and to pick up a string of smaller diameter drill pipe to drill below the intermediate string. Those arguments notwithstanding, most pressure tests are done after the cement has been placed and supposedly cured. Our only question is, what is the fluid in the annulus? Simply put, we do not know. About the best we can come up with is that in the worst case, it is the same as the mud the casing was run in. Assuming the displacement fluid in the casing is the same density as original mud, then this case will give a uniform differential pressure test to the entire casing string. Since most regulations specify a surface pressure for the test, this is the most legitimate form of the pressure test. Changing the mud in the casing before the test is obviously not a good idea.

Drilling stage—burst loads

There are only two general cases of burst loads that occur in the drilling stage of well construction. They are the maximum mud density used in the casing before the next casing string is set and the pressure from a kick.

Drilling—maximum mud density

We always know, or should know, the maximum mud density we will use in drilling below a casing string to reach the next casing point. What we never know is the fluid in the annulus. So again we take a worst case scenario that is within reason. For surface casing we generally assume something like freshwater for surface casing and maybe saltwater for intermediate casing. Some would assume the mud the casing

was run in and others might assume formation pressure. While a formation pressure gradient might sound most reasonable, we must also consider depletion of zones covered by the casing that are being produced in other wells. That applies mostly to production casing, but formation pressures as backup are seldom used in most cases. For simplicity (and lack of data), most use freshwater or saltwater in basic design and use more detailed information for critical wells.

Drilling—well kick

There are three fluids involved in kicks, singly or in combination: gas, oil, and saltwater. Of these, gas is the most severe and dangerous. In considering kicks, we limit ourselves to surface and intermediate casing strings, because production strings are designed as a tubing backup and that is included in the production stage of operations. We normally assume that the kick originates at the highest pressure zone below the casing string, and that in the worst case we have a solid column of the formation fluid (gas, oil, or saltwater) all the way to the surface. All well-control methods are designed to prevent that, but it happens, and when it does, it is too late to change the casing design. There are two approaches to determine the pressure inside the casing: (1) if the pressure of the column of fluid does not exceed the least fracture pressure in the open hole (usually near the shoe) then the pressure of that column is calculated from the kick source zone to the surface, or (2) if the pressure of the kick fluid column exceeds the formation fracture anywhere in the open hole, we assume the kick fluid is flowing into that formation, and we calculate the pressures in the casing using that fracture pressure as the source zone pressure and assume a solid column of the kick fluid from there to the surface.

As already stated, gas is the most severe of these and is usually the basis for our design. There are, however, some areas of the world where there is no gas present, and the design is based on an oil column. Seldom do we design for a saltwater kick, but it is a common possibility in some wells between the surface and intermediate casing strings where there is no gas or oil. As usual, the question of the annular fluid is the same, and again, freshwater, saltwater, or drilling mud are the common options.

Production stage—burst loads

In the production stage of operations, the only affected string is the production string. The exception to that would be a well that has a production liner and utilizes the intermediate string as part of the production string. In that case, the intermediate string must meet the design criteria of both intermediate and production casing.

Production—pressure test

In a production casing pressure test, we almost always assume the backup pressure is the mud in which the casing was run because the test is carried out soon after cementing. If the displacement fluid inside the casing is the same drilling fluid then the pressure test differential will be uniform from top to bottom. If a less dense displacement fluid is used (common with some operators to enhance cement to pipe bonding) then the test should be performed when the displacement fluid is replaced by the more dense workover/completion fluid.

Production—tubing backup

The production casing is a pressure backup for the tubing string. Tubing strings leak, and that is a given. Not always, but it is one of those unfortunate things we cannot predict nor always prevent. Because

Table 3.2 Summary Burst Loading Cases

Burst Loading	*C*	*S*	*I*	*P*
Installation				
Cementing, plugged float	A	A	A	A
Cementing, plug bump	A	A	A	A
Pressure test	S	A	A	A
Drilling				
Max mud dens. below shoe	A	A	A	S
Gas kick (full gas col.)		A	A	S
Oil kick (full oil col.)		A	A	S
Salt wtr. kick (full salt wtr. col.)		A	A	S
Production				
Pressure test			S	A
Tubing backup			S	A
Tubing gas leak			S	A
Stimulation, squeeze			S	A

C, conductor; *S*, surface; *I*, intermediate; *P*, production; A, always applicable; S, sometimes applicable.

the production casing does have some backup in the annulus, it does not have to have the same burst rating as the tubing, except near the surface. What the backup fluid is, is still unknown but generally we may use freshwater or saltwater. You must remember though that the production casing absolutely must contain the well pressure so the worst case is mandatory here.

Production—tubing leak

One of the most severe burst loadings in a gas well results from a near-surface tubing leak. These leaks are not at all uncommon in gas wells. Near-surface tubing corrosion from freshwater condensation mixed with CO_2 to form carbonic acid is quite common in many gas wells. Most operators monitor such corrosion in tubing, but occasional leaks still occur. The result is that wellhead gas pressure is applied to the top of a full column of weighted packer fluid, and the differential pressures on the casing can be very high near the packer. Some casing designers ignore this case altogether. Some operators provide for an emergency relief system on the annulus and/or use a reduced density packer fluid. Some elect to purchase a very expensive casing string.

Production—stimulations, squeeze

A production string must be able to withstand stimulation and squeeze pressures. When such treatments are performed below a retrievable packer or a drillable retainer, only the portion of casing below that tool experiences the treatment burst pressures. On the other extreme hydraulic fracture treatments performed without tubing in the well, subject the entire production string to the treatment pressures. The pressures for high-rate hydraulic fracture treatments can be quite high and are often the critical case for burst design. We will not consider this in our basic design process, but will discuss it in detail in Chapter 7.

A summary of burst loads for different casing strings during three stages of well construction is shown in Table 3.2.

3.6 Specific pressure loads

As we saw in Tables 3.1 and 3.2, different casing strings experience some common types of pressure loads, but also some different types. We will now look at some of these loads as they apply to different strings.

In all our calculations, we will be using specific gravity, $\hat{\rho}$, for density values to make it easier for those working in different unit systems, so $\rho = \hat{\rho}\,\rho_{\text{wtr}}$. We will consistently use a water density, ρ_{wtr}, of 1000 kg/m^3 in SI units and 8.33 ppg in USC units or 62.43 lb/ft^3 should the need arise. Most of our pressure calculations at various depths will be done using liquid gradients:

$$\gamma = g\,\rho = g\,\hat{\rho}\,\rho_{\text{wtr}} \tag{3.2}$$

Using consistent units in a coherent system, e.g., SI, that is all we need. In USC units, we will need some conversion factors, where γ will be in psi/ft (lbf/in.^{2}/ft) and ρ_{wtr} will be in ppg (lb/gal). The specific gravity, $\hat{\rho}$, is dimensionless and independent of our choice of system. We will use water density of 1000 kg/m^3 and 8.33 ppg in all our calculations.

$$\gamma = g\,\hat{\rho}\,C_{\text{ppg}}\,g_{\text{c}}\,\rho_{\text{wtr}} = 32.14\,\hat{\rho}\;(0.052)\left(\frac{1}{32.14}\right)(8.33) \tag{3.3}$$

This is all discussed in Appendix D including derivations of the conversion factors needed for USC units. Since $g \cdot g_{\text{c}} \approx 1$ in all our applications, we will not show it in our numerical calculations when using USC units.[1]

3.6.1 Conductor casing

Conductor casing design is to some extent different from all other casing in a well. Most of the conductor casing is not regular API casing, some is API line pipe, but beyond 20 in. OD, none is API casing. Being of a typically large outside diameter and relatively thin wall thickness, it generally has a low collapse rating. When conductor is set in a drilled hole and cemented, it is usually cemented with an inner string (drill pipe), so there is little differential collapse pressure on the casing. Only rarely is conductor casing capable of pressure control so burst is seldom a consideration. In offshore applications where a diverter (similar to an annular preventer) is installed, its purpose is to divert a shallow gas kick away from the rig to provide enough time for emergency evacuation before the gas breaks through the shallow zones outside the conductor and under the rig. Rarely can conductor hold pressure and prevent gas from breaking through to the surface. As for tension, most conductor casing is set at such shallow depth that tension is not a consideration either. In many land locations, conductor is set by a small rig ("rat hole" rig) before the drilling rig arrives on location. Many offshore platforms have conductor casing installed as part of the platform installation process, though some require an additional conductor string once the rig is on the well. In many water locations, the conductor is driven into the earth with a diesel pile driver hammer. Additional joints are welded to the string as it is driven until it reaches a point where each stroke of the hammer causes negligible additional penetration. The excess and damaged top portion is cut off with a cutting torch. There are also conductor connections (even for drive pipe) that can be installed before the conductor joints are sent to the location, thus eliminating the time consuming welding process

[1] Please note that the conversion factor, g_{c}, does not convert g. It converts the density of water, ρ_{wtr}, from lb/gal to slug/gal. This traditional notation often confuses. Also please note that g_{c} in this edition is a more conventional form and is the reciprocal of the form used in the first edition.

on the rig. There are a number of things to consider with drive pipe such as soil adhesion, elastic response of the pipe to the hammer, hammer sizing and so forth. Where the conductor casing supports a wellhead and additional strings of casing there can be a considerable compressive load.

3.6.2 Surface casing

In this section, we examine the particular loads as they apply to surface casing. Typically, the loads in surface casing are relatively low compared to other casing strings in the well, but many casing failures occur because of under-designed surface casing.

Surface casing collapse loads

The collapse load for surface casing depends on the worst-case scenario anticipated, in which the pressure outside the casing exceeds the internal pressure. There are a number of possibilities, but the most commonly accepted situation assumes that the surface casing is empty inside (usually caused by lost circulation while drilling somewhere below) and has mud pressure on the outside of the same magnitude as when the casing was run. We can modify the internal pressure, if we have some knowledge of the worst case of lost circulation that could be encountered and how far the drilling fluid would drop in the surface casing should that occur. But, in the absence of such knowledge, we should assume the lost circulation situation could be severe enough to empty the surface casing. On the outside of the surface casing, we know the pressure when the casing is run; it is the hydrostatic pressure of the mud column. If the cement is of greater density than the mud (and it usually is) we easily can calculate the pressure contribution of the cement. The question is, what is the pressure after the cement hardens? We can be fairly certain that it will not be as high as the cement pressure before it hardened, but the actual pressure depends on the integrity of the cement job, that is, whether there are channels in the cement or some formations are not cemented properly. Typically, a safe assumption is that the highest pressure outside the casing after cementing is the mud pressure before cementing. It may be less, but it is unlikely to be greater.

Another possibility is a cementing related collapse or post plug-bump collapse where the internal pressure is released after the top wiper plug seats on the top float (plug bump). The liquid phase cement is almost always more dense than the displacement fluid (also a good cementing practice), and the pressure differential could cause a collapse. Such an event is rare, but should always be considered.

Typical surface casing collapse design loads

- Cementing collapse
- Severe lost circulation

Surface casing burst loads

The worst case burst load on the surface casing is based on the maximum anticipated internal pressure and the minimum anticipated external pressure. Let us look at the external pressure first. In collapse, we sought the maximum external pressure, now we are interested in the minimum. The minimum external pressure is likely to occur sometime after cementing. It is believed that, when cement hardens, fluid in the spaces where the cement has channeled or is absent often is similar in density to freshwater or saltwater. For that reason, many assume that the minimum external pressure is equivalent to a freshwater gradient. Some believe that a freshwater gradient is not really likely and they use the mud pressure on the outside, just as we did in collapse. That is also a valid external load but not the most severe that could occur.

The internal pressure for burst is a little more complicated. If we drill a well some distance below the surface casing, encounter a gas kick, and get a large volume of gas in the casing, then the pressures could get quite high. However, if the pressure is very high, the formations at the bottom of the surface casing will fracture and gas flow will go into those formations. That being the case, it does not make sense to design a surface casing string to withstand say, 6000 psi internal pressure, if the formation below the surface casing fractures at 3500 psi. The typical procedure for determining burst load is to assume that the maximum internal pressure is equivalent to the fracture pressure beneath the casing shoe and gas from that point to the surface. In cases where gas is known to not be present, we could use oil or saltwater as the internal fluid. However, gas gives us the most critical load and should always be used unless there is absolute certainty that no gas is present in the zones between the surface casing and the next string of casing.

In addition, there are some other possibilities listed in Table 3.2.

Typical surface casing burst design loads

- Internal pressure—equivalent of gas kick that fractures and flows into formation(s) below the casing shoe
- External pressure—freshwater gradient

Again, we must emphasize there many possibilities and different companies have a variety of approaches. These, however, are simple and should be safe in most cases.

Surface casing load plots

One of the easiest ways to work with casing loads is to construct a set of design load plots. The anticipated loads, such as collapse pressures and burst pressures, are plotted graphically as pressure versus depth. This makes it very easy to visualize the loading, rather than relying on a lot of formulas. (We still need formulas and calculations to construct the load plots, but they require very few calculations.)

3.6.3 Intermediate casing

The intermediate casing loading often is straightforward, like the surface casing, except that the magnitude of the loads generally is greater. For many designs the procedure is exactly the same as our surface casing example.

Intermediate casing collapse loads

Collapse loading in intermediate casing is not often critical, but it can be. Many companies use a mud gradient outside the intermediate casing and no pressure on the inside. This almost always is the case if the intermediate casing later will become part of the production string after a production liner is set. If the intermediate casing will eventually be covered by the production casing or a tieback string, then the issue of collapse load will be different.

Unlike the surface casing, total evacuation seldom occurs nor is even possible in most cases. With very accurate fracture data we could predict the depth to which the fluid inside the casing would fall, but we never have data that reliable. Often when lost circulation is experienced while drilling below intermediate casing, it results in a kick event because of the loss of hydrostatic head. This can be a very serious situation, and the normal procedure is to try to keep the casing full in order to better manage the kick. Obviously, the casing cannot be kept full using drilling mud because it has already fractured a formation and will continue to enter the fracture and the available supply on hand will exhaust quickly. It

is possible that no liquid will stay full to the top, but safety dictates that liquid continuously be pumped into the well to keep formation fluids, especially gas, from reaching the surface if at all possible. This usually means pumping freshwater or seawater to achieve this end. So for our lost circulation collapse load, we will assume the fluid inside the intermediate casing is all freshwater (seawater would be used offshore). Again we do not know what the outside pressure is, but we may conservatively assume it is a mud channel (which is slightly greater than formation pressures).

However, in some cases, intermediate casing is set to allow the drilling of low-pressure formations below the casing. In those cases, it is possible that the casing could be empty or nearly so.

Intermediate casing burst loads

The typical burst load for intermediate casing is similar to that for the surface casing. It assumes a freshwater, saltwater, or drilling mud gradient on the outside and gas pressure on the inside. The maximum gas pressure is assumed to be a full column of gas with a pressure equal to the *lesser* of (1) that attributable to the source formation, or (2) that equivalent to the lowest fracture pressure below the casing shoe. Those are the assumptions we will employ. In addition we also consider the plug-bump pressure and the test pressure prior to drilling out the shoe track.

In the first edition, I included a discussion of a once popular alternate approach called the "maximum load method" developed by Prentice [13]. It is based on the fracture pressure assumption above but allows for a partial mud column in the casing in addition to the gas. This method allows for a lower working pressure BOP stack to be utilized in many cases and consequently results in a considerable cost saving. While the method is sound in principle, it has two serious weaknesses. First, the well must be shut in before gas reaches a critical depth in the casing and certainly before it reaches the surface. Second, a functioning pump and adequate mud supply must be available to replace mud in the casing should any migrate downward into the gas column and flow into the fracture. A failure of either of these two would result in a surface gas pressure exceeding the working pressure of the BOP stack and wellhead. While the method was once quite popular and successful, I believe that no prudent operator is willing to assume such a risk in present times. Consequently, I have excluded it from this edition.

3.6.4 Production casing

As one might imagine, there are a number of different ways to consider the loads in the production casing. One purpose of the production casing is as a backup string for the production tubing, so that it can support the same loads as a tubing string. However, there are some major differences in the maximum loads that a production string might encounter as compared to a tubing string. In some cases, the collapse load might be higher, and in other cases, the burst load might be significantly higher.

Production casing collapse load

The most common approach to collapse loading in a production string is to assume that the worst collapse scenario is one in which the casing is empty and open to the atmosphere. This is not common, but it does happen. Another possibility is to assume that the well always has some amount of liquid or pressure inside it, equal to the formation pressure at the time (usually taken to be the depletion pressure). The situation for each well may be different and can be complex. One should always keep in mind that what may actually occur in the future may be difficult to foresee. Casing often collapses during the producing life of some wells, because later in the life of the well someone attempted some operation that was not foreseen when the casing string was designed.

Production casing burst loads

As far as burst is concerned, the most common procedure is to assume that the casing must withstand the maximum shut-in formation pressure in the form of a gas column for a gas well (or oil for an oil well) from the perforations all the way to the surface. In other words, the production casing is a backup for the tubing as far as burst pressure is concerned. And, there are many ways in which a situation such as that can occur. However, one other situation can be much worse, especially with a gas well. Suppose the tubing is set in a packer and a leak develops in the tubing near the surface. There is no problem with casing burst at the surface, because it was designed for that pressure. But, what happens down-hole because of the gas pressure on top of the packer fluid? The burst load is much higher in a situation like this than with a pure gas column in the casing. Designing for a case like this can lead to a very expensive casing string. Although this particular scenario is often ignored in production casing design, it is not at all an uncommon situation in the producing life of many gas wells. A lot of wells in the world have pressure relief valves on the tubing or casing annulus because of this very situation; the alternative is a possible down-hole rupture of the production casing and an underground blowout.

3.6.5 Liners and tieback strings

Liners and tieback strings are special situations; however, the approach is very similar to that of either the intermediate or production casing. The thing that is different in the load curve for a liner or a tieback is that the load curve is not just for the liner or tieback but for the casing in which it hangs if it is a liner or the liner and tieback combination. Sometimes, liners must meet the requirements of two functions (see Figure 3.1). In other words, a liner or a tieback is never designed by itself but as a contiguous part of another string of casing. The only thing that really differs as far as the load is concerned is the tension load, since it is a separate part of a longer string.

In the figure, we see a well with a production liner and two possibilities for final completion. On the left, the well could be completed as is, with the production liner and the intermediate casing forming

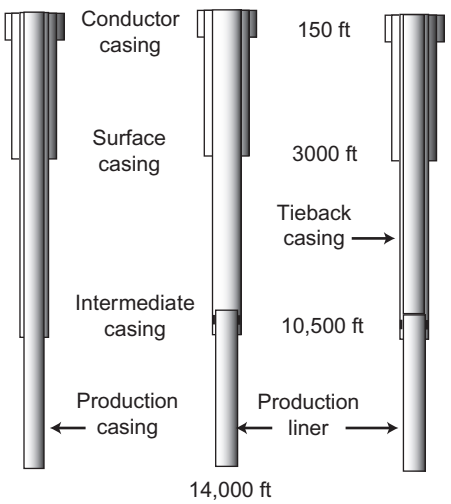

Figure 3.1 The example well with production liner and two completion options.

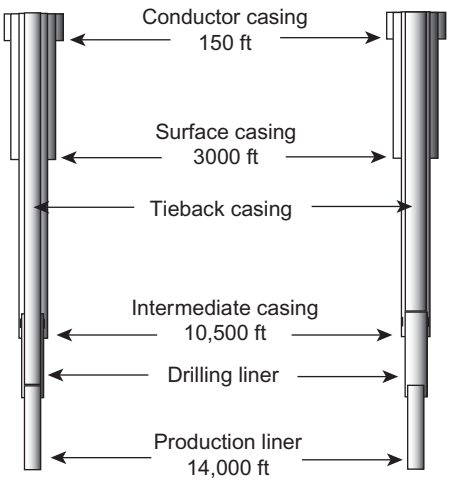

Figure 3.2 The example well with a drilling liner and a production liner.

the final production string. In this case, the intermediate string is designed to function as both the intermediate string and the upper portion of the production string. In the second case, where a tieback is run, the intermediate casing serves only as an intermediate string and the liner and the tieback together serve as the production casing. Figure 3.2 shows another common liner situation.

In this case, there are two liners: a drilling liner and a production liner. On the left, the intermediate casing serves its normal purpose, but it also serves as a portion of a second intermediate string in conjunction with the liner, so both have to be designed as one string and the string has to satisfy both functions. On the right, the drilling liner is tied back to the surface and a production liner run below it. In a case like this, the design depends on when the tieback is run. If the tieback is run immediately after running the drilling liner, the intermediate casing serves as intermediate only until the tieback is run, then the drilling liner and tieback serve as a second intermediate string, and finally, in conjunction with the production liner, they serve as a production string. If the tieback is run after the production liner is run, then the intermediate casing has to be designed to perform its first function as well as a second intermediate string with the drilling liner. Finally, like before, the tieback, the drilling liner, and the production liner all function as the final production string. It may sounds more complex than it actually is, but the only thing to keep straight is to be sure all strings are designed to meet all the required loads to which they will be subjected in their various roles during drilling and production.

3.6.6 Other pressure loads

There is another type of pressure loading that has caused problems in wells in more recent times, and that is collapse and/or burst resulting from thermal loading of fluids trapped in annular spaces. While this type of loading has been common for so many years and easily dealt with in most wells, it has become problematic more recently in subsea completions. For wells that reach the surface, it is common practice (and should be mandatory) to install and maintain pressure gauges on all annuli at the wellhead. If trapped pressure becomes excessive, it can be released at the surface. Not so with subsea completions which generally have no means to monitor annular pressure nor any means of pressure release. In those

types of wells, it is necessary to design the casing to withstand those pressures and to possibly tailor the annular fluids to reduce expansion (not always possible). But in order to quantitatively determine the thermal loads, it is necessary to determine the temperature which involves dynamic heat conduction and convection modeling and knowledge of the volumetric coefficients of thermal expansion, heat conductance, flow properties, compressibility, etc. of the annular fluid. Most of these material properties are also temperature and pressure dependent. A number of papers have addressed this topic, and Halal and Mitchell [14] is a good place to start.

3.7 Example well

The best way to understand the construction of the load plots is with an example. We use the depth selection curve, Figure 2.5 that we plotted in Chapter 2 along with a linear temperature gradient equation, $T = 74 + 0.0018\,h$ and construct a data table for our example well, Table 3.3.

3.7.1 Conductor casing example

For our example well, we will consider 20 in. conductor casing set in a drilled hole at 150 ft.

Conductor casing data

Size: 20
Depth: 150 ft
Mud density: 9.0 ppg

Cementing data

Cement to surface with 1.32 SG cement slurry, use inner string for cementing

Conductor collapse loads

Our example well is an on-shore well and the conductor will be cut off to install the casing head on the surface casing, so it will not be subject to any significant loads. It is not uncommon to float shallow conductor into the hole when using a small conductor rig, though not a recommended practice. The differential pressures at thetop and bottom are

$$\Delta p_0 = p_\mathrm{i} - p_\mathrm{o} = 0 - 0 = 0$$
$$\Delta p_{150} = 0 - 0.052\,(1.08)\,(8.33)\,(150) = -70\,\mathrm{psi}$$

Table 3.3 Example Well Data

Depth (ft)	Fm Press (SG equiv)	Mud Dens (SG)	Frac Press (SG equiv)	Frac Marg (SG equiv)	(°F)
0	1.01	1.02	-	-	74
3000	1.05	1.11	1.48	1.42	128
10,500	1.36	1.42	1.88	1.82	263
14,000	1.78	1.84	1.94	1.88	328

We will use an inner string for cementing so assuming 1.32 SG cement outside and 1.08 SG mud on the inside, the differential pressures are

$\Delta p_0 = p_i - p_o = 0 - 0 = 0$
$\Delta p_{150} = 0.052\,(1.08 - 1.32)\,(8.33)\,(150) = -16\,\text{psi}$

We are considering here fairly consolidated soils. In some near wetland areas, the soils may be almost liquid and could exert higher pressures, but not likely in excess of 1.0 psi/ft gradient (2.31 SG), which would give us −80 psi in the cementing calculation above. Collapse in conductor casing is uncommon in most land wells, but is not uncommon in offshore operations. Large diameter line pipe has a greater diameter to wall thickness ratio and generally a lower yield strength than we normally are accustomed to and a collapsed conductor that renders a platform slot unusable is a very serious matter. Do not ignore the collapse potential of conductor.

Conductor burst load

As we mentioned, conductor seldom provides any pressure containment other than possibly as a diverter. So the only pressure requirement is that it should at least be as strong as the fracture pressure at the shoe which we have no way of determining in most cases. If we make a guess that it cannot be higher than 1.0 psi/ft that gives us 150 psi for our example (it could be higher in some places).

Additional considerations

While it may appear that we just brushed through the conductor loading, we have done more than is usually done for most on-shore applications. Where the conductor will not be supporting a wellhead, we often depend on the pile driving company to recommend and even supply the conductor. In the case of small specialty land rigs that routinely set conductor before the drilling rig moves on location, the choice is sometimes nothing more than the corrugated road culvert material or whatever pipe they can buy cheaply from a salvage supplier. And to some it might come as a surprise but there are still a very large number of wells drilled without conductor casing at all. Where we really have to concern ourselves with conductor casing is where it may support the wellhead (and subsequent casing strings) and in offshore operations and other new areas where we may actually require soil boring samples and other data for which we can justify the higher costs. In some deep water locations, the conductor is jetted into the seabed floor rather than driven or run into a drilled hole.

3.7.2 Surface casing example

Surface casing data

Size: 13-3/8 in.
Depth: 3000 ft
Mud density at shoe ft: 1.11 SG at 3000 ft
Fracture pressure at shoe: 1.48 SG equiv. at 3000 ft
Temperatures: 74 °F at surface, 128 °F at 3000 ft
Max mud dens and temp before next casing string: 1.42 SG, 263 °F at 10,500 ft

Cementing data

Conventional cementing procedure. Cement to surface (required). Lead slurry: 2700 ft, 1.37 SG; tail slurry: 300 ft, 1.85 SG. Use 50% excess on lead slurry to assure cement to surface. Displace with 1.11 SG mud and bump plug with 500 psi above final displacement pressure.

Preliminary calculations

We will be using gradients of the mud, water, and cement in a number of calculations, we will do those separately here.

$$\gamma_{\text{wtr}} = 1.0\ (0.052)\ (8.33) = 0.433\ \text{psi/ft}$$
$$\gamma_{\text{mud}} = 1.11\ (0.052)\ (8.33) = 0.481\ \text{psi/ft}$$
$$\gamma_{\text{frm}} = 1.05\ (0.052)\ (8.33) = 0.455\ \text{psi/ft}$$
$$\gamma_{\text{frac}} = 1.48\ (0.052)\ (8.33) = 0.641\ \text{psi/ft}$$
$$\gamma_{\text{cmt-lead}} = 1.37\ (0.052)\ (8.33) = 0.593\ \text{psi/ft}$$
$$\gamma_{\text{cmt-tail}} = 1.85\ (0.052)\ (8.33) = 0.801\ \text{psi/ft}$$
$$\gamma_{\text{mud-max}} = 1.42\ (0.052)\ (8.33) = 0.615\ \text{psi/ft}$$
$$\gamma_{\text{frm-max}} = 1.36\ (0.052)\ (8.33) = 0.589\ \text{psi/ft}$$

The two "maximum" gradients are the mud density and formation pressure at the formation at 10,500 ft which will be part of the borehole environment before intermediate casing is set.

Cement/fracture check

Because cement density is almost always greater than mud density in surface holes, we should compare the hydrostatic head of the cement with the fracture pressure before proceeding.

$$p_{\text{cmt}} = \gamma_{\text{cmt-lead}}\ L_{\text{cmt-lead}} + \gamma_{\text{cmt-tail}}\ L_{\text{cmt-tail}}$$
$$= 0.593\ (2700) + 0.801\ (300) = 1841\ \text{psi}$$
$$p_{\text{frac}} = \gamma_{\text{frac}}\ h = 0.641\ (3000) = 1923\ \text{psi}$$
$$\therefore\ p_{\text{cmt}} < p_{\text{frac}}$$

This is a rather narrow margin, and in practice we might consider modifying the cement program to avoid possible lost circulation.

Surface casing collapse loads

In Table 3.1, we see there is one collapse situation in the installation stage, one in the drilling stage, and none in the production stage of operations.

Installation—conventional cementing (post plug bump)

The only collapse situation arising from cementing is attributable to the denser cement immediately after the plug has bumped and the internal pressure has been released, post plug-bump collapse loading as shown in Figure 3.3a. The float acts as a check valve to prevent back flow of the cement, and there is a pressure differential between the un-set cement in the annulus and the less dense displacement fluid inside the casing. To calculate the cementing collapse load, we calculate the differential pressures at the surface and at the shoe. But here, the cement gradient is not a constant; it changes at 2700 ft—the interface between the lead slurry and the tail slurry. Consequently, a differential pressure plot will require three points.

$$\Delta p = p_{\text{i}} - p_{\text{o}}$$
$$\Delta p_0 = 0 - 0 = 0\ \text{psi}$$

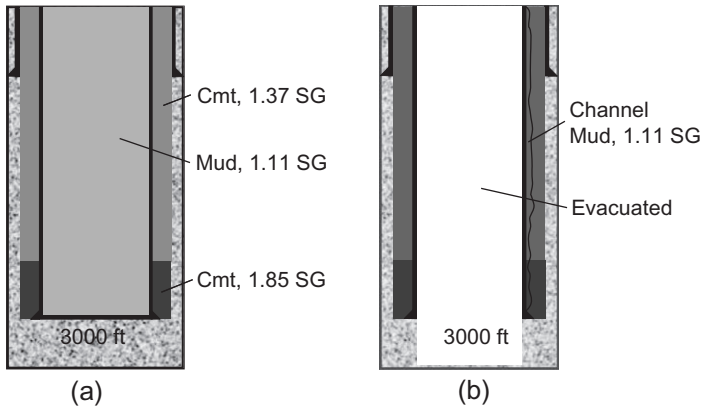

Figure 3.3 Surface casing collapse: (a) cementing, post plug bump and (b) lost circulation, evacuated.

$$\begin{aligned}\Delta p_{2700} &= (\gamma_{\text{mud}} - \gamma_{\text{cmt-lead}})\, L_{\text{cmt-lead}} \\ &= (0.481 - 0.593)\, 2700 = -302 \approx -300 \text{ psi} \\ \Delta p_{3000} &= (\gamma_{\text{mud}} - \gamma_{\text{cmt-tail}})\, L_{\text{cmt-tail}} + \Delta p_{2700} \\ &= (0.481 - 0.801)\, 300 + (-300) = -396 \approx -400 \text{ psi}\end{aligned}$$

This is an insignificant collapse load, and we need not consider it in our design. Recall from Chapter 1 that API standards roundoff pressure ratings to the nearest 10 psi, and we will generally follow that convention except where roundoff in intermediate results may affect subsequent calculations significantly.

Drilling—lost circulation

The most common cause of surface casing collapse is lost circulation. The only question is as to the degree of severity. Will the mud level fall below the surface casing shoe or will it reach equilibrium somewhere inside the surface casing? Most of the time it is somewhere inside the surface casing, but we seldom know where. In an area where we can establish the weakest formation pressure with reasonable certainty, we can actually calculate the mud level in the surface casing. In absence of that data, the safest approach is to assume it is severe enough to drop all the way below the shoe, and this is the approach most designers use. The other question we need answered is, what kind of fluid is on the outside? Surface casing is usually cemented to the surface, but we never rely on the cement to keep any hydrostatic pressure off the casing. We must always assume that the cement job is a failure or at least a partial failure and we cannot know in advance at what depths it will be a failure. The only safe assumption we can make then is that the hydrostatic pressure on the outside of the casing is the formation pressure or the drilling mud pressure when the casing was run. Over time it will likely be the formation pressure, but initially there may be a long channel of drilling mud that was bypassed by the cement slurry and still maintains near original hydrostatic mud pressure. We will always assume then that the fluid pressure in the annulus after the cement has set is equal to the hydrostatic pressure of the mud it was run in. We will calculate a collapse load for severe lost circulation with the surface casing empty and the 1.11 SG drilling mud on the outside (see Figure 3.3b).

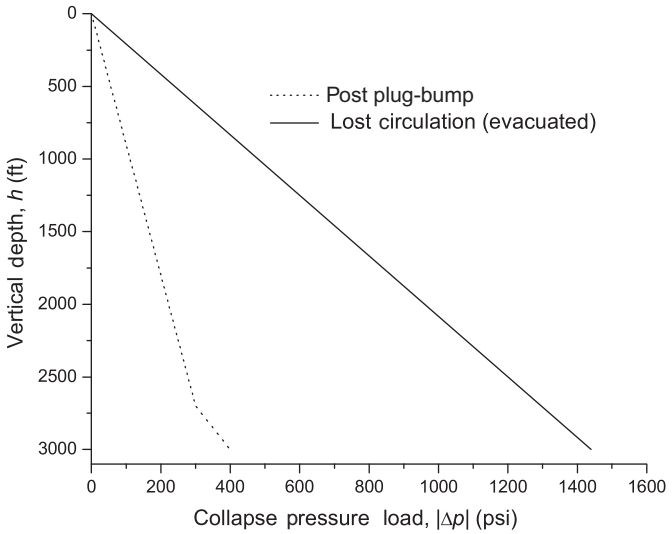

Figure 3.4 Example surface casing collapse loads.

$$\Delta p_0 = 0 - 0 = 0 \text{ psi}$$
$$\Delta p_{3000} = p_\text{i} - p_\text{o} = 0 - \gamma_\text{mud}\, h$$
$$= 0 - 0.481(3000) \approx -1440 \text{ psi}$$

The surface casing collapse load is plotted in Figure 3.4.

Surface casing burst loads

Next, we examine the burst loads for surface casing. Table 3.2 shows three burst loads in the installation stage and four in the drilling stage. It is seldom necessary to calculate all of these once you have done a few. We will do all of these in the installation stage, but will do only two in the drilling stage.

Installation—cementing

Because the cement density is usually greater than the mud density, there is a possibility, though remote, that the float could plug while cement is still inside the casing. We assume that should such an unexpected event happen, some additional amount of pressure will be applied at the surface before the pumps can be stopped. Few actually consider this possibility in casing design, but we will include it here for illustrating the possibility. We have specified our cement volumes in terms of column length in the annulus of the wellbore, so it is necessary to calculate the column length inside the casing. The column lengths are inversely proportional to the ratio of the cross-sectional areas of the inside area to the annular area:

$$k_{\text{i/o}} = \frac{d_\text{bit}^2 - d_\text{o}^2}{d_\text{i}^2} = \frac{17.500^2 - 13.375^2}{12.615^2} = 0.800$$

In this calculation, it was necessary to use an inside diameter, even though we have not yet made a 13-3/8 in. casing selection. So we used a typical inside diameter. The difference is negligible in our load calculations because we never know the hole diameter precisely. One precaution however, this method is not valid in inclined wellbore unless the inclination is constant throughout the interval. If the inclination is not constant (and it seldom is), we must use the measured lengths of the columns along the wellbore path then convert the internal length to vertical depths.

Next we calculate the lengths of the cement columns inside the casing. We are not using a proprietary spacer here since we are cementing to the surface, and we will assume that the lead slurry acts as a scavenger/spacer. Recall also that we are using 50% excess in our lead slurry to assure that we get cement to the surface, so while we used 2700 ft as the column length in the annulus for previous calculations, we must account for the excess when it is inside the casing. So let us calculate the lengths of the cement internally.

$$L_{\text{cmt-lead}} = 0.800\,(1.5)\,(2700) = 3240 \text{ ft}$$
$$L_{\text{cmt-tail}} = 0.800\,(300) = 240 \text{ ft}$$
$$L_{\text{cmt-lead-actual}} = 3000 - 240 = 2760 \text{ ft}$$

We see that the excess lead slurry will actually fill the casing by itself so the worst case here is with either the lead slurry in the casing and mud outside or the tail slurry and lead slurry inside and mud and part of the lead slurry outside. We do not know which so we will calculate both. With only the lead slurry inside, mud outside, and 1000 psi pump pressure, we have

$$\Delta p_0 = 1000 - 0 = 1000 \text{ psi}$$
$$\Delta p_{3000} = 1000 + (0.593 - 0.481)\,3000 \approx 1340 \text{ psi}$$

If on the other hand, the tail slurry is in the casing just as we start to pump the displacement fluid we have to determine the interface depth of the mud and lead slurry on the outside (see Figure 3.5a).

$$L_{\text{lead-outside}} = [3240 - (3000 - 240)]/0.800 = 600 \text{ ft}$$
$$L_{\text{mud-outside}} = 3000 - 600 = 2400 \text{ ft}$$

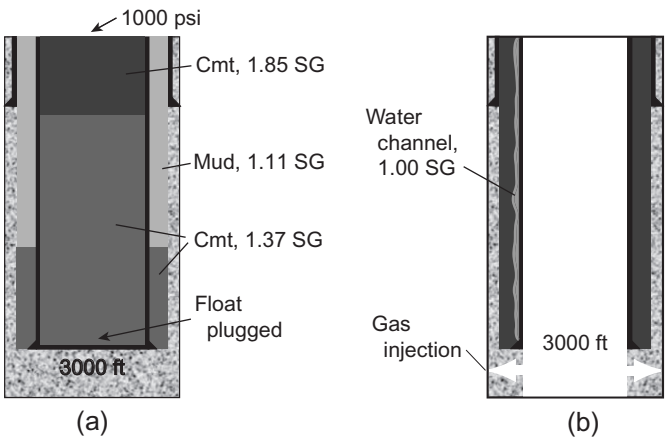

Figure 3.5 Surface casing burst: (a) cementing, float plugged and (b) gas kick.

Now we calculate the pressure differentials at the various fluid interfaces, assume 1000 psi excess surface pressure when the pumps are stopped.

$$\begin{aligned}
\Delta p_0 &= 1000 - 0 = 1000 \text{ psi} \\
\Delta p_{240} &= 1000 + (0.801 - 0.481)\,(240) \approx 1080 \text{ psi} \\
\Delta p_{2400} &= 1000 + 0.801\,(240) + 0.593\,(2400 - 240) - 0.481\,(2400) \\
&\approx 1320 \text{ psi} \\
\Delta p_{3000} &= 1000 + (0.801)\,(240) + 0.593\,(3000 - 240) - 0.481\,(2400) \\
&\quad - 0.593\,(600) \approx 1320 \text{ psi}
\end{aligned}$$

Installation—plug bump

When the top wiper plug bumps at the float collar, the pumping pressure is increased by some amount to assure the plug has actually seated. In our example we have chosen 500 psi as the additional plug-bump pressure. At this point, all cement should be in the annulus, and the casing should be full of displacement fluid. At the surface, the differential pressure is the difference between the inside and annular hydrostatic heads plus the plug-bump pressure.

$$\begin{aligned}
\Delta p_0 &= p_{\text{cmt}-3000} - p_{\text{dspl}-3000} + \Delta p_{\text{bump}} \\
&= 0.593\,(2700) + 0.801\,(300) - 0.481\,(3000) + 500 \\
&\approx 900 \text{ psi}
\end{aligned}$$

At the shoe, the differential pressure is the final surface pressure at the surface (from the previous calculation) minus the annular hydrostatic head.

$$\begin{aligned}
\Delta p_{3000} &= \Delta p_0 + p_{\text{dspl}-3000} - p_{\text{cmt}-3000} \\
&= 900 + 0.481\,(3000) - 0.593\,(2700) + 0.801\,(300) \\
&\approx 500 \text{ psi}
\end{aligned}$$

If we did this correctly, the differential pressure at the shoe is the plug-bump pressure ($\pm$ some roundoff error) because that is the differential pressure we are attempting to put on the plug to be sure it is seated. Note that in these calculations, we are ignoring the length of the shoe track (distance between the float collar and the float shoe—usually 60-70 ft) as being insignificant to our load calculations.

Installation—pressure test

It is customary (and often required) to pressure test casing before resuming drilling. Many regard the plug bump as a pressure test and adjust the bump pressure accordingly. This has a definite advantage in that a pressure test after the cement has cured involves the risk of damaging the cement sheath by radial expansion and axial contraction of the casing if the cement has not properly cured. However, in many areas, regulations require the test prior to resuming drilling and there is no choice. We do not know the hydrostatic pressure outside the casing when this test is conducted. The most likely worst case is that the cement job went badly and left a mud channel from the surface all the way to the bottom. Assuming the test fluid in the casing is also drilling mud, then any pressure applied to the surface gives us a constant differential test of the entire string equal to the applied surface pressure. We will assume that here and that the 1500 psi test pressure required gives a $\Delta p = 1500$ psi at all points in the surface casing string.

Drilling—maximum mud density

As we drill down to the next casing point (10,500 ft), we will increase the mud density up to 1.42 SG. This does create a differential pressure on the casing though it is generally insignificant, but for illustration, we will calculate it. Again, we have no idea what the annular pressure is but a worst case assumption might again be a freshwater channel from top to bottom.

$$\Delta p_0 = 0 - 0 = 0 \text{ psi}$$

$$\Delta p_{3000} = (\gamma_{\max} - \gamma_{\text{wtr}})\, h = (0.615 - 0.433)\, 3000 \approx 550 \text{ psi}$$

Drilling—gas kick

The worst case drilling burst load on surface casing usually occurs during a gas kick. Table 3.2 lists two other possibilities: an oil kick and a saltwater kick. Oil and saltwater kicks present less severe burst loading than gas, assuming the same formation pressure at the source of the kick. There are areas in the world where there are no gas bearing formations, so we will also present an oil kick example for the intermediate casing. In a gas kick, the worst case scenario is one in which gas gets all the way to the surface. There are two possibilities: (1) the source pressure is low enough that the pressure resulting from a full gas column does not exceed the fracture pressure of any formation below the casing shoe (the less common of the two), and (2) the gas pressure does exceed the fracture pressure of a formation below the shoe, and in this case, the surface pressure is that of a column of gas from the fractured zone to the surface with the fracture pressure as the maximum pressure in the casing (the more common of the two).

A significant difficulty in this type load calculation is determining the source pressure. Normally we would think the highest formation pressure below the casing would be the one to use, and that is true for an intermediate string or surface string that requires only a production string below it. In those two cases, we know the highest pressures we will encounter. But for surface casing followed by an intermediate casing string to be set in a pressure transition zone the kick may come from a higher pressure zone than was planned to be cased off by the intermediate string. For example, suppose an intermediate string is to be set in a zone with a 1.50 SG equivalent pressure. We calculate the gas pressure to the surface and find that it does not result in fracture of any formation below the surface casing shoe. We may use that gas pressure in calculating the surface casing burst load, and that is typical. But suppose that as we are drilling this well, we encounter the transition zone prematurely and inadvertently drill into a zone below it with a 1.70 SG equivalent pressure. This is not uncommon and is how many gas (and saltwater) kicks occur. In such a case, the gas column usually fractures a formation below the surface casing shoe. Gas flows into this zone at its fracture pressure (an underground blowout), and if the gas column does reach the surface, its pressure is dictated by the fracture pressure of the fractured zone it is flowing into rather than its source zone. This is generally the worst case scenario and the one we will use in our example (see Figure 3.5b).

First we will determine if gas from the formation at 10,500 ft will fracture the formation at the casing shoe. If not, then we will look at the formation pressures a little below 10,500 ft in case we inadvertently drill beyond the planned casing seat because of geological uncertainty (or carelessness). Our maximum formation pressure at 10,500 ft is 1.36 SG equivalent, and our fracture pressure at the shoe at 3000 ft is 1.88 SG equivalent.

$$p_{\text{frac}} = 0.641\ (3000) \approx 1920 \text{ psi}$$

That is a relatively low fracture pressure. The gas pressure at 10,500 ft is

$$p_{10500} = 0.589\,(10500) \approx 6180 \text{ psi}$$

Using Equation (3.1), the gas pressure at the surface casing shoe is:

$$p_{3000} = 6180 \exp\left[\frac{16\,(3000 - 10500)}{1545\left(460 + \frac{128+263}{2}\right)}\right] \approx 5490 \text{ psi}$$

That exceeds the fracture pressure of 1920 psi by a considerable margin, so in this case, the formation at the shoe will fracture and we will assume a gas column from there to the surface.

$$p_{3000} = p_{\text{frac}} \approx 1920 \text{ psi}$$

Knowing the gas pressure is 1920 psi at 3000 ft, we calculate the gas pressure at the surface:

$$p_0 = 1920 \exp\left[\frac{16\,(0 - 3000)}{1545\left(460 + \frac{74+128}{2}\right)}\right] \approx 1820 \text{ psi}$$

This gives us a maximum surface pressure of 1820 psi and a nasty underground blowout, but the casing and BOP are safe if we use 3000 psi rated BOP and design our surface casing accordingly. Those are the pressures inside the surface casing, what do we use outside? At the surface, we use atmospheric pressure which is zero for our purposes, but what fluid is in the annulus. As already discussed, the heaviest fluid in the annulus would be our drilling mud when the casing is run. We could also use a gradient equivalent to our formation pressure at the shoe or possibly salt water. The worst case we could have for surface casing would be freshwater. Your company may have its own policy, but for surface casing, we will use a freshwater density of 1.0 SG. ($\gamma_{\text{wtr}} = 0.433$).

$$\Delta p_0 = p_{\text{i}} - p_{\text{o}} = 1820 - 0 = 1820 \text{ psi}$$

$$\Delta p_{3000} = 1920 - 0.433\,(3000) \approx 620 \text{ psi}$$

So now we plot our burst load lines in Figure 3.6.

3.7.3 Intermediate casing example

The intermediate casing loading is often straight forward like the surface casing, except that the magnitude of the loads is generally greater. In many strings of intermediate casing, the maximum pressure from a gas kick is not sufficient to fracture any formation below the shoe, and hence, the maximum surface pressure will be from a full column of gas.

Intermediate casing data

Size: 9-5/8 in.
Depth: 10,500 ft
Mud density at shoe ft: 1.42 SG at 10,500 ft
Fracture pressure at shoe: 1.88 SG equiv. at 10,500 ft
Temperatures: 74 °F at surface, 263 °F at 10,500 ft
Max mud dens and temp before next csg string: 1.84 SG, 326 °F at 10,500 ft

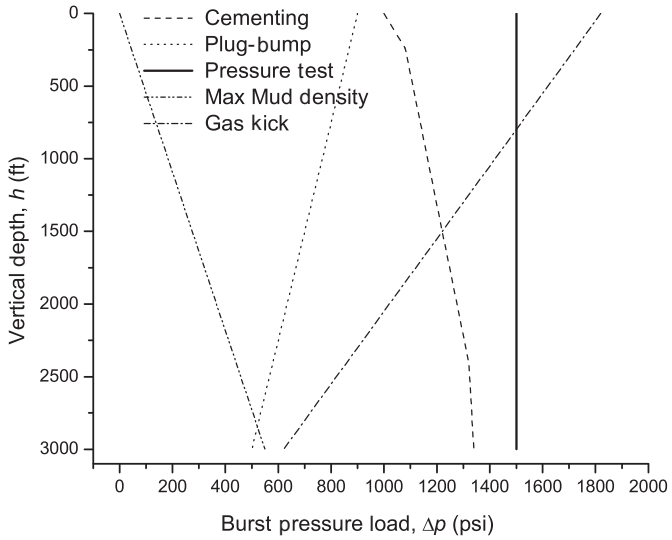

Figure 3.6 Example surface casing burst loads.

Cementing data

Cement to 500 ft inside surface casing, 1000 ft tail slurry at 1.91 SG, 7000 ft lead slurry w/50% excess at 1.44 SG, 1000 ft spacer at 1.44 SG, displace plug w/1.42 SG mud, bump plug with 1000 psi above final displacement pressure.

Preliminary calculations

Here, we calculate the gradients we will be using for the intermediate casing.

$$\gamma_{\text{wtr}} = 1.0\ (0.052)\ (8.33) = 0.433 \text{ psi/ft}$$
$$\gamma_{\text{mud}} = 1.42\ (0.052)\ (8.33) = 0.615 \text{ psi/ft}$$
$$\gamma_{\text{frm}} = 1.36\ (0.052)\ (8.33) = 0.589 \text{ psi/ft}$$
$$\gamma_{\text{frac}} = 1.88\ (0.052)\ (8.33) = 0.814 \text{ psi/ft}$$
$$\gamma_{\text{cmt-lead}} = 1.44\ (0.052)\ (8.33) = 0.624 \text{ psi/ft}$$
$$\gamma_{\text{cmt-tail}} = 1.91\ (0.052)\ (8.33) = 0.827 \text{ psi/ft}$$
$$\gamma_{\text{mud-max}} = 1.84\ (0.052)\ (8.33) = 0.797 \text{ psi/ft}$$
$$\gamma_{\text{frm-max}} = 1.78\ (0.052)\ (8.33) = 0.771 \text{ psi/ft}$$

The two "maximum" gradients are the mud density and formation pressure at the formation at 14,000 ft which will be part of the borehole environment before production casing is set.

Cement/fracture check

Cement density is almost always greater than mud density in intermediate holes, and we should compare the hydrostatic head of the cement with the fracture pressure before proceeding. Because the cement slurry is not designed to reach the surface, we must consider the consequences of the 50% excess in

the lead slurry. Since the lead slurry is more dense than the drilling mud (1.44-1.42), we must assume the greatest hydrostatic pressure would occur if the hole were perfectly in-gauge (exactly 12-1/4 in. diameter), and the excess cement would increase the column length of the lead slurry by 50%. So instead of a 7000-ft column, we would have $1.5(7000) = 10,500$ ft, which would fill the annulus by itself. So if we have a 1000 ft of tail slurry, the maximum length of the lead slurry would be $10500 - 1000 = 9500$ ft. We now calculate the pressures.

$$
\begin{aligned}
p_{\text{frac}} &= 0.814\,(10500) \approx 8550 \text{ psi} \\
p_{\text{max cmt}} &= 0.827\,(1000) + 0.624\,(9500) \approx 6760 \text{ psi} \\
\therefore p_{\text{max cmt}} &< p_{\text{frac}}
\end{aligned}
$$

Intermediate casing collapse loads

There are three collapse loads shown in Table 3.1, and they are collapse caused by the cement slurry after the plug is bumped and the internal pressure is released, and two lost circulation scenarios. In the drilling category, we will only need one of the lost circulation scenarios and not both.

Installation—cementing

Post plug-bump collapse is the only case we need examine for this operational stage. We already saw in our preliminary calculations that the worst case for annular pressure is a gauge hole where the lead slurry reaches the surface. That will be our assumption here. The fluid inside the casing is 1.42 SG mud, and in the annulus is 1.44 SG cement from surface to 9500 ft and 1.91 SG mud from 9500 to 10,500 ft.

$$
\begin{aligned}
\Delta p_0 &= p_{\text{i}} - p_{\text{o}} = 0 - 0 = 0 \text{ psi} \\
\Delta P_{9500} &= (0.615 - 0.624)\,9500 \approx -90 \text{ psi} \\
\Delta p_{10500} &= -90 + (0.615 - 0.827)\,1000 \approx \ -300 \text{ psi}
\end{aligned}
$$

As with the surface casing, the post plug-bump collapse load is insignificant.

Drilling—lost circulation

As previously discussed, lost circulation always poses a collapse possibility for intermediate casing. We will assume here that in the event of lost circulation, the casing will be kept full of water to avoid a kick. Again we do not know what the outside pressure is, but we may conservatively assume it is a mud channel (which is slightly greater than formation pressures).

In the case of freshwater in the pipe:

$$
\begin{aligned}
\Delta p_0 &= 0 \\
\Delta p_{10500} &= (0.433 - 0.615)\,10500 \approx -1910 \text{ psi}
\end{aligned}
$$

Should we prefer to assume an empty intermediate casing:

$$
\Delta p_{10500} = (0 - 0.615)\,10500 \approx -6460 \text{ psi}
$$

We now plot the first two possibilities in Figure 3.7 as our collapse loads.

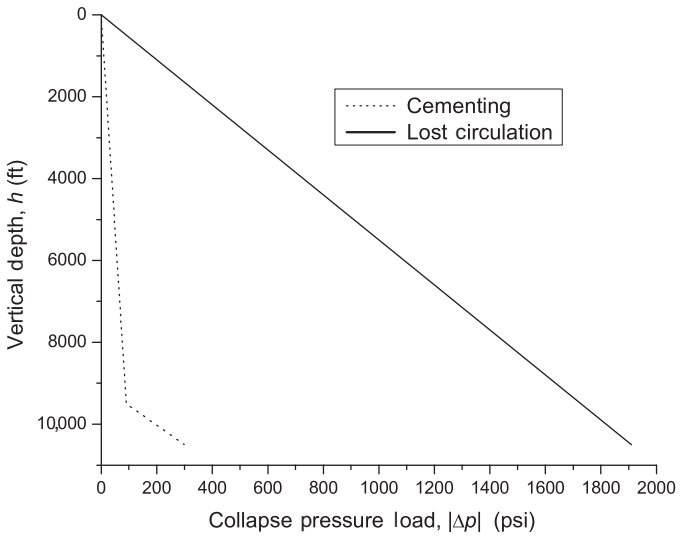

Figure 3.7 Example intermediate casing collapse loads.

Intermediate casing burst loads

For the intermediate casing, we must consider three burst loads in the installation stage. In the drilling stage, we need only calculate the cementing load and one of the three kick cases. We will calculate the gas kick as it is the most severe, but for illustration, we will also calculate the oil kick as an example for those who do not have gas to contend with.

Installation—conventional cementing

Again we mention that it is a rare occurrence that a float should plug with the cement still inside the casing, but we will again illustrate the possibility.

In the intermediate casing, the installation burst possibilities are the same as in the surface casing. First, we look at the possibility of the float plugging or the annulus packing off while the cement is still in the casing and the cementer pumping up to 1000 psi before shutting down, and we need the ratio of column lengths inside to outside.

$$k_{\mathrm{i/o}} = \frac{d_{\mathrm{bit}}^2 - d_{\mathrm{o}}^2}{d_{\mathrm{i}}^2} = \frac{12.25^2 - 9.625^2}{8.681^2} = 0.762$$

Next we calculate the lengths of the cement columns inside the casing. Recall also that we are using 50% excess in our lead slurry to assure that we get cement to the surface. While we used 7000 ft as the column length in the annulus for previous calculations, we must account for the excess when it is inside the casing. So let us calculate the lengths of the cement internally.

$$L_{\mathrm{spac}} = 0.762\,(1000) = 762 \text{ ft}$$
$$L_{\mathrm{lead}} = 0.762\,(1.5)\,(7000) = 8001 \text{ ft}$$
$$L_{\mathrm{tail}} = 0.762\,(1000) = 762 \text{ ft}$$

$$L_{\text{total}} = 762 + 8001 + 762 = 9525 \text{ ft}$$
$$L_{\text{mud}} = 10500 - 9525 = 975 \text{ ft}$$

There are two ways to look at this. One case would be that the spacer has reached the shoe and there is 975 ft of displacement fluid in the casing on top of the tail slurry. The other case of 975 ft of mud ahead of the spacer just as the last of the tail slurry is pumped into the pipe gives a greater differential burst pressure near the surface and through the string, although there is not a significant difference. The latter is the case we will use. With the mud ahead, spacer, lead slurry, and tail slurry just into the pipe and 1000 psi additional pressure before the pump can be stopped we have

$$\Delta p_0 = 1000 - 0 = 1000 \text{ psi}$$
$$\Delta p_{762} = 1000 + (0.827 - 0.615)\,(762) \approx 1160 \text{ psi}$$
$$\Delta p_{8763} = 1160 + (0.624 - 0.615)\,(8001) \approx 1230 \text{ psi}$$
$$\Delta p_{9525} = 1230 + (0.624 - 0.615)\,(762) \approx 1240 \text{ psi}$$
$$\Delta p_{10500} = 1240 + (0.615 - 0.615)\,(975) \approx 1240 \text{ psi}$$

Installation—plug bump

Next to consider is the plug bump which is identical to the placement pressure with the addition of the bump pressure.

$$\begin{aligned}\Delta p_0 &= \Delta p_{\text{bump}} + p_{\text{max cmt 10500}} - p_{\text{dspl 10500}} \\ &= 1000 + 0.827\,(1000) + 0.624\,(9500) - 0.615\,(10500) \approx 1300 \text{ psi}\end{aligned}$$
$$\Delta p_{9500} = 1300 + (0.615 - 0.624)\,(9500) \approx 1210 \text{ psi}$$
$$\Delta p_{10,500} = \Delta p_{\text{bump}} = 1000 \text{ psi}$$

The final result in a plug-bump calculation should always be equal to the additional plug-bump pressure (within some roundoff error).

Installation—test pressure

Pressure testing the casing after cement has set and before drill out with the same mud used to drill the hole will result in a differential pressure equal to the test pressure. We will use 2500 psi as the test pressure and no calculations are required.

After drilling a few feet below the shoe, it is usually the case with intermediate casing to perform a shoe integrity test before weighting up the mud and drilling farther. The integrity test pressure is equivalent to the maximum mud density that will be used in drilling below the shoe. The reason this test is performed before weighting up the mud is so that if it will not hold the pressure, then possible remedial steps can be taken with minimum mud loss. Otherwise if the mud had already been weighted up to 1.84 SG, a fracture during the test would result in loss of more expensive mud and the mud density would have to be reduced back to 1.42 SG before taking remedial steps. With a column of 1.42 SG mud, the surface pressure necessary to test the casing to the equivalent of 1.84 at the shoe is

$$p_{0\,\text{test}} = (0.797 - 0.615)\,10500 \approx 1910 \text{ psi}$$

Like the casing test pressure, this pressure results in the same differential pressure all the way to bottom since we are assuming 1.42 SG mud in the annulus after cementing. This is less than the test pressure of 2500 psi, so it is not considered in the burst loading.

Drilling—maximum mud density

The maximum mud density anticipated below 10,500 ft is 1.84 SG. We will assume that the fluid outside the casing is a channel of 1.42 SG mud in which it was run.

$$\Delta p_0 = 0$$

$$\Delta p_{10500} = (0.797 - 0.615)\, 10500 \approx 1910 \text{ psi}$$

This is the same as the integrity test differential pressure.

Drilling—gas kick

The worst case is that of a severe kick that results in the casing being full of gas at either a pressure attributable to the zone of the kick or the weakest fracture pressure below the shoe whichever results in the least pressure at the surface. This is exactly the situation we examined at the surface casing though here we have a better fix on the maximum pressure than in the surface casing application because we plan to stop at the producing formation. (In some cases, though, there is a possibility of drilling into higher pressures below the target zone and that must always be considered.) So for our example, we can see that the maximum formation pressure of 1.78 SG occurs at 14,000 ft. The fracture gradient at the 10,500 ft shoe is 1.88 SG equivalent. We now calculate the formation pressure at 14,000 ft and the gas pressure at the intermediate shoe from the formation pressure.

$$p_{\text{fm}-14000} = (0.770)\, 14000 = 10,780 \text{ psi}$$

$$p_{\text{gas}-10500} = 10,780 \exp\left[\frac{16\ (10500 - 14000)}{1545\left(460 + \frac{263+326}{2}\right)}\right] \approx 10,270 \text{ psi}$$

$$p_{\text{frac}-10500} = (0.816)\, 10500 \approx 8570 \text{ psi}$$

From these calculations, we find the formation gas pressure will exceed the fracture pressure at the shoe by about 1700 psi. We will then assume that the formation will fracture at the shoe, gas will enter that formation and that the maximum surface pressure will be determined by the fracture pressure at the shoe. With the fracture pressure at the shoe as the gas pressure at 10,500 ft, we can now calculate the gas pressure at the surface.

$$p_{\text{gas}-0} = 8570 \exp\left[\frac{16\ (0 - 10500)}{1545\left(460 + \frac{74+263}{2}\right)}\right] \approx 7210 \text{ psi}$$

We have our top and bottom internal pressures. The outside pressure at the top is zero, so it remains to determine the outside pressure at the bottom. What is the fluid outside the casing? Earlier we used the mud in which the casing was run, 1.42 SG. When our kick occurs it is now several days (or weeks?) later. Perhaps the annular space now has the pressure of the formations. Perhaps in setting the cement gave up free water to form a freshwater channel. We cannot know with any degree of certainty what is behind

the casing. Rather than debate this as many individuals and companies continue to do we will select the worst case which is fresh water. This is a bit inconsistent with what we did with the test pressures and shoe tests, but this one is critical and failure always has disastrous results. So, using freshwater as a backup, the differential pressures for burst are

$$\Delta p_0 = 7210 - 0 = 7210 \text{ psi}$$

$$\Delta p_{10500} = 8570 - 0.433\,(10500) \approx 4020 \text{ psi}$$

Drilling—oil kick

Some producing areas in the world do not have any potential for a gas kick but do have the possibility of an oil kick. Almost no treatment on casing design considers an oil kick, so let us use this same example and assume the production is oil rather than gas. Assume an oil gradient instead of gas and assume that the oil in our well is 35 API gravity at 60 °F. First we will determine if the oil pressure from the formation at 14,000 ft can cause fracture at the shoe. The average temperature of the oil from bottom to surface is $(326 + 74)/2 = 200$ °F, and that gives us an average API gravity of approximately 46. Then using the API formula relating specific gravity and API gravity

$$\text{Specific gravity} = \frac{141.5}{\text{API Gravity} + 131.5} = \frac{141.5}{46 + 131.5} = 0.80$$

We can then convert that to a gradient as follows

$$\gamma_{\text{oil}} = 0.052\,(0.80)\,(8.33) = 0.347 \text{ psi/ft}$$

(Please note that this is all approximate, but close enough for casing design.) For a column of oil from 14,000 to 10,500 ft, the pressure at 10,500 ft would be:

$$p_{\text{oil}(10500)} = 10774 - 0.347\,(14000 - 10500) \approx 9560 \text{ psi}$$

The oil pressure exceeds the shoe fracture pressure so the bottom pressure with oil will also be the shoe fracture pressure, and the pressure differential at the shoe will be the same as with the gas. Using the fracture pressure at the shoe, 8570 psi, we calculate the surface pressure differential with oil:

$$\Delta p_{0\text{oil}} = 8570 - 0.347\,(10500) \approx 4930 \text{ psi}$$

The intermediate casing burst loads are plotted in Figure 3.8.

3.7.4 Production casing example

Production casing requires some slightly different considerations from the previous strings. It serves as a pressure backup for the tubing string and must necessarily retain its integrity for the life of the well. Generally, no drilling will take place below it. But in cases where possible deepening at a later date may be contemplated, then it must also be designed as an intermediate string for the deepening operations.

Production casing data

Size: 7 in.
Depth: 14,000 ft
Formation pressure at shoe: 1.78 SG equiv. at 14,000 ft
Mud density: 1.84 SG at 14,000 ft

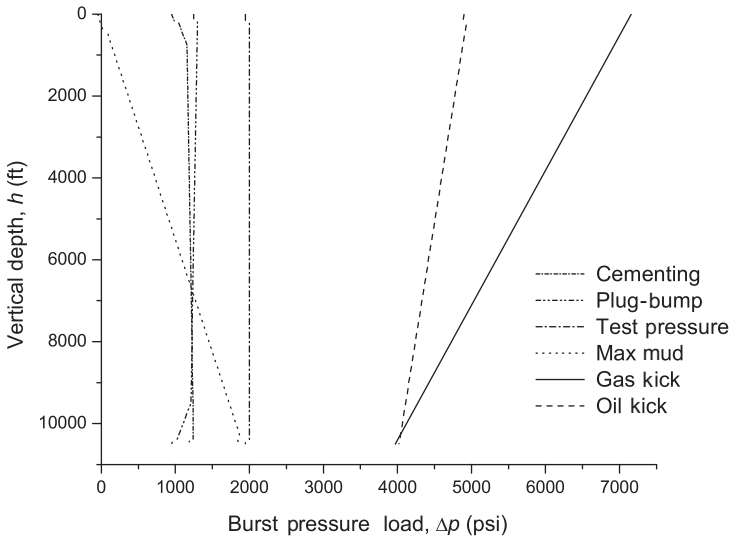

Figure 3.8 Example intermediate casing burst loads.

Fracture pressure at shoe: 1.94 SG equiv. at 14,000 ft
Temperature at surface and shoe: 74 °F, 326 °F
Production: gas and condensate
Completion: 2-7/8 in. tubing with wire line set packer just above perforations near bottom.

Cementing data

Cement to intermediate casing with 500 ft overlap, 1000 ft tail slurry at 1.99 SG, 3000 ft lead slurry at 1.87 SG ppg, 1000 ft spacer (1.84 SG) and displace plug w/1.20 SG brine, bump plug with 1200 psi above final displacement pressure. Use 25% excess on all cement.

Preliminary calculations

Here we calculate the gradients we will be using for the production casing.

$$\gamma_{\text{wtr}} = 1.0\ (0.052)\ (8.33) = 0.433 \text{ psi/ft}$$
$$\gamma_{\text{mud}} = 1.84\ (0.052)\ (8.33) = 0.797 \text{ psi/ft}$$
$$\gamma_{\text{frm}} = 1.78\ (0.052)\ (8.33) = 0.771 \text{ psi/ft}$$
$$\gamma_{\text{frac}} = 1.94\ (0.052)\ (8.33) = 0.840 \text{ psi/ft}$$
$$\gamma_{\text{cmt-lead}} = 1.87\ (0.052)\ (8.33) = 0.810 \text{ psi/ft}$$
$$\gamma_{\text{cmt-tail}} = 1.99\ (0.052)\ (8.33) = 0.862 \text{ psi/ft}$$
$$\gamma_{\text{spcr}} = 1.84\ (0.052)\ (8.33) = 0.797 \text{ psi/ft}$$
$$\gamma_{\text{displ}} = 1.20\ (0.052)\ (8.33) = 0.520 \text{ psi/ft}$$

Cement/fracture check

This conventional cementing job is designed to reach 500 ft up into the intermediate string set at 10,500 ft. It calls for 25% excess on both the lead and tail slurries. Since both are more dense than the drilling mud, we must assume the longest possible cement columns, i.e., a gauge hole diameter. So instead of a 3000 ft lead column, we would use $1.25(3000) = 3750$ ft. Likewise with the tail slurry, we would use $1.25(1000) = 1250$ ft. We now calculate the worst case pressures.

$$
\begin{aligned}
p_{\text{frac}} &= 0.840\,(14000) \approx 11,760 \text{ psi} \\
p_{\text{max cmt}} &= 0.810\,(3750) + 0.862\,(1250) + 0.797\,(14000 - 3750 - 1250) \\
&\approx 11,290 \text{ psi} \\
\therefore p_{\text{max cmt}} &< p_{\text{frac}}
\end{aligned}
$$

Production casing collapse loads

Production collapse loading is one of the most important considerations in casing design. It is not just a matter of determining the collapse loading during initial completion and production, but designing for the loading throughout the life of the well. The worst case of collapse loading in production casing will seldom occur early in the life of the well but often years after the completion. A collapse of the production casing at any point in the life of the well often results in abandonment of the well at that time.

Installation—evacuated

A string may be run empty or partially empty. If it is intentional, then the design should account for this loading. For the most part, the only occasion to run casing empty is in the case of extended reach and long horizontal sections where the intent is to reduce borehole friction by reducing the gravitational contact force. Even in those cases, the entire string cannot be empty. A fully empty string will not run any farther into a highly deviated hole than the same string fully filled because the buoyancy increase in the lower portion is negated by the buoyancy increase of the upper portion which provides the force to push the lower portion into the hole (see Chapter 7). If the empty string is the result of inadvertent failure to fill the casing while running, then it is a breakdown in supervision. The case of a fully evacuated production string during the production stage is a definite possibility and we will address it later.

Installation—cementing

The cementing collapse situation arises at post plug bump when the cement is still in liquid form and the internal displacement pressure is from a brine displacement fluid with a lower density than the drilling mud. The reason many operators do something similar to this on a production string is to help assure a good bond between the casing and the cement. Once the cement is set, and before perforating, the less dense brine is displaced with a normal density completion fluid. This change in internal pressure increases the contact force between the casing and the cement sheath for a better seal.

$$
\begin{aligned}
\Delta p_0 &= 0 \text{ psi} \\
\Delta p_{9000} &= (0.520 - 0.797)\,9000 \approx -2490 \text{ psi} \\
\Delta p_{12750} &= -2490 + (0.520 - 0.810)\,3750 \approx -3580 \text{ psi} \\
\Delta p_{14000} &= -3580 + (0.520 - 0.862)\,1250 \approx -4010 \text{ psi}
\end{aligned}
$$

Production—evacuation

As explained earlier in this chapter, total evacuation of a production string during the producing life of the well is not a rare occurrence. We are going to design for that case here. The only remaining question is, what are the annular loads? Initially the pressure might be that of the mud in which the casing was run, but later it will probably regress to the formation pressure. It may be neither of those, but it should not be greater than that of the mud in which it was run.[2] We do not know when or if that regression might take place so we will elect to use the mud in which the casing was run.

$$\Delta p_0 = 0 \text{ psi}$$

$$\Delta p_{14000} = 0 - 0.797\,(14000) \approx -11,160 \text{ psi}$$

Production—stimulation, squeeze

We also discussed earlier the mechanism for production casing collapse during a squeeze or stimulation treatment. We will assume that during such an event, the fluid density in the casing should be equivalent to the formation pressure or slightly higher, so it is a matter of the maximum differential pressure between the formation pressure and formation fracture pressure. For our example, here it is

$$\Delta p_{\text{sqz}-14000} = (0.771 - 0.840)\,14000 \approx -970 \text{ psi}$$

We see that this is inconsequential compared to our conventional collapse load, and we can ignore it. But you need to be aware of these types of operations because there can be instances where they are not insignificant. The relevant production collapse loads are plotted in Figure 3.9.

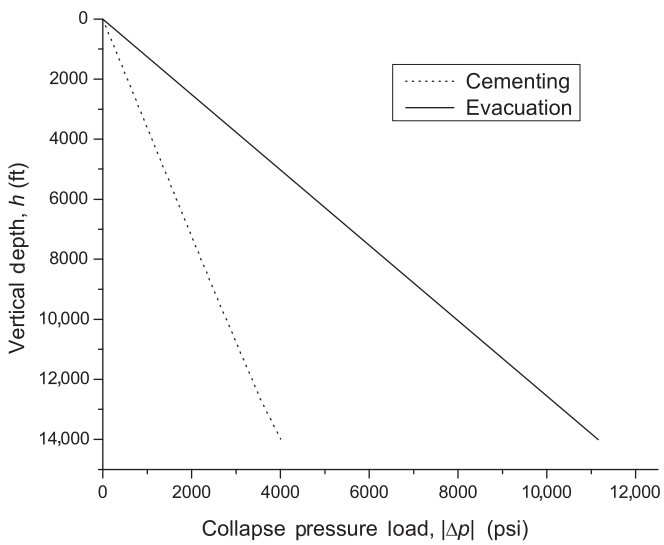

Figure 3.9 Example production casing collapse loads.

[2] There is a possibility of trapped pressure equivalent to the cementing pressures, but these should dissipate in a relatively short time.

Production casing burst loads

The burst loads for production casing are a bit different for production casing as compared to intermediate and surface casing. The cementing and plug-bump loads are similar, but the burst loads are not governed by a well kick, but by the producing zone as a backup for the tubing should it fail.

Installation—conventional cementing

Here too, we examine the possibility of a plugged float or annulus bridge forming to stop the pumping of the cement. Since the displacement fluid in this case is 1.20 SG brine, the greatest differential burst pressure will occur just before the displacement fluid starts to enter the casing.

We must calculate the cement column lengths in the casing, and we begin by calculating the internal to annular ratio assuming a gauge hole diameter.

$$k_{\mathrm{i/o}} = \frac{d_{\mathrm{bit}}^2 - d_{\mathrm{o}}^2}{d_{\mathrm{i}}^2} = \frac{8.5^2 - 7.00^2}{6.094^2} = 0.626$$

Using this ratio, we calculate the column lengths inside the casing (including the excess as usual).

$$\begin{aligned} L_{\mathrm{spacer}} &= 0.626\,(1000) = 626 \text{ ft} \\ L_{\mathrm{lead}} &= 0.626\,(1.25)\,(3000) = 2348 \text{ ft} \\ L_{\mathrm{tail}} &= 0.626\,(1.25)\,(1000) = 783 \text{ ft} \\ L_{\mathrm{mud}} &= 14000 - 2348 - 783 - 626 = 10,243 \text{ ft} \end{aligned}$$

Now we will calculate the differential pressures.

$$\begin{aligned} \Delta p_0 &= 1000 - 0 = 1000 \text{ psi} \\ \Delta p_{783} &= 1000 + (0.862 - 0.797)\,783 \approx 1050 \text{ psi} \\ \Delta p_{3131} &= 1050 + (0.810 - 0.797)\,2348 \approx 1080 \text{ psi} \\ \Delta p_{14000} &\approx 1080 \text{ psi} \end{aligned}$$

It was not necessary to calculate additional differential pressures below 3131 ft because the spacer and mud densities inside are the same as the mud density outside so there is no change in differential pressure from 3131 to 14,000 ft.

Now we must pose a question: Is this actually the worst case? This is how we handled it in the previous examples, but something is different here. We are using a less dense displacement fluid. When the lead cement reaches the float, what is the pumping pressure just before the float plugs? Is it negative as before or is it positive?

$$\begin{aligned} p_{\mathrm{pump}} &= 0.797\,(14,000) - 0.810\,(2348) - 0.862\,(783) - 0.520\,(10,869) \\ &\approx 2930 \text{ psi} \end{aligned}$$

This amount of pressure obviously calls into question our previous calculation as the worst case of float plugging. We must now calculate this case again using the differential pump pressure, 2930 psi, plus a pump increase of 1000 psi prior to shut off and using the column lengths previously calculated.

$$\Delta p_0 = 3930 - 0 = 3930 \text{ psi}$$
$$\Delta p_{10869} = 3930 + (0.520 - 0.797)\,(10869) \approx 920 \text{ psi}$$
$$\Delta p_{11652} = 920 + (0.862 - 0.797)\,783 \approx 970 \text{ psi}$$
$$\Delta p_{14000} = 970 + (0.810 - 0.797)\,2348 \approx 1000 \text{ psi}$$

This gives us a somewhat different burst profile than when displacing with the same drilling mud that is in the annulus, and this should always be kept in mind.

Question—why did this last calculation show a differential pressure at the shoe equal to our excess differential pressure of 1000 psi when the first calculation did not, 1080 psi? It is because we did not take into account the fluid column differential pressure when determining the effect of the additional 1000 psi pump pressure in the first step. The differential fluid column pressure at the surface would have been −80 psi (which would not show on a gauge) because the fluid was falling and not in equilibrium, so our actual excess pump pressure to give us a 1000 psi differential at the shoe would have actually been 920 psi.

Installation—plug bump

Next we calculate the plug-bump burst load. Using the maximum cement column from previously, we calculate the surface displacement pressure when the plug reaches the top float and when the plug is bumped with 1200 psi additional. (You will notice we have already calculated the first two quantities below in the installation collapse loading, but we repeat them here for clarity.)

$$p_{\text{max cmt}-14000} = 0.862\,(1.25)\,(1000) + 0.810\,(1.25)\,(3000) + 0.797\,(1000) + 0.797\,(8000) \approx 11,290 \text{ psi}$$
$$p_0 = 11290 - 0.520\,(14000) = 4010 \text{ psi}$$
$$p_{0\text{bump}} = 4010 + 1200 = 5210 \text{ psi}$$

Next we calculate the differential burst pressures at the annulus density change depths at surface, 9000, 12,750, and 14,000 ft. We have already made parts of these calculations, but we will show them in full once more.

$$\Delta p_0 = p_\text{i} - p_\text{o} = 5210 - 0 = 5210 \text{ psi}$$
$$\Delta p_{9000} = 5210 + (0.520 - 0.797)\,9000 \approx 2720 \text{ psi}$$
$$\Delta p_{12750} = 2720 + (0.520 - 0.810)\,3750 \approx 1630 \text{ psi}$$
$$\Delta p_{14000} = 1630 + (0.520 - 0.862)\,1250 \approx 1200 \text{ psi}$$

The final result in a plug-bump calculation should always be equal to the additional plug-bump pressure (within some roundoff error).

A light density displacement fluid would usually be replaced by a completion fluid before pressure testing the casing, so the pressure test would then assume both the same fluid inside and outside the casing (remember we discount any cement support once it has set). So whatever pressure we elect for a test pressure is uniform from top to bottom. If the well is to be stimulated through the casing the test pressure should be equivalent to the highest stimulation pressures anticipated.

Production—tubing backup

We consider that the packer or seal assembly might leak or fail during production, so that the packer fluid is produced with the gas, resulting in a full column of gas in the annulus between the tubing and production casing. This necessitates our requirement that the production casing should be designed as a full pressure backup for the tubing. We will select our burst load line accordingly. This well will be a gas well, and since the bottom hole formation pressure is equivalent to 1.78 SG, we can calculate a gas pressure at the surface using methane.

$$p_{\text{fm}-14000} = (0.771)\,14000 \approx 10,790 \text{ psi}$$

$$p_0 = 10790 \exp\left[\frac{16\,(0-14000)}{1545\left(460+\frac{74+326}{2}\right)}\right] = 8660 \text{ psi}$$

What kind of fluid would we have outside the production casing? Inside the intermediate casing the initial fluid should be drilling mud and cementing spacer. After some years, the solids may settle and the fluid might be close to freshwater in density. What about below the intermediate casing shoe? Or what if the cement top did not reach the intermediate shoe because of lost circulation while cementing? We cannot know these things when designing the casing string, and we cannot change the design once in the hole so about the worst case we can have is freshwater. With that in mind then, the differential loading pressures are

$$\Delta p_0 = 8660 - 0 = 8660 \text{ psi}$$

$$\Delta p_{14000} = 10790 - 0.433\,(14000) \approx 4730 \text{ psi}$$

That bottom pressure differential is obviously not possible at the perforations or possibly some distance from the perforations. But we are going to assume it is a worst case for our design. Many would use a formation pressure gradient on the outside, which is more likely in the earlier few years of the well but unlikely if we have solids settling in the upper annulus inside the intermediate casing. Your experience and judgment must come into play here.

In this simplified approach, we calculated a net burst pressure at the shoe and at the surface. We connected them with a straight line. Implicit in this is the assumption that both the liquid outside the casing and the gas or liquid inside the casing have constant densities from the shoe to the surface. For the most part, that is reasonable for the liquids, but we know that the gas density varies with depth, since it is temperature and pressure dependent. Our gas equation is exponential, so how does this affect our two-point calculation? The answer, perhaps surprisingly, is not very much with methane. For a plot of the equation used in this example using only 2 points as here and also using 140 points see Figure 3.10. While hardly discernible on the plot, the 140-point, incremental calculation gives a value of 8637 psi at the surface versus 8660 psi for the two-point calculation we used here. So for the purposes of basic casing design, this nonlinearity of the gas density usually is ignored.

Production—tubing leak

We must consider one additional burst scenario here and that is one of a shallow tubing leak in a gas well. If we have a weighted packer fluid behind the tubing and the tubing leaks at or near the surface (not the least uncommon) then we must consider one additional burst case with well head pressure on top of the packer fluid. Let us assume that this example has a weighted packer fluid (1.84 SG) in the tubing annulus and the packer is just above the perforations near the bottom of the hole . The differential pressure at the

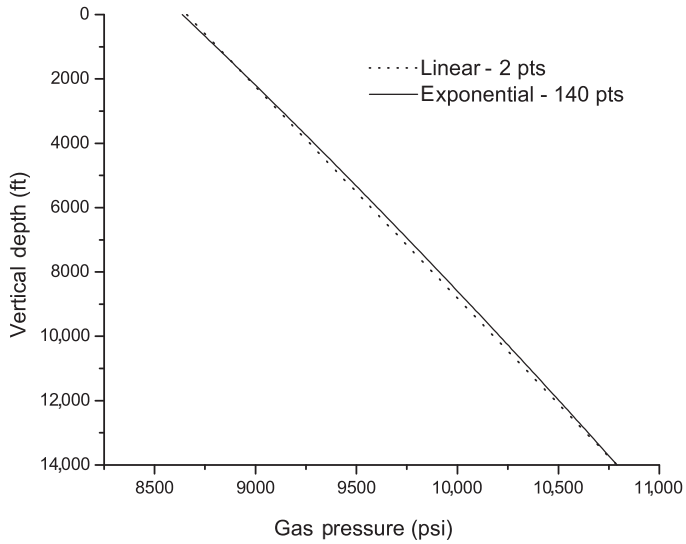

Figure 3.10 Methane gas equation plotted with 2 points and with 140 points.

top is still 8660 psi as before. But if a near-surface tubing leak results in 8660 psi gas pressure on top of the packer fluid, then the differential pressures at the top and bottom are now:

$$\Delta p_0 = 8660 \text{ psi}$$
$$\Delta p_{14000} = 8660 + (0.797 - 0.433)\, 14000 \approx 13,760 \text{ psi}$$

Many ignore this type of event in production casing design, but it does happen and we should consider it in our example design.

We can see that this almost triples the burst load at the bottom of the casing. This might require a very expensive casing string, but the reality is that it is not uncommon to develop a tubing leak at or near the surface. Could we expect to rely on the cement to resist such a burst load? Some operators do, but it is a really bad idea for reasons we have already mentioned. This is a point where we really may legitimately question the use of a freshwater gradient outside the pipe. For a production string, as in our example, for an over-pressured interval at 14,000 ft and below the intermediate casing, it is a stretch of the imagination to visualize a freshwater gradient outside the production casing. In this case, it is much more reasonable to assume something closer to formation pressures rather than a freshwater gradient. Let us look at a gradient equivalent to the formation pressure, 1.78 SG, behind the casing, which is slightly less than the mud the casing was run in:

$$\Delta p_{14000} = 8660 + (0.797 - 0.771)\, (14000) \approx 9020 \text{ psi}$$

While this value is still quite high, it is about the minimum burst load we can reasonably expect if our well develops a tubing leak at or near the surface in the early life of the well, before the zone depletes (see Figure 3.11).

Another point that should be made, is that we used methane in our gas calculations, which is a worst-case scenario. In an actual design for the production casing, it would be much more useful to use the actual gas that will be produced rather than methane. That would result in lower surface pressures than what we calculated. For our example well, we use the loads we calculated here, but the point is that,

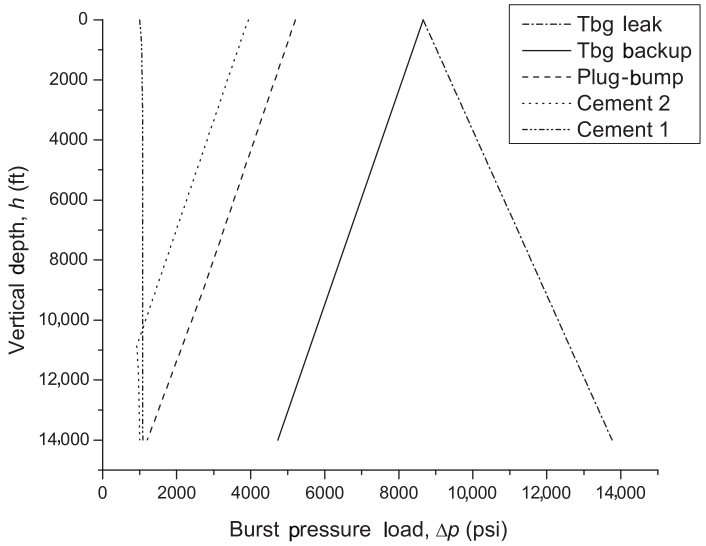

Figure 3.11 Example production casing burst loads.

when designing a production casing string for a gas well, we should consider the best data we have rather than rely on the simplifications we use for designing other strings in the well.

3.8 Closure

It should be pointed out with emphasis that the loads used in this chapter are more or less typical, but still they represent a number of simplifying assumptions. One always should evaluate the possibilities in each individual well rather than rely on common practice. More and more often, new wells are drilled in fields with depleted reservoirs present. This may change significantly the load curves for a particular well, and one should always be wary of using common "recipes" for the loads in these types of wells.

Our example load plots for collapse and burst are complete. We have not mentioned load plots for axial tension yet. That is because the well itself does not impose the axial load (discounting borehole friction and curvature for now). The axial load is not determined until we make our preliminary selection of pipe for the well, because it is a function of the weight of the specific pipe and the density of the drilling fluid. We address the axial load in the next chapter, where we use these curves to arrive at basic casing designs for all three of our example casing strings.

Design loads and casing selection

4

Chapter outline head

Casing and Liners for Drilling and Completion. http://dx.doi.org/10.1016/B978-0-12-800570-5.00004-8

4.1 Introduction

In the previous two chapters, we covered the first three steps of basic casing design:

1. Determined casing depths
2. Selected casing sizes
3. Developed pressure load plots for collapse and burst

And in this chapter, we continue the process to make our initial casing design, then refine it to account for combined loads. Our method will proceed as follows:

- Develop design loads for collapse and burst.
- Select casing for collapse and burst design.
- Develop axial load plots.
- Develop axial design plots.
- Adjust preliminary casing selection for axial loads.
- Refine basic design/selection for combined loads.

As previously discussed, casing selection is primarily a two-step procedure when done manually. Just like writers make a first draft then revise it to make it better, we make a preliminary casing selection based on published strength properties of the tube then refine it, if necessary, to account for the effects of combined loads. It is very easy to use the published values to get a preliminary design; and when used with appropriate design factors, many of these preliminary designs become a final design with no need for further refinement. However, the currently published values for collapse, burst, and tension are based on tests and formulas that assume no other loads are present in the casing. In other words, the collapse rating you see in the tables is the collapse rating with no tension in the tube; the collapse rating is lower if the tube is in tension, but such a value does not appear in any standard tables. We begin with the initial selection process then discuss ways to refine it for combined loading.

In this chapter, we will take a slightly different approach from the last where we first discussed the different types of pressure load scenarios for each type of casing, conductor, surface, intermediate and production. All the calculations involved were basic hydrostatics, so we postponed those for the examples near the end of the chapter. The stages of design covered in this chapter will be approached differently. The load types and procedures will be exactly the same for all the strings except, for the magnitudes of the worst case collapse and burst loads. The calculations involved though, will be of several types, all best learned from examples. Therefore, we will select one of our example casing strings and take it through the remainder of the design process. Then near the end of the chapter, we will repeat the process for each of the other example strings. For simplicity we will select the surface casing string as our learning example.

4.2 Design factors

A design factor[1] is a margin applied to a load or structural strength to account for uncertainty as to the load, the structural properties, or both. The way design factors were historically applied in oilfield casing design was directly to the magnitude of the load. In years past this was also the norm in most construction processes.

[1] The old term, "safety factor," is no longer used because of the growing malignancy of tort litigation where the connotation was construed to mean something never intended.

$$S \geq k_{\mathrm{D}} L, \quad k_{\mathrm{D}} > 1$$

In this approach S is the strength of the structure, L is the load, and k_{D} is the design factor which is almost always greater than unity. In this context we might call it a load design factor.

$$\mathrm{S} \geq k_{\mathrm{DL}} \mathrm{L}, \quad k_{\mathrm{DL}} > 1$$

In this case we have labeled our design factor, k_{DL} , as a load factor. We could also use an alternative approach with a strength design factor, k_{DS} , as

$$k_{\mathrm{DS}} S \geq L, \quad k_{\mathrm{DS}} < 1$$

The two approaches are mathematically equivalent. For example, if we select a strength design factor, $k_{\mathrm{DS}} = 0.80$, which is akin to common oil field practice of restricting loads so that they do not exceed 80% of the yield strength of a tube, then our design criterion would look like this.

$$0.80\, S \geq L$$

This is down-rating the strength by 20%. From this we can easily see that an equivalent statement is

$$S \geq \frac{1}{0.80} L = 1.25L \quad \rightarrow \quad k_{\mathrm{DL}} = 1.25$$

Notice that on one side, we reduced the strength by 20%, but the equivalent procedure increased the load by 25%. Although they are equivalent mathematically, there is a difference in meaning. In construction industries and civil engineering in general, there is recognition of two distinct types of uncertainty. One is an uncertainty in the structural strength, and the other is an uncertainty in the loads.

$$k_{\mathrm{DS}}\, S \geq k_{\mathrm{DL}}\, L, \; k_{\mathrm{DS}} < 1, \text{ and } \; k_{\mathrm{DL}} > 1$$

Here k_{DS} accounts for possible variations and loss of the strengths of materials used in the construction, and k_{DL} accounts for possible overloading of the structure (which is not uncommon for bridges, buildings, etc.). The justification for such an approach is easy to understand because the two are not necessarily related.

For our purposes though, we will follow oilfield tradition and use a single design factor, k_{D}. We could use either a strength factor, $k_{\mathrm{D}} = k_{\mathrm{DS}}$, a load factor, $k_{\mathrm{D}} = k_{\mathrm{DL}}$, or a composite factor like $k_{\mathrm{D}} = k_{\mathrm{DL}}/k_{\mathrm{DS}}$ (if applied to the right hand side of the equation or the reciprocal if applied to the left). Since our collapse and burst loads in basic casing design are usually selected to be the worst case in our simple scenarios, it would seem to make more sense to use a strength factor rather than a load factor, and this is what some current software does. However, for manual casing design that can lead to potential errors because it has to be calculated for each different type of casing considered for use in the string, and you cannot look at a strength table to spot-check for errors since the table values are never plotted graphically. We can, however select a strength factor and "convert" it by taking the reciprocal. For example, if we want to consider down rating the tubular strength by say 20%, then we can then use the reciprocal as a design factor on the right-hand side of the equation and plot the design load alongside the load plot.

$$0.80\, S \geq L \quad \rightarrow \quad S \geq \frac{1}{0.80} L = 1.25\, L \quad \rightarrow \quad k_{\mathrm{D}} = 1.25$$

While this appears to make perfect sense for collapse and burst since we are dealing with fair certainty as to the worst case loads, what about tension? Why do we use much larger design factors in tension than in burst or collapse? If we use a 1.25 design factor in burst and collapse and a 1.6 design factor in tension, what does that imply? Why would we down rate the material by 20% in collapse and burst,

then 37.5% in tension? That makes no sense. In tension loading, the biggest variant is the load, not the strength of the tube. The simple buoyed axial load does not account for friction in the borehole which can be significant. In a highly deviated well we usually have to calculate an estimate of the friction load (with torque and drag software), but we still apply a significant design factor because of the considerable uncertainty. In plain speak, we do not know the actual or worst case friction load in a casing string before the well is drilled, no matter how sophisticated the friction software we have at hand.

So in the end, the only reasonable approach is to use the approach with two design factors, one for strength of the structure (casing string), and the other for the load uncertainty. We can combine them into a single composite factor, and it matters not a whit which side of the equation we put it on as long as we get the numerator and denominator correct for the side we plan to use. We are going to always put it on the right side. We do this because it is much easier to use in a manual design procedure, and it reduces the chance for calculation error. In other words, the design line adjacent to the load line and the strength values of the casing come directly from the tables with no adjustment or down-rating applied. We will use the following convention:

$$S \geq k_D L \quad \text{where} \quad k_D = \frac{k_{DL}}{k_{DS}} \geq 1 \quad \text{with} \quad k_{DL} \geq 1 \quad \text{and} \quad 0 < k_{DS} \leq 1$$

Now we address the actual values of the design factor. There was a time when there were some industry recommended standards that most oil companies seemed to accept, even though almost everyone deviated from them from time to time. Of the companies that have specific design factor policies, few agree with each other as to what they should be. And almost no company will publish their design factors, not because of safety issues or secrecy but because of lability issues. Here is a range of the commonly used design factors.

- Design factor, tension: 1.6-2.0
- Design factor, collapse: 1.0-1.125
- Design factor, burst: 1.0-1.25

Table 4.1 presents a range of the commonly used design factors.

We reiterate: these are not industry standards nor are they recommendations. They are merely some common industry values that have been used for well over sixty years in many, many casing design applications. Your company will likely have its own design factors, and usually the design factors will vary depending on the type of well and possibly its proximity to populated areas. You may question the design factors of 1.0 in. the table chart which amounts to no design factor at all. Those are sometimes used when the possibility of a worst case scenario is so extremely remote that it is almost nonexistent. An example might be a surface casing collapse load plot that assumes the casing is completely empty, yet no such lost circulation problem in that particular geologic area has ever occurred. That explanation is not to justify a 1.0 design factor, but to explain why it is sometimes used by some companies.

In some countries, Canada being an example, minimum design factors are specifically required by regulatory agencies and also the loading requirements to which they will be applied. In such cases you

Table 4.1 Common Design Factors, k_D

Collapse	Burst	Tension
1.0-1.125	1.0-1.25	1.6-2.0

Table 4.2 Minimum Design Factors for Alberta [15]

	H_2S pp <0.34 kPa	H_2S pp ≥0.34 kPa	H_2S pp >500 kPa	CO_2 pp >2000 kPa
Collapse[a]	1.0	1.0	1.0	1.0
Burst	1.0	1.25	1.35	1.35
Tension[b]	1.6	1.6	1.6	1.6

[a]Casing evacuated internally.
[b]No allowance for buoyancy.

are not limited to those loads and factors. You can use more severe loading cases and higher design factors as long as the design meets the regulatory minimum. In Alberta, Canada, where many wells have high H_2S or CO_2 concentrations in the produced fluids, specific minimum design factors are required by regulation. While these may be subject to change, they are listed in Table 4.2 where H_2S and CO_2 concentrations are listed in terms of partial pressure (pp). There are provisions for using reduced design factors in Alberta under some circumstances, where the casing to be used has met certain test requirements. Table 4.2 shows some Alberta minimum design factors and loading conditions [15] and is presented here as an illustration only, and you should always seek out the most current version for actual casing design.

4.2.1 Design margin factor

When we make our final casing selection, including all adjustments and refinements, we know that some portions of the selection strength will exceed one or two of the three design criteria (collapse, burst, or axial) by a fairly significant amount, while very close to the design factor for the other load. For example, one section of the casing we select based on the burst design load may far exceed our tensile requirements. What we would like to have is some measure of how much margin we have between our design loads and the actual strengths of the casing in our selection. This gives us a quick reference as to which are the most critical loads in our final selection. We do this with what we will call a design margin factor[2], k_M.

$$k_M \equiv \frac{S}{k_D\,(L)} \geq 1.0 \tag{4.1}$$

where, as before, k_D is the design factor, S is the strength rating of the casing (collapse, burst, or tension), and L is the load. The design margin should always have a value of 1.0 or greater, where a value of 1.0 indicates that the strength of the casing is exactly the same as the design load. A value less than 1.0 indicates the strength is less than the design load, and an error has been made in the selection. By comparing the design margins for the different loads, one can easily see which loads are the most critical in the string.

The design margin factor will be calculated as the very last step in our basic design procedure.

[2] Some call this design margin factor a "safety factor," but I find this somewhat confusing terminology, especially for those of my generation who are still so accustomed to its original connotation.

4.3 Design loads for collapse and burst

To make a preliminary selection of specific casing for a casing string, it is first necessary to apply design factors to the collapse and burst loads. The result is called a design load, and we employ the design load in the form of a plot or design line. The best way to illustrate the process is to use an example, and for now we will use the example surface casing load plots we developed in the previous chapter. The selection of design factors for this example is arbitrary, with the primary intent being that of illustrating different possibilities. In practice, one would weigh the choice of design factors in light of company standards, experience in an area, perceived risk, and so forth. Those are decisions we cannot examine here.

EXAMPLE 4.1 Surface Casing Collapse and Burst Design Loads

Recall that it is 13-3/8 in. casing to be set at 3000 ft. We arbitrarily select design factors:

Collapse, $k_D = 1.125$
Burst: $k_D = 1.125$

First, we refer to the surface casing collapse loadplot from the previous chapter, Figure 3.4, and see that the evacuated lost circulation collapse load is the worst case. And the following two points are plotted.

$$\Delta p_0 = 0\,\text{psi}$$
$$\Delta p_{3000} = -1440\,\text{psi}$$

In the calculations we used a sign convention to differentiate between collapse, <0, and burst, >0. This helps avoid confusion in the calculation stage, but for the load and design plots we will use absolute values since the casing collapse and burst ratings are all positive values in standard tables. We multiply these two values by our design factor to get the design collapse load.

$$\Delta p_0 = 1.125\,|(0)| = 0\,\text{psi}$$
$$\Delta p_{3000} = 1.125\,|(-1440)| = 1620\,\text{psi}$$

We plot these design values on the same plot with our maximum load plot (see Figure 4.1). It is not necessary to show both on the same plot, but it greatly aids visually in seeing the relative magnitude of the result and also for spotting any error.

From Figure 3.6, the worst case burst load is the gas kick where the differential pressures are

$$\Delta p_0 = 1820\,\text{psi}$$
$$\Delta p_{3000} = 620\,\text{psi}$$

We multiply these values by the burst design factor

$$\Delta p_0 = 1.125\,(1820) \approx 2050\,\text{psi}$$
$$\Delta p_{3000} = 1.125\,(620) \approx 700\,\text{psi}$$

Likewise we plot these values with our maximum burst load (see Figure 4.2).

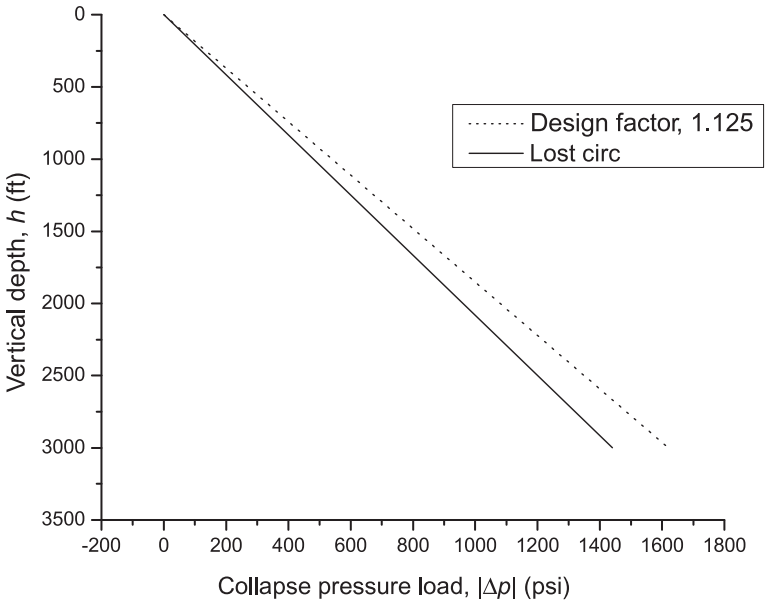

Figure 4.1 Collapse design load for surface casing example.

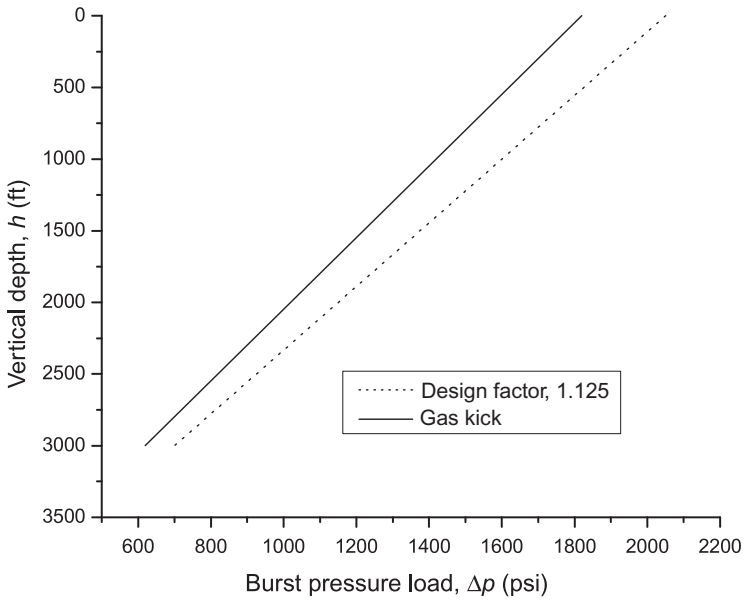

Figure 4.2 Burst design load for surface casing example.

4.4 Preliminary casing selection

We are now ready to select the casing that will meet our design requirements in collapse and burst. We constructed design plots that show the specific collapse and burst requirements, but many choices of casing meet those requirements. So what are some of the things we need to consider at this point?

We have so many variables and choices that we could spend a great deal of time discussing all the possibilities. The most prevalent consideration is cost, or perhaps we should say minimum cost. Minimum cost, however, can be misleading, because that does not necessarily translate to the market price of the casing. Cost also includes logistics, transportation, availability, current inventory, and so forth. Many considerations go into the selection process. In the examples used here, we stay with some rather simple choices, but keep in mind that there are additional considerations.

4.4.1 Selection considerations

There are a number of considerations that come into play in making a preliminary selection of casing to meet the calculated pressure loads. These are weight, grade, connections, design strengths, and simplicity of the resulting string.

Weight and grade

In selecting the casing for our string, we often are presented with a choice of a particular weight and grade of pipe versus a different weight or grade, both of which might satisfy our design. For example, we might have a choice between 7 in. 23 lb/ft N-80 and 7 in. 26 lb/ft K-55, either of which might satisfy a design. The most obvious selection criterion might be cost or availability, as previously mentioned, but what else might enter into the decision? A thicker wall pipe might offer better corrosion or wear life; hence, we might choose the thicker wall 26 lb/ft K-55. But, if it is a directional well where the pipe is below the critical inclination angle,[3] then the heavier it is, the greater the force required to push it in the hole. In that case the 23 lb/ft N-80 might be a better choice. Also the preferred or available bit size or completion equipment dimensions can enter into the selection process, so that one might favor a specific limit on the internal diameter reduction of a thicker wall pipe. The choice of grade of pipe also is significantly affected by the presence of corrosive fluids or hydrogen sulfide.

Connections

In the process of selecting casing to meet our load requirements, we are confronted with many different types of connections. What type do we need? For most normal pressure applications, we can use standard API ST&C or LT&C couplings; but for higher pressures and temperatures, bending in curved wellbores, rotating torque, high-tensile loads, gas containment, and so forth, integral and proprietary connections may be necessary. In those cases, one must refer to the proprietary manufacturer's specifications and recommendations. We can comment on a couple of things though. If there is considerable borehole friction or problems with unconsolidated formations, then one should consider the use of beveled couplings or integral connections to reduce sliding friction. These can significantly reduce frictional drag on the casing. Another consideration is clearance problems, both in the open hole section and inside

[3] The critical inclination angle, denoted α_{cr}, is the inclination angle below which nothing will move by its own weight, approximately 70° ±. See Chapter 7 for derivation and more details.

of existing casing strings. In some cases, flush-joint casing might be the choice because of clearance problems, and in other cases, special clearance couplings might be the choice. There are just too many variables to construct a decision chart for all the different possibilities.

Design strengths

In selecting casing that meets our design requirements, we rely on published values of strengths for the various sizes and types of casing. The source of these design strengths is API Bulletin 5C2 [9], which essentially is a collection of tables listing the dimensions and strengths of the various sizes and grades of API casing. The source of the strength values for these tables is the collection of formulas published in API Bulletin 5C3 [10]. These formulas have been used for many years with good success.

It is also necessary to specify what we mean by collapse strength and burst strength as used in this text for basic casing design. What we call the collapse strength is listed in API Bulletin 5C2 as "Collapse Resistance." It is the minimum external pressure at which the pipe collapses, as calculated from formulas in API Bulletin 5C3. It assumes no internal pressure or axial load on the pipe. The burst strength as we use it here, is listed in API Bulletin 5C2 as "Internal Yield Pressure." It is the internal pressure at which the inner wall of the pipe or coupling yields, as calculated from the formulas in API Bulletin 5C3. It is not the pressure at which the pipe actually ruptures or bursts, but we use it as the limiting pressure. It assumes no external pressure or axial load on the pipe. These explanations will suffice for now, but more detailed discussions are in Chapter 6.

In recent times, certain limitations have been recognized with some of the formulas of API Bulletin 5C3, and an effort is well underway to revise these in light of modern manufacturing processes and casing requirements. Currently, in ISO/TR 10400 [11], the new formulas are published, but they are not yet officially adopted into the API tables at the time of this writing. For now, we take all strength values from the current API Bulletin 5C2 and formulas from API Bulletin 5C3. When or if these documents are revised, they will not affect this basic design procedure, other than to change the published strength values slightly. We discuss the new formulas and approaches in Chapter 6, but for now, we just mention this to inform you that at least some of the published strength values we use are likely to change in the future, but those changes do not affect the basic casing design procedures we use.

Simplicity—the key to success

One thing to always keep in mind about different weights and grades of pipe, as well as connections, is that the fewer different types you have in a single string, the better. The more different types you have, the easier it is for a mistake to occur while running it in the hole. For every point in our design where we change from one type connection to another, we require a crossover sub or joint. In fact, if we are prudent operators, we require two crossovers on location for each of those points, in case one is damaged while running the casing. Not many things can be worse than running a string of 10-3/4 in. casing to 10,000 ft and damage a crossover joint by cross-threading it when the casing is 2000 ft from bottom. Yes, it does happen! If you do not have a spare, then you have to pull 8000 ft of 10-3/4 in. casing out of the hole, laying it down in singles as you pull it. Another thing you will learn if you ever have to pull casing, is that often the mill end of the coupling will back out instead of the field end, so you need backup tong jaws that fit the coupling as opposed to the pipe body, as were used when running the

casing. You also will discover that casing made up to the maximum recommended makeup torque often has galled threads when it is backed out and requires that a good number of the joints be replaced. These are things we must avoid. The casing running process with most rigs of the world is an intense and continuous operation. To stop or interrupt the process, even momentarily, in many areas, will cause the string to stick off bottom. Pipe is rolled off pipe racks or off-loaded from barges as it is being run into the wellbore and usually part, if not most, of this operation occurs at night. Hence, the simpler the design, the less is the likelihood of a costly mistake. Today, in many cases, the rig costs are so high compared to the casing costs that there is no cost benefit to having more than one type of casing in a particular string. In those cases, we might choose just one weight, grade, and connection that meets all the load criteria and disregard any cost savings of multiple weights or grades as inconsequential compared to the rig cost. This is common on many offshore wells and remote wells. However, that does not apply for most wells drilled in the world, and we would not learn much about casing design if we were to adopt that philosophy here.

Another point about simplicity is that the best way to let people in the field know that you are inexperienced and have never run any casing yourself is to send a casing design and casing string to the field that has several short sections of various weights, grades, or connections that might require crossover joints. Most operators seldom run a section of different type of casing that is less than 1000 ft in length and some set 2000 ft as a minimum. There is almost never any justification for running a section less than 500 ft in length, except in short strings of conductor and surface casing. A justifiable exception is sometimes made to use few thicker wall joints at the top of a string for wear, wellhead support, or gauge control where that same pipe is also used in the string further down hole.

EXAMPLE 4.2 Surface Casing—Preliminary Selection

For this example, we will assume that Table 4.3 lists the 13-3/8 in. casing available in our inventory for this particular well.

We can begin with either the burst or collapse, and it is really immaterial which we choose. For most surface casing strings, collapse usually is more critical than burst, and the initial selection for collapse often satisfies the requirements for burst, too. That said, we start with collapse using the design plot we previously constructed (Figure 4.1). We typically start at the top of the design plot and the lowest collapse strength pipe we have and see where the collapse rating of that section intersects our design line. In this case, the pipe with the lowest collapse rating, the 54.5 lb/ft K-55 which has a collapse rating of 1130 psi, can be run to a depth of 2100 ft before its collapse rating is exceeded on our design plot (see Figure 4.3). At that point, we go to the casing with the next higher collapse rating; it is 61 lb/ft K-55 with a collapse rating of 1540 psi. We see that rating is exceeded by our design plot at a depth of about 2850 ft. Then, we select the casing with the next

Table 4.3 Available 13-3/8 in. Casing for the Surface Casing Example

Wt. (lb/ft)	Grade	Conn.	ID (in.)	Clps Press (psi)	Int Yld (psi)	Jt Strength (klbf)
54.5	K-55	ST&C	12.615	1130	2730	547
61	K-55	ST&C	12.515	1540	3090	633
68	K-55	ST&C	12.415	1950	3450	718
68	N-80	ST&C	12.415	2260	5020	963
72	N-80	ST&C	12.347	2670	5380	1040

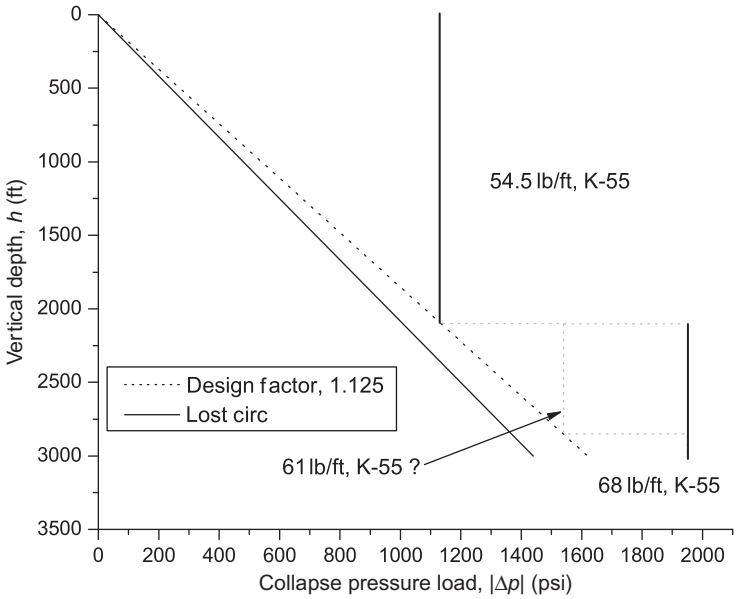

Figure 4.3 Preliminary selection based on collapse for surface casing example.

higher collapse rating, which is 68 lb/ft K-55 with a collapse rating of 1950 psi, which exceeds our maximum collapse design load of 1620 psi at bottom.

So our collapse design is satisfied by a string of 13-3/8 in. K-55 casing with 54.5 lb/ft from 0 to 2100 ft, 61 lb/ft from 2100 to 2850 ft, and 68 lb/ft from 2850 to 3000 ft. This string will work and probably is the least costly string we could run using our available inventory. However, remember what we said about simplicity. We have a 150 ft section of casing on bottom. What should we do about this? There is nothing wrong with it as far as our design is concerned, but do we really want to send three different sections of pipe to the location, one of which is only 150 ft in length (five joints)? No, we are going to opt for simplicity.

We have some obvious choices for simplifying this casing string. One is that we could just extend the 61 lb/ft section all the way to bottom and assume that the chances are slim that it would ever experience the worst-case collapse load. But there is a serious problem with that approach. Suppose a joint in that casing string happened to be defective, and actually collapsed during the drilling of this well, not in the bottom 150 ft, but somewhere above that point. It clearly is not the fault of the design, but rather, a defective joint. Such would be clear to us as engineers, but in a litigation proceeding how clear will it be to a trial judge or jury of peers who may not have even passed high school math. The hard fact is this: You selected a design criteria, and you did not adhere to it. Whether or not it actually was a contributing factor to the failure may be lost to them, along with your credibility as an engineer. This is not some remote possibility; this is the reality of today's world. The point here is that, if you select a design factor of 1.125 in. collapse, stay with it. Never change your design factor for some type of convenience that is unrelated to the mechanics involved.

At this point, we elect to simplify our design by eliminating the 61 lb/ft section and using 68 lb/ft pipe from 2100 to 3000 ft (Figure 4.3). Many operators would have just elected to run 68 lb/ft all the way from surface to 3000 ft. That might be the best choice if the additional cost is not a consequence. Here though, we are learning casing design, and that choice would teach us nothing.

Now that we have made our selection based on the collapse design load, we check that selection for burst and adjust it if necessary. To do this, we plot the burst ratings of our selected casing string on the burst load chart (see Figure 4.4). We see that the burst rating of the casing string exceeds the burst design at all points.

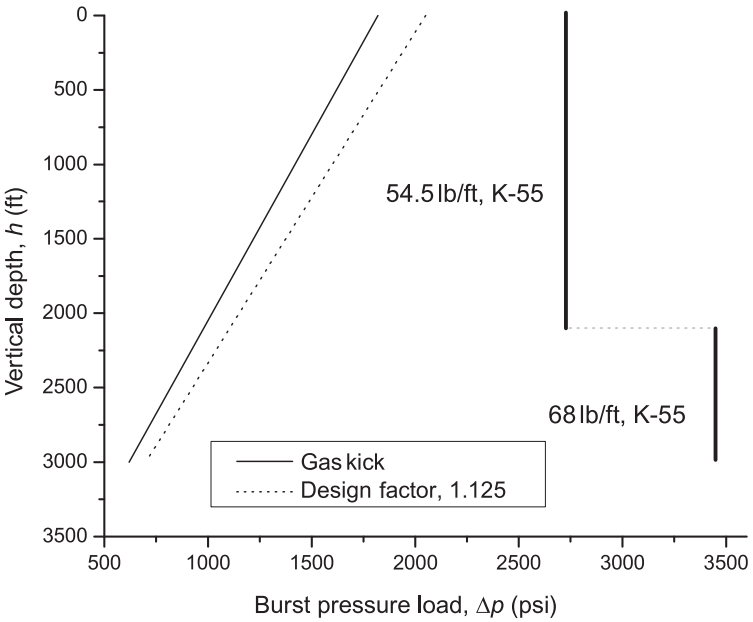

Figure 4.4 Preliminary collapse selection compared to burst design for surface casing example.

It is typical that a surface casing sting that meets the collapse requirement also meets or exceeds the burst requirements without necessity of modification, but sometimes it does not. In any case, we always check it to be sure.

This concludes the preliminary selection process. Once we conclude this step, we can determine the weight of the string and the axial loads.

4.5 Axial loads and design plot

We did not consider axial loads at the time we made our collapse and burst load plots for the simple reason that we cannot know the axial loads until we know the weight of the casing. Therefore, we selected casing that would satisfy our design parameters for both collapse and burst, and having made that preliminary selection, we now determine the axial loads and possibly adjust our selection if the axial loads are too great for the casing we selected for collapse and burst.

There are four sources of axial load (tension or compression) in a casing string:

- Gravitational forces (weight and buoyancy)
- Borehole friction
- Bending
- Temperature changes

The axial load in a casing string at any point from gravity or weight is a function of the buoyancy of the drilling fluid and the inclination of the wellbore. The borehole friction is a function of gravity, buoyancy, borehole inclination, and curvature, and also the axial load in the pipe. In the case of a curved wellbore,

the axial load is a function of the friction, but the friction itself is also a function of the axial load; in other words, they are not independent of each other. We are not going to address directional wells or borehole friction at this time but will discuss them in Chapter 7.

There are a number of considerations when it comes to determining the design criteria for axially loaded casing. Here are a few questions we might have:

- Weight of casing—in air or buoyed weight?
- Borehole friction—how much?
- Design factors—an over-pull margin or a design factor?

We discuss these in the following sections.

4.5.1 Axial load considerations

We have postponed any detailed discussion of axial load until now. As already mentioned, we cannot calculate axial loads until we have a preliminary selection for which to make the calculations.

Weight of casing

When we work with casing in a wellbore, we must consider its weight and the amount of tension in the string from that weight. What measure do we use for the weight? Do we use the weight of the casing in air or the buoyed weight of the casing in the drilling fluid in the hole? As hard as it may be to believe, this question has no universally accepted answer in oilfield practice today. Many use the weight in air, claiming that it gives an extra margin of safety. Others say the buoyed weight is more realistic. We prefer the buoyed weight, but will illustrate both methods.

Borehole friction

We know that there is friction in a wellbore, and as we move the pipe, the friction increases or decreases the axial load in the casing, depending on whether the pipe motion is up or down. In directional wells, we have software that can predict the friction with reasonable accuracy while we are in the design process. For "vertical" wells, we know there is some amount of friction, but we have no means of calculating it, unless we assume some wellbore path and use software as we would for a directional well. We can measure the pickup and slack-off weight while drilling the well, whether it is a vertical well or a directional well. The problem with this is that we usually have to design and purchase the casing string far in advance of the time when we can measure the actual friction in a particular well. Also, the friction load we measure with the drill string is not the same as the friction load the casing string experiences. For most near-vertical wells, we do not consider the friction specifically, but we allow for it with a design factor. That is one reason the design factor for the axial load is usually larger than the design factors for collapse or burst. We have a much better chance of predicting the worst-case loading for collapse and burst than in tension. At least, we have a better chance when we are sitting in an office several months before the well is drilled. We discuss borehole friction in much more detail in Chapter 7, but for now, we assume we can avoid estimating it if we select an appropriate design factor.

Axial load design factors

When it comes to the tensile design of casing, there are two schools of thought. One is to use a design factor, say 1.6, and the other is to use a specified amount of over-pull, say 100,000 lbf. It is quite common

to use both and say that the design should incorporate whichever one leads to the strongest design. In cases where the design factor results in the higher value, that usually is the case only near the surface and the over-pull is greater near the bottom.

The significance of the design factor or over-pull is especially critical in casing design, because of the borehole friction and the fact that its magnitude generally is not known when the casing string is designed. Friction force opposes the motion of the pipe, so we might think that it is of little significance in the design, since it reduces the axial tension only as the casing is run into the well. While that is true, there are two other considerations. One is that, if we intend to reciprocate the casing during cementing (as is desirable for a good primary cement job), then the friction increases the axial tensile load when the pipe is in an upward motion. The second, and extremely important, consideration is that, if a problem is encountered in running the casing, the casing string may have to be pulled out of the hole before reaching bottom. While this is rare, it does happen. So the design factor or over-pull must account for the fact that the casing might be subjected to the full amount of friction in an upward motion. That is one reason for the popularity of an over-pull margin rather than a typical design factor. It is easier for the driller if he knows that he can safely pull a certain amount, say, 100,000 lbf, above the weight of the casing string, and this margin is a constant for the entire string.

4.5.2 Types of axial loads

We consider three forms of axial load. Each has its particular use, but not necessarily in casing design. The three forms are:

- The unbuoyed axial load is simply the weight of the casing string in air. (Remember we do not consider "air" as having any mass or buoyancy in our design process.)
- The effective axial load is determined from Archimedes' principle, which gives us the total buoyed weight, but does not give us any information about the axial load *within* the casing string itself.
- The true axial load is determined from the actual gravitational hydrostatic forces acting on the tube and is valid for all bodies.

The first of these was a common approach for many years because of its simplicity and additional design margin, but it is a load the casing never experiences in the borehole. The second is very common and is probably used more when buoyancy is considered than the true axial load. It is simple to calculate, but it is problematic in that it is a fictitious load that is only correct at the top of the casing string. The third is the actual load in the casing, and unfortunately, a bit more tedious to calculate.

The buoyed weight of the casing in drilling fluid is the most realistic approach for designing casing to withstand axial loads. It is the true axial load that we will use for our designs in the examples.

Unbuoyed Axial Load

The unbuoyed weight of a casing string, or the "weight in air" as it is often called, is simply

$$w = g\,\rho_\ell\,L \tag{4.2}$$

If we chose to use the weight of the casing in air, the design process is quite simple. The drawback to the approach is that it often leads to an over design of the string, since the casing is never actually suspended in air. While the weight in air approach was quite common at one time, it is less favored by most operators today. However, it is still the method required by regulation in some locales.

Effective Axial Load

The effective axial load as we define it, is calculated using Archimedes' principle, in that the buoyant force is equal to the weight of a fluid displaced by the submerged portion of a body. For convenience we use a buoyancy factor, k_b, based on the density difference between that of the body and the fluid. The buoyancy factor multiplied by the weight of the casing in air gives the buoyed weight of the casing.

$$\bar{w} = k_b \, (g \, \rho_\ell \, L) \tag{4.3}$$

The buoyancy factor is calculated as

$$k_b = 1 - \frac{\rho_{mud}}{\rho_{steel}} \tag{4.4}$$

and is explained in more detail in Appendix A (Equation (D.19)) if you are not already familiar with the topic.

We will not use the effective axial load here, but to calculate the effective axial load at any point we could use the following procedure:

$$\hat{F}_j = g \, k_b \sum_{i=1}^{j} \rho_{\ell \, i} \, L_i \tag{4.5}$$

where we sum the buoyed weights of each section up to the top of some section, j, and for the total buoyed weight of a string with n sections we just set $j = n$ and sum over the entire string.

As already stated, the effective axial load is a fictitious load except for a single point in a casing string, the very top of the string. Why does anyone use it then? Most likely because it is so simple, but more disturbingly is the possibility they do not understand what it is. As to its simplicity, yes, but consider a case where the fluid inside the casing is different from the fluid in the annulus. How does that affect our simple buoyancy factor equation above? Clearly stated, the effective axial load is of no use in determining the axial load in casing design because it does not give us the axial load! That said, does the effective axial load have any use at all? The answer to that is emphatically, yes. It is used in determining the point of neutral stability for lateral buckling in tubular strings. It has been used correctly for many years in calculating the length of drill collars needed to prevent lateral buckling in drill pipe. We will discuss lateral buckling in Chapter 6, and again, see Appendix A for more detailed discussion on buoyancy.

True Axial Load

The term, true axial load, is redundant, but we use it anyway to differentiate from the effective axial load which is so pervasively present in oilfield usage. The true axial load is the actual axial load in the buoyed pipe. More specifically it is the axial component of the weight of the pipe less the force from hydrostatic pressure acting on the net cross-sectional areas of the pipe that are perpendicular to the longitudinal axis of the pipe (discounting friction forces for now). It can be a tedious calculation when done manually, but is easily programmed into a spreadsheet or some such software. Two things are important to remember when doing the calculations:

1. Always work with vertical depths, never measured depths. The gravitational force, mg, is vertical, so the axial load is affected only by the axial components of its weight and hydrostatic forces (neglecting friction for now, see Chapter 7).
2. Two calculations are necessary at every point where the pipe cross-sectional area changes—one just below the change and one just above the change. The pressure at that point will cause a discontinuity shift in the axial load plot.

Calculating true axial load

Calculating the true axial load is a process of determining the buoying forces from pressure acting on cross-sectional areas of the casing where those buoying forces act upon the unbuoyed weight of the casing string. Those buoyancy points occur at the bottom of the casing string and at any point in the string where the internal diameter changes (the outside diameter is a constant in all but a few rare tapered string applications). But do not be misled into thinking that all these buoyant forces are in the opposite direction to the gravitational forces. Whenever the internal diameter of a section is greater than the section below it (very common) the pressure force ("buoyant"?) is downward and adding to the gravitational force.

The formulas and procedure for calculating true axial load are developed in Appendix A and will be illustrated with an example in the next section.

$$F_j^{\downarrow} = -p_0 A_0 + p_1 A_1 + \sum_{i=2}^{j} p_i \left(A_i - A_{i-1}\right) + \sum_{i=1}^{j-1} w_i L_i \quad j = 1, \ldots, n \tag{4.6}$$

$$F_j^{\uparrow} = -p_0 A_0 + p_1 A_1 + \sum_{i=2}^{j} p_i \left(A_i - A_{i-1}\right) + \sum_{i=1}^{j} w_i L_i, \quad j = 1, \ldots, n \tag{4.7}$$

where

j = section number where forces are being calculated in step

n = total number of sections in string

i = node number, section number (starting at bottom with node and section 1)

A_0 = total cross-sectional area of casing at bottom, $0.25\pi d_o^2$

A_i = internal cross-sectional area of casing in section i, $0.25\pi d_i^2$

p_0 = pressure outside casing at bottom of string

p_i = pressure inside casing at node i

w_i = unbuoyed linear weight of casing in section i ($w = g\,\rho_\ell$)

L_i = vertical length of section i

$F_j^{\downarrow}$ = axial force in the bottom of section j

$F_j^{\uparrow}$ = axial force in the top of section j

Note: Mathematically, the convention is that when a summation index, i, is initially greater than the summation limit, j or $j-1$, then the summation is zero. And in a case where $j - 1 < 0$, then the summation is zero. This is standard in mathematics, but be cautioned that this is not always consistent in some programming languages.

While those formulas lend themselves easily to programming, they are a bit confusing if doing the calculations manually because they separate the bottom and top loads of each section and calculate them separately. When doing the calculations manually we prefer to do them sequentially without having to repeat so many of the calculations in the summations.

Here is a simple procedure for manual calculation of the true axial load:

1. Calculate the cross-sectional areas: $A_0, A_1, \ldots, A_n$.
2. Calculate the unbuoyed weight of each section: $W_i = w_i L_i$.
3. Calculate the pressure at each node: $p_0, p_1, p_2, \ldots, p_n, p_{n+1}$.
4. Starting at the bottom, calculate the force at the bottom of section 1, $F_1^{\downarrow}$, then the top of section 1, $F_1^{\uparrow}$, bottom of section 2, $F_2^{\downarrow}$, top of section 2, $F_2^{\uparrow}$, etc.

The procedure would then go in sequence as follows:

$$F_1^{\downarrow} = -p_0 A_0 + p_1 A_1$$
$$F_1^{\uparrow} = F_1^{\downarrow} + W_1$$
$$F_2^{\downarrow} = F_1^{\uparrow} + p_2 (A_2 - A_1)$$
$$F_2^{\uparrow} = F_2^{\downarrow} + W_2$$
$$\vdots$$
$$F_j^{\downarrow} = F_{j-1}^{\uparrow} + p_j \left(A_j - A_{j-1}\right) \tag{4.8}$$
$$F_j^{\uparrow} = F_j^{\downarrow} + W_j \tag{4.9}$$
$$\vdots$$
$$F_n^{\downarrow} = F_{n-1}^{\uparrow} + p_n (A_n - A_{n-1})$$
$$F_n^{\uparrow} = F_n^{\downarrow} + W_n$$

Notice that we always start at the bottom of the casing string. That is because the pressure at a node has no effect on the forces below it.

Before we leave this section, it may or may not be obvious to you that since both the true axial load and the effective axial load are the same at the surface, they must be somehow related. They are. The relationship between the true axial load, F, and the effective axial load, $\hat{F}$, is given by

$$F = \hat{F} - (A_o p_o - A_i p_i) \tag{4.10}$$

where A_o and A_i are the outside and inside cross-sectional areas of the casing, respectively, and p_o and p_i are the outside and inside pressures, respectively. You can see from this relationship that at the surface, where $p_o = p_i = 0$, then $F = \hat{F}$ as we would expect. In fact, from this relationship you may see an easier way to calculate the true axial load. Calculate the effective axial load first, and then use the above to adjust it to the true axial load. There will however, be a small (but insignificant) difference in the results of the two methods. The difference arises from the fact that the API linear density ("weight") of the casing is the nominal density and not the actual density.

4.5.3 Axial load cases

Similar to the collapse and burst loads there are more than one case for axial load in the well construction process. The two cases we always check occur in the installation stage of operations. There are some special cases that occur in the production stage that involve high pressure stimulations and thermal effects. These last two will not be included in our basic design, but will be discussed in Chapters 6 and 7 in the appropriate context. The axial load cases are shown in Table 4.4

Table 4.4 Summary Axial Loading Cases

Axial Loading	*C*	*S*	*I*	*P*
Installation				
Running	A	A	A	A
Plug bump	A	A	A	A
Production				
Stimulation			S	S
Thermal effects			S	S

C, conductor; *S*, surface; *I*, intermediate; *P*, production; A, always applicable; S, sometimes applicable.

The axial calculation methods in the previous section are the bases of both cases. The running case is exactly the calculation in the previous section. In the running case, $p_1 = p_0$ because the fluid inside is usually equal to the fluid in the annulus. Also in the running case, the surface pressure is zero so $p_{n+1} = 0$.

The plug-bump case differs in that $p_1 \neq p_0$ because of the difference between the hydrostatic head of the annular and internal columns, and with the addition of the additional pump pressures for displacement and plug bump. Likewise $p_{n+1} \neq 0$ because the surface pressure is the differential displacement pressure plus the additional plug-bump differential. These pressures are already determined in the burst load calculations and are then included in pressure calculations for substitution into Equations (4.6) and (4.7).

We will now show examples using the surface casing we previously selected to meet the collapse and burst designs.

EXAMPLE 4.3 Surface Casing Example—Axial Load, Running Case

Referring to Figure 4.5, we calculate the forces as before. For example

$F_1^{\downarrow}$ = force at the bottom of section 1

$F_1^{\uparrow}$ = force at the top of section 1

So, the force at the top of section 1 is equal to the force at the bottom of section 1 plus the weight of section 1:

$$F_1^{\uparrow} = F_1^{\downarrow} + W_1$$

To make it easier we will calculate all of the cross-sectional areas first.

$$A_0 = (\pi/4)(13.375)^2 = 140.500 \text{ in}^2$$

$$A_1 = (\pi/4)(12.415)^2 = 121.055 \text{ in}^2$$

$$A_2 = (\pi/4)(12.615)^2 = 124.987 \text{ in}^2$$

Then the section weights:

$$W_1 = 68(900) = 61,200 \text{ lbf}$$

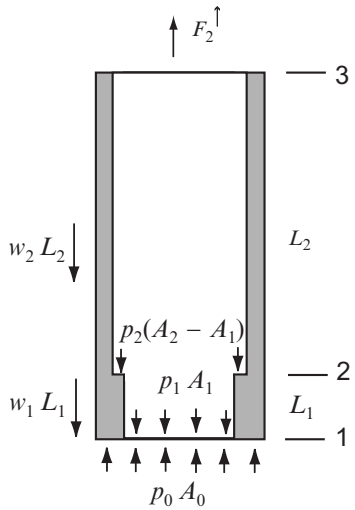

Figure 4.5 Example surface casing schematic.

$W_2 = 54.5(2100) = 114,450\,\text{lbf}$

And the nodal pressures:

$p_0 = 0.052(1.11)(8.33)(3000) = 1440\,\text{psi}$

$p_1 = 0.052(1.11)(8.33)(3000) = 1440\,\text{psi}$

$p_2 = 0.052(1.11)(8.33)(2100) = 1010\,\text{psi}$

Calculate the true axial load at the bottom of each section and at the top of the well using Equations (4.8) and (4.9). Since the fluid inside and outside are the same the pressure at the shoe is the same inside and outside.

$F_1^{\downarrow} = -p_0 A_0 + p_1 A_1 = 1440\,(-140.500 + 121.055) = -28,000\,\text{lbf}$

$F_1^{\uparrow} = F_1^{\downarrow} + W_1 = -28000 + 61200 = 33,200\,\text{lbf}$

$F_2^{\downarrow} = F_1^{\uparrow} + p_1\,(A_2 - A_1) = 33200 + 1010\,(124.987 - 121.055) = 37,170\,\text{lbf}$

$F_2^{\uparrow} = F_2^{\downarrow} + W_2 = 37170 + 114450 = 151,620\,\text{lbf}$

Before proceeding we will now calculate the unbuoyed axial load and the effective axial load for comparison. We will not use those loads in our design, but it is important to see how they compare.

EXAMPLE 4.4 Surface Casing—Unbuoyed and Effective Axial Loads

There are two sections of casing in the surface string, 900 ft of 68 lb/ft on bottom and 2100 ft of 54.5 lb/ft casing on top. The mud density is 1.11 SG.

The unbuoyed axial casing load is

$F_{3000} = 0$

$F_{2100} = 68\,(900) = 61,200\,\text{lbf}$

$$F_0 = 61200 + 54.5\,(2100) = 175,650\,\text{lbf}$$

Recall that in USC units $g \cdot g_c \approx 1$. Had we been working in SI units, g would have appeared in the calculation.

The effective axial load is calculated with a buoyancy factor:

$$k_b = 1 - \frac{\rho_{mud}}{\rho_{steel}} = 1 - \frac{1.11\,(62.34)}{490} = 0.873$$

The effective axial load is obtained by multiplying the unbuoyed axial load by the buoyancy factor:

$$F_{3000} = 0$$

$$F_{2100} = 0.873\,(68)\,(900) = 53,430\,\text{lbf}$$

$$F_0 = 53430 + 0.873\,(54.5)\,(2100) = 153,340\,\text{lbf}$$

See Figure 4.6 for a comparison of the unbuoyed and effective axial loads with the true axial load. Note that the effective axial load is the same as the unbuoyed load at bottom, 0 lbf, and roughly the same as the true axial load at the top. If our theory is correct they should give exactly the same results at the top, but here we see they do not. There is a difference of 1690 lbf as calculated. Roundoff error? No, roundoff plays a small part, but the significant reason is that the nominal weight of the casing is not the actual weight, and it affects these calculations differently.

Note the true axial load plot on the left. It actually is in compression at the bottom, because of the hydrostatic pressure on the cross-sectional area of the tube at the bottom. Note also that, as you move up the plot from bottom to 2100 ft, the plot shifts slightly. That is because of the difference in

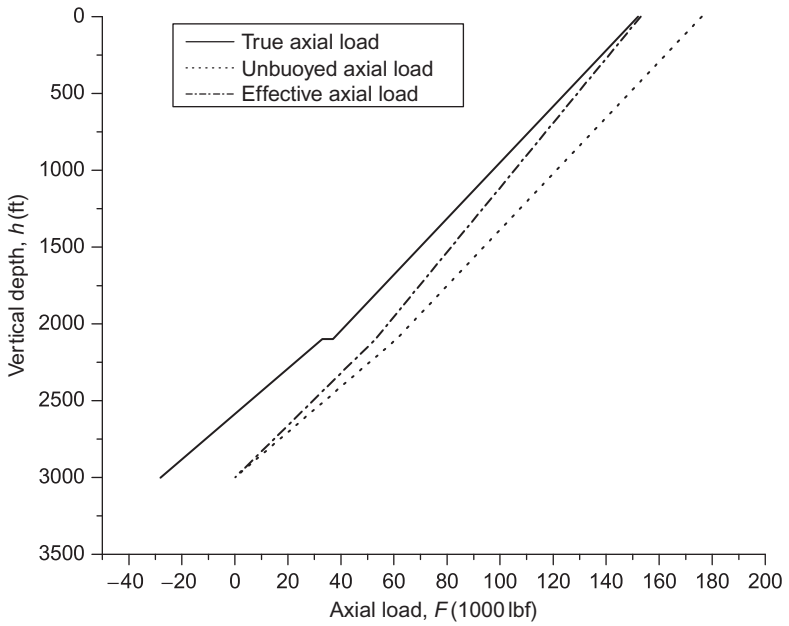

Figure 4.6 Surface casing example: comparison of types of load calculation methods.

cross-sectional area of the 54.5 lb/ft and the 68 lb/ft casing at that point. The tension increases, meaning that the net hydrostatic force is acting downward, because the internal diameter of the 68 lb/ft casing below is smaller than the internal diameter of the 54.5 lb/ft pipe above. (Had the heavier pipe been on top, the plot would have shifted in the opposite direction.) It is important to note: The pressure acting at the point of change in cross-sectional area has no effect on the axial load in the casing below that point, only on the casing above that point.

Another thing to note about these plots is that the unbuoyed load plot essentially parallels the true load plot, except for the change in cross-sectional area. It is much easier to calculate manually, since there are no differences in cross-sectional areas and hydrostatic pressures to consider. That is why, in the past, many used this as the basis for their design (along with an appropriate design factor). And, as stated previously, many still use it, especially when doing manual calculations for calculating the axial load. Some also justify its use by stating that, since we do not know the magnitude of borehole friction in the well when we are designing the casing string, the axial load in air is a safer approach.

Next we will calculate the plug-bump case of axial loading, again using the surface casing as an example.

EXAMPLE 4.5 Surface Casing Example—Axial Load, Plug-Bump Case

The casing sizes and depths will be exactly the same as the previous example. The pressures will however, be different because of the different fluids in the annulus and inside the casing, the displacement pressure, and the differential plug-bump pressure. These pressures were all calculated in the previous chapter and are:

$p_0 = 1840\,\text{psi}$
$p_1 = p_0 + 500 = 2340\,\text{psi}$
$p_3 = 900\,\text{psi}$ (0 psi in previous example)

The only pressure calculation we must make is

$$p_2 = 900 + 0.052\,(1.11)\,(8.33)\,(2100) = 1910\,\text{psi}$$

Now we have all the data to make the true axial load calculations.

$$F_1^{\downarrow} = -p_0A_0 + p_1A_1 = -1840\,(140.500) + 2340\,(121.055) = 24,750\,\text{lbf}$$

$$F_1^{\uparrow} = F_1^{\downarrow} + W_1 = 24750 + 61200 = 85,950\,\text{lbf}$$

$$F_2^{\downarrow} = F_1^{\uparrow} + p_1\,(A_2 - A_1) = 85950 + 1910\,(124.987 - 121.055) = 93,460\,\text{lbf}$$

$$F_2^{\uparrow} = F_2^{\downarrow} + W_2 = 93460 + 114450 = 207,910\,\text{lbf}$$

As you might expect, the axial load is greater during plug bump. This is often the case and points out the necessity to calculate the tension in plug bump.

We will use only the true axial loads in our design. We now plot both the running case and the plug-bump case (see Figure 4.7). Obviously the plug-bump case is the more severe loading for this casing string.

Before continuing we need to cover one more case, not critical to our axial design but of some significance when we discuss combined loading. This case might be called the post plug-bump axial load. The cement is in place and the bump pressure is released. It is identical to the running case except now the external fluid contains cement.

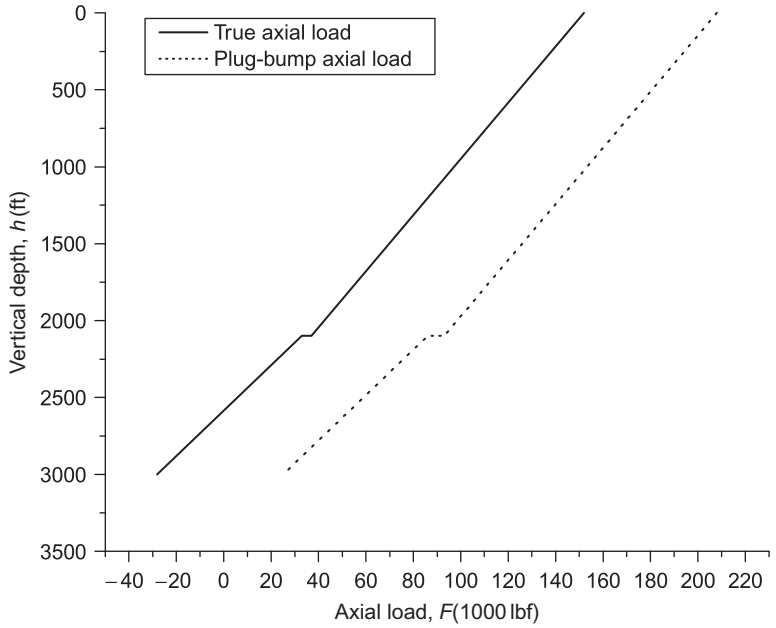

Figure 4.7 Axial loads for surface casing example.

EXAMPLE 4.6 Surface Casing Example—Axial Load, Post Plug Bump

In this example the internal pressure has been released and the casing is buoyed on the outside by cement and mud (or in this particular example, all cement). The only variable that differs here is the outside pressure at the shoe. Now $p_0 = 1840$ psi as in the last example, and all the internal pressures are the same as the running case.

$$F_1^{\downarrow} = -p_0 A_0 + p_1 A_1 = -1840\,(140.500) + 1440\,(121.055) = -84{,}200\,\text{lbf}$$

$$F_1^{\uparrow} = F_1^{\downarrow} + W_1 = -84200 + 61200 = -23{,}000\,\text{lbf}$$

$$F_2^{\downarrow} = F_1^{\uparrow} + p_1\,(A_2 - A_1) = -23000 + 1010\,(124.987 - 121.055)$$

$$= -19{,}030\,\text{lbf}$$

$$F_2^{\uparrow} = F_2^{\downarrow} + W_2 = -19030 + 114450 = 95{,}420\,\text{lbf}$$

4.5.4 Axial design loads

After calculating the axial loads, we next develop a design load plot. We previously discussed two possibilities, a design factor and an over-pull margin. We could use either, or possibly both. For example, we might select both an axial load design factor of 1.6 and an over-pull margin of 100,000 lbf for instance. Figure 4.8 shows those two criteria applied to the surface casing true axial load previously calculated.

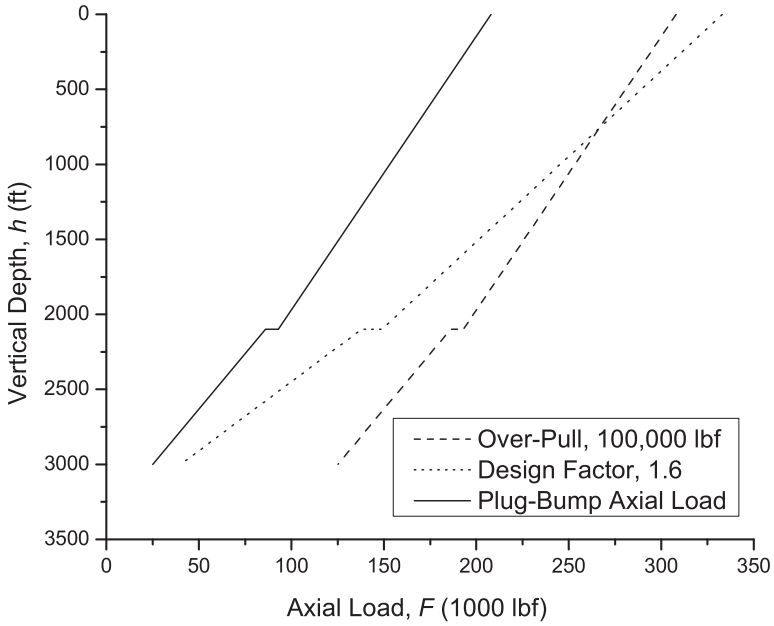

Figure 4.8 Example surface casing design loads.

In axial loading, the design factor is a bit different from collapse and burst loading. The latter two of these design loads assume a static environment where the worst case loads are accounted for. Is that true of the axial load? What if we cannot get the casing to bottom and have to pull it out of the hole? Most would say that is accounted for when we use a larger design factor. But is that correct? Notice that an axial design factor has a decreasing margin with depth and gives no margin at all near bottom. That is fine for a static casing string where tension is minimal near bottom, but if we should have to pull it out of the hole before cementing, there is no tensile margin in the lower part of the design load. But that may not be the case if we have to move the pipe upward, even for reciprocation while cementing. Most drillers know that there is a predetermined amount above the weight of a drill string that they can safely apply should the drill string become stuck. This is called an over-pull margin and 100,000 lbf seems to be a most common value. When it comes to reciprocating casing while cementing, almost no one on location has any idea of the safe limit above the string weight. The over-pull margin is uniform from bottom to top, and that is why many prefer it to the axial design factor. Most casing strings that are adequate in severe collapse loading near bottom tend to have sufficient joint strength too, but this is something to keep in mind. For our axial designs we are going to consider both a design factor and an over-pull margin. The axial selection will be based on the more critical of the two.

In this case, the design factor of 1.6 is less than the 100,000 lbf over-pull except near the surface, so we use both as the design lines. In Figure 4.9, we plot the casing we already selected to meet the collapse and burst requirements, and we find that it easily exceeds the tension requirements also. This is fairly typical of many surface strings, but the tensile design should always be checked to be certain.

At this point we might consider our surface casing design complete, and for many this might be true. However, we are going to add one more step to our design process. We are going to consider the effect of tension in the string and how it reduces the collapse resistance.

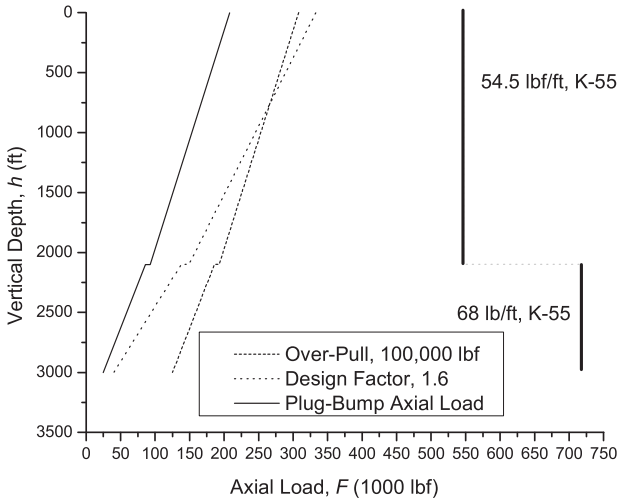

Figure 4.9 Burst preliminary selection compared to axial design loads for surface casing example.

4.6 Collapse with axial loads

All casing is loaded with a combination of loads, such as tension, internal pressure, and external pressure. The significance of this is that, in the case of combined loads, the table values we used for collapse, burst, and tension are not valid. For instance, the collapse value of the 13-3/8 in. 54.5 lb/ft K-55 casing was listed as 1130 psi. But that value is valid only if there is no axial tension or compression in the casing. In the presence of tension, the collapse value is lower, and in the presence of compression, the collapse value may be higher. So we look at combined loads as they apply to axial tension and collapse to determine whether or not we need to refine our casing design.

The combined loads of tension and collapse in casing is often referred to as biaxial loading, usually meaning a combination of axial tension and collapse loads. This implies that the loading is on only two of the principal axes of the casing which is not true. All casing in a borehole is always loaded on all three principal axes: the radial, tangential, and longitudinal axes. What the term refers to is a simplification of three-dimensional loading into a two-dimensional case for ease of handling. The application in casing design is called biaxial design and it works sufficiently well for most basic applications. In fact, it works so well that few have ever seen need to go to anything more sophisticated. We will discuss all this in detail in Chapter 6, and for now we will use a two-dimensional simplification here.

4.6.1 Combined loads

Casing designs for many wells ignore altogether the effects of combined loads, and many operators have never suffered any consequences for having done so. There are two reasons that the deleterious effects are rarely seen. First, a large-enough design factor in collapse has been used, so that combined loading effects are never seen. Second, and most prevalent, is that the actual loads on the casing strings have been lower than the worst-case design loads. However, casing failures from combined loading do occur. And, when they happen, the consequences are serious to the extent that the well may be lost.

The subject of combined loading is a bit complicated, and there are several approaches that work. We will delay any discussion on the topic until Chapter 6, but we need some tool now that we can use for basic casing design. So for now, we introduce a simple and useful equation for use in calculating the reduction in collapse rating caused by axial tension. Again, we will leave any explanation and discussion for Chapter 6.

$$k_{\text{clps}} = \sqrt{1 - \frac{3}{4}\left(\frac{F}{A_t Y}\right)^2} - \frac{1}{2}\left(\frac{F}{A_t Y}\right) \tag{4.11}$$

where k_{clps} is a collapse rating reduction factor at a point in tension, F is the axial tension at that point, A_t is the cross-sectional area of the tube, and Y is the yield strength of the tube.

Where do we apply this formula? The answer may seem obvious: any point where a casing strength line intercepts the collapse design line in our collapse charts. The next question is whether or not the casing is in tension at that point. If no, then there is no need to consider that point, but if yes, then there is definitely going to be a reduction in the collapse rating. For example, our surface casing collapse design plot with preliminary selection shows such a point at 2100 ft (see Figure 4.3).

The next step is to determine whether or not the casing is in tension at that point, and if so, how much. And here is where a dilemma arises: which axial load curve do we use? If you have never considered this, you are far from alone. Combined loads are almost never a combination of the worst case design loads because these never occur at the same time. In our surface casing example, the worst case collapse load which is the one we must consider, occurs during a serious lost circulation event while drilling and after the surface casing is cemented. What is the tensile load in the pipe then? We do not know! We calculated three load cases: running, plug bump, and post plug bump. If our borehole was perfectly vertical and the surface casing is concentric to the borehole, then the answer is easy—the post plug-bump load. But we know such a configuration is not possible in reality; the casing does contact the borehole wall, and there is friction. Realistically, all three of our axial load cases are hypothetical and may never actually exist.

We could make legitimate arguments for a number of scenarios. In an ideal vertical well with no friction, we could list the sequence like this:

- Prior to cementing, the casing is in the running state.
- At plug bump the casing has been stretched by the pressure and is in the plug-bump state.
- As soon as the pressure is released, casing contracts into the post plug-bump state.

That would suggest the post plug-bump curve as the logical choice, and referring to Figure 4.10 we see that the critical collapse point is actually in compression and no adjustment is needed. But if we consider friction (and we must) the sequence may be quite different:

- While cementing we reciprocate the pipe with enough movement at the surface to assure the entire string moves up and down.
- Reciprocation almost always ends on a down-stroke so that the cementing head is at its lowest position where it was installed. Much of the lower casing is most likely in compression.
- Did reciprocation cease before or after plug bump?
  - If before plug bump, was the plug-bump pressure significant enough to overcome frictional resistance and actually stretch the casing into the calculated plug-bump state?
  - If after plug bump, then the calculated plug-bump pressure has no significance in the later collapse loading.
- If casing was actually stretched into the plug-bump state, is the cement buoyancy and tension in the casing (from the plug bump) sufficient to contract the pipe into the calculated post plug-bump state?

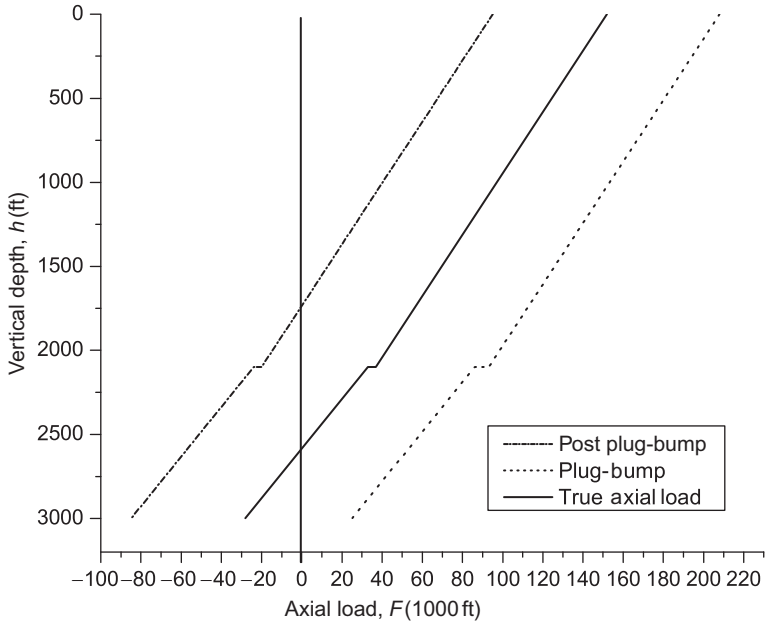

Figure 4.10 Three buoyed axial load cases for example surface casing.

For the most part these questions are unanswerable. For many years most casing strings were designed using the unbuoyed axial load and the worst case collapse case as the combined loads. It worked well and still does, but perhaps it also results in over-design. For our examples, I will use the running case of the true axial load (buoyed), but it is up to you or your company policy as to what you will use in your designs.

EXAMPLE 4.7 Surface Casing Example—Combined Collapse and Tension

From Figures 4.3 and 4.10 and Table 4.3 we get our data:

$$h = 2100\,\text{ft}$$
$$p_{\text{clps}} = 1130\,\text{psi}$$
$$F = 37{,}160\,\text{lbf}$$
$$Y = 55{,}000\,\text{psi}$$
$$A_{\text{t}} = 0.25\pi\left(13.375^2 - 12.615^2\right) = 15.513\,\text{in}^2$$

Substituting into Equation (4.11)

$$k_{\text{clps}} = \sqrt{1 - \frac{3}{4}\left(\frac{F}{A_{\text{t}}Y}\right)^2} - \frac{1}{2}\left(\frac{F}{A_{\text{t}}Y}\right)$$
$$= \sqrt{1 - \frac{3}{4}\left(\frac{37160}{15.513\,(55000)}\right)^2} - \frac{1}{2}\left(\frac{37160}{15.513\,(55000)}\right)$$
$$= 0.9775$$

Now we calculate the reduced collapse strength of the casing:

$$\tilde{p}_{\text{clps}} = 0.9775\,(1130) = 1105\,\text{psi}$$

Obviously now our setting depth of 2100 ft for the top section will not meet our design requirements. What we require is a design margin factor of 1.00 or higher (recall $k_{\text{M}} = \tilde{p}_{\text{clps}}/(k_{\text{D}}\Delta p)$. In our case, $k_{\text{D}}\Delta p = 1130$ from our design line, and

$$k_{\text{M}} = \frac{1105}{1130} = 0.98 < 1.00$$

So to meet our design requirements for collapse we will have to adjust our selection by moving the bottom of the 54.5 lb/ft section to a shallower depth to reduce the collapse load on the bottom of the section. For this example, we will move the bottom of the section up to 2000 ft. This is just a guess, and we will examine a better method later. At 2000 ft our collapse design load is 1080 psi. But something else occurs when we make this adjustment; we reduced the collapse load, but we had to lengthen the bottom section and the result is an increase in tension. This is the nature of the process. We must also recalculate the axial load for the change, and this is where a spreadsheet or some other program can be very useful. We are not going to show the calculations, but the axial tension at 2000 ft is 43,770 lbf and

$$k_{\text{clps}} = \sqrt{1 - \frac{3}{4}\left(\frac{43770}{15.513\,(55000)}\right)^2} - \frac{1}{2}\left(\frac{43770}{15.513\,(55000)}\right)$$
$$= 0.9734$$

The increased tension reduces the collapse rating a bit more.

$$\tilde{p}_{\text{clps}} = 0.9734\,(1130) = 1100\,\text{psi}$$

but

$$k_{\text{M}} = \frac{1100}{1080} = 1.02 > 1.00$$

Our adjustment was successful.

You may question why we used the collapse design load and the axial load rather than the axial design load. Keep in mind that we are working with the collapse design in this process. The axial design load applies only to the axial design, and is not relevant to the collapse design.

4.7 Example well

In this section, we will finalize our basic casing design for all four of our example strings. We used the surface string as an example throughout this chapter so we will not repeat those calculations, but we will do the conductor, intermediate, and production strings through the entire sequence.

4.7.1 Conductor casing example

From the previous chapter we determined that our maximum collapse load might be as high as 70 psi and possibly 80 psi. The worst burst load we estimated to be about 150 psi. The lowest grade of 20 in. API line pipe is Schedule 10 grade A with a 0.25 in. wall thickness. It is pressure tested to 600 psi so it is more than adequate for burst. API does not give a collapse rating for line pipe, but we can calculate it from API formulas (in Chapter 6) and it is 94 psi. This gives us a design factor of 1.18 which should

be sufficient. But since there is considerable uncertainty in our loading we might opt for a Schedule 20 grade A with a calculated collapse pressure of 320 psi. If we consider casing instead of line pipe, the lightest API 20 in. casing is 94 lb/ft H-40 which has a collapse rating of 520 psi. For some operators, this might be preferable to line pipe.

4.7.2 Surface casing example

We have used our surface casing as an example so far in this chapter and will not repeat those calculations here, but we will now calculate the design margins for this string.

Surface Casing—Design Margin Factors

Recall that we defined the design margin as the strength of the actual casing selected divided by the design load ($k_D \cdot$ Load). The actual loads were not necessarily calculated at all the depths that we need to check, but we can either get the values from our load plots or we may easily calculate them from the calculated end points using a linear interpolation since our load lines are all linear. Remember too that we adjusted the section depths for combined collapse and tension so the depth of the top section is not the same as our initial selection. Here I have calculated the load values rather than try to read them from the load plots. We will begin with the collapse design and show the calculation results in a tabular form (Table 4.5).

The depths listed in the table are at the bottom of each section where the maximum collapse loading occurs. Next we calculate the design margins for burst (Table 4.6). In these calculations the largest burst load is at the top of each section so the depths in our table will be at the top of each section, rather than at the bottom as in the collapse loading.

Finally, we calculate the axial design margin (Table 4.7). Here too, the maximum axial load is at the top of each section and in this example the over-pull margin was greater than the design factor at both points.

This completes our basic surface casing design. We have designed for collapse, burst and axial loading. Additionally we have accounted for a reduction in collapse resistance caused by tension. The final design is summarized in Table 4.8.

Table 4.5 Surface Casing Collapse Design Margin Factors

Section	Depth (ft)	Strength (psi)	Load (psi)	k_D	Design (psi)	k_M
2	2000	1130	960	1.125	1080	1.05
1	3000	1950	1440	1.125	1620	1.20

Table 4.6 Surface Casing Burst Design Margin Factors

Section	Depth (ft)	Strength (psi)	Load (psi)	k_D	Design (psi)	k_M
2	0	2730	1820	1.125	2050	1.33
1	2000	3450	800	1.125	900	3.83

Table 4.7 Surface Casing Axial Design Margin Factors

Section	Depth (ft)	Strength (klbf)	Load (klbf)	k_D or Over-pull	Design (klbf)	k_M
2	0	547	209	100	309	1.77
1	2000	718	93	100	193	3.72

Table 4.8 Example 13-3/8 in. Surface Casing Design Summary

Section	Depth (ft)	ID (in.)	Wt. (lb/ft)	Grade	Conn.	Design Margin, k_M		
						Clps	Brst	Axial
2	2000	12.615	54.5	K-55	ST&C	1.05	1.33	1.77
1	3000	12.415	68	K-55	ST&C	1.20	3.83	3.72

Mud density: 1.11 SG.
Design factors, k_D: 1.125 (clps and brst), 1.6 or 100,000 OP (axial).

4.7.3 Intermediate casing example

We follow exactly the same procedure here as with the surface casing. For this example, we will use the following design factors:

- Collapse: 1.125
- Burst: 1.20
- Axial: 1.6 or 100,000 lbf over-pull (whichever is greater)

Intermediate casing example—collapse and burst design loads

From the pressure loads we calculated in Chapter 3, we will now apply the design factors for collapse and burst to give us the pressure design loads.

Intermediate Casing Example—Collapse Design Load

From Chapter 3 the collapse pressures for the intermediate casing are:

$$\Delta p_0 = 0$$

$$\Delta p_{10500} = 1910\,\text{psi}$$

Applying the design factor, $k_D = 1.125$, we calculate the collapse design load at the shoe as

$$\Delta p_{10500} = 1.125\,(1910) = 2150\,\text{psi}$$

We plot the collapse design in Figure 4.11.

Intermediate Casing Example—Burst Design Load

Again referring to the pressure loads calculated in Chapter 3 the burst loads are:

$$\Delta p_0 = 7210\,\text{psi}$$

$$\Delta p_{10500} = 4020\,\text{psi}$$

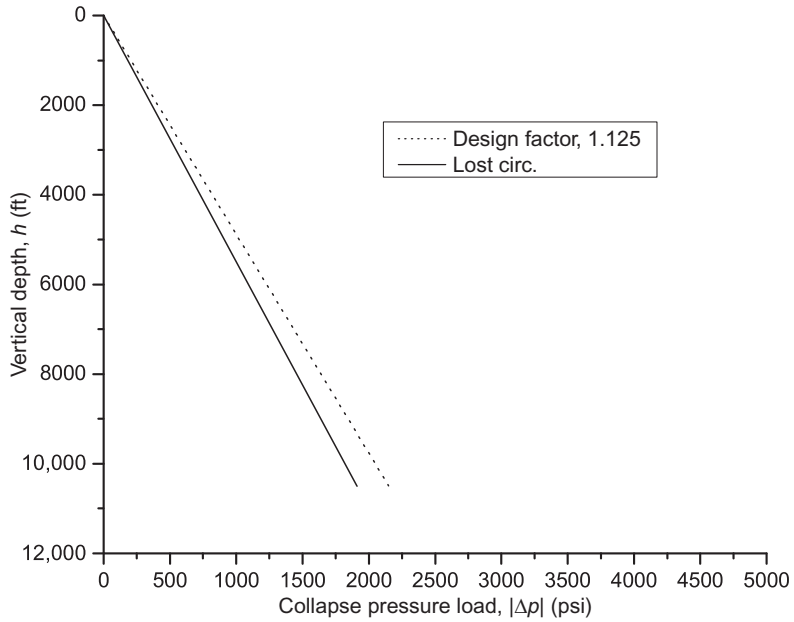

Figure 4.11 Collapse design load for intermediate casing example.

The design burst load is then

$$\Delta p_0 = 1.20\,(7210) \approx 8650\,\text{psi}$$
$$\Delta p_{10500} = 1.20\,(4020) \approx 4820\,\text{psi}$$

Figure 4.12 is a plot of the intermediate casing burst design load.

Intermediate casing example—preliminary selection

We assume that we have available the 9-5/8 in. casing of Table 4.9 in our inventory for use in this well.

Note that, since we elected to drill an 8-1/2 in. hole from the bottom of the intermediate casing to total depth, we may have a problem with some of the casing in this inventory. If we use any 53.5 lb/ft casing in the intermediate string, it must be specially drifted for an 8-1/2 in. bit. The 58.4 lb/ft casing cannot be used at all unless we use a smaller bit, and we do not consider that an option for our well.

In a precursory examination of the available pipe and the loads, we can see almost immediately that the collapse loading is very small, and the weakest pipe in our inventory easily could sustain the maximum collapse load. We also note that the burst load is relatively high and the first three items in our inventory will not even sustain the burst load at the bottom of the string, where the burst load is the lowest. Therefore, it looks like the best place to start the selection is with the burst design, and that is fairly typical of intermediate strings run to protect lower-pressured formations from higher pressures below. In the cases where the intermediate casing is run to protect low-pressure formations below, we would probably start with the collapse selection first. Again, it really makes no difference whether we

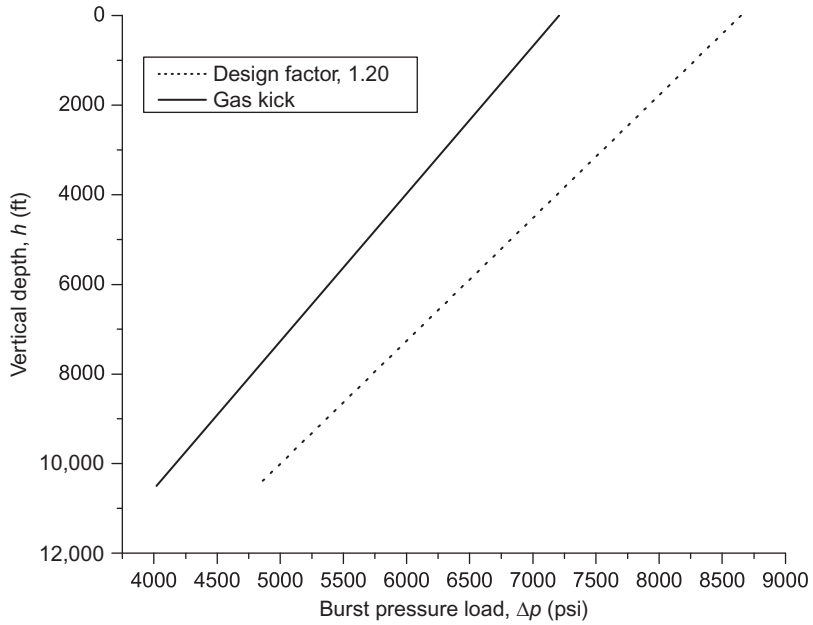

Figure 4.12 Burst design load for intermediate casing example.

Table 4.9 Available 9-5/8 in. Casing for the Intermediate Casing Example

Wt. (lb/ft)	Grade	Conn.	ID (in.)	Drift (in.)	Clps Press (psi)	Int Yld (psi)	Jt Strength (klbf)
36	K-55	ST&C	8.921	8.765	2020	3520	423
40	K-55	ST&C	8.835	8.679	2570	3950	486
40	K-55	LT&C	8.835	8.679	2570	3950	561
40	N-80	LT&C	8.835	8.679	3090	5750	737
43.5	N-80	LT&C	8.755	8.599	3810	6330	825
47	N-80	LT&C	8.681	8.525	4750	6870	905
53.5	N-80	LT&C	8.535[a]	8.379	6620	7930	1062
58.4	N-80	LT&C	8.435[b]	8.279	7890	8650	1167
43.5	P-110	LT&C	8.755	8.599	4420	8700	1105
47	P-110	LT&C	8.681	8.525	5300	9440	1213
53.5	P-110	LT&C	8.535[a]	8.379	7950	10,900	1422

[a]Drift ID is less than bit diameter.
[b]Nominal ID is less than bit diameter.

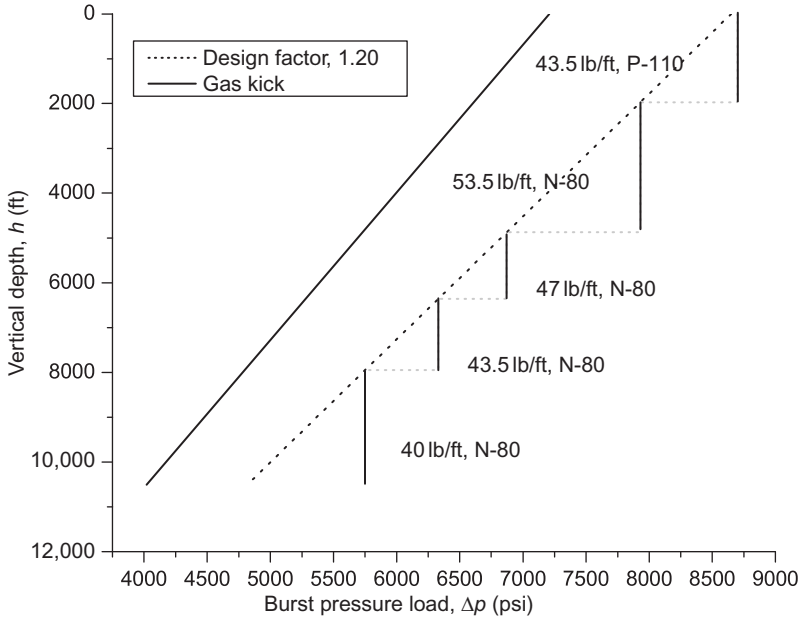

Figure 4.13 Preliminary selection for burst for intermediate casing example.

start with the collapse or burst selection, but if we start with the most critical one first it usually results in less revision.

Intermediate Casing Example—Burst Selection

We start our burst selection at the top of the string and plot the various sections as to their burst ratings onto the design plot, see Figure 4.13.

While the selection process was done graphically in that figure, you should also understand how it is done with calculations. Most of the depths and pressures I use in this and other examples are calculated rather than read from the small graphs used as illustrations in this text.[4] The calculations are easy to do since our design load lines are linear. The only precaution I would advise, is to be careful about roundoff if you do this manually. It is easy to accumulate roundoff errors such that when you calculate your design margin later, it may be slightly less than 1.00 at some critical points. A spreadsheet does not roundoff internally to the same degree, but only in the displayed results, hence it may give different answers from manual calculations rounded off at each step.

Calculating Burst Selection Depths

The burst pressures are:

$$\Delta p_0 = 8650\,\text{psi}$$
$$\Delta p_{10500} = 4820\,\text{psi}$$

[4] Full-size graphs on sheets such as 8.5 × 11 in. or A-4 are read with sufficient accuracy, but not these small versions, so I have calculated the values to keep the examples more accurate for our purposes.

Calculate pressure gradient:

$$\gamma = \frac{\Delta p}{\Delta h} = \frac{4820 - 8650}{10500 - 0} = -0.36476\,\text{psi/ft}$$

The pressure, p, at any depth, h, may be calculated from the linear equation

$$p = p_0 + \gamma h \tag{4.12}$$

In our application for selecting depths for particular types of casing where p is the burst pressure rating of the pipe, p_{brst}, we rearrange Equation (4.12) to calculate the depth at which the design pressure is equal to the burst pressure rating of the casing:

$$h = \frac{1}{\gamma}(p_{\text{brst}} - p_0) \tag{4.13}$$

For our example, we will set this up in tabular form as you can easily do with a spreadsheet to do any number of these calculations (see Table 4.10).

In this selection, we selected some 40 lb/ft N-80, 43.5 lb/ft N-80, 47 lb/ft N-80, and 53.5 lb/ft N-80, and 43.5 lb/ft P-110 casing in the string (refer back to Figure 4.13). This might constitute an optimum design from an engineering point of view, but do we really want to run something like this in our well? There is also a problem with this selection in that the drift diameter is less than the 8-1/2" bits we plan to use in drilling below it. So if we stay with this selection, the 53.5 lb/ft pipe must be specially drifted to be sure that an 8-1/2 in. bit will pass through it. What if it will not pass through enough pipe in our inventory to fill out this section? We would then extend the 43.5 lb/ft P-110 from top to 5200 ft. And that brings up another point. If this well is in a hard rock area, where we will be drilling for a long time below the intermediate casing, do we think that the 43.5 lb/ft pipe has enough wall thickness to sustain the wear caused by the rotating tool joints and still maintain sufficient burst resistance. This is not an easy question to answer, but is quite typical, because wear often is a problem with intermediate strings, and the worst wear often occurs nearer the surface than further down-hole. We discuss wear later in Chapter 7 and bring it up at this point only because this is the kind of question that often arises with intermediate casing.

There are a number of alternatives to this selection that would simplify the string considerably and reduce the chances for errors on location in running a string with five different sections. A simple alternative is to run only 43.5 lb/ft casing giving us a single wall thickness in our string. We initially

Table 4.10 Calculated Tops of Intermediate Casing for Burst

Casing	Internal Yield, p_{brst} (psi)	Section Top, h (ft)[a]
9-5/8 43.5 lb/ft P-110	8700	-
9-5/8 53.5 lb/ft N-80	7930	1974
9-5/8 47 lb/ft N-80	6870	4880
9-5/8 43.5 lb/ft N-80	6330	6360
9-5/8 40 lb/ft N-80	5750	7950

[a] $h = (p_{\text{brst}} - p_0)/\gamma = (p_{\text{brst}} - 8650)/(-0.36476)$.

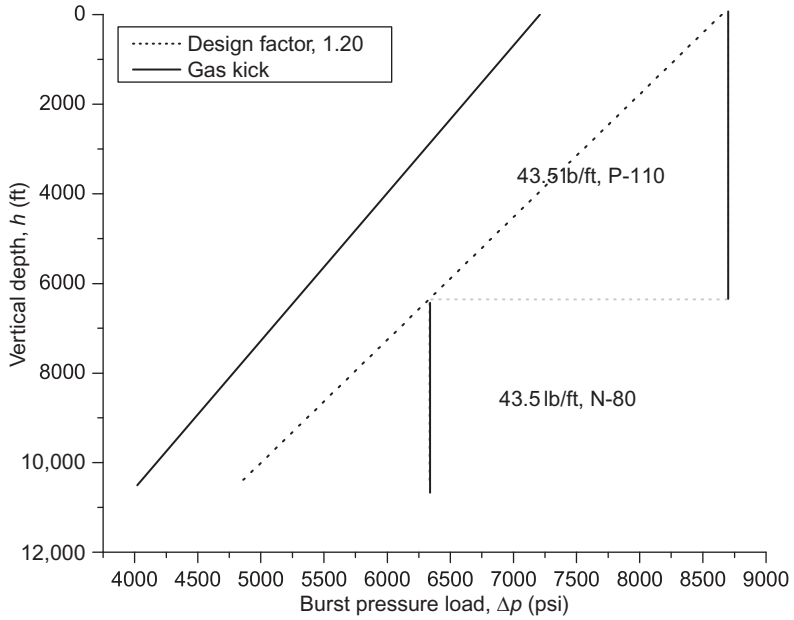

Figure 4.14 Alternate preliminary burst selection for intermediate casing example.

assumed that this well is being drilled in soft formations and we will only drill 3500 ft below this casing string. It should drill fairly rapidly, but always keep in mind the caveat about wear we mentioned above when making a choice like this. The simpler selection is shown in Figure 4.14.

A quick check shows that all the casing we selected easily exceeds the collapse design requirements, so we will not plot that.

Intermediate casing—axial load

Now that we have our preliminary intermediate casing selection, we can calculate the axial loads. This is greatly simplified in this case because even though we have two sections, they both have the same wall thickness.

Preliminary Axial Calculations

$$A_0 = (\pi/4)\,(9.625)^2 = 72.760\,\text{in}^2$$

$$A_1 = (\pi/4)\,(8.755)^2 = 60.201\,\text{in}^2$$

$$W_1 = w_1\,L_1 = 43.5\,(10500) = 456{,}750\,\text{lbf}$$

Installation—Axial Running Case

Calculate the pressure inside and outside the shoe.

$p_0 = 0.052\,(1.42)\,(8.33)\,(10500) = 6458\,\text{psi}$

$p_1 = p_0 = 6458\,\text{psi}$

Calculate the sectional forces.

$F_1^{\downarrow} = -p_0 A_0 + p_1 A_1 = 6458\,(60.201 - 72.760) = -81{,}110\,\text{lbf}$

$F_1^{\uparrow} = F_1^{\downarrow} + W_1 = -81110 + 456750 = 375{,}640\,\text{lbf}$

Installation—Axial Plug-Bump Case

Calculate the annular cement pressure and the internal pressure at the shoe.

$p_0 = 0.052\,(8.33)\,[(1.91)\,(1000) + (1.44)\,(9500)] = 6753\,\text{psi}$

$p_1 = 6753 + 1000 = 7753\,\text{psi}$

Calculate the sectional forces.

$F_1^{\downarrow} = -p_0 A_0 + p_1 A_1 = -6753\,(72.760) + 7753\,(60.201)$

$= -24{,}610\,\text{lbf}$

$F_1^{\uparrow} = F_1^{\downarrow} + W_1 = -24610 + 456750 = 432{,}140\,\text{lbf}$

The plug-bump load is obviously the greater, so we will plot it and use our design factor of 1.6 and an over-pull to get the axial design load, see Figure 4.15.

Next we check to see hour preliminary burst selection compares to our tension design in Figure 4.16. We can see that it easily satisfies the axial load requirements.

Intermediate casing—combined load adjustments

We now check our intermediate string to see if any adjustments are required for combined loading. Referring to Figure 4.17 we see that the collapse values are far exceeded by the casing collapse ratings, so there is no need for a tension/collapse check on the intermediate string.

Intermediate casing—design margin factors

Recall that we defined the design margin as the strength of the actual casing selected divided by the design load ($k_D \cdot$ Load). The actual loads were not necessarily calculated at all depths that we need to check, but we can either get the values from our load plots or we may easily calculate them from the calculated end points using a linear interpolation since our load lines are all linear. Here I have calculated the load values rather than try to read them from the load plots.

The depths listed in Table 4.11 are at the bottom of each section where the maximum collapse loading occurs. Next we calculate the design margins for burst (Table 4.12). In these calculations the largest burst load is at the top of each section so the depths in our table will be at the top of each section, rather than at the bottom in the collapse loading.

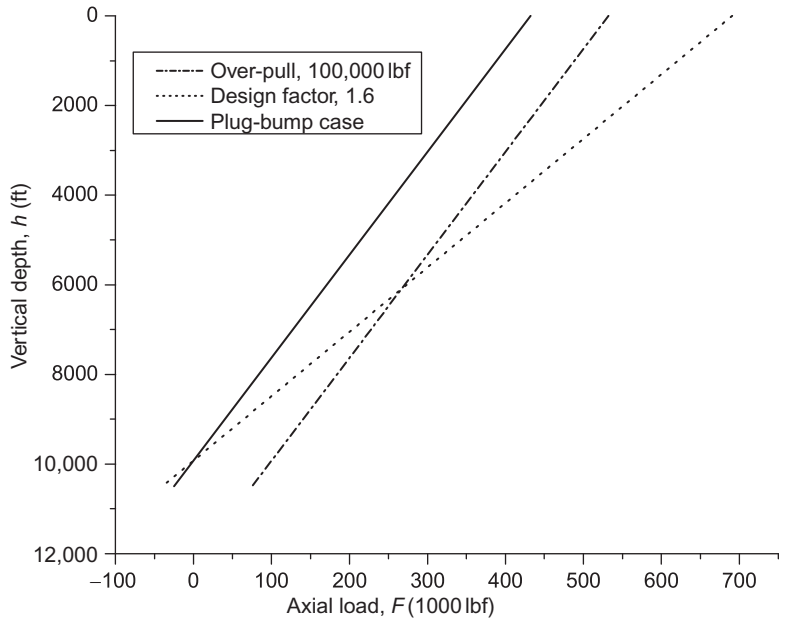

Figure 4.15 Axial design loads for intermediate casing example.

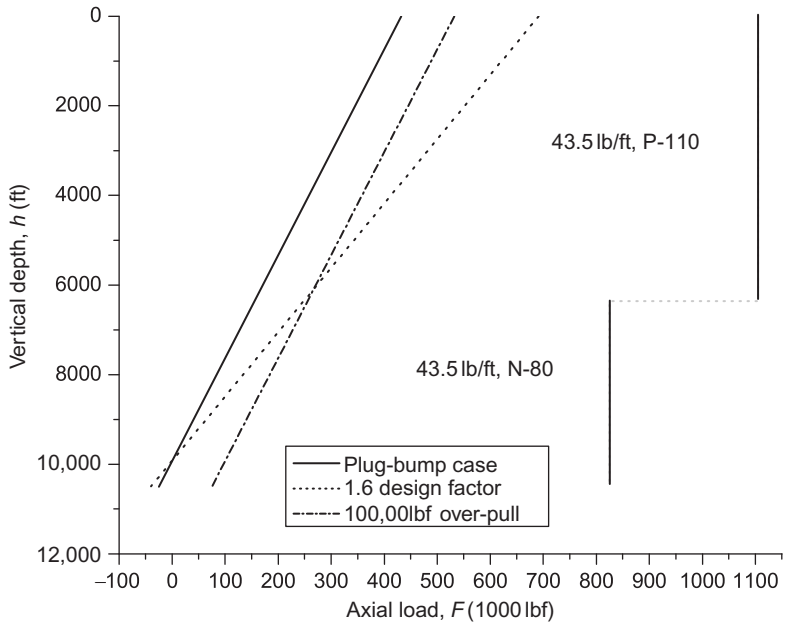

Figure 4.16 Preliminary selection, axial strength for intermediate casing example.

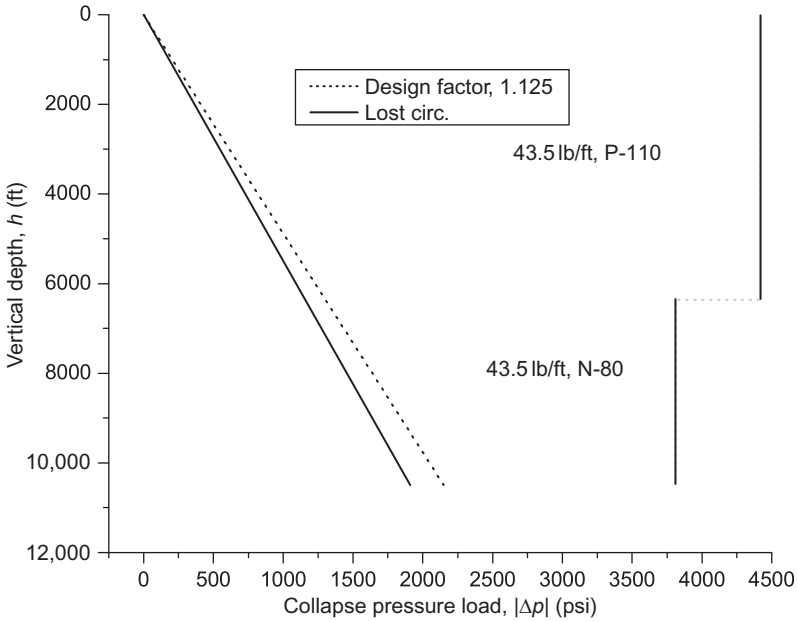

Figure 4.17 Preliminary selection, collapse strength for intermediate casing example.

Table 4.11 Intermediate Casing Collapse Design Margin Factors

Section	Depth (ft)	Strength (psi)	Load (psi)	k_D	Design (psi)	k_M
2	6360	4420	1157	1.125	1300	3.40
1	10,500	3810	1910	1.125	2150	1.77

Table 4.12 Intermediate Casing Burst Design Margin Factors

Section	Depth (ft)	Strength (psi)	Load (psi)	k_D	Design (psi)	k_M
2	0	8700	7210	1.20	8650	1.01
1	6360	6330	5278	1.20	6330	1.00

Finally we calculate the axial design margin (Table 4.13). Here too, the maximum axial load is at the top of each section and in this example the over-pull margin was greater than the design factor at both points.

This completes our basic intermediate casing design. We made our preliminary selection based on the burst design load, and that selection also satisfies the collapse and axial design loads. Additionally

Table 4.13 Intermediate Casing Axial Design Margin Factors

Section	Depth (ft)	Strength (klbf)	Load (klbf)	k_D or Over-pull	Design (klbf)	k_M
2	0	1105	427	100	527	2.10
1	6360	825	150	100	250	3.30

Table 4.14 Example 9-5/8 in. Intermediate Casing Design Summary

Section	Depth (ft)	ID (in.)	Wt. (lb/ft)	Grade	Conn.	Design Margin, k_M		
						Clps	Brst	Axial
2	6360	8.755	43.5	P-110	LT&C	3.40	1.01	2.10
1	10,500	8.755	43.5	N-80	LT&C	1.77	1.00	3.30

Mud density: 1.42 SG.
Design factors, k_D: 1.125 clps, 1.20 brst, 1.6 or 100,000 OP (axial).

we found that no correction for a reduction in collapse resistance caused by tension was necessary. The final design is summarized in Table 4.14.

4.7.4 Production casing example

Finally, we come to the production casing, which is the last casing string in our example. We expect that it should be capable of containing full well pressure throughout the producing life of the well. It should not collapse if the well becomes depleted significantly or during any operations conducted in the wellbore during work overs or stimulations. For the 7 in. production casing at 14,000 ft, we use the following design factors:

- Collapse: 1.125
- Burst: 1.20
- Axial: 1.6 or 100,000 lbf over-pull

We apply the collapse design factor to our collapse load to get the collapse design

$$\Delta p_{14000} = 1.125\,(11160) \approx 12{,}560\,\text{psi}$$

and plot the results on our load plot, Figure 4.18

Then the burst design:

$$\Delta p_0 = 1.2\,(8660) \approx 10{,}390\,\text{psi}$$

$$\Delta p_{14000} = 1.2\,(4730) \approx 5680\,\text{psi}$$

which is plotted in Figure 4.19:

Note that we did not use the burst load plot we generated assuming a near surface tubing leak. In practice, we might have chosen that load plot, even though it is not common practice in most designs. We should also note that the inventory of available casing will not suffice for that load case, and we

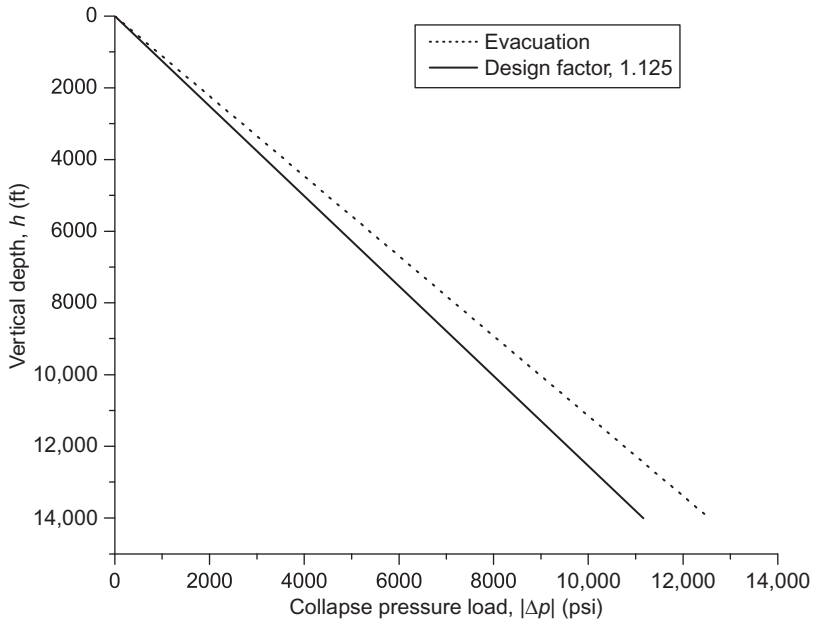

Figure 4.18 Collapse design load for example production casing.

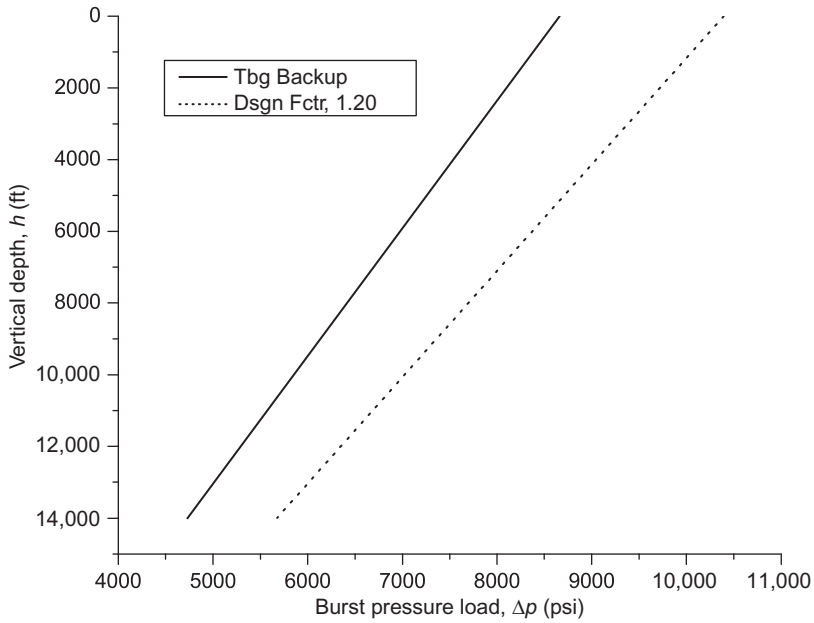

Figure 4.19 Burst design load for example production casing.

Table 4.15 Available 7 in. Casing for the Production Casing Example

Wt. (lb/ft)	Grade	Conn.	ID (in.)	Drift (in.)	Clps Press (psi)	Int Yld (psi)	Jt Strength (klbf)
26	N-80	LT & C	6.276	6.151	5410	7240	519
29	N-80	LT & C	6.184	6.059	7030	8160	597
32	N-80	LT & C	6.094	5.969	8600	9060	672
35	N-80	LT & C	6.004	5.879	10,180	9240	746
38	N-80	LT & C	5.920	5.795	11,390	9240	814
26	P-110	LT & C	6.276	6.151	6230	9960	693
29	P-110	LT & C	6.184	6.059	8530	11,220	797
32	P-110	LT & C	6.094	5.969	10,780	12,460	897
35	P-110	LT & C	6.004	5.879	13,030	12,700	996

would have to opt for higher strength casing with proprietary connections. Given an adequate inventory for selection the design is quite simple. However, we do not choose that load case here because some very important points in this example would not be illustrated had we done so, and the purpose of this example is to illustrate as many points as possible.

Now that we generated the design plots for collapse and burst it is time to begin selecting specific casing for the example well.

Table 4.15 shows the 7 in. casing available to us for this production string.

We will start with the collapse load for the evacuated production string. We know that the burst design load will require higher pressures near the surface, so we stop our collapse selection at about the halfway point. This selection shown in Figure 4.20 will meet our collapse design requirements.

We then continue with the burst selection by plotting the preliminary selection for collapse with the burst design curves (plotting the burst strengths now) and continuing with the upper portion to meet the burst design requirements. Figure 4.21 shows the results. Though this might be the lowest cost selection (in some cases), it is not a good design as it contains too many sections. We see that there is a section of 29 lb/ft pipe in the middle of the section that should definitely be eliminated. The modified selection is shown in Figure 4.22. In practice we might want to simplify this design further, but we are going to leave it as it is so that we can see how to deal with the combined collapse and tensile loads.

Production casing example—axial loads

Next we check the axial loading for the various cases (Figure 4.23).

- Installation—running
  - Inside: mud, 1.84 SG
  - Outside: mud, 1.84 SG
- Installation—plug bump
  - Inside: 1.20 SG + 1200 psi above differential displacement pressure
  - Outside: tail slurry 1.99 SG (1000 ft + 25%), lead slurry 1.91 SG (3000 ft + 35%), spacer and mud 1.84 SG

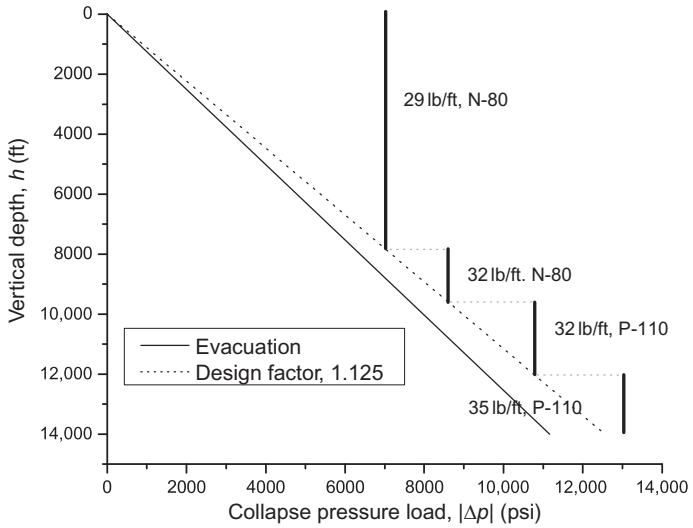

Figure 4.20 Preliminary selection based on collapse design for example production casing.

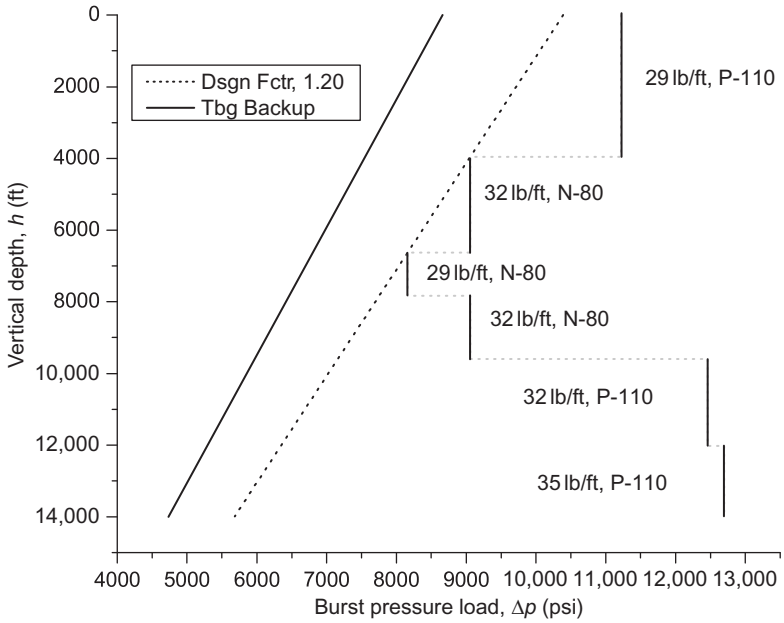

Figure 4.21 Preliminary selection for burst and collapse designs for example production casing.

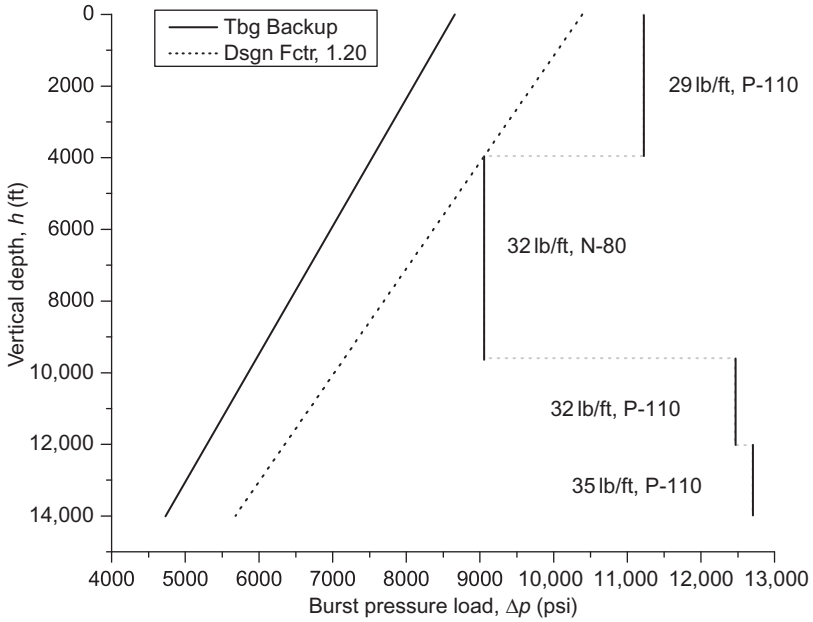

Figure 4.22 Alternate burst and collapse preliminary selection for example production casing.

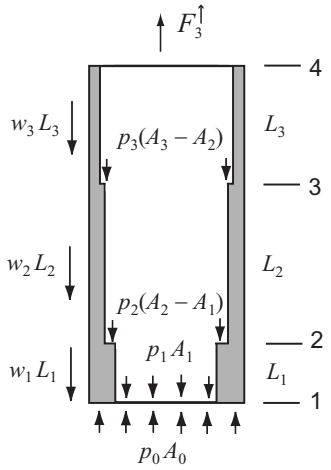

Figure 4.23 Axial schematic for example production string.

Preliminary Calculations

- Cross-sectional areas

$A_0 = (\pi/4)\,(7.000)^2 = 38.485\,\text{in}^2$

$A_1 = (\pi/4)\,(6.004)^2 = 28.312\,\text{in}^2$

$A_2 = (\pi/4)\,(6.094)^2 = 29.167\,\text{in}^2$

$A_3 = (\pi/4)\,(6.184)^2 = 30.035\,\text{in}^2$

- Section weights

$W_1 = w_1 L_1 = 35\,(1979) = 69,265\,\text{lbf}$

$W_2 = w_2 L_2 = 32\,(8067) = 258,144\,\text{lbf}$

$W_3 = w_3 L_3 = 29\,(3954) = 114,666\,\text{lbf}$

Running Case

- Calculate pressures

$p_0 = p_1 = 0.052\,(1.84)\,(8.33)\,(14000) = 11{,}158\,\text{psi}$

$p_2 = 0.052\,(1.84)\,(8.33)\,(12021) = 9581\,\text{psi}$

$p_3 = 0.052\,(1.84)\,(8.33)\,(3954) = 3151\,\text{psi}$

- Calculate section forces

$$F_1^{\downarrow} = -p_0 A_0 + p_1 A_1 = 11158\,(-38.485 + 28.312)$$
$$= -113{,}510\,\text{lbf}$$

$$F_1^{\uparrow} = F_1^{\downarrow} + W_1 = -113510 + 69265 = -44,245\,\text{lbf}$$

$$F_2^{\downarrow} = F_1^{\uparrow} + p_2\,(A_2 - A_1) = -44245 +$$
$$9581\,(29.167 - 28.312)$$
$$= -36{,}053\,\text{lbf}$$

$$F_2^{\uparrow} = F_2^{\downarrow} + W_2 = -36053 + 258144 = 222{,}091\,\text{lbf}$$

$$F_3^{\downarrow} = F_2^{\uparrow} + p_3\,(A_3 - A_2) = 222091 +$$
$$3151\,(30.035 - 29.167)$$
$$= 224{,}826\,\text{lbf}$$

$$F_3^{\uparrow} = F_3^{\downarrow} + W_3 = 224826 + 114666 = 339{,}492\,\text{lbf}$$

Plug-Bump Case

- Calculate pressures

$$p_0 = 0.052\,(8.33)\,[(1.99)\,(1250) + (1.87)\,(3750) + (1.84)\,(9000)]$$
$$= 11{,}288\,\text{psi}$$
$$p_1 = 11{,}288 + 1200 = 12{,}488\,\text{psi}$$
$$p_2 = 12488 - 0.052\,(8.33)\,(1.20)\,(14000 - 12021)$$
$$= 11{,}459\,\text{psi}$$
$$p_3 = 12488 - 0.052\,(8.33)\,(1.20)\,(14000 - 3954)$$
$$= 7266\,\text{psi}$$

- Calculate section forces

$$F_1^{\downarrow} = -p_0 A_0 + p_1 A_1 = -11288\,(38.485) + 12488\,(28.312)$$
$$= -80{,}858\,\text{lbf}$$
$$F_1^{\uparrow} = F_1^{\downarrow} + W_1 = -80858 + 69265 = -11{,}593\,\text{lbf}$$
$$F_2^{\downarrow} = F_1^{\uparrow} + p_2\,(A_2 - A_1) = -11593 + 11459\,(29.167 - 28.312)$$
$$= -1796\,\text{lbf}$$
$$F_2^{\uparrow} = F_2^{\downarrow} + W_2 = -1796 + 258144 = 256{,}348\,\text{lbf}$$
$$F_3^{\downarrow} = F_2^{\uparrow} + p_3\,(A_3 - A_2) = 256348 + 7266\,(30.035 - 29.167)$$
$$= 262{,}655\,\text{lbf}$$
$$F_3^{\uparrow} = F_3^{\downarrow} + W_3 = 262655 + 114666 = 377{,}321\,\text{lbf}$$

The plug-bump load is the highest (Figure 4.24) so we will apply the design factors to it and then check our burst/collapse selection to see if it is adequate in axial load design.

For the production casing example, we use the true axial load in the plug-bump stage in 1.82 SG mud and a design factor of 1.6 or 100,000 lbf over-pull. Then we plot these on in Figure 4.25 for designing the tension.

As can be seen in Figure 4.26, we are fortunate that the string we selected for collapse and burst also meets the design load for tension. While this is often the case with higher pressures, the general case is that deeper wells with lower pressures require adjustment of the preliminary selection for tension. This selection is adequate as is. Now we will check the effect of the axial loads on collapse.

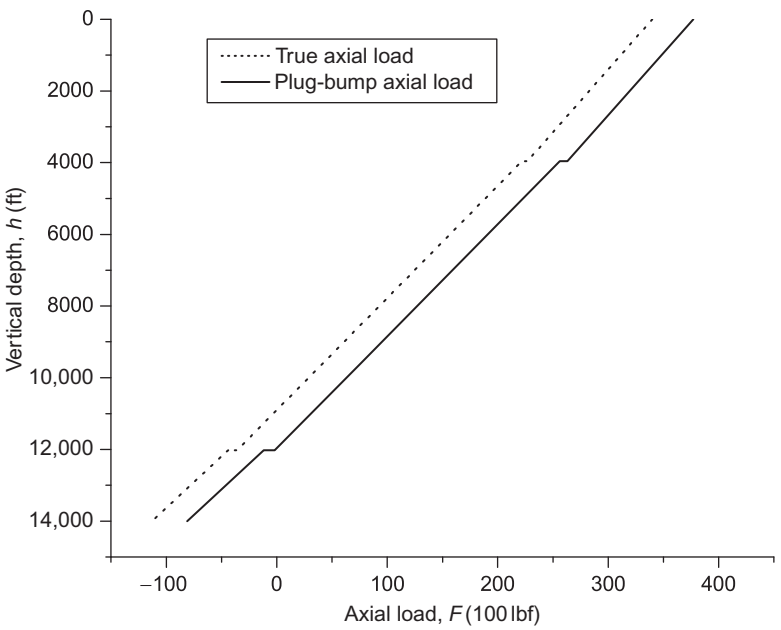

Figure 4.24 Axial loads for example production casing.

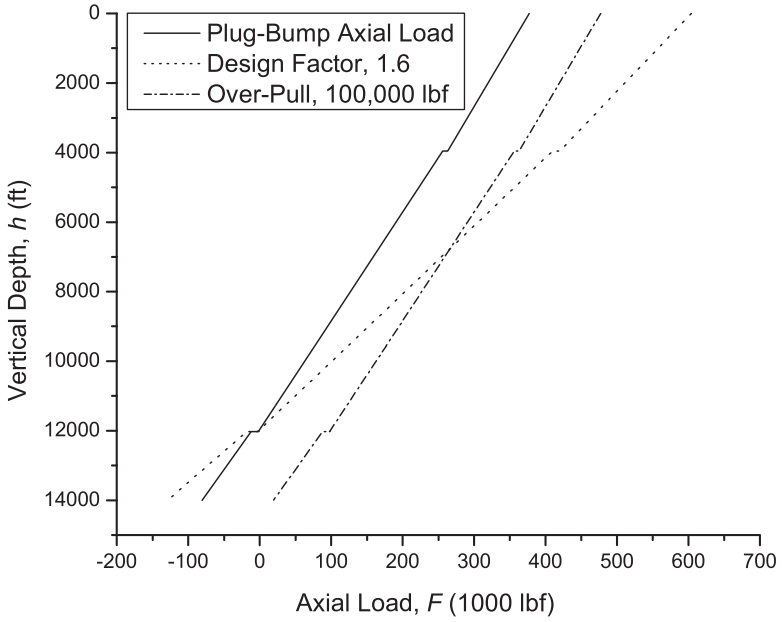

Figure 4.25 Axial design load for example production casing.

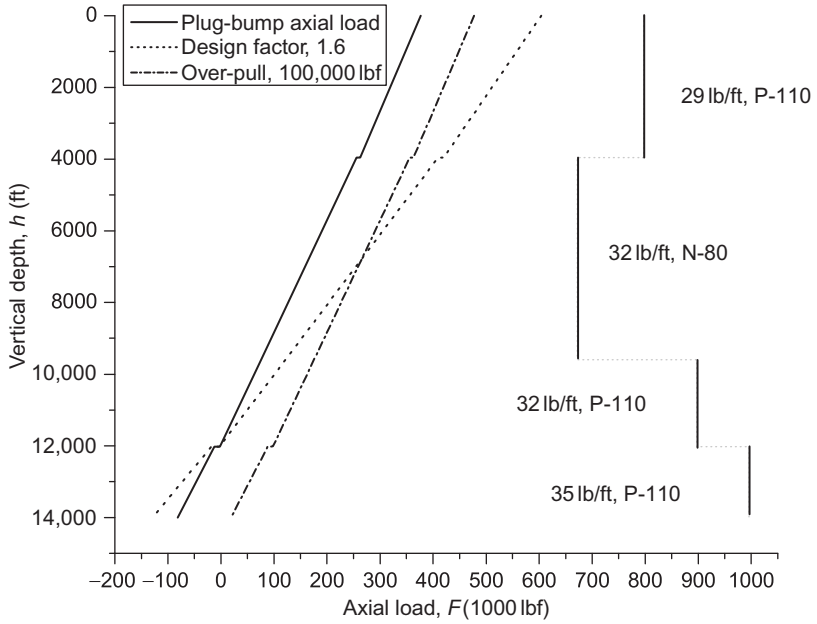

Figure 4.26 Preliminary selection axial strength and axial design for example production casing.

Production casing—combined loading

Examining our collapse design plot with the casing selection (Figure 4.20), we see that there are possibly two critical points (where the casing collapse rating intercepts the design line). These occur at 12,021 ft and 9590 ft. At 12,021 ft the casing is actually in axial compression. This will tend to increase the collapse resistance (though we seldom make any adjustments for that since it is a benefit). At 9590 ft, however, there is a tensile load of 41,739 lbf. and the collapse design load is 8600 psi While we could read an adequate value from a large size plot, this value was calculated from the slope of the load curve for this example, rather than read from the small plot in this text. We employ the same simple formula used for the surface casing (Equation (4.11)) to calculate the reduced collapse value.

$$k_{\text{clps}} = \sqrt{1 - \frac{3}{4}\left(\frac{F}{A_{\text{t}}\,Y}\right)^2} - \frac{1}{2}\left(\frac{F}{A_{\text{t}}Y}\right)$$

$$= \sqrt{1 - \frac{3}{4}\left(\frac{41739}{9.317\,(80000)}\right)^2} - \frac{1}{2}\left(\frac{41739}{9.317\,(80000)}\right) = 0.971$$

The reduced collapse rating of the 32 lb/ft N-80 section is

$$\tilde{p}_{\text{clps}} = k_{\text{clps}}\, p_{\text{clps}} = 0.971\,(8600) = 8351 \text{ psi}$$

and the design margin is

$$k_{\text{M}} = \frac{8351}{8600} = 0.971 < 1.00$$

which requires that we adjust our collapse selection.

We will try what we did for the surface casing and raise the section bottom to 9500 ft. The tension value at 9500 ft will be greater than at 9590 ft, but we will not have to recalculate the axial load curve because both this section and the one below it have the same wall thickness so the axial load line will not change. And furthermore, the axial load gradient is 32 lbf/ft (the linear weight of the casing) so it is easy to calculate the tension value at any point in this section, $F = 41{,}379 + 32(90) = 44{,}619$ lbf. The collapse design load at 9500 ft is 8519 psi.

$$k_{\text{clps}} = \sqrt{1 - \frac{3}{4}\left(\frac{44619}{9.317\,(80000)}\right)^2} - \frac{1}{2}\left(\frac{44619}{9.317\,(80000)}\right) = 0.969$$

The reduced collapse rating of the 32 lb/ft N-80 section is

$$\tilde{p}_{\text{clps}} = k_{\text{clps}}\, p_{\text{clps}} = 0.969\,(8600) = 8333 \text{ psi}$$

and the design margin is

$$k_{\text{M}} = \frac{8333}{8519} = 0.978 < 1.00$$

which still does not meet our requirements.

We will try a 200 ft move this time so that the bottom of the N-80 section is at 9300 ft. The tension is 50,659 lbf and the collapse design load is 8340 psi.

$$k_{\text{clps}} = \sqrt{1 - \frac{3}{4}\left(\frac{50659}{9.317\,(80000)}\right)^2} - \frac{1}{2}\left(\frac{50659}{9.317\,(80000)}\right) = 0.964$$

The reduced collapse rating of the 32 lb/ft N-80 section is

$$\tilde{p}_{\text{clps}} = k_{\text{clps}}\, p_{\text{clps}} = 0.964\,(8600) = 8290\,\text{psi}$$

and the design margin is

$$k_{\text{M}} = \frac{8290}{8340} = 0.994 < 1.00$$

We are getting closer, but we are still not there. We can keep guessing and get close in a couple of more steps, but this is a tedious process, and we have enough data now that we can use a numerical iterative technique like a secant method, or we can use a graphical method.

Suppose we say our calculation process here is some function of the depth, h, that we will call $f(h)$, where if we select the correct value of h, then our design margin factor will be equal to 1.00. So we say $f(h) = 1.00$ or $f(h) - 1.00 = 0$. So we seek a depth, h, such that

$$y = f(h) - 1 = 0$$

We already have calculated three points (two would have sufficed) so let's stop and plot them.

$$y_1 = f(h_1) - 1 = f(9590) - 1.000 = 0.971 - 1.000 = -0.029$$

$$y_2 = f(h_2) - 1 = f(9500) - 1.000 = 0.978 - 1.000 = -0.022$$

$$y_3 = f(h_3) - 1 = f(9300) - 1.000 = 0.994 - 1.000 = -0.006$$

We plot these points and extrapolate to $y = 0$ and read the value of h that will satisfy our function. We can see in Figure 4.27. We see that a depth of 9220 ft should be the correct adjusted depth, so we will check it. At 9220 ft the tension is 53,219 lbf, and the collapse design load is 8269 psi.

$$k_{\text{clps}} = \sqrt{1 - \frac{3}{4}\left(\frac{53219}{9.317\,(80000)}\right)^2} - \frac{1}{2}\left(\frac{53219}{9.317\,(80000)}\right) = 0.962$$

The reduced collapse rating of the 32 lb/ft N-80 section is

$$\tilde{p}_{\text{clps}} = k_{\text{clps}}\, p_{\text{clps}} = 0.962\,(8600) = 8273\,\text{psi}$$

and the design margin is

$$k_{\text{M}} = \frac{8273}{8269} = 1.00$$

This interpolated depth is correct.

Production casing—design margin factors

Finally we calculate the design margin factors and summarize the results. Note that we did change the depth of the bottom of section 3 to account for the combined load effects.

The depths listed in Table 4.16 are at the bottom of each section where the maximum collapse loading occurs.

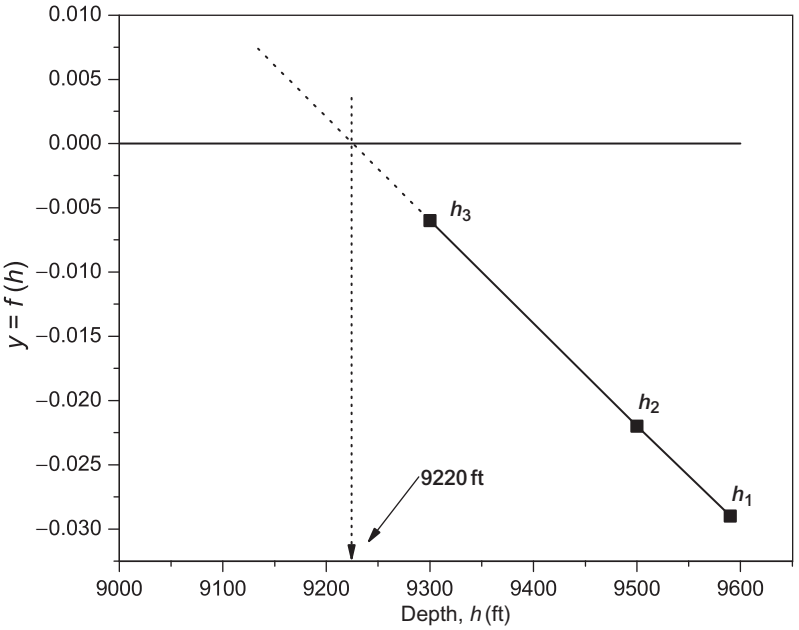

Figure 4.27 Collapse/tension interpolation.

Next, we calculate the design margins for burst. In these calculations the largest burst load is at the top of each section so the depths in Table 4.17 are at the top of each section, rather than at the bottom as in the collapse loading.

Finally, we calculate the axial design margin. Here too, the maximum axial load is at the top of each section, and in this example the over-pull margin was greater than the design factor at both points (see Table 4.18).

This completes our basic production casing design. We made our preliminary selection based on both the collapse and the burst design loads, and that selection also satisfies the axial design loads. Additionally we found it necessary to apply a correction for a reduction in collapse resistance caused by tension. The final design is summarized in Table 4.19. Remember that in this table, the collapse margin is calculated at the bottom of each section (the depth shown in the table), but the burst and axial margins

Table 4.16 Production Casing Collapse Design Margin Factors

Section	Depth (ft)	Strength (psi)	Load (psi)	k_D	Design (psi)	k_M
4	3954	8530	3152	1.125	3546	2.41
3	9220	8273[a]	7350	1.125	8269	1.00
2	12,021	10,780	9582	1.125	10,780	1.00
1	14,000	13,030	11,160	1.125	12,555	1.04

[a]Reduced collapse for tension.

Table 4.17 Production Casing Burst Design Margin Factors

Section	Depth (ft)	Strength (psi)	Load (psi)	k_D	Design (psi)	k_M
4	0	11220	8660	1.20	10,392	1.08
3	3954	9060	7550	1.20	9060	1.00
2	9220	12,460	6072	1.20	7286	1.71
1	12,021	12,700	5286	1.20	6340	2.00

Table 4.18 Production Casing Axial Design Margin Factors

Section	Depth (ft)	Strength (klbf)	Load (klbf)	k_D or Over-pull	Design (klbf)	k_M
4	0	797	377	1.6	603	1.32
3	3954	672	256	1.6	410	1.64
2	9220	897	89	100	189	4.75
1	12,021	996	−12	100	88	11.32

Table 4.19 Example 7 in. Production Casing Design Summary

Section	Depth (ft)	ID (in.)	Wt. (lb/ft)	Grade	Conn.	Design Margin, k_M		
						Clps	Brst	Axial
4	3954	6.184	29	P-110	LT&C	2.41	1.08	1.32
3	9220	6.094	32	N-80	LT&C	1.00	1.00	1.64
2	12,021	6.094	32	P-110	LT&C	1.00	1.71	4.75
1	14,000	6.004	35	P-110	LT&C	1.04	2.00	11.32

Mud density: 1.84 SG.
Design factors, k_D: 1.125 clps, 1.20 brst, 1.6 or 100,000 OP (axial).

are calculated at the top of each section (which is the bottom of the next higher section as shown in the depth column).

4.8 Additional considerations

Generally, cost is the overriding factor in deciding which type of casing to select when several types of casing satisfy the load requirements of the design. Obviously, we could select a string of some weight of P-110 grade pipe that might meet all our design criteria easily. However, the cost of such a string would far exceed that of a string made up of several weights of N-80, K-55, and even some P-110, if required. For the designs in this chapter, our basic premise was to try to select the lowest grade first,

then the lowest weight, because that is how costs tend to run. We also tended to stay away from the heaviest weight in any grade, since that usually is a special item, not readily available and often with too small an internal diameter to use common bit and tool sizes. Market costs vary considerably, and we do not attempt to put casing costs into our examples here, but in general, the lower the grade, the lower is the cost. The other thing that complicates the cost picture is the inventory status within a company and the availability of certain weights and grades. It may be more costly to purchase some K-55 casing than to use some N-80 already owned by the company or the company's partners in some joint venture. These considerations may override what we tend to call an optimum design based on a common scale of prices.

One important point that we have not discussed that should be mentioned here is the depth selections that appear in our designs. Casing does not come in lengths that are readily arranged to satisfy our exact design depths. Each section is always going to be a little shorter or longer than our design specifications. And to add to that uncertainty, the pipe as purchased is tallied in a pipe yard "threads-on" and usually with the protectors on also. Further the tally process is typically somewhat sloppy.[5] Once the pipe is on location, and tallied accurately, the rig supervisor is going to have to "fit" the pipe on location to the design. In all likely hood he or she will not have any idea as to whether it is better to make a particular section a little longer or a little shorter in length than the design. The truth is that it should be inconsequential, as long as the difference is not more than the length of a joint. But sometimes the measurement differences between what is shipped and what is on location require a bigger difference. We can alleviate this problem by adjusting our design to make it easier in the field, and here is where the design margin factors can help us. For example, look at our final design summary for the 7 in. production casing (Table 4.19) keeping in mind that the collapse design margin factor is calculated at the bottom of each section and the burst and axial design factors are calculated at the top of each section. We can see the bottom of section 2 has a design margin factor of 1.00 at its bottom at 12,021. We could easily raise the bottom of that section to an even 12,000 ft or even higher thus raising the margin a little and also giving the field supervisor a round number to aim for with the casing on location. But, if we raise the bottom of section 2 it will also raise the top of section 1. The burst and axial margins at the top of section 1 will then be reduced slightly, but they are 2.00 and 11.34, respectively, so a small reduction is of no consequence. There are any number of adjustments we might make, but the result is that we essentially have to do the selection process all over from the beginning to avoid confusion.

Table 4.20 shows a possible conservative revision to allow flexibility in the field for fitting the casing on hand to the design. Essentially, this was a reworking of the entire selection procedure from the start.

Table 4.20 Example 7 in. Production Casing Design Summary—Alternate Field Design

Section	Depth (ft)	ID (in.)	Wt. (lb/ft)	Grade	Conn.	Design Margin, k_M		
						Clps	Brst	Axial
4	4500	6.184	29	P-110	LT&C	2.11	1.08	1.32
3	9100	6.094	32	N-80	LT&C	1.01	1.02	1.75
2	11,800	6.094	32	P-110	LT&C	1.02	1.70	4.67
1	14,000	6.004	35	P-110	LT&C	1.04	1.98	10.06

Mud Density: 1.84 SG.
Design factors, k_D: 1.125 clps, 1.20 brst, 1.6 or 100,000 OP (axial).

[5] Believe me on this issue. I worked in a pipe yard one summer as a teenage truck swamper.

I added 2% to the design factors (except at the surface and bottom depths which are fixed) and rounded the results to an even 100 ft, always favoring the conservative direction. It still required a combined load adjustment to the bottom of section 3 which calculated exactly at 9200 ft, but I raised that to 9100 ft to allow more flexibility at the rig site. This may seem a pointless exercise if you are satisfied that any field variation in "fitting" the actual casing to your design is not a significant concern. This step does go beyond normal practice, and few would ever go to the trouble. It is not an engineering consideration except in a most critical well, but depending on your professional situation, it can be a liability issue. If you are employed by a substantial company, it is probably a waste of time, but if you are a consultant or with a small organization, you soon learn that being right can still cost you a considerable amount in attorney fees just to prove it.

4.9 Closure

In the basic designs for surface casing, intermediate casing, and production casing that we just examined, we used a variety of design factors. Typically, a company has a set of design criteria for a specific area or field or even one used company wide and stays with those criteria for all designs.

Another point we should make is that we selected from our inventory of pipe without explanation as to why we chose one as opposed to another. Many possible combinations would work just as well as the selections we made. In general, the choice between two different types of casing for a particular section is based on

- Cost
- Availability
- Simplicity of design
- Minimum number of crossovers
- Wear considerations
- Weight in highly deviated or horizontal wells

The basic casing design process we considered so far in this text is adequate for the vast majority of all wells drilled in the world every year. What we presented was more or less a method for basic casing design. Also, we briefly covered some aspects of combined loading with little explanation. Again, the reason was to give the reader who has made it thus far through this text the ability to do basic casing design. We could have gone a bit further and also included some simple formulas for curved wellbores, but at some point, we have to stop and say that we have covered an adequate amount for basic casing design and some additional topics will require a better understanding of the underlying principles.

This page intentionally left blank

Installing casing

5

Chapter outline head

5.1 Introduction

Many of the problems that occur with casing are not problems with design, but problems with handling and running practices. Some companies have specific running practices, but they vary little from the basics. Several things must be kept in mind when transporting, handling, and running casing. Most fall in the category of common sense.

5.2 Transport and handling

Transport of casing is truly one of the most important of all casing handling processes, yet it is seldom given due consideration. Ordinarily, it is just assumed that this requires no attention as those who are

Casing and Liners for Drilling and Completion. http://dx.doi.org/10.1016/B978-0-12-800570-5.00005-X

doing it know what they are doing. Anyone who has ever worked in a pipe yard, boat dock, loaded a truck or boat would find such an assumption laughable. Therefore, it is essential here to suggest some guidelines.

5.2.1 Transport to location

Some casing gets damaged on the way to the location and on the location prior to running. There is no good reason for this to happen as often as it does. It is something that almost always could be avoided, but it still happens from time to time. Whether casing is loaded on trucks, boats, or barges, it must be adequately protected. This means not only care in handling while transferring from racks to trucks, to boat, to rig, all joints should have thread protectors in place and no cables or hooks should be used that can cause damage to the protectors or the pipe. On racks, trucks, or boats the casing should be placed carefully with wood stripping between layers. The casing should be secured so that it cannot move during transport, and strapping is preferable to steel chains.

5.2.2 Handling on location

Once the casing is on location it is off-loaded from trucks onto pipe racks or off work boats or barges onto the rig itself. In some cases rack capacity is limited, and the casing must remain on barges and be transferred to the rig as it is being run. Whatever the procedure, it is imperative that the casing be subjected to as little transfer as possible so as to reduce the chances for damage. All transfer must be done using good practices to prevent damage to the casing. Another important consideration is that the final transfer, whether to the racks or onto a barge must be done so that the casing is in the proper sequence in which it will be run into the hole. It is not acceptable to try to swap the order of pipe on the racks during the running process. Such an endeavor will most likely lead to errors. All transfers must be considered when the pipe is loaded at the pipe yard. For instance if the casing must be loaded onto trucks for transport to a dock, loaded directly from the trucks onto work boats, and then off-loaded onto the rig, all of these transfers must be taken into account so that the order of the pipe does not have to be shuffled at the rig. There is usually too little rack space on most offshore rigs to do this, and it is much easier to do it in a pipe yard when the pipe is loaded the first time.

Whether or not a company requires some type of electro-magnetic inspection on location is a matter of policy and the type of well that is being drilled. However, there are several things that are essential:

- Casing should be drifted on location to be sure that no damage has caused a reduction of the internal diameter, and also to be sure that nothing is lodged inside the pipe (it happens).
- The thread protectors should be removed and the threads cleaned with a solvent to remove any unknown type of lubricant on the threads.
- The cleaned threads should be visually inspected.
- In offshore locations where bare metal rusts in a matter of minutes, the threads should be lubricated as soon as they are inspected with the same lubricant that will be used when the string is run in the hole.
- In most cases, the protectors on the pin end should be cleaned and reinstalled.
- Do not place any type of equipment, such as casing spiders or tongs, on top of the casing that is on the pipe racks. This is not always possible on many small offshore rigs, but it is a bad practice that should be avoided.

5.3 Pipe measurements

One of the most critical aspects of running casing is the pipe tally or pipe measurement. The importance of this simple task cannot be overemphasized. The success of the entire well depends on it being

done correctly. So, who is responsible for the measurements, the rig crew? Absolutely not! The final responsibility of the pipe measurements is with the operator's representative on location, and who is in charge of the well. If the operator's representative does not personally do the physical measurement, then he or she should at the very minimum witness and record a duplicate of the measurement. There is no excuse for botching this simple procedure, yet it continues to happen all too often.

As to the actual measurement procedure, there are many variations on how and when to do it. Most often, it is done when the pipe is off-loaded at the rig onto the rig pipe racks. The best methods involve removing the protectors (from both ends) and numbering each joint with a paint type marker (not chalk) that will remain on the pipe until it goes in the hole. After a layer of pipe is measured and before it is covered with another layer, the recorded measurements should be inspected to ascertain that the joint numbers of the first and last casing joints on the layer correspond to the numbers of the recorded measurements. Then the measurements should be reviewed for any joints whose lengths vary significantly from the others. If a short or long joint is spotted in the tally, then that joint should be physically checked on the rack to be sure the recorded value is not a mistake. Most practical systems involve recording the joint measurements in a tally book or on some form that lists the joints in groups of 10. As the total length of each group is summed, the total length for each 10-joint group will be ten times the average length of joint in that group. If a mistake has been made in the measurements or in the addition, it is often easy to spot using that method.

Accuracy is essential in pipe measurements, but it is incredible as to how often so little attention is given to this phase of the process. Whatever system you use, it should be simple and consistent. The final responsibility for an accurate tally lies with the company representative on the location—not the roughnecks or roustabouts. One more time; there is no excuse for an incorrect casing tally!

5.4 Wrong casing?

Everyone who is involved in casing design and installation should be aware of an insidious mishap that does occur. Sometimes a joint (or more) of the wrong type gets into a sting of casing. Unfortunately, it is not usually discovered until it is too late—after the casing has been run and cemented. Such occurrences are always attributed to human error. But what is not always understood, is that it is not always a random error. For instance, a pipe yard loading-crew accidentally drops a joint of casing, damaging the threads. That is a random accident. They then "correct" this random accident by taking a replacement joint from another rack making sure that they picked one with the same color coupling! Even when we think we take great care, things can mysteriously go wrong. One such instance involved an intermediate string for a critical well with high H_2S content. The operator sent an engineer to the steel mill to witness the rolling, testing, and inspection of the string. He also stayed to witness the loading of the string onto barges at the mill, and met the barges at the destination port to witness the off-loading onto reserved pipe racks in the pipe yard, and later the loading onto trucks to the rig. On location the pipe was drifted, run, and cemented. Later during the drilling process the operator ran a wire-line caliper to monitor any wear in the casing. And what did they find? One joint in that string was the wrong wall thickness (one size less than all the rest)! Where did it come from? That was never solved, but the point here is that the most sophisticated design ever done is useless if this sort of mistake happens in the field. The casing process is always more than the design.

5.5 Crossover joints and subs

When the pipe is measured, that is the time to check all of the crossover joints (if any are required) as to correct threads and placement in the string on the racks or in a separate location where they can be added to the string when needed. Be sure the crossovers are included in the tally. There should be at least one spare for each different type of crossover used—you cannot wait for a replacement if one should be damaged during the running process. Crossovers for proprietary connections should be cut only by a machine shop or manufacturer licensed to cut that specific thread. The legal issue is one thing, but an improperly cut thread can cause failure of the string.

Crossover subs or couplings for API ST&C and LT&C threads need special comment. A short pin will make up into a long coupling, so no crossover is normally required when ST&C is run above LT&C. The reverse is not true, because a long pin will not make up properly into a short coupling. Some operators get around this crossover issue by purchasing an LT&C coupling and sending it to the rig as a crossover. The idea is that, when it comes time to make up the LT&C pipe into the top of the ST&C, the short coupling will be removed and the long coupling installed on the short pin. That sounds easy, but it is a poor practice. It often comes as a surprise that the short coupling may not back off easily. We cannot predict the torque required to remove a coupling that was installed at the mill. It may come off easily if the pipe is relatively new, but if the pipe has been sitting on a rack in the hot sun for two or three years it might require so much torque that the threads are galled and ruined in the removal process. This is not uncommon. It is also not uncommon to see a rig crew use a cutting torch to heat or even cut a coupling to get it off. So it is far better to have a dedicated crossover joint or sub (and a spare) for each place one is needed. The cost saved by purchasing an LT&C coupling for a crossover is miniscule compared to the potential cost if something goes wrong.

5.6 Running casing

The running procedures are important, not only for the success of the well, but also for personnel safety. Many injuries occur during the running process because of the relatively large size and weight of the casing, the length of the joints, and the unfamiliarity of regular drilling crews with the procedures. For those fortunate enough to work on rigs that have automated pipe handling systems, it may seem hard to imagine the crude casing running procedures that are common to many drilling operations.

The running procedure itself must be looked upon as a critical operation in the well. It should not be hurried, but should be smooth and efficient as far as time is concerned. Typically, the worst thing that can happen during the running procedure (aside from personnel injury) is to have to stop for some reason. In many parts of the world, it might be possible to stop the operation for several hours or even a day without sticking the casing. In other parts of the world, if the operation is stopped for half an hour, the casing will never be moved again. For that reason, all of the equipment must be in good working order and a certain amount of redundancy is desirable.

5.6.1 Getting the casing to the rig floor

Usually the pin protectors are removed before the pipe is picked up to the V-door of the rig, so as not to slow the make-up process on the rig floor. In this case, the pin should be protected with a quick-release type rubber protector during this time and until it is up on the rig floor ready to stab.

5.6.2 Stabbing process

The stabbing process (fitting the pin of a new joint into the box of the previous joint to begin the makeup process) is critical to prevent damage to the casing. All rigs do not have or use adjustable stabbing boards. It is still quite common to see jury-rigged stabbing boards that are nothing more than some $2'' \times 8''$ boards tied to derrick cross members. Where available, there are mechanical stabbing arms that can greatly ease the stabbing process. These aids are not available in many locales, so whatever means are employed, it is important that they allow for accurate stabbing of the joints to prevent thread damage. In some cases, this means shelter from winds that can cause difficulty and misalignment. Some proprietary connections require clamp-on stabbing guides to protect sealing surfaces and threads during the stabbing process. Where such guides are recommended, they should always be used.

5.6.3 Filling casing

In general, the casing should be filled with mud as it is being run into the well. An adequate fill line should be rigged up to assure that the filling operation will not slow the running process. In any event, you should visually assure the casing is full at least every few joints, even if it means slowing the running process until you see the mud at the surface inside the casing. It is especially important to be sure that the first joints of casing run are full because of the buoyancy effect if they are empty. If the first joints of casing are empty they may actually begin to float or at least lag behind the elevators as they go in the hole. This is a recipe for disaster because some casing tools with integral slips may actually open without a load and allow the casing to fall to bottom. It has happened.

Some companies use self-fill or differential-fill type float equipment to aid or replace the surface fill procedure. Where it works, it is fine, but when it does fail (and it sometimes does) it can cause serious problems if you are not aware that it has failed and is not allowing fluid into the casing. Casing collapse can result. Another objection that many operators have with this type of equipment is that it may allow hole debris to enter the casing at the bottom. Once on bottom and circulation is initiated, it may plug the float equipment, and there is no way to circulate it out short of running pipe inside the casing to the float to clean it out. If debris should remain in the casing after circulation and is pushed down to the float collar with the bottom cement wiper plug and plugs the float, then one is left in the precarious position of having all the cement inside the casing and no way to pump it in either direction. Self-fill or differential-fill float equipment has been most successful in hard rock areas, and it has failed mostly in areas of unconsolidated formations. If you use such equipment, just be aware of the possibilities for failure—it is much safer to fill from the surface.

5.6.4 Makeup torque

All connections should be made up to the proper specified torque while running. Most casing crews have all the standard torque values, but it is good practice to check and be sure that everyone is in agreement. There are different types of thread lubricant available for environmental considerations, high pressures and temperatures, and many have different frictional resistance. The correct type of thread lubricant and clean threads are essential for getting the correct amount of torque and seal. For critical applications there are special services that measure both torque and the number of revolutions of the pipe to be sure that the maximum torque did not occur before the coupling was fully made up.

Another point about proper torque is its measurement. The torque of a typical casing tong is measured with a hydraulic transducer in the tong line. In other words it actually measures tension in the tong line

and not torque. The torque gauge is calibrated such that it multiplies the length of the tong arm times the tension in the tong line to give the torque. That only works correctly if the tong line is perpendicular to the tong arm when the torque measurement is made. If the angle is more or less than 90°, then the actual torque will be less than that shown on the gauge. A few degrees is not going to make an appreciable difference, but it is not uncommon to see casing tongs rigged up with a considerable deviation from the proper 90°.

One last but most important point about make-up: The best casing design with the best quality pipe can fail if the casing is not properly made up on the rig.

5.6.5 Thread locking

One of the true disasters associated with casing is the disengagement of the bottom joint (or several joints) after the casing has been cemented and operations have resumed to drill out the cement inside the casing. The torque from the rotating bit drilling out the cement and float equipment in the bottom two joints starts to turn the casing, and the bottom joint(s) back out at a connection. Once this happens, there is usually no remedy; the hole has been junked and must be abandoned. This is slightly more prevalent with the trend to use PDC bits rather than roller bits in drilling out the floats and cement because of higher torque values. The reason that this sort of thing happens is not the bit, but that the cement around the bottom joints is incompetent, usually because has not yet reached a satisfactory strength. It happens most often on surface casing, where the temperature at the shoe is relatively low, and the cement does not set as fast as expected, or the operator is in a hurry to start drilling and does not allow sufficient time for the cement to set. While those are cementing issues which we will not cover here, there steps that can be taken in the running process of the casing to prevent such an event.

Most operators secure the connections on the bottom joints up to one joint above the float collar to prevent accidental back off of the casing while drilling out cement. There are chemical kits consisting primarily of a thermoset polymer used to “glue” the connections. The resin and hardener are mixed and applied in place of thread lubricant to the cleaned connections on the float equipment and bottom joints. There are a couple of problems associated with such a practice. One is that most use the compound only on the field make-up part of the connection. They assume that the mill end will not back off. This is a poor practice. If you are going to use the locking compound you should remove the couplings and “lock” all the threads, not just the field threads. (The mill ends might best be treated in a pipe yard prior to shipping to the rig.) The second problem is that, if something goes wrong and the casing string has to be pulled back out of the hole before reaching bottom, those connections cannot be easily broken out. That presents something of a dilemma in that if you do it you are safe from backing off the pipe, but if you have to pull the pipe you cannot easily undo it. You actually can heat the pipe with a welding torch to a temperature where the polymer will break down and the pipe can be backed out. But those joints should be replaced and not run back in the hole. An alternate procedure to the tread locking compound is that of tack welding the couplings on the lower joints. This was common practice for many years before the polymer compounds were available and is still common in some areas. However, welding on casing couplings can lead to serious problems and should be avoided at least for couplings with higher yield strengths than K-55.

When is thread locking necessary? As already mentioned, the cause of casing back-off while drilling float equipment is almost always caused by drilling out before the cement has had sufficient time to harden. Hence, the risk of a joint backing off is most acute on the surface casing or a cemented conductor casing because the temperatures are relatively low and the cement sets relatively slowly. In the case of deeper intermediate strings the issue is less critical because the temperatures are higher

and it often takes much longer to change out BOPs, drill strings, and other equipment in order to resume drilling below the intermediate casing. In the case of stage cementing equipment, there is little need to lock the threads of the stage tools. For a joint to back-off at a stage tool, the joints below it must also rotate, and this is almost impossible for a stage tool that is a few thousand feet above the casing shoe.

5.6.6 Casing handling tools

A wide variety of elevator and spider assemblies are available to run casing. Some elevators are called square shouldered (see Figure 5.1a). They have no slip elements. Instead, they have an internal diameter that will fit around the casing body but is too small for a coupling to pass through; they are hinge opening. The spider may be similar to the elevator and hinged or large enough for the coupling to pass through with some type of slip assembly built in, or there may be just a simple set of manual slips.

Elevators and spiders increase in sophistication from there. We assume that anyone who runs casing knows to select an elevator and spider combination of sufficient strength to suspend the casing safely. There is one important point to make in this regard though. The elevator and spiders normally used to run heavy casing strings (see Figure 5.1b and c) are rated at 500 tons (1,000,000 lbf) or even 1000 tons (2,000,000 lbf) and have an internal slip assembly that is either manually activated with an external lever or is air or hydraulically actuated.

These are very good tools for the purpose of running heavy strings of casing. The problem is that even a heavy string of casing is not "heavy" when it starts in the hole. The efficiency and ease with which the manual lever operates the slips is such that it is possible for someone on the rig floor to easily open the slips even with a few hundred feet of casing suspended in the spider. A similar problem can occur when the pipe is in the elevator and an obstruction is hit, causing the load on the elevator to momentarily ease so that the slips jump open. The result in either case is a portion of a casing string dropping in the hole and going to bottom. For this reason, it is often preferred to start a long string of casing in the hole with lower weight capacity rated tools, then switching over to the 500 ton tools when the casing is at the bottom of the surface casing or some other point where the running process can be paused to switch the elevator and spider. The possibility of such an event may sound remote, but there

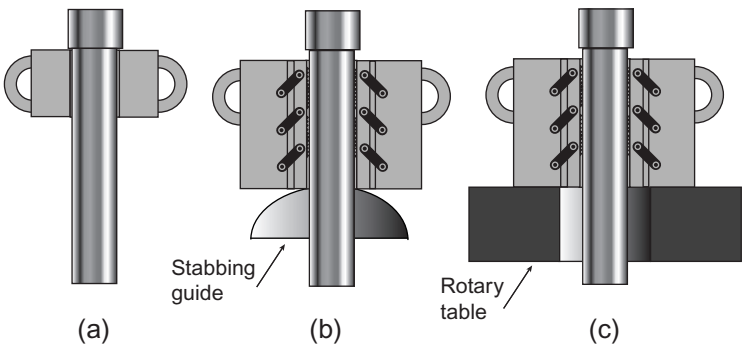

Figure 5.1 Casing tools: (a) wrap-around square-shouldered elevator, (b) slip-type casing elevator with stabbing guide, and (c) slip-type casing spider.

are a number of these instances in many companies' annals of bad events. In one case a casing crew member slipped and fell against the release lever on a spider and dropped 400 ft of 13 3/8″ casing to the bottom of a 5000 ft well. In another case, the crew was not filling the 7 5/8″ casing properly, and as the driller lowered the casing, it was buoyed enough so that it did not descend at the same rate as the elevator. The elevator slips opened. No one realized the elevator slips were open until the driller stopped the elevator above the spider and the casing kept on going right through the spider before anyone had time to react. Approximately 1100 ft of 7 5/8″ casing fell 12,000 ft before it stopped. The well had to be sidetracked.

One additional point about casing tools: a spare elevator/spider combination should be on the rig in case there is a problem with the primary tools. There will not be time to order a replacement if one fails.

5.6.7 Running casing in the hole

There several considerations to keep in mind while actually running casing. These include the running speed, getting casing all the way to bottom, what to do if it does not get to bottom, and whether or not to tag the bottom of the hole with the casing or stop just above bottom.

Running speed

Running casing is an intense operation; in cases where differential sticking is likely, it is even more so. There is often the temptation to run it too fast. But because casing is of a larger diameter than the drill string, the annular clearance is smaller, and the displacement and surge pressures in the annulus are usually higher that when running a drill string in the hole. If a formation is fractured during the running process, then the tendency to differentially stick the casing off bottom is increased, and the chances of getting a good cement job are usually decreased considerably depending on where the fracture occurs. There are formulas for calculating surge pressures. Almost no one ever uses them. A sure way to get into trouble running casing is to rely on some dubious value of the fracture pressure from some unknown source and a formula that may or may not model the actual mud rheology and hole conditions. A rule of thumb is that casing should be run in the hole at a slower rate than the drill string. Another is to observe the delay and rate at which the mud spills over the bell nipple, and if there is a noticeable delay between the rate of displacement and the mud being displaced from the borehole, then the casing is being run too fast for that particular mud. It is mostly a matter of experience and the known conditions of the specific borehole. The point here is: Do not attempt to run the casing too fast; it is not a race.

Getting casing to bottom

What should we do if the casing will not go to the bottom? When this happens (and it sometimes does) there is a tough decision to make. Should we rig up to circulate and try to wash past an obstruction or should we start out of the hole immediately? There are no firm rules on this because there are so many variables. In many places it is possible to install a circulating head (or top drive) and wash through an obstruction. In other situations where differential sticking is prevalent the act of turning on the pump to circulate is the equivalent of saying, "This is where I want to stick my casing string." You cannot rotate a casing string to free it like drill pipe.

One should always decide before starting in the hole what the risks are, and what the decision will be should something stop the casing from going to bottom. It is much easier to make such a tough decision before starting in the hole than when a problem arises during the running process.

Tagging bottom

We might also mention the issue of tagging the bottom of the hole with the casing. Some say that it should not be done because it can possibly plug the float shoe or even stick the casing in cuttings or fill on bottom. There is legitimacy to this line of thinking. Others do routinely tag bottom to verify their pipe measurements. I was schooled in the "do not tag bottom" discipline and never had a problem, but I have seen a couple of cases where followers of that mode of thinking set the production casing shoe above the bottom of the pay, and that can also be problematic.

In recent years it has become common practice when setting liners in Level 4 multi-lateral wells (where the upper portion of the cemented liner is washed over and milled out flush with the junction) to tag bottom as a depth reference so as to avoid cementing the liner with a coupling in the window. If a liner coupling (or any liner connection) is in the window when the liner is cemented, the coupling or connection will be partially milled in the wash-over operation. The result is a loose section of milled pipe above the connection as well as a loose, partial coupling in the wellbore. Do not make the foolish assumption that the cement will hold it in place. Lateral wellbores have been lost to re-entry in such cases.

Another important point along these lines: We hate to admit that it happens, but sometimes we find that the casing stops 42 ft from bottom, or maybe even 83 ft, or some such multiple of the pipe length range being used. This sort of thing happens too often, and the embarrassment of having made a mistake in the tally or joint count is only secondary to the reality that it could also end your current employment. Check your records quickly and make your decision, because the result of trying to wash pipe to bottom that is already on bottom may only compound your problems.

5.6.8 Highly deviated wells

Directional and highly deviated wells pose a special set of conditions. borehole friction may be quite high, and borehole stability problems may complicate the situation even further. Unlike most nearly vertical wells, the hookload does not always increase as the casing nears bottom. It often decreases as more casing enters the highly deviated portion and must be pushed in the hole (see Figure 5.2).

Obviously if the hookload goes to zero, we have nothing more to push the casing with, and the casing will go no further. (A top drive rig will allow us to add additional force, but it may not be enough either.)

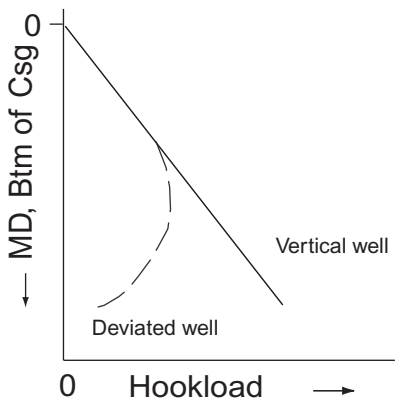

Figure 5.2 Decreasing hook load as casing is run into highly deviated wells.

If it is not on bottom, then our only hope is to be able to pull it out of the hole. Will our design allow the casing to be pulled out of the hole with the amount of borehole friction that is in this well? It is essential in highly deviated wells that we incorporate borehole friction into our design and running procedures. We will discuss borehole friction in Chapter 7.

5.7 Cementing

Cementing is a totally separate topic from this textbook, but it is a critical phase of well construction and is closely related to casing design as we have already seen in our basic design process. Therefore, it is necessary that we mention a few relevant points, since a bad cement job can render the entire casing process utterly useless.

While cements and cementing is a complex technological discipline in itself, there are two simple, but fundamental rules that are crucial to successful cementing:

- Get the mud out.
- Use ample cement.

Those may seem overly simplistic, but they summarize succinctly the requirements of a successful cement job. Accomplishing the first is the crucial requirement of primary cementing, and we will discuss that in more detail. The second tells us that cement is cheap compared to the consequences of a bad cement job, so do not skimp on the amount of cement you use, that is, more is usually better in most cases.

5.7.1 Mud removal

Casing is run into a borehole that is filled with drilling mud which has remained more or less static for a number of hours. Most drilling fluids begin to gel or become more viscous in the borehole with time. As the casing is run some of the mud is displaced by the casing. This displaced mud is usually the less viscous mud. Once the casing is in place it is mostly in contact with the wall of the borehole, that is it is eccentric to the borehole. The circulating velocity is the slowest where the casing is closest to (or touching) the borehole wall, making mud removal difficult in that area. The gelled mud must be removed in order to get a successful primary cement job. Here are some of the necessary steps:

- High circulation rates (but below fracture pressure)
- Pipe movement (rotation or reciprocation) and with scratchers where possible
- Pipe centralization (minimum of 70% of concentric clearance)
- Adequate precirculation prior to starting cement into casing (minimum of two hole volumes)
- No delay between precirculation and starting cement into casing
- Adequate preflush contact time (rule of thumb: 10 minutes minimum)

For horizontal wells where pipe movement is usually not possible we add two more.

- Remove all cuttings from horizontal lateral
- 0% free water in cement slurry

Of course, there are many other considerations as to cement type and chemistry, rheology, formation lithology, cement/mud/spacer/preflush compatibility, and so forth, but this listing covers the mechanical aspects associated with the casing string.

Once the casing string is on bottom, a cementing head is placed on top, and the well is precirculated prior to starting the cement into the casing. This step is of considerable importance in removing gelled mud. Scratchers can aid in this removal by breaking up the gelled mud for easier removal by circulation. Contrary to common belief, it is not the filter cake that must be removed, but the gelled mud. This circulation is done at high circulation rates, but below the fracture pressure of any exposed formations. A minimum volume of two hole volumes (sans casing) is required, and some companies require 2.5 hole volumes. Very important: start the cement immediately after the precirculation because the mud will start to gel again as soon as circulation stops. Precirculation and cement pumping should be a continuous operation if possible.

In the areas where bonding is critical centralizers are run to better center the pipe so that all the gelled mud is displaced and a uniform cement sheath around the casing is assured. Cementing companies recommend that adequate centralizer spacing should give a minimum of 70% of the concentric clearance, between casing and the hole, minimum clearance $= 0.7(r_{\text{hole}} - r_{\text{csg}})$. The closer the casing is to the borehole wall, the less likely the gelled mud in that area will be removed because the least resistant flow path is on the side with the greatest clearance. A concentric profile provides the maximum resistance to annular flow, and therefore, the greatest efficiency in removing the gelled mud. Figure 5.3a shows typical poor results in a well where casing is not centralized and the gelled mud was not sufficiently removed.

Pipe movement (reciprocation and/or rotation) is very effective in aiding the removal of the gelled mud. The difficulties associated with pipe movement involve a number of considerations. Which is more effective, rotation or reciprocation? The consensus favors rotation. Rotation is frequently used for relatively short liners with integral, shouldered connections. The limitation in all cases is that the rotating torque must not exceed the maximum makeup torque of the liner connections. Because of the liner hanger, reciprocation is not recommended; one does not want to reciprocate a liner only to find out that the hanger will not set once the cement is in place. So, given that rotation is best, where does that leave us with a long casing string? In general, we do not ever attempt to rotate a full casing string because the torque required to rotate a full string far exceeds the maximum makeup torque of most coupled connections, for example, ST&C, LT&C, Buttress. Reciprocation is the only alternative, and this must be taken into account in the axial design. In a vertical well, we generally use a sufficient design factor to account for some amount of friction in picking up the casing on the up-stroke, but in a deviated well the friction can be significant and must be accounted for separately (see Chapter 7).

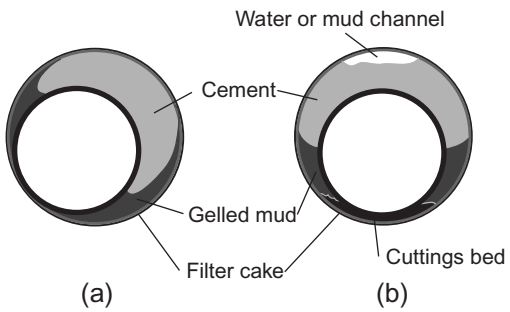

Figure 5.3 Poor cementing: (a) un-centralized vertical well and (b) un-centralized horizontal lateral with poor cuttings removal.

Horizontal wells exhibit additional complications because drilled cuttings are more difficult to remove. The casing tends to lie on the bottom of the borehole in the cuttings bed, and since the pipe is even harder to move because of friction, movement is often ignored. Shown in Figure 5.3b is a typical result in a horizontal lateral where cuttings were not sufficiently removed, the casing was not centralized, and was not moved during cementing. It also illustrates another common problem in cementing a horizontal lateral as a mud or water channel has formed along the top of borehole because of too much free water in the cement slurry.

5.8 Landing practices

There is no standard practice for landing casing after it has been cemented. It is assumed that the casing is now fixed at the top of the cement. (The fixed point is often referred to as the freeze point). The casing above the freeze point can actually buckle laterally and even into a spiral or helix because of its weight, the weight of the fluids inside, and/or a change in temperature. Only in rare cases would this buckling actually result in damage to the casing because the relatively small annular clearance limits the severity of the postbuckling displacements, but it could cause wear problems in intermediate casing strings where drilling will continue below. In production strings it may cause difficulty in running production equipment. As already mentioned, the severity of the postbuckled deformation is limited by the clearance between the casing and borehole wall which is normally relatively small, but it can be considerable in a washed out area. We will discuss lateral buckling in Chapter 6.

Four landing procedures are common and were once mentioned as recommended practices in a number of publications (but no longer). Roughly they are as follows:

- Land the casing with the same load on the wellhead as the hook load after cementing.
- Land the casing with tension at the top of the cement which is assumed to be the freeze point.
- Land the casing with the neutral point (axial tension/compression) at the freeze point.
- Land the casing with compression at the freeze point.

You can see that some of those are in opposition (the second and last), and none are in agreement. There are operating companies that have selected one of these (with possible variations) and are adamant that theirs is the best method to use. One problem with all this is that, once the casing is on bottom and cemented, we are not really certain what happens down hole when we land (or hang) the casing at the surface. Is the freeze point at the top of the cement or is the pipe stuck somewhere above the top of the cement? Do we even know where the top of the cement is? In some cases there is a limitation on what the wellhead equipment can support. There is also the question of the type of hanger used—a slip-type hanger gives us considerable flexibility (if we can get it down into the casing head properly) whereas a mandrel-type hanger cannot be adjusted once the pipe is on bottom or cemented.

It is generally agreed by most operators though that the casing should not buckle above the freeze point. That means that the effective axial load should be in tension if at all possible everywhere above the freeze point. Do not be misled into using the true axial load, the neutral point for buckling is the point where the effective axial load is equal to zero. Anything above that point should have an effective tensile load. (You learned to calculate the effective load in Chapter 4 so it should be no problem for you.) If the casing will be heated by circulating or by produced fluids you should take into account that the heat will expand the casing and reduce the tension, and possibly even put part of the noncemented casing in compression. (Temperature effects are covered in Chapter 6.) If you are using a mandrel-type hanger instead of a slip type, and in many situations you have no choice, then there is no way to adjust

the axial load above the top of the cement after it has set. In that case you should, if possible, design the cementing job such that the cement top is well above the neutral point. You may also be able to rotate the pipe while cementing or before cementing. This will serve to allow the pipe to overcome any residual frictional force from going in the hole and work the neutral point to the shoe (except in horizontal wells). However, before you elect to rotate the casing you must be sure that the torque required for rotation does not exceed that maximum recommended make-up torque of the casing connections. It usually does exceed the maximum for 8-rd couplings and many other non-shouldered type connections.

One significant problem, as far as lateral casing buckling, is concerned is hole washout and bad cement or no cement in those washed out intervals. In the presence of heated circulating fluid or produced fluids, buckling in this interval can occur. That is not a landing problem, but rather, it is a cementing problem that must be addressed. Along these same lines is the presence of a stage tool in a casing string. Often a stage tool will be used some distance above the top of the lower stage of cement. This means that there is an unsupported section of casing that is fixed at both ends (at the stage tool and at the top of the lower stage cement), and a significant rise in temperature can cause lateral buckling of the casing in that unsupported interval.

5.8.1 Maximum hanging weight

There are limits on the amount of weight that may be hung on a casing hanger:

- Tensile strength of the casing string
- Maximum support strength of wellhead and support casing
- Support rating of the casing hanger
- Collapse rating of the top casing joint when using slip-type hanger

The first limitation in the above list is a matter of proper casing design such that if tension above the string weight is to be applied (e.g., preventing thermal buckling), the additional tension must be included in the design loads. The second item is a matter of structural integrity of the supporting casings or platform and is beyond the scope of our discussion. The third item applies primarily to slip-type hangers, and one need refer to the hanger manufacturer's rating for the particular hanger to be used. There is also the case of weight and wellhead pressures exceeding the rating of the casing head such that the hanger actually causes the head to expand, but that is rare and most wellhead manufacturers have eliminated those problems from their equipment. The last item concerning the collapse load of a slip-type hanger on casing can sometimes be a serious problem for heavy strings of casing (see Figure 5.4). The weight of the casing forces the slip segments downward which in turn imposes a radial, compressive force on the outside of the casing in the slip area. Such a force can exceed the collapse resistance of the casing.

A simple formula can be used to estimate the collapse load imposed by a slip-type casing hanger.

$$p_{\text{hgr}} = k_{\text{D}} \frac{W}{A_{\text{slip}} \tan \phi} \tag{5.1}$$

where

$p_{\text{hgr}} =$ external casing pressure from hanger
$k_{\text{D}} =$ design factor
$W =$ hanging weight of casing

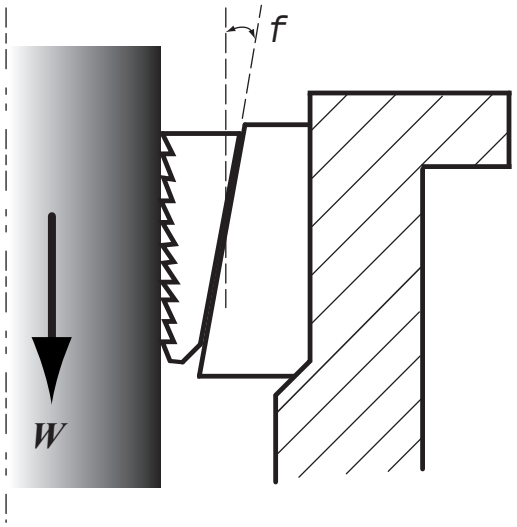

Figure 5.4 Slip-type casing hanger.

$A_{\text{slip}} =$ apparent gross contact area of slips

$\phi =$ taper of slips and hanger (measured from vertical)

To be as consistent as possible, the pressure load from this equation should be compared to the combined tension-collapse pressure rating of the casing. As to the design factor it is a matter of company policy, but a commonly used design factor is 2.0.

EXAMPLE 5.1 Slip Hanger Collapse Load

From our continuing example the 7″ production casing has the following data:

- Buoyed casing string weight at surface: 339,000 lbf
- Type of 7″ casing at surface: 29 lb/ft, P-110
- Nominal collapse rating: 8530 psi
- Hanger taper: 25°
- Hanger slip length: 10 in.

Using a design factor of 2.0, determine if the entire buoyed weight of the string can be hung on the hanger. The reduced collapse rating of the casing with 339,000 lbf tension is: 7271 psi[1]

$$p_{\text{hngr}} = 2.0\frac{339{,}000}{\pi\ (7)\ (10)\tan 25} = 6612\,\text{psi}$$

This value is well below the reduced tension-collapse rating of the casing.

In this example, case the casing may be hung safely with the full buoyed weight on the hanger without danger of collapse. Whenever doing this type of calculation it is important to know whether the

[1] As calculated from the traditional API method in the next chapter.

angle of the slip segments is measured from the horizontal or vertical. If the angle is measured from the horizontal it must be subtracted from 90° before using in this formula. It is also important to compare to the reduced collapse rating of the casing rather than the published nominal collapse rating, though many assume the design factor of 2.0 is sufficient to ignore the combined collapse/tension effect.

5.9 Closure and commentary

This chapter closes out the casing design and installation portion of this textbook, and from here on the topics become considerably more technical in nature though still sprinkled with a lot of precautions, suggestions, and opinions based on experience and case histories, most too sensitive to ever see publication. But before moving on there are some things that need to be said, and maybe best said in anecdotal form since written documentation will never see the light of day.

Casing strings fail, but it least they do not fail too often. By far the most common cause of casing failure is corrosion. In fact, I can safely state that corrosion causes more casing failures than all the rest combined. That is a topic we do not cover in this textbook because there are many sources available. So what are the other causes?

Over the last 55 years I have supervised on-site the running of casing strings that number into the hundreds in my earlier years. I have designed, checked, and approved designs for casing strings that number well into the thousands. And having spent most of those years in drilling and completion operations, I have been involved directly, indirectly, or peripherally with numbers into the tens of thousands. I am not trying to impress anyone with my long experience because there are many who have had considerably more. The reason I mention this at all is to emphasize a point: in all those casing strings, I have seen only *one* that failed because of a bad casing design![2] What does this say? I will not attempt to answer that, but offer the two most plausible reasons. Either the design process is so easy everyone can do it correctly, or on the other hand, perhaps we are over designing all our casing strings.

So if the design process, which is the technical emphasis of this textbook, seems to work okay, what are the problems? They are many and varied, but most distill down to some human link in the chain of events that failed, inadvertently, carelessly, intentionally or out of laziness or ignorance. Even a defective joint of casing can in effect be attributed to someone not doing their job properly.

The most common and serious casing problem I have witnessed over the years (aside from corrosion) is the backing off of the shoe track of surface casing while drilling out. It is not a life endangering event but a costly one. In all but one case it resulted in abandonment of the well. This event is always a result human error (though we like to claim otherwise, especially if we are personally responsible). It comes down to two things: not properly thread locking the joints in the shoe track and/or drilling out prematurely. Interestingly, all of these I have personally seen involved H-40 grade casing. That may have other implications because that also means they were relatively shallow casing strings and it is unlikely that the cement had properly cured before drilling took place.

This type of problem is also often exacerbated by a purely non-technical issue. Many wells in North America for instance, are drilled under a "footage" contract, meaning the drilling contractor is paid X dollars per foot drilled down to the intermediate casing point or total depth. The contractor makes

[2] It was a production string that collapsed around a tubing string as in Figure 6.5c, when the string became partially evacuated. It failed because the designer did not take into account the combined effects of tension/collapse, either through omission or ignorance of the method.

his money in the upper part of the hole where the drilling is fast and easy. Waiting for cement to cure sufficiently is costing him money while none is being earned since no drilling is taking place. Most drilling contracts specify a minimum waiting time for cement to cure, but some do not. And when they do, it is often some standard clause that has not been reevaluated in years (if ever) let alone adapted to a particular well or field area. If the operator has no representative on location (and many do not for a footage contract), the waiting time may get shaved a bit. I once had a client who contracted several shallow wells, and typically saw no need for the expense of having a representative on location. The wells were drilled under a footage contract and required only 500 ft of surface casing. I will not detail the resulting problems here, but the contractor had zero hours waiting on cement. Why? Because he did not cement the surface casing. He wrapped the bottom joints with large diameter hemp rope that swelled in the drilling fluid and held the surface casing in place for the three days it took to drill to total depth. Illegal? Yes. Was any of this on the drilling report? No, it reported a conventional cement job and 8 h waiting on cement. A rare occurrence? Sadly, no.

Another casing problem I have seen frequently also involves shallow wells and H-40 grade surface casing. The number of shallow wells drilled in North America with 8-5/8 in. surface casing and 4-1/2 in. production casing is in the hundreds of thousands at minimum. Most of these use H-40 surface casing with a threaded casing head on top. The problem? Not uncommonly, the casing head and BOP stack breaks off the casing at the threads. It is caused by a combination of a poorly stabilized BOP stack, vibrations, settling of the soil beneath the substructure, and so on. The kinds of things that do not normally occur with bigger rigs, but are common to these necessarily low cost operations. Almost all occur in 28 lb/ft H-40 8-5/8 in. casing. It is the minimum weight in that grade and definitely meets the design requirements for these casing strings. The solution is easy and is 100% successful everywhere I have seen it applied—put two joints of 32 lb/ft casing in the top of the string. It works. This is one of those quirks in casing design that we learn from practice, and unfortunately this particular one seems to be learned and relearned time and again. I have seen this one result in expensive forensic failure analysis and even lawsuits (to no avail), while the solution is trivial.

Though I have seen a number of tensile failures in tubing, I have seen only one tensile failure in casing in the form we would normally expect. Five others were from the cyclic pressures and temperatures of hydraulic fracturing in horizontal wells as discussed in Chapter 7. Those resulted from coupling leaks and subsequent erosion but the fracture fluid through the leaks. Though the final failure was in axial tension, I cannot call those true axial failures in the normal sense.

The one axial casing failure I did experience (on a telephone with the on-site drilling foreman) was almost bizarre. A production string of 4-1/2 in. H-40 grade casing was run in a shallow well. It was to be a pumping well, and this was the same type casing that had been run in hundreds of wells in the same field. The cement was being displaced, and just as the top wiper plug landed on the float collar, circulation was lost. The drilling fluid level and cement in the annulus fell rapidly. It fell, and it continued to fall. Then suddenly, the casing parted at the first connection below the elevator. A big surprise. A check of its rated joint strength showed that it certainly had enough tensile strength to be suspended in air all the way to total depth without failure, but the failure occurred because it did not have enough strength to be suspended in air and full of water. The water could not fall out the bottom because of the seated wiper plug. At the time I thought there was nothing we could have done once the annulus fluid started to fall. But I was wrong about that, there was something we could have done had we anticipated such an event. And probably we should have anticipated it since the producing zone was mostly depleted. Do you see what it was? At least we were able to secure the top of the parted casing and complete the well normally. This was an unusual case to be sure, but also it is a reminder that casing design should not become routine even for shallow wells. Oh yes, what could we have done to prevent

the failure? We could have immediately lowered the casing and set it on bottom to relieve the tension—a contingency we later adopted for such instances.

You may have noticed that much of what I have said here involves shallow wells. I started my career drilling relatively deep high pressure gas wells, where considerable effort and care was put into casing design and related practice. Consequently, I encountered few casing problems. It was not until much later when I began working more frequently with shallow wells and older wells that I began to experience real casing problems. Too often it is the routine, the normal, the shallow wells that seem to bite your professional ego the hardest. This is complacency, avoid it.

Running casing is as important as the casing design itself. If the casing is damaged or it does not reach bottom, the success of the entire well is jeopardized. We have looked at some practical aspects in this chapter, and I hope that these may be of use to you. There is much that could have been discussed, but we covered the essence.

This chapter concludes what might be called the basics of casing design and practices. It has been presented as something of a "recipe" for casing design. Though some of the issues were discussed in detail, little was said about where the strength ratings come from, and what their limitations are. The remaining chapters of this text will examine the mechanics of casing and special conditions and applications in more detail.

This page intentionally left blank

Casing performance

6

Chapter outline head

Casing and Liners for Drilling and Completion. http://dx.doi.org/10.1016/B978-0-12-800570-5.00006-1

6.1 Introduction

The first four chaptersof this text were written to provide a basic foundation in casing design. They more or less constitute a recipe, if you will, for basic casing design. That "recipe" should be adequate for designing casing strings for the vast majority of wells drilled in the world. One need not be an engineer to do it successfully, and it is hoped that the preceding chapters were enlightening to those who are not. Beginning with this chapter, we abandon the recipe. From here on, we address a number of topics considered more advanced. The intent here is not to try to teach a method for designing casing for critical wells but to help one understand the principles involved. More and more, we rely on software to do casing design. On the one hand, that is good, because it allows us to make sophisticated calculations and adjustments that require an excessive amount of time if done manually, and which few are actually trained to do in practice. On the other hand, we have people using software to design casing for real wells who are clue-less as to what the software is doing and what the results mean. This is not an exaggeration. In this chapter, we examine some of the topics that may fill a few gaps in the education of many drilling engineers in regard to casing design. The purpose here is to impart a degree of understanding of some of the concepts and terminology for more advanced topics concerning casing and its use. This chapter begins with a brief discussion of design methods and then looks at some of the concepts of solid mechanics as applied to casing and oilfield tubulars in general. We then address the design performance of casing for collapse loading, burst loading, axial loading, and the all important combined loading. Additionally we will briefly cover lateral buckling, dynamic loading, and thermal effects, and we will end the chapter with a brief discussion of expandable casing.

In this chapter we will make use of the concepts of solid mechanics covered in Appendix C. If you are not familiar with that topic or need a refresher, I strongly recommend that you review it before delving into the material that follows. If you are not already thoroughly familiar with the von Mises yield criterion, you must definitely read that section (C.6.3) of the appendix before proceeding.

6.2 Structural design

The design of structures is almost as old as humanity itself. Whether the first "structures" were for shelter, tools, or weapons, the design process from its primitive beginnings has been around a long time. Almost everything we see each day is a structure of some sort. Casing also is a structure, though we may not often think of it in that context. It is a containment structure for the most part, and the design procedures we use are similar in many respects to those of more complex structures.

6.2.1 Deterministic and probabilistic design

There are two general approaches to designing casing or any type of structure. One is a deterministic design method, the process with which we are most familiar. We use published values for the minimum strengths and performance properties of the materials, load scenarios based on observed and hypothetical criteria, and a set of formulas to calculate structural performance with those loads. Then we specify the types and sizes of structural materials required to safely sustain the loads. This is the method used for the design of most common static structures, such as bridges, skyscrapers, television transmission towers, drilling rig masts, and even oilfield casing strings. The other general approach is a probability-based design method, in which we use statistical test data for the strengths and properties of actual materials and probabilistic loading scenarios. This approach often is used in the design of structures subject to dynamic and cyclic loading such as airframes, turbine blades, and so forth, where fatigue failure is a significant or dominant factor. The probabilistic design criteria in these types of structures may also be weighted on the consequences of structural failure. In other words, the critical strengths and loads often are based on things like risk to human life, property value, the environment, and so forth. An example would be the blade of a gas turbine operating in some remote oilfield location as opposed to a jet engine turbine blade on an aircraft flying human passengers across a continent: in other words, a 0.1% probability of failure in 10,000 h of service may be acceptable for the remote oilfield gas turbine, but that same failure probability in an aircraft engine design would likely have aircraft falling out of the sky almost daily, and that is not acceptable. This method can also be applied to static type structures: we see an example of this in the oil field in the design of pipelines, where the published standards for strength often are based on the human population density in the vicinity of the pipeline. A probability-based design must account for the consequences of failure in addition to the probability of a failure. And, to do that, one must have reliable limit data on actual materials or components to work with rather than some limit set by manufacturing standards that allow considerable tolerance. Obviously, the better data we have, the better both methods work, but it is especially important in probability-based design if any significant savings is to be realized.

6.2.2 Design limits

One thing we must get very clear in our heads is that, when we design a casing string (or any other type of structure for that matter), we are not attempting to predict failure. Predicting actual failure is near impossible, even when we have the most complete data we can imagine[1]: in the case of oilfield tubes and borehole conditions, predicting failure is impossible. So our goal is to select some design limits and select our casing such that the anticipated loads do not exceed those limits. Calculating design limits and predicting failure are separate and distinct processes.

A design limit is naturally linked to some strength property of the structural member, which is a tube in our case. Since we already stated that we cannot predict actual failure of the tube, there must be some other property of the tube that we can reliably predict or calculate. The historic design limit for casing, as well as most structures in the world, is the elastic yield point: the stress at which a material goes from elastic behavior to plastic behavior. The elastic yield point or yield stress (sometimes referred to as the yield strength) of a metal such as steel is well defined and relatively easy to determine experimentally. What we never know, however, is the actual yield stress of a particular joint of casing. The only value

[1] If you doubt this, think of the "precision" shear pins used in the oilfield tools and designed to shear at a specified load. How many times have you seen one shear at exactly the specified load?

we have to work with is called a *minimum yield stress*, also which is not a material property. In other words, a joint of casing with a specified minimum yield stress (strength) is sold with the manufacturer's assurance that it will not yield at a lesser value. It may yield at a higher value (also limited by an upper value in most cases), so the only value we have to work with is the *minimum yield stress*, which may or may not be the actual yield stress.

We can (and sometimes do) design beyond the yield stress in some cases of structural design, but working within the plastic regime is quite complex and generally avoided in all but the simplest cases. These usually are cases in which part of the material body or structure remains elastic and the design limit might be selected as the point at which the entire body reaches the yield point (or possibly some point before that state is reached) assuming that no critical members of the structure actually fail before that point is reached. These types of design limits typically are one-time limits and do not consider the effects of cyclical loading (which changes the yield stress value). An example is the new ISO formula proposed for ductile rupture of casing, which we discuss later in this chapter. The only cyclical loading in the plastic regime for oilfield tubulars is in coiled tubing, and we all know (or should know) that coiled tubing has a very short service lifespan because of the cyclic loading in the plastic regime.

6.2.3 Design comments

It is not likely in the near future that more than a small number of companies will be doing probability-based casing designs for more than a relatively few critical wells, as compared to the number of wells drilled in the world each year. Those companies doing this work have their own expertise and criteria for risk, and those criteria cannot necessarily carry over to other companies. For instance, years ago with the advent of tubing-less completions, many looked at it as a way to save money. If you drilled a lot of these wells, you could save a sizeable amount of money. To be sure, there were failures, and the inexpensive wells completed with 2-3/8 in. tubing/casing could not be effectively worked over with the equipment of the day. The larger companies accepted this risk, and the frequency of failed wells (which were usually plugged as expendable) was within reason. But, for a small operator that had only one well or two, a failure sometimes was cause for bankruptcy. That is not acceptable from the small operator's perspective. However, that said, the one benefit of the trend toward probabilistic casing design that every operator, big or small, has realized is a decided improvement in the design formulas and the ways in which certain variations in casing tolerances can be measured and accounted for, even in deterministic design. And even what we call a deterministic design is based on some probabilities of certain critical loading occurrences and possible failures of casing to meet minimum standards. The difference is that, in deterministic design, we do not attempt to quantify those probabilities (see Klever and Tallin [16]).

One last comment should be made. A common mistake is to think that a deterministic design gives us a 100% safe structure at a higher cost, and a probabilistic design gives us a more cost-effective structure but at a slightly greater risk. While that may be true in some particular cases, it is not true in general. In fact, many of the probability-based designs are safer than some deterministic designs. Both methods have their place and applications.

6.3 Mechanics of tubes

Casing is a tube. A tube may serve as a beam, a column, a pressure vessel, or any combination of the three from the standpoint of mechanics. A casing string, to some extent, is all of those. The stress in a

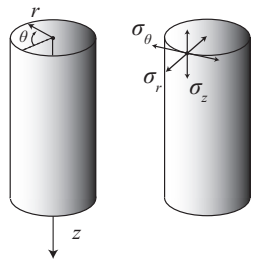

Figure 6.1 Cylindrical coordinate system for a tube, and stress component directions on tube body.

tube is of particular interest to us in light of the yield strength we just discussed, since that is what we need to know to determine if the tube is in an elastic range or not. We are fortunate in many respects that a tube is a fairly easy structure to analyze in an elastic state. In general, we need be concerned with only four stress components for our applications:

- Axial stress
- Radial stress
- Tangential stress
- Torsional stress

To understand these stress components, we first need a convenient coordinate system. One that fits our needs quite well is a circular cylindrical coordinate system, as shown in Figure 6.1, which also shows the first three stress components listed above.

There are three orthogonal coordinate axes, as with a Cartesian coordinate system. The axial coordinate, z, runs along the central axis of the tube; the radial coordinate, r, that runs from the central axis out in any direction; and the tangential coordinate, θ, which is an angular measure about the central axis as measured from some arbitrary reference point. The main difference between this and a Cartesian coordinate system is that two of the coordinate measures are in standard length units and one is an angular measure. Hence, the physical meaning of θ is not the same as z or r. The measure of physical distance in the θ coordinate is $r\theta$. This is a right-hand coordinate system, but it is oriented so that the axial coordinate, z, is in a downward direction. This is intentional so that the z-axis corresponds to the vertical depth (in a well), and furthermore, the compass azimuth (when viewed from above) and the conventional angles of trigonometric functions rotate in the same direction.

6.3.1 Axial stress

The axial stress in a straight tube is merely the axial load divided by the cross-sectional area of the tube:

$$\boxed{\sigma_z = \frac{F_z}{A_t} = \frac{F_z}{\pi\left(r_o^2 - r_i^2\right)} = \frac{F_z}{\frac{\pi}{4}\left(d_o^2 - d_i^2\right)}} \tag{6.1}$$

where

$\sigma_z =$ axial load stress component
$F_z =$ axial load
$r_o, r_i =$ pipe radius, outside and inside walls, respectively
$d_o, d_i =$ pipe diameter, outside and inside walls, respectively

We always assume that the pipe is straight and stress free before it is run in a well. If the pipe is in a curved bore hole, there will be additional stresses in the axial direction from bending, which we will discuss later.

6.3.2 Radial and tangential stress

We should all be thankful to Lamé, who in 1852, worked out the elastic stress solutions in tubes because of internal and external pressure. His solutions for the axial stress resulting from pressure depend on whether the tubes are open on the ends, capped on the ends, or the ends are free or fixed (plane strain). The Lamé solutions for the stress components attributable to pressure are

$$\sigma_r = \frac{r_\mathrm{i}^2 r_\mathrm{o}^2 \left(p_\mathrm{o} - p_\mathrm{i}\right)}{r_\mathrm{o}^2 - r_\mathrm{i}^2} \frac{1}{r^2} + \frac{p_\mathrm{o} r_\mathrm{o}^2 - p_\mathrm{i} r_\mathrm{i}^2}{r_\mathrm{o}^2 - r_\mathrm{i}^2} \tag{6.2}$$

$$\sigma_\theta = -\frac{r_\mathrm{i}^2 r_\mathrm{o}^2 \left(p_\mathrm{o} - p_\mathrm{i}\right)}{r_\mathrm{o}^2 - r_\mathrm{i}^2} \frac{1}{r^2} + \frac{p_\mathrm{o} r_\mathrm{o}^2 - p_\mathrm{i} r_\mathrm{i}^2}{r_\mathrm{o}^2 - r_\mathrm{i}^2} \tag{6.3}$$

$$\Delta\sigma_z = \begin{cases} \frac{p_\mathrm{i} r_\mathrm{i}^2 - p_\mathrm{o} r_\mathrm{o}^2}{r_\mathrm{o}^2 - r_\mathrm{i}^2} & \text{capped ends, both} \quad \text{free ends, one or both} \\ 0 & \text{open ends, one or both} \quad \text{free ends, one or both} \\ \nu\ (\Delta\sigma_\theta + \Delta\sigma_r) & \text{open or capped ends} \quad \text{fixed ends, both} \end{cases} \tag{6.4}$$

where the non-subscripted r is the radius at any point in the wall of the pipe. Please note that although the equations for σ_r and σ_θ may appear identical, they are not; the second equation has a negative sign in front of the first term. Another important point concerns the change in axial stress caused by pressure (Equation (6.4)). Casing in a well is already in a state of axial stress and is subjected to hydrostatic pressure. You must be careful with this equation because it accounts for *change in axial stress caused by change in pressure* from some reference state. Capped-end conditions affect casing only when one end of the casing is free to move. When casing is run in a well, the only time the capped-end condition normally applies is when the top wiper plug is bumped during cementing. After that, the casing is fixed at the top by the wellhead and below by cement. If you want to consider the wellhead a cap, then you must also consider that, for it to move enough to cause an axial stress change in the casing string, it must move every tubular string in the well that is attached to the wellhead, some of which are cemented to the surface. (Some thermal wells allow for wellhead movement.) The second term in the numerator of the capped-end formula is for external pressure that acts on the capped free end, pressure that may or may not be present. Post plug bump is a case in point here. If the ends are fixed, you must know if they were fixed before the pressure change was applied or afterward because the fixed-end axial stress equation is only valid for changes in the axial stress from pressure applied after the ends are fixed.

The general Lamé formulas are useful as they are stated above, but as it turns out we are seldom interested in the stress at various points within the wall of the cylinder, because the maximum stress always is at one of the walls if there is pressure. Which one? It is not intuitive, but whether the greater pressure is internal or external, *yield always occurs at the inner wall first*! (Work it out, if you do not believe it.) If we substitute r_i in place of r to get the Lamé solutions at the *inner wall*, we find they are greatly simplified:

$$\boxed{\sigma_r = -p_\mathrm{i}} \tag{6.5}$$

$$\boxed{\sigma_\theta = \frac{p_\mathrm{i}\left(r_\mathrm{o}^2 + r_\mathrm{i}^2\right) - 2p_\mathrm{o}r_\mathrm{o}^2}{r_\mathrm{o}^2 - r_\mathrm{i}^2}} \tag{6.6}$$

The axial stress change is unchanged from in Equation (6.4). The sum of the radial and tangential stress in that equation is a stress invariant through the wall of the tube, so it does not matter if they are calculated at the inner wall or outer wall, so long as both are calculated at the same place. One more caveat: often you may see the tangential stress equation without the second term in the numerator. That is typical of pressure vessels where there is no external pressure. Many use that form and use the difference between the internal and external pressure as the internal pressure. Don't do that! Yes, it gives close results, but it is a sloppy practice.

There are times when we might need to calculate the radial and tangential stress at the outer wall. In bending and torsion, the tube yields first at the outer wall, so if we are checking for yield in these cases where pressure is also present, we may want to check both the inner and outer walls. The radial and tangential stress components at the outer wall are

$$\boxed{\sigma_r = -p_\mathrm{o}} \tag{6.7}$$

$$\boxed{\sigma_\theta = \frac{-p_\mathrm{o}\left(r_\mathrm{o}^2 + r_\mathrm{i}^2\right) + 2p_\mathrm{i}r_\mathrm{i}^2}{r_\mathrm{o}^2 - r_\mathrm{i}^2}} \tag{6.8}$$

Lamé solutions and yield

Here is an important point illustrated in Figure 6.2 that concerns location of initial yield from pressure: if we apply pressure to casing internally until it yields, will it yield first at the inner wall or the outer wall? Similarly, if we apply pressure to casing externally until it yields, will it yield first at the inner wall or the outer wall? These are not such simple questions as one might think, and the answers are important to know. Despite any apparent simplicity, the answer is that it makes no difference as to whether the pressure causing yield is internal or external, *the casing will always yield first at the inner wall*. This is not intuitive, and if you would like some practice with the Lamé equations you might work this out as an exercise.

The Lamé solutions are extremely useful, but we must be very careful to not use them beyond the yield point. Remember that these are elasticity solutions based on linear elastic material behavior. They are not valid beyond the yield point. If you use them to calculate the stress components for use in the von Mises yield criterion, and the result is greater than the yield, then the calculated stress component

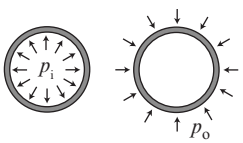

Figure 6.2 Internal and external pressure increasing to yield stress in casing.

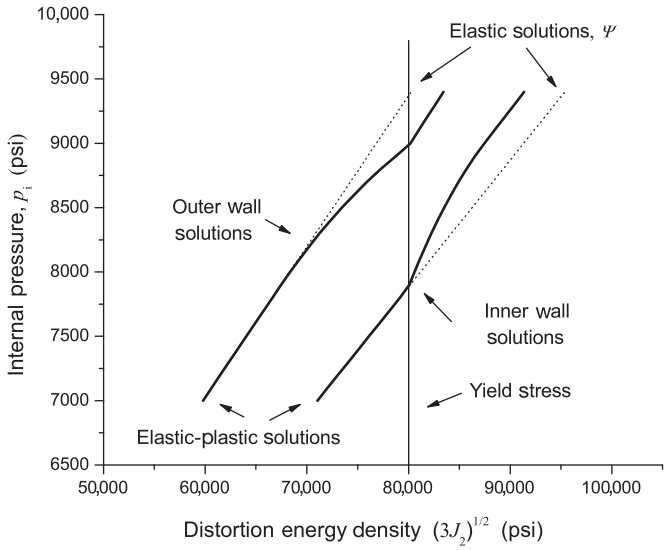

Figure 6.3 Internal pressure causing yield in a fixed-end casing.

values are quantitatively meaningless. In that case, they will tell you only that the initial yield has been exceeded, but not by how much. This is illustrated in Figure 6.3 where we have calculated the yield measure, Ψ, using the Lamé elastic solutions at the inner and outer walls of a tube of the dimensions of 7 in. 23 lb/ft casing with a yield stress of 80,000 psi. We also calculated and plotted the distortional energy density, $\sqrt{3J_2}$, using elastic-plastic theory.[2] Two things are important in this figure. One is that yield occurs first at the inner wall causing the distortional energy density to become nonlinear with respect to the internal pressure, and though the outer wall does not yield until sometime later, the distortional energy density becomes nonlinear well before it actually yields. The second thing to note is that once the yield point is reached at the inner wall, the elastic values of the yield, Ψ, calculated with the Lamé equations become meaningless because the material is no longer elastic. See Appendix C for a discussion on plasticity and an example of a similar analysis with different end conditions.

6.3.3 Torsion

We do not often rotate casing in a borehole. It does help in attaining a good primary cement job, but often the friction in the borehole is such that the torque required to rotate the casing exceeds the maximum recommended makeup torque of the connections such as ST&C, LT&C, buttress, and so on. However, many times, liners are rotated while cementing and casing can be rotated with some proprietary connections or special stop rings inserted to prevent over-makeup of non-shouldered connections, like buttress, ST&C, or LT&C. The equation for the shear stress from torsion in a pipe body is given by

$$\boxed{\sigma_{r\theta} = \frac{2\,r\,T_{\mathrm{q}}}{\pi\left(r_{\mathrm{o}}^4 - r_{\mathrm{i}}^4\right)}} \tag{6.9}$$

[2] The elastic-plastic constitutive equation used in this example is not that of an API steel, but a piecewise linear approximation of a strain hardening steel with a yield stress of 80,000 psi.

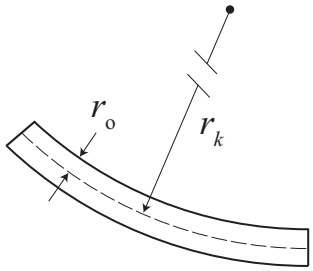

Figure 6.4 Simple planar bending of tube.

where $r = r_o$ to calculate the shear stress at the outer wall where it is a maximum or $r = r_i$ at the inner wall. The torque (rotational moment) in the casing is T_q and it must be in consistent units. In oilfield units it usually is in lbf ft and it must be multiplied by 12 to change it to lbf in. to be consistent with the radii units. In SI units, the torque will be in Joules (N m) so the radii must be in meters so that the stress will be in Pa.

6.3.4 Bending stress

The bending of casing in curved wellbores is discussed in detail in Chapter 7 and derived in Appendix C, so all we present here is a formula for planar bending stress that refers to Figure 6.4:

$$\boxed{\sigma_b = \pm E\frac{r}{r_\kappa}} \tag{6.10}$$

The radius of the pipe is $r = r_o$ at the outside wall where the bending stress is a maximum, and $r = r_i$ if it is desired to calculate the bending stress at the inner wall. The radius of the wellbore curvature is r_κ. It must be in the same units as the radius of the pipe. The bending stress component has a plus sign on the convex side of its curvature as that portion is in tension. On the concave side, it is negative because it is in compression.

The bending stress component is added to the axial stress for determining yield, but it should be remembered that the bending stress is a maximum only along a line running parallel to the central axis in the plane of curvature on the convex side and the concave side. The values calculated in the bending equation are not the bending stress at other points around the circumference of the tube.

6.4 Casing performance for design

In earlier chapters, we took the published values of casing strengths at face value. In this section, we examine some of the formulas from which those strengths are calculated. What are the bases of these formulas? What are their limitation? Are there better formulas or methods? We will address those questions and then look at combined loading and its effects. We will also look at lateral instability (buckling) and the effects of temperature on casing design.

Reiterating what was previously mentioned, we cannot actually predict failure of a joint of casing, and we do not seek a to do so. What we are interested in is a value we can use as a design limit.

A particular joint of casing may fail at that limit or it may not; the important consideration is that it does not fail before that limit point. Historically, yield strength has been used as a design limit, and that continues. However, some of the formulas used in the past were based on some simplifying assumptions and tests that did not realistically model actual loading. For example, the API collapse formulas are based on collapse tests on short samples of casing, and it has been found that joint length plays a part in collapse, i.e., end conditions affect the collapse of short tubes. So, much of what is covered in this part of the chapter might be characterized as design strength formulas and calculations. Most are still based on yield strength or test data. While it may be perfectly acceptable to use conservative formulas in the vast majority of wells drilled in the world, there are deeper, high-pressure, high-temperature wells where such conservative formulas might greatly increase well costs by requiring much higher strengths than is necessary or even available. We examine the current formulas and discuss some of the changes.

6.4.1 Tensile design strength

Casing failure in tension is not common. When it does occur it usually occurs at a connection, and the connection is usually ST&C or LT&C. The failure in those types of connections usually is a result of pull-out rather than fracture of the casing body. In some cases, the pull-out is the result of a split coupling caused by hydrogen embrittlement or over-torque during makeup. As far as tensile strength of casing is concerned, it is specified in two ways by the API and ISO, *pipe body yield* and *joint strength*. The first is the value of the pipe body yield strength exclusive of threads, expressed as axial tension (or compression) rather than axial stress, and the second is the value of the connection strength, which always refers to tension and not compression. The pipe body yield values use the minimum yield strength as the design strength limit. The joint strength is based on the minimum value from formulas that use the minimum ultimate strength and the yield strength separately or in combination.

Pipe body yield

Pipe body strength at yield is the yield stress of the metal multiplied by the specified cross-sectional area of the tube.

$$\boxed{F_{\max} = Y A_t} \tag{6.11}$$

where

$F_{\max}$ = pipe body strength at yield

Y = uniaxial yield strength of pipe

A_t = cross-sectional area of tube, $\pi \left(r_o^2 - r_i^2\right)$

For example, the pipe body yield for 7 in. 23 lb/ft N-80 casing is

$$F_{\max} = 80000 \ (\pi/4) \left(7.000^2 - 6.366^2\right) = 532,000 \text{ lbf}$$

which is the value shown in the published tables. This value is valid for either tension or compression. For ST&C and LT&C couplings, the strength of the connection usually is less than that of the pipe body. For instance, for the above 7 in. 23 lbf/ft N-80 casing with LT&C connections, the joint strength rating is 442,000 lbf, or about 17% less than the pipe body yield, so one must be aware that the joint strength is usually the lesser of the two.

Joint strength

Joint strength is usually the yield strength of a casing connection in tension; however, formulas also are available for the fracture strength of connections, although they are not used often in casing design. The calculation of joint strength depends on the specific type of coupling and includes things such as the makeup length of the threads, the cross-sectional area of the tube under the last full thread, and so forth. Furthermore, the formulas have been adjusted to fit actual tests with various samples of casing connections. The resulting formulas for ST&C, LT&C, buttress, and extreme-line are listed in API 5C3 and ISO/TR 10400. Additionally, one must refer to API 5B to get some of the necessary thread dimensions for use in the formulas. Proprietary thread manufacturers, in general, do not publish their formulas but only the connection strength values. For those reasons, we do not include any joint strength formulas here. Almost no one actually uses them, since the results are published in many tables. The thing we must point out as a precautionary note is that one should always check both the body strength and connection strength for any casing design. And remember, the strength of connections in compression is not addressed by API standards.

6.4.2 Burst design strength

The traditional API formula for what we commonly refer to as burst is not actually a formula for burst or pipe rupture but a yield formula for internal pressure. It is based on a thin-wall tube that assumes yield takes place across the entire wall thickness at a single pressure. It also includes a design factor to account for the 12.5% variation in wall thickness allowed by API casing specifications (API Spec 5C2 or ISO 11960). The result is a formula for the internal yield pressure:

$$\boxed{p = 0.875\, Y \frac{d_o - d_i}{d_o}} \tag{6.12}$$

This formula known as the Barlow formula was derived from three-dimensional shell theory assumptions and is adequate for basic casing design, but it leaves a lot to be desired. For one thing, it assumes that yield occurs throughout the pipe wall at the same time, which it does not. What is lost by the assumption of a thin-wall cylinder with a uniform stress throughout the wall of the cylinder? We can use the Lamé elastic formulas along with a yield criterion to determine the yield at the inner wall for a thick-wall tube and compare the results. In the absence of any axial load or axial constraints, that is, the pipe is free to move axially and the ends are not capped, the Lamé formulas give the stress components at the inner wall as

$$\sigma_r = -p_i \tag{6.13}$$

$$\sigma_\theta = \frac{p_i\left(r_o^2 + r_i^2\right) - 2p_o r_o^2}{\left(r_o^2 - r_i^2\right)} \tag{6.14}$$

In absence of axial stress, at internal yield, the following holds for the von Mises yield criterion:

$$Y = \left\{\frac{1}{2}\left[(\sigma_\theta - \sigma_r)^2 + (\sigma_r)^2 + (-\sigma_r)^2\right]\right\}^{\frac{1}{2}} \tag{6.15}$$

If the external pressure is zero, that is, $p_o = 0$, then we can solve this equation for the internal pressure at yield in terms of the yield strength of the pipe and the internal and external diameter of the pipe. The result is

$$\boxed{p_\mathrm{i} = Y\frac{d_\mathrm{o}^2 - d_\mathrm{i}^2}{\sqrt{3d_\mathrm{o}^4 + d_\mathrm{i}^4}}} \tag{6.16}$$

This equation is the thick-wall equivalent of Equation (6.12), except it does not account for a tolerance in the wall thickness. The wall thickness is accounted for in ISO 10400 by calculating an internal diameter based on the tolerance in the wall thickness such that, for this equation,

$$\boxed{\tilde{d}_\mathrm{i} \equiv d_\mathrm{o} - 0.875\,(d_\mathrm{o} - d_\mathrm{i})} \tag{6.17}$$

This definition uses the standard API tolerance; however, other values could be used for specific situations where the actual tolerance is known as opposed to the specified maximum tolerance of 12.5%.

EXAMPLE 6.1 Comparison of Burst Equations

Using 7 in. 26 lbf/ft P-110 casing in this example, the Barlow (Equation (6.12)), gives an internal pressure at internal yield

$$p = 0.875\,Y\frac{d_\mathrm{o} - d_\mathrm{i}}{d_\mathrm{o}} = 0.875\,(110000)\,\frac{7.000 - 6.276}{7.000} \approx 9960\,\mathrm{psi}$$

whereas Equation (6.16) using Lamé's pressure equation and von Mises yield criterion gives

$$\tilde{d}_\mathrm{i} = d_\mathrm{o} - 0.875\,(d_\mathrm{o} - d_\mathrm{i}) = 7.000 - 0.875\,(7 - 6.276) = 6.367\,\mathrm{in.}$$

$$p_\mathrm{i} = Y\frac{d_\mathrm{o}^2 - \tilde{d}_\mathrm{i}^2}{\sqrt{3d_\mathrm{o}^4 - \tilde{d}_\mathrm{i}^4}} = 110000\frac{7.000^2 - 6.367^2}{\sqrt{3\,(7.000)^4 + 6.367^4}} \approx 9900\,\mathrm{psi}$$

From this example we see that there is only a slight difference in the two. The formula based on thick-wall tubes will usually be slightly conservative. The problem with the API Barlow formula, though, is that it is valid only if the pipe has no axial stress. It also assumes that any external pressure can be accounted for by subtracting it from the internal pressure and using the difference, $\Delta p = p_\mathrm{i} - p_\mathrm{o}$, as the internal pressure (as long as $\Delta p > 0$). Some do the same thing with the Lamé formula for tangential stress, which is not good practice, because it does not give the same result as when both internal and external pressures are used.

Ductile rupture formula

The current ISO/TR 10400 [11] includes new formulas for ductile rupture as differentiated from internal yield. Few, if any, oilfield tubulars actually fail in rupture when the internal wall surface reaches the yield point, which is the basis for the conventional API/ISO formulas for "burst" or, more correctly, internal yield. If the material were perfectly plastic, it would quickly yield all the way through the wall thickness as the pressure is increased and rupture, but that is not the way most oilfield tubulars behave (coiled tubing excepted). Unless they are very brittle, they are made of a strain-hardening material, so that once the yield stress has been exceeded, the stress still increases before

ultimate failure occurs, as discussed in Appendix C. The recent ISO formulas take that into account by actually modeling the material behavior in the plastic regime. In addition, certain defect sizes are taken into account, so that the pipe may more realistically model actual casing. Even fracture growth is considered.

To use these formulas, one must have more specific data than is conventionally published. In particular, one needs inspection results for the casing to be used or at least have a specific inspection in mind and know that casing not meeting those standards will be culled from this particular application. We are going to present only some basics of the formulas here, but before using these formulas, one should definitely read the discussion in ISO/TR 10400 (Appendix B) and some of the associated references. The primary ductile rupture formula in ISO/TR 10400 includes a capped-end effect such that the internal pressure generates an axial stress from the pressure effect on the end caps. For a capped-end effect to be realized, one end of the tube must be free to move in relation to the other end, so that the axial stress is a function of the internal pressure. This almost never happens with casing in a well except in the plug-bump case, since one end of the casing is cemented (fixed) and the other attached to a wellhead. Unless the wellhead is free to move, the capped-end effect does not occur. One could argue that the wellhead may move, but its movement is considerably restricted by the other strings of pipe also attached to the wellhead, in addition to the fact that the conductor and surface casing are usually cemented at the surface. For casing, the pressure effects are almost always those of fixed ends not capped ends. That being said then, the ISO design formula for the internal pressure at ductile rupture with capped ends is

$$\boxed{p = 2k_1 U \frac{\tilde{t}_w - k_2\,\delta}{d_o - \tilde{t}_w + k_2\delta}} \tag{6.18}$$

where

p = internal pressure at ductile rupture

U = minimum tensile strength of casing

d_o = outside diameter of casing

$\tilde{t}_w$ = reduced wall thickness from the tolerance, e.g., $(0.875\,t_w)$

$k_1 = \left[\left(\frac{1}{2}\right)^{n+1} + \left(\frac{1}{\sqrt{3}}\right)^{n+1}\right]$ = correction factor

k_2 = burst strength factor, 1.0 for Q&T or 13Cr steels,
default 2.0 for others not specifically measured

δ = depth of imperfection in wall thickness

n = dimensionless hardening index for true stress/strain
curve from uniaxial tensile test

This formula is called a design formula, which calculates rupture assuming certain minimum values for the quantities in the formula, such as the minimum tensile strength. This is derived from a limit state formula, which predicts rupture for a specific sample where the quantities just listed are known exactly for that sample. Some of these quantities can be calculated from measurements or tests. Table 6.1 suggests values for the hardening index, n, in the absence of actual test data. A hardening index, as used here, is a means of approximating a uniaxial stress-strain curve for a particular material, with a curve fit

Table 6.1 ISO Suggested Hardening Index Values [11]

API Grade	Hardening Index, n
H-40	0.14
J-55	0.12
K-55	0.12
M-65	0.12
N-80	0.10
L-80	0.10
C-90	0.10
C-95	0.09
T-95	0.09
P-110	0.08
Q-125	0.07

to an idealized material, such as a Ramberg-Osgood material [17], or a Ludwik power-law material [18]. No conversion factors are required if you use consistent units.

We use this formula to determine the ductile rupture pressure for the same casing in the previous example.

EXAMPLE 6.2 Ductile Rupture Formula

Using the same casing as in the previous example and assuming our casing inspection rejects all defects in excess of 5% of the wall thickness, we determine the variable quantities for use in equation (P-110 casing has a minimum ultimate tensile strength of 125,000 psi):

$$\tilde{t}_w = 0.875\, t_w = 0.875\,(0.362) = 0.317\,\text{in.}$$

For the hardening index, we use $n = 0.08$ for P-110 (Table 6.1) and calculate the correction factor:

$$k_1 = \left[\left(\frac{1}{2}\right)^{n+1} + \left(\frac{1}{\sqrt{3}}\right)^{n+1}\right]$$

$$= \left[\left(\frac{1}{2}\right)^{0.08+1} + \left(\frac{1}{\sqrt{3}}\right)^{0.08+1}\right] = 1.026$$

The maximum allowable depth of the wall thickness defect in the selected casing is

$$\delta = 0.05\,(0.362) = 0.0181\,\text{in.}$$

For the burst strength factor we use 2.0, the default value. We substitute these values into Equation (6.18):

$$p = 2k_1 U \frac{\tilde{t}_w - k_2\,\delta}{d_o - \tilde{t}_w + k_2\delta}$$

$$= 2\,(1.026)\,(125000)\,\frac{0.317 - 1.0\,(0.0181)}{7 - 0.317 + 1.0\,(0.0181)} \approx 11,440\,\text{psi}$$

We can see that this value is about 14% higher than the current API formula in the previous example. Part of this is attributable to the capped-end effect. As we will later see with the von Mises yield criterion, internal yield is higher in the presence of axial tension, which is what we have with a capped-end effect.

An additional ISO ductile rupture formula accounts for external pressure and arbitrary axial loading. It is a nonlinear limit state formula, see ISO10400/TR [11] pages 25-30. One difficulty with that formula is that for a fixed end tube such as casing cemented at the bottom and fixed to a wellhead at the top, the axial load is not a constant, but is a function of the pressure as in the Lamé formula for fixed ends, $\sigma_z = \sigma_{z0}\nu(\Delta\sigma_r + \Delta\sigma_\theta)$, Equation (6.4). But beyond the yield point, σ_r and σ_θ are elastic-plastic stress components, not proportional to the pressure, as in the capped end case. Finally though, one should note that the ductile rupture formulas take into account material behavior in a plastic regime. In our discussion on plastic behavior in Appendix C, we pointed out that materials become history dependent in this regime, so these formulas are valid only if the loading exceeds the yield stress and proceeds to rupture. If the loading stops once yield has been exceeded but short of the rupture value, then the formulas are valid for subsequent loading only if the loading path is exactly the same as before, once the new yield value is exceeded. Therefore, the use of the ductile rupture formulas is a highly questionable endeavor, especially for cyclic loading in casing beyond the yield point. At least in my opinion and experience with plasticity [19].

Coupling performance with internal pressure

In some configurations, casing couplings will yield before the pipe body or will leak at a lesser internal pressure than that which will yield the pipe body. There are formulas in ISO 10400 to calculate these values for API round thread and buttress threads. It is rare that anyone ever needs to use these formulas because the values are listed in the tables of casing properties in API 5C2. Because of this and the need to refer to actual thread specifications, I do not include them here. The important point to remember is that *in some casing the coupling is weaker than the pipe body in internal yield and/or leak pressure rating*.

6.4.3 Collapse design strength

Casing collapse is actually two phenomena (1) an instability (radial buckling), and (2) collapse (post-buckling). The collapse rating of casing usually (but not always) refers to the pressure at which the pipe becomes radially unstable and the actual collapse is the behavior after the instability is reached and usually takes place at a lower pressure than the buckling pressure. Casing collapse possibly is the most common type of failure after corrosion and wear. There have been cases of collapse resulting from defective casing joints, but the cause often is one of not accounting for the actual collapse load on the casing. This is especially true where the casing is in tension and subjected to a collapse load. Perfectly round casing with a uniform wall thickness is quite resistant to collapse pressure. If there is a variation in the wall thickness because of eccentricity or defects, the cross section is ovalized, or the collapse loading is other than hydrostatic pressure (e.g., borehole stability problems), then failure from collapse usually occurs at lesser loads. The typical post-buckling collapse mode is shown if Figure 6.5a where the casing tends to flatten in cross section. Collapse also depends on outside support of the casing (see Figure 6.5b) in that casing with little outside clearance or partially supported by cement may begin to collapse into the configuration illustrated or the partial support may prevent total collapse. Another mode (Figure 6.5c) is common in production casing where tubing is present.

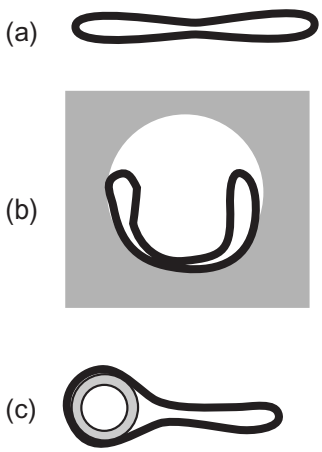

Figure 6.5 Common collapse modes: (a) unsupported collapse, (b) partially supported collapse (e.g., cement or coupling), and (c) unsupported collapse with tubing inside.

Sometimes partially collapsed casing may be restored with an internal casing roller, but fully collapsed casing, is usually a total loss. It may be possible to mill out, and sometimes even recover, a collapsed portion of the casing. When a tube begins to buckle in collapse (collapse is a form of buckling), the buckle propagates along the tube at a much lower pressure than what caused the initial collapse. The buckle propagation pressure may be on the order of 60 – 65% of the initial collapse pressure if the casing is unsupported. For an undersea, welded pipeline, the entire line may collapse because of a defect in one joint. For this reason, many undersea pipelines now include rings, called buckle arrestors, welded to the pipe at various intervals so that, if a collapse should occur, it will not propagate the full length of the submerged pipeline.

Fortunately, in a casing string, a hydrostatic-induced collapse typically is limited to one joint, because as the buckle propagates, it usually stops at a coupling. In the case of a threaded coupling, the propagation stops because the collapse of the pipe inside a coupling does not transfer the load to the other pin inside the coupling. It also opens the interior of the casing to external pressure, so that the pressure differential is relieved. In the latter case, it becomes what is known as a *wet buckle*, and it tends to stop at that point. In the case of integral joints, the propagating buckle usually is stopped by the increased thickness of the pipe upset. In that case, the upset serves as a "buckle arrestor." In the case of flush joint casing, the buckle might continue to propagate until the pressure differential is less than the buckle propagation pressure, or it may stop if it becomes a wet buckle from an opening at one of the collapsed connections. An extreme example is coiled tubing that has no connections; if it collapses, the buckle propagates until the pressure differential is less than the propagation pressure. There are formulas for collapse strength but not for buckle propagation. Buckles have been observed to propagate at pressures of about 65% or so of the initial collapse pressure (see Yeh and Kyriakides [20]; Kyriakides, Babcock, and Elyada [21]; Chater and Hutchinson [22]). For an exhaustive treatment see also the excellent book on offshore pipelines by Kyriakides [23].

Interestingly the case of casing collapsed around tubing is often one of the easiest to repair because maximum dimension of the collapsed casing is less than the ID of the un-collapsed casing. The tubing

itself is almost never collapsed and provides a passage through the collapsed casing for a chemical cutter, can be easily cut internally itself, and provides a smooth internal surface for a spear. Since the maximum dimension of the collapsed casing is less than the un-collapsed casing it can be retrieved once cut free.

Traditional API collapse formula

The API formula for collapse is not a single formula, but rather four:

- Yield strength collapse formula
- Plastic collapse formula
- Transition collapse formula
- Elastic collapse formula

Each formula has a range for which it is valid, depending on the yield strength of the material and the ratio of the outside diameter to the wall thickness.

Yield collapse formula

$$\boxed{p_{\mathrm{YC}} = 2Y\left[\frac{(d_{\mathrm{o}}/t_{\mathrm{w}}) - 1}{(d_{\mathrm{o}}/t_{\mathrm{w}})^2}\right]} \tag{6.19}$$

Valid range:

$$(d_{\mathrm{o}}/t_{\mathrm{w}}) \leq \frac{A - 2 + \sqrt{(A-2)^2 + 8\,(B + C/Y)}}{2\,(B + C/Y)} \tag{6.20}$$

Plastic collapse formula

$$\boxed{p_{\mathrm{PC}} = Y\left[\frac{A}{(d_{\mathrm{o}}/t_{\mathrm{w}})} - B\right] - C} \tag{6.21}$$

Valid range:

$$\frac{A - 2 + \sqrt{(A-2)^2 + 8\,(B + C/Y)}}{2\,(B + C/Y)} < (d_{\mathrm{o}}/t_{\mathrm{w}}) \leq \frac{Y\,(A - F)}{C + Y\,(B - G)} \tag{6.22}$$

Transition collapse formula

$$\boxed{p_{\mathrm{TC}} = Y\left[\frac{F}{(d_{\mathrm{o}}/t_{\mathrm{w}})} - G\right]} \tag{6.23}$$

Valid range:

$$\frac{Y\,(A-F)}{C+Y\,(B-G)} < (d_o/t_w) \leq \frac{2+B/A}{3B/A} \tag{6.24}$$

Elastic collapse formula

$$\boxed{p_{EC} = \frac{46.95\times 10^6}{(d_o/t_w)\,[(d_o/t_w)-1]^2}} \tag{6.25}$$

Valid range:

$$(d_o/t_w) > \frac{2+B/A}{3B/A} \tag{6.26}$$

where

d_o = outside diameter
t_w = nominal wall thickness
Y = yield stress of pipe
p_{YC} = collapse pressure, yield pressure formula
p_{PC} = collapse pressure, plastic formula
p_{TC} = collapse pressure, transition formula
p_{EC} = collapse pressure, elastic formula

As with most API formulas, the units are not consistent, so for USC units with dimensions in inches and psi the API constants in those formulas are calculated with:

$$\boxed{\begin{aligned}
A &= 2.8762 + 0.10679\times 10^{-5}Y + 0.21301\times 10^{-10}Y^2 - 0.53132\times 10^{-16}Y^3\\
B &= 0.026233 + 0.50609\times 10^{-6}Y\\
C &= -465.93 + 0.030867Y - 0.10483\times 10^{-7}Y^2 + 0.36989\times 10^{-13}Y^3\\
F &= \frac{46.95\times 10^6\left[\dfrac{3B/A}{2+(B/A)}\right]^3}{Y\left[\dfrac{3B/A}{2+(B/A)}-(B/A)\right]\left[1-\dfrac{3B/A}{2+(B/A)}\right]^2}\\
G &= FB/A
\end{aligned}} \tag{6.27}$$

For SI units, where yield stress is in MPa and diameter in mm, the collapse formulas and range formulas are the same, but the API constants are calculated from the following formulas:

$$
\begin{aligned}
A &= 2.8762 + 0.15489 \times 10^{-3} Y + 0.44809 \times 10^{-6} Y^2 - 0.16211 \times 10^{-9} Y^3 \\
B &= 0.026233 + 0.73402 \times 10^{-4} Y \\
C &= -3.2125 + 0.030867 Y - 0.15204 \times 10^{-5} Y^2 + 0.77810 \times 10^{-9} Y^3 \\
F &= \frac{3.237 \times 10^5 \left[\dfrac{3B/A}{2 + (B/A)} \right]^3}{Y \left[\dfrac{3B/A}{2 + (B/A)} - (B/A) \right] \left[1 - \dfrac{3B/A}{2 + (B/A)} \right]^2} \\
G &= FB/A
\end{aligned}
\tag{6.28}
$$

Numerical values of the constants are listed in tables in API 5C3 and elsewhere. They are of little use though, because the values calculated with those constants are already published in API 5C2 and many other sources. However, when one finds it necessary to calculate collapse for some casing not having a standard yield value (the only time one would need the values of the constants), the table values of the constants are of no use.

One of the tedious tasks in using these equations for manual calculations is the process of calculating the API constants and then going through the range formulas in order to determine which collapse formula to use. It is easy to program this process in a spreadsheet, but there is another way to do this. A useful chart (see Figure 6.6) can be used instead, without calculating any of the constants. Once the correct formula is determined from the chart, then one need calculate only those API constants appearing in that formula. The API range formulas are only valid for API yield values from 40,000 to 125,000 psi. These range formulas result from curve-fitting of data, and they behave quite badly outside the range of

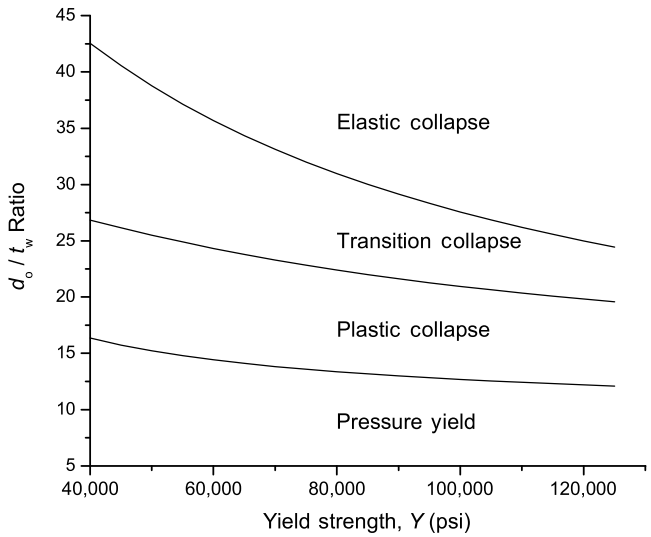

Figure 6.6 Valid range for API collapse formulas.

API yield values, especially in the low range below 40,000 psi. In other words, *do not extrapolate these curves outside the yield value range shown in the figure*.

The yield collapse formula is based on the external pressure that causes yield to occur at the inner wall of the casing, so that the yield strength is the design limit. Usually, the pipe will not collapse at that pressure. The elastic collapse formula is based on elastic stability and does not depend on the yield strength of the casing. The plastic collapse and the transition collapse formulas are based on tests done on casing samples, and the formulas essentially are curves fitted to the test results. The end of each range for the various formulas is the intersection of the curves for each formula.

Improved collapse formula

There are difficulties with the traditional API collapse formulas other than that they are not valid for collapse in combination with tension; for instance, only the elastic collapse formula is valid in tension. Also, the collapse tests on which they were based were performed with very short sections of casing, and work done in recent years has shown that the values in those tests were affected by the end conditions. In the more recent ISO/TR 10400 standard, a new approach is recommended. The new formulas are based on work originally done by Tamano, Mimaki, and Yanagimoto [24] and recently published by Klever and Tamano [25]. The full formula contains terms for inclusion of defects, ovality, eccentricity, and so forth. Although not yet accepted universally, it is an improvement on the traditional API formulas, plus it has the advantage of being able to include known data about the specific pipe for a casing string and can be used in probabilistic casing design methods. The formula essentially contains a yield collapse formula and an elastic collapse formula and accounts for the transition between those two:

$$p_{\text{clps}} = \frac{p_{\text{elas}} + p_{\text{yld}} - \left[\left(p_{\text{elas}} - p_{\text{yld}}\right)^2 + 4p_{\text{elas}}p_{\text{yld}}H_{\text{t}}\right]^{\frac{1}{2}}}{2\left(1 - H_{\text{t}}\right)} \tag{6.29}$$

where

$$p_{\text{elas}} = \frac{0.825\,(2E)}{\left(1 - \nu^2\right)\left(\frac{d_{\text{o}}}{t_{\text{w}}}\right)\left(\frac{d_{\text{o}}}{t_{\text{w}}} - 1\right)^2} \tag{6.30}$$

is the elastic collapse portion, and

$$p_{\text{yld}} = 2k_{\text{y}}Y\left(\frac{t_{\text{w}}}{d_{\text{o}}}\right)\left(1 + \frac{t_{\text{w}}}{2d_{\text{o}}}\right) \tag{6.31}$$

is the yield collapse portion.

In these formulas, k_{y} is a bias factor for yield collapse, and H_{t} is a decrement factor for the transition region between elastic and plastic collapse. These values can be determined from actual tests of the casing to be used or one can use the default values in the tables of ISO/TR 10400, as shown in Table 6.2.

These results from this method will vary slightly from the values calculated with the traditional formulas from API 5C3. The new method is considered to be more accurate.

The procedure for calculating reduced tension/collapse using this method is much easier than the traditional API method. We will show examples of both methods of collapse combined with tension

Table 6.2 Collapse Yield-Bias and Transition-Decrement Factors from ISO 10400 [11]

	Cold Rotary Straightened		Hot Rotary Straightened	
API Grade	H_t	k_t	H_t	k_t
H-40	0.164	0.910	n/a	n/a
J-55	0.164	0.890	n/a	n/a
K-55	0.164	0.890	n/a	n/a
M-65	0.164	0.880	n/a	n/a
L-80	0.164	0.855	0.104	0.865
L-80 9Cr	0.164	0.830	n/a	n/a
L80 13Cr	0.164	0.830	n/a	n/a
N-80 as rolled	0.164	0.870	n/a	n/a
N-80 Q&T	0.164	0.870	0.104	0.870
C-90	n/a	n/a	0.104	0.850
C-95	0.164	0.840	0.104	0.855
T-95	n/a	n/a	0.104	0.855
P-110	0.164	0.855	0.104	0.855
Q-125	n/a	n/a	0.104	0.850

later in this chapter, but for now, we look at an example of a collapse calculation with the new formula in the absence of tension.

EXAMPLE 6.3 Using the Improved Collapse Formulas

We apply these new formulas to determine the collapse rating of 7 in. 32 lb/ft N-80 casing. We calculate the wall thickness first:

$$t_w = \frac{1}{2}(d_o - d_i) = \frac{1}{2}(7.000 - 6.094) = 0.453\,\text{in}$$

Next, we calculate the elastic collapse using Equation (6.30):

$$p_{elas} = \frac{0.825\,(2E)}{(1-\nu^2)\left(\frac{d_o}{t_w}\right)\left(\frac{d_o}{t_w}-1\right)^2}$$

$$= \frac{0.825\,(2)\left(30\times10^6\right)}{\left(1-0.28^2\right)\left(\frac{7.000}{0.453}\right)\left(\frac{7.000}{0.453}-1\right)^2}$$

$$= 16,641\,\text{psi}$$

then, the yield collapse, using Equation (6.31):

$$p_{yld} = 2k_y Y\left(\frac{t_w}{d_o}\right)\left(1+\frac{t_w}{2d_o}\right)$$

$$= 2\,(0.870)\,(80000)\left(\frac{0.453}{7.000}\right)\left(1+\frac{0.453}{2\,(7.000)}\right)$$

$$= 9300\,\text{psi}$$

Now, we use these values in Equation (6.29) to calculate the collapse rating of the casing:

$$p_{clps} = \frac{p_{elas} + p_{yld} - \left[\left(p_{elas} - p_{yld}\right)^2 + 4p_{elas}p_{yld}H_t\right]^{\frac{1}{2}}}{2\left(1 - H_t\right)}$$

$$= \frac{16641 + 9300 - \left[(16641 - 9300)^2 + 4\,(16641)\,(9300)\,(0.164)\right]^{\frac{1}{2}}}{2\,(1 - 0.164)}$$

$$\approx 8060\,\text{psi}$$

This is the value of collapse we would read from a table that uses the proposed new collapse formula (recall that API rounds values to the nearest 10 psi). It is a bit lower than the current published value of 8600 psi calculated using the current API formulas. Partly, this reflects that many of the early API tests used short tube samples, which generally gave higher collapse values. Also, the new formula distinguishes between cold and hot rotary straightened pipe. We used the cold value here, but N-80 is one grade that is straightened by either method.

6.5 Combined loading

Almost always, casing is subjected to some type of combined loading. Here are the most common individual types:

- Tensile and compressive loads attributable to gravitational forces, borehole friction, hydrostatic forces, and bending forces
- Collapse and burst loads from hydrostatic pressures
- Torsion loads from borehole friction

There are various ways to calculate a design limit for combined loading. Most of them work, but some are quite misleading and can cause serious problems if one does not understand the limitations. We are going to look at a simple method that has been around for more than 150 years and in publication for almost 100 years. It has proven effective throughout all those years in all engineering design applications.

6.5.1 A yield-based approach

As we have already stated we generally use the yield strength (elastic limit) as our design limit. So, what we would like to have is some method of quantifying the combined loads into a single value to compare with some simple strength or stress value for the material of the tube. For example, if Y is the yield stress determined from a uniaxial test and Ψ represents the combined load, we might compare them thus:

$$Y > \Psi \quad \rightarrow \quad \text{no yield} \tag{6.32}$$

$$Y \leq \Psi \quad \rightarrow \quad \text{yield} \tag{6.33}$$

where Ψ is a yield measure as defined in Appendix C. This is exactly what we looked at with the von Mises yield criterion previously. The only practical difficulty we have at this point is that casing loads generally are known in terms of axial force, pressure (internal and external), and possibly torque. We

need stress values for the von Mises yield criterion. We make use of the Lamé formulas for those stress components. The yield-based approach is best illustrated by an example.

EXAMPLE 6.4 Combined Loads in a Yield-Based Approach

Suppose we have a point in a casing string where the internal pressure is 4000 psi, the external pressure is 4000 psi, and the true tension in the pipe at this point is 160,000 lbf. Our casing is 7 in. 23 lb/ft, K-55. It has an internal diameter of 6.366 in. We increase the pressure at the surface to 4000 psi to test it for a planned stimulation; the internal pressure at our point of interest will be 8000 psi. Will the pipe yield under this load?

First of all, we want to determine where the pipe will yield first, at the inner wall or the outer wall. Internal or external pressure always causes yield at the inner wall first, as mentioned previously. We have no bending or torque in the pipe, which always causes yield at the outer wall first. So, we require the yield condition at the inner wall. Second is that the test pressure of 4000 psi is applied after the casing is cemented and hung off at the surface (i.e., the ends are fixed), so we must account for the effect of that pressure change on the axial stress.

Determine the axial stress before the pressure test:

$$\sigma_{z_0} = \frac{F_z}{A_t} = \frac{160000}{\frac{\pi}{4}\left(7.00^2 - 6.366^2\right)} = 24,040\,\text{psi}$$

Determine the radial stress before the pressure test using the Lamé equation for the inner wall (Equation (6.5)):

$$\sigma_{r_0} = -p_i = -4000\,\text{psi}$$

Determine the radial stress when the test pressure is applied:

$$\sigma_r = -8000\,\text{psi}$$

Determine the tangential stress before pressure test using the Lamé equation for the inner wall (Equation (6.6)):

$$\sigma_{\theta_0} = \frac{p_i\left(r_o^2 + r_i^2\right) - 2p_o r_o^2}{\left(r_o^2 - r_i^2\right)}$$

$$= \frac{4000\left[(7/2)^2 + (6.366/2)^2\right] - 2\,(4000)\,(7/2)^2}{(7/2)^2 - (6.366/2)^2}$$

$$= -4000\,\text{psi}$$

Determine the tangential stress when the test pressure is applied:

$$\sigma_\theta = \frac{8000\left[(7/2)^2 + (6.366/2)^2\right] - 2\,(4000)\,(7/2)^2}{(7/2)^2 - (6.366/2)^2} = 38,260\,\text{psi}$$

Determine the incremental radial and tangential stress from the test pressure:

$$\Delta\sigma_r = \sigma_r - \sigma_{r_0} = -8000 - (-4000) = -4000\ \text{psi}$$

$$\Delta\sigma_\theta = \sigma_\theta - \sigma_{\theta_0} = 38260 - (-4000) = 42,260\,\text{psi}$$

Then, using the Lamé equation for fixed end tubes (Equation (6.4)), calculate the change in axial stress caused by the test pressure:

$$\Delta\sigma_z = \nu\,(\Delta\sigma_\theta + \Delta\sigma_r) = 0.28\,(42260 - 4000) = 10,710\,\text{psi}$$

The axial stress including the test pressure effects is

$$\sigma_z = \sigma_{z0} + \Delta\sigma_z = 24040 + 10710 = 34,750\,\text{psi}$$

Now, using the three stress components calculated in the presence of the test pressure, we want to determine whether or not yield will occur. Since there is no torsion, these values are principal stress components and may be plugged directly in to the von Mises yield formula:

$$\Psi = \left\{\frac{1}{2}\left[(\sigma_\theta - \sigma_r)^2 + (\sigma_r - \sigma_z)^2 + (\sigma_z - \sigma_\theta)^2\right]\right\}^{\frac{1}{2}}$$

$$\Psi = \left\{\frac{1}{2}\left[(38260 + 8000)^2 + (-8000 - 34750)^2 + (34750 - 38260)^2\right]\right\}^{\frac{1}{2}}$$

$$\Psi = 44,610\,\text{psi}$$

Finally, check the yield condition:

$$Y = 55,000\,\text{psi}$$

$$\Psi = 44,610\,\text{psi}$$

$$Y > \Psi \quad \rightarrow \quad \text{no yield}$$

In this case, there is no yield. The combined load in this example is approximately 90% of the yield strength of the pipe. Questions might arise: How close to the yield strength would we design if we were aware of these calculations? What would be a reasonable limit? What are the recommended design factors for combined loading? Those are good questions, and there are no standard answers. Some operators would go up to 80% of the yield in a case like this, which would amount to a design factor of 1.25. That might be acceptable for a one-time occurrence, where the specifics are known in detail. If we were spot checking a conventional casing design for a well that had not been drilled, we might want to think again. In those cases, our confidence level might be somewhat less, so we might set a 1.6 design factor as an absolute minimum. You are on your own in this area, unless your company has some particular policy.

One other caveat about using yield stress as a limiting point in combined loading is that it does not account for collapse at loads lower than the yield strength of the casing. You should always check the collapse using the combined load collapse formulas of API or ISO, which are covered in the next two sections.

6.5.2 A simplified method

There is a very simple method for adjusting casing to account for combined tension/collapse loads. It has been used by a number of operating companies for many years, and when combined with design

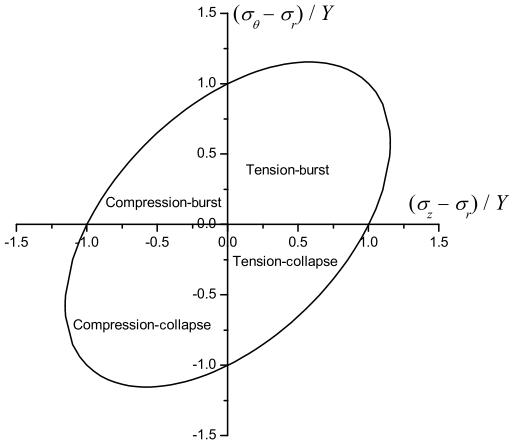

Figure 6.7 The two-dimensional von Mises yield criterion.

factors, it has proven workable for most normal vertical wells. It has its basis in a more theoretical context but has been simplified for easy use. Some would say it is oversimplified and that is an accurate statement, because it departs from theory and the results tend to be somewhat conservative. It is based on a 2D plot of the von Mises yield criterion where it intercepts the $\sigma_\theta - \sigma_z$ principal stress plane (see Figure 6.7).

Here is how the method works: We take the tension load of the casing at the point of interest, and divide it by the joint tensile strength of the casing to get a decimal fraction. Then, we then locate that point on the horizontal tension/compression axis. From there, we go down vertically to the point of intersection with the ellipse. From that intersection, we go left horizontally to the vertical burst/collapse axis and read the collapse fraction. We multiply the collapse rating of the pipe by that fraction. That gives us a reduced collapse rating of the casing under that amount of tensile load.

EXAMPLE 6.5 Simplified Tension/Collapse Adjustment

- Joint tensile strength = 547,000 lbf
- API collapse rating = 1130 psi
- Tensile load = 61,200 lbf

We determine the fraction of tensile load to the tensile strength:

$$\frac{61200}{547000} \approx 0.1$$

We go to the positive 0.1 point on the horizontal axis, down to the intersection with the ellipse, then horizontally to the vertical axis, where we read a value of 0.94. We multiply the collapse rating by this fraction to get a reduced collapse rating:

$$0.94\,(1130) \approx 1060\,\text{pasi}$$

This value of 1060 psi is taken to be the reduced collapse rating at that point. If our design plot has a higher value, then we must adjust our casing string accordingly.

The chart in this method is based on a yield criterion for steel known as the von Mises yield criterion, which we discuss in detail in Appendix C. A formula can be derived from the plot for the quadrant concerning tension and collapse:

$$k_{\text{clps}} = \sqrt{1 - 0.75k_{\text{tens}}^2} - 0.5k_{\text{tens}} \tag{6.34}$$

where

k_{clps} = fraction of collapse rating, i.e., $\tilde{p}_{\text{clps}}/p_{\text{clps}}$ (reduced clps /clps rating)

k_{tens} = fraction of tensile rating, i.e., F/F_{tens} (tens load/joint tens strength)

To calculate the reduced collapse pressure of casing with axial tension, the factor calculated in Equation (6.34) is multiplied by the published collapse pressure (without tension):

$$\tilde{p}_{\text{clps}} = k_{\text{clps}}\, p_{\text{clps}} \tag{6.35}$$

This method should be used with caution: perhaps I should not even include it here, but it has been in common use for many years by many people for non-critical wells and with success. It is not the API method for calculating tension/collapse combined loads, nor is it the improved method of the ISO. It might be called a quick-and-dirty method that proved successful in many normal pressured wells all over the world before the days of electronic calculators and computers. While that approach is simple in its graphical form, it is not as well accepted if one is actually going to do the calculations. The reason for this is that the graph is based on stresses rather than loads and joint strength. The joint strength of a tube in tension is based on the connection strength rather than the cross-sectional area of the tube itself.

I have intentionally presented the 2D von Mises yield criterion in Figure 6.7 in a format too small for use because I do not want you to use this method. If you are intent on using it however, you can plot a larger one for yourself using Equation (6.38).

You may also note that the chart in this procedure shows a reduction of burst strength in axial compression. Additionally, it shows an increase in collapse strength in axial compression and an increase in burst strength in axial tension. While this is true, almost no one uses a simple chart like this for those cases in practice. Increases in burst or collapse resistance from axial loads are seldom considered in basic casing design. Likewise, a case of reduced burst, which almost always results from axial compression from thermal expansion, is not considered using such a simple method. These types of combined loads are generally considered only in more-advanced designs and more-sophisticated methods are used rather than reading simple values from a chart like this. We discuss those issues later.

6.5.3 Improved simplified method

A more consistent way of expressing the reduced collapse fraction based on stresses is as follows:

$$\boxed{k_{\text{clps}} = \sqrt{1 - 0.75\left(\frac{F}{A_{\text{t}}Y}\right)^2} - 0.5\frac{F}{A_{\text{t}}Y}} \tag{6.36}$$

where

Y = yield strength

F = axial load

A_{t} = cross-sectional area of tube body

and the reduced collapse rating is calculated with Equation (6.35). This is the formula we used in Chapter 4. A similar approach was proposed by Wescott, Dunlop, and Kimler [26] that attempts to account for the difference in the thickness of the tube body and the area under the threads. Their formula is

$$\boxed{k_{\text{clps}} = \sqrt{1 - 0.932\left(\frac{F}{A_t Y}\right)^2} - 0.26\frac{F}{A_t Y}} \tag{6.37}$$

where the variables are the same as in Equation (6.36).

EXAMPLE 6.6 Simple Formulas for Reduced Collapse

Using Equation (6.34) in our previous example, we get the same conservative collapse value we got from the plot in Figure 6.7 (assuming we can read the graph accurately):

$$k_{\text{clps}} = \sqrt{1 - 0.75 f_{\text{tens}}^2} - 0.5 f_{\text{tens}}$$

$$= \sqrt{1 - 0.75\left(\frac{61200}{547000}\right)^2} - 0.5\left(\frac{61200}{547000}\right) = 0.939$$

$$\tilde{p}_{\text{cpls}} = k_{\text{clps}} p_{\text{clps}} = 0.939\,(1130) \approx 1060\,\text{psi}$$

If, instead, we use Equation (6.36) for this example, we get a slightly higher value for the reduced collapse:

$$k_{\text{clps}} = \sqrt{1 - 0.75\left(\frac{61200}{\frac{\pi}{4}\left(13.375^2 - 12.615^2\right)(55000)}\right)^2}$$

$$- 0.5\left(\frac{61200}{\frac{\pi}{4}\left(13.375^2 - 12.615^2\right)(55000)}\right) = 0.962$$

$$\tilde{p}_{\text{clps}} = k_{\text{clps}}\, p_{\text{clps}} = 0.962\,(1130) \approx 1090\,\text{psi}$$

Using Equation (6.37) we get

$$k_{\text{clps}} = \sqrt{1 - 0.932\left(\frac{61200}{547000}\right)^2} - 0.26\left(\frac{61200}{547000}\right) = 0.965$$

$$\tilde{p}_{\text{clps}} = 0.965\,(1130) \approx 1090\,\text{psi}$$

The difference in the last two equations in that example is that Equation (6.36) is based on the von Mises ellipse:

$$x^2 - xy + y^2 = 1 \tag{6.38}$$

and Equation (6.37) is a modified version that uses the axial load and the joint strength as developed by Wescott et al. [26], based on the ellipse:

$$x^2 - 0.52xy + y^2 = 1 \tag{6.39}$$

The axial stress formula (6.36) has been used for many years with success and generally is preferable to the conservative method of Equation (6.34). Recall that Equation (6.36) is the one we used in our example designs in Chapter 4, and it also appears in the minimum casing design requirements of the AEUB as the preferred formula [15]. The second formula (6.37) currently appears in the catalog of a major casing manufacturer and has seen many years of use. It might appear that the differences between these formulas are a bit trivial, but since they appear in various sources, usually without explanation, my purpose here has been to explain the differences.

6.5.4 Traditional API method

Because collapse is a stability and post-buckling event, we cannot use a strictly yield based approach like we considered earlier. However, since a yield value appears in three of the four API collapse formulas (elastic collapse is not affected by yield strength), yield certainly plays a role in collapse.

The traditional API method for calculating the effects of combined loads has a basis in the von Mises yield criterion, and the method is published in API Bulletin 5C3. The reason it is referred to here as the "traditional" API method is because it may be phased out with the adoption of the newer ISO/TR 10400 standards. But, as of this writing, the traditional method has not been officially replaced.

We will derive and show the equations for this method, but the method may be summarized as follows: The API method uses the fractional axial stress, σ_z/Y, to calculate a fractional tangential stress, σ_θ, using an equation for the lower right-hand quadrant of the 2D plot of the von Mises yield criterion (see Figure 6.7). This method assumes the radial stress, σ_r, from internal pressure is negligible, so that the tangential stress, σ_θ represents the yield strength in collapse. The fractional tangential stress is then multiplied by the original uniaxial yield strength of the pipe to give us a "reduced" yield value. This reduced yield value is then substituted into one of the four API collapse formulas to calculate the reduced collapse rating of the pipe. Although this method is not especially good engineering, it is preferable to the previous simplified methods. It is *extremely important* to understand though, that *the presence of tension does not actually reduce the yield strength of the tube, but merely moves the loading stress to a different position on the yield criterion curve* so that we are using a different value from that of the uniaxial yield. This value is referred to as a "reduced" yield because all the off-axis values on the yield curve in the lower right-hand quadrant of the Figure 6.7 are less than unity.

Earlier in this chapter, we used a 2D version of the von Mises yield surface (Equation (6.36)). That is where the traditional API-based approach begins. The von Mises yield surface in two dimensions is

$$\frac{\sigma_1 - \sigma_2}{Y} = \frac{\sigma_3 - \sigma_2}{2Y} \pm \sqrt{1 - \frac{3(\sigma_3 - \sigma_2)^2}{4Y^2}} \tag{6.40}$$

where σ_1, σ_2, and σ_3 are the three principal stress components. In the absence of shear components, such as torsion, the three principal stress components are σ_θ, σ_r, σ_z and we may substitute them into Equation (6.40) to get a convenient form for our use:

$$\frac{\sigma_\theta - \sigma_r}{Y} = \frac{\sigma_z - \sigma_r}{2Y} \pm \sqrt{1 - \frac{3(\sigma_z - \sigma_r)^2}{4Y^2}} \tag{6.41}$$

We purposely set the stress components in that order, so that the radial stress is the one we want to subtract from the other components. The radial stress is the negative value of the internal pressure (recall that yield from internal or external pressure always occurs at the inner wall first). If it is zero, we can leave it out, but in any event, we should know its value, so for now we rewrite it with the internal pressure:

$$\frac{\sigma_\theta + p_i}{Y} = \frac{\sigma_z + p_i}{2Y} \pm \sqrt{1 - \frac{3(\sigma_z + p_i)^2}{4Y^2}} \tag{6.42}$$

Plotted it is an ellipse exactly like Figure 6.7 except $-p_\mathrm{i}$ is substituted for σ_r and the terms, $(\sigma_\theta - \sigma_r)$ and $(\sigma_z - \sigma_r)$, become $(\sigma_\theta + p_\mathrm{i})$ and $(\sigma_z + p_\mathrm{i})$, respectively.

Now, here is how API uses this 2D formulation. API assumes that the tangential stress becomes an effective yield stress for collapse. So, we define an effective yield stress in collapse as

$$\tilde{Y} \equiv -\sigma_\theta \tag{6.43}$$

We may rewrite Equation (6.42), adjusting the signs to account for the fact that the tangential stress is compressive (negative) in a collapse situation:

$$\tilde{Y} = Y\sqrt{1 - \frac{3}{4}\left(\frac{\sigma_z + p_\mathrm{i}}{Y}\right)^2} + \frac{p_\mathrm{i} - \sigma_z}{2} \tag{6.44}$$

This is essentially the API formula, except the API version assumes that the internal pressure is negligible or zero and, hence, uses the following formula:

$$\boxed{\tilde{Y} = Y\sqrt{1 - \frac{3}{4}\left(\frac{\sigma_z}{Y}\right)^2} - \frac{\sigma_z}{2}} \tag{6.45}$$

This formula is used to calculate a reduced yield value, $\tilde{Y}$. That reduced yield value then is used in the appropriate API collapse formula, from the earlier section on API collapse, to determine the reduced collapse value caused by the tension.

EXAMPLE 6.7 Traditional API Method

Using data from the production casing example in Chapter 4: 7 in. 32 lb/ft N-80 casing (ID = 6.094 in.) and an axial load at the bottom of that section of 41,739 lbf, we want to determine the reduced collapse strength of the casing.[3] The published API collapse value with no tension is 8600 psi.

We calculate the reduced yield using Equation (6.45):

$$\tilde{Y} = 80000\sqrt{1 - \frac{3}{4}\left(\frac{41739}{\frac{\pi}{4}\left(7.000^2 - 6.094^2\right)(80000)}\right)^2}$$

[3] Normally we would roundoff such a value, but we use the same value as in the example production casing so as to compare results of the various methods.

$$-\frac{1}{2}\left[\frac{41739}{\frac{\pi}{4}\left(7.000^2-6.094^2\right)}\right]$$

$$= 77,666\,\text{psi}$$

We now must determine which API collapse formula to use. To do that, we need the value of d_o/t_w:

$$\frac{d_o}{t_w} = \frac{d_o}{0.5\,(d_o - d_i)} = \frac{7.000}{0.5\,(7.000-6.094)} = \frac{7.000}{0.453} = 15.453$$

We also need the API formula constants at the reduced yield strength. Without showing the calculations, we calculate them from the formulas shown in the section on API collapse formulas (6.27):

$A = 3.062736$

$B = 0.065539$

$C = 1885.482$

$F = 1.993754$

$G = 0.042664$

We start with the range limit for yield collapse and Equation (6.20) using those constants and d_o/t_w = 15.453:

$$(d_o/t_w) \le \frac{3.062736-2}{2\,(0.065539+1885.482/77666)} + \frac{\sqrt{(3.062736-2)^2+8\,(0.065539+1885.482/77666)}}{2\,(0.065539+1885.482/77664)}$$

$$= 13.127$$

We see that our value of d_o/t_w is greater than that, so we must then check the formula for the upper range formula for plastic collapse formula which is Equation (6.22):

$$(d_o/t_w) \le \frac{77666\,(3.062736-1.993754)}{1885.482+77666\,(0.065539-0.042664)} = 22.769$$

Our d_o/t_w is within the range of the plastic collapse formula, so we use Equation (6.21) to calculate the reduced collapse strength of the casing:

$$\tilde{p}_{PC} = 77666\left[\frac{3.062736}{15.453} - 0.065539\right] - 1885.482 \approx 8420\,\text{psi}$$

This shows a reduction of 180 psi in the collapse resistance of the casing in tension. It is not much in this case, but it might put our design below the minimum design factor, in which case, we might have to adjust the design to compensate.

So far we have only accounted for collapse pressure in the form of a differential pressure, but the magnitude of the internal pressure does have some effect in combined loading. The traditional API method does account for this in the form of a correction for the presence of internal pressure.

$$\boxed{\tilde{p}_{clps} = p_{reduced} + p_i\left(1 - \frac{2t_w}{d_o}\right)} \tag{6.46}$$

It should be noted that the inclusion of internal pressure in our combined loading for collapse means that to use differential pressures as we did in our basic collapse load plots and design procedure we must subtract the internal pressure from the results of Equation (6.46). This complicates the basic design procedure somewhat. In the previous example, we did not add a pressure correction for internal pressure and use the actual external pressure as the collapse pressure, since our example production casing was designed assuming no internal pressure. But we will now illustrate a case where there is internal pressure in the following example.

EXAMPLE 6.8 Internal Pressure in API Traditional Method

In the case of the 7 in. 32 lb/ft production casing in the previous example, we examined the reduction in collapse resistance at a point where the tension was 41,739 lbf. In Chapter 4, we compared the reduced collapse pressure to the differential collapse pressure to adjust for combined loading using Equation (6.36), and made design adjustments accordingly. In that case the casing was evacuated so there was no concern for any internal pressure. But for this example let us assume that there is an internal pressure from, say a brine workover fluid, and the internal pressure is 3000 psi. What is our reduced collapse pressure in this case?

Just as in the previous example we use Equation (6.45) to calculate a reduced yield and then the plastic collapse formula to get a reduced collapse pressure of 8420 psi as compared to 8600 psi with no axial load. Then we substitute into Equation (6.46) as the p_{reduced} value:

$$\tilde{p}_{\text{clps}} = 8420 + 3000\left(1 - \frac{2\,(0.453)}{7.000}\right) \approx 11,030\,\text{psi}$$

This is the reduced collapse pressure with an internal pressure of 3000 psi. For comparison let us look at the differential load pressures with no internal pressure and with the 3000 psi internal pressure.

1) $\Delta p_{\text{clps}} = p_{\text{i}} - p_{\text{o}} = 0 - 8420 = -8420\,\text{psi}$
2) $\Delta p_{\text{clps}} = p_{\text{i}} - p_{\text{o}} = 3000 - 11030 = -8030\,\text{psi}$

What this illustrates is that the presence of internal pressure actually reduces the differential collapse resistance of the casing a bit further. Most casing designs do not account for this. However, in most cases, the presence of internal pressure reduces the magnitude of the differential loading so the additional reduction in collapse resistance may not be significant.

The necessity of determining which API collapse formula is applicable, as well as calculating the API constants for those formulas makes this a tedious process when done manually. In the case of standard yield strengths, like 80,000 psi, for instance, there are tables in API 5C3 and ISO/TR 10400 specifying the values of the five constants, but for our case of a yield of 77,664 psi, a nonstandard yield value, all the constants must be calculated. There are five constants in all, though only two appear in the transition collapse formula. In this case, all five had to be calculated to determine the correct formula to use. One can easily program the API method into a spreadsheet and avoid the tedium and inherent errors in doing the calculations manually.

The current API method does not account for combined loads in combination with burst. It is seldom considered in casing design, but when it is, the yield-based approach is used because burst is not a stability type event like collapse.

6.5.5 The API traditional method with tables

One need not do the preceding calculations to use the traditional API method. Tables published in API Bulletin 5C2 allow one to look up the reduced collapse value directly. For instance, in the example, we

could use Table 4 in API 5C2 [9]. It is in terms of axial stress rather than axial load, but it also gives the cross-sectional area of the tube to make the axial stress calculation easier if you have not already calculated it.

$\sigma_z = 41739/9.317 = 4480\,\text{psi}$

The table gives the collapse pressure corresponding to axial stress in 5000 psi increments, so for zero axial stress, the collapse pressure is 8610 psi, and at 5000 psi axial stress, the collapse value is 8400 psi. We may do a linear interpolation for 4480 psi axial load and get a collapse value of 8420 psi (rounded to nearest 10 psi) which is the value we got with the traditional API calculation method.[4] If you do not have a spreadsheet programmed for the API method, it is much easier to use Table 4 in API Bulletin 5C2.

6.5.6 Improved API/ISO-based approach

The proposed new API/ISO formula for combined tension and compression begins something like the current API method as far as calculating a reduced collapse strength, in that it first uses an equation to calculate a reduced yield value. The equation for calculating the reduced yield is

$$\tilde{Y} = \frac{1}{2}\left(\sqrt{4Y^2 - 3(\sigma_z)^2} - \sigma_z\right) \tag{6.47}$$

It is the same as the equation we used to calculate the reduced yield strength in the current API method with no internal pressure (Equation (6.45)) although in a slightly different form. The reduced yield from this formula then is used in Equation (6.31) to calculate a reduced yield collapse, which then is used in Equation (6.29) along with the elastic collapse from Equation (6.30) to calculate a reduced collapse strength without internal pressure. If there is internal pressure, then a correction using Equation (6.46) may be added. This internal pressure correction is called a simplified method in ISO/TR 10400 and gives results to an accuracy of ±5% when $0 \le \sigma_z/Y \le 0.4$. Outside that range, one should refer to ISO/TR 10400 for the more rigorous internal pressure correction method (currently listed in Appendix H of ISO 10400 [11]). This is an iterative solution technique.

EXAMPLE 6.9 Improved API/ISO Collapse Formula

We apply these new formulas to determine the reduced collapse rating of the 7 in. casing in the previous examples. In Section 6.4.3 we calculated the wall thickness (0.453 in.) and the collapse value without tension, which was 8060 psi, so we do not repeat those.

Now, we use an axial tension of 41,739 lbf to determine the reduced yield using Equation (6.47):

$$\tilde{Y} = \frac{1}{2}\left(\sqrt{4Y^2 - 3\left(\frac{F_z}{A_t}\right)^2} - \frac{F_z}{A_t}\right)$$

[4] If you noticed, we used a collapse value of 8600 psi in all our design calculations which is the value listed in the main tables of API 5C2. However, in Table 4 as mentioned above, it is listed as 8610 psi. The API formulas give a value of almost exactly 8605 psi depending on the precision of your calculating device. So this apparently accounts for why it is rounded to two different values in the main tables and Table 4 of API 5C2.

$$= \frac{1}{2}\left(\sqrt{4(80000)^2 - 3\left(\frac{41739}{\frac{\pi}{4}\left(7^2 - 6.094^2\right)}\right)^2} - \frac{41739}{\frac{\pi}{4}\left(7^2 - 6.094^2\right)}\right)$$

$$= 77,666 \text{ psi}$$

Note again that this is exactly the reduced yield value we calculated using the traditional API method in the earlier example. This method differs from the traditional method in the manner in which the reduced yield is used once calculated. The reduced yield value is then used in Equation (6.29). We may use the elastic collapse value of 16,641 psi that we calculated in Section 6.4.3 with Equation (6.30) because it is independent of yield strength, but we must re-calculate a reduced yield collapse value using Equation (6.31).

$$\tilde{p}_{\text{yld}} = 2k_{\text{y}}Y\left(\frac{t_{\text{w}}}{d_{\text{o}}}\right)\left(1 + \frac{t_{\text{w}}}{2d_{\text{o}}}\right)$$

$$= 2\,(0.870)\,(77666)\left(\frac{0.453}{7}\right)\left(1 + \frac{0.453}{2\,(7)}\right)$$

$$= 9028 \text{ psi}$$

Now, we plug this value and the elastic collapse value into Equation (6.29):

$$p_{\text{clps}} = \frac{p_{\text{elas}} + p_{\text{yld}} - \left[\left(p_{\text{elas}} - p_{\text{yld}}\right)^2 + 4p_{\text{elas}}p_{\text{yld}}H_t\right]^{\frac{1}{2}}}{2\,(1 - H_t)}$$

$$= \frac{16641 + 9028 - \left[(16641 - 9028)^2 + 4\,(16641)\,(9028)\,(0.164)\right]^{\frac{1}{2}}}{2\,(1 - 0.164)}$$

$$\approx 7870 \text{ psi}$$

The traditional API method gives a reduction of 180 psi from the published API collapse value of 8600 psi. This formula gives a reduction of 730 psi, from the published API collapse value. However, if one calculates the collapse value without tension using the improved formulas, the unloaded collapse value is 8060 psi, so this example is a reduction of 190 psi. The question is really whether the unloaded collapse value is 8600 psi as per the traditional API formulas or 8060 psi as given by the improved formulas. From the discussions in ISO/TR 10400 and the notes leading to the improved formulas, it would appear to favor the new formulas. All indications are that the newer formulas are better, but until the old ones are declared obsolete they will still be used by many.

6.6 Lateral buckling

Much has been written over the years about lateral buckling of oilfield tubulars. Some of it has been good, some a bit misinformed, and some even has been ludicrous. Lateral buckling is called columnar buckling in most areas of structural engineering, but lateral buckling of oilfield tubulars differs from the common concepts of columnar buckling as it is understood by most structural engineers. In most structural applications where gravity is considered, the load on the column is at the top of the column as opposed to the bottom as in our case. In those cases, gravitational forces tend to contribute to the tendency of a column to buckle. In the case of oilfield tubulars, the loading is a bit different. Usually,

the top of the column (casing or tubing) is fixed and the buckling load is caused by a reactive force on the bottom. The reactive force is caused by the weight of some portion of the column resting on bottom, some pressure force on the bottom, or a combination of both. Many refer to lateral buckling of casing as simply buckling. However, collapse is a form of buckling called radial buckling. There is also axial buckling, in which the casing is crushed in an axial direction. And, we could include torsional buckling. This section is about lateral buckling. Lateral buckling occurs when the casing becomes unstable and displaces laterally disproportionately to the magnitude of a very small lateral force.

6.6.1 Stability

The best way to visualize the concept of stability is with a simple and commonly used illustration. In Figure 6.8, three balls are in equilibrium on three surfaces. In case (a), a ball rests at the low point on a concave surface. The ball is in static equilibrium; in other words, it will not move unless some force is applied to it. If we nudge the ball with some small force, it will move slightly then return to its original position as soon as the small force, called a perturbation, is removed. Also note that to move it further from its initial position requires an increasing force the farther it is moved. This ball is in a state of stable equilibrium. In case (b), the ball rests on a flat horizontal surface. It is also in a state of static equilibrium. If a small force is applied, the ball will move. It will continue to move with no requirement that the force be increased as in the first case. It will stop when the force is removed, or if its environment is frictionless, it will continue to move at constant velocity until another force is applied to stop it or it falls off the edge of the surface. It will not return to its original position, however. We call this case conditionally stable equilibrium or sometimes neutrally stable equilibrium. The third case, (c), also is in static equilibrium, though, from a practical standpoint, we might have a bit of trouble comprehending how someone could get a ball to balance on the high point of convex surface. Nevertheless, it is easy to understand that, if we apply even the smallest of perturbations to this ball, it will roll off the surface. Once it starts to move, no additional force is required to keep it rolling away from its static equilibrium point. We call this condition unstable equilibrium. This last condition is the type of instability that concerns us with buckling of casing.

How does lateral buckling occur? If you consider the type of lateral or columnar buckling shown in most engineering texts, you will see something like Figure 6.9a.

Typically, these are weight-less columns with a vertical load applied at the top and the bottom either hinged or fixed. The initial buckling mode is in the form of a single curve. Other modes are possible (usually at higher loads), leading to sinusoidal-type configurations with an increasing number of nodes. These additional nodes are mostly theoretical, because once the column buckles into a single curve, the other modes are not possible unless some constraints are applied. A perfect beam with a perfectly applied axial load (as is the case of our mathematical models) never buckles laterally unless some perturbation

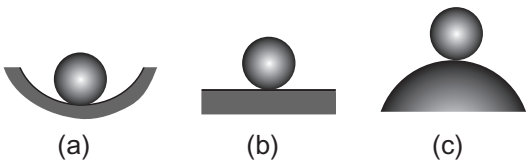

Figure 6.8 Equilibrium states: (a) stable, (b) neutrally stable, and (c) unstable.

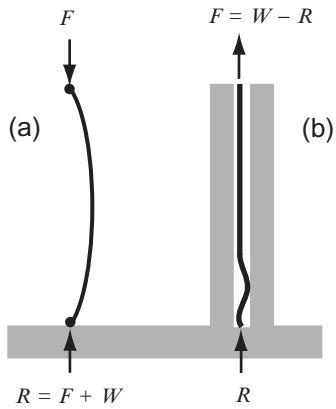

Figure 6.9 Lateral buckling: (a) typical structural column and (b) casing in borehole.

is applied. In other words, we could keep applying a load until the column yields in compression and deforms axially in a plastic regime, until it is just a lump of metal on the ground. For instance, the equation[5] for the elongation or compression of an elastic tube is

$$\Delta L = \frac{2F + w L^2}{2\pi \left(r_o^2 - r_i^2\right) E} \tag{6.48}$$

Nowhere in that equation is any allowance for lateral buckling, because there is no inherent instability in the formula itself. Lateral buckling has to be determined in other ways. As to casing in a wellbore, it usually is fixed on bottom with cement and has lateral constraint in the form of a borehole wall, Figure 6.9b. Buckling in this case is affected by the weight of the casing, and we see that only the lower part of the casing is buckled, because the buckling is caused by axial compression at the bottom from the weight of the casing. As the distance from the bottom increases, the axial compression decreases. When casing buckles in this manner, it initially may be in the shape of a sinusoidal curve, with decreasing frequency as the distance from the bottom increases, until a point is reached where there is no buckling. It may be even more extreme and form a helical shape in the wellbore, with decreasing pitch as the distance from bottom increases.

It would seem intuitive, then, that for lateral buckling to occur in casing, it would have to be caused by a compressive load and some small perturbation. For many years, it was assumed that, if casing was hung in tension throughout the full string or at least the portion of the string above the top of the cement, then lateral buckling could not occur. That sounds intuitively simple, and that was the assumption up until papers by Lubinski [27] and by Klinkenberg [28] and several discussions of those papers.

The Woods stability model

In 1951, in a discussion of the paper by Klinkenberg [28], Henry Woods [29] presented an example illustrating the buckling neutral point in a simple way that became something of a classic. It essentially showed that, contrary to popular intuition, lateral buckling could occur in casing in tension (under certain

[5] See Appendix C for derivation.

pressure conditions). Much of what had been done previously was based on intuition combined with an unfortunate lack of understanding of hydrostatics.

Woods, however, based his analysis on the theory of elastic stability, using a thought experiment with a weight-less tube in a hypothetical test chamber. The model as Woods set it up illustrates his point quite well, but it has been criticized because it does not model something that can occur in reality, even under the most ideal of conditions. I have modified his thought experiment to one that more realistically models an actual wellbore situation. This modified version gives exactly the same results and is perhaps more realistic in terms of our experience with casing in boreholes, see Figure 6.10. A weight-less tube is installed in a pressure test chamber, fixed at the lower end, and free at the upper end. While the upper end is free to move, it is closed internally with a frictionless pressure seal that does not move. There is also a frictionless pressure seal on the outside of the tube, between the upper chamber and lower chamber. The lower chamber, representing a wellbore annulus, has a pressure p_o, and inside the tube the pressure is p_i. The top chamber is open to the atmosphere, and the tube is held in tension at the top by a suspended weight, W. The tube is long enough that its stiffness against bending is negligible. Also, the chambers are large enough that the pressures in the lower chamber remains constant. Woods then said, if one could apply a small lateral force to the tube in the large chamber such that the tube would deflect laterally by a small amount, then the top of the tube would slide downward some small amount δL. And the suspended weight would rise by the same displacement, δL. The following volume changes would occur:

$$\delta V_o = -\pi r_o^2 \, \delta L$$

$$\delta V_i = \pi r_i^2 \, \delta L$$

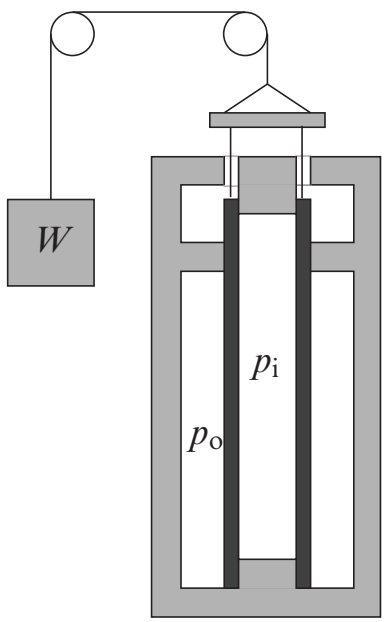

Figure 6.10 A modified Woods model.

Since pressure is in each of the places where volume changes occur, a change in potential energy in each place is equal to the change in volume times the pressure, and the total change in potential energy, $\delta\Pi$ is given by

$$\delta\Pi = \delta V_{\mathrm{o}} p_{\mathrm{o}} + \delta V_{\mathrm{i}} p_{\mathrm{i}} + \delta L\, W$$

$$\delta\Pi = \pi r_{\mathrm{o}}^2 \delta L p_{\mathrm{o}} - \pi r_{\mathrm{i}}^2 \delta L p_{\mathrm{i}} + \delta L\, W$$

The last term is the force, W, acting on the tube. We may express it in terms of axial stress as

$$W = A_{\mathrm{t}} \sigma_z = \pi \left(r_{\mathrm{o}}^2 - r_{\mathrm{i}}^2 \right) \sigma_z$$

We can substitute the axial stress into the equation:

$$\delta\Pi = \pi r_{\mathrm{o}}^2 \delta L p_{\mathrm{o}} - \pi r_{\mathrm{i}}^2 \delta L p_{\mathrm{i}} + \pi \left(r_{\mathrm{o}}^2 - r_{\mathrm{i}}^2 \right) \delta L\, \sigma_z$$

For this system to remain stable, the change in potential energy must be zero or positive:

$$\pi r_{\mathrm{o}}^2 \delta L p_{\mathrm{o}} - \pi r_{\mathrm{i}}^2 \delta L p_{\mathrm{i}} + \pi \left(r_{\mathrm{o}}^2 - r_{\mathrm{i}}^2 \right) \delta L\, \sigma_z \geq 0$$

$$\sigma_z \geq \frac{\pi r_{\mathrm{i}}^2 p_{\mathrm{i}} - \pi r_{\mathrm{o}}^2 p_{\mathrm{o}}}{\pi \left(r_{\mathrm{o}}^2 - r_{\mathrm{i}}^2 \right)}$$

We could then write the stability condition in a number of ways, four of which follow:

$$\boxed{\sigma_z \geq \frac{A_{\mathrm{i}} p_{\mathrm{i}} - A_{\mathrm{o}} p_{\mathrm{o}}}{A_{\mathrm{o}} - A_{\mathrm{i}}}} \tag{6.49}$$

$$\boxed{\sigma_z \geq \frac{ri^2 p_{\mathrm{i}} - r_{\mathrm{o}}^2 p_{\mathrm{o}}}{r_{\mathrm{o}}^2 - r_{\mathrm{i}}^2}} \tag{6.50}$$

$$\boxed{F_z \geq A_{\mathrm{i}} p_{\mathrm{i}} - A_{\mathrm{o}} p_{\mathrm{o}}} \tag{6.51}$$

$$\boxed{\sigma_z \geq \frac{1}{2} \left(\sigma_\theta + \sigma_r \right)} \tag{6.52}$$

The last version was derived using the Lamé formulas. Recall that the sum of the tangential stress and the radial stress is constant through the wall of the pipe, so it makes no difference whether they are calculated at the inner or outer wall, as long as both are calculated at the same point.

What Woods's model illustrates is the difference between the change in potential energy by a slight increase in the internal volume of the tube and slight decrease in the annular volume in addition to mechanical work done on the weight. If the deflection results in an increase in potential energy, then the tube is stable, whereas if it results in a decrease in potential energy, then it is unstable. If there is no change in potential energy, then it is conditionally stable. Obviously, if the internal pressure is

sufficiently greater than the external pressure, then the system is unstable, even when the axial stress is positive or in tension. Likewise, with a sufficiently higher external pressure, the system is stable when the axial stress is compressive. This particular article by Woods turned around a lot of thinking about landing practices for casing. His results have been generally accepted.

One of the most important concepts to come from the Woods' model is the concept of the neutral point as to lateral buckling. One interesting aspect of the equilibrium points derived from this model is in Equation (6.51). That might look vaguely similar to something we saw in Chapter 4, where we examined the relationship between the true and effective axial loads. If we rearrange it slightly, it shows that, at the neutral point,

$$F_z + (A_o p_o - A_i p_i) = 0 \tag{6.53}$$

Now, it should look familiar, because the left-hand side is exactly the effective load. So, at the neutral point for lateral buckling,

$$\boxed{\hat{F}_z = F_z + (A_o p_o - A_i p_i) = 0} \tag{6.54}$$

stating that the effective axial load is zero at the buckling neutral point. It can be seen that the condition of stability is exactly the same as the neutral point of an effective load curve calculated using a buoyancy factor as opposed to a true axial load curve. The neutral point in buckling is the point at which the effective load curve goes from compression to tension; that is, the point where the effective load is zero. If the pipe is off bottom, then the neutral point is at the bottom of the string, and *no amount of hydrostatic pressure can cause the string to buckle as long as its effective density (the pipe and its contents if closed ended) is greater than the fluid it is in*. Such was the basis for determining the length of the drill collars necessary in a bottom hole assembly to prevent lateral buckling of the drill pipe while rotating—a mode that leads to early failure in drill pipe. The simple formula

$$L_{DC} A_t \, (\rho_{steel} - \rho_{fluid}) \, g = W_{bit}$$

equates the buoyed weight of drill collars of length, L_{DC} and cross-sectional area, A_t to the desired weigh on the bit, W_{bit}. We can regroup the equation as

$$L_{DC} \, (A_t \rho_{steel}) \left(1 - \frac{\rho_{fluid}}{\rho_{steel}}\right) g = W_{bit}$$

where the first term in parentheses is the linear density of the drill collars and the second term in parentheses you will recognize as the buoyancy factor so

$$L_{DC} \, \rho_l \, k_b \, g = W_{bit}$$

and rearranging to solve for the length of the drill collar assembly

$$L_{DC} = \frac{W_{bit}}{\rho_l \, k_b \, g} \tag{6.55}$$

Standard practice called for two or three additional collars so that the neutral point was always within the drill collar string and not in the drill pipe at any time while rotating.

This simple formula worked well for many years, and still does because it is correct. Unfortunately, the consequences of this stability issue got lost for some in the 1960s, when some erroneously thought the transition point from axial compression to axial tension (the true axial load as calculated in

Chapter 3) should be the criterion instead. Only in an unbuoyed system where they are identical, is that true. There was no change in drill string failure rate by going to the true axial load which always required more drill collars, but at least it was a boon to rental tool companies. If one bought into that erroneous notion, then one would require drill collars even for rotating drill pipe off bottom since it is always in axial compression near the bottom of the string without drill collars. This of course, was ludicrous and fortunately most began to see that. The issue here is one of *stability and not axial compression*. Sadly that fact is still lost on many who should know better, and is still found in places from which it should have long since been purged.

Somewhat related to that error was also a notion that "drill pipe tool joints are not designed to drill in compression." That was nonsense back then, and is patently obvious today as we drill horizontal wells with drill pipe in compression all the time. Apparently this thinking arose from the fact that drilling with drill pipe in compression caused premature failure in the connections where the failure rate in drill collars in compression was much less. But even early on, when that view was widely held, many small drill collars had exactly the same connections as some drill pipe. The only difference was that some of the drill collar connections had a small relief area between the last thread and the connection shoulder whereas drill pipe tool joints usually did not. This allows more flexing in the connection with less fatigue failure, and that in itself is a clue to the reality of the problem. What seems to have gotten lost in all of this, both then and even now, is that all pipe (drill pipe, drill collars, tubing, and casing) that is in the unstable region will likely buckle laterally.[6] With the exception of tubing, the buckling itself is seldom a problem. It is the rotation while in the buckled configuration that causes the serious issues, especially in drill pipe. Contrary to what was a popular opinion for so long is that drill collars buckle too. The difference between drill pipe and drill collar buckling is the severity of the bending in the buckled configuration—slight for drill collars and more severe for drill pipe.

Here are some things you should understand about lateral buckling.

- Lateral buckling is a stability phenomenon.
- All pipe below the neutral point as determined with Equations (6.49)–(6.52) is unstable—always assume that it will buckle.
- The severity of buckling in drill pipe is greater than that of drill collars because of the respective clearance in the borehole.
- Lateral buckling itself seldom causes pipe failure.
- It is the rotation while in the buckled configuration that causes premature failure, not the buckling itself.
- Considerable care is taken in proper makeup torque with drill collars, but such is seldom the case with drill pipe.

Lateral stability is important in all phases of drilling and completions and often seems to be one of the least well understood. Having covered possibly more than enough on stability, we now turn to how it affects casing.

6.6.2 Lateral buckling of casing

As previously stated, lateral buckling of tubulars in wells has been a considerable topic for many years. It is quite a bit different from the structural engineer's typical columnar buckling, in that it is constrained by the walls of a bore hole. Possibly even more significant is that the buckling load is caused by a relative displacement from the bottom of the suspended column, and the resultant force at the bottom of the column is caused by both gravity and the elastic resistance of the column acting in the same direction.

[6] We are discussing vertical boreholes for now and will address inclined wellbores later.

Very little in typical columnar buckling of structures applies globally to a casing string because of the nature of the loading and the post-buckling constraints, but they are quite similar locally where we ignore the effects of gravity except in the form of an axial load.

Like most buckling, lateral buckling has bifurcation points into different modes. Few slender stand-alone structural columns ever reach a second bifurcation point because post-buckling deformation does not allow for it. Lateral buckling of tubes in wellbores does often result in additional bifurcations into additional modes. The first mode of lateral buckling is something like a single curve, which may become sinusoidal because of the borehole constraints and end conditions. In its most severe mode though, it becomes helical in shape. Most of us have seen a permanent helix in a recovered tubing string, work string, or tail pipe that was compressed beyond its yield strength.

For purposes of analysis we may (and do) idealize the post-buckling configuration as sinusoidal or helical locally, but because of the nature of the loading in a borehole, the configuration cannot be perfectly sinusoidal nor perfectly helical on a larger scale. The situation is even more complicated in an inclined wellbore (and all are inclined to some degree) because the constraint is not only curved axially, but also radially, and there is a definite gravitational force component transverse to the constraint (borehole) axis.

For the most part, buckling of casing in wellbores is not the problem it is with tubing or drill pipe. The primary reason for this is that the clearance between casing and the borehole wall is relatively small in most wells. So, even when it is buckled, the degree of buckling is so small in most cases that there are few serious consequences. If the buckling is severe enough, the casing actually could yield or fail. This is rare and almost always a consequence of some geotectonic activity, like subsidence, fault movement, and so forth. And, severe cases do happen with large temperature fluctuations. Less severe cases of buckling can have serious consequences too. One is the possibility of extensive casing wear in an intermediate string while drilling to the next casing point. Another is the difficulty of running and retrieving completion equipment in a buckled production string. So, for these reasons, we try to avoid any lateral buckling in casing. If we are using a slip-type casing hanger, we have some control over the final axial load in the non-cemented portion of the casing string. We may even be able to take into account possible thermal expansion and design our casing such that we can pull enough tension to avoid buckling. If we are using a mandrel-type hanger, there is not much we can do other than to try to support the casing with cement. When the top wiper plug is bumped at the end of the cement job and internal pressure is released, we have to live with whatever axial stress is in the non-cemented portion. The final motion with a mandrel hanger is always downward.

One of the most insidious forms of buckling can occur in a cemented section where there is an interval of bad cement and we have no means of controlling the axial load in the casing, no matter what type of hanger we have at the surface. Serious problems have arisen when casing in one of these sections of an intermediate string experiences increased temperatures from drilling and circulation in higher-temperature zones below the intermediate casing, as is discussed later in this chapter.

I end this part of the discussion with a comment about helical post-buckling. Most of the papers on the subject are based on experiments with rods under axial compression in tubes to simulate pipe inside a borehole. Mathematically, they are modeled as one-dimensional, two-point boundary value problems with a single degree of translational freedom at each boundary, one of which is static, and the other subjected to an axial load. There are three rotational degrees of freedom at each end as being understood but not constrained. In none of the early papers or experiments is torsion considered, and in fact some have mentioned that torsion is of no significance. It is interesting that in none of those rod experiments are any rotational degrees of freedom considered, especially rotation about the axial coordinate. So how

is torsion ruled out other than by intuition? What is the perturbation that causes the tube to bifurcate into a helix rather than another sinusoidal mode? Here is something we should understand about a helix: a straight rod (or tube) forced axially into a helix will require a rotation (twist) of 2π radians for each cycle of the helix if it is to be torsion free. If one end of the tube is not allowed to *rotate freely* with respect to the other end then there will be torsion in the tube. Likewise, when a helical buckle is released by pulling tension in the pipe, a full 2π rotation of the tube is required for each cycle of the helix if it is to be torsion free.[7] Logically one would assume from this that a right-hand rotation of a drill string at the surface and drag on a bit at the bottom would enhance the tendency for pipe to buckle somewhat helically (with a left-hand pitch) as a first mode rather than sinusoidally, yet torsion is not included in our basic buckling formulas. Why not? Any helically buckled tube that makes contact with a borehole or casing wall will have friction that will affect the freedom to rotate as helical pitch changes, and torsion will become a factor in the pitch of the helix and the stress state of the tube. So? I am posturing intuitively here, and have no intent or desire for getting personally involved in tubular buckling analysis. I mention all this to perhaps give you pause for thought.

Buckling in a vertical wellbore

The published work on buckling of vertical structural columns could fill a small library. As interesting as all that may be to some, it is of little practical consequence in casing design for reasons already mentioned. That is why this is the shortest section in this book. Seldom are real wellbores vertical. *If you do have a near-vertical wellbore and the effective load is in compression, assume the casing will buckle; you do not need a formula.*

Buckling in an inclined wellbore

It is a bit more difficult for casing to buckle in an inclined wellbore, because gravity tends to hold it to the low side of the bore hole. It can start to move away from the low side, but the farther it moves, the more it has to move up the side of the wellbore. In one sense, it is like the ball resting in the low point of a concave surface in Figure 6.8, but that analogy is only for visualizing the gravitational effect; it does not tell us much about buckling. Here is a formula for buckling in a straight but inclined wellbore (Dawson and Paslay [30]):

$$\boxed{F_{\text{crit}} = 2\sqrt{\frac{4EI\, g\, k_{\text{b}}\, \rho_{\ell}\, \sin\alpha}{\Delta r}}} \tag{6.56}$$

where

F_{crit} = critical axial buckling force

ρ_{ℓ} = linear density of casing

k_{b} = buoyancy factor

Δr = concentric radial clearance between pipe and hole $(r_{\text{h}} - r_{\text{o}})$

g = local acceleration of gravity

[7] Any cowboy who has ever thrown a lasso or rig hand who has pulled a coiled water hose knows this intuitively.

E = Young's elastic modulus

I = second area moment of tube cross section

α = borehole inclination angle

Commonly we see this equation with the buoyed linear weight, $\bar{w}$, where $\bar{w} = g\, k_\mathrm{b}\, \rho_\ell$, but this time I have included all the terms for clarity. One particular reason for this is that for close to 17 years, almost everywhere it was published in USC units, the buoyed linear weight, $\bar{w}$, is stated in lbf/ft and all other length units in inches in the notation tables at the end of those papers, even in the original paper. To be fair, I can verify that the calculations in the original paper were definitely done correctly, and it is only the notation table at the end that is erroneous. It appears that the calculations in most of the other papers were done correctly also. In practice though, that has not always been the case, because many have taken the formula as stated in those papers and used it without noticing the inconsistency (and I include myself). While the error is a small careless error that was repeated without discernment, it is no small error if you do not make this correction in your calculations. The correct critical buckling load is about 70% less than the load calculated using the wrong units as stated in those papers. So, if you use USC units, you should ignore the units given in those papers and use consistent units.

Of particular note regarding this equation is that as the inclination angle goes to zero (vertical wellbore), the critical buckling load in this formula also goes to zero, implying that any compression in a vertical well will cause buckling. We are using buoyed weight in this formula so the equation is referring to the actual stability point, and as stated in the previous section on vertical wellbores, if the effective axial load is zero or less then assume that the pipe will buckle. It is not necessary to switch to a different formula as the inclination angle approaches zero as some recommend. From a practical viewpoint, this is the only formula needed for a straight section of borehole whether vertical or inclined.

This formula works pretty well for casing, but it does not take into account any wellbore curvature. Wellbore curvature was considered by He and Kyllingstad [31] and then later by Mitchell [32] in the course of resolving differing published formulations. This is Mitchell's solution:

$$F_\mathrm{crit} = \frac{2\,E\,I\,r_\kappa}{\Delta r}\left[1 + \sqrt{1 + \frac{g\,k_\mathrm{b}\rho_\ell\,\Delta r\,r_\kappa^2\,\sin\bar{\alpha}}{EI}}\,\right] \tag{6.57}$$

where $\bar{\alpha}$ is the average inclination angle over the short interval being considered. Later, Mitchell advanced his study to include the effects of couplings. In that paper [33], he recommended that the radial clearance be calculated with the coupling radius as opposed to the pipe body radius; that is, $\Delta r = r_\mathrm{h} - r_\mathrm{cpl}$.

One should remember that all lateral buckling formulas are approximate, at the very best. Some have sweeping assumptions that may or may not be realistic. The two just discussed have been used extensively, and they are reasonable. They do not account for the effects of torsion, connections, and so forth. Mitchell continues to work in the area of tubular buckling in wellbores and has taken some of those things into account. For anyone interested in the subject, his papers on the subject are a good source.

6.6.3 Axial buckling of casing

Axial buckling of casing may be described as a crushing or collapsing effect in the longitudinal axial direction of the tube. It is usually characterized as a composite of faceted triangular faces and folds in its configuration. It can also take the form similar to that of a bellows in some thin wall configurations.

It always involves yield of the material. True axial buckling of casing is rare. When it does occur, such buckling is usually in conjunction with lateral buckling or bending in the presence of high axial loads. There are structural formulas for axial buckling, but in the case of casing, it is so rare that we typically consider compressive axial yield or lateral buckling criteria as limits instead.

6.7 Dynamic effects in casing

The effects of motion is not generally considered in casing design because for the most part casing is in a quasi-static mode. The exception occurs when casing is lowered into the hole where there is a sequence of motion states: a static state, an acceleration state, a constant velocity state (more or less), a de-acceleration state, and then another static state. This cycle is repeated for each joint in the string. The dynamic states in this cycle are relatively benign as far as inertial forces are concerned and are usually ignored. The initial acceleration is gravitational and relatively small. The constant velocity is also relatively small on the order of a few feet per second. The only significant inertial force comes from the de-acceleration at the end of each cycle. Obviously the longer the casing string, the more significant the force. Drillers intuitively understand this and can even feel it in the brake lever and actual rig floor motion. They can, and usually do, monitor the magnitude of the force on the weight indicator. In other words, these natural dynamic effects are almost never a problem, and hence, they are seldom ever considered in design of the string except in very deep wells.

There is one dynamic event that is not routine and is sometimes considered, and that is the *emergency stop*. It may be intentional with the sudden application of the brake or unintentional with a premature setting of the slips while the pipe is still in motion. The latter of those two is obviously the most drastic and severe load generator. There is a sudden change in momentum and also a shock impulse. Both deserve examination.

6.7.1 Inertial load

Inertial loading of casing strings occurs when we initiate motion and cease motion. Each happens once for each joint added to the casing string. There is also the possibility of an inadvertent change in momentum caused by hitting an obstruction in the borehole or setting the spider slips while the casing is still in motion. It is Newton's second law in practice:

$$\mathbf{F} = \dot{\mathbf{p}} = \dot{m}\dot{\mathbf{u}} + m\ddot{\mathbf{u}} \tag{6.58}$$

where force is equal to the time rate of change of momentum. And in our case where mass is constant and we consider only one dimension,

$$F = m\ddot{u} \tag{6.59}$$

The fundamental equation of structural dynamics is an expansion of that equation which I have rearranged from the traditional form so that you might easily see that it is the same equation with more force terms (still in one-dimensional form).

$$ku + c\dot{u} + f = m\ddot{u} \tag{6.60}$$

Forces are on the left and acceleration on the right. The first term, is an elastic force proportional to displacement (or deformation). The second term is called a damping term that is proportional to

the velocity. The third term does not normally appear, and it is a forcing function, which I have added here to account for forces independent of displacement or velocity. Most structural dynamics analyses are based on this equation. It does have a serious flaw in that almost nowhere is damping force linearly proportional to the velocity, but it is part of the classical method because it lends to closed form solutions of the equation not otherwise possible, and to some extent it is accurate enough for rudimentary analysis. It the case of a casing string that term would be insignificant compared to frictional damping and friction damping which would be accounted for in the third term. But in a curved borehole it would be much more complicated as the contact force is a function of all the other terms.

That is all fundamental and easily understood. The question is how do we apply that to casing design? And additionally, should we even consider it in casing design? Almost no one considers inertial forces in casing design. The only way to properly do an inertial force analysis would be with an explicit type finite element analysis, which should include borehole friction. That is beyond what we can address here. However, many who do choose to include dynamic effects, usually employ the rigid body shock load addressed in the next section rather than any consideration of inertial forces.

6.7.2 Shock load

There is a popular formula that has found its way into some casing design contexts that seems to be used frequently without much due consideration. It is

$$\Delta\sigma = \dot{u}\sqrt{E\,\rho} \tag{6.61}$$

where $\Delta\sigma$ is the impulse change in axial stress, $\dot{u}$ is the relative velocity of the pipe in relation to some stationary, rigid object impacted, E is Young's modulus, and ρ is the density of the steel. This formula is usually presented in oilfield context complete with a value for $\sqrt{E/\rho}$ lumped in with several conversion factors into a single numerical value I will denote as C for now. So the formula is presented as

$$\Delta\sigma = C\dot{u}$$

with little or no explanation given as to what C is. Whether or not you or your company choose to use it is immaterial here, but if we do choose to use it, we should understand it and be able to explain why we use it. The derivation by Timoshenko [34] is as good as any and it comes from a thought experiment in which there is an impact of a rigid body on the end of a static elastic bar suspended horizontally (so that gravity plays no role). The velocity, $\dot{u}$, in the equation is the velocity of the rigid body. The other assumption is that a flat face of the rigid body impacts the end face of the bar perfectly across its surface. Although Timoshenko used a solid bar, the equation is equally valid for a prismatic tube.

If we consider USC units where $E = 30 \times 10^6$ lbf/in^2, $\rho = 490$ lb/ft^3, and velocity, $\dot{u}$ in ft/s, then $C \approx 1780$ with $\Delta\sigma$ in psi. In consistent SI units, $E = 2.068 \times 10^{11}$ Pa and $\rho = 7850$ kg/m^3, then $C = 4.029 \times 10^7$ and neither contains nor requires any unit conversion factors.

Now we examine this equation. Notice in particular that mass, m, of neither the tube nor the rigid body is present, so an inertial force, $\dot{\mathbf{p}}$, is not included. This is a purely theoretical impulse load only, and it does not account for any inertial force. The result is a compressive elastic wave propagating down the length of the tube. If the other end of the tube is free, the impulse will reflect and travel back through the length of the tube as a tensile wave of equal magnitude (in theory). We could in a thought experiment imagine a negative impact on the end and generate a tensile impulse wave at impact similar to suddenly

setting slips on a moving joint of casing. Or we could assume a situation where the bottom of the casing strikes a ledge or bridge while being run in the hole, thus generating a compressive wave. The equation will work either way. In theory such a shock wave can propagate the length of the tube and reflect back and forth for an infinite length of time. If an end is free it reflects back as an opposite type of wave, that is, a tensile wave reflects back as a compressive wave and vice versa. If an end is fixed it reflects back in the same mode, a tensile wave reflects back as a tensile wave and a compressive wave as a compressive wave.

The speed at which casing is lowered into a borehole is relatively slow, say on the order of 5-8 ft/s. Let us look at casing being lowered at 8 ft/s and apply the formula.

$$\Delta\sigma = 1780\,(8) = 14,240\,\text{psi}$$

That would likely represent a worst case scenario and is not an alarming number. It is about 18% of the yield of N-80 casing and would likely be compensated for in a design factor if ignored completely. In almost all cases where the spider slips are prematurely set, the casing is almost already stopped, so the speed would be much slower. The impulse formula gives results that we can reasonably accept and possibly that is why its use is seldom questioned.

That being understood, let us examine another case that is not so intuitively reasonable. Suppose we have a rigid plate attached to one end of a joint of casing that is suspended horizontally as in Timoshenko's derivation. Now we have an archer with a modern compound bow who releases a rigid-tipped arrow at 300 ft/s that passes internally through the length of the joint striking the rigid plate at the other end. Bam! The impulse, $\Delta\sigma$, is 534,000 psi! That is about 6.7 times the minimum yield strength of N-80 casing and almost 5 times the minimum ultimate strength. Can such an event cause the casing to actually part in tension? Perhaps now, this equation does not appear so reasonable as before when it gave results we could easily accept.

In the real world, there is no such thing as a rigid body nor an instantaneous transfer of force as in the theoretical model. It just cannot happen. Any rig floor hand can tell you that a rotary table (or rig floor) is not a rigid body because it definitely moves any time you set the weight of pipe in the slips. Furthermore, in a borehole, an elastic wave attenuates fairly rapidly because of the viscous borehole fluids, frictional contact with the borehole wall, and the presence of non-uniformly spaced couplings. The reflection of such a wave at the end is almost nil except in very short lengths of pipe. If this were not the case, the problem of real-time telemetry from down-hole tools would have been laid to rest over decades ago. The shock load from premature setting of slips is an impact loading between two elastic bodies, not an elastic body and a rigid body. The choice to use or not use this formula is entirely yours.

6.8 Thermal effects

So far we have not discussed temperature and how it affects casing design, except in brief. We now look at two aspects of temperature effects on casing, its magnitude and the change in magnitude.

6.8.1 Temperature and material properties

An engineering rule of thumb in most structural applications is that we do not consider temperature effects on the properties of many structural metals until the temperature exceeds 50% of the melting temperature of the metal; that is, $T \geq 0.5T_{\text{m}}$. Most casing applications easily fall below that point. Steel

properties do vary with temperature and naturally they are dependent on the alloy composition. There are no API standards or open source data for API tubulars, but like all steels, there is some effect. How much effect is open to question. Some discussion and charts were published by Holliday [35] as examples. They indicate that most grades retain about 90% of their yield up to around 700 °F (∼ 370 °C). There is no universally accepted threshold temperature at which one should start down-rating the yield strength from temperature, although some companies definitely have their own standards. I am not about to recommend a threshold temperature, but certainly at some point, one might consider reducing the yield value of casing to around 90% or so.

Geothermal and steam injection wells, for instance, not only have high temperature environments but also large changes in temperature. Those high-temperature environments are not considered here.

6.8.2 Temperature changes

The thermal consideration in most casing design is not the actual temperature *per se* but the change in temperature. Temperature change causes casing to expand or contract. When casing is run in the hole, the mud has been in a static condition for several hours before the casing reaches bottom. The temperature of the mud may or may not be close to an equilibrium state, depending on how long circulation has been static, but in most wells it is relatively close to static equilibrium (or more accurately, a steady state in the earth's natural heat flux). Once casing is on the bottom and circulation begins, the temperature profile moves further away from the static thermal equilibrium state again. Much depends on the difference between the surface and down-hole temperatures, circulation rates, circulation time, and so forth. As circulation continues, the lower part of the hole normally is cooled below its static temperature and the upper part of the hole is warmed above its static temperature. Once cement is in place and circulation ceases, temperatures begin to return to the static thermal equilibrium state. We do not know how close to the static profile the temperature is when the cement sets. There may be some added axial compressive stress in the lower part of the casing as it warms, and there may be added tensile stress in the upper portion of the well as it cools. This amount of stress generally is ignored in most casing design, and in most cases, it likely is nowhere near any critical value. But when we start to produce the well, the casing is exposed to a different thermal profile than it experienced before. Now, fluids from the formation travel up the hole and warm the upper part of the casing. No cooler fluids circulate downward from the surface to offset the warming. More of the casing in the upper part of the hole expands, and the axial stress change is toward compression. Whether it actually goes into compression or not depends on how much tension was in the pipe initially and how much the temperature is increased.

We can show the effects of temperature change on uniaxial stress in casing with a 1D, thermoelastic version of Hooke's law:

$$\boxed{\sigma = \sigma_0 + E\,\varepsilon - E\,\alpha_{\mathrm{T}}\,\Delta T} \tag{6.62}$$

where

$\sigma =$ uniaxial stress

$\sigma_0 =$ initial stress (before deformation or temperature change)

$E =$ Young's elastic modulus (material dependent)

$\varepsilon =$ uniaxial strain (change in length/original length)

$\alpha_{\mathrm{T}} =$ coefficient of linear thermal expansion (material dependent)

$\Delta T = T_t - T_0 =$ change in temperature from initial state to some time, t

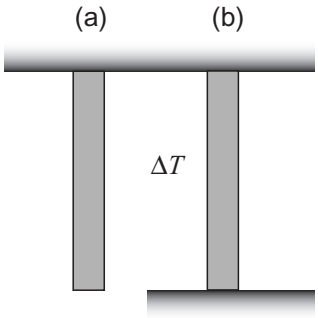

Figure 6.11 Thermal effects: (a) suspended tube and (b) constrained tube.

In general, both the elastic modulus and the coefficient of thermal expansion are functions of temperature, but within a limited range, they are sufficiently constant that we assume them to be so here. With that assumption, this equation looks straightforward, and it is.

The simplicity of that equation can be misleading because temperature effects are not always intuitive. For instance, we can say that a temperature change can cause a strain without causing a stress, and it can also cause a stress without a strain.

Look at the vertical tube in Figure 6.11a. A metal tube (or casing string) is suspended from the top end and free at the lower end. If we heat that tube by some amount, ΔT, then it will expand and get longer; that is, we induced a thermal strain in the tube. But, have we changed the stress? No, we have not. In this case, the total positive uniaxial strain we might measure is equal to the thermal strain; that is, $\varepsilon = \alpha_{\mathrm{T}}\,\Delta T$, so the stress in the bar at any point has not changed, it still is equal to the initial stress, σ_0, which in this example is the body force of gravity.

Now examine the tube in Figure 6.11b. This tube is constrained at both ends. If we apply the same temperature change to this tube, it tries to expand, but it cannot (we will assume it does not buckle laterally). The tube has not gotten longer, so we have not caused any strain; that is, $\varepsilon = 0$. But, have we changed the stress in this bar? Absolutely. We changed it by the amount, $-E\,\alpha_{\mathrm{T}}\,\Delta T$, a negative value, since the change in stress is compressive. What we see here is that the product of the coefficient of thermal expansion and the change in temperature, $\alpha_{\mathrm{T}}\,\Delta T$, is something like an "effective strain." If we substitute values into the uniaxial thermoelastic Hooke's law we can calculate the change in axial stress in casing with fixed ends (as in Figure 6.11b) in USC units as

$$\Delta\sigma = \left(30 \times 10^{6}\right)\left(6.9 \times 10^{-6}\right)\Delta T$$

$$\boxed{\Delta\sigma = 207\ \mathrm{psi/^{\circ}F}} \tag{6.63}$$

and in SI units

$$\Delta\sigma = \left(206.8 \times 10^{6}\right)\left(12.42 \times 10^{-6}\right)\Delta T$$

$$\boxed{\Delta\sigma = 2568\ \mathrm{Pa/^{\circ}C}} \tag{6.64}$$

In the uniaxial case, it was relatively simple, and we can use this simple equation to calculate changes in axial stress in casing if we know the magnitude and the end conditions. It begins to get a bit more complicated in three dimensions:

$$\sigma_{ij} = \sigma_{0\,ij} + C_{ijkl}\,\varepsilon_{kl} - \delta_{ij}\frac{E}{1-2\nu}\,\alpha_{\mathrm{T}}\,\Delta T \tag{6.65}$$

If you are familiar with index notation, this will make sense to you, if not please refer to Appendix C. We are not going to use this equation, but I show it for reference because you need to see that the 1D form (Equation (6.62)) does not simply translate into 2D and 3D applications. The temperature terms only apply in the three coordinate axes directions. For composite materials, this gets much more difficult, in that the thermal coefficient is not necessarily the same in all directions nor is the elastic modulus. One additional thing we might mention so that you do not go through life thinking that things are too simple. In the unconstrained bar, we said no stress is caused by heating the bar. That is true only if the bar is thin and heated slowly and uniformly, so that the temperature is always uniform throughout the bar. If it is thick and we heat it rapidly and/or locally, then we induce some amount of stress within the bar until the temperature becomes uniform throughout.[8]

One of the important points that come out of thermoelasticity is that we are dealing with changes in stress and strain. Too often undergraduate engineers are taught Hooke's law (in one dimension) as

$$\sigma = E\,\varepsilon$$

and left at that. Most applications assume an initial stress-free state, but you should always think of Hooke's law should as

$$\sigma = \sigma_0 + E\,\varepsilon$$

because nothing in a wellbore is stress free.

In casing design, thermal effects usually lead to a situation of compression (note the negative sign in the Hooke's constitutive equation). That is something we are not accustomed to seeing in basic casing design, except in bending and borehole friction in inclined wells, which we cover in the next chapter. To determine the thermal effects in casing, we must know a number of things that we do not consider in most wells. The major thing we need to know, obviously, is the change in temperature. This can be measured in actual wells, but we also can use a heat transfer software model to estimate it. We must also know if the casing is free to move or not, and this we often do not know and cannot determine except at the wellhead and top of cement (where we assume it is not free to move). We already covered the effect of pressure changes on axial stress when the pipe is constrained at the ends, and we might have to incorporate that into our thermal stress calculations, too. The best way to illustrate the thermal stress is with examples, where we can see the assumptions we must make along the way and how we might decide the question as to what additional data we require for a particular application.

EXAMPLE 6.10 Thermal Effects on an Unbuoyed Casing String

Referring to Figure 6.11b, assume that, initially, the tube is at a constant temperature throughout its length. Let us also assume that it is hanging by its own unbuoyed weight before the lower end was constrained. Its

[8] In some hypersonic flight vehicles, localized heating can occur so rapidly that inertial forces are generated that can cause yielding even in an unconstrained tube like Figure 6.11a.

cross-sectional area is 7.55 in.^{2}, its linear density 26 lb/ft, and its total length is 10,000 ft (it is 7 in. casing). We will assume a coefficient of linear thermal expansion of 6.9×10^{-6}/°F. The tensile force at the top is

$$F_0 = g\,\rho_\ell\,h = 26\,(10000) = 260,000\,\text{lbf}$$

and, at the bottom, it is zero. If we set our z-coordinate axis at the top with a positive direction downward, then the axial stress at any point is

$$\sigma_z = \frac{F_0}{A_\text{t}} - \left(\frac{\rho_\ell}{A_\text{t}}\right) z$$

where A_t is the cross-sectional area of the bar (or tube). Now, if we apply a constant temperature change to this bar, we can calculate the axial stress at any point by

$$\sigma_z = \sigma_0 + E\,(\varepsilon_z - \alpha_\text{T}\,\Delta T) = \frac{F_0}{A_\text{t}} - \left(\frac{\rho_\ell}{A_\text{t}}\right) z - E\,\alpha_\text{T}\,\Delta T$$

since $\varepsilon_z = 0$, because the bar is constrained. If we change to temperature in the bar by increasing it 100 °F, the axial stress at the top is

$$\sigma_z = \frac{F_o}{A_t} - \left(\frac{w}{A_t}\right) z - E\,\alpha_\text{T}\,\Delta T$$

$$= \frac{260000}{7.55} - \frac{26}{7.55}\,(0) - 30 \times 10^6 \left(6.9 \times 10^{-6}\right) 100$$

$$\approx 13,700\,\text{psi}$$

At the bottom, the axial stress is

$$\sigma_z = \frac{F_o}{A_t} - \left(\frac{w}{A_t}\right) z - E\,\alpha_\text{T}\,\Delta T$$

$$= \frac{260000}{7.55} - \frac{26}{7.55}\,(10000) - 30 \times 10^6 \left(6.9 \times 10^{-6}\right) 100$$

$$\approx -20,700\,\text{psi}$$

The bar is in compression at the bottom and in tension at the surface, although the tension at the top now is less than before the temperature change.

Let us now look at another example, this one in a wellbore.

EXAMPLE 6.11 Thermal Effects on Hanging Weight

Suppose we have a well with a string of 7 in. 26 lb/ft L-80 casing in a vertical well. The top of the cement is at 10,000 ft, and the well is perforated in a zone at 14,000 ft. After the cement sets, the hook load is 275,000 lbf, and we calculate the true axial load at the top of the cement is 13,000 lbf. We pull an additional 50,000 lbf on the casing above its hook weight and set it in a slip-type hanger. We run a shut-in temperature survey in the well and find the temperature at the top of the cement is 220 °F and its gradient is linear to a surface temperature of 70 °F; that is, $T = 70 - 0.015h$, where h is the vertical depth. Below that point, we find that the formations are much hotter, and the temperature at 14,000 ft is 370 °F. To keep this simple, let us say that our heat transfer model predicts that, with the anticipated production rate, the heat transfer will reach a near steady state with a temperature increase of 150 °F uniformly along the casing string. We ignore any stresses caused by any temperature change between the time the cement set and the temperature survey was

run and any effects from the possible expansion of fluids in the annulus outside the 7 in. casing, although expansion of trapped fluids is not something we can ignore in many cases (see Halal and Mitchell [14]). We also assume that the pipe stays straight and does not buckle. The cross-sectional area of our casing is 7.55 in.^2.

We would like to determine the following.

- The axial stress in the casing at the top of the cement
- The axial stress in the casing at the surface
- The amount of tension at the surface to avoid any compression in the casing from the temperature increase during production

Since the casing is constrained at the top and the bottom (wellhead and cement), there is no axial strain from the change in temperature. Assuming a coefficient of linear thermal expansion of $6.9 \times 10^{-6}/^{\circ}\text{F}$, the axial stress at the top is

$$\sigma_z = \sigma_o - E\alpha_{\text{T}}\,\Delta T$$

$$= \frac{275000 + 50000}{7.55} - 30 \times 10^6 \left(6.9 \times 10^{-6}\right) 150$$

$$\approx 12,000\,\text{psi}$$

and, at the top of the cement, it is

$$\sigma_z = \sigma_o - E\alpha_{\text{T}}\,\Delta T$$

$$= \frac{13000 + 50000}{7.55} - 30 \times 10^6 \left(6.9 \times 10^{-6}\right) 150$$

$$\approx -23,000\,\text{psi}$$

The top of the casing is still in tension, but the bottom is in compression. What is the magnitude of the compressive force at the bottom?

$$F_z = \sigma_z A_t = -23000\,(7.55) \approx -173,600\,\text{lbf}$$

Suppose we are concerned about buckling. What amount of tension should we pull so that the casing does not go into compression at the top of the cement with this amount of temperature change?

$$\frac{F_z + 13000}{7.55} - 30 \times 10^6 \left(6.9 \times 10^{-6}\right) 150 = 0$$

$F_z \approx 221,000$ lbf (additional at the bottom)

$F_z = 275000 + 221000 = 496,000\,\text{lbf}$ (total hanging weight at surface)

Assuming we use proprietary couplings with a higher tensile strength, the pipe body yield of this casing is only 604,000 lbf, leaving us with a tensile design factor of about 1.22, which is very low. If we down-rate the yield to 90%, as mentioned earlier, then we must look at other options. Additionally, we must consider whether our wellhead and conductor would support that amount of weight. We actually might have to live with some amount of buckling in the lower section of this casing string. In that case, we also have to determine the limit of our connections in compression near the bottom. There

are no formulas for determining the compression strength of API connections. Some manufacturers of proprietary connections have compression strength data for their couplings, although that information usually is not published. See Jellison and Brock [36] for a discussion of connections in compression. An alternative approach would be to bring the cement higher to a point where the casing tension is greater, but one also must consider that cemented casing is not necessarily immune to coupling failure in compression with large temperature increases.

The preceding is a simple calculation, and you will note, we made a lot of simplifying assumptions. We did not consider any inclination and friction in the bore hole that would resist pipe motion, and we assumed that the temperature change would be constant along the entire length of the string. However, we can use simple calculations like that to spot-check thermal stresses at various points to determine if we need a more in-depth investigation.

One particular thermal problem has occurred in a number of cases of intermediate casing strings where abnormally high temperatures are encountered when drilling below the intermediate string. It involves a cemented intermediate string through a washed out interval of the borehole where the casing is virtually un-cemented, but the casing on either side of that interval is securely cemented. When the higher temperature zones below the casing are being drilled the circulating temperature in the casing increases markedly. At some point the casing in the un-cemented interval buckles laterally. Any damage from the buckle is not necessarily critical or even noted, but as drilling continues a hole is worn in the casing fairly quickly. Let us look at an example of this.

EXAMPLE 6.12 Thermal Buckling

Referring to the constrained bar in Figure 6.11b and assume it is 7-5/8 in. casing with an ID of 6.875 in. We will assume the un-cemented interval is 50 ft in length and for our purposes we will assume the axial load in this section of casing is negligible for now. First of all we need a buckling formula, and we will use an Euler column formula for fixed ends (cemented in our case):

$$F_{\text{cr}} = \frac{4\pi^2 EI}{L^2}$$

We calculate the axial second area moment

$$I = I_a = \frac{\pi}{64}\left(d_{\text{o}}^4 - d_{\text{i}}^4\right) = \frac{\pi}{64}\left(7.625^4 - 6.875^4\right) = 56.269\,\text{in}^4.$$

then the critical buckling force is

$$F_{\text{cr}} = \frac{4\pi^2 EI}{L^2} = \frac{4\pi^2\left(30\times10^6\right)(56.269)}{[12\,(50)]^2} = 185,118\,\text{lbf}$$

This force will give us an axial stress of

$$\sigma_z = \frac{F}{A_{\text{t}}} = \frac{4\,(185118)}{\pi\left(7.625^2 - 6.875^2\right)} = 21,674\,\text{psi}$$

Now, how much change in temperature is required to give us a compressive stress of 21,674 psi? From Equation (6.63) we determine that the constrained thermal stress is 207 psi/°F.

$$\Delta T = \frac{21674}{207} = 105\,^\circ\text{F}$$

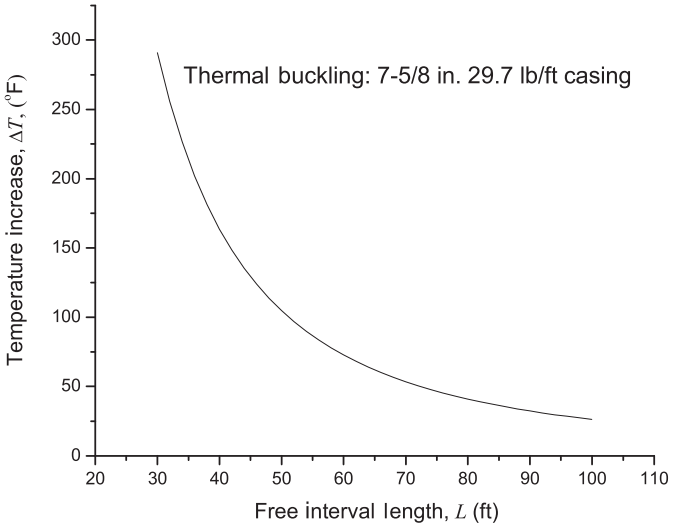

Figure 6.12 Thermal buckling as a function of free pipe length and temperature increase, 7-5/8 in. 29.7 lb/ft casing.

We could repeat this calculation and make a chart for this particular 7-5/8 in. casing as to free length and temperature change (Figure 6.12).

There is much more we could say about thermal effects, but in general we do not know the temperatures very accurately unless the well has been static for some period of time. A circulating or flowing well is a forced convection heat exchanger and, the time for the temperature to equalize to the steady state geothermal normal is usually unknown for most wells.

6.9 Expandable casing

Two problems with casing sizes sometimes arise in the drilling of wells, both of which can increase the well costs and possibly prevent a well from reaching its objective:

- Unanticipated conditions that require an additional casing string of casing after the well has been started.
- Known conditions that require multiple casing strings for a well before it has been started.

In the first case, the sizes and depths already are selected, and one or more strings may be set before the need for an additional string arises. Unexpected borehole stability or pressure problems may require an additional string that was not originally planned for. Another problem of similar nature is the possibility that a planned casing string may stick before reaching its planned depth and thereby necessitate an additional string. In these cases, an additional casing string or liner must be set and the final casing string at total depth will be smaller than desired, unless some contingency was included in the original plan to allow for such an event. The second case is becoming more common in some areas, especially where depleted zones may be present. Typically, we think in terms of a surface string, an intermediate string, and a production string, possibly with a liner somewhere in that mix, but basically three or four strings. Occasionally, we may even find it necessary to run five or six strings, counting liners. In recent

times, however, we are seeing wells that require 7 or even as many as 10 strings of casing to reach an objective. A conventional approach to this problem requires some very large boreholes and large casing sizes to reach the total depth with a final casing string size that allows for adequate production. In each of these cases, size and clearance become serious problems.

One answer to these problems is expandable casing. This is a type of casing with connections that can be run through conventional casing (or other expandable casing) then expanded to a larger diameter than a conventional string run through that same size pipe. While this is a relatively new technology, it has seen some good success in numerous applications. However, it is not necessarily a panacea, as there are drawbacks, too.

6.9.1 Expandable pipe

Expandable casing is not your typical casing product. First of all, it must be ductile enough that it can be expanded without rupturing and still have sufficient strength to function properly. We discuss plastic material behavior in Appendix C, so we do not rehash that here, but this is exactly the type of material behavior involved in the expansion process. Consequently, it does not come in standard API grades, weights, and so forth. Likewise, there are no published standards of performance properties but rather those are set by the manufacturer. Most expandable pipe is not seamless pipe, since the wall thickness has to be much more uniform than most seamless pipe. It is manufactured from flat plate steel that has been precisely rolled to be within close tolerances. Seamless pipe can be used and is being used in some expandable applications, but the wall thickness must be very carefully rolled to within close tolerances. You can imagine the results of the expansion process if the wall thickness is not uniform before the expansion begins; most of the expansion will take place in the portions where the wall thickness is the thinnest. Additionally, the connections must be expanded, since it must be run as individual joints. When you consider the amount of expansion of the pipe body and the threaded connections, you come to appreciate the technology of the process, in that it is not nearly as simple as it might first appear. Obviously, for the performance properties of the expanded pipe to be reasonable, the expansion process must be uniform.

6.9.2 Expansion process

Two basic processes are used for expanding pipe, and they essentially are the same two processes that have been around since the early 1960s when the first internal casing patches were introduced. Of course, they have seen considerable improvement since that introduction. One process involves a swaging operation in that an internal swaging mandrel is run with the expandable casing, and it expands the pipe from the bottom up as it is pushed or pulled through the tube. This typically is a hydraulic process. The other process employs a roller-type device that expands the casing from the top down, using a tapered device with rollers that expand the casing as the device is rotated with a work string. One thing that must be kept in mind, though, is the elastic unloading discussed previously about elastic-plastic behavior. If we expand a tube plastically, it always exhibits some amount of elastic shrinking from its plastic state when unloading. This means that it has to be expanded to a slightly larger diameter than its final diameter to account for the elastic unloading once the expansion tool is removed.

The swaging process uses a mandrel with a circular cross section that is in the bottom of the expandable casing as it is run. The mandrel can be either a solid piece or of a type that allows for retraction and retrieval through a smaller diameter. In its expanded position, it is pumped and/or pulled

through the casing from the bottom upward and expands the casing as it moves upward (Figure 6.13). This may be accomplished hydraulically, with a mechanical pulling force, or a combination of both, as long as the casing is not allowed to move as it is being expanded. It is a positive type of expansion, in that, for the mandrel to pass through, the casing must expand to the diameter of the mandrel. Advantages of this process are that it imparts a true hoop stress (uniform tangential stress) to the casing being expanded. If the wall thickness of the casing is uniform and the material is isotropic, then the hoop stress is truly uniform around the circumference. The expanded tube should be round. A perceived disadvantage is that the swaging process induces an axial stress in the pipe as it is being pumped or drawn through the pipe. Whether or not this is an actual disadvantage seems to be more of a marketing argument than a technical one. Usually a special coating is applied internally to reduce the friction. If the mandrel is a one-piece device and for some reason it cannot be pulled through the entire expandable casing, then it cannot be removed unless it can be milled up. This was always an argument against the earlier mandrel-type casing patch tool, yet it was the only truly successful one on the market. Again, marketing forces played a dominant role in that discussion too. This may not be a problem with retractable-type mandrels, though they lack the simplicity of a single piece mandrel.

The roller-type process was in use long before the expandable casing patch was introduced in the 1960s. It traditionally was used to try to restore partially collapsed casing. The roller process is simple, in that the process starts from the top and expands the casing as it is rotated downward into the expandable or collapsed pipe. It has the advantage that it can be removed at any time, replaced, and then resume the operation where it stopped. The historic problem with rollers is that they do not work very well, at least in the fixed version. A roller device does not induce true uniform hoop stress in a tube, because it contacts the casing at only a finite number of points, usually three or four. The old roller-type casing patches typically failed because they never were round in cross section once expanded, since the rollers had only three contact points. Expanders with four rollers were introduced and had better success than three rollers but still never were as successful as the swage-type process. The use of casing rollers to restore partially collapsed casing historically enjoyed limited success primarily because of the point contact with the casing wall and the elastic unloading between contact points. It is an inferior process for longer sections of expandable casing.

6.9.3 Well applications

At the beginning, we mentioned the unanticipated well problem as a possible application for expandable casing. For someone who has been involved in drilling operations for a period of time, this usually is the first application that comes to mind. Expandable casing could be used in such an application as a temporary means of getting past some troublesome zone. Originally, the availability and lead time required for the expandable pipe to be a readily available solution for this type of problem was limited. The expandable casing had to be ordered and available as a backup for a particular well before the actual need arose. This changed in time and is not so critical a limitation now. Another drawback to expandable casing as an unplanned contingency string is the cementing issue. If the expandable string is to be reliably cemented, then the hole in which it is to be placed must be either under-reamed to a larger diameter than the bit that will pass through the casing above it or it must be drilled initially to a larger diameter as with a bi-center bit. These are not necessarily amenable to unanticipated situations that may arise and require an additional casing string. As it currently stands, expandable casing is a planned part of the casing program and for that application, it has proven quite successful.

The cementing process in regard to expandable casing is a bit different from conventional casing cementing. The usual procedure is to displace the cement prior to expanding the casing. This requires

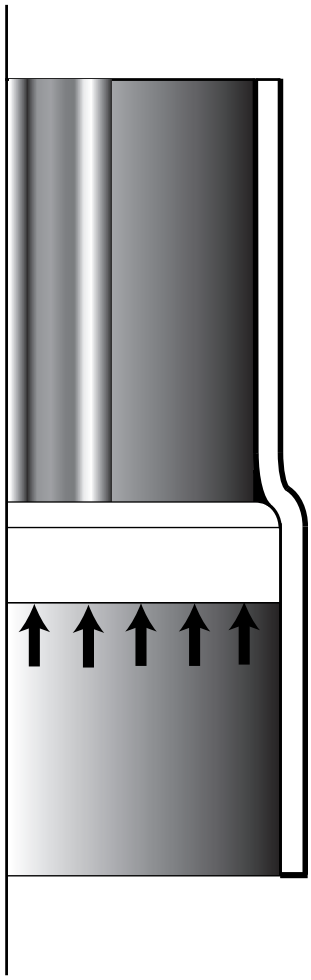

Figure 6.13 Schematic of a mandrel-type casing expansion tool.

that the casing expansion be completed before the cement begins to harden. The expandable casing can be reciprocated and even rotated during the displacement process prior to expansion, so in that respect, it is no less effective than a conventional liner cementing job. The biggest differences may be the cement near the top of the liner and whether or not one wants cement in the annulus above the liner before the expansion process begins. As the casing is expanded, the mud and cement in the annulus must be displaced somewhere, and it goes into the annulus between the running string and the previously set casing. If cement actually is displaced into this space above the expandable liner, then there is a considerable discomfort factor until the expansion is complete and this cement can be circulated out of the wellbore. For the most part though, since the expandable casing is used for a temporary drilling liner, it is not critical to have cement all the way to the top of the liner. Most expandable casing is run as a liner and the final part of the expansion process is the expansion of the overlap in which some type of elastomer seals on the outside of the expandable casing seal against the casing through which it has

been run. Once that seal has been established there is no way to displace cement into the annulus short of perforating and squeezing, so the seal itself must be considered adequate.

6.9.4 Collapse considerations

The collapse rating of expandable casing is usually less than what one is accustomed to in similar sizes of conventional casing. This is mostly because of the thinner wall of the expanded tubes as compared to API tubes. The thinner wall is the tradeoff we accept for the larger internal diameter which is the primary reason we choose the expandable tube. In the discussion on plasticity, we mentioned that a material that strain hardens in plastic tension may gain yield strength in that direction, but in the process, it loses yield strength in compression. Also, if the casing wall does not expand uniformly, then the collapse strength is less than if it had expanded uniformly. With conventional casing, we can inspect its wall thickness and eccentricity before it is run in the hole. With expandable casing, there is no way to know with certainty the final wall thickness and any eccentricity until after it is in the hole and expanded. Since it has been cold-worked, it has different material properties and is no longer isotropic.

The most noted change is in the collapse strength. It has been suggested that one could use the traditional API formulas with the post-expansion diameter and reduced wall thickness, both of which can be reliably predicted, along with the pre-expansion API grade to calculate a post-expansion collapse value. Such a procedure will not work, because the pre-expansion yield value is no longer valid. The pipe has not only been expanded radially, but has undergone a bending cycle around the nose of the mandrel all the while in a state of axial tension. It is no longer isotropic and the yield surface size and location relative to the original $\sigma_1 = \sigma_2 = \sigma_3$ axis are not known. In short, we do not know what the post-expansion collapse value is and we have no formula from which to calculate it. Some recent investigations in this area has been done by Klever [37], but we are still far from having a reliable method.

Consequently, the most obvious practical application for expandable casing is as an intermediate string or a drilling liner that eventually will be cased with conventional casing. This is no insignificant niche, and in those applications, it can be invaluable. In Chapter 3 we used a total evacuation scenario for production casing collapse load. We would not attempt this with expandable casing. This is not to say that it cannot be used as a production liner at all, but to do so requires considerable forethought as to the pressure environment throughout the life of the well so that severe evacuation never occurs.

The significant advantage of expandable casing is illustrated in Figure 6.14 which shows a conventional casing program for a particular application along with an alternative utilizing expandable casing. The advantage of expandable casing in the well plan is readily apparent, in that the total depth now can be reached with the same size conventional casing on bottom and smaller casing at shallow depths. There are several possible variations. While this may not be applicable for the most common wells drilled in the world, it represents a considerable advantage in those costly wells that do fall outside the common category.

6.10 Closure

We covered a lot of ground in this chapter. Some topics we covered in more detail than others. This is not to slight any particular topic, but the material in this chapter in conjunction with Appendix C easily could constitute a separate book. In the next chapter, we look at inclined and curved wellbores. Much of

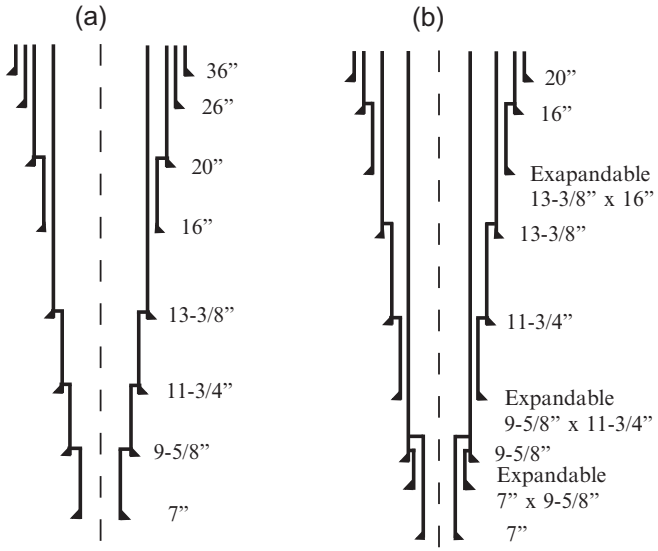

Figure 6.14 Well schematic (a) conventional and (b) expandable casing.

what was covered in this chapter and the previous one will carry over into it and will be further explained as to how it applies in those circumstances.

We have barely scratched the surface of mechanics of tubes, but we have gone far beyond what most petroleum engineers and engineers coming into drilling and completion engineering from other disciplines, such as electrical or chemical engineering, normally have been exposed to at an undergraduate level. This should help you understand much of what is written in the literature on the behavior of casing. Some of the terminology appearing in the petroleum literature is a bit convoluted at times, but most of it represents the honest efforts of those dedicated to trying to solve the problems of casing loading and design. I strongly encourage you to study Appendix C as a foundation and a supplement to this chapter.

The formulas and methods we have discussed in this chapter and elsewhere are sound and adequate for design of off-the-rack API casing. Because of the fairly wide variations in manufacturing tolerances allowed by API and the limited properties data published for such casing, these formulas necessarily lead to conservative designs in most cases. With stricter manufacturing control and an availability of more specific property data on specific batches of casing, we can certainly do better designs for critical wells.

This page intentionally left blank

Casing in directional and horizontal wells

7

Chapter outline head

Casing and Liners for Drilling and Completion. http://dx.doi.org/10.1016/B978-0-12-800570-5.00007-3

7.1 Introduction

Many wells drilled each year are directional wells, and an increasing number of those are horizontal wells. In one sense, all wells are inclined to some degree, and the phenomena we are about to discuss affect them too, even though we usually ignore them when it comes to casing design for "vertical" wells. We are now ready to consider wells in which these phenomena cannot be ignored. What are they? There are principally two: borehole friction and borehole curvature.

Simply put, borehole friction affects the axial load in casing by resisting its motion. An upward motion of the casing increases the tension, and a downward motion decreases the tension. If the casing is rotated, this too adds a torsion load to the casing—something we never consider in basic casing design. Borehole curvature causes bending stresses in casing. Historically, this stress was ignored in most casing designs, until horizontal wells began being drilled. Even then, it is surprising how many casing strings are still designed for horizontal wells that do not take bending into account, possibly because the bending-stress magnitude is not understood to be significant. For example, a string of 7 in. K-55 casing run through the build section of a medium-radius well with a radius of curvature of 400 ft will have a bending stress amounting to near 40% of its yield strength, and that does not account for additional stress from friction, gravity, or pressure. Bending stress is not insignificant in horizontal wells.

In this chapter, we look at borehole friction and curvature and their effects on casing design. We also consider combined loads in directional wells with some examples of how we do the calculations.

7.2 Borehole path

Before we get into the effects of friction and curvature in boreholes, we should examine the borehole path, or more specifically, how it is quantified. The basic measurement tools for determining the borehole path are an *inclinometer* for measuring the borehole inclination (the deviation angle, α, of the borehole from vertical), a *magnetic compass* for measuring the borehole direction (azimuth angle, β, from magnetic north), and the *drill pipe measurements* for determining the length, Δs, along the borehole path between directional survey points. The resulting data defines a spatial direction vector at each survey point using α and β. The drill pipe measurement, Δs, is the distance between two of the vectors as *measured along the borehole path between them*. Contrary to what is often assumed, that is not enough information to specify the location of a second survey point even when the first of the two is known exactly.

This is not like plotting points on a Cartesian coordinate system because we do not know the coordinates of the second vector. All we know is the distance from the first point as measured along the borehole path. Mathematically, the second point could be anywhere within a sphere of radius, $r = \Delta s$. Considering an actual drilling assembly, we know that is not the case since there is a limit to how much such an assembly will flex, but we also know that the greater the value of Δs, the greater the uncertainty. This brings us to the crux of all directional calculation methods: *we must always assume that we know the shape of the borehole path between survey points*.

There are a number of calculation methods that have seen use, each differing by the assumptions made as to the shape of that path. Earlier methods assumed segmented straight-line paths averaged between survey points. Everyone knew straight-line segments were not as accurate as curved segments, but these were almost essential assumptions because even those methods required trig tables and a mechanical or electric-mechanical calculator which were adding machines with the capability to also

multiply and divide. Slide rules had trig functions, but did not have nearly the precision required. As digital computers and hand-held electronic calculators came along it became possible to consider curved borehole paths which is where we are today. Before you dismiss all the older methods out of hand, you should realize that as Δs is decreased in size (number of survey points in a given interval increased) all of the methods then and now converge to the same result.

The method used almost exclusively today is known as the *minimum curvature method* as proposed by Taylor and Mason [38] in 1972. They arrived at their method by minimizing a quadratic curve that would give the minimum path length between two survey points and having the same vector directions as the survey vectors at the two ends. Their result is that the borehole path between two survey points is approximated by a segment of a circle in a plane. The details of Taylor's and Mason's minimum curvature method are presented in Appendix E. Additionally a borehole path interpolation scheme based on the minimum curvature method is presented for more accurate calculation of contact force for use in borehole friction and casing wear calculations.

Possibly the most serious limitation on mechanics of tubes in boreholes is the lack of accurate data on borehole geometry. No one really believes that a borehole path calculated by the minimum curvature method with survey points spaced 90 ft or more apart is very accurate. The single biggest problem with this and all methods of this type is that all errors and inaccuracies are cumulative. The location of each survey point is calculated from the location of the previous survey point and every error and inaccuracy carries over to the next survey. Hence we have what is called a *cone of uncertainty* that increases in radius with depth, see Wolff and De Wardt [39]. We do not know where the wellbore is, but we can reasonably assume that it is somewhere in that cone. With the digital instruments of today we can eliminate reader error, but there is still inherent inaccuracy in the measurements themselves. We typically assume that a gyroscopic survey instrument run on wireline is more accurate than a magnetic instrument run on drill pipe. True, the gyroscopic instruments are more precise, but the real question is, are the *results* more accurate? We do not know because we do not have a way to compare them—we do not have a well in which we know with certainty the location of the bottom of the hole.[1] Think about it. I hate to dispel another common misconception, and that is that wireline depth measurements are more accurate than drill pipe depth measurements. No. The opposite is true, if the drill pipe is measured accurately in tension in the elevators while tripping into the hole. Wireline takes a different path through a borehole than drill pipe; it takes all the shortcuts, the shortest route. Accelerometer tests have shown that down-hole wireline tools do not necessarily move at the same speed as the depth counter on the surface reel, and in fact there are times when they are not even moving in the same direction. And you will not likely find that in print. My point here is to make you aware that to some extent, many of our analyses that depend on borehole geometry are only precise as academic exercises, but they are still useful approximations in our applications.

7.3 Borehole friction

Friction is a resistance to motion between two bodies or media. We all studied it in basic physics or engineering courses and learned a so-called friction law for rigid bodies. It is not a law of physics at all, but you might not guess that from the way it is often presented in basic physics texts. Friction is quite complex by its very nature, and the simple friction relationship most of us learned does not hold up well

[1] Actually there was one. It was drilled near the Grand Canyon in the USA and intersected the canyon wall, so its location was determined precisely. I know of no other.

in many real-life situations. However, it is a simple relationship, and it works well enough for numerous practical applications, ours included.

7.3.1 The Amontons-Coulomb friction relationship

The simple friction relationship is often referred to as the *Coulomb friction law* or a bit more accurately as the Amontons-Coulomb friction law. It was originally the outcome of two postulates by Amontons in 1699 and has been understood in its present form since about 1790, when Coulomb added a third postulate to it.

- Frictional force is proportional to the weight of the body being moved (Amontons, 1699).
- Frictional force is independent of the apparent contact area (Amontons, 1699).
- Frictional resistance is independent of the sliding velocity (Coulomb, 1790).

That is the simple friction relationship we all learned and is stated mathematically as

$$\boxed{F \leq \mu N} \tag{7.1}$$

It says that the frictional force, F, is less than or equal to a friction factor, μ, multiplied by the normal contact force, N, *normal* meaning perpendicular to the contact surface. The relationship is necessarily an inequality, because the product of the friction factor and the normal contact force is equal to the frictional force only when the force opposite the friction force is equal to or greater than that product. In other words, if the force applied to generate motion of a body is less than μN, then the frictional force is equal to the applied force and not that product. Once the body is in motion, the friction force is equal to μN and independent of the applied force, as long as the motion is sustained. In 1699, Amontons considered objects sliding on a level surface, so he used weight instead of contact force in his postulate.

What are the assumptions in that relationship? There are several, and they often are not mentioned in basic texts.

- The contact surfaces are smooth.
- The contact surfaces are dry (uh, oh!).
- The contact surfaces do not deform.
- The friction factor is a constant, that is, not affected by the heat generated.

We could add more, but that about covers the areas of our interest. We should discuss these limitations briefly.

When we require that the surfaces are smooth, we are talking about a matter of scale. On a microscopic scale, even smooth surfaces are not what we would consider smooth. There are numerous asperities that are elastically deformed, plastically deformed, fractured, melted, fused, and so forth, as two surfaces slide relative to one another. But these microscopic asperities are small compared to the entire surface area, and the distribution of the asperities on the smooth surfaces is relatively uniform. Casing sliding in a borehole is generally on a scale that allows the use of such a relationship.

What about deformation of the contact surfaces? Suppose we have a string of casing with LT&C couplings and a string of identical-weight casing with tapered integral connections. Which is going to slide in the hole (or out of the hole) easier? No question about it, the casing with the tapered connections will slide easier than the casing with the square shouldered couplings, even though both may have identical contact force. The friction relationship does not account for couplings gouging a borehole wall. But again, that is a matter of scale, since a long string of casing has many connections (asperities?)

of uniform size. Their gross effect might be legitimately included in a friction factor. In other words, the coupling shape can be accounted for by the friction factor if we are considering numerous joints of casing.

What can we say about the effects of lubrication? Can the Amontons-Coulomb dry-friction relationship work for lubricated surfaces? In general, the answer is no, but again it depends on scale and the accuracy desired. If the lubrication is consistent, the dry-friction relationship can give reasonably practical results. By *consistent*, we mean that the friction factor does not vary significantly with contact force. The walls of a borehole usually are coated with a filter cake and the borehole contains some type of liquid drilling fluid. This provides considerable lubrication as the casing slides along the borehole wall. If the casing couplings scrape the filter cake off portions of the wall as it slides, that changes the friction factor; in other words, the friction factor may increase in those areas. Another thing that may happen is that, with removal of some of the filter cake, the casing in contact with permeable formations may tend to be forced harder against the wall from the difference in hydrostatic pressure in the borehole and formation pore spaces. In this case, the contact force has increased. We may reasonably account for some of these things by lumping all we do not know into some average friction factor. The one inconsistency we may encounter, though, is that the friction factor may vary with pipe diameter, weight, coupling shape, and so forth. This brings up a question of terminology.

Is such a composite factor as we just described, a *friction coefficient* in the sense of the Amontons-Coulomb relationship or is it something else that we might refer to as a *friction factor*? Is such a distinction really necessary? We could argue those points either way (and some do). Our use here is more as a composite (or catch-all) factor and we are going to use the term, *friction factor*, and the variable name, μ, in our borehole friction discussion. Just keep in mind that μ, as we use it, is not a value that you can look up in some table in a handbook on friction.

The single question that most often arises about the Amontons-Coulomb relationship concerns the postulate that the frictional force does not depend on the apparent area of contact. If that is true, then why do racing cars have wide tires rather than narrow? The simple answer is that the postulate is true, but racing tires are much more complicated. Briefly, the crux of the matter is the last qualification mentioned, the one regarding heat. For the most part, a narrow tire of the same composition gives the same frictional resistance on a given race car as a wide one—at low speeds. At high speeds, several things come into play, and heat is a major one. Wide tires distribute the heat over a larger area, and the heat is dissipated to the atmosphere more quickly. There is also the matter of wear or ablation of the tire. A narrow tire with a much smaller area of compound in contact with the track wears in its radial dimension much faster than a wider tire. In fact, a narrow tire might make only a few laps before it would have to be replaced. On a wet track, racers have to switch to grooved tires, which actually reduce the contact area. This is a matter of hydrodynamics, where the narrower contact areas tend to cut through the lubricating layer of water, whereas the slick tires tend to "float" on top of it. That is totally off the subject at hand, but it comes up in almost every discussion of the Amontons-Coulomb friction relationship, so that is why we address it. Still on the issue of heat, a good example of a breakdown of the simple friction relationship is automobile brakes. This is a practical example of heat affecting the friction factor significantly. Brakes are said to "fade" when they get hot, in other words the friction factor is reduced with heat. That is true in most cases of friction. Fortunately, we generally need not be concerned about the heat of friction affecting the motion of casing in a bore hole. However, it can significantly affect casing wear from internal drill pipe rotation.

Most of the preceding discussion on the limitations of the Amontons-Coulomb friction relationship has to do with linearity. In other words, the assumption of the relationship is that the friction factor is a constant. As long as the friction factor is not a function of the contact force, Equation (7.1) is simple and

easy to use. Also, linearity means that if we change our mud properties to reduce the friction factor by 25%, for instance, then we also reduce the frictional force by 25%. Likewise, if we reduce the contact force by some amount, we also reduce the friction force by the same amount. Or, if we change our casing design by increasing the wall thickness of the casing in a horizontal section of a well, we increase the friction force in that part of the hole proportionally.

Before we leave this friction relationship, there is one other important point to cover that relates to casing design. When most of us learned the simple version of friction, we were taught that two friction factors apply to a particular problem, a static friction factor, μ_s, being the larger, and a kinetic (or dynamic) friction factor which we label simply, μ, without subscript because it is the only one of interest in our applications.

That means the force to initiate motion is greater than the force required to sustain the motion once initiated. Which do we use for casing design? It might seem obvious that a static friction factor is more realistic, since motion of the pipe ceases and initiates for each connection made up in the casing string. This might not seem worth the concern, if we are considering the running process, but if we are going to reciprocate the casing while cementing or if we encounter an obstruction in the bore hole before reaching bottom and have to pull the casing out of the hole, it may be a serious concern. The caveat about static friction factors is that they are problematic except for rigid bodies. We see an example of that on the rig weight indicator all the time. When pipe is picked up off bottom we see the weight indicator increase gradually until some maximum point is reached, then it drops back to a slightly lower value. That pretty much seems to confirm what we have been taught about static and kinetic friction factors, but reconsider what we actually observe. When the driller starts to pick up the pipe, we see it moving through the rotary as the weight indicator reading increases. Some of the pipe already is moving before we reach the peak load. And, before the final peak is reached, a lot of the pipe is moving. The pipe is not a rigid body like the simple objects we encountered in basic friction applications. Once the entire string of pipe is in motion, the situation is fairly simple, since it is moving more or less as a rigid body and an approximate kinetic friction factor pretty well predicts the resistance to motion. But, what about the initiation stage? What is going on there? Obviously, if some of the pipe is in motion, we cannot assume a single static friction factor and apply it to the entire string. This brings up a basic flaw in the Amontons-Coulomb friction relationship as a step-function. Suppose we have a rigid body with a total weight, W, resting on a flat surface, as in Figure 7.1. We apply a gradually increasing force, P, to the body, and the friction force, F, resists any motion.

As P increases so does the value of F, which is equal to P, until it reaches its maximum value, $P = F = \mu_s W$. As P continues to increase, the value of the friction force decreases suddenly to its maximum dynamic value of $F = \mu W$. It remains at that value as long as $P \geq F = \mu W$. This is shown in Figure 7.2.

Once motion is initiated and $P = F = \mu W$, the motion is quasi-static. If $P > F = \mu W$ then the motion is characterized by Newton's second law, $P - \mu W = m\ddot{u}$.

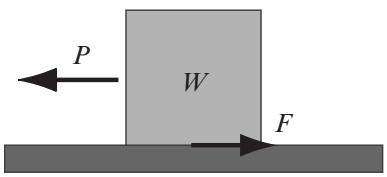

Figure 7.1 A rigid body of weight, W, at rest on a flat surface.

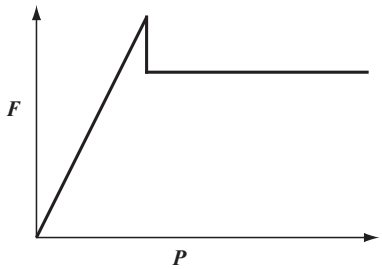

Figure 7.2 Static friction force increases until motion is initiated, then changes to a kinetic friction force.

An extensible body, however, does not behave like that. Suppose now, we model the same rigid body with four pieces instead of one and connect them with massless springs to simulate elastic extensibility. The total weight is the same, W, but each segment now weighs one fourth the total, $W/4$. This is illustrated in Figure 7.3.

We stipulate that initially the segments are all static, and there is no load in the connecting springs. In this case, as we apply a force, P, we see that initially the only body acted on until motion is initiated is the one on the left. No force is transmitted to the next segment until the first one moves. As the static friction in the first segment is overcome, the friction force drops back to the kinetic value. As we continue to increase the force, P, the same thing takes place successively in each of the other segments, but when the final segment is set in motion the total difference between the maximum static friction force and the maximum dynamic friction force is only one-fourth that of the previous rigid body example. The friction force for the segmented example is shown in Figure 7.4.

Now, suppose we divide the body into an infinite number of segments attached by massless springs. We could say that the difference between the static friction and dynamic friction disappears altogether,

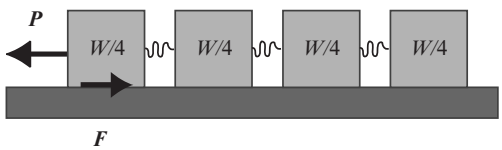

Figure 7.3 Extensible body model.

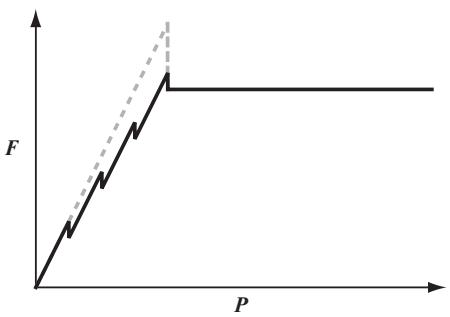

Figure 7.4 Friction force in a segmented body.

and it does, at least in this model. However, some would argue that the weight of each segment goes to zero; and while that argument may at first seem valid, it does not affect the limit. Since the static friction factor is greater than the kinetic friction factor, we can show the friction force at any time as the sum of the segments in motion times the kinetic friction factor plus the weight of one static segment times the static friction factor.

$$\mu < \mu_s \quad \rightarrow \quad F = \mu \frac{W}{n}(n-i) + \mu_s \frac{W}{n} \tag{7.2}$$

where n is the total number of segments, $n - i$ is the number of segments in motion, and i is the current number of static segments. We can take the limit of the friction force as the number of segments goes to infinity:

$$\lim_{n\to\infty} F = \mu W \lim_{n\to\infty}\left(\frac{n-i}{n}\right) + \mu_s \lim_{n\to\infty}\left(\frac{w}{n}\right) \tag{7.3}$$

$$\lim_{n\to\infty} F = \mu W (1) + \mu_s (0) \tag{7.4}$$

$$\lim_{n\to\infty} F = \mu W \tag{7.5}$$

That may be a bit over simplified, but what we have shown is that, for an extensible body, a static friction factor does not exist in the context of the linear Amontons-Coulomb friction relationship. This is not to say that a static friction factor does not exist even though all bodies are extensible to some degree, but that there are serious deficiencies in the linear Amontons-Coulomb friction relationship in regard to extensible bodies. It also points out that, for casing in a borehole, we cannot assume some value for a static friction factor, as with a rigid body, and use it for predicting the initiating force with any degree of accuracy.

So, as to calculating casing loads with friction, we are pretty comfortable with a kinetic friction factor. We know that it will take more force to initiate motion, but to determine a static friction factor for a particular well is not addressed because it is not possible. All we can truthfully say is that we require some amount of force greater than the kinetic friction force to initiate motion in a casing string that has come to rest. Another thing that we may notice in many boreholes is that the initiating force often increases with time. That usually is a sign of differential sticking, which in terms of friction translates into increased contact force rather than a different friction factor. In many such cases, the friction factor becomes a catch-all for all those things we cannot quantify otherwise.

There is another important concept to understand when dealing with directional wells: There is some critical inclination angle at which a body is at static equilibrium with movement impending. In common engineering terms, this is known as the *angle of repose*, except in that case the angle of is conventionally measured from horizontal. Since we measure inclination from the vertical, we simply call it a *critical inclination angle*, α_{cr}, meaning that any casing in the well where the inclination is greater than this value will not slide under its own weight; that is, it has to be pushed into the hole.

The critical inclination angle depends on the friction factor, and it can be derived as follows (Figure 7.5):

$$W\cos\alpha_{cr} - \mu W \sin\alpha_{cr} = 0$$

$$1 - \mu\frac{W\sin\alpha_{cr}}{W\cos\alpha_{cr}} = 0$$

$$\tan\alpha_{cr} = \frac{1}{\mu}$$

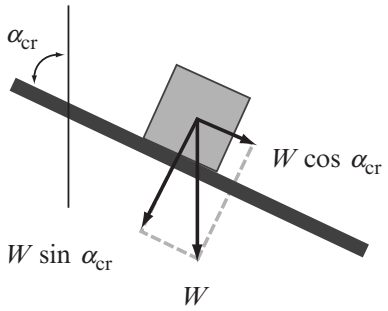

Figure 7.5 Critical inclination angle.

then

$$\boxed{\alpha_{cr} = \tan^{-1} \frac{1}{\mu}} \tag{7.6}$$

Since we know the friction factor only approximately, this formula at best gives us an idea as to where in our borehole the casing will cease to slide from its own weight. For example, if an open hole friction factor is 0.4, then the critical inclination angle, $\alpha_{cr} = 68°$. We know, then, that we cannot expect the casing to slide from its own weight and must be pushed anywhere the inclination exceeds 68°. All of us have seen similar limiting values in relation to wire line logging tools in directional wells.

7.3.2 Calculating borehole friction

A number of commercial friction software models on the market calculate borehole friction, probably to the point that hardly anyone cares how they work as long as they give reliable results. One does not really have to have software, since the calculations can be done manually, although it is a tedious process. In addition to the tedium, doing borehole friction calculations manually is error prone, in that if an error is made, it carries through to all the subsequent calculations. One can fairly easily program one of the models into a spreadsheet and get results as accurate as any commercial software, although the commercial software has numerous options to make life much easier.

Some assumptions are common to all the current models for borehole friction:

- The Amontons-Coulomb friction relationship is valid.
- The tubular string is a rigid body in translation.
- The tubular string is a rigid body in rotation.
- The tube has no bending stiffness.
- The tube is in contact with the bore hole everywhere.

The first assumption already has been discussed adequately. The second, third, and fourth assumptions are referred to collectively as the *soft string* assumptions. None of them is true, but that needs explanation. If the entire string is in translation or rotation, it does not matter if it is extensible or not because we are primarily interested in the value of friction when the entire string is in translation or rotation and not some intermediate values when only a portion of the string is in motion. The fourth assumption is that bending the pipe around a curve does not add to the contact force. In other

words, the contact force required to bend the tube is ignored. This is reasonable for drill pipe in most cases, and even for casing in most situations, so we can generally accept this assumption. Some of the commercial software now includes contact force caused by bending stiffness.[2] The fifth assumption, regarding discontinuous contact, might be questioned, however. Without better data than we currently get regarding the borehole path and shape, it is not possible to determine where the pipe is in contact with the borehole wall and where it is not. This is not a serious limitation, though, because of the first assumption in the list. Since the Amontons-Coulomb friction relationship is independent of the area of contact, the portion of the pipe that is not in contact is accounted for in the contact force where the pipe is in contact. From a practical standpoint, the current torque-and-drag software works quite well.

Most of the commercial software is based on the model of Johancsik, Frieson, and Dawson [40], which is a difference equation that uses the buoyed specific weight of the pipe in its calculations. The result is an effective axial load. Another model was formulated by Sheppard, Wick, and Burgess [41]. It is in the form of a differential equation and it ultimately produces the true axial load, with the effective axial load as an intermediate step. One might question why the commercial models use the former instead of the latter. It was published first, it is easy to program, and not many people use the true axial load for casing design in directional wells, because the unfortunate truth is that many do not understand the difference. When programmed, the second model actually does the same thing in terms of buoyed specific weight and results in an effective axial load, but it also shows how to take that result one step further to calculate the true axial load. The issue is inconsequential from a practical standpoint, in that both models produce the effective axial load and one goes a step further to produce the true axial load. The true axial load formulas of Sheppard et al. may also be used with the Johancsik et al. model results to determine the true axial load. The differential equation of Sheppard et al. is not solvable in closed form, except in the case of a single plane, that is, constant azimuth, and the assumption that the borehole curvature is that of a segment of a circle between survey points. (A circle-segment well path between surveys is the basic assumption of the minimum curvature method currently used in directional drilling.) Such closed-form solutions are derived in Appendix E. However, the single-plane, or 2D, closed-form solution is of little practical use, because it can be used only for idealized single-plane well paths and it results in two closed-form equations. The two solutions occur because at points where the contact is on the high side of the hole, the gravitational force subtracts from the contact force, and when the contact is on the low side of the hole, the gravitational force adds to the contact force. An incremental calculation method must be used to determine when to switch from one solution to the other. A number of tests were done using the closed-form solution to test the accuracy of numerical techniques for solving Johancsik et al.'s difference equation and Sheppard et al.'s differential equation. A simple incremental method was used in Johancsik et al.'s equation. An Euler method, a second-order Taylor series, and a fourth-order Runge-Kutta method were used for solving Sheppard et al.'s differential equation. As it turns out, the simple incremental method gave almost identical results with the difference equation as the more sophisticated fourth-order Runge-Kutta method for the differential equation, when the same number of increments were used. The Euler method never approached the order of accuracy of the other methods, even with twice the number of increments. The net result is that

[2] In their paper, Taylor and Mason [38] state that a quadratic borehole path should be adequate, and they could see no need for a higher order curve. Well, not quite. The minimum curvature borehole path is a quadratic spline which is a class C^1 curve at the junctions (survey points) meaning that the slope (first derivative) is continuous at the survey points, but not the curvature (the second derivative). To get an adequate well path to include bending, we really need class C^2 smoothness at the junctions. Of course this requires a cubic spline and more assumptions. Where bending stiffness is added to software it is a patchwork of sorts, but while hardly as mathematically elegant as continuous curvature at the junctions, it works well enough.

a simple incremental solution to either equation gives acceptable results, as long as one uses a sufficient number of subintervals between survey points. The following is the differential equation of Sheppard et al. [41]:

$$\boxed{\frac{\mathrm{d}\hat{F}}{\mathrm{d}s} = \bar{w}\cos\alpha \pm \mu\left[\left(\hat{F}\frac{\mathrm{d}\alpha}{\mathrm{d}s} + \bar{w}\sin\alpha\right)^2 + \left(\bar{w}\,\frac{\mathrm{d}\beta}{\mathrm{d}s}\sin\alpha\right)^2\right]^{\frac{1}{2}}} \tag{7.7}$$

where

$\hat{F} =$ effective axial load

$\bar{w} =$ buoyed linear weight of casing, $\bar{w} = k_{\mathrm{b}}\, g\, \rho_{\ell}$

$s =$ coordinate along the casing central axis

$\mu =$ friction factor

$\alpha =$ inclination angle

$\beta =$ azimuth angle

The first term on the right is the gravitational contribution to the axial load, and the second term is the frictional contribution, that is, the friction factor multiplied by the contact force. The $\pm$ sign is determined by whether the pipe motion is into the well (negative) or out of the well (positive). Two things to note about this equation are that the axial load appears on both sides of the equation and the contact force always is positive. In a straight section of bore hole, the axial load is dependent on the contact force, but the contact force is not dependent on the axial load. In that case, the axial load disappears from the contact force term. In a curved bore hole, the axial force is dependent on the contact force as in a straight section, but also the contact force is dependent on the axial load. The differential equation may be solved numerically as an initial-value problem using a second-order Taylor method or a fourth-order Runge-Kutta method. As previously mentioned, an Euler method does not give very good results, even with a significantly greater number of increments. An incremental formulation of the Sheppard et al. equation gives equally good results as the more sophisticated Taylor and Runge-Kutta techniques with sufficient number of increments. The initial condition at the bottom of the hole is $\hat{F}(0) = \hat{F}_0$ which accounts for any weight set on bottom. The incremental form of Johancsik et al. [40] is

$$\boxed{\hat{F}_n = \hat{F}_0 + \sum_{i=1}^{n}\left[(s_i - s_{i-1})\,\bar{w}_i\cos\left(\frac{\alpha_{i-1}+\alpha_i}{2}\right) \pm \mu_i N_i\right]} \tag{7.8}$$

where the contact force is given by

$$\boxed{\begin{aligned} N_i \;= (s_{i-1} - s_i)\Bigg\{&\left[\bar{w}_i\sin\left(\frac{\alpha_{i-1}+\alpha_i}{2}\right) + \hat{F}_{i-1}\left(\frac{\alpha_i - \alpha_{i-1}}{s_{i-1}-s_i}\right)\right]^2 \\ &+ \left[\hat{F}_{i-1}\left(\frac{\beta_i - \beta_{i-1}}{s_{i-1}-s_i}\right)\sin\left(\frac{\alpha_{i-1}+\alpha_i}{2}\right)\right]^2\Bigg\}^{\frac{1}{2}} \end{aligned}} \tag{7.9}$$

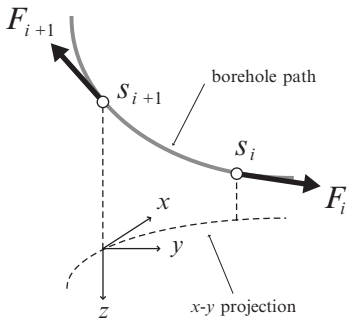

Figure 7.6 Node numbering system for borehole friction calculations.

In this last equation, the angle measurements must be in radians. (When angles appear in formulas outside of trigonometric functions, they are almost always in radians.) The numbering of the nodes starts at the bottom of the hole with node 0 and proceeds to the top as seen in Figure 7.6.

Using these formulas one may write a simple spreadsheet program to do the calculations of borehole friction for casing design.

To convert the values of effective load at any node to true load, one may use the formula from Chapter 4:

$$F_i = \hat{F}_i - (p_o A_o - p_i A_i) \tag{7.10}$$

There are times when we might consider rotating the casing while cementing. This is not often done in highly inclined or horizontal wells because of the significant amount of friction. However, if it can be done at a torque less than the maximum recommended makeup torque of the connections, then there is a possibility of doing it. After all, getting a good cement job in a horizontal well is difficult enough as is, and everything we could do to displace the mud is worthwhile. The differential form of the torsion equation is

$$\frac{dT_q}{ds} = r_o \mu \left[\left(\bar{w} \sin\alpha + \hat{F} \frac{d\alpha}{ds} \right)^2 + \left(\hat{F} \frac{d\beta}{ds} \sin\alpha \right)^2 \right]^{\frac{1}{2}} \tag{7.11}$$

where r_o is the outside radius of the casing. This is also a one-dimensional differential equation with the boundary condition, $T_q(0) = T_{q\,0}$ at the bottom of the tube, although that would be zero for most casing strings. We could solve this initial-value problem using a second-order Taylor method or a fourth-order Runge-Kutta as previously mentioned. We could just as easily cast this equation in an incremental form, where it becomes

$$T_{q\,n} = T_{q\,0} + \sum_{i=1}^{n} r_i \mu_i N_i \tag{7.12}$$

and the normal contact force is calculated by Equation (7.9) as in the axial friction case. In this case, the axial load used to calculate the normal contact force is not itself a function of the contact force, so it may be calculated separately for use in Equation (7.9) from the following.

$$\hat{F}_i = \hat{F}_o + \sum_{k=1}^{i} (s_{k-1} - s_k)\, \bar{w}_k \cos\left(\frac{\alpha_{k-1} + \alpha_k}{2}\right) \tag{7.13}$$

An incremental approach such as this and the one for sliding friction are used in most commercial software. And, as previously mentioned, numerical techniques do not give better solutions when applied directly to the differential form as long as a sufficient number of increments are used.

The drawbacks to using these models for casing design are the lack of actual friction factors and the idealized well plan as opposed to the actual hole as drilled.

Common Friction Factors

There are no tables of values in which to look up friction factors for boreholes. There are some average values for water-based drilling fluids:

- 3.0-4.0 for an open hole.
- 2.0-2.5 for a cased hole.

If one were using an oil-based mud, those values might be reduced by 30-50%. In practice, measurements of the actual hook load are made in the field, and the values are plugged into a commercial torque-and-drag model, which iteratively finds a friction factor that gives results matching the field measurements. This is of great benefit during drilling operations but of little use if the casing is being designed before the well is drilled, unless one has data from previously drilled wells. Even if we have the correct friction factor, the next problem facing the casing designer is the well path.

In a conventional L-shaped horizontal well plan, for instance, the vertical portion of the well plan is exactly that—vertical! There is no friction in that portion of the hole according to the models. And the rest of the hole also is totally smooth with no tortuosity. The actual hole is quite different, there is friction in the "vertical" section, and none of the rest of the well is quite as smooth as the planned well path. How do we deal with that? One possibility is to use the data from a similar well with some possible adjustments. Some commercial software have a way to impose some tortuosity on the planned well path in the form of a sinusoidal curve or some type of random "noise" curve. Both are good, but they require some experience to know how much tortuosity to use. One other method is to add an inclination of a few degrees to the "vertical" section of the plan and use a "high" friction factor for casing design. Figure 7.7 shows the calculated true axial load for upward motion of 5-1/2 in. casing in an actual well plan and the true axial load in this well as it was actually drilled.

For most wells, it is not critical what method is used, as long as it is recognized that one cannot use a perfect well path plan to design a casing string for a real well. Long-reach and high-pressure wells may require a lot more planning and even considerable effort to drill the well as nearly smooth and close to the planned path as possible.

The result of the friction calculations just discussed is a load curve similar to Figure 7.7 that we would employ for designing our casing string for tensile loads. In that particular curve, the friction is calculated for an upward motion of the casing string once on bottom, similar to what we would expect if reciprocating the casing while cementing. We can plot these curves either in terms of effective axial load or true axial load, depending on how we intend to design our casing string. If we expect to rotate the casing while cementing, we would also want a plot of the rotating torque from friction, so that we might verify whether or not the connections of our string will permit rotation. Maximum recommended makeup torque generally is the limiting factor in rotating most casing strings. The main point here is that, in highly deviated wells, we do not use the simple vertical well assumptions we used in Chapter 4.

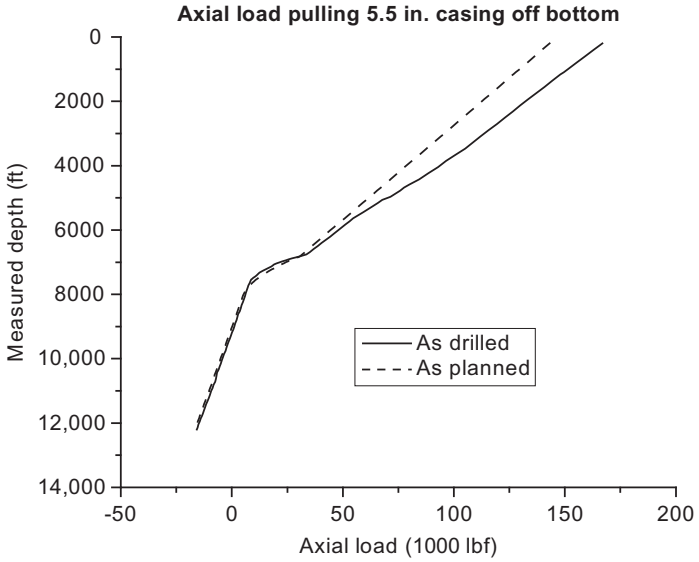

Figure 7.7 Drag friction distribution for 5-1/2 in. casing being pulled off bottom in a horizontal well, as planned and as drilled.

That having been said, there is one other important point: The friction curves do not account for bending stresses in the pipe attributable to borehole curvature. That is a later topic.

7.3.3 Torsion

All torsion in wellbores is a result of frictional resistance to rotation, hence, torsion in casing is almost never considered. There are few occasions where casing can be rotated in horizontal wells because the torque required to rotate casing usually exceeds the maximum makeup torque of the connections. There are instances however where liners can be (and are) rotated while cementing. Sometimes liners have been rotated to get to bottom and to help clean the hole while circulating.

One thing we must include here is that *slotted liners should never be rotated*. Tests have shown that they easily fail at less than a third the torque required to fail a solid liner and the failure occurs so easily that there is no indication at the surface that the liner has failed. There are some slotted liners sold as capable of being rotated liners, but tests (unpublished unfortunately) have shown that they fail just as easily.

7.4 Casing wear

Casing wear is a serious problem in many intermediate strings and some surface strings. It often is the reason that an intermediate string cannot be used as a production string in combination with a production liner. Reduced wall thickness or a hole in the pipe can be disastrous. There is no good way to repair badly worn pipe so that it will contain higher internal pressures other than to run a new string inside it with the accompanying reduction of internal diameter. Hence, it is quite important to prevent or minimize casing wear.

The primary mechanism for casing wear is the rotation of drill pipe, although the tripping of the drill pipe also contributes to the wear but to a lesser degree. Two things are necessary for the wear to occur, and these are fairly obvious: contact force and movement of the drill pipe (rotation and sliding). The rate of wear depends on a number of things, such as

- Magnitude of contact force
- Rotation speed
- Lubricity of the drilling fluid
- Relative hardness of the drill pipe tool joints and casing
- Presence of abrasives

Of course, the total amount of wear depends on all these plus the time duration during which wear occurs. Typically, we measure the amount of wear as a percentage of reduction in the wall thickness, with 100% meaning that the wall thickness is completely worn through. Reduction of wall thickness is a linear measure and therefore somewhat misleading. The amount of metal removed under a specific set of conditions generally is a linear function of time, but the reduction of wall thickness is not. Figure 7.8 illustrates why it is not.

It is easy to see that, as the tool joint wears into the wall of the casing, more volume of metal must be removed in relation to the amount of penetration. So, while the rate of metal removed may be linear with time or cumulative revolutions, the reduction in actual wall thickness is not. We can see that, initially, the wall thickness reduction is quite fast, but as it progresses, it becomes much slower because of the increasing volume of metal that must be removed for a corresponding reduction in wall thickness.

Prevention of casing wear is of utmost concern in most wells. Historically, most of what was known about preventing wear came from common sense and experience. We have long known that rough hard-banded tool joints can wear a hole in casing as quickly as a mill. Even heat galling can take place when the lubricity of the mud is low and the contact force is high. And, no matter what precautions are taken, if there is sand in the mud, all wear mechanisms are accelerated. Even with rubber pipe protectors, the presence of sand causes wear, since the sand grains can become embedded in the rubber itself. So, assuming we know to keep abrasives to a minimum and hard-banded tool joints out of the casing while rotating, where do we install the pipe protectors to reduce wear? It was once thought that we could make

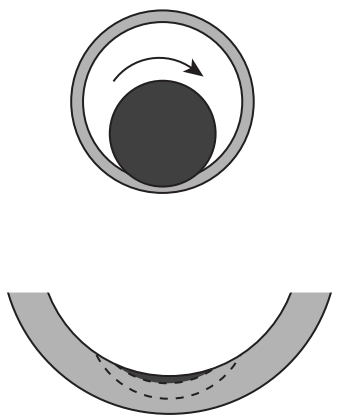

Figure 7.8 Increasing volume of metal with reduction in wall thickness.

a plot of dog-leg severity (hole curvature) to determine where the critical wear areas were. Historically, this proved unreliable. In general, casing wear is not a function of the magnitude of the dog-leg severity. The worst wear in casing typically occurs nearer the surface rather than deeper and often where the magnitude of the dog-leg severity is typically less than 1° or 2° per 100 ft, as opposed to deeper in the well where the dog-leg severity might exceed 4°/100 ft, for example. Another approach that proved more useful is a plot of the difference between successive dog-leg severity measurements. While that is a much better indication of the areas of most severe wear, it too can be grossly misleading in some parts of the well. Until casing was studied more seriously, that remained the only tool readily available to most operators for determining the best location for pipe protectors. Most operators just ran them on every joint or so in the upper half of the casing as a precaution.

A lot of work has been done to try to quantify wear in casing, and software is available to predict the amount of wear. The results of such predictions have been mixed at best and, in many cases, have been totally unreliable. The difficulty in quantifying wear is in quantifying all the variables that affect the process. In other words, one has to know pretty accurately the time spent rotating, the penetration rate, the lubricating properties of the mud, the rotation speed, the type and concentration of solids and abrasives in the drilling fluid, and so forth. However, this is not a dismissal of such software by any means. While it has proven relatively poor at quantifying actual casing wear, it is extremely good at predicting where the critical wear areas in a casing string are located. For any given mud system and amount of rotating time, the areas of most severe wear are those areas that experience the greatest amount of contact force between the tool joints and casing. That contact force is quite easy to quantify, at least to the accuracy needed.

An investigation was done several years ago with this type of software run *post priori* on several wells that had experienced holes worn in the casing. Good drilling data were available, as well as caliper logs that had been used to locate the holes, and of course, directional surveys, which are essential for use of the software. The results were a bit disappointing. In none of these particular wells did the software predict a hole in the casing, even though each actually had a hole worn through the casing. In fact, the worst wall thickness loss predicted in any of the wells by the software was slightly more than 50%. But, the important point again is that where the software predicted the worst wear to occur was exactly where the holes were (see Figure 7.9). In addition to the wear curves, the contact force curves were plotted for comparison in Figure 7.10, and in fact, the wear curves and contact force curves were almost identical, except of course for the scale. The conclusion of that particular study was that, while the software was not very good at quantifying the amount of wear, it was excellent for determining the critical wear areas. It also was found that a contact force curve by itself was adequate for predicting where pipe protectors were needed while drilling below those strings of casing. And that, ultimately, is what we want to know, because we cannot know with certainty the exact properties of the mud system, abrasives content, and rotating time prior to drilling below the casing. However, we do know the shape of the hole we just cased, and the planned well path below the casing well enough to predict the amount of contact force on the casing string we have just installed.

The other useful indicator mentioned, differential dog-leg severity essentially is the difference between the dog-leg severity at one point and that at the previous point. While it often gives a similar plot to the two above, it gives misleading results near the bottom of the casing string because it cannot account for the reduction in contact force caused by smaller values of axial tension.

Rotating contact force can be calculated from the borehole friction formulas presented earlier in Equations (7.9) and (7.13), and they easily can be programmed into a spreadsheet. Most commercial torque-and-drag software also generates a contact force curve. But, to use the contact force for determining the need for pipe protectors, one must have directional survey data, and in the case of

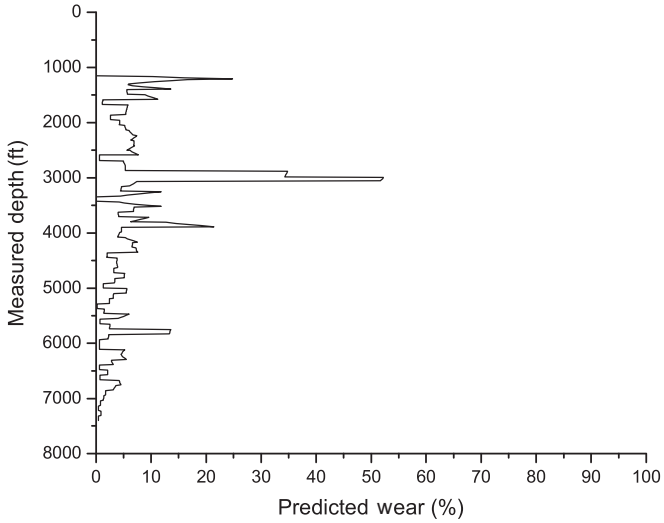

Figure 7.9 Results from casing wear software, showing the predicted amount of wear in a particular well. This casing string had a hole in it at about 3000 ft.

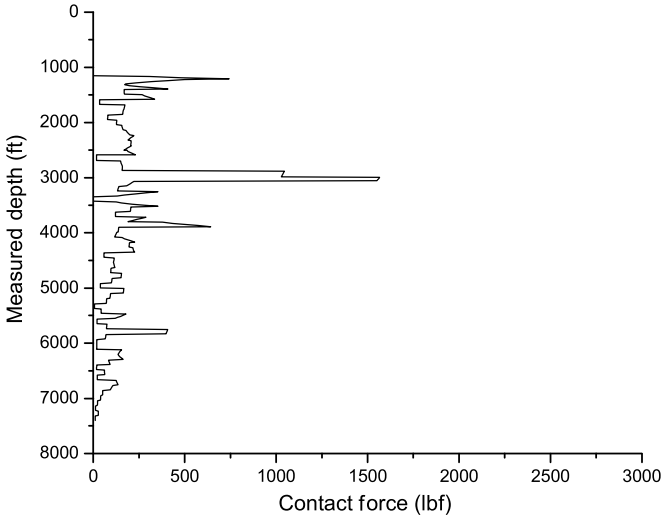

Figure 7.10 Contact force for same well.

vertical wells, this may not be available. Many companies feel that if a well requires an intermediate string for over-pressured reservoirs below, then it should also have a gyro survey run in the intermediate casing in the event it becomes necessary to drill a relief well to kill a blowout. In those cases, the gyro survey can serve both purposes. There really is no reason for not being able to determine where the casing wear will be most severe and where pipe protectors should be placed in a drill string. Given that knowledge and common sense as regard to wear mechanisms, casing wear should not be a severe problem.

7.5 Borehole collapse

One of the early concerns in horizontal drilling was a borehole stability issue related to the way in which the *in situ* stress field is oriented to a horizontal borehole. Because the largest of the *in situ* stress components, the overburden stress, σ_v, acts in a vertical direction it was feared that borehole collapse would be a potential problem. And in some cases that proved to be true. However, the dilemma was: Will it, or will it not be a problem? Lacking any quantitative data, many operators elected to run some type of liner into the horizontal section as a sort of insurance policy just in case. But rather than run a full string of casing or conventional liner and cement it in place which is quite expensive, most chose to run a slotted or perforated liner instead. As insurance against borehole collapse it is probably a reasonable choice. Unfortunately, from a completion perspective it is probably the worst choice one can make for a horizontal well. Unless you can get it out of the borehole later (and you should assume you cannot), there is nothing else you can do with that wellbore as far as monitoring production or zonal isolation for testing or stimulation. In short, there is nothing effective you can do other than accept what the well produces. Additionally, a slotted liner is a very poor means of sand control, its original purpose. The problem inherent with this type of completion is that most of the flow along the lateral takes place outside the liner and does not enter the liner until it is near the heel of the lateral. There is no way to run any kind of production profile to plan a stimulation. There is no way to spot a stimulation treatment where it is most needed and one cannot even use diverting agents to perform an effective stimulation. If the well starts to produce saltwater there is no way to determine where it is being produced and no way to isolate it or shut it off. The hard fact is that once you install a slotted liner in a horizontal lateral you have precluded all remaining options for managing the production from that lateral.

All that said, there are some better options even with slotted liners. One of the more successful is slotted (or pre-perforated) liner sections along with blank sections and external casing packers. Inflatable casing packers have long been favored, though their reputation has often suffered somewhat over the years, mostly from haphazard placement practices and inadequate evaluation than from actual failure of the packer itself. In recent years, swelling type packers have become quite popular in many such applications. And of course a conventional casing string or liner is always an option, whether cemented or with some type of zonal isolation packers. The critical point here is that whatever means one takes to insure against borehole collapse the most important consideration in the selection process is the future management of production in the wellbore.

7.5.1 Predicting borehole collapse

There are methods for predicting borehole failure through collapse, and they are discussed briefly in Appendix E. The problem that we face in casing design is that we seldom have the data and/or expertise to do a proper analysis. Typically, most such stability analyses are done for drilling purposes, but critical

for casing design is the issue of pressure depletion during the life of the well. A horizontal wellbore that is stable during drilling (even under-balanced) may later become unstable later in its producing life as the pore pressure declines. These are issues we cannot address here, except to develop an awareness for the potential problems.

There is one somewhat related issue that we must consider, and this is probably a good place. Often times in earlier horizontal drilling operations one would hear someone claim that their borehole had collapsed "halfway through the build section." Mostly, such incidents have occurred while running drill pipe back in a hole after a bit trip. But the same phenomenon has also occurred when running casing into a horizontal well where it hits an obstruction about halfway through the build section where the inclination is about 45° or so. Casing failures have occurred in such instances, and I have included a real-life example later in this chapter. The usual description of such an event has been that the drill pipe encountered an obstruction, the driller circulated, rotated, and washed through the obstruction, and a "bunch of cuttings came across the shale shaker." The conclusion: "borehole collapse." Or is it? If you examine the example borehole stability curves in Appendix E you will note that the most critical stability inclination is 90°, not some intermediate value like 45°. If the borehole collapsed at the midpoint in the build section, it would collapse from that point all the way down, yet in these instances the lower part of the hole was always open. There are instances where there is an unstable shale zone on top of the pay zone and the transition from the shale to the pay zone is near the midpoint of the build section. In those cases such an explanation might certainly be valid, but most of these "collapses" were reported where such was not the case. The true explanation in most of these cases was (and still is) a cuttings removal problem. The part of a build section between about 40° to 60° is the most difficult part of a hole to clean of drilled cuttings. In the horizontal section, cuttings tend to settle to bottom and are removed with a combination of agitation from pipe rotation, proper mud rheology, and circulation rate. In the build section, however cuttings may settle to the low side of the hole where the circulating velocity is low, but they also start migrating back down the hole and form accumulations. In fact lab experiments have shown that along the low side of the hole there actually can be a flow of cuttings in the opposite direction of the circulation. Drillers are accustomed to making a bit trip and finding a few feet of "fill" on bottom after a trip, but in a horizontal well the fill is not on bottom but in the build section and it is usually more severe. So, cuttings removal in these wells is critical in the casing process.

7.5.2 Designing for borehole collapse

What are the forces on casing during a borehole collapse? If there is any one topic in casing design that begs a good solution this is it. The one thing we can say is that, with the possible exception of salt flow, it is not likely to be a uniform radial pressure load. The problem with a collapsing borehole is that the loading on the pipe is seldom uniform like a hydrostatic pressure. It can be different in every case, depending on the geometry of the borehole cross section (seldom a perfect circle), the formation stress field, the formation material, formation heterogeneities, etc. The ultimate design process will likely be some sophisticated finite element procedure that cannot be replicated by simple manual calculations. There is one simple method that has been used, though not particularly good. That is a unidirectional distributed load as shown in Figure 7.11.

In the figure the distributed load f is acting in a vertical direction uniformly across the surface of the pipe. An approximate solution to this problem was derived by Nester et al. [42]. And it is stated as

$$Y > \frac{2 f r_o}{3 (r_o - r_i)} \tag{7.14}$$

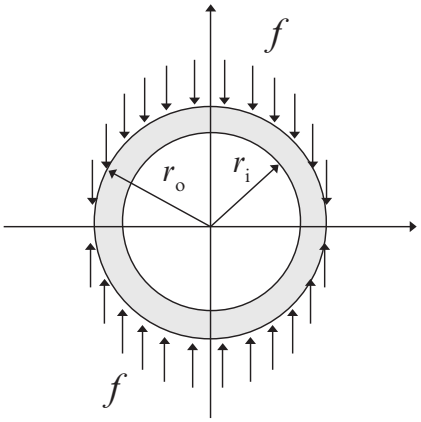

Figure 7.11 A possible non-uniform, transverse loading on casing.

The only questions are what value to use for the distributed traction load, f and some would suggest using the value of the overburden stress, $f = \sigma_v$. That might be a bit severe and can lead to selecting some very heavy pipe in a horizontal section where friction is directly proportional the pipe weight. A more reasoned choice might be $f = \sigma_v - p_{depl}$, where p_{depl} is the pore pressure at depletion. If you do choose to use this formula, you should definitely also check the conventional radial collapse because this formula will sometimes give you a lesser collapse value.

Effect of perforations

Another design concern that many have is the effect of perforating on casing collapse strength in borehole collapse. Crushing tests performed by King [43] led to the following conclusions:

1. Shot densities of 4-8 shots per foot have little effect on crush resistance.
2. Shot densities of 12-16 shots per foot with 60^o phasing have little effect on crush resistance.
3. Phasing of 0°, 90°, or 120° with 12-16 shots per foot significantly reduce crush resistance, especially when a line of perforations is 90° to the load direction.

Salt flow and geotectonic activity

In some parts of the world salt beds behave as a visco-plastic liquid, though the flow rate is quite slow. Consequently the hydrostatic pressure exerted by the salt is equal to the overburden stress, σ_v discussed in Appendix E. This pressure is much higher than ordinary pore pressures and can easily collapse a conventionally designed casing string. One solution is the use of special thick-walled casing with wall thicknesses on the order of 1-1.5 in. Other solutions have been successfully applied, such as two concentric casing strings with cement between the two strings. If the salt flow is radially symmetric (i.e., hydrostatic) in nature the problem is similar to conventional collapse except with higher external pressures. The difficulty arises when the flow is not symmetric and we are back to the quandary mentioned above—how to model a non-uniform borehole collapse. These are not common design considerations, but for those interested, equations for collapse of concentric

casing-cement-casing strings with uniform radial loading have been proposed by Marx and El-Sayed [44], and for non-uniform loads by El-Sayed and Khalaf [45].

As to geotectonic activity such a fault movement and subsidence, the prognosis is grim. These forces of nature can move mountains, and there is no casing string that can resist such forces. In the case of fault motion the most successful approach has been to under-ream the hole across the fault and cement the casing below and above the expanded hole section. This allows some amount of movement of the fault before it eventually collapses and shears the casing. Similarly, un-cemented casing in subsidence intervals allow some flexibility in the casing string to postpone eventual failure. The hard fact is that all you can do is delay the time of casing failure; you cannot prevent it.

7.6 Borehole curvature and bending

Curved boreholes add stress to casing, and often that added stress is quite significant. A general lack of understanding of this has led to casing failures in the build sections of a number of horizontal wells. We now examine the effects of borehole curvature and the resulting bending stresses in casing.

But, before we get into particulars, we need to see a couple of formulas, because we encounter them time and again in working with curved boreholes. Curvature is the change in angle with respect to the distance along the path, or mathematically,

$$\boxed{\kappa \equiv \frac{\mathrm{d}\theta}{\mathrm{d}s}} \tag{7.15}$$

where

$\kappa =$ curvature

$\theta =$ reference angle (inclination angle in 2D wellbore)

$s =$ distance along curved path (wellbore length measurement)

The curvature may be expressed in two forms: as curvature, meaning a change in angle as just shown, or a radius of curvature, r_κ:

$$\boxed{r_\kappa = \frac{1}{|\kappa|}} \tag{7.16}$$

There is a mathematical quirk here, in that the curvature can be either positive or negative (as we defined it), but the radius of curvature always is positive, since a negative radius is meaningless.

Curvature is measured in units of reciprocal length, that is, L^{-1}. In oilfield parlance, curvature is called by a colorful term, *dogleg severity*, in reference to a crooked hole. It usually is measured in degrees per 100 ft or degrees per 10 m. To convert from curvature as used in oilfield terminology to radius of curvature and vice versa, we need a formula. In USC units this is

$$\kappa = \frac{18000}{\pi\, r_\kappa} \tag{7.17}$$

$$r_\kappa = \frac{18000}{\pi\, \kappa} \tag{7.18}$$

where

$\kappa =$ curvature (dogleg severity), degrees/100 ft

$r_\kappa =$ radius of curvature, ft

In SI units, the conversion formula is

$$\kappa = \frac{1800}{\pi\, r_\kappa} \tag{7.19}$$

$$r_\kappa = \frac{1800}{\pi\, \kappa} \tag{7.20}$$

where

$\kappa =$ curvature (dogleg severity), degrees/10 m

$r_\kappa =$ radius of curvature, m

There are two other versions of curvature in metric units, degrees per 30 m and degrees per 100 m. The former is numerically approximately the same as degrees per 100 ft and was used for a number of years but is fading from popularity. When using degrees per 30 m, the numerator is 5400. The latter measure, degrees per 100 m, was common about 20 years ago but does not see much use today.

We employ two conventions in referring to curvature here:

- Although we often use radius, r_κ, to quantify curvature, the descriptions *small* or *large values of curvature* refer to the values of κ. Hence, a large radius refers to a small curvature and vice versa.
- Measure of curvature in boreholes always is assumed to be taken at the central axis of the bore hole.

One more comment on curvature is in order. As we defined it in Equation (7.15) we are using curvilinear coordinates. In Cartesian coordinates curvature takes on a more complicated form and is conventionally defined as:

$$\kappa = \left| \frac{\mathrm{d}^2 y/\mathrm{d}x^2}{\left[1 + (\mathrm{d}y/\mathrm{d}x)^2\right]^{\frac{3}{2}}} \right|$$

In most instances the derivative in the denominator is small when squared so the equation reduces to $\kappa \approx \left|\mathrm{d}^2 y/\mathrm{d}x^2\right|$. The absolute value is taken in the conventional form, but for our applications we allow for the negative value also because curvature has sign significance in borehole applications (build sections and drop sections).

7.6.1 Simple planar bending

Calculating bending stresses can be a formidable undertaking in general. Even the planar bending problem is a two-dimensional elasticity boundary-value problem, and several assumptions usually are adopted so that a simple solution may be obtained from a one-dimensional ordinary differential equation, a derivation of which is given in Appendix C. These *ad hoc* assumptions are known variously as Euler-Bernoulli beam theory, *planar beam theory*, or simply just *beam-bending theory*. No theory really is involved, but merely a set of *a priori* assumptions about the way a beam deforms in bending that allows for an analytic solution to the more complicated boundary-value problem. For the case of tubes, such as casing, these are the typical assumptions:

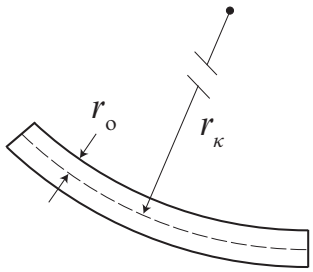

Figure 7.12 Simple planar bending of tube.

- The tube initially is straight.
- The tube cross section is symmetric about the central longitudinal axis.
- All cross sections normal to the longitudinal axis before bending remain normal to the axis after bending.
- The central longitudinal axis (neutral axis) experiences no axial strain
- The tube radius is small compared to the length.
- The bending deflections are small in comparison to the length, so that the radius of the tube remains constant in all directions.

The result of these assumptions is an equation for the axial strain:

$$\varepsilon_s = -y\frac{\mathrm{d}\theta}{\mathrm{d}s} \tag{7.21}$$

where y is a coordinate in the bending plane with origin at the neutral axis (center), θ the angle in the plane of curvature, and s an axial coordinate along the neutral axis of the tube. Substituting this into a one-dimensional constitutive equation (Hooke's law) gives us the axial bending stress:

$$\sigma_\mathrm{b} = \sigma_s = E\,\varepsilon_s = -E\,y\,\frac{\mathrm{d}\theta}{\mathrm{d}s} \tag{7.22}$$

It is obvious that the maximum stress occurs at the point where y is equal to the outside radius of the pipe, r_o. But we might want to determine the stress at the inner wall also in cases of internal pressure, so we will just leave off the subscript with the understanding that $r_\mathrm{i} \le r \le r_\mathrm{o}$ The term, $\mathrm{d}\theta/\mathrm{d}s$, is the curvature of the bent tube, which is the reciprocal of the radius of curvature, r_κ So, in practical form (Figure 7.12), the equation becomes

$$\boxed{\sigma_\mathrm{b} = \pm E\frac{r}{r_\kappa}} \tag{7.23}$$

where

$\sigma_\mathrm{b} =$ bending stress, (+) for tension, (−) for compression

$E =$ Young's elastic modulus

$r =$ radius of pipe where stress is determined (i.e., inside or outside)

$r_\kappa =$ radius of curvature of borehole path

It is important that the units used are consistent. In USC units, the radius of the pipe usually is in inches and the radius of curvature of the borehole path usually is in feet, so they must be converted to the

same unit (it does not matter which). In SI units, both measures should be in meters. Young's modulus usually is in units of psi, kPa, or MPa, and the bending stress is in the same units.

It is necessary to remember the assumptions of this formula before using it, especially with tubes. As a tube bends, its cross section tends to ovalize rather than remain circular. The pipe radius in the bending plane is reduced as the cross section becomes ovalized, and the formula no longer is valid. Since there is no simple way to determine the point at which the shape is too ovalized to use the formula, the tendency is to ignore it, since it will over-predict the maximum bending stress when the pipe is slightly ovalized. That makes the formula possibly a bit conservative in casing design. For long and medium radius of curvature wells, it seems to work well for all but larger diameter, thin-wall pipe. For short-radius wells, it should be used with caution, and again, it would depend on the pipe diameter and wall thickness. That may seem to avoid the specific, but for certain, we can say that it becomes meaningless if the yield point is exceeded. In addition to the tendency to become oval the cross section changes in another way. The compressive side becomes thicker and the tensile side becomes thinner. This causes the neutral axis to shift also. These effects are negligible for small bending deflections, but do not ignore the possibilities. And since in the case of oval deformation, Equation (7.23) will over predict the stress (the effective value of r_o is reduced), it may still be considered as a conservative approach.

7.6.2 Effect of couplings on bending stress

One limitation of the simple bending formula, as we typically apply it, is that it assumes the casing is in contact with the borehole wall along its entire length and its curvature is the same as that of the bore hole. This does not account for an amount of standoff from the couplings. The coupling standoff allows for local bending with a smaller radius of curvature than that of the bore hole, therefore possibly a higher bending stress from axial tension or compression loading in the pipe. In the tensile case, the couplings are assumed tangent to the borehole wall, so that if the pipe between couplings is not in contact with the borehole wall, then the tension tends to straighten the joint between couplings. The result is that the greatest bending stress in the joint is in the pipe body near the couplings, until the pipe makes contact with the borehole wall, then the maximum bending stress in the pipe may be at some other point. In the compression case, the casing between couplings is forced toward the borehole wall in a compressive mode and the bending stress is higher near the couplings. Once pipe body contact with the borehole wall is made in compression, the point of maximum curvature and bending stress may be at some other point in the tube. This is illustrated in Figure 7.13.

An equation for determining the maximum bending stress with connections was derived for the tension case by Lubinski [46] in 1961, and later derivations were done for both tension and compression by Paslay and Cernocky [47] in 1991. Lubinski's equation initially was developed to account for the

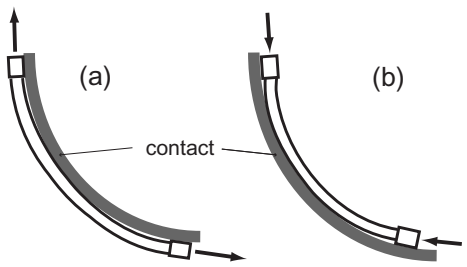

Figure 7.13 Effects of couplings in bending: (a) tension and (b) compression.

standoff of drill-pipe tool joints and the effects this had on the fatigue of drill pipe rotating in tension in curved boreholes. His equation later began to appear in conjunction with casing design in curved wellbores. His equation (and all that follow in this discussion) assumes that the borehole curvature is constant and in a plane between casing couplings, the coupling length is small compared to the length of the joint, the couplings are in contact with the borehole wall, and the couplings are tangent to the borehole curvature at the point of contact. Also assumed is that, since the coupling is relatively small in length, its entire length is in contact with the wall and it does not bend. These are reasonable assumptions. Although not in Lubinski's original form, his equation from 1961 can be written as follows:

$$\sigma_{\mathrm{b}} = \lambda_{\mathrm{b}} E \frac{r_{\mathrm{o}}}{r_{\kappa}} \tag{7.24}$$

which is essentially the same as our previous bending equation (7.23), except for the factor, λ_{b}, which has been called a *bending-stress magnification factor*. Note that there is no $\pm$ in this equation, since Lubinski's equation is valid only in tension. Lubinski's bending-stress magnification factor is

$$\lambda_{\mathrm{b}} = \frac{\varphi}{\tanh(\varphi)} \tag{7.25}$$

where

$$\varphi \equiv \frac{\ell}{2}\eta \tag{7.26}$$

and

$$\eta \equiv \sqrt{\frac{|F_s|}{E I_{\mathrm{a}}}} \tag{7.27}$$

where

$\ell =$ joint length between couplings

$F_s =$ axial load along curvilinear borehole path (tension in this case)

$E =$ Young's modulus of elasticity

$I_{\mathrm{a}} =$ axial second area moment of tube cross section

The second area moment of the tube cross section about an axis passing through the center of the tube perpendicular to its longitudinal axis is

$$I_{\mathrm{a}} = \frac{\pi}{4}\left(r_{\mathrm{o}}^4 - r_{\mathrm{i}}^4\right) = \frac{\pi}{64}\left(d_{\mathrm{o}}^4 - d_{\mathrm{i}}^4\right) \tag{7.28}$$

A reminder, use consistent units. Note also that we used the absolute value of the axial load in this formula. In this particular equation, we are talking about tension, but later we use the same quantities for equations in which the axial load is in compression, a negative value, and the square root would be a complex number. We choose this slight modification so that we may use the same nomenclature later in both the tension and compression states. And, in that context, we could resume use of the $\pm$ sign in Equation (7.24), once the equations for λ_{b} are derived for the compression case.

The limitation of this equation of Lubinski's is that the casing does not contact the borehole wall between the couplings. Simply stated, if there is contact, the equation is not valid. That notwithstanding,

his equation has appeared in various places to show that coupling standoff is important in casing design, but without mention of the contact limitation. One cannot just plug numbers into Lubinski's equation without understanding its limitations. One must always determine the valid range for a specific application.

The maximum displacement, y_{max}, from a straight configuration to contact by the midpoint of the casing between couplings, as written by Lubinski, is

$$y_{max} \approx \frac{\ell^2}{8R} + \omega \tag{7.29}$$

This gives the approximate maximum displacement of the midpoint of an initially straight pipe deflected to the point of contact with the borehole wall. The second term, ω , is the standoff from the coupling, defined as

$$\omega \equiv r_{cpl} - r_{csg} = \frac{d_{cpl} - d_{csg}}{2} \tag{7.30}$$

where

$\omega =$ standoff

$r_{csg} =$ outside radius of casing

$r_{cpl} =$ outside radius of coupling

$d_{csg} =$ outside diameter of casing

$d_{cpl} =$ outside diameter of coupling

As previously mentioned, Paslay and Cernocky [47] did additional work in this area. They solved the problem in both tension and compression and cast it in a slightly different format, which lends itself to computer programming. The tension case results in a formula for each of the three possibilities: no contact, point contact, and wrap contact. The first two are self-explanatory, and the wrap contact is reached when the curvature of the pipe in contact with the bore hole begins to follow the curvature of the bore hole. Since there are both tension and compressive axial-loading possibilities, the pipe can take six modes of deformation:

- Mode 1. Tension, no contact
- Mode 2. Tension, point contact
- Mode 3. Tension, wrap contact
- Mode 4. Compression, no contact
- Mode 5. Compression, point contact
- Mode 6. Compression, wrap contact

Paslay and Cernocky derived equations for all six modes, plus four equations necessary to define the transition between modes (two for tension and two for compression). I present their results with very little explanation, and one should read their paper for a full understanding of the derivations.

Mode 1. tension, no contact

The bending-stress magnification factor for this mode is

$$\lambda = \varphi \frac{\cosh \varphi}{\sinh \varphi} \tag{7.31}$$

This equation is equivalent to Lubinski's equation (7.25). The nomenclature for this equation and all the following remain the same as previously defined.

Mode 2. tension, point contact

Point contact begins when the tension is such that

$$1 - \cosh\varphi + \left(\frac{\varphi}{2} - \frac{2\,\eta\,\omega\,R}{\ell}\right)\sinh\varphi = 0 \tag{7.32}$$

This nonlinear equation in φ must be solved numerically for values of tension, F_s, contained in η and φ, to establish the value of tension at which contact is established. The equation for the bending-stress magnification factor for point contact is

$$\lambda_b = \frac{\varphi\left[(\sinh\varphi - \varphi) - \left(\frac{\varphi}{2} + \frac{2\,\eta\,\omega\,R}{\ell}\right)(\cosh\varphi - 1)\right]}{2\,(\cosh\varphi - 1) - \varphi\sinh\varphi} \tag{7.33}$$

Mode 3. tension, wrap contact

Wrap contact begins when the curvature in the casing first begins to equal that of the bore hole where the two are in contact. Wrap contact begins when the magnitude of the tension is such that

$$\frac{\varphi}{2}(\cosh\varphi + 1) - 2\,\sinh\varphi + \left(\frac{2}{\varphi} - \frac{2\eta\,\omega\,R}{\ell}\right)(\cosh\varphi - 1) = 0 \tag{7.34}$$

This nonlinear equation must be solved numerically to determine the value of the axial tension at which the wrap contact begins. The equation for the bending-stress magnification factor in wrap contact is

$$\lambda_b = \frac{\frac{\xi^2}{2} + \eta^2 R\,\omega\,(\cosh\xi - 1) - \xi\,(\sinh\xi - \xi)}{\xi\,\sinh\xi - 2\,(\cosh\xi - 1)} \tag{7.35}$$

where we must first solve the following nonlinear equation numerically for ξ:

$$\frac{\xi^2}{2}(\cosh\xi + 1) - 2\xi\,\sinh\xi + \left(2 - \eta^2 R\,\omega\right)(\cosh\xi - 1) = 0 \tag{7.36}$$

Paslay and Cernocky state that the solution of interest is in the range

$$\varphi \le \xi \le \eta\,R\cos^{-1}\left[\frac{R}{R+\omega}\right] \tag{7.37}$$

Mode 4. compression, no contact

The equation for no contact in compression is.

$$\lambda_b = \frac{\varphi}{\sin\varphi} \tag{7.38}$$

Mode 5. compression, point contact

When the compression load in the casing reaches a magnitude at which point contact is made, the following condition is satisfied:

$$1 - \cos\varphi - \left(\frac{\varphi}{2} + \frac{2\,\eta\,\omega\,R}{\ell}\right)\sin\varphi = 0 \tag{7.39}$$

It must be solved numerically to obtain the axial load at which point contact occurs.

The Paslay and Cernocky bending stress magnification factor for point contact in compression is a bit more complicated, in that there are three possibilities as to where the maximum bending-stress occurs. The maximum could occur at the coupling, the midpoint of the joint, or under some circumstances, at another location in the pipe. One must determine the first two, then determine if the third possibility exists and, if so, its magnitude. Once those are calculated, the maximum of the three is the bending-stress magnification factor.

At the coupling,

$$\Lambda_{\text{cpl}} = \frac{\varphi\left[\left(\frac{2\,\eta\,\omega\,R}{\ell} - \frac{\varphi}{2}\right)(1 - \cos\varphi) + \varphi - \sin\varphi\right]}{2\,(1 - \cos\varphi) - \varphi\sin\varphi} \tag{7.40}$$

At the midpoint,

$$\Lambda_{\text{mid}} = \frac{\varphi\left[-\left(\frac{2\,\eta\,\omega\,R}{\ell} - \frac{\varphi}{2}\right)(1 - \cos\varphi) + \varphi\cos\varphi - \sin\varphi\right]}{2\,(1 - \cos\varphi) - \varphi\sin\varphi} \tag{7.41}$$

Two additional quantities are needed to determine the possible third point:

$$\Gamma = \frac{\varphi\left[\left(\frac{2\,\eta\,\omega\,R}{\ell} - \frac{\varphi}{2}\right)\sin\varphi + 1 - \cos\varphi\right]}{2\,(1 - \cos\varphi) - \varphi\sin\varphi} \tag{7.42}$$

$$\Omega = \tan^{-1}\left(\frac{\Gamma}{\Lambda_{\text{cpl}}}\right) \tag{7.43}$$

Then, the third possible bending-stress moment is

$$\Lambda_s = \Lambda_{\text{cpl}}\cos\Omega - \Gamma\sin\Omega \qquad \Leftrightarrow \qquad 0 < \Omega < \varphi \tag{7.44}$$

If Ω is outside the valid range, then Λ does not exist and the maximum bending-stress moment will be either at the midpoint or the coupling. The maximum bending-stress factor is the maximum absolute value of the three possibilities:

$$\lambda_{\text{b}} = \max\left(\left|\Lambda_{\text{cpl}}\right|, \left|\Lambda_{\text{mid}}\right|, \left|\Lambda_s\right|\right) \tag{7.45}$$

Mode 6. compression, wrap contact

When the compression load in the casing reaches a magnitude such that wrap contact begins, the following condition is satisfied:

$$\frac{\varphi}{2}(1 + \cos\varphi) - 2\sin\varphi + \left(\frac{2}{\varphi} - \frac{2\,\eta\,\omega\,R}{\ell}\right)(1 - \cos\varphi) = 0 \tag{7.46}$$

As before, this must be solved numerically to determine the axial compressive load at which wrap contact begins.

The bending-stress magnification factor for wrap contact in compression has two possibilities: The maximum is at the coupling or some other point between the coupling and the midpoint. Since the casing curvature at the midpoint is the same as the borehole curvature, the bending magnification factor there is unity.

At the coupling,

$$\Lambda_{\text{cpl}} = \frac{\frac{\xi}{2} - \eta^2 \omega R\,(1 - \cos\xi) + \xi\,(\xi - \sin\xi)}{\xi \sin\xi - 2\,(1 - \cos\xi)} \tag{7.47}$$

where we must first solve the following nonlinear equation numerically for ξ:

$$\frac{\xi^2}{2}\,(1 + \cos\xi) - 2\xi \sin\xi + \left(2 - \eta^2\,\omega R\right)(1 - \cos\xi) = 0 \tag{7.48}$$

Paslay and Cernocky do not give a range for the solution, but it appears the range given in Equation (9.32) might be at least a starting point.

We then calculate two more quantities:

$$\Gamma = \frac{\left(\frac{\xi}{2} - \eta^2 \omega R\right)\sin\xi + \xi\,(1 - \cos\xi)}{\xi \sin\xi - 2\,(1 - \cos\xi)} \tag{7.49}$$

and

$$\Omega = \tan^{-1}\left(\frac{-\Gamma}{\Lambda_{\text{cpl}}}\right) \tag{7.50}$$

Then, we calculate a stationary value of the bending-stress factor at some location in the pipe, if it exists:

$$\Lambda_s = \Lambda_{\text{cpl}} \cos\Omega - \Gamma \sin\Omega \quad \Leftrightarrow \quad 0 < \Omega < \xi \tag{7.51}$$

If Ω is outside the specified range, then Λ_{s} does not exist. Paslay and Cernocky recommend assigning a value of unity in that case, if it is used in a computer program. A value of unity is equivalent to saying there is no bending-stress magnification at that point. Then, the maximum bending-stress magnification factor for this joint of pipe is the maximum of the absolute values of Λ_{cpl} and Λ_{s}:

$$\lambda_{\text{b}} = \max\left(\left|\Lambda_{\text{cpl}}\right|, |\Lambda_s|\right) \tag{7.52}$$

Comments on bending-stress magnification

As can be seen, calculation of the bending stress magnification factors of Paslay and Cernocky is not exactly something that can be done manually. These formulas may be programmed for computer implementation, but the programming is not trivial. Paslay and Cernocky were interested primarily in drill-pipe fatigue, and they mention solving the transition equations for the standoff quantity that we labeled ω. In that context, the equations are linear and solved easily. That may be of some use in selecting a drill-pipe string with various options as to tool joint dimensions, but in most casing design, the standoff, ω, is a fixed quantity, and our primary interest in the transition equations is in the value of the *axial load* that determines the transition point from one mode of contact to another, so that we might

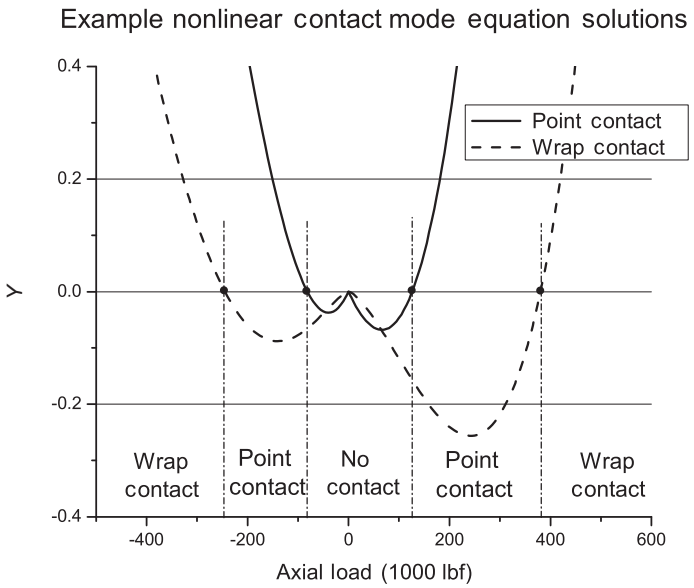

Figure 7.14 Typical behavior of transition equations for tension and compression. The compression equation has additional solutions farther to the left (solutions at $Y = 0$).

apply the appropriate equation for the bending-stress magnification factor, λ_b. In terms of the axial load, which is contained in the variables, η and φ, these equations are nonlinear and must be solved numerically. All the nonlinear equations that must be solved numerically have been recast here to avoid singularities in the numerical solutions, so they may not exactly resemble those of Paslay and Cernocky. However, some of these equations have local minima and maxima and multiple roots, so they are best solved with a bracketing technique, such as the bisection method. It might be of some help to see a plot of some of the nonlinear equations that determine the contact mode transition points, and an example is shown in Figure 7.14. This figure is for a specific casing size and borehole curvature so it will vary for different casing sizes and borehole curvature.

The two equations that define the transition between tensile modes are relatively easy to solve with a simple bracketing method, such as a bisection method. However, for small values of curvature, κ, (or large radius, r_κ), there is a range for which contact is physically impossible and will result in an infinite root. That condition, which is not addressed by Paslay and Chernocky, can be quantified as

$$\omega > \sqrt{r_\kappa^2 + \left(\frac{\ell}{2}\right)^2} - r_\kappa \tag{7.53}$$

Another characteristic of the tensile modes is that, when the curvature is small, the value of the tensile load at which point contact occurs is far greater than the joint strength of the casing, so there is no point in searching for a root if it lies beyond the joint strength.

The two transition equations for compression exhibit especially bad behavior, as equations with trigonometric functions often do over a wide range of values. As previously mentioned, the equations of Paslay and Cernocky have been recast here to avoid numerical singularities, but they still produce multiple roots. The first roots for these two equations tend to lie close to the origin for large curvature

and further away for smaller values of curvature. From a computational standpoint, this means that a combination procedure that first brackets the root starting very near the origin, then proceeds to locate the root within the bracket, is a good approach. The physical meaning of the additional roots to these equations does not appear to have been explored, but Mitchell [33] has done work in lateral buckling of drill pipe in curved boreholes and shows that the Paslay and Cernocky equations underpredict the bending-stress magnification in cases where compressive loading causes lateral buckling. The reason for the higher bending-stress magnification in those cases is that the lateral buckling is out of the plane of the wellbore curvature to which the Paslay and Cernocky equations are confined.

It is does not seem to have been mentioned in any of the discussions on the bending-stress magnification factor as to the nature of the axial load used for actual calculations. Simple bending, as described by Equation (7.23), is independent of axial loading, but the bending-stress magnification factor, λ_b, is not. That raises the question as to whether we use the true axial load or the effective axial load to calculate λ_b. The largest factors in tension arise from use of the effective axial load, which has no compression in the string. More accurate results should come from the true axial load, however, the compressive axial load in the bottom portion of the string begs a few questions. First, the values of λ_b in the compressive section are usually minimal except in the case of a horizontal (or other highly deviated well), where a significant amount of casing is below the critical angle point. Secondly the compression formula does not consider lateral buckling which generally will not be planar as required in the assumptions.[3]

When one calculates the bending-stress magnification factors for a particular casing design, one may be alarmed at their magnitudes, which easily may range between 1 and 4, yet for some reason, this process rarely is considered in actual casing design. One excuse might be that it is not something that can be calculated easily, but surely if casing failures actually occur because of bending-stress magnification, then everyone would have a computer program to calculate it. The most probable reason that we do not recognize problems caused by bending-stress magnification is likely because, in most casing strings, the highest value of tension occurs near the surface, where the curvature often is relatively small. It is not unusual to see bending-stress magnification factors of over 5 in such instances, but the bending stress attributable to borehole curvature is so small that, when multiplied by a large magnification factor, it still is only a small percentage of the yield strength of the casing, especially when we are inclined to use relatively large design factors in tension loading. This is not to say that it can be ignored, but that it does not seem to cause problems in most wells (or at least that we recognize as such). Bending-stress magnification should certainly be considered for casing design in deeper wells and any well where the combined loading may be close to the yield of the casing.

We definitely do not attempt an example calculation here, but Figure 7.15 shows an example of the bending stress magnification factors for an actual horizontal well. And, as would be expected from our discussion, they are highest near the surface.

These factors were calculated to check a previously designed casing string for the specific borehole in which it would be run. While the results might tend to be cause for apprehension because of the large magnitudes, the overall effect in this well is negligible, as will be seen in a following section of this chapter devoted to combined loading in directional wells. The combined loading for this well is shown with and without bending-stress magnification in that section in Figure 7.16. It can be seen there that

[3] Personally, I run both along with both an upward and downward friction calculation (using software of course), and almost always opt for the effective load for a design check as it is more conservative.

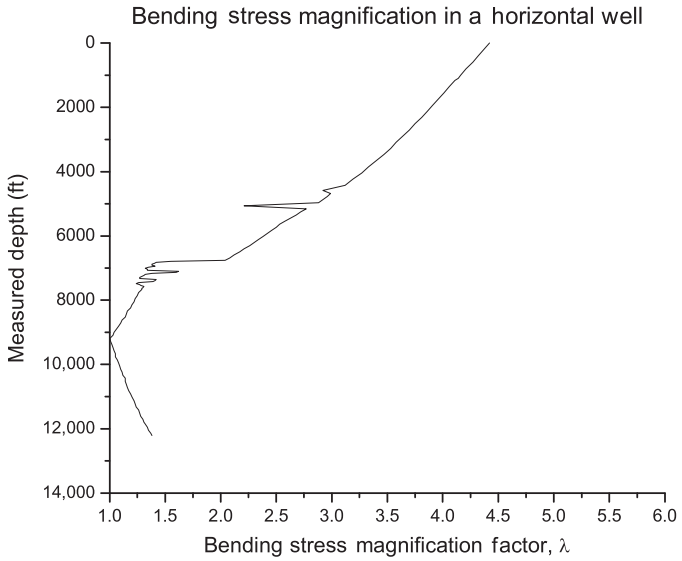

Figure 7.15 Bending stress magnification factor for a horizontal well.

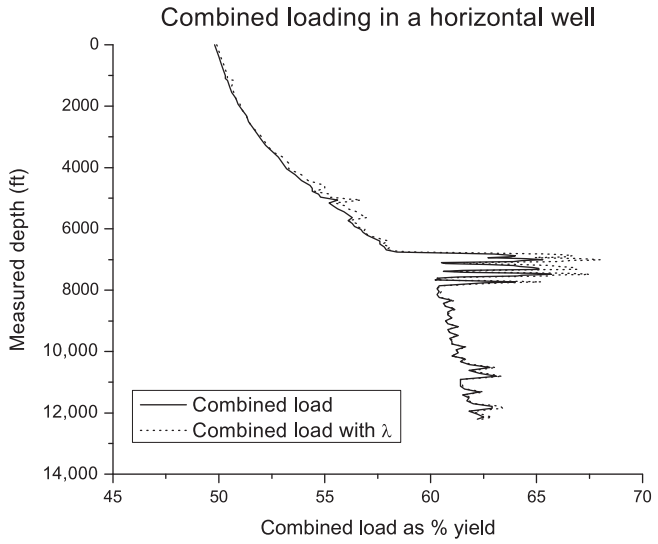

Figure 7.16 Combined loading in a horizontal casing string.

the only significance of the bending-stress magnification is in the build section of the well, as one would intuitively expect.

The transition point equations as I have formulated them here are all nonlinear because I have used the coupling standoff, ω, as a given, and then calculated the axial load at the mode transition points. However, as I mentioned above, Paslay and Cernocky formulated the algorithm using the axial load as the given and calculating the standoff at the transition points using linear equations. In our case

of known actual standoff that method could be used to calculate the standoff at the transition points and then determine into which mode bracket the actual standoff belongs. That might be a preferable approach for some who would rather not program as many nonlinear equations.

One last comment is in order here. Paslay and Cernocky assumed a constant curvature, κ, and couplings tangent to the borehole wall. Those are reasonable assumptions and really the only way to obtain closed form solutions. Implicit in the assumption of tangent couplings is the assumption that the curvature remain constant or nearly constant at least one joint length either side of the joint in consideration. That is not a serious restriction, given the approximate nature of assumed geometry, but the stress magnification could be more severe (or less) if the borehole path varied from that smooth curvature.

7.6.3 Effects of bending on coupling performance

There are no standards on coupling performance in bending other than what some companies and manufacturers established for themselves. API Bulletin 5C3 and a 2004 draft of ISO 10400 contained two formulas for "joint strength of round thread casing with combined bending and internal pressure." Oddly, there were no terms in those two formulas to quantify the bending or pressure. The first edition of this text included those two formulas (with a note of considerable skepticism). The release version of ISO/TR 10400 [11] made no such mention of bending or internal pressure. Therefore those two formulas do not appear in this edition.

One way that combined bending and axial load was handled historically amounted to multiplying the maximum bending stress times the cross-sectional area of the tube, adding it to the axial load, then comparing that sum to the joint strength of the casing. The best recommendation that could be made here is no recommendation at all, as no particular method inspires much confidence. One thing that should be understood about the eighth-rd thread in a bending situation, though, is that it is considered a poor choice by most operators. V-shaped threads have a tendency to "jump out" or override one another because the shape is conducive to this, and possibly more so in the presence of a thread lubricant. Most operators of horizontal wells elect to use a thread with a more squared profile as opposed to a V-shaped profile, because it lessens the possibility of jump-out. A buttress thread has a square contact in tension but is somewhat tapered in compression. A buttress-type thread has performed successfully in medium-radius wells for many operators. Most proprietary threads are a better choice, and in critical wells, the proprietary threads that tend to interlock are a much better, although more expensive solution. Some proprietary thread manufacturers publish bending performance data for their connections, and these can be quite useful.

7.7 Combined loading in curved boreholes

We examined combined loading in the previous chapter. Perhaps, the most common occurrence of failure from combined loading is in horizontal wells or highly deviated wells. Primarily, this is caused by the addition of the bending stress, which can be quite significant in magnitude. Our approach to casing design for these wells is to use conventional load curves for burst and collapse. Then, the tension design is based on a load curve that includes the effects of both gravity and friction, so it will be quite different from casing hanging in a vertical well. A typical curve like this was shown earlier in Figure 7.7. John

Greenip [48] illustrated a simple method for designing casing strings in highly deviated wells, using torque-and-drag curves like we discussed in an earlier section on borehole friction. He went a step further to include bending stress, which he converted to an "equivalent axial load" by multiplying the bending stress by the cross-sectional area of the tube so that it might be considered part of the tensile load. That equivalent axial load is added to the axial load from the borehole friction curves in the appropriate places to constitute a tensile load curve for casing selection. The procedure produces an adequate design for most directional wells and has been used successfully by numerous operators. Here, we assume that we designed a casing string by that method or something similar, and we now are ready to check it for the effects of combined loading, especially in the build section.

Although none of the single loads, such as tension, bending, or burst, may exceed the yield strength of the pipe individually, it is quite possible that the combination of the loads may exceed the yield strength. And there are no handy charts to adequately show the effects of the combined loads often encountered in highly deviated wells. It is easy to check the combined loads at critical points manually to determine whether we need to make adjustments to a design or not. We also could do this with a spreadsheet and check the entire string. Next is an example of a horizontal well in which there was a casing problem. The operator had drilled the vertical part of the hole and a build section to an inclination of 90°. The company was running 7 in. casing, and about halfway through the build section, the casing hit an obstruction, which is not unusual in a horizontal well, if the drilled cuttings are not sufficiently cleaned out of the bore hole.[4] The operator took immediate action. He put a circulating head on the casing, then tried to wash through the obstruction. At first unsuccessful, the driller slacked off the brake even further. As hard as it may be to understand, he set the entire string weight on the obstruction. The shoe plugged and the internal pressure at the surface rose to 3000 psi before he was able to shut off the pumps and pick up the string off bottom to relieve the pressure. The operator pulled the casing out of the well and found one of the joints in the build section had buckled and crushed. Here are the data and calculations for this actual case.

EXAMPLE 7.1 Combined Loading in Curved Wellbore

Data at 6000 ft (TVD):

- Casing OD = 7.0 in.
- Casing ID = 6.366 in.
- Casing grade = K-55 ($Y = 55{,}000$ psi)
- Young's modulus = 30×10^6 psi
- Axial compression = –122,000 lbf (from torque and drag estimate)
- Radius of curvature = 300 ft
- External pressure = 3000 psi
- Internal pressure = 6000 psi

Determine if combined loads will yield pipe.

1. Calculate the axial stress:

$$\sigma_z = \frac{-122000}{\frac{\pi}{4}\,(7.0^2 - 6.366^2)} = -18,331 \text{ psi}$$

[4] The build section of horizontal wells is notoriously difficult to clean because cuttings tend to migrate down the low side of the hole at inclination angles between 45° and 60°, even at relatively high circulating rates.

2. Calculate the bending stress:

$$\sigma_{\mathrm{b}} = -\frac{30 \times 10^6 \ (7.0/2)}{12\,(300)} = -29,167 \text{ psi}$$

Note that we had to get the radius of curvature into the same units as the pipe radius.

3. Calculate the pressure effect using at the outside wall using the Lamé equations:

$$\sigma_r = -3000 \text{ psi}$$

$$\sigma_\theta = \frac{-3000(3.5^2 + 3.183^2) + 2(6000)(3.183)^2}{3.5^2 - 3.183^2} = 25,694 \text{ psi}$$

4. The maximum axial stress at the external wall is the preceding axial stress plus the bending stress:

$$\sigma_z = -18331 - 29167 = -47,498 \text{ psi}$$

5. Since there is no torque, these are principal stress components and can be plugged directly into the von Mises criterion:

$$\Psi = \sqrt{\frac{1}{2}\left[(-3000 - 25694)^2 + (25694 + 47498)^2 + (-47498 + 3000)^2\right]}$$

$$\Psi \approx 63,900 \text{ psi}$$

$$63,900 > 55,000 \quad \rightarrow \quad \text{yield}$$

Clearly, this combined load value is well above the yield strength of the casing. This casing string, in fact, did fail. The operator was not aware that the combined loading could be that significant. In this case, the operator was lucky to get the casing out of the hole. Others have encountered similar circumstances and found the lower part of the casing string missing when they pulled the string out of the hole. In this case, we calculated the combined load at the outer wall of the casing, assuming that, since the maximum bending stress occurs at the outer wall, that would be the critical location. But, the maximum stress from pressure occurs at the inner wall, and if we calculate it at the inner wall, we find that the combined load there would be slightly less at 63,700 psi. In this case, it was not obvious as to whether the maximum combined load would occur at the inner wall or outer wall, but it did appear obvious that, since the pipe was in compression, it would occur on the concave side of the curve. One should be careful about such assumptions, however. While the maximum combined load typically occurs on the concave side when the pipe is in compression and on the convex side when it is in tension, that is not true in general because of the influence of the pressure.

It is relatively easy to program the Lamé equations and the von Mises yield criterion in a spreadsheet to calculate the combined loading for a well for use in casing design. From a directional survey, one needs the measured depths, true vertical depths, and radius of curvature between survey points. From a torque-and-drag model, one needs the true axial loads for motion in both directions, so that one may check for the worst-case scenario. Additionally, one needs the pipe dimensions and specific weights, the fluid densities, applied pressures, and so forth. One does not actually need both directional and friction software to get this data, as it all can be programmed into a single spreadsheet. The addition of a bending-stress magnification factor would be a bit cumbersome in a spreadsheet though, but it can be done. One convenient way to look at combined loading in casing design is in a plot of the

combined load as a percentage of pipe yield stress. Figure 7.16 shows the combined load in an actual L-shaped horizontal well as a percent of the yield of the casing. This is a rather simple case, where the entire string is a single weight and grade of casing, 5-1/2 in., 17 lb/ft, N-80. The operator plans to do multiple hydraulic fracture treatments in this well at high rates and pressures. The combined load is calculated for a burst scenario, where the fracture treatment might screen out with a full column of fracture fluid and proppant such that the pressure equalizes at maximum surface treatment pressure.

A plot like this figure provides an easy way to visualize the effects of combined loading. If necessary, a casing string can be modified to compensate for the combined loading effects. One last reminder though, combined loading using a von Mises yield criterion does not account for connection strength nor collapse prior to yield, as mentioned in previous chapters.

7.8 Casing design for inclined wells

The example well we used in Chapters 2–4 was for a vertical well. How would we design casing for a directional well with the same fracture and formation pressure data? The answer is that we would follow exactly the same procedure using vertical depths and pressures as before and we would reach a point as at the end of Chapter 4 with a completely designed casing program adequate for our directional well to which we would add the following steps:

Intermediate Casing

- Calculate borehole friction for intermediate string and adjust axial design if necessary.
- Calculate combined loads for intermediate string in curved portion of wellbore and adjust design if necessary.
- Calculate the section lengths of the casing for purchasing and running (as opposed to the vertical lengths in the design.
- Calculate contact force on intermediate string for placement of drill pipe protectors while drilling to total depth. This can only be done after the intermediate hole is drilled and before drilling below the intermediate casing.

Production Casing

- Calculate borehole friction for production string and adjust axial design if necessary.
- Calculate combined loads for production string in curved portion of wellbore and adjust design if necessary.
- Calculate the section lengths of the casing for purchasing and running (as opposed to the vertical lengths in the design.

Let us illustrate these items in examples, first lets us establish the well geometry and data. Typically we would have this data in a well profile plan provided by a service company according to our specifications, in other words, they would do all the calculations. But for our example we will make the specifications and do the calculations ourselves.

EXAMPLE 7.2 Directional Well Profile

Using data from our example well in previous chapters we will say the vertical depth is 14,000 ft as before. Our target zone at 14,000 ft is 8000 ft horizontally from the surface location and we will drill a horizontal

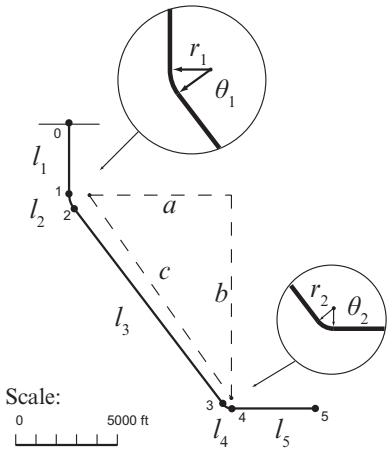

Figure 7.17 Example directional well profile.

lateral from that point an additional 3000 ft in length. That is the entirety of our data for this well plan, a surface location and a target at the beginning of a lateral and a target at the end of the lateral. From there on, it is up to us as to how we drill the hole. Optimizing a borehole path is not the topic of our endeavor here, so we will just arbitrarily select a common approach. We will drill a vertical hole to 3000 ft and set surface casing. At 500 ft below the surface casing we will begin the directional drilling with an upper build section with a radius of 1000 ft. We will hold a constant inclination angle to near the top of the lateral at which point we will drill a lower build section with a radius of 500 ft. Upon reach a horizontal inclination at our first target we will drill the lateral for an additional 3000 ft. A profile of this plan is shown in Figure 7.17.

Data

$$\text{vertical depth} = 14,000 \text{ ft}$$

$$\text{hz displ.} = 11,000 \text{ ft}$$

$$a = 7000 \text{ ft}$$

$$b = 10,000 \text{ ft}$$

$$l_1 = 3500 \text{ ft}$$

$$l_5 = 3000 \text{ ft}$$

$$r_1 = 1000 \text{ ft}$$

$$r_2 = 500 \text{ ft}$$

Using the given data and Figure 7.17 we may calculate the additional quantities needed. The only clarification needed is to recognize that the line, c, is not parallel to l_3, so the angle, θ_2 requires a bit more attention.

Calculations

$$c = \sqrt{a^2 + b^2} = \sqrt{7000^2 + 10000^2} = 12,207 \text{ ft}$$

$$l_3 = \sqrt{a^2 + b^2 - r_2^2} = \sqrt{7000^2 + 10000^2 - 500^2} = 12,196 \text{ ft}$$

$$\theta_2 = \frac{\pi}{2} - \left[\sin^{-1}\left(\frac{a}{c}\right) + \sin^{-1}\left(\frac{r_2}{c}\right)\right]$$

$$= \frac{\pi}{2} - \left[\sin^{-1}\left(\frac{7000}{12207}\right) + \sin^{-1}\left(\frac{500}{12207}\right)\right] = 0.91912 \text{ rad}$$

$$\theta_1 = \frac{\pi}{2} - \theta_2 = \frac{\pi}{2} - 0.91912 = 0.65167 \text{ rad } (\approx 37^\circ)$$

$$l_2 = r_1\,\theta_1 = 1000\,(0.91912) = 919 \text{ ft}$$

$$l_4 = r_2\,\theta_2 = 500\,(0.65167) = 326 \text{ ft}$$

Calculate the measured depths of the nodes:

$$s_1 = l_1 = 3500 \text{ ft}$$

$$s_2 = s_1 + l_2 = 3500 + 919 = 4419 \text{ ft}$$

$$s_3 = s_2 + l_3 = 4419 + 12196 = 16,615 \text{ ft}$$

$$s_4 = s_3 + l_4 = 16615 + 326 = 16,941 \text{ ft}$$

$$s_5 = s_4 + l_5 = 16941 + 3000 = 19,941 \text{ ft}$$

Calculate the vertical depths of the nodes:

$$h_1 = s_1 = 3500 \text{ ft}$$

$$h_2 = h_1 + r_1 \sin\theta_1 = 3500 + 1000 \sin(0.65167) = 4107 \text{ ft}$$

$$h_3 = h_2 + l_3 \sin\theta_2 = 4107 + 12207 \sin(0.91912) = 13,812 \text{ ft}$$

$$h_4 = h_3 + r_2 - r_2 \sin\theta_1 = 13812 + 500 - 500\sin(0.65167) = 14,000 \text{ ft}$$

$$h_5 = h_4 = 14,000 \text{ ft}$$

It is an exercise in trigonometry, but to avoid common mistakes remember that inclination is measured from vertical (θ_1 is the same as the inclination angle, θ_2 is not, even though they may appear otherwise), and always work in radians and convert to degrees when finished.

Now that we have those calculations done we need to determine the measured depths of our casing sections. First, we do the 9-5/8 in intermediate casing which has two sections with the transition point at a vertical depth of 6360 ft and the bottom at 10,500 ft.

EXAMPLE 7.3 Intermediate Casing Section Lengths

We calculate the lengths, ℓ, of the two sections, starting with the top section, ℓ_2. The bottom section length, ℓ_1, is all in the inclined straight section.

$$\ell_2 = s_2 + \frac{6360 - h_2}{\cos\theta_1} = 4419 + \frac{6360 - 4107}{\cos(0.65167)} = 7253 \text{ ft}$$

$$\ell_1 = \frac{10500 - 6360}{\cos\theta_1} = \frac{10500 - 6360}{\cos(0.65167)} = 5207 \text{ ft}$$

Table 7.1 Example 9-5/8 in. Intermediate Casing

Section	Weight (lb/ft)	Grade	Vert. Depth (ft)	Meas. Depth (ft)	Sect. Length (ft)
2	43.5	P-110	6360	7253	7253
1	43.5	N-80	10500	12460	5207

We summarize the results in Table 7.1.

Next we will determine the borehole friction for this casing string. We do these calculations with software programmed from the equations earlier in this chapter using only six survey points (at the nodes in Figure 7.17) because this is a smooth well plan. Because of the smoothness of the planned profile we will use higher than average friction factors to account for some amount of tortuosity in the well as drilled. We will use a factor of 0.3 in. the cased hole and 0.5 in. the open hole. The vertical section of the well will have zero contact no matter what friction factor we select, we will assume an increasing inclination angle up to 4° in that section. We will also employ the interpolation algorithm in Appendix E to add nodal points so as to generate a usable graph that we would not get with only six surveys. The friction load is plotted in Figure 7.18 along with the axial strengths of the casing.

As you can see, the casing strength is well above the friction load. You may notice that the friction load is based on the effective axial load instead of the true axial load. Both the Johancsik et al. [40] and the Sheppard et al. [41] models calculate borehole friction using the effective stress as is this case. This curve can be corrected to a true axial load with friction using Equation (7.10), but given the approximate nature of our method of using a smooth well plan profile and increased friction factors to account for tortuosity, it is hardly worth the effort since it usually has to be done manually. Most commercial

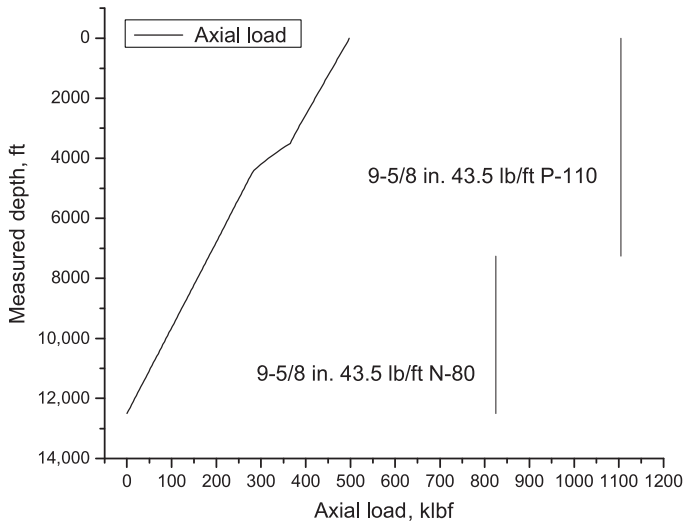

Figure 7.18 Example intermediate casing, axial load with friction (upward motion case).

software can be "tricked" into giving a true axial load by applying a "bit weight load" equivalent to the buoyant pressure load at the bottom, but this only works if the entire casing string is the same wall thickness.

A point regarding that friction curve is that there exists a pervasive misconception that in a directional well with friction, the true axial load does not exist because most of the string is "out of the shadow of the casing top." That is pure bunk, and where such a notion came from is a mystery (I have seen this actually taught in industry training courses). The only time the pressure effects are not distributed throughout a string of pipe is when the pressure has changed while the pipe is static and the change in pressure is not sufficient to cause the pipe to move axially and redistribute the new pressure forces. But if you move the pipe again the changed pressure effects will be distributed in the pipe as a true axial load.

We should also check the combined load in the intermediate casing from the bending, axial load, and burst pressure.

EXAMPLE 7.4 Intermediate String Combined Loading

We will examine the combined loading just inside the top of the build section where the radius of curvature is 1000 ft. The axial load at this point taken from Figure 7.18 at 3500 ft is 365 klbf. We will assume that the internal pressure when the casing is set is 2150 psi and the external pressure is 1520 psi. The internal pressure in burst is 7660 psi and the external pressure is still 1520 psi (these values all interpolated from data in Chapter 3). The casing is 9-5/8 in. 43.5 lb/ft P-110 (ID = 8.755 in.).

We will assume that yield will first occur at the inner wall.

Determine the initial axial stress:

$$\sigma_{z_0} = \frac{F_z}{A_t} = \frac{365000}{\frac{\pi}{4}\left(9.625^2 - 8.755^2\right)} \approx 29,060 \text{ psi}$$

Determine the bending stress

$$\sigma_b = \frac{30 \times 10^6 \,(4.8125)}{12\,(1000)} \approx 12,030 \text{ psi}$$

Determine the initial radial stress the Lamé equation for the inner wall (Equation (6.5)):

$$\sigma_{r_0} = -p_i = -2150 \text{ psi}$$

Determine the radial stress when the burst pressure is applied:

$$\sigma_r = -7660 \text{ psi}$$

Determine the tangential stress before pressure test using the Lamé for the inner wall (Equation (6.6)):

$$\sigma_{\theta_0} = \frac{p_i\left(r_o^2 + r_i^2\right) - 2p_o r_o^2}{\left(r_o^2 - r_i^2\right)}$$

$$= \frac{2150\left[(9.625/2)^2 + (8.755/2)^2\right] - 2\,(1520)\,(9.625/2)^2}{(9.625/2)^2 - (8.755/2)^2}$$

$$\approx 5150 \text{ psi}$$

Determine the tangential stress when the test pressure is applied:

$$\sigma_\theta = \frac{7660\left[(9.625/2)^2 + (8.755/2)^2\right] - 2\,(1520)\,(9.625/2)^2}{(9.625/2)^2 - (8.755/2)^2} \approx 63,480 \text{ psi}$$

Determine the incremental radial and tangential stress due to the test pressure:

$$\Delta\sigma_r = \sigma_r - \sigma_{r_0} = -7660 - (-2150) = -5510 \text{ psi}$$

$$\Delta\sigma_\theta = \sigma_\theta - \sigma_{\theta_0} = 63480 - 5150 = 58,330 \text{ psi}$$

Then, using the Lamé equation for fixed end tubes (Equation (6.4)), calculate the change in axial stress due to the test pressure:

$$\Delta\sigma_z = \nu\,(\Delta\sigma_\theta + \Delta\sigma_r) = 0.28\,(58330 - 5510) = 14,790 \text{ psi}$$

The axial stress including the test pressure effects is

$$\sigma_z = \sigma_{z_0} + \sigma_\mathrm{b} + \Delta\sigma_z = 29860 + 12030 + 9700 = 55,880 \text{ psi}$$

Now, using the three stress components calculated in the presence of the test pressure, we want to determine whether or not yield will occur. Since there is no torsion, these values are principal stress components and may be plugged directly in to the von Mises yield formula:

$$\Psi = \left\{\frac{1}{2}\left[(\sigma_\theta - \sigma_r)^2 + (\sigma_r - \sigma_z)^2 + (\sigma_z - \sigma_\theta)^2\right]\right\}^{\frac{1}{2}}$$

$$\Psi = \left\{\frac{1}{2}\left[(63480 + 7660)^2 + (-7660 - 55580)^2 + (55580 - 62480)^2\right]\right\}^{\frac{1}{2}}$$

$$\Psi = 67,660 \text{ psi}$$

Finally, check the yield condition:

$$Y = 110,000 \text{ psi}$$

$$\Psi = 67,660 \text{ psi}$$

$$Y > \Psi \quad \rightarrow \quad \text{no yield}$$

The combined load is nowhere near the yield strength of this casing section.

At this point we could calculate the bending stress magnification factors and the contact forces for determining placement of drill pipe protectors to protect the intermediate casing from wear. Neither of these two would be of much use when run on a smooth well plan profile. In practice, we would do a bending stress magnification check with actual survey data as the drilling is nearing the casing point. As to the contact force calculations we could do those once the drilling reaches the casing point and sometime before the drill string is picked up to drill out. A more accurate contact force calculation could be made from a gyro survey made inside the casing, but this is seldom done except in a well where wear might be an extremely critical element of the drilling operation.

Table 7.2 Example 7 in. Production Casing (Alternate Selection)

Section	Weight (lb/ft)	Grade	Vert. Depth (ft)	Meas. Depth (ft)	Sect. Length (ft)
4	29	P-110	4500	4910	4910
3	32	N-80	9100	10700	5790
2	32	P-110	11800	14090	3390
1	35	P-110	14000	19940	5850

Next, let us calculate the lengths of sections for the production casing.

EXAMPLE 7.5 Production Casing Lengths

$$\ell_4 = s_2 + \frac{4500 - h_2}{\cos\theta_1} = 4419 + \frac{4500 - 4107}{\cos(0.65167)} = 4910 \text{ ft}$$

$$\ell_3 = s_2 + \frac{9100 - h_2}{\cos\theta_1} = 4419 + \frac{9100 - 4107}{\cos(0.65167)} = 10,700 \text{ ft}$$

$$\ell_2 = s_2 + \frac{11800 - h_2}{\cos\theta_1} = 4419 + \frac{11800 - 4107}{\cos(0.65167)} = 14,090 \text{ ft}$$

$$\ell_1 = s_5 = 19,940 \text{ ft}$$

The results of these section length calculations are shown in Table 7.2. We calculate the production casing axial load with borehole friction. This time the calculation is a bit more complicated by the fact that there are four sections of casing (only three different weights though) and both cased hole and open hole friction factors.The results are shown in Figure 7.19, and as in the intermediate string there is adequate tensile strength in the original selection.

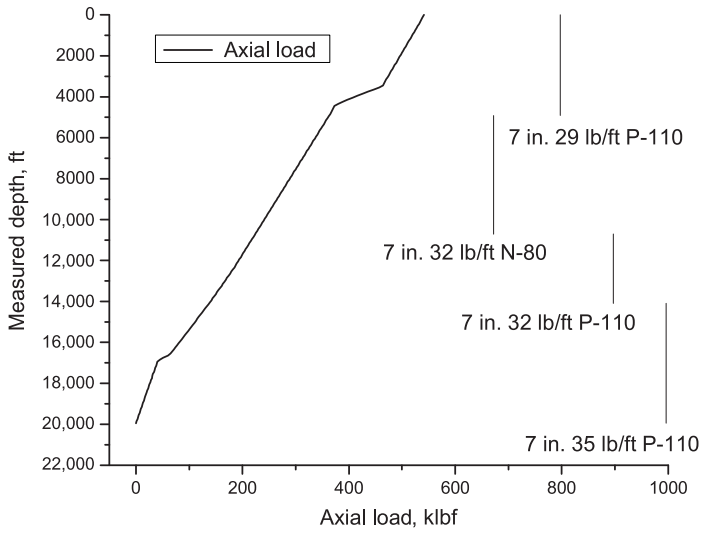

Figure 7.19 Example production casing, axial load with friction (upward motion case).

The maximum combined load might occur at the top of the upper build section if the plug bumps the float collar during an upward motion of the pipe while reciprocating during the cement displacement.

EXAMPLE 7.6 Combined Loads for Production Casing

Data

- Pipe data (at top of upper build section 3500 ft): 7.000 in. OD, 6.184 in. ID, P-110
- Radius of curvature of upper build section: 1000 ft
- Tension with friction from Figure 7.19: 460,000 lbf
- Pressures from plug-bump case (Chapter 3): $p_i = 6820$ psi, $p_o = 2790$ psi
- Additional tension from plug-bump case (Chapter 4): 38,000 lbf

Calculate Stress Components

$$\sigma_z = \frac{460000 + 38000}{\frac{\pi}{4}\left(7.000^2 - 6.184^2\right)} \approx 58,940 \text{ psi}$$

$$\sigma_r = -6820 \text{ psi}$$

$$\sigma_\theta = \frac{6820\left(3.500^2 + 3.092^2\right) - 2\,(2790)\left(3.500^2\right)}{3.500^2 - 3.092^2} \approx 29,890 \text{ psi}$$

$$\sigma_b = \frac{30 \times 10^6\,(3.5)}{12\,(1000)} = 8750 \text{ psi}$$

$$\sigma_z = 58940 + 8750 = 67,690 \text{ psi}$$

Check for Yield

$$\Psi = \left\{\frac{1}{2}\left[(29890 + 6820)^2 + (-6820 - 67690)^2 + (67690 - 29890)^2\right]\right\}^{\frac{1}{2}}$$
$$\approx 64,530 \text{ psi}$$

$64,530 \text{ psi} < 110,000 \text{ psi} \quad \rightarrow \quad$ no yield

There is no combined load problem with this casing string. In a well like this we always design the well path with a long radius curve for the upper build section to avoid high friction and bending forces where the axial forces are high. If we were to plan a hydraulic fracture treatment through this string we would repeat this calculation with the maximum internal treatment pressure.

7.9 Hydraulic fracturing in horizontal wells

Ironically, the initial impetus for horizontal wells was that it is a way to overcome the limitations of hydraulic fracturing. Hydraulic fracturing was, and still is problematic in that the direction of hydraulic fractures cannot be controlled. It is a given—determined by the *in situ* stress field which we cannot

change. Unfortunately, hydraulic fractures almost always orient in the least desirable direction for maximum productivity (see Appendix E for detailed explanation), whereas a horizontal well can be drilled in a direction for best productivity. Few envisioned early on that hydraulic fracturing would ever be necessary in horizontal wells, but that changed quickly as it became obvious that hydraulic fracturing could considerably enhance productivity in horizontal wells in low permeability formations. Hydraulic fracturing in horizontal wells in some areas was common for more than a decade before the shale gas boom began, and it is now almost routine in those shale formations.

Casing in horizontal wells was also rare in the beginning. For one thing, there was no point in it for most of the formations then being drilled, because no zonal isolation was necessary. Secondly, it was expensive compared to a vertical well. And technically it was hard to do successfully. Getting casing to bottom and adequately cemented posed new problems not experienced in vertical wells. But there were good reasons to run casing in some areas because zonal isolation and stimulation are not easily accomplished in open hole completions. There was also the possibility of borehole collapse because of formation instability, but few operators understood that well enough to predict or quantify any possible problems. Many operators opted to run slotted liners as insurance against borehole collapse, and while that sounded like an inexpensive and easy solution at the time (and unfortunately still does to many), it is possibly the worst completion choice one can make. Except for possible borehole support, it virtually eliminates any further completion or production options such as production monitoring (most flow is outside the liner until it nears the heel end), selective stimulation, zonal isolation, and so forth. It is also the poorest sand control method in the industry. I have already made this point, but it is critically important and bears repeating: *Once a slotted liner is in place, all further options are eliminated*, unless you can get it out later, and good luck with that.[5]

7.9.1 Casing design consideration

In addition to the items already covered, there are some special considerations concerning the design of casing strings for hydraulic fracturing stimulations in horizontal wells, especially as they apply to the high-pressure, high-volume treatments for shale formations.

- Relatively high treatment pressures
- Pressure cycling
- Temperature cycling

High treatment pressures

There is little that we need add to what we have already covered as far as internal pressure is concerned. The pressures we experience in these high-volume fracture treatments is not in itself a complicated issue. It is a source of high casing costs not normally encountered in these areas since these high pressures are not intrinsic to the normal producing phase of the wells. That may lead to a discounting of its importance, and some have paid the price with a very expensive fracturing stage going through casing leaks rather than into the intended zone.

The only burst design question here is one of determining the burst pressure load for the fracture job. The anticipated treatment pressures are dependent on depth, casing size, formation properties,

[5] The exception to that caveat is the use of short slotted sections in a conventional liner with inflatable or swelling casing packers between to achieve true zonal isolation; many of those have been quite successful.

length and nature of the perforated interval, pumping rate, and the density and rheology of the fluids being pumped. We are highly dependent on the service companies for much of this information until we have experience of our own in a particular area. Once we are given the maximum anticipated surface pumping pressure though, we can make adequate pressure load calculations for a casing string design.

Worst case burst

When pumping the fracture fluid containing the maximum concentration of proppant at the maximum rate, we may experience a critical event that can happen and often does—a *screen-out* occurs. A screen-out is an event where the proppant bridges in the perforations and blocks entry of additional proppant. Very quickly, all flow into the perforations is blocked and no further pumping into the formation is possible. This can happen while pumping at the highest rates. Pressure can build very rapidly to a static state where there is a hydrostatic column of proppant filled fluid in the casing and possibly a high shut-in pressure at the surface. There is a compensating factor in that when screen-out occurs the pressure at the perforations (less the hydrostatic head) is somewhat less than at the surface because of the circulating friction loss in the casing. This may allow shut down before the shut-in surface pressure acts upon the entire casing string above the perforations. But the pressure difference is overcome very quickly at high pumping rates and the shut-in pressure can exceed the current surface pumping pressure. Some would add an additional margin, yet many assume it is reasonable to use the maximum pumping pressure as the surface shut-in pressure during a screen-out and that the fluid in the wellbore is the fracture fluid with maximum concentration of proppant. The crux of the matter is that we do not always know the surface pumping pressure, but we can set allowable limits based on our design, and enforce those limits during the fracture treatment. We can then calculate a differential burst pressure as in Chapter 3.

The only remaining question is the density of the fluid in the wellbore. In most treatment proposals (and post-treatment reports) we read something like, "5 lb/gal #2 Ottawa sand." What does that mean in terms of density? If the fracture fluid is, say 9.0 lb/gal, does that mean that the fluid with the sand proppant is 14.0 lb/gal? No, it does not. It is the weight of sand added to a gallon of the fracture fluid. We cannot know the density of the combined fluid unless we know the density of the proppant, and when we can find that number it is often stated in something like "lb/ft^3." That is hardly a useful number either because that is not the actual density of proppant but the bulk density of the proppant. (A cubic foot of sand in a sack may have a mass of 100 lb, but its density is not 100 lb/ft^3.) Most fracture service companies have appropriate tables and you can calculate the density of the mixture from those.

$$\rho_{\text{frac}} = \frac{V_{\text{fluid}}\,\rho_{\text{fluid}} + V_{\text{prop}}\,\rho_{\text{prop}}}{V_{\text{fluid}} + V_{\text{prop}}} \tag{7.54}$$

One can easily measure the density of a sample of the proppant using a mud balance, a graduated cylinder, and water.

Once you know the density of the fracture fluid with proppant, then the worst case scenario at a screen-out is easily calculated as in Chapter 3:

$$\Delta p = p_{\text{surf}} + h\,\rho_{\text{frac}} - p_{\text{o}}$$

In addition to that you should also include a test pressure check that would take place before the well is perforated.

Pressure and temperature cycling

One of the more insidious problems that has been encountered in the high pressure, high volume, multi-stage fracture treatments in recent times is that of coupling leaks. I have been involved in the forensics of several cases and the most likely source of the majority of these leaks is the cycling of pressure and temperature with the multiple stages. While none of the temperature or pressure cycles came near the pressure rating of the couplings, the cyclic loading appeared to have a significant effect. In several cases the pressure cycles were on the order of 9000-10,000 psi and the temperature cycles on the order of 100 °F. Here is an example based on an actual well in the Marcellus shale in the USA.

EXAMPLE 7.7 Temperature and Pressure Cycle for a Fracture Stage

Assume that there is a section of casing between two fixed (cemented or stuck) points. We determine the magnitude of the maximum differential axial stress in a stimulation cycle during winter conditions.

- Casing: 5-1/2 in. 20 lb/ft. P-110, 4.778 in.ID
- Initial down-hole pressure: $p_i = p_o = 3000$ psi
- Maximum surface treating pressure cycle: $\Delta p = 10,000$ psi
- Maximum temperature change: $\Delta T = -100\,^{\circ}\text{F}$ (cold fracture fluid, near freezing point)

First we calculate the initial stress from the hydrostatic pressure:

$$\sigma_r = -3000 \text{ psi}$$

$$\sigma_\theta = \frac{3000\left(2.750^2 + 2.389^2\right) - 2\,(3000)\left(2.750^2\right)}{2.750^2 - 2.389^2} = -3000 \text{ psi}$$

We do not know the axial stress, but for this example we are calculating the change in axial stress caused by the pressure and temperature cycle. Now we assume the maximum pressure cycle and calculate the change in stress caused by the change in pressure.

$$\Delta\sigma_r = -13000 - (-3000) = -10,000 \text{ psi}$$

$$\Delta\sigma_\theta = \frac{13000\left(2.750^2 + 2.389^2\right) - 2\,(3000)\left(2.750^2\right)}{2.750^2 - 2.389^2} - (-3000)$$
$$= 71,530 \text{ psi}$$

$$\Delta\sigma_z = 0.28\,(-10000 + 71530) = 17,230 \text{ psi}$$

Notice that there is now a change in the axial stress of the casing because of the change in internal pressure. We used the Lamé fixed end formulas here.

Next we calculate the change in axial stress from the contraction caused by the cold fracture treatment fluid. This particular well was fractured in winter where the fracture fluid had to be warmed to slightly above the freezing point to prevent freezing. Normally we might not consider such a drastic reduction of bottom-hole temperature, but in the case of such large volumes of treatment at a relatively shallow depth it is easy to lower the casing temperature to very near the surface temperature.

$$\Delta\sigma_T = -E\alpha\,\Delta T = -30 \times 10^6 \left(6.9 \times 10^{-6}\right)(-100) = 20,700 \text{ psi}$$

Finally we calculate the differential stress cycle of a treatment stage.

$$\Delta\sigma_z = 17230 + 20700 = 37,930 \text{ psi}$$

In that example we used the extreme values that could be encountered in a single fracture stage, and we see that the results are not at all critical to the axial yield strength of the casing. Even though we do not know the initial axial stress, it is most likely a compressive stress since this is a horizontal lateral and the casing was pushed into the hole at that point. This particular calculation was made in trying to determine why a casing string failed after the fourth stage of a multi-stage fracture treatment. Several similar failures were also reported and examined, and it hardly seemed likely that the magnitude of pressure-temperature change was severe enough to cause a coupling failure—all the failures were in couplings. Down-hole videos of two failures verified the coupling failures. Severe erosion had taken place and the couplings appeared to not be made up fully. In either case, once a coupling started to leak, the fracture fluid and sand proppant began to quickly erode the threads and couplings. Great care was exercised in the running process (because a previous string had a similar failure), and it seemed unlikely that the connection was not fully made up. Had that been the case, the failure would more likely have occurred during the first fracture stage, rather than the fourth. It is most plausible that the additional separation occurred after the failure—possibly during a cycle of increased axial tension as in the example.

All of the failures investigated in this area and another area (where temperature was not a factor) failed in couplings. There are a number of possibilities such as improper makeup of connections, improper amount or type of thread compound, and the axial and radial cycling that caused the couplings to leak. After the first incident, considerable care had been taken to assure the first two were not the problem. Because the threads were interference type (API 8rd and buttress) it appeared likely that the cycling was causing a breakdown in the sealing effectiveness of the thread compound. The obvious solution appeared to be to employ a metal-to-metal seal connection, or at least one in which the pins contact a shoulder sufficiently so that the threads themselves do not cycle between tension and compression. Two successful and inexpensive solutions have been used, one is the use of insert stop-rings for buttress couplings as used in drilling with casing to prevent additional makeup while rotating the casing, and the other is a special buttress connection with an extended pin so that the two pins contact each other and form a shoulder. In both these cases the connections can be made up to the point where an axial tension/compression cycle does not cause movement in the threads.

7.9.2 Field practices

There is a significant paradox in designing and selecting casing for a horizontal well that will undergo high-pressure, high-volume, multi-stage hydraulic fracturing. On the one hand, the fracture pressures demand a substantial casing string, and on the other, the resulting well will be low pressure and require only a minimal casing string design. In other words we design and install a high pressure casing string in a well that will never need it again once it starts producing (unless additional fracturing is done later in the well's life). That is one reason for seeking a low cost solution to the leak problems just discussed.

There is an associated problem that has also concluded with an expensive fracture stage going through a coupling leak instead of the intended target zone. That problem involves the field practice. A low pressure well does not need a 10,000 psi wellhead. This has been recognized from almost the beginning of hydraulic fracturing in the 1950s. The solution was then, and still is, a *Christmas tree saver*, a device installed on the wellhead that isolates the top of the wellhead from the casing so that the wellhead is never subjected to the high treatment pressures. And here is where field practice comes into play—casing should be adequately tested to the maximum anticipated treatment pressure *before* the day of the treatment in case there is a leak. And a small leak should never be ignored because it will definitely get much bigger during a large volume treatment. This test requires extra time, equipment, and expense, but

the cost of pumping the first fracture stage into a casing leak well above the pay zone and the subsequent task of repairing the resulting hole should be incentive enough. It has happened.

Finally, there is the process of running and cementing a casing string in horizontal well. Getting the casing to bottom (or the end of the lateral) is one task. Getting an adequate cement job is the other. The less the friction the easier the first. Here are some points on friction reduction:

- Smooth borehole with as little tortuosity as possible
- Minimize contact force in the lateral (lighter weight, higher strength casing)
- Minimize friction factor (friction reducers in mud—oil, plastic beads, ground walnut shells, etc.)
- Beveled couplings on casing
- Centralizers

Those are all self-explanatory, but recalling the friction equation from earlier in this chapter, $F = \mu N$, you can see that it is a linear relationship and lowering either the friction factor or contact force (or both) will also reduce the friction force proportionally. The last item, centralizers, is thought to be a bit controversial. If you get the hole clean, centralizers are an aid to getting casing in a horizontal section, if you do not clean the hole prior to running the casing, the centralizers can be an impediment. As far as the cementing goes, rigid centralizers are preferred and are good if the formation is competent. If the formation is soft, the bow type are better for friction reduction, especially the "double-bow" type which provide better rigidity and standoff. Cementing was discussed in Chapter 5.

There have been a number of problems in horizontal wells where getting to bottom has been difficult—pinched pins from rotating, damaged connections or buckled joints from trying to push or jar casing past obstructions, and so on. A possible aid is the use of insert-stop rings or long pin buttress connections as mentioned previously which may allow for rotation of the casing string, but do not ever attempt to rotate ST&C or LT&C casing.

7.10 Closure

Directional wells and horizontal wells place additional loads on casing that are not present in vertical wells. We looked at the effects of friction and curvature in this chapter and saw the extent of these types of loadings. We also examined the combined effects of tension or compression, pressure, and bending in these types of wells to get a feel for the relative significance. What one should get from this chapter is an understanding of the loads in these types of wells and a certain amount of comfort in being able to check conventional designs for these types of wells.

Appendix A: Notation, symbols, and constants

Chapter outline head

The symbols and notation used in continuum solid mechanics are not standardized. Among disciplines, mathematicians tend to adhere to particular notation conventions, engineers to others, physicists to yet others, and so on. Further, various authors within disciplinary groups tend have their own particular preferences too. Adding to that is the fact that there are just too many different variables, types of variables, and types of operators for the Roman and Greek alphabets to avoid repetition. Therefore, I have tried to use some of the more common conventions within the mechanics community, and use them in as consistent a manner as possible. There are some variable and operator representations that are consistent through the entirety of the text. But strict consistency is not practical, so some variables of lesser importance may be represented by the same letter or symbol as others. In those cases such duplication should be obvious from the context and will be defined on first usage.

Please note that some of the mathematical symbols appearing in this appendix are not used in this text. They are included for consistency and completeness in relation to some of those that are used.

Variables

A strict adherence to *algebraic convention* is used for representation of variables in that a variable consists of a single kernel only, and further specification is indicated with subscripts and superscripts.[1] This text also conforms to current ISO mathematical standards for *slanted variables* to distinguish between variables and operators. This is especially important for upper case Greek characters which in past traditions were non-slanted in all occurrences and often causing confusion.

I have tried to make all equations, especially in-line equations (those appearing in a line of text), absolutely clear by including enough delimiters to avoid confusion even where their inclusion might appear redundant.

Subscripts and superscripts

The standard convention used here is that italicized subscripts and superscripts signify a variable quantity, e.g., the subscript, i, in x_i is a variable indicating the coordinate directions as in three-dimensional

[1] The use of multi-letter variable names should only appear in computer algorithms and programs as their appearance in equations is both sloppy and confusing.

space, x_1, x_2, x_3. Non-italicized subscripts or superscripts are descriptors, e.g., the plain text subscript, i, in d_{i} denotes the inside diameter of a tube. This practice is not standard with ISO, but is with many science texts. The one exception I have made is with the linear density symbol where ISO specifies, ρ_l but with a non-italicized subscript would appear as ρ_{l}, both of which can be easily misinterpreted, so I have opted for ρ_ℓ to avoid confusion.

A.1 Mathematical operators and symbols

These are some of the more common operators and symbols that are useful in our text, and though we may seldom use many of them they are listed here for reference.

Mathematical Operators and Symbols

$\therefore$	therefore
$\forall$	for all
$\in$	in
$\rightarrow$	to, as in A to B, or implies, as in A implies B
$\Rightarrow$	if, if A then B
$\Leftrightarrow$	iff, if and only if, B if and only if A
$\oplus$	addition operation
$\odot$	scalar multiplication operation
$\otimes$	vector multiplication operation
$\emptyset$	null or empty set
V	a vector space
$\mathbb{R}$	space of real numbers
$\mathbb{C}$	space of complex numbers
$\mathbb{E}^3$	Euclidean space (manifold) (3D)
$\cdot$	inner product operator
$\times$	cross product operator
grad	grad or gradient
$\boldsymbol{\nabla}$	grad operator
div	div or divergence
$\boldsymbol{\nabla}\cdot$	div or divergence operator
curl	curl
$\boldsymbol{\nabla}\times$	curl or curl operator
∞	infinity
$\sum$	summation
$\propto$	proportional to
$\lfloor\ \rfloor$	row vector, $1 \times n$

$\{\ \}$	column vector, $n \times 1$
$[\ ]$	matrix, $m \times n$
$[\ ]^{\mathrm{T}}$	transpose of a matrix, $n \times m$
$^{\mathrm{T}}$	transpose operator (superscript T)
$\vert\ \vert$	absolute value of a scalar
$\Vert\ \Vert$	magnitude of a vector or a norm
$\det[\ ]$	determinant (the common notation $\vert\ \vert$ is not used here to avoid confusion)
δ	delta, a small variation
Δ	Delta, an increment
δ_{ij}	Kronecker delta
$C^0, \ldots, C^\infty$	smoothness (C^2 is continuous in its second derivative, C^∞ is infinitely differentiable and smooth)

Points, Vectors, Tensors

$\mathbf{x}, \mathbf{y}, \mathbf{z}$	typical points in a mathematical space
$\mathbf{u}, \mathbf{v}, \mathbf{w}$	typical vectors
$\mathbf{0}$	zero vector
$\mathbf{T}, \mathbf{S}$	typical tensors, 2-order

A.2 Standard ISO and traditional solid mechanics variables and symbols

Physical dimensions for mass, length, time, and force and temperature are given by the symbols M, L, t, F, and T, respectively.[2]

Scalar Variables

m	mass, M
ρ	mass density, $\mathrm{M/L^3}$
ρ_ℓ	linear density, M/L
v	specific volume $(1/\rho)$, $\mathrm{L^3/m}$
p	pressure (energy density), $(\mathrm{F\,L})/\mathrm{L^3} \ \rightarrow \mathrm{F/L^2}$
s	distance (along a curvilinear path), L
T	temperature, T
t	time, t
V	volume, $\mathrm{L^3}$
ν	Poisson's ration, dimensionless

[2] Although force is not a fundamental unit, $\mathrm{F = M\,L/t^2}$, we will use F here for simplicity.

I_a second area moment, axial, L^4
μ dynamic friction factor, dimensionless
μ_s static friction factor, dimensionless
Z gas compressibility factor, dimensionless
α_T coefficient of linear thermal expansion, T^{-1}
β_T coefficient of volumetric thermal expansion, T^{-1}
I_1, I_2, I_3 stress invariants, F/L^2
J_2, J_3 deviatoric stress invariants ($J_1 = 0$), F/L^2
σ principal stress component (eigenvalue), F/L^2
σ' principal deviatoric stress component (eigenvalue), F/L^2
τ_o octahedral stress, F/L^2

Some of the scalar symbols may have a subscripted 0, as h_0, meaning a reference value. When preceded by a Δ the meaning is an incremental value such as Δh means $h - h_0$.

Points

$\mathbf{X}, \mathbf{x}$ coordinate points or coordinate systems (context dependent)
X_1, X_2, X_3 coordinate points or axes in $\mathbf{X}$
x_1, x_2, x_3 coordinate points or axes in $\mathbf{x}$

Vectors

Direct notation:

$\mathbf{F}$ force, F
$\mathbf{M}$ moment, F L
$\mathbf{T}_q$ torque, F L
$\mathbf{p}$ linear momentum, M L/T
$\mathbf{h}$ angular momentum, M L/T
$\mathbf{r}$ radius vector (from origin), L
$\mathbf{F}_g$ weight ($m\mathbf{g}$), F
$\mathbf{g}$ local gravitational acceleration,[3] L/t^2
$\mathbf{u}$ linear displacement vector, L
$\dot{\mathbf{u}}$ linear velocity, L/t
$\ddot{\mathbf{u}}$ linear acceleration, L/t^2

Index notation:

F_i force, F
M_i moment, F L

[3] Gravitational acceleration is a vector.

$T_{\mathrm{q}\,i}$ torque, F L
p_i linear momentum, M L/T
h_i angular momentum, M L/T
r_i radius vector (from origin), L
$F_{\mathrm{g}\,i}$ weight (mg_i), F
g_i local gravitational acceleration,[4] L/t^2
u_i linear displacement vector, L
$\dot{u}_i$ linear velocity (v is not used), L/t
$\ddot{u}_i$ linear acceleration (a is not used), L/t^2

Second-Order Tensors[5]

Direct notation:

T or **S** stress tensor, F/L^2
S′ deviatoric stress tensor, F/L^2
E strain tensor, dimensionless

Index notation:

σ_{ij} stress tensor, F/L^2
σ'_{ij} deviatoric stress tensor, F/L^2
ε_{ij} strain tensor, L/L

Vector/tensor subscript variables (always in *italics*)

i,j,k general coordinate indices: 1,2,3
l,m,n also general coordinate indices: 1,2,3
x,y,z rectangular Cartesian coordinates
r,θ,z circular cylindrical coordinates, $(-\pi \leq \theta \leq \pi)$
r,θ,ϕ spherical coordinates, $(-\pi \leq \theta \leq \pi, 0 \leq \phi \leq \pi)$

A.3 Casing and borehole application-specific variables

A_{t} cross-sectional area of tube, $A_{\mathrm{t}} = \pi(r_{\mathrm{o}}^2 - r_{\mathrm{i}}^2)$, L^2
d_{i} inside tube diameter, L
d_{o} outside tube diameter, L

[4] We usually omit the subscript on g_i because we typically use an earth-oriented coordinate system, but this is not always the case.
[5] Here these symbols are for small strain and displacements, other notation is defined in the very few places where needed.

g_i local gravitational acceleration,[6] $\mathrm{L/s^2}$
g_0 standard gravitational acceleration, $\mathrm{L/s^2}$
g_c USC conversion factor (see Appendix B)
h vertical depth of a point in a borehole, L
k_b buoyancy factor, dimensionless
k_{clps} collapse rating reduction factor, dimensionless
k_D design factor, dimensionless
k_M design margin factor, dimensionless
ℓ length along a curvilinear path, e.g., $s_2 - s_1$, L
L a straight length or vertical length, e.g., $h_2 - h_1$, L
p pressure, $\mathrm{F/L^2}$
p_i inside or internal pressure, $\mathrm{F/L^2}$
p_o outside or external pressure, $\mathrm{F/L^2}$
Δp differential pressure load, $\Delta p \equiv p_i - p_o$, $\mathrm{F/L^2}$
r_i inside tube radius, L
r_o outside tube radius, L
r_h radius of hole (borehole), L
r_{cpl} radius of coupling, L
r_κ radius of curvature for borehole path, L
s coordinate distance along a curvilinear path, L
Δs distance along a curvilinear path between two points on that path, L
t_w pipe wall thickness ($r_o - r_i$), L
T temperature, T
T_m temperature at melting point, T
T_q torque, FL
w linear weight of tube ($w = g\,\rho_\ell$), F/L
$\bar{w}$ buoyed linear weight of tube ($\bar{w} = k_b\,g\,\rho_\ell$), F/L
Y uniaxial yield stress, $\mathrm{F/L^2}$
α inclination angle, rad. or deg. depending on context
β survey azimuth, rad. or deg. depending on context
α_{cr} critical inclination angle, rad. or deg. depending on context
γ specific weight or fluid gradient, usually with subscript identifier, $(\mathrm{F/L^2})/\mathrm{L}$
κ borehole path curvature, ($\kappa = r_\kappa^{-1}$), $\mathrm{L^{-1}}$
λ_b bending stress magnification factor, dimensionless

[6] We usually omit the coordinate subscript on g because we typically use an earth-oriented coordinate system, but this may not always be the case.

μ composite kinetic friction factor, dimensionless

μ_s composite static friction factor, dimensionless

ρ_ℓ tube linear density, mass per unit length of tube ($\rho_\ell = \rho\, A_t$), M/L

$\hat{\rho}$ specific density (water = 1.0), dimensionless

ρ_f density of fluid, M/L^3

ρ_s density of steel (see Appendix B), M/L^3

Ψ yield measure ("fictitious von Mises equivalent stress"), $FL/L^3 \rightarrow F/L^2$

This page intentionally left blank

Appendix B: Units and material properties

Chapter outline head

B.1 Introduction

In this textbook, I have written all of the equations and formulas in their physical form without conversion factors. Any numerical values appearing in them are physical or mathematical constants. Any consistent set of units from a coherent unit system may be used without conversion factors. In this appendix, we will list some conversion factors that are often required between metric and English systems, as well as some commonly required within inconsistent English systems.

Additionally, a number of material property values as used in this textbook are also listed, as well as some physical constants.

B.2 Units and conversions

All physical phenomena are independent of the units used to measure them, and consequently, all units of measure are arbitrary. Hence, most systems developed over the centuries are based on convenience of usage. In the latter quarter of the twentieth century most of the world adopted a standard system called the SI system. It too is an arbitrary system, but it is also what is called a *coherent system*. A coherent system allows use of the equations of mechanics and physics without need of conversion factors. Despite the many advantages of such a system, there are vestiges of other systems still in use, especially in the oilfields of the world. By far, the most prevalent oilfield usage is a mixture of units mostly in the English engineering system, but hardly consistent. It is referred to in ISO standards as the USC (US Customary) system. Almost every calculation done with this system requires conversion factors making it cumbersome as well as confusing. We will not debate the issue of unit systems here, but we use the USC system in this text because of its overwhelming prevalence in the world's oilfields.

Table B.1 shows a comparison of four common systems.

The SI, the English absolute, and the English gravitational systems shown in the table are coherent systems. The English engineering system is not coherent. Almost no one uses the English absolute system as the poundal is almost unknown. While the English gravitational system is used frequently in engineering where Newton's second law is applicable, commercial scales that measure mass in slugs are non-existent. A slug is $g_c m$ where m is in lb and $g_c = (1/32.174049)\,\text{lbf} \cdot \text{lb}^{-1} \cdot \text{ft}^{-1} \cdot \text{s}^2$. Depending on

Table B.1 Common Systems of Units

Physical Quantity	International SI	English Absolute	English Gravitational	English Engineering
Length	m	ft	ft	ft
Force	N	pdl	lbf	lbf
Mass	kg	lb	slug	lb
Time	s	s	s	s
Stress/pressure	Pa (N/m^2)	pdl/ft^2	lbf/ft^2	psi ($lbf/in.^2$)
Energy/torsion	J (N m)	pdl ft	lbf ft	lbf ft
Density	kg/m^3	lb/ft^3	$slug/ft^3$	lb/ft^3

Table B.2 Consistent Units in SI and English Gravitational Units with Smaller Scale Subsets

Physical Quantity	International		English Gravitational	
	SI	SI (mm)	(ft)	(in)
Length	m	mm	ft	in.
Force	N	N	lbf	lbf
Mass	kg	ton (10^3 kg)	slug	$lbf\,s^2/in.$[a]
Time	s	s	s	s
Stress/pressure	Pa (N/m^2)	MPa (N/mm^2)	lbf/ft^2	psi ($lbf/in.^2$)
Energy/torsion	J (N m)	mJ (10^{-3}J)	lbf ft	lbf in.
Density	kg/m^3	ton/mm^3	$slug/ft^3$	$lbf\,s^2/in.^4$ [b]

[a] $lbf\,s^2/in. = slug/12$.
[b] $lbf\,s^2/in.^4 = slug/12^4$.

the scale of interest we may choose other sets of consistent units within those two systems which also do not require conversion factors. Table B.2 shows both the SI and English Gravitational systems in two sets of consistent units depending on the scale being used.

Table B.3 shows some of the more common conversion factors required to convert various USC units to consistent SI units and Table B.4 lists conversion factors to convert common USC units into the consistent English gravitational system.

Mass and force

One of the more confusing things about the USC system is in dealing with mass, lb, and force, lbf, especially in gravitational loads. Under the force of earth's standard gravity the two have the same numerical value, and that was the intent of the definition of a pound-force. In our context the local gravity seldom varies enough from the standard value to make any significant difference in our calculations.[1] The net result is that we often omit the acceleration of gravity from Newton's second law when the only force is that of gravity. USC units require a conversion factor which, for lack of anything better, I will call g_c. So that the weight of an object is given by

$$W = m\,g = g_c\,m\,g$$

[1] If we want to get even more technical, the centrifugal force of the earth's rotation opposes the gravitational force so the weight of an object is a maximum at the poles and a minimum at the equator.

Table B.3 Conversion of Common USC Units to Consistent SI

Physical Quantity	USC		SI
Length	1 ft	=	0.3048 m[a]
	1 in.	=	0.0254 m [a]
Area	1 ft^2	=	0.09290304 m^2 [a]
	1 $in.^2$	=	0.64516×10^{-3} m^2 [a]
Volume	1 ft^3	=	0.028316846592 m^3 [a]
	1 gal (US)	=	$3.785411784 \times 10^{-3}$ m^3
	1 bbl	=	0.158987294928 m^3
Force	1 lbf	=	4.4482216152605 N
Mass	1 lb	=	0.45359237 kg[a]
	1 slug	=	14.593903 kg
Density	1 lb/ft^3	=	16.018463374 kg/m^3
	1 lb/gal	=	0.119826427317 kg/m^3
Pressure/stress	1 psi	=	6894.75729317 Pa
Torsion/energy	1 lbf ft	=	1.35581794833 J
Pressure gradient	1 psi/ft	=	22620.5947939 Pa/m
Linear mass gradient	1 lb/ft	=	1.48816394357 kg/m
Linear weight gradient	1 lbf/ft	=	14.5939029372 N/m

[a]Conversion is exact.

Table B.4 Conversion of Common USC Units to Consistent English Gravitational Units

Physical Quantity	USC		Consistent Eng. Grav.
Length	1 in.	=	1/12 ft[a]
Area	1 $in.^2$	=	1/144 ft^2 [a]
Volume	1 $in.^3$	=	1/1728 ft^3 [a]
	1 gal (US)	=	231/1728 ft^3 [a]
	1 bbl	=	9702/1728 ft^3 [a]
Force	1 lbf	=	1 lbf[a]
Mass	1 lb	=	1/32.174049 slug
Density	1 lb/ft^3	=	1/32.174049 $slug/ft^3$
	1 lb/gal	=	0.23250165 $slug/ft^3$
Torsion/energy	1 lbf ft	=	1 lbf ft[a]
Pressure gradient	1 psi/ft	=	144 $lbf/ft^2/ft$[a]
Linear mass gradient	1 lb/ft	=	1/32.174049 slug/ft
Linear weight gradient	1 lbf/ft	=	1 lbf/ft[a]

[a]Conversion is exact.

Table B.5 Some Other Common Oilfield Units Within the USC System

Physical Quantity	USC		USC
Area	1 acre	=	43,560 ft^2 [a]
Volume	1 bbl	=	42 gal(US)[a]
	1 ft^3	=	1728/9702 bbl[a]
Density	1 lb/ft^3	=	231/1728 lb/gal(US)[a]
	1 lb/gal	=	1728/231 lb/ft^3 [a]
Pressure gradient	1 lb/gal	=	0.052 psi/ft
	1 lb/ft^3	=	1/144 psi/ft[a]

[a]Conversion is exact.

where m is in lb and $g_c = (1/32.174049)\,\text{lbf} \cdot \text{lb}^{-1} \cdot \text{ft}^{-1} \cdot \text{s}^2$. The net result of this is that numerically, $g_c \cdot g \approx 1$ and therefore gets omitted from many equations where USC units are used. That is fairly straight forward, but confusion often arises in the case of inertial forces when Newton's second law is

$$F = m\,\ddot{u} = g_c\,m\,\ddot{u}$$

In this case, $g_c\,\ddot{u} \neq 1$ in general unless the acceleration, $\ddot{u}$ is equal to the gravitational acceleration, g. We might make one more important point to remember. Though we seldom write it as such, g is actually a vector and not a scalar. So properly written, the weight equation is $\mathbf{W} = m\,\mathbf{g} = g_c\,m\,\mathbf{g}$, and Newton's second law is $\mathbf{F} = m\,\ddot{\mathbf{u}} = g_c\,m\,\ddot{\mathbf{u}}$ when expressed in USC units. Always remember too that g_c is a conversion factor in the USC system for converting engineering system mass units, lb, into consistent gravitational system mass units, slug, and has nothing to do physically with gravitational acceleration. *Please note that g_c as it appears in this edition is the reciprocal of that used in the first edition*. The usage here is more conventional. Other common USC units in oilfield usage are shown in Table B.5.

B.3 Material properties

Solid materials used in this text are all API steel for which there is little data published, and some is inferred from calculation examples in some of the API standards. For properties of steel in Table B.6 we see that Poisson's ratio is only 0.28 which is the value used in ISO/TR 10400 [11] rather than the

Table B.6 Steel Properties Used in This Text

Symbol	Description	SI[a]	USC[a]
ρ	Density	7850 kg/m^3	490 lb/ft^3
E	Young's modulus	206.8 GPa	30×10^6 psi
G	Shear Modulus	75.8 GPa	11×10^6 psi
ν	Poisson's ratio	0.28	0.28
α	Thermal exp. coef.—linear[b]	$12.42 \times 10^{-6}\,°C^{-1}$	$6.9 \times 10^{-6}\,°F^{-1}$
β	Thermal exp. coef.—volume[b]	$37.26 \times 10^{-6}\,°C^{-1}$	$20.7 \times 10^{-6}\,°F^{-1}$

[a]Property values will vary with composition.
[b]Actual values may vary significantly with temperature range and composition.

Table B.7 Other Constants and Properties Used in This Text

Symbol	Description	SI	USC
ρ_w	Water density (4 °C)	1000 kg/m^3	8.33 lb/gal
g_0	Standard gravity	9.80665 m/s^2	32.174049 ft/s^2

Table B.8 Standard Constants and Values Used in Gas Equations

Symbol	Description	SI[a]	USC[a]
R	Gas constant	8314.462 J/K/mol	1545.349 ft lbf/R/lb-mol
g_0 [b]	Std Gravity	9.80665 m/s^2	32.174049 ft/s^2
M_{C_1}	C_1 mass	16 g/mol	16 lb/lb-mol

[a]In proper units for use in gas equations of Appendix D.
[b]Commonly used when local value of g is not known.

common value used for steel, 0.3. The coefficients of thermal expansion given here are the ones used in the text and are average values for carbon steel in the 70-220 °F range. Actual values may vary considerably with temperature range and metal composition. Other properties and gas constants used in this text are given in Table B.7 and Table B.8, respectively.

This page intentionally left blank

Appendix C: Basic mechanics

Chapter outline head

C.1 Introduction

This appendix is intended as a foundation level introduction to the mechanics of solids. This material is generally taught on a graduate level, but I think it is important for those seriously working with oilfield tubulars who have not studied this subject to any extent, to have a basic reference or refresher source. There are excellent references on the topic, but most are difficult for those whose interest comes about from an interest in tubulars in oilfield applications. I attempted something similar in the first edition of this textbook, but was constrained from presenting what I thought was an adequate treatment. It felt to me like starting a trip but stopping before getting anywhere. This appendix is more complete, but still very brief. It assumes an understanding of undergraduate calculus, linear algebra, and matrix operations.

In our field of endeavor we are working in an environment in which we assume a three-dimensional Euclidean spatial geometry, $\mathbb{E}^3$, and that time, t, is represented as a monotonically increasing real value. Further, we assume that Newtonian mechanics is sufficiently accurate for our applications. These are nothing more than the assumptions of classical mechanics as taught in basic physics and engineering courses that have served us well for many years and still do so in our everyday macroscopic world. However, classical mechanics deals with points, point masses, point loads, and rigid bodies. These are mathematical conveniences that do not physically exist in our universe, let alone in our macroscopic world. We still employ them for convenience in many applications, but in our applications, all material bodies have mass and volume (and hence, density), and all material bodies are deformable. The only deformation phenomena taught in traditional classical mechanics courses are modeled with springs (usually without mass). So, here we must add an additional assumption as to the nature of material bodies, and that is that they are *continuous* on the scale in which we are working. In other words, we may ignore the molecular, atomic, and subatomic substructure and discontinuities of a material and assume a continuous material for whatever order of differentiation we may require. This extension to classical mechanics is known as continuum mechanics and is what engineers work with every day. It applies to both solids and fluids, though our concentration here will be on solids.

Our goal is to employ continuum mechanics to construct mathematical models of the material bodies and events we are investigating. It is a simple task to do an experiment, record the data, plot the data to show the results. For example, we might apply several tensile loads to a bar and record the stretch in the bar for each load. A plot would give us a performance curve for that bar and might prove useful for some specific application. What if we want to use a different size bar or use a different material for the bar? Our plot is useless as a model because all it does is "output the input." We seek to make models that can *predict* behavior for different input. This appendix is a brief introduction/refresher to this topic.

C.2 Coordinates

Before we explain the index notation that we will be using, we need a coordinate system, because index notation always refers to a coordinate system. Figure C.1 illustrates a right-hand Cartesian coordinate system similar to the one we employ in the various chapters. Note, however, that the coordinate axes are not labeled x, y, z, but x_1, x_2, x_3. We just as easily could have labeled them y_1, y_2, y_3; z_1, z_2, z_3; x'_1, x'_2, x'_3; or even X_1, X_2, X_3. In this notation, the letters, x, x', and X refer to specific coordinate systems, and we may have as many or as few as we need for a specific use (typically, we seldom need more than two). The numbered subscripts, 1, 2, and 3, refer to the three axes of those specific coordinate systems.

Once we have the coordinate system established, we can refer to a point in that coordinate system. So, instead of referring to a point by its three coordinates, x_1, x_2, x_3, we can simply refer to the point as x_i where $i = 1, 2, 3$.

The letter index, i in this case, is assumed to include all three axes, so it is not necessary to write out the range of the index, i, except in cases where other subscripts might cause confusion.

We used a Cartesian coordinate system as an example, but we are not limited to Cartesian coordinates. For instance in a circular cylindrical coordinate system we may still number the axes as 1, 2, 3, instead of r, θ, z. The only thing we have to be careful about in other coordinate systems is the physical meaning of some of the quantities, but we do not concern ourselves with that for now.

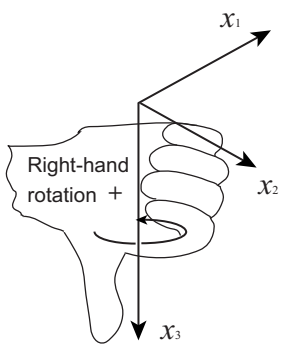

Figure C.1 A right-hand Cartesian coordinate system.

The greatest advantage to numbered coordinate systems is in computation. Computers do not do q_x, q_y, q_z or $q_x\hat{\mathbf{i}}, q_y\hat{\mathbf{j}}, q_z\hat{\mathbf{k}}$ very well at all. The computational baggage of such notations is excessively inefficient.[1]

One important point to remember is that the physical entities which we will encounter that are represented by scalars, vectors, and tensors are coordinate invariant, meaning that they do not depend on our selection of coordinates. While their numerical components take on different values in different coordinate systems, the physical entity itself is invariant. Once a coordinate system is assigned to such an entity, it becomes unique and its values are fixed in any other coordinate system we may later choose. This will repeated time and again in case you miss it here.

C.3 Notation convention

The notation used in continuum mechanics is relatively simple, at least it is simple *after* you understand it. The difficulty in understanding is for the most part a difficulty in explaining it, and that is my challenge, not yours.

There are three general notational schemes employed in engineering mechanics: *algebraic*, *direct*, and *index* notations. The first is the most common and is taught from an early age on through most undergraduate engineering curricula. It can become extremely cumbersome when dealing with the most common entities of mechanical phenomena, vectors and tensors. The second finds popularity in the discipline of mathematics where its compactness is an asset to a discipline primarily interested in qualifying mathematical and physical phenomena rather than quantifying them. The third one, once thought the domain of mathematicians, is a shorthand version of the first and an expansion of the second. Let us look at an example in way of clarification.

Let us assume a vector, $\mathbf{q}$, represents a steady-state heat flux across a material boundary at some point. Assume also that $\mathbf{q} = \mathbf{q}(x, y, z)$. We would like to find the gradient of that vector by taking the spatial derivative of it. In one-dimensional space this is written simply as $\mathrm{d}q/\mathrm{d}x$.In three dimensions it becomes a little more complicated because $\mathbf{q}$ has three components, $q_x\hat{\mathbf{i}}, q_y\hat{\mathbf{j}}, q_z\hat{\mathbf{k}}$. The gradient vector is given by:

- Algebraic notation:

$$\begin{bmatrix} \dfrac{\partial q_x\hat{\mathbf{i}}}{\partial x\hat{\mathbf{i}}} & \dfrac{\partial q_x\hat{\mathbf{i}}}{\partial y\hat{\mathbf{j}}} & \dfrac{\partial q_x\hat{\mathbf{i}}}{\partial z\hat{\mathbf{k}}} \\ \dfrac{\partial q_y\hat{\mathbf{j}}}{\partial x\hat{\mathbf{i}}} & \dfrac{\partial q_y\hat{\mathbf{j}}}{\partial y\hat{\mathbf{j}}} & \dfrac{\partial q_y\hat{\mathbf{j}}}{\partial z\hat{\mathbf{k}}} \\ \dfrac{\partial q_z\hat{\mathbf{k}}}{\partial x\hat{\mathbf{i}}} & \dfrac{\partial q_z\hat{\mathbf{k}}}{\partial y\hat{\mathbf{j}}} & \dfrac{\partial q_z\hat{\mathbf{k}}}{\partial z\hat{\mathbf{k}}} \end{bmatrix}$$

- Direct notation

$$\nabla\mathbf{q} \quad \text{or} \quad \operatorname{grad}\mathbf{q}$$

- Index notation

$$q_{i,j}$$

[1] We will use x, y, z in most of our discussions and derivations for clarity, but never for programmed computation.

Algebraic notation can become exceedingly verbose mathematically as in the above example. Some would shorten that example by omitting the unit coordinate vectors, $\hat{\mathbf{i}}$, $\hat{\mathbf{j}}$, $\hat{\mathbf{k}}$, as being understood. The direct notation is the most compact of all in that it seldom refers to a coordinate system at all, because scalars, vectors, and tensors are independent of any coordinate system used to reference them. Index notation is similar to direct notation in its compactness, but it always refers to components (the subscripts) in some coordinate system.[2] In continuum mechanics the indices (subscripts) always take the values of 1, 2, 3 in three dimensions, 1, 2 in two dimensions, and in relativity 0, 1, 2, 3. You may have noticed the comma in the indices "$q_{i,j}$." It denotes partial differentiation (more on that later).

From that example, index notation should obviously have some appeal. It is:

- Logical
- Economical and compact
- Easily learned

We will introduce index notation in the next section. But before leaving this section we want to emphasize an extremely important point. A vector or tensor will have different component values in different coordinate systems, but they are the same entity and do not depend on the coordinate system you select. *All vectors and tensors are independent of any reference coordinate system.*

C.3.1 Index notation

In a previous finite element textbook I co-authored, I was told that it is forbidden to present index notation to undergraduates. I think this is nonsense. It takes only a few minutes to understand the basics of index notation for small deformations in Cartesian coordinate systems, and after a little practice and familiarity, one would wonder why this was never taught sooner. It greatly simplifies the appearance of the equations of mechanics and, I believe, enhances understanding. Index notation is simply this: Coordinates are numbered and noted with subscripts.[3] That is it! That is the whole idea! It was more or less formalized by Einstein to make life easier in dealing with the geometric analogy of general relativity where there are four dimensions in non-Euclidean space-time. We use a much more modest version though.

Conventions of index notation

The power of the index notation is not merely the handy way to denote coordinates, but in additional conventions that greatly reduce the amount of writing we have to do. We cover some of those now.

[2] As long as we use orthogonal coordinate systems such as Cartesian or cylindrical the indices will all appear as subscripts. In more general coordinate systems indices may appear as both subscripts and superscripts. We will not use non-orthogonal coordinates here.

[3] In some coordinate systems, the axes are not orthogonal. There, we must use both superscript and subscript indices. But we are not going to concern ourselves with that degree of complexity here. See Simmonds [49] for a good foundation level book on vectors and tensors.

Summation convention

Any index repeated in a term is automatically summed over its entire range (3). For example,

$$a_{ij}\,x_j = c_i \quad \rightarrow \quad \sum_{j=1}^{3} a_{ij}\,x_j = c_i \qquad i = 1,2,3$$

In the summation convention, a non-repeated index is called a *free index*, and the repeated index is called a *dummy index*. In the example, i is a free index, and j is a dummy index.

Range convention

Any free (not repeated) index is implied to take on all possible values of its range (3). For example,

$$a_{ij}\,x_j = c_i \quad \rightarrow \quad \begin{aligned} a_{11}\,x_1 + a_{12}\,x_2 + a_{13}\,x_3 &= c_1 \\ a_{21}\,x_1 + a_{22}\,x_2 + a_{23}\,x_3 &= c_2 \\ a_{31}\,x_1 + a_{32}\,x_2 + a_{33}\,x_3 &= c_3 \end{aligned}$$

Nuances

The dummy index may be changed without affecting the meaning. The following is acceptable because changing the dummy index does not change the meaning, since it only implies a sum over the range:

$$a_{ij}\,x_j = a_{ik}\,x_k$$

The free index may not be changed within an equation, unless we change all occurrences of that particular index. For example,

$$a_{ij}\,x_j = c_i \quad \leftrightarrow \quad a_{kj}\,x_j = c_k$$

The two equations are equivalent but the following is not:

$$a_{ij}\,x_j \neq a_{kj}\,x_j$$

because the free index is not consistent on both sides.

A repeated index on a single variable is called a *contraction*:

$$a_{ii} = a_{11} + a_{22} + a_{33}$$

A dummy index can be repeated only once in a term. The following expressions are meaningless: C_{iiii} , ϵ_{iii} , $a_i b_i c_i$

We might think of indexed quantities as matrices, although that is not necessarily the purpose. Two examples follow:

$$a_i = \begin{Bmatrix} a_1 \\ a_2 \\ a_3 \end{Bmatrix} \qquad b_{ij} = \begin{bmatrix} b_{11} & b_{12} & b_{13} \\ b_{21} & b_{22} & b_{23} \\ b_{31} & b_{32} & b_{33} \end{bmatrix}$$

When considered in terms of matrix algebra, the first index is the row number and the second is the column number. (Caution: While this is the most common practice, some use the opposite convention:)

$$c_i = a_j b_{ij} \quad \rightarrow \quad \left\{ \begin{array}{c} c_1 \\ c_2 \\ c_3 \end{array} \right\} = \left[\begin{array}{ccc} b_{11} & b_{12} & b_{13} \\ b_{21} & b_{22} & b_{23} \\ b_{31} & b_{32} & b_{33} \end{array} \right] \left\{ \begin{array}{c} a_1 \\ a_2 \\ a_3 \end{array} \right\}$$

$$= \left\{ \begin{array}{l} a_1 b_{11} + a_2 b_{12} + a_3 b_{13} \\ a_1 b_{21} + a_2 b_{22} + a_3 b_{23} \\ a_1 b_{31} + a_2 b_{32} + a_3 b_{33} \end{array} \right\}$$

In index notation, it makes no difference whether we write

$$c_i = a_j b_{ij} \qquad \text{or} \qquad c_i = b_{ij} a_j$$

as long as we keep the indices in the correct order, but the order of the indices does make a difference; for instance, in general,

$$a_j b_{ij} \neq a_j b_{ji}$$

Partial derivatives

Partial derivatives with respect to spatial coordinates occur frequently in solid mechanics, and index notation allows for a shortcut in notation by using a comma to denote partial differentiation.

$$f_{i,j} \equiv \frac{\partial f_i}{\partial x_j} \qquad f_{i,jk} \equiv \frac{\partial^2 f_i}{\partial x_j \, \partial x_k}$$

We also use summations in derivatives; for instance,

$$u_{i,ij} = \left\{ \begin{array}{l} \dfrac{\partial^2 u_1}{\partial x_1 \partial x_1} + \dfrac{\partial^2 u_2}{\partial x_2 \partial x_1} + \dfrac{\partial^2 u_3}{\partial x_3 \partial x_1} \\ \dfrac{\partial^2 u_1}{\partial x_1 \partial x_2} + \dfrac{\partial^2 u_2}{\partial x_2 \partial x_2} + \dfrac{\partial^2 u_3}{\partial x_3 \partial x_2} \\ \dfrac{\partial^2 u_1}{\partial x_1 \partial x_3} + \dfrac{\partial^2 u_2}{\partial x_2 \partial x_3} + \dfrac{\partial^2 u_3}{\partial x_3 \partial x_3} \end{array} \right\}$$

Note that the result is still a 3×1 vector.

It becomes readily apparent that index notation can save a lot of space and effort in presenting mathematical expressions. It is not necessary to write out such long expressions, and it also lends itself well to computer algorithms.

This is enough to get us started. We will add to this as needed in context of certain applications. The important things to remember for now are the ideas of the indices and the summation convention. It is a simple concept at this level, and one only need a little practice to master it.

C.4 Scalars, vectors, and tensors

Most of you are already familiar with scalars and vectors. Tensors are perhaps not quite so familiar to many bachelor level engineers except perhaps in the form of matrices. What follows is not by any

means a thorough treatment, but I hope sufficient to grasp the basic concepts and to clear up any possible misconceptions.

C.4.1 Scalars

Scalars are nothing more than single numbers. Here, they will always be real numbers, and they obey the simple addition and multiplication rules of ordinary arithmetic. In our context, pressure, mass, density, and temperature are commonly encountered scalars. Obviously they are not necessarily constants, but can be functions of space and time. They may also have the physical dimensions of some vectors and tensors, like ft/s or psi and so forth. We can often speak of them in terms of *scalar fields* over some volume of space, such as a temperature field or pressure field. And since a scalar field is a function of space we can determine its spatial gradient at different points (its rate of change within that space in different directions). Its gradient, however, is not a scalar, but is a vector because it is assigned a direction as well as a magnitude. The $\mathrm{d}p/\mathrm{d}x$ in Darcy's one-dimensional flow rule is an example of a pressure gradient in one direction—it is a vector, the gradient of a scalar pressure field in the x-direction.

C.4.2 Vectors

Now we turn to the traditional engineering concept of a vector as a special case of a general algebraic vector. A simple definition of a geometric or physical vector is a quantity with both a magnitude (or length) and a direction in some space, e.g., displacement, velocity, momentum, and so forth in $\mathbb{E}^3$. Mathematically such a vector is an ordered n-tuple such as $(u_1, u_2, u_3, \ldots, u_n)$ which may or may not represent any physical phenomena. It may be expressed in a number of notations, for example, a displacement vector, $\mathbf{u}$, may be written variously as:

1. $\mathbf{u}$
2. $(u, v, w)\,\mathbf{e}$
3. $\left(u\,\hat{\mathbf{i}}, v\,\hat{\mathbf{j}}, w\,\hat{\mathbf{k}}\right)$
4. $u\,\hat{\mathbf{i}} + v\,\hat{\mathbf{j}} + w\,\hat{\mathbf{k}}$
5. $\left(u_x,\ u_y,\ u_z\right)$
6. (u_1, u_2, u_3)

The first of these is called direct notation, used primarily in mathematics where the component values in any particular coordinate system are seldom important. While it is quite compact, it is a bit abstract for most engineers whose primary interest is in numerical results. Form 2 above is a slightly expanded general form where $\mathbf{e}$ is understood as a set of base vectors of some coordinate system. These are not necessarily unit base vectors nor is the coordinate system necessarily orthogonal. Forms 3 and 4 are expansions commonly used in undergraduate engineering texts where $\hat{\mathbf{i}}$, $\hat{\mathbf{j}}$, and $\hat{\mathbf{k}}$ are unit base vectors in a Cartesian coordinate system and u, v, and w are the three component magnitudes, respectively. These two examples are very easy to visualize as physical quantities, especially when numerical values are assigned to the components. But in the age of computers they are extremely cumbersome to the point of being an impediment to computation because they involve three different variable names as well as three different coordinate names for the same vector. Number 5 illustrates the components with a single name but with component subscripts denoting three coordinate directions. This form is very common, but is still un-handy for machine computation and becomes even messier when we get to tensors later. The last form is more computationally efficient in that the variable has a single name and the indices are sequential numbers rather than characters. In the more efficient index notation we commonly write that same displacement vector simply as

$u_i \quad \text{where} \quad i = 1, 2, 3$

or simply, u_i, where the index, i, is assumed to take the range of some spatial coordinate system directions. In other words, u_i represents all three of the components of $\mathbf{u}$ in our coordinate system. More formally we might write the vector, $\mathbf{u}$ as a vector sum of its components:

$$\mathbf{u} = \sum_{i=1}^{3} u_i \, \hat{\mathbf{e}}_i$$

This then brings us back to the summation convention of index notation where the above may be written more simply as

$$\mathbf{u} = u_i \hat{\mathbf{e}}_i = u_1 \, \hat{\mathbf{e}}_1 + u_2 \, \hat{\mathbf{e}}_2 + u_3 \, \hat{\mathbf{e}}_3$$

where the expansion is understood but seldom written.

I have included a set of unit base vectors, $\hat{\mathbf{e}}_i$, similar to the familiar $\hat{\mathbf{i}}$, $\hat{\mathbf{j}}$, $\hat{\mathbf{k}}$, into the mix here as a formality where

$$\hat{\mathbf{e}}_1 = (1, 0, 0)$$

$$\hat{\mathbf{e}}_2 = (0, 1, 0)$$

$$\hat{\mathbf{e}}_3 = (0, 0, 1)$$

For clarity $\mathbf{u}$ might be written more fully as

$$\begin{aligned}
\mathbf{u} &= u_i \hat{\mathbf{e}}_i \\
&= u_1 \hat{\mathbf{e}}_1 + u_2 \hat{\mathbf{e}}_2 + u_3 \hat{\mathbf{e}}_3 \\
&= u_1 (1, 0, 0) + u_2 (0, 1, 0) + u_3 (0, 0, 1) \\
&= (u_1, 0, 0) + (0, u_2, 0) + (0, 0, u_3) \\
&= (u_1, u_2, u_3)
\end{aligned}$$

In most applications base vectors are understood, do not change, and are omitted for simplicity, so our displacement vector is usually written simply as u_i with the base vectors being understood but not written. The written economy of index notation is becoming readily apparent and will become more so as we progress. We do, however, need to understand base vectors and basis in a little more depth before we proceed.

Base vectors

When we wish to work with vectors in component form, we must have some *basis* to which they refer. For example, $\mathbf{u}$, refers to a vector in direct notation and requires no coordinate system or *basis*, however when we cast the same vector in component form, u_i for instance, there is an implied basis to which the subscript refers. The basis itself is comprised of a set of *base vectors*. In three-dimensional Euclidean space, $\mathbb{E}^3$, there are three base vectors and u_i means $(u_1, u_2, u_3)\mathbf{e}$ where $\mathbf{e}$ is the basis or $u_1\mathbf{e}_1, u_2\mathbf{e}_2, u_3\mathbf{e}_3$ where $\mathbf{e}_1, \mathbf{e}_2, \mathbf{e}_3$ are the base vectors of the basis $\mathbf{e}$. The three base vectors are not necessarily unit valued nor orthogonal in general. When they are orthogonal we call $\mathbf{e}$ an *orthogonal basis*. When they are both orthogonal and unit valued, as $\hat{\mathbf{e}}_1, \hat{\mathbf{e}}_2, \hat{\mathbf{e}}_3$, we call the basis $\hat{\mathbf{e}}$ an *orthonormal basis*.

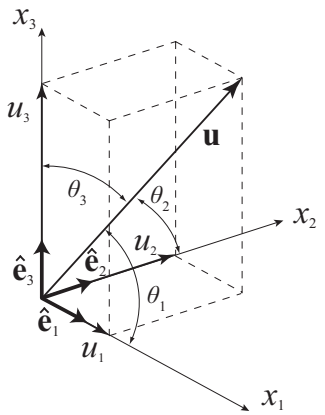

Figure C.2 Rectangular components of a vector.

Most commonly we work with orthonormal bases on which we define a Cartesian coordinate system. The components of a vector in such a basis are the projections of the vector onto the basis vectors. For example, consider the vector, $\mathbf{u}$, with magnitude, u, in a Cartesian coordinate system with an orthonormal basis:

$$\mathbf{u} = u_1\hat{\mathbf{e}}_1 + u_2\hat{\mathbf{e}}_2 + u_3\hat{\mathbf{e}}_3 \tag{C.1}$$

The vector components, u_1, u_2, u_3, are the projections of $\mathbf{u}$ onto their respective base vectors, $\hat{\mathbf{e}}_1, \hat{\mathbf{e}}_2, \hat{\mathbf{e}}_3$ with the angles $\theta_1, \theta_2, \theta_3$, as shown in Figure C.2 and given by

$$u_1 = u\cos\theta_1, \quad u_2 = u\cos\theta_2, \quad u_3 = u\cos\theta_3 \tag{C.2}$$

where the length of the vector, $u = \|\mathbf{u}\|$ is defined in the next section.

The bases we have described here are relatively simple, but the topic can get much more complicated in some applications, as in curvilinear coordinate systems for example. In cases where displacements and/or strains are of significant magnitude a basis assigned to a point in a material body that was initially orthonormal in an undeformed reference configuration may not be orthonormal in the resulting deformed configuration. That being said, *we will not include basis vectors in our notation beyond this point except where necessary for clarity.*

Vector magnitude

The *magnitude* (or "length") of a vector representing some physical quantity is obviously an important property and its coordinate components by themselves may not directly express what we need to know about a particular vector. For example, a displacement (vector), $\mathbf{u}$, of some point in a material body may be represented in coordinate form as (u_1, u_2, u_3), but that does not tell us the magnitude of the total distance that point has moved. There are many mathematical operations where knowledge of the magnitude of a vector is necessary. The *magnitude*, u, of a vector, $\mathbf{u}$ is defined by

$$\boxed{u = \|\mathbf{u}\| \equiv \sqrt{(u_1)^2 + (u_2)^2 + (u_3)^2} \geq 0} \tag{C.3}$$

The magnitude of a vector is either positive or zero, and in most contexts a zero vector is a point and not a vector. An important point: When squaring vector (and tensor) components it is wise to always use parentheses to avoid confusion, e.g., use $(u_i)^2$ or $(u_2)^2$ instead of u_i^2 or u_2^2, respectively. While we will seldom use superscripted vector or tensor components in this text, more general vector and tensor analyses do, and omitting the parentheses can cause confusion. The exception will be when we are using second-order derivatives like $\partial^2 u_2/\partial x_2^2$ where parentheses might cause even worse confusion.

Unit vectors

A unit vector is a vector whose magnitude is unity (1). Any non-zero vector can be unitized so that its magnitude is unity, and its direction is unchanged. A unit vector, $\hat{\mathbf{u}}$, for instance is defined as

$$\hat{\mathbf{u}} \equiv \frac{\mathbf{u}}{\|\mathbf{u}\|} \tag{C.4}$$

In index form we might express it as

$$\hat{u}_i = \frac{u_i}{u} = \frac{u_i}{\sqrt{(u_1)^2 + (u_2)^2 + (u_3)^2}} \tag{C.5}$$

It is quite important to note that a component, $\hat{u}_i$, of a unit vector, $\hat{\mathbf{u}}$, is not equal to unity (unless the other two components are equal to zero), so $\hat{u}_i$ always denotes the components of a unit vector and not components that are themselves unity in value.

Polar and axial vectors

So far we have assumed that vector orientation is obvious from the physical quantities they represent, but that is not always the case. *Polar vectors*, also called *true vectors*, are the vectors we are most accustomed to using. They have the property that when transformed by coordinate rotations they maintain their correct orientation. For example if we consider a reflection of some event or a transform from a right-hand coordinate system to a left-hand system, a polar vector will still retain the proper orientation for the quantity it represents. On the other hand, an *axial vector*, or *pseudo-vector*, is oriented by some established convention and when transformed into a reflection or from a right-hand to left-hand coordinate system it will generally point in the opposite direction from the quantity it represents. Examples of axial vectors are torque (moment), angular momentum, and electro-magnetic flux which are oriented by convention rather than obvious physical entities. Typically axial vectors arise from a cross product such as $\mathbf{f} \times \mathbf{u} = \boldsymbol{\tau}$ which might represent force×length = torque, an axial vector. Torque does not have an intuitive "direction" like force, so the direction of the torque vector is assigned by convention as it is a mathematical construct of a special operation on two vectors.

C.4.3 Coordinate invariance

What we have covered about vectors so far has been illustrated in Cartesian coordinate systems which is where we work for the most part, and we think of a vector as an ordered 3-tuple (or ordered triple if you prefer) whose components are dependent on the particular coordinate system chosen. But mathematically, *a vector is an objective entity*, and *it is coordinate invariant*. In other words it represents the same entity, independent of any coordinate system in which it is cast. Once it is quantified in component form in any coordinate system it is *absolutely unique*. It may be transformed into other

coordinate systems where its components may take different numerical values, but it is still the same unique vector. This is an *extremely important point to remember*.

C.4.4 Vector operations

The basic operations of vectors are addition and multiplication, and there is no operation called "division" in vector (or tensor) operations. Vector addition and multiplication take different forms from the arithmetic of scalar numbers. Additionally, there are several special operators that are unique to vector (and tensor) operations. We will introduce two especially useful operators immediately, and though they are tensors, it is not essential to understand tensors at this point.

Kronecker delta and permutation symbol

Before we get into specific vector operations it is advisable to introduce two tensor operators and an identity that relates them. They are extremely useful in applying index notation to vector (and tensor) operations. These are the *Kronecker delta* which is a 2-order tensor and the *permutation symbol* which is a 3-order tensor in our usage. For now let us be satisfied that a 2-order tensor has two subscripts and a 3-order tensor has three.

The *Kronecker delta*, is written in index notation as δ_{ij}, a delta with two coordinate subscripts in orthogonal coordinate systems. It is defined simply as

$$\boxed{\delta_{ij} \equiv \begin{cases} 1 & \text{if } \ i = j \\ 0 & \text{if } \ i \neq j \end{cases}} \tag{C.6}$$

Where i and j take on the values $1, 2, 3$. It might also be thought of as an *identity tensor* since in matrix form it is written

$$\mathbf{I} = \left[\delta_{ij}\right] = \begin{bmatrix} 1 & 0 & 0 \\ 0 & 1 & 0 \\ 0 & 0 & 1 \end{bmatrix}$$

as $\mathbf{Iv} = \mathbf{v}$. Its usefulness will soon become apparent as we proceed.

The *permutation symbol* or permutation tensor is a 3-order tensor which in Cartesian coordinate systems is defined as

$$\boxed{\epsilon_{ijk} \equiv \begin{cases} 0 & \text{if any two indices are equal} \\ 1 & \text{when } i, j, k \text{ are an even permutation of } 1, 2, 3 \\ -1 & \text{when } i, j, k \text{ are an odd permutation of } 1, 2, 3 \end{cases}} \tag{C.7}$$

The idea of even and odd permutations is easily visualized in Figure C.3 so that (1,2,3), (2,3,1), (3,1,2) are *even* permutations, and (3,2,1), (2,1,3), (1,3,2) are *odd* permutations. The permutation symbol is a shortcut for computing determinants and cross products which we will soon encounter. In those contexts it serves as a notational device, hence the term, *permutation symbol*, however, in a more general context it is a 3-order tensor called the *Levi-Civita tensor* where it can take $\pm$ values other than 1 in its even and odd permutations. We will not encounter that form in this text, but you should be aware that we are employing a special case of the more general form.

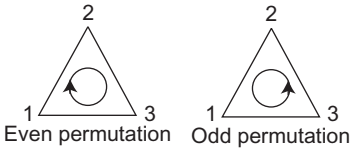

Figure C.3 Even and odd permutations.

The permutation symbol and Kronecker delta are related in Cartesian coordinates by a relationship called the ϵ-δ *identity*:

$$\boxed{\epsilon_{ijk}\epsilon_{ipq} = \delta_{jp}\delta_{kq} - \delta_{jq}\delta_{kp}} \tag{C.8}$$

which is used in computing a triple cross product that we will see later.

Vector addition

All engineers are familiar with vector addition in a geometric context where vectors are graphically arranged head to tail, and and a resultant vector (the vector sum) is drawn from the first tail to the last head. For computational work that is a bit primitive and we use the component form instead. For example the sum **w** of two vectors, **u** and **v** is

$$\mathbf{w} = \mathbf{u} + \mathbf{v}$$
$$\mathbf{w} = (u_1 + v_1,\ u_2 + v_2,\ u_3 + v_3)$$
or
$$w_i = u_i + v_i$$

Inner product

Often we find need to multiply two vectors in a manner that produces a scalar value. This is variously referred to as *inner product*, *dot product*, *scalar product*. The *inner product* between two vectors, **u** and **v** is defined as

$$\boxed{\mathbf{u} \cdot \mathbf{v} \equiv \|\mathbf{u}\|\,\|\mathbf{v}\|\,\cos\theta, \qquad 0 \le \theta \le \pi} \tag{C.9}$$

where $\|\mathbf{u}\|$ and $\|\mathbf{v}\|$ are the magnitudes of **u** and **v**, respectively, and θ is the angle between the two vectors (see Equation (C.3) for vector magnitude). An inner product of a vector with itself or "square" of a single vector, is given by

$$\mathbf{u}^2 = \mathbf{u}\cdot\mathbf{u} = \|\mathbf{u}\|^2 \cos 0 = \|\mathbf{u}\|^2 \tag{C.10}$$

From the definition Equation (C.9) we can see that the inner product between any two different unit base vectors, $\hat{\mathbf{e}}_1$, $\hat{\mathbf{e}}_2$, $\hat{\mathbf{e}}_3$ of an orthonormal coordinate system is zero since $\theta = \pi/2$ and $\cos \pi/2 = 0$ and the inner product of a unit base vector with itself as in Equation (C.10) is equal to 1. Hence,

$$\hat{\mathbf{e}}_1 \cdot \hat{\mathbf{e}}_2 = \hat{\mathbf{e}}_2 \cdot \hat{\mathbf{e}}_3 = \hat{\mathbf{e}}_3 \cdot \hat{\mathbf{e}}_1 = 0$$
$$\hat{\mathbf{e}}_1 \cdot \hat{\mathbf{e}}_1 = \hat{\mathbf{e}}_2 \cdot \hat{\mathbf{e}}_2 = \hat{\mathbf{e}}_3 \cdot \hat{\mathbf{e}}_3 = 1$$

We could as easily express the above two equations as the Kronecker delta:

$$\hat{\mathbf{e}}_i \cdot \hat{\mathbf{e}}_j = \delta_{ij} \tag{C.11}$$

Typically we are working with the component form of vectors in some orthonormal coordinate system so the inner product of $\mathbf{u}$ and $\mathbf{v}$ is

$$\begin{aligned}\mathbf{u} \cdot \mathbf{v} &= \left(u_1\hat{\mathbf{e}}_1 + u_2\hat{\mathbf{e}}_2 + u_3\hat{\mathbf{e}}_3\right) \cdot \left(v_1\hat{\mathbf{e}}_1 + v_2\hat{\mathbf{e}}_2 + v_3\hat{\mathbf{e}}_3\right) \\ &= (u_1 v_1 + u_2 v_2 + u_3 v_3) \\ &= u_i\, v_i\end{aligned}$$

or using the Kronecker delta as a substitute for the orthonormal base vectors,

$$\mathbf{u} \cdot \mathbf{v} = \left(u_j\, v_k\right)\, \delta_{jk} = u_i\, v_i$$

An inner product of a vector with itself is often encountered and is

$$\mathbf{u} \cdot \mathbf{u} = (u_i)^2 = u_i\, u_i = u_1\, u_1 + u_2\, u_2 + u_3\, u_3$$

There are several other uses for the inner product of two vectors. From the definition of the inner product (Equation (C.9)), we may find the angle between two vectors $\mathbf{u}$ and $\mathbf{v}$ as

$$\cos\theta = \frac{\mathbf{u} \cdot \mathbf{v}}{\|\mathbf{u}\|\, \|\mathbf{v}\|} \tag{C.12}$$

or

$$\theta = \cos^{-1}\left(\frac{u_i\, v_i}{\sqrt{(u_i)^2\ (v_i)^2}}\right) \tag{C.13}$$

Also considering two vectors, $\mathbf{u} \neq \mathbf{0}$ and $\mathbf{v} \neq \mathbf{0}$, if the inner product, $\mathbf{u} \cdot \mathbf{v} = \mathbf{0}$ then $\mathbf{u}$ and $\mathbf{v}$ are perpendicular vectors, i.e.,

$$\mathbf{u} \cdot \mathbf{v} = 0 \quad \Rightarrow \quad \mathbf{u} \perp \mathbf{v} \quad (\mathbf{u}, \mathbf{v} \neq \mathbf{0}) \tag{C.14}$$

This is sometimes useful in computational work to test whether or not two vectors are perpendicular.[4]

The inner product is a form of *contraction* which refers to any tensor operation which results in a tensor (or vector) of an order less than the original. In this definition we are talking of tensors in general of any order including scalars and vectors.

We might also mention at this point that in many engineering contexts, the "dot" is often omitted from the notation and is to be assumed by the context. For example $a = \mathbf{uv}$ might be used, and in this case it should be obvious that a is a scalar and $a = \mathbf{u} \cdot \mathbf{v}$ is the implied meaning since that is the only possible product of two vectors, $\mathbf{u}$ and $\mathbf{v}$, that can produce a scalar.

[4] In practice, the finite arithmetic of computers will seldom compute inner products as exactly zero from roundoff and truncation, so if such a test is required one must test an absolute value of the inner product against some arbitrarily small positive constant or variable depending on the application, for example, "If abs(Prod)<Small then Prod = 0.0e00," where Prod is the inner product and Small = 1.0e-10 or something within reason.

Open product

An open product of two vectors produces a tensor called a *dyad*. We have not yet covered 2-order tensors, but for explanation of this vector operation just consider them to be 3×3 matrices for the time being. For example

$$\mathbf{T} = \mathbf{u} \otimes \mathbf{v} \tag{C.15}$$

where $\mathbf{T}$ is a dyad tensor produced from the open product of two vectors, $\mathbf{u}$ and $\mathbf{v}$. In Cartesian coordinates we could express it as

$$T_{ij} = u_i v_j = \begin{bmatrix} u_1v_1 & u_1v_2 & u_1v_3 \\ u_2v_1 & u_2v_2 & u_2v_3 \\ u_3v_1 & u_3v_2 & u_3v_3 \end{bmatrix} \tag{C.16}$$

Upon examination you will see that this dyad tensor is symmetric, i.e., $\mathbf{T} = \mathbf{T}^{\mathrm{T}}$ or $T_{ij} = T_{ji}$ because the vector components are scalars and multiplication of scalars is commutative.

The open product is also called a tensor product, but that name is a bit confusing and will not be used here. In fact we will not have need for the open product in this text but include it should you encounter it elsewhere.

Cross product

The *cross product* or *vector product* is another type of multiplication of two vectors, $\mathbf{u}$ and $\mathbf{v}$, that yields a third vector, $\mathbf{w}$ that is perpendicular to the plane containing the original two vectors.

$$\mathbf{u} \times \mathbf{v} = \mathbf{w} \tag{C.17}$$

The magnitude of the cross product may be defined as

$$\boxed{\| \mathbf{u} \times \mathbf{v} \| \equiv \|\mathbf{u}\| \, \|\mathbf{v}\| \, \sin\theta, \qquad (0 \leq \theta \leq \pi)} \tag{C.18}$$

and by convention its direction is perpendicular to the plane containing the original two vectors and directed like a right hand coordinate system as in $\mathbf{u} \rightarrow \mathbf{v} \rightarrow \mathbf{u} \times \mathbf{v}$ shown in Figure C.4.

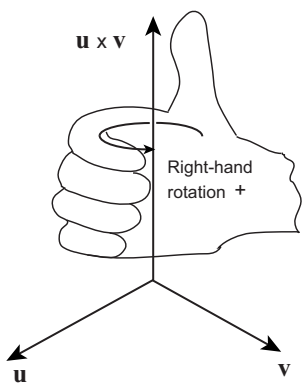

Figure C.4 Cross product, right-hand convention.

Because the cross product results in an axial vector it is *not commutative*. In other words

$$\mathbf{u} \times \mathbf{v} = -(\mathbf{v} \times \mathbf{u}) \tag{C.19}$$

so that the commuted magnitude is the same but the orientation is in the opposite direction. A cross product is *distributive over addition*

$$\mathbf{u} \times (\mathbf{v} + \mathbf{w}) = \mathbf{u} \times \mathbf{v} + \mathbf{u} \times \mathbf{w} \tag{C.20}$$

A cross product is *not associative*.

$$\mathbf{u} \times (\mathbf{v} \times \mathbf{w}) \neq (\mathbf{u} \times \mathbf{v}) \times \mathbf{w} \tag{C.21}$$

An oftentimes useful property of the cross product is its use calculating a unit normal vector to a plane defined by two vectors. Given two vectors, $\mathbf{u}$ and $\mathbf{v}$, then a unit normal vector, $\hat{\mathbf{n}}$, to those two vectors and a plane they define is

$$\hat{\mathbf{n}} = \frac{\mathbf{u} \times \mathbf{v}}{\|\mathbf{u} \times \mathbf{v}\|} \tag{C.22}$$

Somewhat similar to the inner product, the angle between $\mathbf{u}$ and $\mathbf{v}$ is given by

$$\sin\theta = \frac{\|\mathbf{u} \times \mathbf{v}\|}{\|\mathbf{u}\| \, \|\mathbf{v}\|}, \qquad (0 \leq \theta \leq \pi) \tag{C.23}$$

or

$$\theta = \sin^{-1}\left(\frac{\|\mathbf{u} \times \mathbf{v}\|}{\|\mathbf{u}\| \, \|\mathbf{v}\|}\right) \tag{C.24}$$

Computing a cross product

The defining equation for the cross product (Equation (C.18)) given previously is not particularly useful if one does not know the angle between the two vectors. The magnitude of the cross product is usually calculated from the components of the two vectors in a Cartesian coordinate system as

$$\mathbf{u} \times \mathbf{v} = \det \begin{bmatrix} \hat{\mathbf{e}}_1 & \hat{\mathbf{e}}_2 & \hat{\mathbf{e}}_3 \\ u_1 & u_2 & u_3 \\ v_1 & v_2 & v_3 \end{bmatrix} \tag{C.25}$$

Suppose now we want to calculate a vector, $\mathbf{w}$, using the above equation by cofactor expansion on the first row for the determinate.

$$\mathbf{w} = \mathbf{u} \times \mathbf{v} = \det \begin{bmatrix} \hat{\mathbf{e}}_1 & \hat{\mathbf{e}}_2 & \hat{\mathbf{e}}_3 \\ u_1 & u_2 & u_3 \\ v_1 & v_2 & v_3 \end{bmatrix}$$

$$= (u_2 v_3 - u_3 v_2)\,\hat{\mathbf{e}}_1 + (u_3 v_1 - u_1 v_3)\,\hat{\mathbf{e}}_2 + (u_1 v_2 - u_2 v_1)\,\hat{\mathbf{e}}_3$$

Alternatively, we may make use of the permutation symbol so that the direct notation equation for $\mathbf{w}$ above may be expressed in index notation as

$$w_i = \epsilon_{ijk}\, u_j\, v_k \tag{C.26}$$

Let us use this equation to calculate the three components of $\mathbf{w}$. First let is calculate w_1 so the free index i is 1 and $w_1 = \epsilon_{1jk} u_j v_k$. Recall that the permutation symbol is zero if any two indices are the same, so that leaves only two possibilities, ϵ_{123} which is an even permutation, and ϵ_{132}, an odd permutation. Therefore,

$$w_1 = \epsilon_{123} u_2 v_3 + \epsilon_{132} u_3 v_2 = (1) u_2 v_3 + (-1) u_3 v_2 = u_2 v_3 - u_3 v_2$$

which is exactly what we calculated using the determinate form above. Now we calculate the remaining two components, w_2 and w_3.

$$w_2 = \epsilon_{231} u_3 v_1 + \epsilon_{213} u_1 v_3 = (1) u_3 v_1 + (-1) u_3 v_2 = u_3 v_1 - u_1 v_3$$

$$w_3 = \epsilon_{312} u_1 v_2 + \epsilon_{321} u_2 v_1 = (1) u_1 v_2 + (-1) u_2 v_1 = u_1 v_2 - u_2 v_1$$

There are two combination products with the cross product that are useful to know though they seldom apply in our applications here. The most common is the called the *scalar triple product* which is a triple product of three vectors as in $\mathbf{u} \cdot (\mathbf{v} \times \mathbf{w})$ that gives a scalar value result. Geometrically it calculates the volume of a parallelepiped (Figure C.5) and as such we may write it as

$$\text{vol}\,(\mathbf{u}, \mathbf{v}, \mathbf{w}) = |\,\mathbf{u} \cdot\, (\mathbf{v} \times \mathbf{w})| \tag{C.27}$$

and it forms a right-hand system, and by symmetry it is invariant under cyclic permutation, i.e.,

$$\mathbf{u} \cdot\, (\mathbf{v} \times \mathbf{w}) = \mathbf{w} \cdot\, (\mathbf{u} \times \mathbf{v}) = \mathbf{v} \cdot\, (\mathbf{w} \times \mathbf{u}) \tag{C.28}$$

Notice that in Equation (C.27) we used absolute value notation on the result of the scalar triple product result because in that particular context a volume is a positive scalar. The scalar triple product always yields a scalar value, but it is not necessarily positive.

Another cross product is often called the *triple cross product* or *triple vector product* and is given by

$$\mathbf{u} \times\ (\mathbf{v} \times \mathbf{w}) = (\mathbf{u} \cdot \mathbf{w})\, \mathbf{v} - (\mathbf{u} \cdot \mathbf{v})\, \mathbf{w} \tag{C.29}$$

Similarly

$$(\mathbf{u} \times \mathbf{v})\ \times \mathbf{w} = (\mathbf{u} \cdot \mathbf{w})\, \mathbf{v} - (\mathbf{v} \cdot \mathbf{w})\, \mathbf{u} \tag{C.30}$$

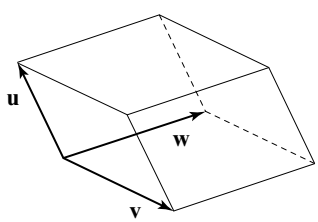

Figure C.5 Parallelepiped formed by scalar triple product.

and is a different vector from Equation (C.29). Computing the triple vector product for $\mathbf{t} = \mathbf{u} \times (\mathbf{v} \times \mathbf{w})$ in component form makes use of the ϵ-δ identity (Equation (C.8)) as

$$\begin{aligned} t_i &= \epsilon_{ijk}\, u_j \left(\epsilon_{kpq}\, v_p\, w_q\right) \\ &= \epsilon_{kij}\, \epsilon_{kpq} \left(u_j\, v_p\, w_q\right) \\ &= \left(\delta_{ip}\delta_{jq} - \delta_{iq}\delta_{jp}\right)\, u_j\, v_p\, w_q \\ &= \left(u_j\, w_q\, \delta_{jq}\right) v_p \delta_{ip} - \left(u_j\, v_p\, \delta_{jp}\right) w_q \delta_{iq} \\ &= (u_r\, w_r)\; v_i - (u_r\, v_r)\; w_i \end{aligned}$$

This is the component form of Equation (C.29) above and also serves as a proof of the ϵ-δ identity.

Before leaving the cross product, we should understand that it is a special case of a more general vector operation called variously the *wedge product*, the *outer product*, or the *exterior product*. We will not encounter those forms in this text because they refer to a more general case in vector spaces of dimensions greater than three.

C.4.5 2-Order tensors

We have mentioned before that scalars and vectors may be thought of as tensors of 0-order and 1-order, respectively, because they obey similar rules. However, in common usage of continuum mechanics, "tensor" refers to a 2-order tensor. And that is the custom we will follow from here on unless we specify otherwise. Like a vector, a *tensor is an objective entity*, and *it is coordinate invariant*. It only takes on numerical values when it is quantified in some coordinate system at which time it becomes *absolutely unique* even though its components may have different numerical values when transformed into other coordinate systems.

The definition of a tensor is usually unsatisfying for most engineers when first encountered: *A tensor is a linear operator that transforms a vector into another vector*. So its definition tells us what it does, but before we get into tensor operations let us cover a few things about what it is in terms of representation. In our context we typically think of a tensor as being represented as a 3×3 matrix in some coordinate system.

In direct notation we indicate a tensor in boldface upper case like, $\mathbf{T}$ for instance. In component index form we might represent the same tensor as T_{ij} where i, j each take all values of 1, 2, 3, in three dimensions (or 1, 2 in two dimensions), so there are nine tensor components in three dimensions. In matrix form the first subscript refers to the matrix row number and the second to the matrix column number.[5] For example

$$\mathbf{T} = T_{ij} = \begin{bmatrix} T_{11} & T_{12} & T_{13} \\ T_{21} & T_{22} & T_{23} \\ T_{31} & T_{32} & T_{33} \end{bmatrix}$$

Possibly the best starting point is with three examples. Simmonds [49] uses one I particularly like called the *projection operator* that projects a vector onto another vector. It is quite commonplace in many applications (including this text) and is defined as

[5] While this is common in most of mechanics, some texts use an opposite convention, especially some mathematical texts as well as some of Truesdale's work [50, 51].

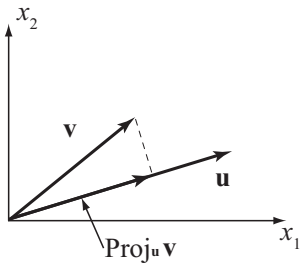

Figure C.6 Projection operator.

$$\text{Proj}_{\mathbf{u}}\mathbf{v} \equiv \left(\mathbf{v} \cdot \hat{\mathbf{u}}\right)\hat{\mathbf{u}} \tag{C.31}$$

which is illustrated geometrically in Figure C.6. The vector, $\mathbf{u}$, is generally not a unit vector, but must be unitized for the projection calculation using Equation (C.4) or (C.5).

While $\text{Proj}_{\mathbf{u}}$ does not fit so nicely into our notion of a tensor as a 3×3 matrix it is nevertheless a linear operator that transforms one vector, $\mathbf{v}$ into another with magnitude $\mathbf{v} \cdot \hat{\mathbf{u}}$ in the direction of $\mathbf{u}$, it does meet the definition of a tensor. Notice the projection tensor is equivalent to projecting a vector onto a basis vector to calculate its component in that direction as shown previously in Equations (C.1) and (C.2) and as illustrated in Figure C.2.

An example of a tensor is the Kronecker delta which we have already used and may represent as a 3×3 matrix

$$\mathbf{I} = \left[\delta_{ij}\right] = \begin{bmatrix} 1 & 0 & 0 \\ 0 & 1 & 0 \\ 0 & 0 & 1 \end{bmatrix}$$

which we earlier called an identity matrix because $\mathbf{I}\,\mathbf{v} = \mathbf{v}$ when used with a vector or in matrix form

$$\mathbf{I}\mathbf{v} = \delta_{ij}\,v_j = \begin{bmatrix} 1 & 0 & 0 \\ 0 & 1 & 0 \\ 0 & 0 & 1 \end{bmatrix} \begin{Bmatrix} v_1 \\ v_2 \\ v_3 \end{Bmatrix} = \begin{Bmatrix} v_1 \\ v_2 \\ v_3 \end{Bmatrix}$$

It "transforms" a vector into itself.

Another common tensor, $\mathbf{T}$, forms the Cauchy stress relationship whereby the stress tensor at a point on a surface (a physically real surface or an imaginary interior surface) transforms a unit vector normal to that surface, $\hat{\mathbf{n}}$, into the equivalent traction vector (distributed load vector), $\mathbf{t}$, acting on the surface at that point as in $\mathbf{t} = \hat{\mathbf{n}}\,\mathbf{T}$.

Further discussion of tensors requires an understanding of tensor operations which is the next section.

C.4.6 Tensor operations

Similar to vectors, tensors have analogous operations of addition and multiplication with somewhat different rules from scalars or vectors. Tensors add as we would expect, but multiplication is somewhat different.

Dyadic tensor product

The *dyadic tensor product* is a tensor operation on a vector as $\mathbf{v} = \mathbf{T}\,\mathbf{u}$. Some authors use a dot notation, $\mathbf{v} = \mathbf{T}\cdot\mathbf{u}$, but more commonly it is omitted and we will not use it here. We have already shown an example of a dyadic tensor product as Cauchy's stress relationship, $\mathbf{t} = \hat{\mathbf{n}}\,\mathbf{T}$, as the product of a vector and a tensor. In general dyadic products are not commutative, $\mathbf{u}\,\mathbf{T} \neq \mathbf{T}\,\mathbf{u}$ unless $\mathbf{T}$ is symmetric, i.e., $\mathbf{u}\,\mathbf{T} = \mathbf{T}\,\mathbf{u} \;\Leftrightarrow\; \mathbf{T} = \mathbf{T}^{\mathrm{T}}$. In our work here, most of the tensors we use will be symmetric and that sometimes leads to carelessness. In index notation we have more flexibility, for example

$$\mathbf{u}\,\mathbf{T} = u_i\,T_{ij} = T_{ij}\,u_i$$

and

$$\mathbf{T}\,\mathbf{u} = T_{ij}\,u_j = u_j\,T_{ij}$$

are all valid, as long as we keep the indices in the proper sequence to indicate the proper summation. However, the second forms in each of the above, while correct, are considered sloppy practice and should be avoided as many common computational errors result from improper index notation.

A dyadic product, $\mathbf{v} = \mathbf{T}\,\mathbf{u}$, written in matrix form would be

$$\begin{Bmatrix} v_1 \\ v_2 \\ v_3 \end{Bmatrix} = \begin{bmatrix} T_{11} & T_{12} & T_{13} \\ T_{21} & T_{22} & T_{23} \\ T_{31} & T_{32} & T_{33} \end{bmatrix} \begin{Bmatrix} u_1 \\ u_2 \\ u_3 \end{Bmatrix} \tag{C.32}$$

and $\mathbf{v} = \mathbf{u}\,\mathbf{T}$ would be written as

$$\begin{Bmatrix} v_1 & v_2 & v_3 \end{Bmatrix} = \begin{Bmatrix} u_1 & u_2 & u_3 \end{Bmatrix} \begin{bmatrix} T_{11} & T_{12} & T_{13} \\ T_{21} & T_{22} & T_{23} \\ T_{31} & T_{32} & T_{33} \end{bmatrix} \tag{C.33}$$

Again, Equations (C.32) and (C.33) are equivalent if $\mathbf{T}$ is symmetric, $\mathbf{T} = \mathbf{T}^{\mathrm{T}}$ or $T_{ij} = T_{ji}$.

Tensor product

The *tensor product* of two tensors is one that results in another tensor. Such operations occur frequently in continuum mechanics applications. It is commonly written as

$$\boxed{\mathbf{T} = \mathbf{U}\,\mathbf{V}} \tag{C.34}$$

Some authors use a dot as in $\mathbf{T} = \mathbf{U}\cdot\mathbf{V}$, but most omit it as we will here. The best way to understand the operation is to cast it in index notation in Cartesian coordinates as

$$\boxed{T_{ij} = U_{ik}V_{kj}} \tag{C.35}$$

where it is seen as the simple multiplication of two 3×3 matrices. The tensor product forms a real vector space, and as such obeys all the rules. It is not, however, commutative, in that $\mathbf{U}\,\mathbf{V} \neq \mathbf{V}\,\mathbf{U}$. But

$$\mathbf{U}\,\mathbf{V} = \left[\mathbf{V}^{\mathrm{T}}\mathbf{U}^{\mathrm{T}}\right]^{\mathrm{T}} \tag{C.36}$$

Inner product of two tensors

The *inner product* of two tensors is a product that results in a scalar value. For example

$$\mathbf{U} : \mathbf{V} = U_{ij}V_{ij}$$
$$= U_{11}V_{11} + U_{12}V_{12} + U_{13}V_{13} + \cdots + U_{33}V_{33} \tag{C.37}$$

There is another form where

$$\mathbf{U} \,.\, \mathbf{V} = U_{ij}V_{ji}$$
$$= U_{11}V_{11} + U_{12}V_{21} + U_{13}V_{31} + \cdots + U_{33}V_{33} \tag{C.38}$$

If either tensor is symmetric ($\mathbf{U} = \mathbf{U}^{\mathrm{T}}$ or $\mathbf{V} = \mathbf{V}^{\mathrm{T}}$) then they are the same form. The inner product is commutative, is associative with addition and scalar multiplication, and $\mathbf{U} : \mathbf{U} > 0$ when $\mathbf{U} \neq \mathbf{0}$.

Curvilinear coordinates

Before moving on, this is an appropriate place to bring up an important point. The previous examples of matrix representations of dyadic products are only valid for rectangular Cartesian coordinate components. Things become much more complicated in curvilinear coordinates where the components of a tensor in a coordinate system are not the same as the physical components they represent. We alluded to this earlier when we talked about "distances" in a cylindrical coordinate system where θ, is not the same type of coordinate as r and z. For example, the dyadic product, $v_i = T_{ij}u_j$, expressed in matrix form in Equation (C.32) is only valid in rectangular coordinates. In more general coordinates it would be written as $v_i = T_{ij}u^j$ where v_i is a covariant vector and u^j is a contravariant vector (see Simmonds [49]). This is not said to confuse the issue, but to make you aware of more general concepts that we are specializing in our treatment.

C.4.7 Coordinate transforms

Quite often it becomes necessary to transform the components of a vector or tensor from one coordinate system into another. In working with tubes in boreholes one finds it is quite often useful to employ a global coordinate system that is earth oriented to account for a downward vertical gravitational force and some compass orientation of the borehole itself. However, it is more convenient when working with some segment of a borehole or a tube within a borehole to use a local coordinate system oriented in relation to the segment of the borehole or the tube. Were it not for the gravitational force component, our work could be greatly simplified, but that is almost never our case and we are constantly faced with working with two coordinate systems in the same analysis.

The topic of coordinate transformation is quite easy, but as a consequence, almost no textbook on tensor analysis gives an adequate explanation for someone who actually intends to apply such a transform in actual calculations. Furthermore, the notation can cause considerable confusion to the practitioner. I will try to remedy that here by explaining coordinate transforms as something you are actually going to apply in practice since it is essential in our applications.

A transform between Cartesian coordinates whose origins are coincident is easily accomplished by a 3×3 orthogonal rotation matrix, $[Q]$. Such an orthogonal matrix has some interesting and specific properties.

$$[Q]\,[Q]^{\mathrm{T}} = [Q]^{\mathrm{T}}\,[Q] = [I]$$

$$[Q]^{\mathrm{T}} = [Q]^{-1}$$

$$\det[Q] = \det[Q]^{\mathrm{T}} = 1$$

where the superscript, T, denotes the transpose of the matrix, $[Q]$.

In index notation, given that $[Q] = Q_{ij}$, then the above may be stated as[6]

$$Q_{ik}\,Q_{jk} = Q_{ki}\,Q_{kj} = \delta_{ij}$$

$$Q_{ji} = Q_{ij}^{-1}$$

$$\det Q_{ij} = \det Q_{ji} = 1$$

One must be very careful about index notation in regard to transposed matrices. The general custom is to always use free indices in alphabetical order, and therefore free indices in reverse order would indicate a transpose matrix form, e.g., if $[Q] = Q_{ij}$ then $[Q]^{\mathrm{T}} = Q_{ji}$. Unfortunately this is not always so clear or adhered to consistently, as we will discuss later.

To understand the orthogonal rotation matrix, we should see how it is defined. The standard derivation is correct, but can lead to misunderstanding if not followed closely. Consider two coordinate systems, $\mathbf{x}$ and $\mathbf{x}'$, with orthogonal base vectors, $\mathbf{e}_i$ meaning $\mathbf{e}_1, \mathbf{e}_2, \mathbf{e}_3$ and $\mathbf{e}'_i$ meaning $\mathbf{e}'_1, \mathbf{e}'_2, \mathbf{e}'_3$, respectively, then

$$\mathbf{e}_i \cdot \mathbf{e}_j = \delta_{ij} \qquad \text{and} \qquad \mathbf{e}'_i \cdot \mathbf{e}'_j = \delta_{ij} \tag{C.39}$$

because the base vectors are orthogonal. Note especially here that the index on $\mathbf{e}_i$ refers to the number of the base vector, e.g., $\mathbf{e}_2$, and not to its individual components.

A vector, $\mathbf{u}$, may be expressed in either coordinate system as

$$\mathbf{u} = u_j \mathbf{e}_j = u'_j \mathbf{e}'_j \tag{C.40}$$

If we want to transform a vector, u_j from the original coordinate system, $\mathbf{x}$, to a new coordinate system, $\mathbf{x}'$, we use the vector equality as expressed in the above equation and rearrange it to the following:

$$\mathbf{e}'_j\,u'_j = \mathbf{e}_j\,u_j \tag{C.41}$$

We multiply both sides by $\mathbf{e}'_i$ we get

$$\left(\mathbf{e}'_i \cdot \mathbf{e}'_j\right) u'_j = \left(\mathbf{e}'_i \cdot \mathbf{e}_j\right) u_j \tag{C.42}$$

Since $\mathbf{e}'_i \cdot \mathbf{e}'_j = \delta_{ij}$ then

$$u'_i = \left(\mathbf{e}'_i \cdot \mathbf{e}_j\right) u'_j \tag{C.43}$$

[6] Strictly speaking, Q_{ij} refers to specific components of the matrix, $[Q]$, and hence the second two equalities are not correct for individual components of the matrix, but are meant in this context to denote the entire matrix in index notation.

At this point we define the transform matrix as

$$Q_{ij} \equiv \left(\mathbf{e}'_i \cdot \mathbf{e}_j\right) = \cos\theta_{ij} \tag{C.44}$$

From this we can see that

$$\boxed{u'_i = Q_{ij}\, u_j} \tag{C.45}$$

or in direct notation

$$\mathbf{u}' = Q\,\mathbf{u} \tag{C.46}$$

If we wish to perform the inverse operation, recall that $[Q]^{\mathrm{T}} = [Q]^{-1}$ so pre-multiplying both sides by Q^{T} gives

$$Q^{\mathrm{T}}\mathbf{u}' = \mathbf{u} \tag{C.47}$$

or

$$Q_{ji}u'_i = u_j \tag{C.48}$$

Here, we must always exercise caution with indices to distinguish between the transform matrix and its transpose. We will always use Q_{ij} for the components of $[Q]$ and Q_{ji} for the components of its transpose, $[Q]^{\mathrm{T}}$. Be aware that some authors do differ in this notation.

In general form the transform matrix, $[Q]$, is written as

$$[Q] = \begin{bmatrix} \cos\theta_{11} & \cos\theta_{12} & \cos\theta_{13} \\ \cos\theta_{21} & \cos\theta_{22} & \cos\theta_{23} \\ \cos\theta_{31} & \cos\theta_{32} & \cos\theta_{33} \end{bmatrix}$$

In matrix form the row numbers refer to the components of the transformed vector and the column numbers refer to the components of the vector being transformed. For example, $u'_1 = Q_{11}u_1 + Q_{12}u_2 + Q_{13}u_3$. In some texts you might see the components written as $Q_{i'j}$ as to keep the meaning clear, but we will not do that here as it encumbers the notation considerably. Now comes the confusing part; *the angle θ_{ij} is the angle measured from the original ith coordinate to the new jth coordinate*. For example, θ_{13} is the angle from x_1 to x'_3 which appears contrary to the notation of row and column numbers we have just stated, but that is how it is measured.

For a simple example, assume that the $\mathbf{x}'$ coordinate system is formed by a rotation of the $\mathbf{x}$ system by an angle, θ, counterclockwise about the x_3 axis as in Figure C.7. This is a right-hand rotation in a right-hand coordinate system so θ is a positive rotation angle. The angle between the x_1 axis and the x'_1 axis is θ hence the Q_{11} component is $\cos\theta$. Next, the angle between x_1 and x'_2 is $\theta + \pi/2$, so $Q_{12} = \cos(\theta + \pi/2) = \sin\theta$. The angle between x_1 and x'_3 is π so $Q_{13} = cos\pi = 0$. The second row of $[Q]$ is done similarly. $Q_{21} = \cos(\pi/2 - \theta) = -\sin\theta$. Then $Q_{22} = \cos\theta$ and $Q_{23} = \cos\pi = 0$.

This completes the first two rows of Q_{ij}, and you should be able to see the pattern now. The first subscripts of θ_{ij}, the row numbers, i, are the axes of the original coordinate system from which θ is measured, and the second subscripts, j, the column numbers, are the transformed axes to which θ is

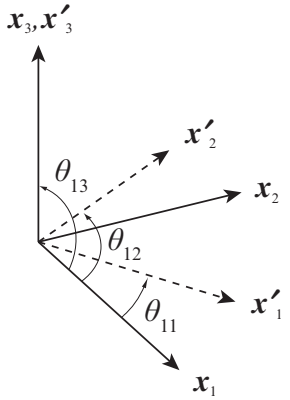

Figure C.7 Example of positive rotation of θ about the x_3 axis.

measured. For completeness, the last row is $Q_{31} = \cos\pi = 0$, $Q_{32} = \cos\pi = 0$, $Q_{31} = \cos 0 = 1$. We may write it in matrix form as

$$[Q] = Q_{ij} = \begin{bmatrix} \cos\theta & \sin\theta & 0 \\ -\sin\theta & \cos\theta & 0 \\ 0 & 0 & 1 \end{bmatrix}$$

It may seem obvious at this point that the general case will usually be much more complicated than a simple rotation about a single axis and the values of θ_{ij} will be much more tedious to calculate than that simple example. The good news is that any configuration can be determined by three consecutive rotations, each about a single axis. For many applications, two consecutive rotations is all that is required. *Any orientation can be achieved by a rotation about an axis of the original system followed by second rotation about an axis of the transformed system, followed by a third rotation about an axis of the second transformed system.* In other words, we only have to determine three rotation angles at maximum. And we may combine those three rotations into a single matrix if it is one we may be continually using for a particular application. In common practice of evaluating borehole stress components, we will require only two rotations rather than three.

$$[Q] = [Q'][Q]$$

Tensor and matrix multiplication is associative but not commutative in general, so *the order of multiplication is critical* because $[Q'][Q] \neq [Q][Q']$. Hence, *the sequence of rotations proceeds from right to left*.

That being understood, three axial rotation forms are all we will ever require, and we will seldom need more than two of them for most transformations in our context.

$$\left[{}^1Q\right] = \begin{bmatrix} 1 & 0 & 0 \\ 0 & \cos\theta_1 & \sin\theta_1 \\ 0 & -\sin\theta_1 & \cos\theta_1 \end{bmatrix}$$

$$\left[{}^{2}Q\right] = \begin{bmatrix} \cos\theta_2 & 0 & \sin\theta_2 \\ 0 & 1 & 0 \\ -\sin\theta_2 & 0 & \cos\theta_2 \end{bmatrix}$$

$$\left[{}^{3}Q\right] = \begin{bmatrix} \cos\theta_3 & \sin\theta_3 & 0 \\ -\sin\theta_3 & \cos\theta_3 & 0 \\ 0 & 0 & 1 \end{bmatrix}$$

The superscripts on these denote the axis of rotation. If you examine these you will notice a pattern that will make it very easy to remember these three transforms. A value of 1 always appears on the diagonal of the row/column for the axis of rotation. The other elements of that row and column are 0. The other two elements on the diagonal are always $\cos\theta$. The remaining two elements are always $\sin\theta$ with the lower left of those two always negative. Remembering that and the right-hand convention of rotations, you will never have to look any of this up again. Now how do we apply this?

For a general transform consisting of a rotation of θ_3 about the x_3 axis followed by rotation of θ_2 about the x_2' axis we would have

$$Q_{ij} = {}^{2}Q_{ik}\,{}^{3}Q_{kj} = \begin{bmatrix} \cos\theta_2 & 0 & \sin\theta_2 \\ 0 & 1 & 0 \\ -\sin\theta_2 & 0 & \cos\theta_2 \end{bmatrix} \begin{bmatrix} \cos\theta_3 & \sin\theta_3 & 0 \\ -\sin\theta_3 & \cos\theta_3 & 0 \\ 0 & 0 & 1 \end{bmatrix}$$

$$= \begin{bmatrix} \cos\theta_2\cos\theta_3 & \cos\theta_2\sin\theta_3 & \sin\theta_2 \\ -\sin\theta_3 & \cos\theta_3 & 0 \\ -\sin\theta_2\cos\theta_3 & -\sin\theta_2\sin\theta_3 & \cos\theta_2 \end{bmatrix}$$

Notice that in the summation convention the subscripts of the two rotation matrices are not in alphabetical order as we required earlier, but we formed the two matrices, ${}^{2}Q_{ij}$ and ${}^{3}Q_{ij}$, properly first, then changed the inner indices to dummy indices to indicate the matrix multiplication. While this is shown for illustration, this particular transform occurs frequently in analyses regarding boreholes.

Transforming vectors

The transform of a vector, $\mathbf{u} = u(x_i) = u_i$ to the new coordinate system, $\mathbf{u}' = u'(x_i') = u_i'$, is simple in direct notation.

$$\mathbf{u}' = Q\,\mathbf{u}$$

or

$$\mathbf{u}' = \mathbf{u}\,Q^{\mathrm{T}}$$

The order is important because matrix multiplication does not in general commute. In index notation it may be written any number of ways, each correct, but possibly confusing when actually calculating.

$$u_i' = u_j Q_{ij} = u_j Q_{ji} = Q_{ij} u_j$$

or even

$$u_i' = u_k Q_{ik} = u_k Q_{ki} = Q_{ik} u_k = Q_{ki} u_k$$

Remember, we may use any indices we choose but *the free index must always signify the row index of the original* $[Q]$ *matrix as we defined it above*. While this is mathematically a trivial point, it is one of the most frequent sources errors in student programming. So, whatever notation you choose, *be consistent in its use*.

EXAMPLE C.8 Coordinate Transform of a Vector

Suppose $u_i = (1, 1, 1)$ and our new coordinate system represents a rotation of $\pi/2$ (90°) counterclockwise about the x_3 axis so that our coordinate transform tensor in matrix form is

$$Q_{ij} = \begin{bmatrix} 0 & 1 & 0 \\ -1 & 0 & 0 \\ 0 & 0 & 1 \end{bmatrix}$$

then

$$u_i' = Q_{ij} u_j = \begin{bmatrix} 0 & 1 & 0 \\ -1 & 0 & 0 \\ 0 & 0 & 1 \end{bmatrix} \begin{Bmatrix} 1 \\ 1 \\ 1 \end{Bmatrix} = \begin{Bmatrix} 1 \\ -1 \\ 1 \end{Bmatrix}$$

Alternatively we could do it **u** as a row vector and Q^{T} as

$$Q_{ji} = \begin{bmatrix} 0 & -1 & 0 \\ 1 & 0 & 0 \\ 0 & 0 & 1 \end{bmatrix}$$

then

$$u_i' = u_j Q_{ji} = \begin{bmatrix} 1 & 1 & 1 \end{bmatrix} \begin{bmatrix} 0 & -1 & 0 \\ 1 & 0 & 0 \\ 0 & 0 & 1 \end{bmatrix} = \begin{bmatrix} 1 & -1 & 1 \end{bmatrix}$$

In the above example we assumed that a row vector and a column vector were equivalent for our transformation, but in non-orthogonal coordinates that is not necessarily the case.

Transforming tensors

The transformation of tensor components from one coordinate system to another is quite similar to that of vectors in that the transformation matrix, $[Q]$, is exactly the same. The difference is that the 2-order tensor has nine components represented as a 3×3 matrix, and requires two multiplications instead of one.

$$\mathbf{T}' = Q\ \mathbf{T}\ Q^{\mathrm{T}}$$

In index notation where $[Q] = Q_{ij}$ one possibility is

$$T_{ij}' = Q_{ip}\, T_{pq}\, Q_{jq}$$

EXAMPLE C.9 Tensor Transform

Assume the same transform matrix, $[Q]$ as in Section C.4.7 and a tensor

$$T_{ij} = \begin{bmatrix} 1 & 2 & 3 \\ 4 & 5 & 6 \\ 7 & 8 & 9 \end{bmatrix}$$

then the transform is

$$\begin{aligned} T'_{ij} &= \begin{bmatrix} 0 & 1 & 0 \\ -1 & 0 & 0 \\ 0 & 0 & 1 \end{bmatrix} \begin{bmatrix} 1 & 2 & 3 \\ 4 & 5 & 6 \\ 7 & 8 & 9 \end{bmatrix} \begin{bmatrix} 0 & -1 & 0 \\ 1 & 0 & 0 \\ 0 & 0 & 1 \end{bmatrix} \\ &= \begin{bmatrix} 0 & 1 & 0 \\ -1 & 0 & 0 \\ 0 & 0 & 1 \end{bmatrix} \begin{bmatrix} 2 & -1 & 3 \\ 5 & -4 & 6 \\ 8 & -7 & 9 \end{bmatrix} \\ &= \begin{bmatrix} 5 & -4 & 6 \\ -2 & 1 & -3 \\ 8 & -7 & 9 \end{bmatrix} \end{aligned}$$

where we started the matrix multiplication from the right. It makes no difference as to which matrix multiplication is done first as long as you do not commute the matrix sequence.

As a quick error check when transforming tensors manually, recall that the sum of the diagonal elements of the transformed matrix will be the same as the sum of the diagonal elements of the original matrix. Also, if the original matrix is symmetric, then the transformed matrix will also be symmetric. These checks are no guarantee against errors, but if either of these fail there is definitely an error.

C.5 Kinematics and kinetics—strain and stress

The two fundamental tensor quantities of the mechanics of deformable bodies are strain and stress. In general, strain is a measure of kinematics, kinematics meaning movement in space as a result of force or energy—displacement, translation, deformation. Stress on the other hand is a measure in kinetics, kinetics meaning the forces and energy that provide motion.

C.5.1 Deformation and strain—kinematics

All real materials are deformable. But it is perfectly appropriate in many cases to assume that certain objects behave as rigid bodies and do not deform, since in many cases we are not interested in deformation or the magnitude of deformation does not affect our observations or calculations. An example would be picking a casing string up off bottom in a well to reciprocate the pipe while cementing. When we first begin to pull on the pipe, it is stretching. The top is moving, but the casing shoe is not. Once we pull a certain amount, the entire string is moving. If we are trying to determine the maximum load required to reciprocate the pipe, then we are not interested in the load as the pipe is stretching before the entire string is moving. We are interested only in the load from gravity and friction when the entire string is moving. This is modeled as a rigid body motion and the deformation or stretch in the pipe has no significance in this context. A rigid body motion may be a *translation* and/or a *rotation in*

space. A body moves from one position to another without deformation. A rotary table rotates while drilling, and that is a rigid body motion for most applications. Certainly, there is some amount of deformation in the individual parts, but that is of no interest if we are interested in penetration rate as a function of rotary speed. If we are interested in bit speed as a function of rotary speed, however, we might consider the deformation of the drill pipe in torsion as a possible fluctuating variable. If we are interested in the burst pressure of a casing string, the burst value is based on a deformation of the casing.

Deformation by itself is not that meaningful. For instance, if a casing string is stuck, we pick up on it to try to free it, and we pull maybe 6 ft or 2 m through the rotary table. Is that significant? We cannot answer such an important question with only the amount of information given. If it is stuck at a depth of 10,000 ft, then a 6 ft or 2 m stretch is not very much. But, if the casing is stuck near the surface that deformation could be quite significant. So, what we need is a measure that gives us some idea of how significant the stretch is.

One way to measure deformation, then, is simply the stretch divided by the original length. That is a simple measure of strain and satisfactory at low values for uniaxial deformations. However, if we were to measure the wall thickness of the pipe very accurately, we also would find that, as the pipe stretched and got longer, the wall thickness decreased slightly. One simple definition of strain in three dimensions is

$$\boxed{\varepsilon_{ij} = \frac{1}{2}\left(u_{i,j} + u_{j,i}\right)} \tag{C.49}$$

where u_i is the deformation in one of the three axis directions. This definition of strain, called the *Cauchy infinitesimal strain*, is the measure most commonly used for small strains. Suppose, for our pipe example from above (with a "strain" measure $\Delta L/L = 0.0006$), the x_3 coordinate is vertical and downward in a weight-less environment (for simplicity), so that the strain from the 6 ft stretch is uniform along the entire length of the tube down to 10,000 ft, that is, $\mathrm{d}u/\mathrm{d}x_3$ is a constant all along the length of the pipe, then

$$\varepsilon_{33} = \frac{1}{2}\left(u_{3,3} + u_{3,3}\right) = \frac{1}{2}\left(\frac{\partial u_3}{\partial x_3} + \frac{\partial u_3}{\partial x_3}\right) = \frac{1}{2}\left(0.0006 + 0.0006\right) = 0.0006$$

This is fairly straightforward, but note that there are a total of nine strain components instead of one, and the others may not be zero. In fact, not all will be zero. Because, as we said, when we stretch the pipe in one direction, there is a change in the other dimensions as well. Those other changes may be insignificant or they may not. In addition to the strain definition given by Equation (C.49), the Cauchy infinitesimal strain, there are other definitions of strain. We save those for later. The Cauchy strain tensor may be written as a matrix:

$$\varepsilon_{ij} = \begin{bmatrix} \varepsilon_{11} & \varepsilon_{12} & \varepsilon_{13} \\ \varepsilon_{21} & \varepsilon_{22} & \varepsilon_{23} \\ \varepsilon_{31} & \varepsilon_{32} & \varepsilon_{33} \end{bmatrix} \tag{C.50}$$

Large deformations

We are not going to cover large deformations in this text, but we should mention a few things that are important. Most all of the engineering mechanics problems we solve are based on small deformations

and infinitesimal strains. The world gets a lot more complicated when we consider finite or large deformations and finite or large strains.

Strains within the elastic limit of metals like steel are very small, and we are quite safe in that respect. Where we get into trouble with even small strains is when the displacements become finite, so that even though the strains are very small, the geometry of the deformed body changes measurably.

In our area of interest this is most common in the bending of tubes in curved wellbores. Such a problem is classified as one with nonlinear geometry. The rule of thumb is that deflection of any structural member with a length to radius of gyration ratio of 10:1 or greater should be considered as one of nonlinear geometry. That means that most problems we address regarding lateral deflection of casing (or tubing or drill pipe) should be considered as geometrically nonlinear.

In the linear geometry of small deformations and infinitesimal strains we need only consider one coordinate system—the original reference coordinate system. Once we move to the next step up in complexity, finite deformations and infinitesimal strains, we must now include an additional coordinate system, the current or deformed coordinate system. This presents additional complexities as to how we define strain. If the reference coordinate system is designated the **X**-coordinate system and the deformed coordinate system is the **x**-coordinate system then we have two measures of the strain:

$$E_{ij} = \frac{1}{2}\left(u_{i,j} + u_{j,i} + u_{k,i}u_{k,j}\right) = \frac{1}{2}\left(\frac{\partial u_i}{\partial X_j} + \frac{\partial u_j}{\partial X_i} + \frac{\partial u_k}{\partial X_i}\frac{\partial u_k}{\partial X_j}\right)$$

and

$$e_{ij} = \frac{1}{2}\left(u_{i,j} + u_{j,i} - u_{k,i}u_{k,j}\right) = \frac{1}{2}\left(\frac{\partial u_i}{\partial x_j} + \frac{\partial u_j}{\partial x_i} - \frac{\partial u_k}{\partial x_i}\frac{\partial u_k}{\partial x_j}\right)$$

Very few textbooks deal with large deformations to any extent, and it sometimes becomes a matter of self study to piece together a workable knowledge of the topic. One place to begin is the book by Fung [52].

C.5.2 Stress—kinetics

Our early concept of stress was most likely that it is a "distributed load" as opposed to a "point load." That is all right for many simple engineering calculations, but it is quite misleading when we advance to more complicated problems. First of all, we need to recognize that, in the real world, there is no such thing as a point load. A point load is a mathematical convenience that exists only in theory and calculations. All real loads are distributed loads. Think about it this way; if we could apply a true point load of 100 lbf to the surface of a steel block, what would happen? If it is truly a point load, the contact area shrinks to zero, the pressure exerted by the load goes to infinity, and the steel block fails at the point of contact. Of course, this does not happen in the real world, because the contact area is not zero, so the load actually is distributed over some area, even though it may be very small. So, even though true point loads do not exist, we use them in our calculations for convenience. Now, back to the distributed load, is a distributed load that we typically measure in psi (lbf/in.^{2}) or Pa a stress? No, it is not. Just because it has the same units of stress does not make it a stress.

What is a distributed load then? Some call it a stress vector. This is an unfortunate bit of terminology that has become entrenched in elementary mechanics. If you want to use that term, you have plenty of company, but it can be confusing to call two totally different things stress. A distributed load is a vector, it has magnitude and direction, but stress is never a vector. The proper name for a distributed load is a *traction* or *traction vector*, and it is a directional load (force) distributed over some area of contact.

Something else worth noting is that you cannot apply a stress. You can apply only traction; stress is a result of the traction. But, most important, remember that stress itself is never a vector.

We have said that stress is a tensor. What is a tensor? That is a good question for which there is not a good answer. Or at least, there is no good answer that would ever satisfy an engineer. A tensor is a mathematical quantity that transforms according to certain rules (which were illustrated previously, but we lack space to explain here). Also, when we speak of a tensor, we typically are talking about a 2-order tensor, such as stress (or strain). There are other tensors of different orders as well.

The stress tensor for small displacements and strains is called the Cauchy stress tensor. In component form, σ_{ij}, it has nine components and is typically written as a 3×3 matrix.

$$\left[\sigma_{ij}\right] = \begin{bmatrix} \sigma_{11} & \sigma_{12} & \sigma_{13} \\ \sigma_{21} & \sigma_{22} & \sigma_{23} \\ \sigma_{31} & \sigma_{32} & \sigma_{33} \end{bmatrix}$$

In our applications it is real-valued and symmetric, $\sigma_{ij} = \sigma_{ji}$, such that $\sigma_{12} = \sigma_{21}, \sigma_{13} = \sigma_{31}, \sigma_{23} = \sigma_{32}$, thus reducing the number of different components to six.

Figure C.8 shows the sign convention of the components. All of the components shown are positive in value. For example, σ_{11} to the right is on the positive x_1 face of the block and is pointed in the positive x_1 direction, hence it is positive in sign. On the left side there is a component of σ_{11} pointing in the negative x_1 direction, but it is on the negative x_1 face of the block so it too is a positive component. The off-diagonal or shear components of the stress matrix follow a similar convention. The shear component, σ_{12}, is on the positive x_1 face and is pointed in the positive x_2 direction. On the negative face (not shown) σ_{12} would point downward in the negative x_2 direction and hence is also positive. The first subscript denotes the face and the second denotes the direction. Considering the diagonal components, $\sigma_{11}, \sigma_{22}, \sigma_{33}$, positive is tension, and negative is compression.

A very important formula that relates the stress tensor and a traction vector is known as Cauchy's formula[7] and is

$$\mathbf{t} = \hat{\mathbf{n}}\,\mathbf{T} \qquad \rightarrow \qquad t_i = n_j\,\sigma_{ij} \tag{C.51}$$

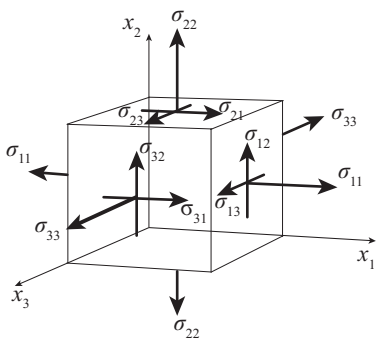

Figure C.8 Stress sign convention.

[7] A derivation of this important formula appears in every book on continuum mechanics. We will not take space to derive it here because we are not going to use it.

where $\mathbf{t}\,(t_i)$, $\hat{\mathbf{n}}\,(n_j)$, and $\mathbf{T}\,(\sigma_{ij})$ are a traction vector acting on a surface with a unit normal vector, and the stress at the point of contact, respectively. The surface need not be a physical surface, but can be an imaginary one drawn within a material body itself.

One final point before we move on. It is misleading to assume that we can always determine a uniaxial stress by dividing a uniaxial load by the cross-sectional area of the material body. This is true only for a prismatic bar, that is, one with a constant cross section, but it is not true near the ends of the bar, where the loads are applied. We cannot determine the axial stress in a tube under a thread cut into the tube by dividing the axial load by the cross-sectional area under the thread. Likewise, we cannot calculate the uniaxial stress in a coupling, connection, or upset in a tube in a similar fashion. Whenever the cross-sectional area of a tube changes, the stress field at the change and in the near vicinity of the change is more complicated than a single uniaxial component. In the case of a connection, additional complication comes from the addition of tangential, radial, and shear stress components in the connection itself. Saint-Venant's principle, however, effectively states that, at some distance away from the ends of a long tube (or point of change in diameter), the stress field becomes uniaxial, and there we are safe in dividing the cross-sectional area by the axial load to get the uniaxial stress component. For all practical purposes, that distance is relatively short in oilfield casing, but in a strict interpretation of the theory, it is valid only for tubes of infinite length.

Stress invariants

Some things about a stress tensor are invariant no matter how we may rotate our coordinate system. These are called *stress invariants*, and three are associated with a symmetric stress tensor:

$$I_1 = \sigma_{ii} \tag{C.52}$$

$$I_2 = \frac{1}{2}\left[(I_1)^2 - \sigma_{ij}\sigma_{ji}\right] \tag{C.53}$$

$$I_3 = \frac{1}{3}\left[3I_1I_2 - (I_1)^3 + \sigma_{ij}\sigma_{jk}\sigma_{ki}\right] \tag{C.54}$$

You might well ask, of what use are those three invariants? There are a number of times when those are useful, but one use that is of importance is to find the three principal stress components. We can expand the determinant in the following equation to get a cubic equation in terms of the above stress invariants, from which we can solve for the three principal stress components:

$$\det\left[\sigma_{ij} - \sigma\,\delta_{ij}\right] = 0$$

where σ is a principal stress component and δ_{ij} is the Kronecker delta. We will return to methods to determine the principal stress components and their directions after the next section.

Deviatoric stress

To understand a yield stress and plastic material behavior, it is necessary to learn about one other type of stress component and its invariants, the deviatoric stress. The stress tensor may be decomposed into a spherical (or hydrostatic) stress and a deviatoric stress. The spherical stress is that part of the stress tensor that is basically equal in all directions, that is, just like hydrostatic pressure. The deviatoric

stress is what is left after the spherical stress is taken out. One way of thinking about it is that the spherical stress might be said to be the part of the stress tensor trying to compress a material body (or pull it apart) uniformly in all directions and the deviatoric part of the stress is what attempts to distort its shape.

In terms of the three principal stress components, the spherical stress is

$$\sigma_{\text{spherical}} = \frac{\sigma_1 + \sigma_2 + \sigma_3}{3} \tag{C.55}$$

We could then calculate the three principal deviatoric stress components by subtracting the spherical stress from each principal stress component:

$$\begin{aligned}
\sigma_1' &= \sigma_1 - \frac{\sigma_1 + \sigma_2 + \sigma_3}{3} \\
\sigma_2' &= \sigma_2 - \frac{\sigma_1 + \sigma_2 + \sigma_3}{3} \\
\sigma_3' &= \sigma_3 - \frac{\sigma_1 + \sigma_2 + \sigma_3}{3}
\end{aligned} \tag{C.56}$$

If we do not have the principal stress components, we can calculate the deviatoric stress from the stress tensor components as

$$\sigma_{ij}' = \sigma_{ij} - \delta_{ij}\frac{\sigma_{kk}}{3} \tag{C.57}$$

There are several things to note here. The off-diagonal components of the deviatoric stress tensor are the same as the regular stress tensor. The only components that are changed are the ones on the diagonal. Each of those has subtracted from it one third of the sum of the diagonal components, which is $I_1/3$. Now, the deviatoric stress also has similar invariants:

$$I_1' = \sigma_{ii}' = 0$$

$$I_2' = \frac{1}{2}\left[\left(I_1'\right)^2 - \sigma_{ij}'\sigma_{ji}'\right] = -\frac{1}{2}\sigma_{ij}'\sigma_{ji}'$$

$$I_3' = \frac{1}{3}\left[3\left(I_1'\right)\left(I_2'\right) - \left(I_1'\right)^2 + \sigma_{ij}'\sigma_{jk}'\sigma_{ki}'\right] = \frac{1}{3}\sigma_{ij}'\sigma_{jk}'\sigma_{ki}'$$

But rather than use the same notation as the regular stress invariants, it is customary to define these deviatoric stress invariants as follows:

$$J_1 \equiv I_1' = 0 \tag{C.58}$$

$$J_2 \equiv -I_2' = \frac{1}{2}\sigma_{ij}'\sigma_{ji}' \tag{C.59}$$

$$J_3 \equiv I_3' = \frac{1}{3}\sigma_{ij}'\sigma_{jk}'\sigma_{ki}' \tag{C.60}$$

Note that we defined J_2 as $-I_2'$. There is a purpose to that in later applications, but use care in that some authors do not use this convention.

We show an example of the deviatoric stress when we discuss yield stress in the section on plasticity.

Principal stress components

As already stated, the stress tensor is invariant under any coordinate system and that only the component values vary. In Cartesian (and other orthogonal systems) it is possible to find a coordinate system in which all the off-diagonal components of the stress matrix disappear leaving only the diagonal components. These three diagonal values are called the *principal stress components* of a stress tensor. The principal stress components are the *eigenvalues* of the stress matrix and their direction vectors are the *eigenvectors*. Recall from your linear algebra that a system of linear equations $[A]\{x\} = \{C\}$ has a unique solution if and only if the coefficient matrix, $[A]$, is non-singular, i.e., $\det[A] \neq 0$. For a homogeneous system, $[A]\{x\} = \{0\}$, with a non-singular, $[A]$, the unique solution is $\{x\} = \{0\}$, and is called the trivial solution. If the homogeneous system is singular, $\det[A] = 0$, then there is no unique solution, and there may be an infinite number of them which will include the trivial solution.

In mathematical terms the eigenvalues, σ, make the matrix $[\sigma_{ij} - \delta_{ij}\sigma]$ singular, such that there are nontrivial solutions to the homogeneous set of equations, $[\sigma_{ij} - \delta_{ij}\sigma]\{x_j\} = \{0\}$. The nontrivial solutions, $\{x_j\}$ are the eigenvectors. Singular systems are of no interest to us except to solve for the eigenvalues and eigenvectors which are the principal stress components and their direction vectors. In matrix form we express the singular equation set as

$$\begin{bmatrix} \sigma_{11} - \sigma & \sigma_{12} & \sigma_{13} \\ \sigma_{21} & \sigma_{22} - \sigma & \sigma_{23} \\ \sigma_{31} & \sigma_{32} & \sigma_{33} - \sigma \end{bmatrix} \begin{Bmatrix} x_1 \\ x_2 \\ x_3 \end{Bmatrix} = \begin{Bmatrix} 0 \\ 0 \\ 0 \end{Bmatrix} \tag{C.61}$$

Here the eigenvalues are of a value that makes the stress matrix singular. Since one characteristic of a singular square matrix is that its determinant is zero, we solve for the eigenvalues (principal stress components) by setting the determinant of $\left[\sigma_{ij} - \sigma\delta_{ij}\right]$ equal to zero:

$$\det\left[\sigma_{ij} - \sigma\delta_{ij}\right] = 0 \tag{C.62}$$

or in matrix form as

$$\det\begin{bmatrix} \sigma_{11} - \sigma & \sigma_{12} & \sigma_{13} \\ \sigma_{21} & \sigma_{22} - \sigma & \sigma_{23} \\ \sigma_{31} & \sigma_{32} & \sigma_{33} - \sigma \end{bmatrix} = 0 \tag{C.63}$$

When we expand that determinant, we get a *characteristic equation* whose coefficients are the three stress invariants:

$$\sigma^3 - I_1\sigma^2 + I_2\sigma - I_3 = 0 \tag{C.64}$$

When the stress tensor is symmetric (always the case in our applications), that cubic equation has three real roots, which are the three principal stress components. Any cubic equation always has a closed form solution, meaning there is a formula we can use to find the three principal stress components.

General formula

The characteristic equation may be solved for the real roots, the principal stress components, as follows:

$$a = \frac{1}{9}\left(I_1^2 - 3\,I_2\right) \tag{C.65}$$

$$b = \frac{1}{54}\left(2I_1^3 - 9I_1I_2 + 27I_3\right) \tag{C.66}$$

1. *If* $a^3 + b^2 > 0$ then there are three real and unequal roots (principal stress components) and the equation may be solved by the trigonometric method as follows.

$$\phi = \cos^{-1}\left(\frac{a}{\sqrt{b^3}}\right) \tag{C.67}$$

$$\sigma_1 = -2\sqrt{a}\ \cos(\phi/3) - I_1/3 \tag{C.68}$$

$$\sigma_2 = -2\sqrt{a}\ \cos[(\phi + 2\pi)/3] - I_1/3 \tag{C.69}$$

$$\sigma_3 = -2\sqrt{a}\ \cos[(\phi - 2\pi)/3] - I_1/3 \tag{C.70}$$

2. *If* $a^3 + b^2 = 0$ then there are three real roots and at least two are equal. These roots may be solved with the following which involves complex arithmetic (the results are real valued, but the intermediate arithmetic will involve complex numbers).

$$A = \sqrt[3]{-b + \sqrt{b^2 + a^3}} \tag{C.71}$$

$$B = \sqrt[3]{b + \sqrt{b^2 + a^3}} \tag{C.72}$$

$$\sigma_1 = -(A + B) \tag{C.73}$$

$$\sigma_2 = \frac{A+B}{2} - \frac{A-B}{2}\sqrt{-3} \tag{C.74}$$

$$\sigma_3 = \frac{A+B}{2} + \frac{A-B}{2}\sqrt{-3} \tag{C.75}$$

3. *If* $a^3 + b^2 < 0$ then there is one real root and two conjugate complex roots, i.e., the tensor is not real valued and symmetric. We do not consider this case since our stress tensor is symmetric.

Polar coordinates

In tubes where $\sigma_{rz}, \sigma_{\theta z} = 0$.

$$\sigma_1 = \frac{\sigma_\theta + \sigma_z}{2} + \sqrt{\left(\frac{\sigma_\theta - \sigma_z}{2}\right)^2 + \sigma_{r\theta}^2} \tag{C.76}$$

$$\sigma_2 = \frac{\sigma_\theta + \sigma_z}{2} - \sqrt{\left(\frac{\sigma_\theta - \sigma_z}{2}\right)^2 + \sigma_{r\theta}^2} \tag{C.77}$$

$$\sigma_3 = \sigma_r \tag{C.78}$$

and in tubes where there is no torsion, i.e., $\sigma_{r\theta} = 0$, then

$$\sigma_1 = \sigma_\theta \tag{C.79}$$

$$\sigma_2 = \sigma_z \tag{C.80}$$

$$\sigma_3 = \sigma_r \tag{C.81}$$

Principal deviatoric stress components

The characteristic equation for the principal deviatoric stress is:

$$\left(\sigma'\right)^3 + J_2\sigma' + J_3 = 0 \tag{C.82}$$

This is similar to the characteristic equation for principal stress components except that J_1 is zero and does not appear.

General Formula

Similar to solving for roots of the cubic characteristic equation for principal stresses we set:

$$a = -J_2/3 \tag{C.83}$$

$$b = -J_3/2 \tag{C.84}$$

1. *If* $(J_3/2)^2 - (J_2/3)^3 < 0$ then

$$\phi = \cos^{-1}\left(\frac{B}{\sqrt{A^3}}\right) \tag{C.85}$$

$$\sigma_1' = 2\sqrt{a}\ \cos\left(\phi/3\right) \tag{C.86}$$

$$\sigma_2' = 2\sqrt{a}\ \cos\left[\left(\phi + 2\pi\right)/3\right] \tag{C.87}$$

$$\sigma_3' = 2\sqrt{a}\ \cos\left[\left(\phi - 2\pi\right)/3\right] \tag{C.88}$$

2. *If* $(J_3/2)^2 - (J_2/3)^3 = 0 \ \rightarrow\ J_2/J_3 = 3/2$ then

$$A = \sqrt[3]{-b + \sqrt{b^2 + a^3}} \tag{C.89}$$

$$B = \sqrt[3]{b + \sqrt{b^2 + a^3}} \tag{C.90}$$

$$\sigma_1 = A + B \tag{C.91}$$

$$\sigma_2 = -\frac{A+B}{2} + \frac{A-B}{2}\sqrt{-3} \tag{C.92}$$

$$\sigma_3 = -\frac{A+B}{2} - \frac{A-B}{2}\sqrt{-3} \tag{C.93}$$

3. *If* $(J_3/2)^2 - (J_2/3)^3 > 0$ then the stress tensor is not real valued and symmetric.

And as before, step 2 above involves complex arithmetic. There are any number of software programs available that will do these calculations, if you are not familiar with programming complex

variables. And there are other approaches that can avoid complex arithmetic altogether (see Allen and Haisler [53]), but are too long to go into here.

Principal stress directions

After solving for the principal stress components (or deviatoric principal stress components), we may also need the orientation of the components, the eigenvectors. To do this we plug an individual principal stress component into Equation (C.61) and solve for its eigenvector. If there are three different roots we will have to do this three times to solve for all three eigenvectors. While this is easy to say, it is not a simple as that, because each eigenvalue makes the coefficient matrix, $[\sigma_{ij} - \delta_{ij}\sigma]$ singular, and thus rendering an infinite number of solutions. But the important characteristic of these solutions is that the values are always in the same proportion to each other, which is all we need to define a vector and which we can easily make unit vectors using Equation (C.4). One way to do this is to set one of the solution components to unity and solve the set for the other two.

$$\begin{bmatrix} \sigma_{11} - \sigma_1 & \sigma_{12} & \sigma_{13} \\ \sigma_{21} & \sigma_{22} - \sigma_1 & \sigma_{23} \\ \sigma_{31} & \sigma_{32} & \sigma_{33} - \sigma_1 \end{bmatrix} \begin{Bmatrix} 1 \\ x_2 \\ x_3 \end{Bmatrix} = \begin{Bmatrix} 0 \\ 0 \\ 0 \end{Bmatrix} \tag{C.94}$$

We can then use two of those three equations to solve for the components, x_2, x_3. Traditionally we make the eigenvector a unit vector with Equation (C.5). And we repeat the process for each principal stress component.

Comments on stress

There are a number of ways we can use the stress invariants, I_1, I_2, I_3 and the deviatoric stress invariants, J_2, J_3 in applications. For example, if we calculate the principal stress components, σ, we do not have to solve another cubic equation for the principal deviatoric stress components because

$$\sigma' = \sigma - I_1/3 \tag{C.95}$$

Another way to get the principal deviatoric stress components without solving the characteristic equation is to calculate another stress quantity called the octahedral stress, τ_o.

$$\tau_0 = \sqrt{\frac{2}{3} J_2} \tag{C.96}$$

then

$$\phi = \cos^{-1}\left(\sqrt{2}\ \frac{J_3}{\tau_o^3}\right) \tag{C.97}$$

Then the principal deviatoric stress components are then

$$\sigma_1' = \sqrt{2}\ \tau_o \cos\left(\frac{\phi}{3} + \frac{4\pi}{3}\right) \tag{C.98}$$

$$\sigma_2' = \sqrt{2}\ \tau_o \cos\left(\frac{\phi}{3}\right) \tag{C.99}$$

$$\sigma_3' = \sqrt{2}\,\tau_o \cos\left(\frac{\phi}{3} + \frac{2\pi}{3}\right) \tag{C.100}$$

From these results we can back into the principal stress components with Equation (C.95)

$$\sigma = \sigma' + I_1/3 \tag{C.101}$$

This involves a few more steps, but avoids solving the cubic characteristic equation totally.

One last comment. The notion of principal stress components raises an interesting question. Since stress is independent of any coordinate system and may be represented mathematically as a symmetrical stress tensor that can always be resolved into three principal stress components in any coordinate system such that the "shear" components disappear, then is shear stress a physical reality or just a mathematical notation? Or posing it another way, if for any stress, we can orient our coordinate system such that the shear components disappear, is there actually such a physical entity that we can designate as shear stress or is it just a name for the off-diagonal components of a stress matrix? What I am driving at here is that shear components of stress are nothing more than the mathematical names for components of stress in particular directions and are not some separate kind of physical stress as much common usage tends to imply. The unfortunate use of separate variable names, σ and τ, for diagonal and off-diagonal components, respectively, of a stress matrix as if they are somehow a different type of stress, has contributed greatly to the misunderstanding. While the orientation of stress at some point in a material body or structure is obviously very important, it is that orientation with regard to a material body or structure that may be critical rather than some separate physical entity of the stress tensor. As one wise soul once stated it, "A material cannot 'feel' a shear component, only the principal components."

C.6 Constitutive relationships

Suppose we have a solid cube of some material that measures 1 meter on each edge, and it is lying on a flat surface. We know the weight of the cube. We apply a downward force of a known magnitude on top of that object. If we are asked, What is the force on the flat surface?, we have an easy problem. It is Newtons third law, and the answer is the force on the surface is the weight of the cube plus the force we applied to the top of the cube. If we approach it slightly differently and instead of measuring the force we apply on top we instead measure how much we actually compress that cube vertically, by say 0.2% of its original height (see Figure C.9). We now have a different problem in determining the resultant force on the flat surface.

We know that it is equal to the weight of the cube plus whatever force is necessary to compress the cube by 0.2%. In order to solve this problem we need to know something about the material the cube is made of, and more specifically how the material responds to a compressive load. Such a relationship is called a constitutive equation and in this case it is a simple one-dimensional version of Hookes law.

$$\sigma_z = E\frac{\mathrm{d}u}{\mathrm{d}z}$$

This simple relationship relates a load (stress), to a deformation gradient (strain), by means of a constant, Young's modulus, which is a property of the material. There are many constitutive relationships in every day use though we do not often think of them as such. Here are two one-dimensional examples.

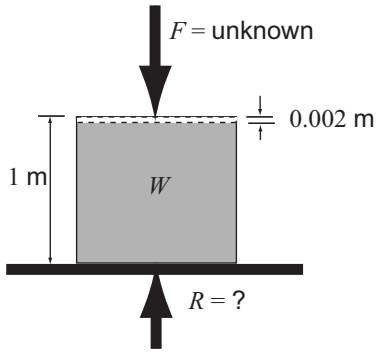

Figure C.9 Force, displacement, and reaction.

$$q = -k\frac{\mathrm{d}T}{\mathrm{d}x}$$

$$v = \frac{k}{\mu}\frac{\mathrm{d}p}{\mathrm{d}x}$$

The first is Fouriers law of heat conduction that relates heat flux to a temperature gradient by means of a material property, the conductivity. The second is Darcy flow that relates fluid flux to a pressure gradient with two material properties, permeability and viscosity.

There are many types of material behavior, for example, elastic, plastic, viscoelastic, viscoplastic. Elastic behavior could be subdivided into linear elastic, non-linear elastic, hyper-elastic, and viscoelastic. If one were to apply a load to a material and plot the load curve (load versus deformation) such as a stress-strain curve, one could not really understand much about a materials behavior. It is only when the load is removed that we can begin to understand its behavior. For example, look at the material load curve in Figure C.10a. What type of behavior is this? We might be tempted to say it is elastic-plastic since it looks like what we have often seen to illustrate how a metal behaves elastically up to a yield point and then becomes plastic beyond the yield point. But in truth, all we can say for this example without more information is that its behavior is non-linear.

Now let us reveal the unloading behavior on that same material, Figure C.10b. We see that it returns to the same point that we started. So when the load is removed it has no permanent deformation. It is by definition elastic.

The defining criteria for elastic behavior is that if a body is subjected to a load and the load is later removed it will return to its original state. But we notice something else about this material load curve.

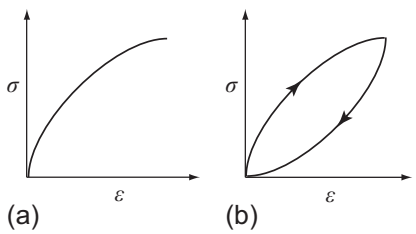

Figure C.10 Nonlinear behavior: (a) loading curve and (b) loading and unloading curves with a hysteresis loop.

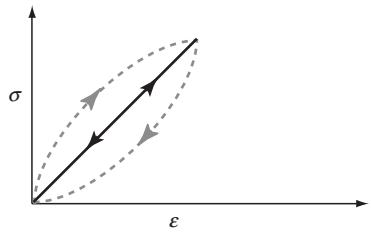

Figure C.11 Slow loading and unloading cycle. Linear elastic material?

It did not return by the same path with which it was loaded (a hysteresis loop). What could explain that? Time. It is a rate-dependent behavior, in other words it is viscoelastic. The shape of this load curve depends on the loading and unloading rate. The loading and unloading curve does not tell us the rate at which the load was applied or removed. For example, we could load the same material very slowly and remove the load also very slowly. We might get a loading and unloading curve that would look like the straight path in Figure C.11. If you were not aware of the time dependent curves you might assume that it is a linear elastic material. And it is, albeit at very slow rates of loading. Many materials that we might consider linear elastic are actually rate dependent materials. Porous formation rock in most wells is an example.

Appearances can be deceiving. We are not going to concern ourselves with rate dependent materials here, but the point is important, do not jump to conclusions that are not justified.

C.6.1 Elasticity

We said that an elastic material is one in which the material returns to its original state after an applied load is removed. A linear elastic material[8] is one whose loading path and unloading path are the same straight line. The constitutive behavior of a linear elastic material is modeled by Hooke's law, as mentioned before. It is called a *law*, but it is not a law of physics or nature. It is just a convenient relationship that models the behavior of certain materials within a very limited range of deformation. We might even say that we are very fortunate that it does, even though its range is quite small, because almost every structure or machine we come into contact with daily is designed using this constitutive relationship. Hooke's law written in three-dimensional tensor form is

$$\sigma_{ij} = C_{ijkl}\,\varepsilon_{kl} \tag{C.102}$$

If we were to write that out in matrix form, the stress and strain tensors would each contain 9 terms and the elastic modulus would contain 81 terms. All are symmetric (except in the presence of body moments—usually electro-magnetic). For an isotropic material, one whose material properties are the same in all directions, Equation (C.102) can be simplified considerably. We can use a contracted notation (called *Voigt notation*) and write the stress and strain in vector form and the elastic modulus as a 6×6 matrix:

[8] We should note that, when we refer to an elastic material, we are speaking to only a particular range of a particular material's behavior. Materials may exhibit different types of behavior in different load ranges.

$$\begin{Bmatrix} \sigma_{11} \\ \sigma_{22} \\ \sigma_{33} \\ \sigma_{23} \\ \sigma_{13} \\ \sigma_{12} \end{Bmatrix} = \frac{E}{(1+\nu)(1-2\nu)} \begin{bmatrix} 1-\nu & \nu & \nu & 0 & 0 & 0 \\ \nu & 1-\nu & \nu & 0 & 0 & 0 \\ \nu & \nu & 1-\nu & 0 & 0 & 0 \\ 0 & 0 & 0 & \frac{1-2\nu}{2} & 0 & 0 \\ 0 & 0 & 0 & 0 & \frac{1-2\nu}{2} & 0 \\ 0 & 0 & 0 & 0 & 0 & \frac{1-2\nu}{2} \end{bmatrix} \begin{Bmatrix} \varepsilon_{11} \\ \varepsilon_{22} \\ \varepsilon_{33} \\ \varepsilon_{23} \\ \varepsilon_{13} \\ \varepsilon_{12} \end{Bmatrix}$$

where we have now included Poisson's ratio, ν. This is a bit more complicated than the simple one-dimensional form, but often a number of simplifying assumptions, such as plane strain or plane stress, can be adopted to reduce it to two dimensions for a number of applications. We are not going to use this constitutive relationship, but merely show it so that you can see what it looks like.

C.6.2 Plasticity

We defined an elastic material as one in which, when an applied load is removed, the material goes back to its original state. A material is said to behave plastically when an applied load is removed and it does not go back to its original state. In other words, it has undergone some permanent deformation in the loading process. Plasticity is a complex topic and there are exceptions to just about everything, but we are concerned primarily with steel in casing here, so we are going to confine our discussion to that limited scope. Steel behaves more or less as a linear elastic material up to a point, called the *yield point*. When loaded beyond that point, its behavior is said to be plastic, but the elasticity has not disappeared, it is still exhibited when the loads are removed. Figure C.12a shows a load curve for elastic-plastic behavior of a test sample in uniaxial tension.

The loading in this curve is such that the sample is linear elastic up to its yield point, Y, then deforms plastically until the load is removed, at which time, it unloads elastically. The difference between the initial strain (zero here) and the final strain is the permanent deformation of the material in a plastic mode. It is of significance at this time to make mental note of this elastic unloading. When a metal, such as steel, is deformed plastically to a certain size or shape, it will always display some amount of elastic "rebound" or deformation when the load is removed. When coiled tubing is bent plastically onto a reel, a lot of elastic energy is stored on that reel, and if you were to release the end of the tube, you would witness an amount of elastic unloading you might not otherwise imagine.

In many cases, the behavior of the metal at the yield point is somewhat more complicated than that in Figure C.12a. Sometimes the elastic behavior becomes nonlinear before the actual yield stress is reached, and that point is called the *proportional limit*. Ductile steels often exhibit this behavior and

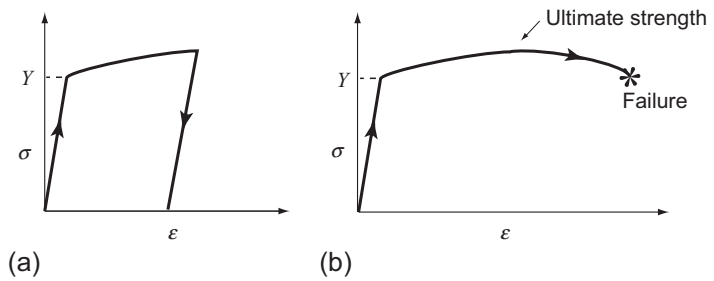

Figure C.12 Uniaxial test, elastic-plastic behavior of steel: (a) loading and unloading and (b) loading to failure.

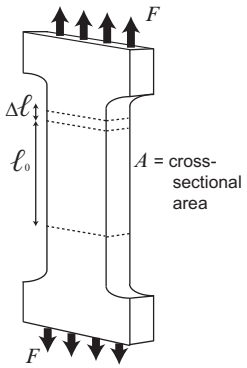

Figure C.13 A typical steel test sample.

materials like cast iron seldom exhibit a distinctive yield point. There are other cases where the stress actually decreases slightly after the yield stress is reached; hence, there is an upper yield stress and a lower yield stress. This is typical of some steel alloys. In many cases, the yield point is indistinct on a stress-strain chart, so the yield point is defined as some arbitrary point offset from the proportional limit by a specified amount of strain (API does this). We do not concern ourselves with those details, but rather assume that, as long as we do not exceed the published yield stress for the casing material, its behavior is linear and elastic up to that point.

What happens if we continue to load the test sample? Figure C.12b shows the uniaxial loading of a sample all the way to failure. At this point, we need to explain a few things. First of all, in this figure, we are looking at a uniaxial load curve. It is plotted as stress versus strain, which we already discussed but we need to understand a bit more. We must emphasize one thing about this figure, and that is in reference to the point labeled as the *ultimate strength*. That is *not a material property*, it is a property of the sample geometry and the test type. It is the point at which the test sample begins to experience significant deformation of its initial geometry in tension. You will observe nothing comparable in a compressive test. While it is not a material property, it is a property in a tube in tension and does have some use—it appears in the current ISO formulas for ductile rupture.

The samples of material used in these tests are relatively small compared to the massive machine in which they are tested. The samples usually look like the one shown in Figure C.13, sometimes colloquially referred to as a *dog bone* sample. The sample is placed in a large machine that pulls it in tension, as the load and stretch are recorded.

The ends are larger than the test portion, so the gripping effects of the machine do not affect the stress in the narrower test portion. The cross-sectional area of the test portion is measured accurately before the test begins. The stretch in the sample is measured by the machine as a displacement, and the load is measured with a pressure transducer, These are recorded on a chart similar to that shown in Figure C.12b. The machine itself is massive in relation to the size of the sample, but nevertheless it has some amount of elastic stretch while pulling tension, as does the wider portion of the sample, so usually an electronic strain gauge is attached to the sample in the thinner area to measure the stretch. The results may be plotted as load versus stretch, which is the raw data from the machine, but that is not of much use unless one is testing a particular structural element or part as opposed to a sample of material like we are considering here. We use the following relationships to get the values for a stress-strain plot:

$$\sigma = \frac{F}{A} \qquad , \qquad e = \frac{\ell - \ell_o}{\ell_o} = \frac{\Delta\ell}{\ell_o}$$

where the stress is the machine-measured load divided by the cross-sectional area of the sample, and the strain is the stretch in the sample section divided by the original length of the sample section.This strain measure is known as the *engineering strain* or the *nominal strain*. These are plotted as in Figure C.12b. Similar tests may be run in compression or cyclical loading.

In looking at Figure C.12b, we see that the material deforms elastically up to the yield point, then begins its plastic deformation, in which a lot of strain takes place with little increase in stress, yet the stress continues to increase up to a point, where it begins to decline until the sample fails. The part of the curve where the stress continues to increase in the plastic range is called *strain hardening*. But what about the part of the curve where it starts to decline. Is this "strain softening" then? This part of the curve can be misleading because of the way we calculated the stress and strain. Our definition holds only for very small deformations. If we actually measured the cross-sectional area of the sample as it stretches, we would find that the area is getting smaller. So, what we have plotted on the vertical axis is not the true stress, but rather the load divided by the original cross-sectional area of the sample, which is commonly referred to as the *engineering stress* or *nominal stress*. And, if we looked at the failed sample, we would see that the most significant decrease in cross-sectional area occurred in only a small part of the length of the sample and the cross-sectional area at the point of failure is possibly less than half the original area. If we were to plot the true stress, we would find that, in many cases, it continues to increase right up to the point of failure; and for some materials, the increase is rather drastic just before failure. We might also note that our measure of strain, e above, is no longer valid either, since the reduction in cross section (called *necking-down*) is quite localized, so that the uniaxial strain in the region of failure is apparently a lot greater than elsewhere along the sample length. The true strain is not $\Delta\ell/\ell_0$ but rather $\mathrm{d}\ell/\ell$, which leads to a *true strain* or *logarithmic strain* measure:

$$\varepsilon = \ln\left(\frac{\ell}{\ell_0}\right) = \ln\left(1 + \frac{\ell - \ell_o}{\ell_0}\right) \tag{C.103}$$

We might also note that the appearance of the sample itself began to change just before failure, in that visible bands of discoloration or surface texture began to appear on the surface of the sample where the area reduction was most pronounced, giving the appearance of some change in the metal itself. These are called *Lüder's bands*, and that is exactly what they indicate. Two things are of importance here. If we tested several samples of the same material, all would fail at different values. That is the nature of materials; we cannot predict the actual load value at which the material fails. We can determine a range of values, but we cannot predict the exact value for any particular sample. If all of the samples were cut in precisely the same way under the same conditions and we could perform rigorous inspections on them, we could get pretty close, but the point is we could not predict the exact failure strength. The second point is this. We said that, if we used a measure of true stress and strain, then we could say that the material never got "weaker" before it failed, and that is often true. However, the sample itself got weaker before it failed, and that is important. In terms of total load, it failed at a load less than the maximum load it was subjected to in the test. If it were a structural member or casing, that would be important. So, while the true stress is important, the load on a structure does not know to reduce itself when the cross-sectional area of a structural member is reduced by plastic deformation. In casing, the apparent stress at the maximum load is called the *ultimate strength*. It is very important to remember that *the ultimate strength is not a material property; it is a property of the sample in uniaxial tension*. Likewise it is a property of a right, prismatic tube like casing. We never want to exceed that maximum load value, no matter how we measure stress or strain.

Now, let us go back to the issue of strain hardening mentioned earlier. Strain hardening in a metal, for the most part, is caused by defects in its crystalline structure, called *dislocations*. All steels have some amount of this type of defect. But *defect* might be a severe term to use in an oilfield context, so perhaps a dislocation should be thought of as an imperfection in the crystalline lattice of a metal. A dislocation is a missing bond at a lattice junction. When a metal is stressed beyond its initial yield point, these dislocations begin to move or migrate. No material physically moves (at least, on an observable scale), but where a bond is missing at a lattice junction, a bond forms, and the missing bond is transferred to the next junction, sort of like the game of musical chairs, where there is one fewer chair than the number of people present. When one person gets up, another takes his or her place. What causes the strain-hardening effect is that as these dislocations begin to accumulate at grain boundaries, there is no other place for them to go, and they begin to resist the deformation of the material. There are other contributing factors, but that is the main one. While most structural steels are strain hardening materials to some degree, some are not. Some brittle steels exhibit very little strain hardening, and failure strength is very close to the yield strength. Some soft steels behave more like what is known as an *elastic-perfectly-plastic material*, in that once yield stress is reached, the material continues to elongate to failure with no increase in stress required. The steel used for coiled tubing closely approximates this latter behavior. Also some strain-softening materials are such that, once yield is reached, continued elongation requires less and less stress.

For a strain-hardening type of steel, if we stop loading a sample before we reach the maximum and remove the load, we know that it unloads elastically as shown in Figure C.12a. What happens if we apply a load again? The answer is that it goes right back up the same path as the unloading path. Furthermore, it does not yield until it reaches the value at which the load was removed before. It may vary with a bit of hysteresis and become slightly nonlinear before yielding again, but after yield, it continues on the same path, as if the unloading never took place. The result, though, is that, on re-loading, it actually yields at a higher value than the original yield value at the start of the test. We could repeat this process any number of times, and each time, we increase the yield value until we reach the top of the curve. So, for a strain-hardening material, we can increase the yield strength by cold working it. Or can we? It all depends on what our application is. Let us look at compression.

If we were to test an identical sample in compression, it would be a mirror image (and upside down) of the one we just showed. And we could compress it to the same point and increase its yield strength in compression just as we did in tension. The question is, then, if we work our sample in tension first then test it in compression, will the yield point in compression be increased just like the one in tension? The answer is no, it would not. In fact, if we increased the yield in tension, then the yield in compression actually would be less than the initial yield. This is called the *Bauschinger effect*. In other words, we cannot have it both ways. Is the amount of reduction in compression equal to the amount of increase in tension? Again the answer is no, the reduction in the compressive yield stress generally is less than the increase in tensile yield stress. We can show this with an ellipse, which we call a *yield surface* in two dimensions for now. We are not plotting strain now but principal stress components in two directions. Up is tension, down is compression. We do not concern ourselves with the transverse component for now. We know that, when we increase the tensile load beyond the yield surface, we increase the yield stress in that direction. One way to think about it would be that the yield surface gets larger. In other words, it expands by the amount we go beyond the initial yield stress, as shown in Figure C.14a. This is known as *isotropic hardening*; the yield surface grows uniformly in all directions.

This means that we also increased the yield strength in compression by the same amount; and we already said that does not happen. Isotropic hardening does not happen, but it is useful in a few

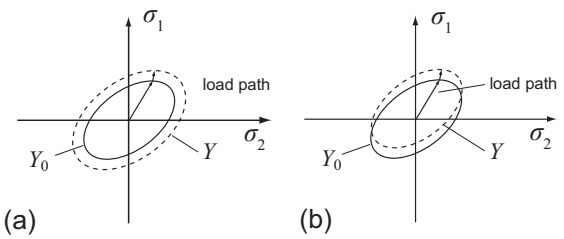

Figure C.14 Strain hardening: (a) isotropic hardening and (b) kinematic hardening.

applications when repeated loading does not cause yielding in different directions. Another possibility might be that the yield surface actually moves as shown in Figure C.14b. Here, the yield surface stays the same size, but it moves as the stress exceeds the yield stress. This model is called *kinematic hardening*

For kinematic hardening in the simple uniaxial case we are discussing, the reduction in yield stress in compression is of exactly the same magnitude as the increase in the tensile yield stress. We already said that does not happen either. What actually takes place is something in between. The yield surface grows, but it also moves. This is called *combined hardening*. And what all this amounts to is this: When working in the plastic regime, we have to keep up with the growth of the yield surface and keep track of where it is. This usually is done with something called *internal state variables*, which are defined by a flow rule to account for the translation of the yield surface and a growth law that accounts for its expansion or hardening. In the simple incremental theory of plasticity, one internal state variable is a second-order tensor that tracks the translation of the yield surface, and the other is a scalar that keeps track of the size of the yield surface. Take into account also that we are not talking about the three-dimensional space we live in, but rather a nine-dimensional stress space. Another point of complication is that, when the stress is on the yield surface (it cannot go past it), the most common plasticity theory requires that plastic strain can take place only in a direction normal to this nine-dimensional hyper-surface. In some plasticity theories, the yield surface is not regular and smooth, like the ellipse we illustrated, and loading paths also may change shape in addition to size and location. Additionally, in larger deformations such as the necking discussed in the uniaxial test previously mentioned, localized rotations within the material begin to occur. These rotations must be tracked, too. At some point, we begin to kid ourselves as to what we know how to do in this strange space. So we are going to drop back a notch or two for now and think about how to stay out of it. Obviously, if we stay inside that yield surface with our stress and do not bump into it, we should stay out of serious trouble. That is the topic of the next section, but let us look at one more scenario first.

One of the most difficult aspects of materials that have been loaded beyond the initial yield point is predicting their properties at a later time, because the loading beyond initial yield makes it a history-dependent material. You cannot predict its future behavior unless you know the history of its loading. For example, suppose we take two identical samples, both with an initial yield strength of 80,000 psi. We subject them both to a uniaxial load of 90,000 psi. In other words, we work hardened them in tension to increase the yield strength (in tension). If we test these two samples, one in tension and one in compression. We find that the tensile sample does indeed yield at 90,000 psi as we expect. But the sample we test in compression does not yield at 90,000 psi, nor even the original 80,000 psi. We find that in compression it yields at say 77,000 psi. This is a case of combined hardening (somewhere between

isotropic and kinematic) which is typical in many metals. By cold working this metal we have moved the yield surface (in stress space) and we have also changed the size.

That example was for a simple uniaxial test. If we had subjected a large sheet of steel to the same uniaxial stress then cut samples from it in various directions, the results would have been even more alarming. The point is that, when a metal is loaded beyond the initial yield point, we cannot possibly predict its behavior, unless we know the history of the loading. And, that not only means the exact loads but also the exact sequence. One oilfield example would be a well subject to large temperature fluctuations from a shut-in state to a flowing state, and back to shut-in. If, in compression from thermal expansion, suppose a portion of the production casing string yields. Take into account that, during the heated stage, the packer fluid also is heated and expands, causing a high internal pressure in the casing. Assume that the casing actually yields at the inner wall with a combined axial compressive stress, a radial compressive stress, and a tangential tensile stress, but because of strain hardening, it does not actually fail in this particular case. Then, the well is shut in for a few days and cools to where that portion of the casing is now in tension and even has a net differential pressure from the outside. Now, the state of stress at the inner wall is axial tension, radial compression, and tangential compression. What is the yield strength of the casing under that load? All we can honestly say is that it differs from what it was before the yield occurred and is probably less, but without knowing the exact history of the loading, we cannot predict the yield in the current state. We may be able to get close enough for "oilfield use" with some appropriate assumptions—or we may not.

The history dependence and the changes in yield are the primary reasons we try to stay out of the plastic regime in most engineering design. We can do fairly well with one-time loading, but when the loading is cyclical and even varies in magnitude and direction with the cycles, it is extremely difficult to get any meaningful results. James F. Bell, who did significant experimental work with large deformation plasticity at Johns Hopkins University, once made the comment that, if you subject a material to varying loads beyond the initial yield point, it may become impossible to even find the yield point experimentally. What that translates to is that incremental plasticity theory works much better as a mathematical concept than it does with real materials.

C.6.3 Yield criteria

A yield criterion is a hypothesis that defines the limit of elastic behavior under any possible state of stress. We call that limit a *yield surface*, although it is a surface in a mathematical sense only. There have been a number of yield criteria over the years, but two have proven quite successful, especially for metals such as steel. The oldest of these is that of Tresca, dating back to 1864. It is a piecewise linear model that in cross section is a hexagon. It found a lot of use before computers became available for computations and still enjoys some use because it lends itself to a number of closed-form solutions that otherwise require a computer and numerical solutions. It does not model real metals very well except in some special cases and is considered outmoded in today's technology.

The other yield criterion that is most used and best models metals like steel is the one attributed to Richard von Mises in 1913, who developed it from theoretical concepts. The idea behind it is that pure spherical stress (hydrostatic pressure) has no effect on the yielding of a material because it acts in direct opposition (compression or tension) to the bonding forces of the atomic structure of a material which are very strong. Assuming a material body is isotropic, a spherical stress causes a material body to compact or expand uniformly, thus preserving its initial shape (but not size). If we subtract the spherical stress from the stress tensor we are left with the deviatoric stress. The deviatoric portion of the stress tensor tends to distort the shape of the material body. It is this distortional or deviatoric

portion of the stress state that causes the material to yield, by shearing action. This concept was first hypothesized by James Clerc Maxwell in 1858 but never published except in his private letters. Later M. T. Huber, in 1905, published a similar hypothesis, but it went unnoticed because it was published in a journal that was not widely read outside his home country (Poland). About 11 years after von Mises's publication, Heinrich Hencky did some work with plasticity, especially in the range beyond the yield point, and his name became associated with it too. So, variously, you will hear it referred to as the von Mises hypothesis, the Maxwell-Mises hypothesis, the Huber-Mises hypothesis, or the Hencky-Mises hypothesis, and so on. That should give fair due to all those who contributed their skills to the idea, but we call it the *von Mises yield criterion* for the sake of brevity. Plotted in principal stress space, the von Mises yield criterion is a circular cylinder, which makes more physical sense than the Tresca criterion. Its biggest disadvantage is that it does not lend itself to closed-form solutions of elastic-plastic problems.

The von Mises yield criterion may be stated mathematically as

$$Y \geq \sqrt{3J_2} \tag{C.104}$$

where Y is the uniaxial yield strength of the material and J_2 is the second deviatoric stress invariant, defined in Equation (C.59). The yield condition is

$$Y > \sqrt{3J_2} \quad \rightarrow \quad \text{no yield} \tag{C.105}$$

$$Y = \sqrt{3J_2} \quad \rightarrow \quad \text{yield} \tag{C.106}$$

$$Y < \sqrt{3J_2} \quad \rightarrow \quad \text{not possible} \tag{C.107}$$

Now, comes a bit of semantics. What is $\sqrt{3J_2}$? It has the units of stress, traction, pressure—is it any of those things? No, it is not. It is a scalar quantity with the same units as stress, traction, or pressure. It is definitely not a stress. You might well ask, then, how can we compare a scalar to the uniaxial yield stress and get anything meaningful? The truth is we are not comparing it to the uniaxial stress component, Y, we are comparing it to the value of $\sqrt{3J_2}$ in which $\sigma_{11} = Y$ and all other stress components are zero. We, in fact, are comparing it to another scalar. In continuum mechanics, $\sqrt{3J_2}$ may be written in several different forms and it is seldom referred to by any particular name in most continuum mechanics textbooks. Properly, $\sqrt{3J_2}$ is *distortional energy density* or *deviatoric energy density*, a scalar value. The distortional energy density is commonly called the *von Mises equivalent stress* or something similar in many contexts. And that is okay as long as you understand what it actually is.

Now we must consider another serious misconception. In the above equations we stated that the distortion energy density cannot exceed the uniaxial yield stress value of a metal (Equation (C.107)). In this case the value of Y is the *current yield stress* and not necessarily the initial yield value. When the loading exceeds the yield stress, the yield surface expands and moves in principal stress space as in the examples shown in Figure C.14.

In our applications we are only concerned with the initial yield value which we take as our design limit in most cases. If we calculate $\sqrt{3J_2}$, and its value exceeds that of the initial yield stress what does that mean? It means that the stress resulting from that particular loading exceeds the yield strength of the material, and that is all we can draw from our calculations. It does not tell us by how much the yield has been exceeded, because all of our calculations (in this textbook) are based on linear elasticity and are not valid beyond the initial yield stress. So any value of $\sqrt{3J_2}$ that we calculate with linear elasticity

and exceeds the yield stress of the material is purely fictitious. Do we then refer to it as the "fictitious distortional energy density" or perhaps the "fictitious von Mises equivalent stress?"

Since I do not mind being labeled an eccentric, and I refer to it as a *yield measure* which is about as apt a description as I can come up with.[9] And I use the symbol, Ψ (Psi), to denote this yield measure. If this violates your sensitivities, then feel free to use whatever you like as long as I have made the point in your mind that if this value exceeds the initial yield stress value, then it is purely fictitious (unless you have calculated it with a valid elastic-plastic constitutive model). So, we define a *yield measure*, Ψ:

$$\Psi \equiv \sqrt{3J_2} = \left\{ \frac{1}{2} \left[(\sigma_1 - \sigma_2)^2 + (\sigma_2 - \sigma_3)^2 + (\sigma_3 - \sigma_1)^2 \right] \right\}^{\frac{1}{2}} \tag{C.108}$$

where Ψ is our yield measure and σ_1, σ_2, σ_3 are the three principal stress components, assuming the material is linear elastic. We also state that $Y \equiv Y_0$, in other words Y is the initial yield strength, and we do not concern ourselves with changes in the yield strength caused by work hardening. The yield condition is

$$Y > \Psi \quad \rightarrow \quad \text{no yield} \tag{C.109}$$

$$Y \leq \Psi \quad \rightarrow \quad \text{yield} \tag{C.110}$$

This may seem a lot like nitpicking. It is.

The best way to comprehend all this is to see a picture of it. Figure C.15 shows a plot of the von Mises yield surface plotted in *principal stress space*, which has only three coordinate axes.

The von Mises yield surface is a cylinder in this space.[10] The central axis of the surface is along the line, $\sigma_1 = \sigma_2 = \sigma_3$. In theory, the ends do not terminate, but we can assume that it extends as far

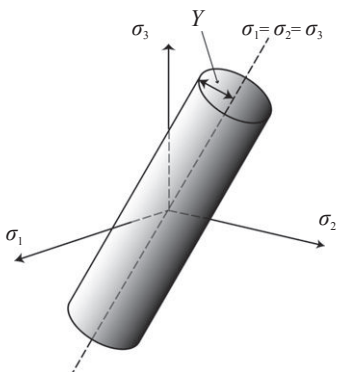

Figure C.15 The von Mises yield surface plotted in principal stress space.

[9] My apologies to readers of the first edition and training manuals where I used a different name for this. Over time I have used at least three different names seeking something appropriate. Mathematically it is a distance measure or metric in principal stress space. I refuse to call it anything with "stress" in the name because it is not a stress.

[10] The intercept of this cylinder with the σ_1-σ_2 plane is a two-dimensional ellipse as already seen in Figure C.14 and will appear later in Figure C.18.

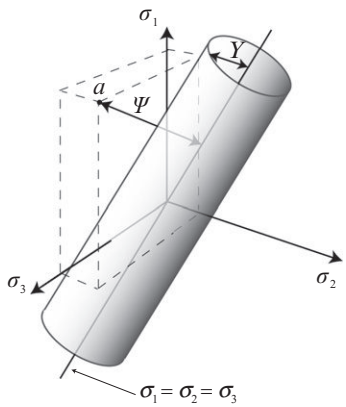

Figure C.16 Example of load that is beyond the boundaries of the von Mises yield surface.

as any load we could practically imagine. (Be careful to not confuse this cylinder with a section of pipe.) The meaning is that any combination of principal stress components that plots on the inside of this cylindrical yield surface does not cause yield and anything on the surface or outside does cause yield. The radius of the cylinder is the uniaxial yield stress of the material. As discussed in the previous section, this yield surface grows and its axis moves about as various combinations of stress exceed its initial boundaries. As it grows and moves, it may no longer retain its shape as a cylinder and may even develop corners. Most plasticity theory demands that the outside of the surface remain convex though. But, as we said, our primary interest is not what happens outside this yield surface but that we keep our casing stress inside it. Another thing that should be apparent with this surface is that the central axis is a spherical stress. You can see that, no matter the magnitude of the spherical stress, it always plots within the cylindrical yield surface, it makes no difference whether it is 1000 psi or 10^6 psi. Spherical stress (compression or tension) cannot cause yield in materials that can be modeled by the von Mises yield criterion.

Figure C.16 shows a case where we calculate a load on casing using elastic assumptions, and we plot that point in principal stress space. You can see that it is outside the yield surface (meaning that the material will yield), and our yield measure is the distance from the central axis to that point. This gives some physical meaning to our yield measure. So the yield measure, Ψ, or $\sqrt{3J_2}$, is actually a *distance measure* in the principal stress space. A distance measure (sometimes called a *metric*) is not a vector but a scalar. It is always positive. You can see that Y is also a distance measure in this space, and although it has the same value of, say, σ_{11} at the yield point in a uniaxial stress-strain test, it is not the same thing. Maybe that does not justify my nitpicking, but at least you can see the point.

As mentioned before, we can write the von Mises yield criterion in several forms, such as Equation (C.108), which is in terms of principal stress components. If the principal stress components correspond to the cylindrical coordinate axes (and they do in absence of torsion) we can write it in terms of the coordinate axes components:

$$\Psi = \left\{ \frac{1}{2} \left[(\sigma_\theta - \sigma_r)^2 + (\sigma_r - \sigma_z)^2 + (\sigma_z - \sigma_\theta)^2 \right] \right\}^{\frac{1}{2}} \tag{C.111}$$

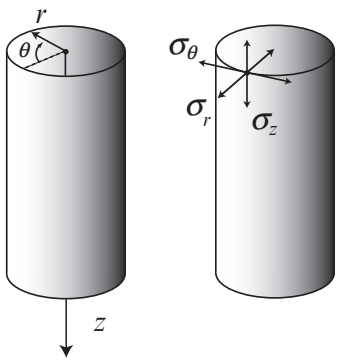

Figure C.17 Principal stress components in cylindrical coordinates.

If the principal stress components do not correspond with the coordinate axes, as when torsion is present, then we have a choice. We can resolve the stress into principal stress components and use Equation (C.108) or we use the expanded version of the von Mises criterion when the axial components of stress are not the principal stress components:

$$\begin{aligned}\Psi &= \left\{\tfrac{1}{2}\left[(\sigma_\theta-\sigma_r)^2+(\sigma_r-\sigma_z)^2+(\sigma_z-\sigma_\theta)^2\right]\right.\\ &\quad\left.+3\left(\sigma_{r\theta}^2+\sigma_{rz}^2+\sigma_{\theta z}^2\right)\right\}^{\frac{1}{2}}\end{aligned} \tag{C.112}$$

In this case, we normally consider only the shear stress from torsion, $\sigma_{r\theta}$ and the other two components of shear are assumed to be zero. If we prefer to get the principal stress components and use the principal stress formula, then

$$\begin{aligned}\sigma_1 &= \frac{\sigma_\theta+\sigma_r}{2}+\sqrt{\left(\frac{\sigma_\theta-\sigma_r}{2}\right)+\sigma_{r\theta}^2}\\ \sigma_2 &= \frac{\sigma_\theta+\sigma_r}{2}-\sqrt{\left(\frac{\sigma_\theta-\sigma_r}{2}\right)+\sigma_{r\theta}^2}\\ \sigma_3 &= \sigma_r\end{aligned} \tag{C.113}$$

When we work with principal stress components, it is immaterial how they are numbered, but the custom is that the largest value is σ_1 and the smallest is σ_3. There are a number of other ways to show the von Mises criterion in equation form. Usually, it is shown in a form that makes sense as to how it relates to deviatoric stress, octahedral stress, principal stress, and the like. One note of caution: Whenever doing manual calculations with the von Mises yield criterion, no matter which formula you use, be careful with the signs, so that you do not run amok. Tension is positive; compression is negative.

Now that we have seen the von Mises yield criteria in equation form and in a graph, let us examine how it applies to casing design. First of all, we hear terms like *biaxial casing design* and *triaxial casing design*. Those terms refer to the coordinate axes and the state in which the principal stress components

are aligned with those coordinate axes. And, in terms of casing, the coordinate axes usually are circular cylindrical coordinates as in Figure C.17. So biaxial casing design refers to two principal stresses aligned with two coordinate axes. The two principal stresses referred to are the axial stress component and the tangential stress component. In a biaxial sense, the radial stress component is ignored. Triaxial design refers to all three. If there is a nonzero shear stress component, as in rotational torsion, then neither of those terms apply as the principal stress components are not aligned with the coordinate axes. Although it is not technically correct, some refer to any three-dimensional stress state as *triaxial*, whether the principal stresses are aligned with the coordinate (or pipe) axes or not, and that is okay as long as we understand the meaning.

Earlier, we employed an ellipse in a two-dimensional chart to correct for the combination of tension and collapse pressure. Essentially, that was a biaxial approach, and that chart is another way to visualize the von Mises yield criterion. If the principal stress components are the tangential, radial, and axial stress components, that is, no shear components, then we can use Equation (C.111) to derive the equation for the ellipse. On the yield surface, $\Psi = Y$, the yield measure is equal to the yield stress:

$$Y = \left\{ \frac{1}{2} \left[(\sigma_\theta - \sigma_r)^2 + (\sigma_r - \sigma_z)^2 + (\sigma_z - \sigma_\theta)^2 \right] \right\}^{\frac{1}{2}}$$

$$Y^2 = \frac{1}{2} \left[(\sigma_\theta - \sigma_r)^2 + (\sigma_r - \sigma_z)^2 + (\sigma_z - \sigma_\theta)^2 \right]$$

$$Y^2 = (\sigma_\theta - \sigma_r)^2 - (\sigma_\theta - \sigma_r)(\sigma_z - \sigma_r) + (\sigma_z - \sigma_r)^2$$

With a bit of algebra, we have gotten the von Mises yield surface into an elliptic equation of the form $r^2 = x^2 - xy + y^2$. This is a quadratic equation we can solve as

$$x = \frac{y}{2} \pm \sqrt{r^2 - \frac{3y^4}{4}}$$

which we can put in a more useful dimensionless form:

$$\frac{x}{r} = \frac{y}{2r} \pm \sqrt{1 - \frac{3y^2}{4r^2}}$$

We can write this in terms of the principal stress components:

$$\frac{\sigma_z - \sigma_r}{Y} = \frac{\sigma_\theta - \sigma_r}{2Y} \pm \sqrt{1 - \frac{3(\sigma_\theta - \sigma_r)^2}{4Y^2}} \tag{C.114}$$

or, equivalently,

$$\frac{\sigma_\theta - \sigma_r}{Y} = \frac{\sigma_z - \sigma_r}{2Y} \pm \sqrt{1 - \frac{3(\sigma_z - \sigma_r)^2}{4Y^2}} \tag{C.115}$$

We can plot either of those as in Figure C.18, which is exactly what we used in Chapter 6.

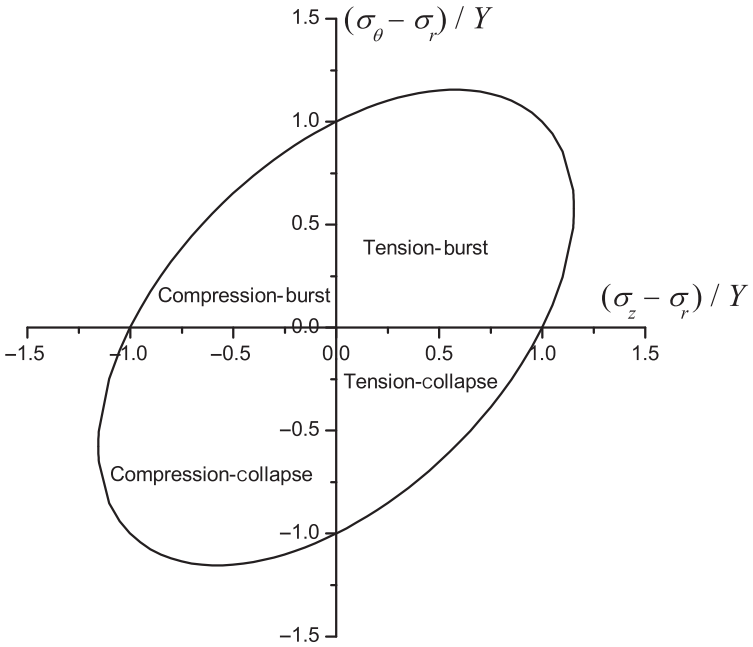

Figure C.18 The von Mises yield criterion in two dimensions.

So far we have not accomplished much. We have taken a three-dimensional surface and plotted it in two dimensions. Since the radial stress is the negative value of the pressure on the wall of the tube, we can substitute that into the equations. Then, if we know the pressure and one other component, we can find the value of the third at the yield surface. However, this is no easier than calculating it, but it does provide a useful way of illustrating an elastic stress state in relation to the yield surface. The basis of so-called biaxial casing design is that we ignore the radial stress, which usually is small compared to the other two components, and we have the following equivalent equations:

$$\boxed{\frac{\sigma_z}{Y} = \frac{\sigma_\theta}{2Y} \pm \sqrt{1 - \frac{3(\sigma_\theta)^2}{4Y^2}}} \tag{C.116}$$

or

$$\boxed{\frac{\sigma_\theta}{Y} = \frac{\sigma_z}{2Y} \pm \sqrt{1 - \frac{3(\sigma_z)^2}{4Y^2}}} \tag{C.117}$$

Those are the biaxial design formulas (we need only one), then we could plot them and the plot would be exactly as before, except we assume the radial stress or pressure at the wall is zero. One always should

remember that the underlying assumption of biaxial casing design is that the radial stress component is relatively small compared to the tangential and axial stress components, and that assumption is not always true.

Before leaving this section, it might be worth illustrating the von Misses yield criterion with an example to show how the hydrostatic pressure (or spherical stress) has no effect on yield.

EXAMPLE C.10 Hydrostatic Pressure Effect on Yield

Suppose a block of steel in the shape of a cube has a yield strength of 40,000 psi. It is loaded three-dimensionally in tension such that the three principal stress components are $\sigma_1 = 80,000$ psi, $\sigma_2 = 50,000$ psi, and $\sigma_3 = 50,000$ psi.

Each of those components is greater than the yield strength of the steel. Will it yield? We calculate the deviatoric stresses to see the hydrostatic pressure effects:

$$\sigma'_1 = 80{,}000 - \frac{80{,}000 + 50{,}000 + 50{,}000}{3} = 20{,}000$$

$$\sigma'_2 = 50{,}000 - \frac{80{,}000 + 50{,}000 + 50{,}000}{3} = -10{,}000$$

$$\sigma'_3 = 50{,}000 - \frac{80{,}000 + 50{,}000 + 50{,}000}{3} = -10{,}000$$

Then we calculate

$$J_2 = \frac{1}{2}\left[(\sigma'_1)^2 + (\sigma'_2)^2 + (\sigma'_3)^2\right]$$

$$= \frac{1}{2}\left[(20{,}000)^2 + (-10{,}000)^2 + (-10{,}000)^2\right]$$

$$= 300 \times 10^6$$

Then, we substitute into the yield criterion to calculate the yield measure:

$$\Psi = \sqrt{3J_2}$$

$$\Psi = \sqrt{3\left(300 \times 10^6\right)}$$

$$\Psi = 30{,}000 \text{ psi}$$

And, we check the yield condition:

$$Y > \Psi \ ?$$

$$40{,}000 > 30{,}000 \quad \rightarrow \quad \text{no yield}$$

For this particular example we did not have to even make the calculations, because we could see that two of the components were 50,000 psi and the third was greater than that, so the hydrostatic stress is

50,000 psi. We subtract that value from 80,000 psi and it leaves us with the equivalent of 30,000 psi in one direction.

In order to better understand the behavior of casing in the plastic regime, we might look at an example of the elastic-plastic behavior at the inner wall of a 7 in, 23 lb/ft tube with an 80,000 psi yield strength. This is not an example of actual API casing, but a tube of the same dimensions with a common strain hardening uniaxial behavior in tension.

EXAMPLE C.11 Elastic-Plastic Behavior of a 7 in. OD Tube

In this example analysis, we will use a 7 in. OD, 6.366 in. ID tube with a yield strength of 80,000 psi. A uniaxial tensile test for a sample of this steel is given in Figure C.19. This data is a piecewise linear plot, which is common for an analysis of this type.

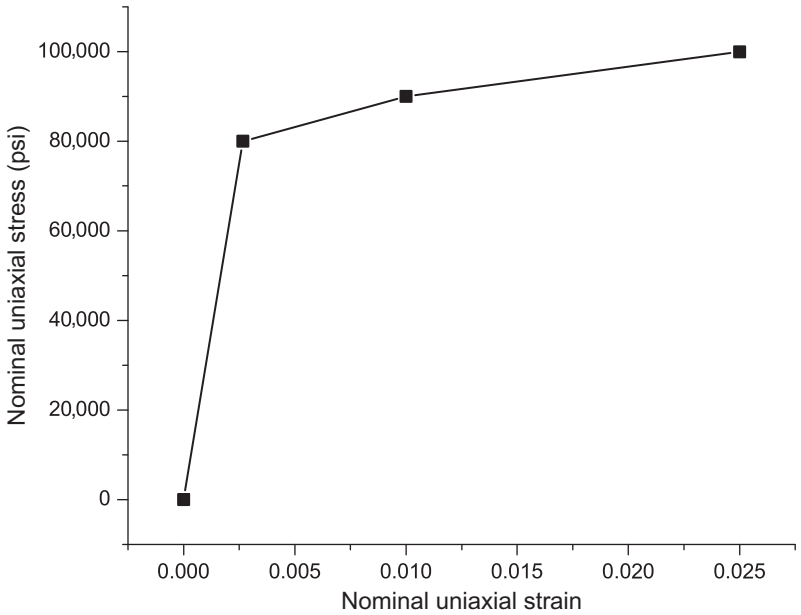

Figure C.19 Uniaxial test data for example material.

We will assume no initial axial stress, and load the tube with increasing internal pressure with no external pressure.

The analysis is done with a special purpose finite element program for nonlinear material behavior. Nonlinear geometry is not considered as the strains are less that 2.5%. Three cases are analyzed, (1) free ends (at least one open), (2) both ends capped (at least one end free), and (3) both ends fixed (capped or not capped has no effect). The results are plotted in Figure C.20.

You will note from the figure that the free end model yields at an internal pressure of about 7250 psi, the fixed end model at about 7900 psi, and the capped end model at about 8050 psi. In the first case the axial stress remains at zero, hence the lower yield pressure. In the latter two cases we have an increase in axial tension caused by "ballooning" in the fixed end case, and end forces from pressure in the capped end case. Recall from the two-dimensional ellipse plot of the von Mises yield criterion that tension increases the burst (internal yield) limit whereas it decreases the collapse resistance.

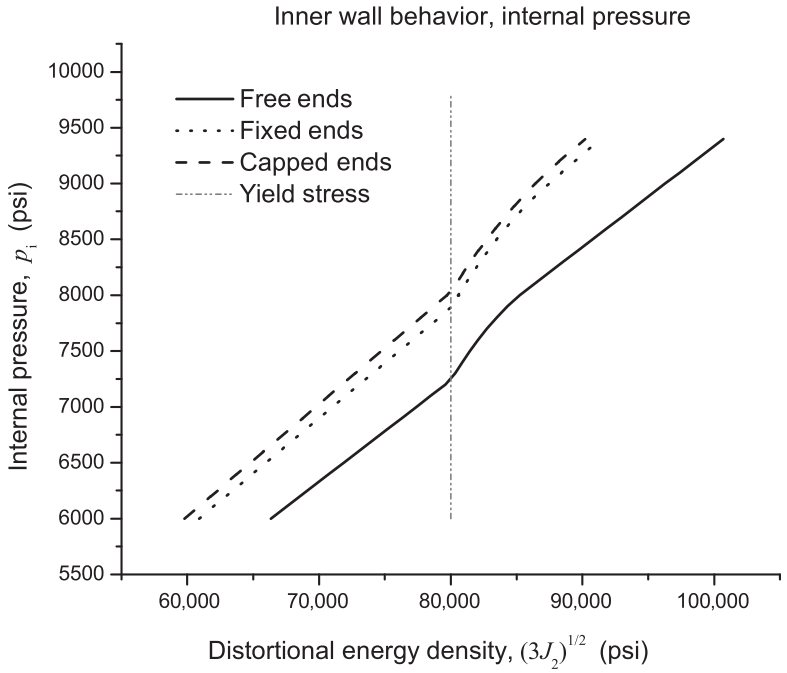

Figure C.20 Internal pressure loading effects on inner wall of 7 in. OD tube.

Another point that should be emphasized is this: once the distortional energy density, $\sqrt{3J_2}$, reaches the yield point, 80,000 psi in this example, the plot becomes nonlinear. The Lamé equations are perfectly valid up to this point and would duplicate exactly the curves from the finite element analysis. Had we employed them beyond that point they would have continued as straight lines with exactly the same slope as before and would not be valid at all. This is why I am adamant about the nomenclature regarding a "yield measure," Ψ, when doing manual calculations using the Lamé equations, because the results are purely fictitious if elastic equations are used beyond the yield point, and they often are when we use them as a check on yielding with combined loads. Another example similar to the above is shown if Chapter 6, Figure 6.3, where we show the simultaneous behavior at both the inner and outer walls of a fixed end model, as well as the error of the elastic equations and Ψ beyond the yield point.

At this point I add a caution. The von Mises yield criterion has no basis in physics, it is what we call *phenomenological*, in that it describes what is observed rather than any underlying principles of physics. The hypothesis has been tested many times for over a century and found to be valid for a number of metals. For many years most experiments showed variations, and the variations were almost always attributed to anisotropy in the samples. Even the famous experiment of Taylor and Quinney [54] which in the eyes of many verified the criterion once and for all, showed some small but disturbing variations also attributed to anisotropy. Over 40 years later Bell [55] revisited their experiment and noted that they had plotted their results as nominal stress versus logarithmic strain. He recalculated their results

using nominal stress versus nominal strain and found "precise agreement" of the Taylor and Quinney experiment with the von Mises criterion.

Before you go away overly enthralled with it, we should consider a quotation from Bernard Budianski [56] of Harvard University, one of the world's foremost solid mechanics experts, "No one really believes Mises' theory is really right. It might be good enough, but it is not really right."

C.7 Natural laws

Many so-called "laws" have appeared in science and engineering over the centuries, but most are merely relationships that are convenient and approximate. There are some naturally occurring laws, however, that are foundational in their nature that we refer to as *natural laws* or sometimes as *laws of physics*. These are the true laws of nature and the foundation on which natural sciences are based. Man did not invent them nor can they be derived from more fundamental axioms. They just are! And always have been as far as we know! Humans eventually discovered them and formulated them into mathematical expressions which are the foundations of science. If we cannot derive them, how do we know they are true? We don't! However, throughout the history of the universe as we know it, man has never seen any evidence that they have ever been violated. Mathematically that is not a proof, but it is overwhelmingly the nearest thing to it that we can imagine.

The natural laws we speak of are called *conservation laws* in that some particular quantity is conserved. The quantity may or may not be some physical quantity like mass for instance, but rather a mathematical quantity like energy.[11] These conservation laws are generally expressed as mathematical equations, and they are reversible as mathematically formulated. But there is another law that is somewhat different in that it is not an equality equation but an inequality from which no quantity can actually be calculated. Yet it constrains all events in our universe by stating that none of these conservation laws is actually reversible in the real universe even though they are formulated as such. While there are conservation laws that apply on a sub-atomic scale we only concern ourselves with the macroscopic scale:

- Conservation of mass
- Conservation of momentum
- Conservation of energy
- Entropy production

C.7.1 Conservation of mass

Those of my generation were taught this law from early on stated as, "Matter can neither be created nor destroyed." Later we learned that it is not true because energy and matter are equivalent, at least on a quantum scale. That said, however, on our macroscopic scale it is fundamental. In our applications where we consider the mass of a body a constant, it is almost trivial

$$\dot{m} = 0 \qquad \rightarrow \qquad \frac{\mathrm{d}m}{\mathrm{d}t} = 0 \tag{C.118}$$

[11] Mass and energy are equivalent in modern physics, as in $E = mc^2$.

In fluid mechanics, conservation of mass is expressed more elaborately and called a continuity equation which we will not need in our work.

C.7.2 Conservation of momentum

There are two types of momentum, *linear momentum* that is concerned with straight-line motion and will be central to our focus, and *angular momentum* which is concerned with rotational motion. Both are vector quantities, the first being a polar vector and the second, an axial vector. For material bodies with uniform density, we may express them, respectively, as

$$\mathbf{p} = m\,\dot{\mathbf{u}} \quad \rightarrow \quad p_i = m\,\dot{u}_i \tag{C.119}$$

and

$$\mathbf{h} = m\,\mathbf{r} \times \dot{\mathbf{u}} \quad \rightarrow \quad h_i = m\,\epsilon_{ijk} r_j \dot{u}_k \tag{C.120}$$

Newton's second law as expressed by Euler says that the change of rate of linear momentum is equal to the applied force (or moment in the case of angular momentum which we will not be using):

$$\mathbf{F} = \dot{\mathbf{p}} = m\,\ddot{\mathbf{u}} + \dot{m}\,\dot{\mathbf{u}} \quad \rightarrow \quad F_i = m\,\ddot{u}_i + \dot{m}\dot{u} \tag{C.121}$$

As we already stated in the previous section that we will not consider cases where mass changes with time, so $\dot{m} = 0$, and we may express conservation of linear momentum as:

$$\boxed{\mathbf{F} = \dot{\mathbf{p}} = m\,\ddot{\mathbf{u}} \quad \rightarrow \quad F_i = m\,\ddot{u}_i} \tag{C.122}$$

where the force, $\mathbf{F}$ is assumed to be the summation of forces, ΣF.

Without going into any details of derivation, we may also express conservation of linear momentum in terms of stress as

$$\boxed{\nabla \cdot \mathbf{T} + \rho\,\mathbf{b} = \rho\,\ddot{\mathbf{u}} \quad \rightarrow \quad \sigma_{ji,j} + \rho\,b_i = \rho\,\ddot{u}_i} \tag{C.123}$$

where the second term is the body force vector (gravity in our case). Though we skipped over angular momentum it does have a consequence in our considerations of the stress tensor in that, in the absence of electro-magnetic body forces, the Cauchy stress tensor is symmetric:

$$\boxed{\mathbf{T} = \mathbf{T}^{\mathrm{T}} \quad \rightarrow \quad \sigma_{ij} = \sigma_{ji}} \tag{C.124}$$

Newton's laws of motion

Newton's laws of motion are not natural laws but are a special case subset of the law of conservation of momentum. They are:

- First law: Objects in motion (or at rest) stay in that motion (or at rest) unless acted upon by some force.

$$\ddot{\mathbf{u}} = \mathbf{0} \tag{C.125}$$

- Second law: Force on a body is equal to the rate of change of momentum (inertia).

$$\mathbf{F} = \dot{\mathbf{p}} = \dot{m}\dot{u} + m\ddot{\mathbf{u}} \tag{C.126}$$

- Third law: Every reaction has an equal and opposite reaction (equilibrium).

$$\sum \mathbf{F} = \mathbf{0} \tag{C.127}$$

The first law is more or less a statement of condition in absence of forces. In statics we employ the third law for equilibrium. In dynamics where mass is constant we generally combine the second and third laws as

$$\sum \mathbf{F} = m\ddot{\mathbf{u}} \tag{C.128}$$

by which D'Alembert became famous for performing a simple algebraic feat as $\sum \mathbf{F} - m\ddot{\mathbf{u}} = \mathbf{0}$.

C.7.3 Conservation of energy

We cannot know the amount of energy present in a system, but what we can know and measure is the change of energy in a system. So the conservation of energy law that we use is one that balances the changes in total energy, not the total energy itself. There are any number of ways to express this law, but we quantify energy in four forms, internal energy, E, kinetic energy, K, heat energy, Q, and mechanical energy (work), W. The energy balance is thus stated as the change in internal energy plus the change in kinetic energy is equal to the heat added plus the work done on the system:

$$\mathrm{d}E + \mathrm{d}K = \mathrm{d}Q + \mathrm{d}W \tag{C.129}$$

or in terms of rate of change[12]

$$\frac{\mathrm{d}E}{\mathrm{d}t} + \frac{\mathrm{d}K}{\mathrm{d}t} = \frac{\mathrm{d}Q}{\mathrm{d}t} + \frac{\mathrm{d}W}{\mathrm{d}t} \tag{C.130}$$

That is a global form of the law. We will not go into the long derivation of the local component form, but give the result here

$$\rho\dot{e} = \sigma_{ij}\dot{\varepsilon}_{ij} + \rho\, r - q_{i,i} \tag{C.131}$$

where $\dot{e}$ is the rate of change of internal energy, $\dot{\varepsilon}_{ij}$ is the strain rate, r is the rate of generation of internal energy, and $q_{i,i}$ is the gradient of heat flux into the system.

In the above form you can see that the conservation of energy is coupled with the conservation of linear momentum through the mechanical energy term, $\sigma_{ij}\dot{\varepsilon}_{ij}$. This creates considerable difficulty in thermal stress analyses because the heat flow depends on the stress-strain rate, but the stress depends on the heat changes. This is often referred to as two-way coupling. For most engineering applications the stress-strain term is considered small and negligible and can be omitted so that the changes in heat and stress can be calculated incrementally in time. This coupling is often called one-way coupling. These will not concern us here, but it is an important point to understand—thermal and mechanical effects are interrelated.

C.7.4 The second law

The second law (of thermodynamics) is not something we find much use for in mechanics since it cannot be used to calculate anything. It is actually a constraint on what is physically possible, and does have

[12] In solid mechanics we may use the simple time derivative as $\mathrm{d}/\mathrm{d}t$ whereas in fluid mechanics we must use the total derivative (or co-moving derivative), $\mathrm{D}/\mathrm{D}t$, which gives the rate of change of a fluid at a particular location as well as the rate of change in the material itself as it moves past that location.

application in formulating some material constitutive equations. In its global form, the total internal entropy, S_i, is defined as

$$\rho \, \mathrm{d}S_\mathrm{i} \equiv \rho \, \mathrm{d}s - \frac{\mathrm{d}q}{T} \geq 0 \tag{C.132}$$

where s is entropy, q is heat flux, T is temperature, and ρ is material density. Stated here in local coordinate form with time dependence, it is

$$\rho \, \frac{\mathrm{d}S}{\mathrm{d}t} = \rho \, \frac{\mathrm{d}s}{\mathrm{d}t} - \left(\frac{q_i}{T}\right)_{,i} - \rho \, r \geq 0 \tag{C.133}$$

In this form the second law is often called the Claus-Duhem inequality. While the law says that the rate of entropy production is either zero or positive the reality is that it is never zero. The importance is that while all the other conservation laws are mathematically reversible the second law tells us that in the real world they are not.

Our macroscopic version of entropy may seem unrelated to the idea of entropy as discussed by physicists, but it is not. There seems to be a prevalent misconception about entropy production in that it has something to do with randomness, and that is a false notion. I suspect it comes from the popular illustration in many elementary physics texts that show a two-chambered box with an opening between the two chambers. Two particles are placed in one chamber and on inspection after some lengthy time interval it is found that there is one particle in each chamber. This has nothing to do with going from orderliness to randomness, it is merely a matter of probabilities. You could perform the same experiment with two dense metal billiard-sized balls in a weight-less environment, and the results would be quite different—they would both be in the same chamber and touching each other. The assumption in the first case is that there is no physical attraction between the particles, and each has a 50% probability of being in either chamber. The probability of each being in separate chambers is about 67%. But the metal balls have a gravitational attraction to each other, and though small, it will eventually pull them together so the probability in that case is 100% that they will both be in the same chamber.

C.8 Field problems

The notion of a field problem stems from the presence of a material body interior domain and its boundary. While various entities will vary within that domain they all obey the definitions and laws we have covered. If we consider a linear elastic mechanical field in a solid (no thermal effects), we have the following equations:

1. Conservation of mass, $\dot{m} = 0$, 1 equation
2. Conservation of linear momentum, $\sigma_{ji,j} + \rho \, b_i = \rho \, \ddot{u}_i$, 3 equations
3. Conservation of angular momentum, $\sigma_{ij} = \sigma_{ji}$, 1 equation
4. Definition of small strain, $\varepsilon_{ij} = 1/2 \, (u_{i,j} + u_{j,i})$, 9 equations
5. Elastic constitutive equation, $\sigma_{ij} = C_{ijkl} \, \varepsilon_{kl}$, 9 equations

We have 23 equations, how may unknowns?

- u_i, 3
- σ_{ij}, 9
- ε_{ij}, 9
- ρ, 1
- b_i, 3

We have 25 unknowns and 23 equations, so we have to eliminate some unknowns (or find more equations). Number 1 does not apply here so we have only 22 equations. We can specify ρ, leaving us with 24 unknowns. We can apply number 3 to make σ_{ij} symmetric so that we now have 18 unknowns and 21 equations. But when we apply number 4, we find that ε_{ij} is also symmetric which reduces the number of equations in number 5 to 6. Now we have 12 unknowns left (u_i, σ_{ij}, and b_i) and 9 equations. We can then specify the body forces, b_i, and we are left with 9 unknowns and 9 equations.

This is an outline of the formulation of a simple linear elastic field problem. Perhaps the best way to understand it is with examples. There are two very important field problems in tubular mechanics that lend themselves to frequent use: tube elongation and simple tube bending. Those we will now illustrate with examples and add a corollary to the second one.

EXAMPLE C.12 Tube Elongation

The elongation (stretch) of a tube is one of the basic field problems in mechanics of tubes. It is easily derived, and an understanding of the derivation is important, because the results may be expressed in many useful forms for a variety of applications. We begin with a vertically suspended tube (or uniaxial bar) as shown in Figure C.21.

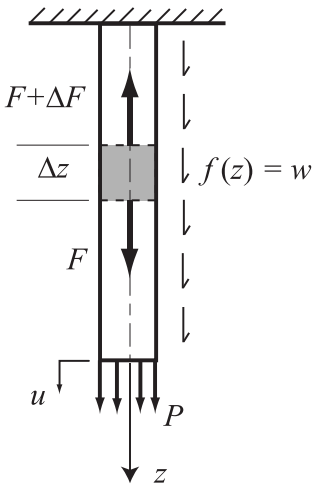

Figure C.21 Vertical tube (or uniaxial bar).

Kinetic Equation (Equilibrium)

$$\frac{\mathrm{d}F}{\mathrm{d}z} + f(z) = 0 \tag{C.134}$$

This is derived from a balance of forces in Figure C.21 above as follows:

$$-(F + \Delta F) + F + \int_z^{z+\Delta z} f(z)\ \mathrm{d}z = 0 \tag{C.135}$$

Divide Equation (C.135) by Δz

$$-\frac{\Delta F}{\Delta z}+\frac{1}{\Delta z}\int_{z}^{z+\Delta z} f\left(z\right)\,\mathrm{d}z=0$$

and take the limit as $\Delta z \to 0$

$$\lim_{\Delta z\to 0}\left(-\frac{\Delta F}{\Delta z}+\frac{1}{\Delta z}\int_{z}^{z+\Delta z} f\left(z\right)\,\mathrm{d}z\right)=\frac{\mathrm{d}F}{\mathrm{d}z}+f\left(z\right)=0 \tag{C.136}$$

Kinematic Equation (Strain)

$$\varepsilon=\frac{\mathrm{d}u}{\mathrm{d}z} \tag{C.137}$$

Constitutive Equation (One-Dimensional)

$$\sigma=E\varepsilon \tag{C.138}$$

Field Equation

Then for a uniaxial tube or bar, $F=A\,\sigma$ and which we substitute into the kinetic equation, (C.136) to get

$$\frac{\mathrm{d}}{\mathrm{d}z}\left(A\sigma\right)+f\left(z\right)=0 \tag{C.139}$$

and substituting the constitutive Equation (C.138) gives

$$\frac{\mathrm{d}}{\mathrm{d}z}\left(AE\,\varepsilon\right)+f\left(z\right)=0 \tag{C.140}$$

and finally substituting the kinematic Equation (C.137) gives the *general governing differential equation* for a uniaxial bar or tube:

$$\boxed{\frac{\mathrm{d}}{\mathrm{d}z}\left(AE\frac{\mathrm{d}u}{\mathrm{d}z}\right)+f\left(z\right)=0} \tag{C.141}$$

Boundary Value Problem

The general governing differential equation has no unique solution. To obtain solutions for specific applications we must now apply some boundary conditions. A one-dimensional equation such as this one has two boundaries, one at each end. For most applications we assume the cross section is prismatic, i.e., the cross-sectional area, A , is constant and Young's modulus, E , is also a constant. For a vertical bar or tube the forcing function, $f(z)$, is attributable solely to the *gravitational force per unit length* and is a constant, $w=g\,\rho_{\ell}$. In this case the differential equation simplifies to:

$$AE\frac{\mathrm{d}^2u}{\mathrm{d}z^2}+w=0 \tag{C.142}$$

Integrate once:

$$AE\int\frac{\mathrm{d}^2u}{\mathrm{d}z^2}\,\mathrm{d}z+\int w\,\mathrm{d}z=AE\frac{\mathrm{d}u}{\mathrm{d}z}+wz+C_1=0$$

at the boundary, $z = L$, $AE\,\mathrm{d}u/\mathrm{d}z = P$ (the end load) and the integration constant

$$C_1 = -(P + wL)$$

Integrate once more:

$$AE\int \frac{\mathrm{d}u}{\mathrm{d}z}\,\mathrm{d}z + \int [w - (P + w\,L)]\,\mathrm{d}z = AEu + \frac{w\,z^2}{2} - (P + w\,L)\,z + C_2 = 0$$

At the boundary where $z = 0$ the displacement $u = 0$ and by inspection we can see that the integration constant, $C_2 = 0$.

Displacement (Stretch)

The displacement at any point, $0 \le z \le L$, then is given by

$$\boxed{u = \frac{1}{AE}\left[(P + w\,L)\,z - w\,\frac{z^2}{2}\right]} \tag{C.143}$$

For the entire tube where $z = L$ the total displacement is:

$$\boxed{u = \frac{1}{AE}\left[P\,L + \frac{w}{2}\,L^2\right]} \tag{C.144}$$

or for a specified displacement the required load is:

$$\boxed{P = \frac{AE\,u}{L} - \frac{w\,L}{2}} \tag{C.145}$$

Incremental Displacement

An incremental displacement from a change in load is:

$$\boxed{\Delta u = \frac{\Delta P L}{AE}} \tag{C.146}$$

Incremental Load

Incremental load required for a given incremental stretch:

$$\boxed{\Delta P = \frac{AE\,\Delta u}{L}} \tag{C.147}$$

Free Pipe

This equation can also be rearranged to give the length of free pipe when measuring an incremental displacement and incremental load:

$$\boxed{L = \frac{AE\,\Delta u}{\Delta P}} \tag{C.148}$$

Note: this equation is only marginally reliable for determining the free point of stuck pipe (especially in open hole) because of borehole friction and lack of precision in a typical weight indicator.

Composite Bar or Tube

If the bar are tube is composed of more than one size (still prismatic in each size) then we can expand the previous formulas.

$$\boxed{\Delta u = \frac{\Delta P}{E} \sum_{i=1}^{n} \frac{L_i}{A_i}} \tag{C.149}$$

and

$$\boxed{\Delta P = \Delta u\, E \left(\sum_{i=1}^{n} \frac{L_i}{A_i} \right)^{-1}} \tag{C.150}$$

A note of caution: Be aware that uniaxial formulas are for continuous tubes and are not valid near connections or the ends. The stress field near connections and ends are not the same as the pipe body and there is no formula that is valid there. As an example, the composite formula above is commonly used for long bars of, say two different diameters, milled from a single piece of stock. There is no connection, but the local stress field near the diameter change is not a simple $\sigma = F/A$. The formula is not valid near the diameter transition (and the two ends where loads are applied). In these types of problems we appeal to Saint-Venant's principle that says the local stress field becomes a uniform uniaxial stress field very quickly as the distance from that local area increases. And in fact it does, and we seldom concern ourselves, but also keep in mind that a fundamental assumption in Saint-Venant's theory is that the bar is infinitely long.

Another important field problem in tubular mechanics is that of planar bending of tubes or beams. The derivation is a bit more involved, but again it is important to understand the assumptions that go into it so that you can also understand the limitations.

EXAMPLE C.13 Planar Beam (Tube) Bending

The so-called theory of simple beam bending in a plane is not an actual theory but a set of ad hoc assumptions as to the nature of the beam in its deformed state. Our beam is a tube so our set of assumptions addresses that as follows.

- Cross sections perpendicular to longitudinal axis before bending remain perpendicular after bending
- Tube cross sections remain circular
- Tube is initially straight and prismatic
- Tube is long in relation to its diameter

The first assumption is often referred to as the classical Euler-Bernoulli assumption, and the others are qualifiers for which the first is true.

A right-hand Cartesian coordinate system is assumed. The downward positive vertical coordinate here is z and the z-displacement is u_z. A horizontal y-coordinate is defined as positive "out of" the page.

Moment, Shear, and Axial Second Area Moment (Definitions)

$$M \equiv \int_A \sigma_{xx}\, z \, \mathrm{d}A \tag{C.151}$$

$$V \equiv \int_A \sigma_{xz} \, \mathrm{d}A \tag{C.152}$$

$$I_\mathrm{a} \equiv \int_A z^2 \, \mathrm{d}A \tag{C.153}$$

These integrations are over a cross-sectional area, A, of the beam (tube). The second area moment, I_a, defined above is an axial second area moment. In the case of a tube, the axis, a, in the subscript is any outside diameter. For this derivation we will take $I_\mathrm{a} = I_y$ so that the diameter used is on the y-axis. We will not include the derivation of I_a, but will give the formulas at the end of the example.

Kinetic Equations (Equilibrium)

Referring to the above free-body diagram we set up equilibrium equations in shear

$$-V + (V + \Delta V) + \int f\,(x)\ \mathrm{d}x = 0 \tag{C.154}$$

and in moment

$$-M + (M + \Delta M) + V\Delta x + \int f\,(x)\ \Delta x \, \mathrm{d}x = 0 \tag{C.155}$$

Similar to the uniaxial tube procedure, we divide these two equations by Δx and take the limit as $\Delta x \to 0$.

$$\frac{\mathrm{d}V}{\mathrm{d}x} + f\,(x) = 0 \tag{C.156}$$

$$\frac{\mathrm{d}M}{\mathrm{d}x} + V = 0 \tag{C.157}$$

It is important to note that these equilibrium equations are specific to the coordinate system and conventions in the free-body diagram (Figure C.22), hence *the signs are specific to that diagram*. You may notice that in other sources the convention may be different, so always use caution when working with beam bending equations.

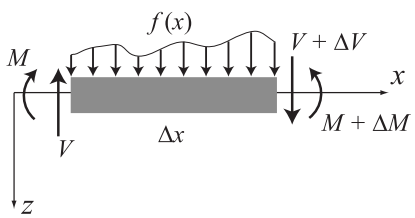

Figure C.22 Tube in simple planar bending, free-body diagram.

Kinematic Equations

It is in the kinematics that our bending assumptions come into play, and we will specifically point them out as they are encountered. The axial displacement from small rotational bending about the *y*-axis is

$$u_x = -z\theta_y \tag{C.158}$$

and, hence, the axial strain is

$$\varepsilon = \frac{\mathrm{d}u_x}{\mathrm{d}x} = -z\frac{\mathrm{d}\theta_y}{\mathrm{d}x} \tag{C.159}$$

Next, we incorporate the Euler-Bernoulli *small rotation* assumption as in Figure C.23 and make the following approximation.

$$\theta \cong \tan\theta = \lim_{\Delta x \to 0} \frac{\Delta u_z}{\Delta x} = \frac{\mathrm{d}u_z}{\mathrm{d}x} \tag{C.160}$$

This is the important simplifying assumption that limits the simple beam bending equation to small rotations.

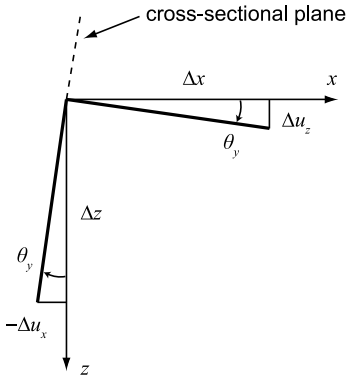

Figure C.23 Small rotation of simple beam (tube).

Constitutive Equation (One-Dimensional)

$$\sigma = E\varepsilon \tag{C.161}$$

Field Equation

Now substitute (C.160) into (C.159)

$$\varepsilon = -z\frac{\mathrm{d}}{\mathrm{d}x}\left(\frac{\mathrm{d}u_z}{\mathrm{d}x}\right) \tag{C.162}$$

then (C.162) into (C.161)

$$\sigma = -Ez\frac{\mathrm{d}}{\mathrm{d}x}\left(\frac{\mathrm{d}u_z}{\mathrm{d}x}\right) \tag{C.163}$$

Now substitute (C.163) into (C.151)

$$M = \int_A -zE\frac{\mathrm{d}}{\mathrm{d}x}\left(\frac{\mathrm{d}u_z}{\mathrm{d}x}\right) z\,\mathrm{d}A = -EI_y\frac{\mathrm{d}^2u_z}{\mathrm{d}x^2} \tag{C.164}$$

then (C.164) into (C.157)

$$V = -\frac{\mathrm{d}}{\mathrm{d}x}\left(-EI_y\frac{\mathrm{d}^2u_z}{\mathrm{d}x^2}\right) \tag{C.165}$$

Finally we substitute (C.165) into (C.156) to get the *governing differential equation for small deflection planar beam bending*:

$$\boxed{\frac{\mathrm{d}^2}{\mathrm{d}x^2}\left(EI_y\frac{\mathrm{d}^2u_z}{\mathrm{d}x^2}\right) + f\,(x) = 0} \tag{C.166}$$

Boundary Value Problem

There are many possible load conditions, so the equation will not be integrated further here for any particular situation. For most tubes E and I are constants, and many useful formulas may be obtained by integration and specification of the value of two or more of these *boundary conditions*:

$$\begin{aligned}
u_z &= \text{transverse displacement}\\
\frac{\mathrm{d}u_z}{\mathrm{d}x} &= \text{slope}\\
\frac{d^2u_z}{dx^2} &= \text{curvature (approximate)}\\
EI_y\frac{\mathrm{d}^2u_z}{\mathrm{d}x^2} &= \text{moment}\\
EI_y\frac{\mathrm{d}^3u_z}{\mathrm{d}x^3} &= \text{shear}\\
EI_y\frac{\mathrm{d}^4u_z}{\mathrm{d}x^4} &= -f\,(x) = \text{the transverse load}
\end{aligned} \tag{C.167}$$

Second Area Moment (Axial)

$$I_\mathrm{a} = \frac{\pi\left(r_\mathrm{o}^4 - r_\mathrm{i}^4\right)}{4} \tag{C.168}$$

or

$$I_\mathrm{a} = \frac{\pi\left(d_\mathrm{o}^4 - d_\mathrm{i}^4\right)}{64} \tag{C.169}$$

where a is any diameter.

Another example closely related to the previous one is that of axial stress in a tube that results from the bending just described. This is an important part of casing design in curved wellbores and is included here.

EXAMPLE C.14 Axial Bending Stress

Along a curvilinear borehole path, s, we may define the curvature at any point as

$$\kappa \equiv \frac{\mathrm{d}\theta}{\mathrm{d}s} \tag{C.170}$$

Likewise we define a radius of curvature as

$$r_\kappa \equiv \left|\frac{1}{\kappa}\right| \tag{C.171}$$

and while the curvature, κ, can be positive or negative, a radius of curvature, r_κ only has meaning when it is positive.

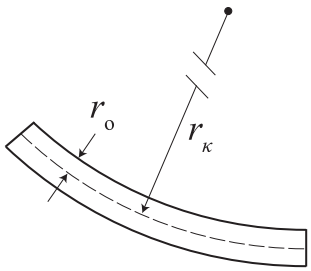

Figure C.24 Simple planar bending of tube.

Similar to Equation (C.159) in the previous example the axial strain is

$$\varepsilon = \frac{\mathrm{d}u}{\mathrm{d}s} = -z\frac{\mathrm{d}\theta}{\mathrm{d}s}$$

Appealing to the small rotation assumptions of the previous example,

$$\theta \approx \frac{\mathrm{d}u}{\mathrm{d}x}$$

as in Equation (C.160) and $\mathrm{d}s \approx \mathrm{d}x$, and wecan express the small strain in Cartesian coordinates as

$$\varepsilon = \frac{\mathrm{d}u}{\mathrm{d}x} = -z\frac{\mathrm{d}\theta}{\mathrm{d}x} = -z\kappa = \frac{-z}{r_\kappa}$$

In the previous example, we assumed a positive z which gave a negative strain. In this case we will assume that z measured from the centroid of the tube can be either positive or negative depending on the direction of the rotation. So that now we say $\pm z$ and substitute into Hooke's one-dimensional constitutive Equation (C.161)

$$\sigma = \pm E\frac{z}{r_\kappa}$$

For the small bending of casing (or any tube) the maximum value of z is the outside radius of the tube, r_o, (Figure C.24), so the maximum axial bending stress is

$$\boxed{\sigma_b = \pm E\frac{r_o}{r_\kappa}} \tag{C.172}$$

Some commentary on those examples is in order. Notice that in Section C.8, we took two differential equations, (C.156) and (C.157), and through a substitution process we ended up with the single Equation (C.166). Did you notice that the first two differential equations are about different entities, force and moment, respectively, and the differential forms (differentiated with respect to length) are in units of F/L and F, respectively? We did the process correctly, but I would like to call to your attention to something else you may encounter. Often you will see those two combined into a single equation equivalent to:

$$\frac{\mathrm{d}V}{\mathrm{d}x} + V + \frac{\mathrm{d}M}{\mathrm{d}x} + f(x) = 0$$

Mathematically this is legitimate since both equations equate to zero, but physically it makes no sense, and you can run amok if you are not careful.

C.9 Solution methods

To understand mechanical theory we cast entities and events in mathematical form which we call models. The mathematical formulation we seek is simple (and elegant if possible) and conveys the essential physical nature of the model. In continuum mechanics these models take the form of field problems defined by differential equations. The ideal is to find a closed-form solution to these equations if possible. Such solutions, referred to as *exact solutions*, are the pinnacle of mathematical modeling. They can be easily taught, printed in a textbook like this, and used by engineers with pencil and paper, a hand held calculator, or laptop computer. We tend to think of such solutions as the ultimate in mechanics. At least that is the prevalent notion in academia. It is not a wrong notion, except where it tends to claim superiority over so-called "numerical approximations." *All solutions are approximate because all models are approximate*. The false faith in so-called "exact solutions" as opposed to "numerical approximations," is unjustified. The truth is that an exact solution to an over-simplified model is not as accurate as a proper numerical solution to a more exacting and complex model that better represents the physical reality. All real problems in mechanics are solved numerically. That may sound a bit brash, but it is true. With the abundance of digital computers it has become possible to easily obtain more accurate solutions to almost any physical problem than with reliance on closed-form solutions used in the past. This is a reality of our time.

Along these lines, the extent to which engineers have in the past avoided nonlinear equations is no longer acceptable. There is plenty of software available to perform these tasks, and plenty of free programming software if you do not have access to commercial versions. Every engineer at this time has been taught numerical methods and some basic programming skill in at least one language to solve simple nonlinear equations and initial value problems.

Unfortunately, when it comes to solid mechanics the situation is not quite as simple because we are dealing with partial differential equations in two and three dimensions. Commercial software is almost mandatory for all but a few who can and do write their own. It is not cheap, and the training and skill level required is not minimal. I am alluding to the finite element method here which was born in structural engineering and has evolved to multi-physics applications today. While training and skill levels are significant barriers in themselves, most commercial finite element software does not do subsurface borehole mechanics very well. Most commercial packages are focused toward simulated loading and behavior of manufactured parts or components and assemblies of such. For example, a rule of thumb says that any structural member whose length to radius of gyration ratio is greater than 10:1

should be analyzed as geometrically nonlinear in any deflection situation. Okay, but that means every joint of oilfield pipe exceeds that 10:1 ratio. What about a 14,000 ft string of 7 in. casing with a ratio of over 90,000:1. It can be done, but not always easily. Most analyses regarding casing can be confined to a local region to evaluate rupture, collapse, buckling and so forth. But to evaluate a full casing string on a global scale, for torque, drag, impact loads, bending stress magnification, inertial reactions to sudden decelerations, and so forth, requires analyses that most commercial software is not well suited for. One of the real complications with the finite element method is contact problems, and especially when friction is included. As we discuss in Chapter 7, the Amontons-Coulomb friction equation is problematic with extensible bodies (like long tubes). Another difficulty is that most calculations with casing in the borehole must start from the bottom of the string and this is sometime difficult to do with commercial software. Some applications are better analyzed with special-built software, as for example, Newman's finite element model [57] as used by McSpadden et al. [58] for a casing path in a borehole. I am not denigrating the finite element method in the least; I think it is one of the most useful tools engineers can have access to. I taught graduate courses in the subject; I co-authored two textbooks on the subject, I have written a at least a couple of dozen specialty finite element programs including one for dynamic aerothermal stress analysis for NASA; I am a believer! But, I find that commercial finite element software is not that well suited for many of the applications we want to address. (At least that is my opinion.)

I think there is one very important point we must always keep in mind regarding casing design. The data we have both *a priori* for the design process and even later as the well is drilled are of varying accuracy and reliability. And among the least accurate is the actual geometry of the borehole path. So even the most sophisticated analytical approaches in casing design must be taken as a fair approximation.

There is no need to detail any of the numerical methods here as there are many excellent sources. For those interested in further reading about numerical methods, I can recommend the one by Burden and Faires [59]. As to finite element methods the standard is Zienkiewicz [60] and his two companion volumes. For those just wanting an introduction in terms of undergraduate level math, I cannot help but recommend one by Huebner et al. [61] that I co-authored.

C.10 Closure

We have covered a lot of deep material in this appendix with a rather sweeping brush stroke, the point being to give you a basic acquaintance with the foundational material to the mechanics of tubes as used in subsurface borehole environments. For those whose interest go deeper there is a wealth of literature on the subject.

For those whose interest is not so much depth but a more complete but systematic approach to what we have covered written in the mathematical language of the undergraduate I can recommend the introductory text to structural analysis by Allen and Haisler [53], and although its primary topic is aerospace structures it just as easily applies to casing.

For those who want to go farther, I can recommend two texts on vectors and tensors. By far, the most popular and enduring is the one by Simmonds [49] often referred to as the "little yellow book." It is short, concise, and easy to understand. My only reservation is his use of the terms "cellar" and "roof" for subscript and superscript coordinate variables which makes for easy initial understanding, but leaves one disadvantaged when encountering the conventional terms, covariant and contravariant, in all the rest of the literature. The other text, by Lebedev et al. [62], is newer, is more complete, and has

several applications to mechanics, but unfortunately, a sparse index. Adequate treatments of vectors and tensors may also be found in the classic text on continuum mechanics by Malvern [63] and the solid mechanics text of Fung [52] and also in his book on continuum mechanics [64]. These last three texts use only subscripted vectors and tensors (covariant) in orthogonal coordinate systems as we do here. A newer text on continuum mechanics by Irgens [65] is quite good if perhaps a bit heavy on math and light on examples. Though intended primarily for physicists, the text by Jeevanjee [66] is excellent in many of its explanations on vectors and tensors as covered in his first three chapters. A good look-up type reference is the classic Bronshtein and Semendyayev *Handbook of Mathematics* [67] now in its fifth English edition.

For those wanting more in-depth coverage of linear algebra there are any number of basic linear algebra texts available. Most authors, myself included, tend to recommend the text they learned from, having never experienced any other unless they taught the subject. I used Kolman [68] which I found to be at least adequate as an introductory text, but it was a fourth edition and it is now in the ninth edition and appears to get poor reviews at Amazon. A more advanced and rigorous book on vector and tensor analysis is by Bowen and Wang [69] that is sufficiently rigid to satisfy most mathematicians, but it is not for the feint of heart. It was originally published in two volumes but has since been reprinted in a Dover paperback edition in one volume. Recently, the introductory linear algebra textbook by Larson and Falvo [70] seems to get the best reviews at Amazon.

This page intentionally left blank

Appendix D: Basic hydrostatics

Chapter outline head

D.1 Introduction to subsurface hydrostatic loads

The pressure loads on tubes in wellbores are for the most part hydrostatic, meaning static or quasi-static, but there are applications where fluid dynamics also come into play during circulation where both pressure and friction from fluid flow also exert loads on the tubes. The biggest drawback to application of pressure loads is that they usually must be calculated from surface measurements with assumed conditions in the wellbore, rather than by direct measurements. Hydrostatics is a fairly simple topic and as such receives relatively brief coverage in basic fluid mechanics courses. Because of this brief coverage and the fact that most such courses deal with near surface hydrostatics with liquids only, the frequent number of misconceptions and intuitive assumptions arising should not be surprising. Almost no one is immune to an occasional blunder (myself included). For those reasons, we will cover hydrostatics in a bit of detail beyond the simplified equation, $p = g\,\rho\,h$, that we are all so accustomed to using.

D.2 Hydrostatic principles

Most simply stated, hydrostatics is the effect of gravity on fluids at rest. To be more precise, we should include temperature which is quite important in wellbore hydrostatics. A better description is: *hydrostatics is the effect of gravity and temperature on fluids at rest*. Before we begin discussion of the calculations of hydrostatics, we should clarify some of the fundamental concepts involved.

D.2.1 Basic concepts

Fluid

A fluid is a material that *cannot sustain a shear load when at rest*. The definition includes both liquids and gases. Or another way, a solid is a material that retains its shape when at rest; a fluid is a material that does not. While both definitions seem to clearly delineate between a fluid and a solid, the division is not quite as distinct as one might hope. What we left out of the definitions is *time*. How much time is allowed for a shear load to dissipate? Seconds? Hours? Years? Centuries? For example, we think of a salt diapir as a solid, yet on a geologic timescale it is more like a fluid. The distinction is not as clear as we would like, but for our purposes the simple definition will apply.

Pressure

We normally think of pressure as a force per unit area. That is a useful description for most applications, but pressure is actually something else: it is *energy density* with physical dimensions $\mathrm{F\,L/L^3}$, that is, energy per unit volume resulting from molecular motion and resistance to compaction. We seldom write it with those dimensions since the length units partially cancel leaving $\mathrm{F/L^2}$ (psi in USC units) which is obviously force per unit area. In the ideal gas equation, $pV = nRT$, the term pV represents energy density times volume which results in the macroscopic energy of that volume of gas. The right hand-side represents the same energy in terms of molecular activity as a function of temperature.

While pressure has the units of force per unit area like a traction vector (a distributed force), it is not a distributed force vector. Pressure, as we encounter it in mechanics is a scalar value, and when we use it as a traction (distributed force), we are actually multiplying it with a unit normal vector to the contact surface as $\mathbf{t} = -p\,\hat{\mathbf{n}}$, and it is negative because the unit normal vector, $\hat{\mathbf{n}}$, is conventionally positive outward from a surface. And while we are referring to a "surface," we should be clear that it is not necessarily a physical surface we refer to, but any surface, physical or imaginary drawn within the fluid itself as in Figure D.3 later in this appendix. Perhaps that is a bit technical, but the important things to remember in our applications are

- Hydrostatic pressure at a point is the same in all directions (it is a scalar not a vector).
- Hydrostatic pressure can only act in a normal direction to a surface (there are no other pressure components acting on a surface at any point).

Archimedes' principle

Simply stated, the brilliant discovery of Archimedes is that the net buoyant force on a body in a fluid is equivalent to the weight of the fluid displaced by that body. It is an extremely useful and simple concept. But the key ideas are that it is a *net force* and it acts only in an *upward vertical direction*. It has no horizontal force component. It says nothing about the distribution of forces acting on a body nor about the distribution of forces within a body. It is most easily applied to a rigid body in an incompressible

fluid. When that is not the case, other things must be taken into account. For instance, consider a rigid body in a compressible fluid where the rigid body density is only slightly greater than that of the fluid at the surface. The body will sink initially, but because of gravity, the density of the compressible fluid will increase with depth so the body may descend only to a point where its density and that of the fluid are equal, and there it will remain suspended. Or consider a case of a compressible body and an incompressible fluid in which the density of the body is slightly less than that of fluid. If placed in a closed tank of incompressible fluid, the body will remain at the top of the tank, but if the pressure inside the tank is increased until the density of the compressed body becomes greater than that of the fluid then it will start to sink. And as it sinks deeper, its density will continue to increase because the hydrostatic pressure is also increasing. It will only stop when it reaches the bottom of the tank. If the pressure on the tank is released, the body may remain on bottom if the hydrostatic pressure is sufficient that the density of the body cannot recover to its initial value. High altitude weather balloons are a buoyancy scenario where both the body and the fluid are compressible. Initially, the *effective density* of the balloon, including its gas content and cargo, is less than that of the surface atmosphere. When released, the balloon will rise. The density of the atmosphere decreases with altitude, but the effective density of the balloon also decreases as its gas expands. Eventually, though, the effective density of the balloon will equal that of the atmosphere at some altitude and the balloon will cease to rise any farther.[1]

D.2.2 Hydrostatic pressure

Another clarification we make in this introduction concerns the fundamental nature of pressure in the macroscopic scale of material bodies. As already stated, pressure at a point has the same magnitude in all directions, and it only acts on a body normal to its surface at a point of contact. It has no tangent component acting on any surface which it contacts. In the sense of pressure acting on the surface of a material body, pressure is a stress which is a scalar, $-p$, multiplied by the identity tensor, $\mathbf{I}$. In matrix form, we would express it as

$$-p\mathbf{I} = -p[I] = -p\begin{bmatrix} 1 & 0 & 0 \\ 0 & 1 & 0 \\ 0 & 0 & 1 \end{bmatrix} = \begin{bmatrix} -p & 0 & 0 \\ 0 & -p & 0 \\ 0 & 0 & -p \end{bmatrix} \tag{D.1}$$

It is what we refer to in solids as a *spherical stress*. Why the negative sign though? Recall Cauchy's formula from Appendix C (Equation (C.51)), $\mathbf{t} = \hat{\mathbf{n}}\,\mathbf{T}$, relating stress the traction at a point on a surface by its action on an outward unit normal vector to that surface. For example, let us assume a flat vertical surface some submerged object. The surface is a positive face perpendicular to a horizontal x_2 Cartesian coordinate as in Figure D.1. At some point on that surface, the magnitude of the hydrostatic pressure is p. So the traction on that surface is

$$t_j = n_i\,\sigma_{ij} = \lfloor 0, 1, 0 \rfloor \begin{bmatrix} -p & 0 & 0 \\ 0 & -p & 0 \\ 0 & 0 & -p \end{bmatrix} = \lfloor 0, -p, 0 \rfloor$$

While that is straightforward, some amount of confusion occasionally tends to arise, especially in buoyancy and subsurface applications. And even when a hydrostatic effect is correct, the explanation sometimes typically offered for the effect may be dead wrong. Take for instance an oft used sample

[1] The altitude is restricted by the capacity and weight of the balloon and cargo, otherwise a weight-less balloon with an infinitesimal elastic modulus and containing hydrogen could reach the upper edge of the atmosphere.

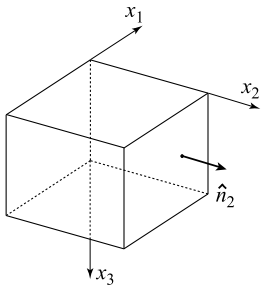

Figure D.1 Solid with outward normal on positive $_2$ face.

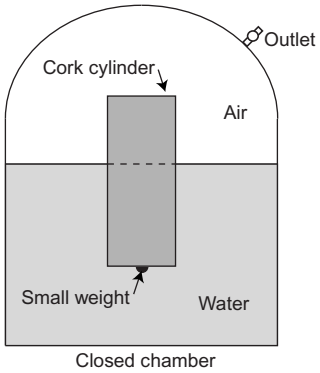

Figure D.2 Floating cork cylinder in chamber.

question from a fundamentals of engineering exam. A cylindrical cork is floating vertically in a chamber half filled with water as in Figure D.2 where a small weight on the bottom keeps the cork cylinder in a vertical position. Initially, the upper part of the chamber contains air at standard atmospheric pressure.

Suppose now that we attach a vacuum pump to the outlet and remove the air from the upper part of the chamber so that it now has a vacuum. The question is: (A) does the cork rise slightly in the water, (B) does the cork maintain the same level in the water, or (C) does the cork sink slightly in the water? The correct answer is C, but the explanation usually given appeals to Archimedes' principle saying that the air has mass and is buoying the cork and hence when it is removed it no longer buoys the cork. While that is true in essence it is quite misleading as stated. The air is not directly buoying the cork, it acts only downward on the top surface of the cork and horizontally on the exposed side of the cork. So how can it buoy the cork? It does so only indirectly by acting on the surface of the water. The only buoying force acting on the cork is on the bottom surface of the cork, where there is no contact with the air. That buoying force is the combined hydrostatic pressure of the water plus the pressure of the air on top of the water, acting in conjunction on the bottom of the cork in an upwards direction. While it might seem that the air pressure on top of the cork and on the surface of the water are the same, they are not. Because the air has mass, the air pressure on the water surface is slightly greater than on the top of the cork.

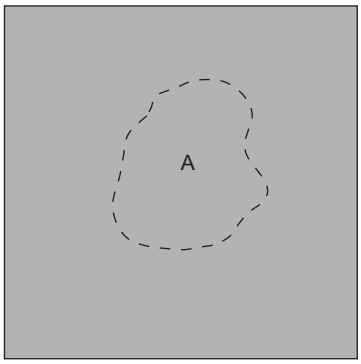

Figure D.3 Imaginary material boundary in a liquid.

Hence the net effect of the air is a buoying force, but only indirectly as the portion of the cork in the air experiences no direct buoying force at all, but rather a downward force from the air pressure on top. The pressure difference between the top of the cork and the surface of the water is indeed small, but still enough to add to the buoyancy force on the bottom of the cork.

Another fiction which arises occasionally is that hydrostatic pressure can cause a free body to move in some direction other than vertically upward. It cannot. If it were true we might design a ship that could cross the oceans without power, a violation of the natural laws. Whenever we observe any material body motion other than vertically upward seemingly caused by hydrostatic pressure, it is caused by a resultant force of the buoyant force on the body and some other applied force or physical constraint, removal of a constraint, or contact with some other body. One of the better and often used illustrations of hydrostatic equilibrium is shown in Figure D.3 where we draw an imaginary boundary in a liquid defining some arbitrary domain, A. The liquid contained within that boundary is in equilibrium with its surroundings. If A is a solid but with the *same density* as the liquid, it is also in equilibrium and will experience no motion caused by hydrostatic pressure.

D.2.3 Compressibility

All materials are compressible; the only distinction is the relative degree as in a particular application. Incompressibility is an assumption we often make in particular applications where material compressibility is negligible or where we ignore it simply because we do not know how to account for it. Unfortunately, the later is more common than we are prone to admit. Contrary to what we have been given to assume in many engineering courses, *water is compressible*. It is significantly less compressible than most metals, only about 0.7% the compressibility of steel at room temperature and atmospheric pressure. It varies with temperature and pressure, for example, at down-hole conditions of 200 °F and 6000 psi it is about 1.1% that of steel.

D.3 Formulation of hydrostatics

All matter on earth is affected by gravity, whether or not we choose to ignore it in some particular application. From Newton's second law, we can derive the fundamental formulation of hydrostatics.

In index notation Newton's second law says

$$f_i = m\,\ddot{u}_i \tag{D.2}$$

where the mass, m, is not a function of time.

The fundamental differential equation of hydrostatics is

$$\boxed{\mathrm{d}p = \rho\, g\, \mathrm{d}z} \tag{D.3}$$

where p is pressure, ρ is the fluid density, g is the local gravitational acceleration, and z is a vertical coordinate measure. In integral form, the fundamental equation is

$$\boxed{\int_{p_0}^{p_h} \mathrm{d}p = \int_{h_0}^{h} \rho\, g\, \mathrm{d}z} \tag{D.4}$$

where in the limits of integration p_0 is the pressure at a reference point, $z = h_0$, and p_h is the pressure at some point $z = h$. Although it is almost never noted formally in these equations, **g** and **z** are actually vectors, but since they are always vectors in the same direction (vertical), only their scalar magnitudes, g and z, are commonly used.

In general ρ and g are not constants, but for most applications at or near the earths surface we assume that at least g is constant. The density, ρ is almost never constant, but over relatively short intervals and isothermal conditions, it may be nearly constant for many liquids. In wellbores, we generally assume that it is constant for most circulating fluids used in wellbore operations because we seldom have accurate fluid property data or accurate knowledge of the wellbore temperature which usually increases with depth but also varies with the forced-convection effects of circulation. For most applications, the assumption of constant density is accurate enough for the approximate nature of the calculations we must make to determine pressure loads in a wellbore. In those cases, the assumptions of constant ρ and g simplify Equation (D.4) to

$$p_h - p_0 = \rho\, g\ (h - h_0) \tag{D.5}$$

While many applications of this equation occur where both $h_0 = 0$ and $p_0 = 0$ leading to the common form of

$$p = \rho\, g\, h \tag{D.6}$$

It is important to remember that such is not always the case and Equation (D.5) is always the basic equation for hydrostatics when ρ and g are constants. It is also important to remember that in many wellbore applications the known pressure, p_0, is at some depth $h_0 > h$ so that $p_0 > p$. Perhaps a less burdensome form to remember to avoid mistakes is

$$\boxed{\Delta p = \rho\, g\, \Delta h} \tag{D.7}$$

D.3.1 Gases

Unlike in the previous equations, we may almost never assume a constant density for gases. Fortunately, we do have an *equation of state* for gases from which we can derive an equation of state for gas density, and from which we can substitute into Equations (D.3) and (D.4) and solve in closed form for some useful approximations for many applications.

We are all familiar with the simple form of this state equation known as the *ideal gas law*, often written as

$$pV = nRT \tag{D.8}$$

where p is the pressure of the gas, V is the gas volume, n is the number of moles, and T is the absolute temperature. R is the "ideal gas constant" which is a conversion factor that converts mass-temperature (MT) to energy (FL) for an "ideal gas." In terms of physical properties, this equation is an energy balance that says "macroscopic energy = microscopic energy" or in physical dimensions, FL = FL. In that form, common in chemistry and physics, the equation is hardly useful in engineering applications where gas pressure is to be calculated. In essence, it relates a macroscopic energy scale to a microscopic one, and we seldom know (or even care) how many moles of gas are present in a particular wellbore or even the earth's atmosphere for that matter. Before we begin to derive a more useful form of this equation, we should examine some of its aspects for better understanding.

Mole

Briefly, the definition of a mole is the amount of a substance that contains the same number of atoms or molecules as the number of atoms in 12 g of ^{12}C (carbon-12). It is a unit of measure defined in the SI system and abbreviated as mol. It is sometimes called a gram mole (g mol), but in many engineering applications a more useful form is the kmol (equivalent to the old kg mol). It is often defined in USC units as a pound-mole (lb-mol) and in some cases an ounce-mole. In any event, it always corresponds to the Avogadro constant of 6.022141×10^{23} atoms or molecules of the substance.

Gas Constant, R

The gas constant is essentially a conversion factor that converts absolute temperature into energy per mole of gas per degree absolute temperature (FL/mol/T).

In working with real gases as opposed to an "ideal gas," we typically employ a compressibility factor, Z, to account for variations from Equation (D.8) as

$$pV = nZRT \tag{D.9}$$

The value of Z is dependent on the composition of the gas, and in general, Z is not a constant but rather, a function of both temperature and pressure.

In order to calculate gas density (physical units, M/L^3) from Equation (D.9) for use in Equation (D.3) or (D.4) we work with n, the number of moles. If we represent the mass of a mole of gas by M, the relationship of a mass of gas, m, to the number of moles, n, is given by

$$n = \frac{m}{M} \tag{D.10}$$

Next we divide both sides of Equation (D.9) by V, the volume of gas, and substitute Equation (D.10) for n,

$$p = \frac{1}{V} nZRT = \frac{1}{V}\frac{m}{M} ZRT \; . \tag{D.11}$$

so that both sides are in terms of energy density. The density of a gas is

$$\rho = \frac{m}{V} \tag{D.12}$$

and substituting this into Equation (D.11), and rearranging to get ρ gives

$$\rho = \frac{pM}{ZRT} \tag{D.13}$$

which is our goal, an equation of state for the density of a gas as a function of temperature and pressure.

Now, we may substitute that into the differential form of the hydrostatic equation (D.3) to get

$$\mathrm{d}p = \frac{pM}{ZRT}\, g\, \mathrm{d}z \tag{D.14}$$

or into the integral form of the hydrostatic equation (D.3) resulting in

$$\int_{p_0}^{p_h} \frac{\mathrm{d}p}{p} = \int_{h_0}^{h} \frac{M}{ZRT}\, g\, \mathrm{d}z \tag{D.15}$$

In wellbore applications the temperature, T, is almost never a constant. One simple approach is to use an average temperature, T_{avg} as a constant in Equation (D.15). The resulting integration is

$$\boxed{p = p_0 \exp \frac{Mg\,(h - h_0)}{ZRT_{\mathrm{avg}}}} \tag{D.16}$$

A slightly different approach for most wellbores is to take the temperature as a linear function of the vertical coordinate, z, such as $T = T_0 + k_{\mathrm{T}}\, z$ where T_0 is the temperature at h_0 and k_{T} is a linear temperature gradient. Substituting this relationship into Equation (D.15) yields

$$\boxed{p = p_0 \left(\frac{T_0 + k_{\mathrm{T}} h}{T_0 + k_{\mathrm{T}} h_0} \right)^{\frac{Mg}{ZRk_{\mathrm{T}}}}} \tag{D.17}$$

The two equations above are adequate for many wellbore hydrostatic calculations where we often use methane as a worst case gas load. Methane has a molecular mass of $M = 16$ g mol and a compressibility factor of $Z \approx 1$. But for more accurate work, we must consider the compressibility factor, Z, which we obviously assumed constant in the above two derivations. In general, it is not constant and is not only material dependent, but also a function of both pressure and temperature. Gases encountered in wellbores are never a single molecular gas but consist of several hydrocarbons and oftentimes include CO_2, H_2S, and even elemental He. If a greater degree of accuracy is required, one must turn to more sophisticated methods. There are a number of correlations and models for use with natural gas. Some are fairly simple requiring only the specific gravity of the gas (air = 1.0) and others more accurate which require a detailed knowledge of the chemical composition of the gas. Those methods will not be covered here, and Equation (D.16) will suffice for our basic design process.

As to the value of the gas constant, R, standard values are readily available in many sources. Table B.8 in Appendix B gives standard values for R along with values for standard gravitational acceleration and M for methane, C_1, in SI and USC units. The confusion often encountered with gas equations in a gravitational environment as in Equations (D.14)–(D.17) is in the units of R and M. Most reference sources give the SI value of R as 8.314462 J K mol, but most standard chemistry references give molecular mass in g/mol which is inconsistent with R and requires a conversion factor in our formulations. In this text we will apply a conversion factor to the gas constant so that $R = 8314.462$ mJ K mol, thus allowing the use of M in standard chemistry units of g mol. This has the advantage that

when working in USC units M will have the same numerical value, though in units of lb/lb-mol instead. The problem in USC units though is complicated not by R or M, but by use of lb and lbf as mentioned earlier in this chapter. The inclusion of the conversion factor, g_c numerically cancels g if the two are numerically equal (and they usually are assumed equal for most applications). The result of that is the conversion is often invisible in the calculations so that R and M appear consistent. Numerically they are, but in terms of units, they are not—yet another reason not to use USC units in serious engineering work.

Again, always keep in mind that the known gas pressure p_0 may be at some depth $h_0 > h$ and that $p_0 > p$ in those cases. If you substitute into the equations correctly this is automatically accounted for, but it is a common source of error in manual calculations.

D.4 Buoyancy

The effects of buoyancy from the presence of fluids in a wellbore are significant. While we may choose to ignore it in certain calculations (unbuoyed design), it is nevertheless always present.

D.4.1 Buoyancy and Archimedes' principle

When we mention buoyancy, Archimedes' principle automatically comes to mind. It is an essential part of hydrostatics, which states that the buoyant force on a submerged, or partially submerged, body is equal to the weight of the volume of fluid displaced by the body. This is quite handy for calculating the buoyed weight of submerged objects, such as casing, without the necessity of determining the hydrostatic forces on the body, which requires details of the body geometry and depths within the fluid. For instance, a cube with dimensions $b \times b \times b$ submerged in a liquid, as shown in Figure D.4, has a buoyant hydrostatic force acting on the bottom cross-sectional area, $b \times b$. We can calculate the force on the bottom easily:

$$F_{\text{bottom}} = -g\rho_{\text{liquid}}\, h\, b^2$$

The force on the top is

$$F_{\text{top}} = g\rho_{\text{liquid}}\, (h - b)\, b^2$$

The net buoying force is the sum of those two (no buoying force on the sides). And the buoyed weight, $\hat{W}$, of the cube can be calculated as

$$\begin{aligned}\hat{W} &= g\rho_{\text{solid}} b^3 + g\rho_{\text{liquid}}\, (h - b)\, b^2 - g\rho_{\text{liquid}} h\, b^2 \\ &= g\left[\rho_{\text{solid}} b^3 + \rho_{\text{liquid}}\left(hb^2 - b^3 - hb^2\right)\right] \\ &= g\left(\rho_{\text{solid}} - \rho_{\text{liquid}}\right) b^3\end{aligned}$$

We see that the depth is irrelevant (assuming the liquid is incompressible) and the buoyed weight depends only on the difference in densities of the solid and the liquid and the volume of the solid (or the displaced liquid), and above equation in its final form is a statement of Archimedes' principle, which can be generalized as

$$\boxed{\hat{W} = g\left(\rho_{\text{solid}} - \rho_{\text{liquid}}\right) V_{\text{solid}}} \tag{D.18}$$

where

$\hat{W}$ = buoyed weight of solid

V_{solid} = volume of solid

ρ_{solid} = density of solid

ρ_{liquid} = density of liquid

Now suppose that, instead of the orientation in Figure D.4, the cube had been oriented with the "bottom" face 60° to the vertical and a "side" face 30° to vertical. The calculation of the buoyed weight is somewhat more complicated but yields the same result. So, it should be obvious that Archimedes' principle is of considerable use in simplifying calculations of buoyed weight of submerged or semi-submerged objects.

A handy relationship we can derive for employing Archimedes' principle is the formula for a buoyancy factor for a body, which is the ratio of the buoyed weight in a liquid to the weight in air. We start with the ratio of a buoyed solid to an unbuoyed solid using the generalized Archimedes' principle above (Equation (D.18)):

$$\frac{\hat{W}}{W} = \frac{g\left(\rho_{\text{solid}} - \rho_{\text{liquid}}\right) V_{\text{solid}}}{g\,\rho_{\text{solid}}\,V_{\text{solid}}} = 1 - \frac{\rho_{\text{liquid}}}{\rho_{\text{solid}}}$$

From that we define the buoyancy factor, k_{b}, as the ration of $\hat{W}/W$ as

$$\boxed{k_{\text{b}} \equiv \frac{\hat{W}}{W} = 1 - \frac{\rho_{\text{liquid}}}{\rho_{\text{solid}}}} \tag{D.19}$$

We could also use specific gravity or specific weights in the formula instead of density.

While Archimedes' principle can be of great use, as we just demonstrated, it can also get us into serious trouble if we are not careful. Here is an important question: Can we use Archimedes' principle to determine a load at some point within a buoyed body? We will examine some examples of axial and moment loads on tubes from buoyancy and gravity shortly.

D.4.2 Fluid density

Throughout this text, we continually use the density of fluids in wellbores to calculate hydrostatic pressures. The common oilfield measure of liquid density is pound per gallon (lb/gal or ppg), which

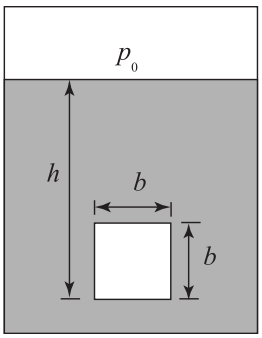

Figure D.4 Solid cube submerged in a liquid.

almost always requires conversion factors every time it is used. Almost anyone who uses that measure has long since committed to memory the necessary conversion factors, but it is still an awkward measure, especially for those accustomed to SI units and in regions where the common engineering density measure, pound per cubic foot, is used instead. Therefore, in the interest of making this text more universal, I use specific gravity (density), $\hat{\rho}$, in referring to the densities of wellbore liquids. This specific gravity is easily multiplied by the density of water in whatever units one may want to use to give the density of the liquid in those units.

That, of course, brings up the question as to what is the density of water to which our measure is specific. Pure water at 4 °C has a density of 1000 kg/m^3, and at 20 °C, it has a density of 998 kg/m^3. Respectively then, those give us densities of 8.345 lb/gal and 8.33 lb/gal or 62.43 lb/ft^3 and 62.32 lb/ft^3. Some will immediately ask to what temperature do we refer when we have to convert the specific gravity into a value of density for a calculation. It is interesting that this question arises in this context, because it almost never arises when one reads a drilling fluid density from a drilling report and uses it in hydrostatic calculations. At what temperature was the density measurement made on the rig, and how does that relate to the temperature and density down hole? Do we ever even consider that? In this text, I use the density of water at 20 °C for the sake of consistency and possibly some notion that it is perhaps closer to the average temperature at which most rig density measurements are made. But I also add that it does not make any difference, because nobody knows the density of the drilling fluid at 4 or 20 °C in the first place. Furthermore, if I work in SI units, I use water at 4 °C just to make my life easier, since the density in kg/m^3 is simply 1000 times the specific gravity rather than 998 times.

D.4.3 Axial load in a vertical tube

Suppose we have a smooth tube suspended vertically in a liquid to some depth, h, as in Figure D.5. We want to know the axial load, F_a, in that tube at point a, some distance, ℓ, from the bottom. The density of the liquid (fluid) is ρ_f, the density of the tube (solid) is ρ_s, and the tube is open at both ends.

We use Newton's third law by saying the force at point a is equal to the buoyed weight of the portion of the tube below that point, and we can calculate that buoyed weight by calculating the displaced volume times the difference in the density of the solid and the fluid, in other words Archimedes' principle:

$$\begin{aligned} \sum F_z &= 0 \\ g\,V\Delta\rho\ - F_a &= 0 \\ F_a &= g\pi\left(r_\mathrm{o}^2 - r_\mathrm{i}^2\right)\ell\,(\rho_\mathrm{s} - \rho_\mathrm{f}) \end{aligned} \tag{D.20}$$

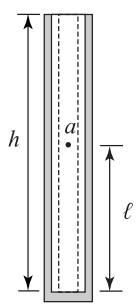

Figure D.5 A smooth open-ended tube suspended vertically in a liquid.

Now, is that correct? Is that really the axial force in the tube at point a? Let us compare to Newton's third law and the actual forces, that is, the body force of the section of tube below point a and the force of the fluid on the bottom of the tube. Assuming there is no pressure at the surface, then

$$\sum F_z = 0$$
$$g\rho_s\pi\left(r_o^2 - r_i^2\right)\ell - g\rho_f\pi\left(r_o^2 - r_i^2\right)h - F_a = 0$$
$$F_a = g\pi\left(r_o^2 - r_i^2\right)(\ell\rho_s - h\rho_f) \tag{D.21}$$

The two methods give different results because $\ell \neq h$. We know that Newton's law with the forces is correct, so what is wrong with using Archimedes' principle in Newton's law? Before we answer that, let us note one thing about the results. If $\ell = h$, then they both give the same results. In other words, the only point where Archimedes' principle can give the correct axial load in the suspended tube is at the surface. The casing in this example is being acted on by forces (at the surface) not accounted for in Archimedes' principle. The problem with Archimedes' principle is that, in general, it cannot be used on part of a body to give the loads within the body itself. This is important to remember, and it is a common mistake. Newton's third law with actual forces gives us the true loads; Archimedes' principle gives us something often termed *effective loads* in the vertical direction. Actually, there are legitimate applications for the effective loads, and we discuss those Chapter 6. For now we consider how Archimedes' principle can give us misleading results.

D.4.4 Axial load in a horizontal tube

Now let us attempt another application using Archimedes' principle. Suppose we have an open-ended tube fixed to a vertical wall and extending horizontally into a liquid, and the central longitudinal axis of the tube is at some depth, h, as in Figure D.6. What is the longitudinal axial load in this horizontal tube (neglecting bending loads caused by gravity for now)? We can see that a pressure load on the end of the tube is acting on the cross-sectional area, so we know there is a compressive axial load in the tube. Can we use Archimedes' principle to determine that load? No, we cannot, because Archimedes' principle applies to gravitational (vertical) loads only. Also we cannot simply multiply the pressure by the cross-sectional area, as we did previously, because it is apparent from the figure that the pressure on the cross section is not the same at all points since the pressure varies with depth. So, let us see how we calculate the load on the end attributable to the liquid pressure, which varies with depth.

We could show this more easily if it were a solid bar with a rectangular cross section, but since our interest is in tubes, we may as well see the details of how it is done. Since pressure varies with depth, we can express the pressure at any point on the tube end as follows:

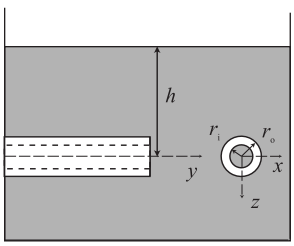

Figure D.6 Horizontal tube, centroid at depth, h.

$$p = p_o + g\rho_f\,(h + r\cos\theta) \tag{D.22}$$

Note carefully the orientation of our coordinate system, because we have adopted the convenient system mentioned earlier for our use in wellbore calculations, and it appears to be upside down to what we are accustomed to seeing; that is, the z-axis is positive downward. The angle, θ, is measured counterclockwise from the positive z-axis. Since the pressure varies over the area of the tube, the force of the pressure on the end of the tube is the pressure integrated over the area of the tube:

$$\begin{aligned}
\sum F_y &= 0 \\
-F - \iint p\,\mathrm{d}A &= 0 \\
F &= -\int_{r_i}^{r_o}\int_0^{2\pi} [p_o + g\rho_f\,(h + r\cos\theta)]\; r\,\mathrm{d}\theta\,\mathrm{d}r \\
F &= -\int_0^{2\pi} \frac{p_o}{2}\left(r_o^2 - r_i^2\right)\mathrm{d}\theta - g\rho_f\int_0^{2\pi}\left[\frac{h}{2}\left(r_o^2 - r_i^2\right) + \frac{r_o^3 - r_i^3}{3}\cos\theta\right]\mathrm{d}\theta \\
F &= -(p_o + g\rho f h)\;\pi\left(r_o^2 - r_i^2\right)
\end{aligned} \tag{D.23}$$

From this result, we see that the force on the end of the tube is equal to the pressure at the center of the tube end times the cross-sectional area of the tube. Is this a general result for any tube, or is it specific for a horizontal tube face? This can be generalized to any inclination and is an important result in fluid statics, in that the force of a fluid of constant density on a submerged flat surface is equal to the pressure at the centroid of the surface times the area of the surface.

D.4.5 Axial load in an inclined tube

We generalize the preceding statement with the following example of an inclined tube. The tube in Figure D.7 is inclined at some angle, α, from vertical. Note that, in oilfield applications, wellbore inclination angles are always measured from vertical not horizontal. So again the pressure at the center of the tube end at its end is given by

$$p = p_o + g\,\rho_f \tag{D.24}$$

where p_o is a surface pressure and h is the depth of the center of the tube end. If we use Newton's third law, again with the subscripts denoting a coordinate direction along the longitudinal axis of the tube, the axial force on the end of the tube is

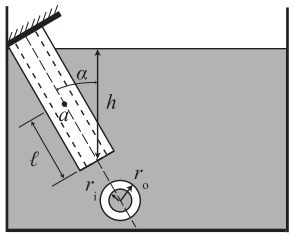

Figure D.7 Tube at a in inclined angle in a liquid.

$$\begin{aligned}
\sum F_s &= 0 \\
-F - \iint p\,\mathrm{d}A &= 0 \\
F &= -\int_{r_\mathrm{i}}^{r_\mathrm{o}} \int_0^{2\pi} \left[p_\mathrm{o} + g\rho_\mathrm{f}\left(h + r\cos\theta\sin\alpha\right)\right] r\,\mathrm{d}\theta\,\mathrm{d}r \\
F &= -\int_0^{2\pi} \frac{p_\mathrm{o}}{2}\left(r_\mathrm{o}^2 - r_\mathrm{i}^2\right)\mathrm{d}\theta - g\rho_\mathrm{f}\int_0^{2\pi}\left[\frac{h}{2}\left(r_\mathrm{o}^2 - r_\mathrm{i}^2\right) + \frac{r_\mathrm{o}^3 - r_\mathrm{i}^3}{3}\cos\theta\sin\alpha\right]\mathrm{d}\theta \\
F &= -\left(p_\mathrm{o} + g\rho_f\,h\right)\pi\left(r_\mathrm{o}^2 - r_\mathrm{i}^2\right) \qquad \text{(D.25)}
\end{aligned}$$

We see then that the result is the same. No matter what the inclination angle the hydrostatic force on the end of the tube is equal to the cross-sectional area of the tube times the pressure at the centroid of the tube end.

Now let us look at the axial force at some point, a, some distance, ℓ, from the end of an inclined tube:

$$\begin{aligned}
\sum F_s &= 0g\rho_s\pi\left(r_\mathrm{o}^2 - r_i^2\right)\ell\cos\alpha - \left[p_\mathrm{o} + g\rho_\mathrm{f}\pi\left(r_\mathrm{o}^2 - r_\mathrm{i}^2\right)h\right] - F_a = 0 \\
F_a &= g\pi\left(r_\mathrm{o}^2 - r_\mathrm{i}^2\right)\left(\ell\rho_\mathrm{s}\cos\alpha - h\rho_\mathrm{f}\right) - p_\mathrm{o} \qquad \text{(D.26)}
\end{aligned}$$

Notice that, as the inclination angle goes to 0° (vertical), Equation (D.26) is identical to Equation (D.21) with the addition of a surface pressure, and when the inclination goes to 90° (horizontal), it is identical to Equation (D.23).

D.4.6 Moment in a horizontal tube

Let us now look at one more example of a horizontal tube and determine the moment in the tube at some point a. We determine the moment about the x-axis, in Figure D.8.

Again we might be tempted to use Archimedes' principle as others have before. We try that using the buoyed weight of the end segment to find the moment at point a about the x-axis:

$$\sum M_x = 0$$

$$\int_{y_a}^{\ell} \pi\left(r_\mathrm{o}^2 - r_\mathrm{i}^2\right) g\left(\rho_\mathrm{s} - \rho_\mathrm{f}\right)\left(y - y_a\right)\,\mathrm{d}y - M_a = 0$$

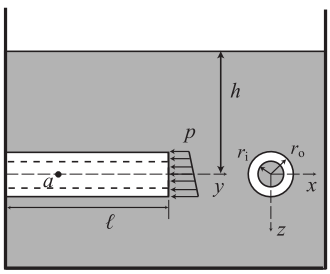

Figure D.8 A fixed horizontal tube.

$$M_a = \frac{(\ell - y_a)^2}{2} \pi \left(r_{\mathrm{o}}^2 - r_{\mathrm{i}}^2 \right) g \left(\rho_{\mathrm{s}} - \rho_{\mathrm{f}} \right) \tag{D.27}$$

That is pretty straight forward and relatively easy. Now, let us do it using the actual forces, and to save a little bit of calculation, we use the center of gravity of the segment as the length of the moment arm:

$$\sum M_x = 0$$

$$\frac{(\ell - y_a)^2}{2} g \left[\rho_{\mathrm{s}} \pi \left(r_{\mathrm{o}}^2 - r_{\mathrm{i}}^2 \right) + \rho_{\mathrm{f}} \int_0^{2\pi} (h + r_{\mathrm{o}} \cos\theta)\, r_{\mathrm{o}}\, \cos\theta \, \mathrm{d}\theta \right.$$

$$\left. - \rho_{\mathrm{f}} \int_0^{2\pi} (h + r_{\mathrm{i}} \cos\theta)\, r_{\mathrm{i}}\, \sin\theta \, \mathrm{d}\theta \right]$$

$$+ g\, \rho_{\mathrm{f}} \int_0^{2\pi} \int_{r_{\mathrm{i}}}^{r_{\mathrm{o}}} (h + r\cos\theta)\, r^2 \cos\theta \, \mathrm{d}r \, \mathrm{d}\theta - M_a = 0$$

$$M_a = \frac{(\ell - y_a)^2}{2} g \left[\rho_s \pi \left(r_{\mathrm{o}}^2 - r_{\mathrm{i}}^2 \right) - \rho_{\mathrm{f}} \pi r_{\mathrm{o}}^2 + \rho_{\mathrm{f}} \pi r_{\mathrm{i}^2} \right] + g\, \rho_{\mathrm{f}} \frac{\pi}{4} \left(r_{\mathrm{o}}^4 - r_{\mathrm{i}}^4 \right)$$

$$M_a = \frac{(\ell - y_a)^2}{2} g\, \pi \left(r_{\mathrm{o}}^2 - r_{\mathrm{i}}^2 \right) \left(\rho_{\mathrm{s}} - \rho_{\mathrm{f}} \right) + g\, \rho_{\mathrm{f}} \frac{\pi}{4} \left(r_{\mathrm{o}}^4 - r_{\mathrm{i}}^4 \right) \tag{D.28}$$

We can see immediately that the results are different. The first term of the result is the moment from gravity, and we see that it is exactly the same as the moment we derived using Archimedes' principle. But the second term is a moment at the end of the tube from the difference in the pressure from the top of the tube to the bottom of the tube. We might call this term a pressure-end moment. Clearly, this term is finite and does contribute to the moment in the tube, so it is not something fictitious that we can arbitrarily disregard. But, how significant is this term in oilfield applications? Let us look at an example to get some idea of the magnitude of that term in an oilfield context. Say, the tube is 9-5/8 in. casing with an inside diameter of 8.681 in., and the fluid is drilling fluid with a specific gravity of 2.0 (16.66 ppg, 124.64 lb/ft^3, or 1996 kg/m^3):

$$g\, \rho_{\mathrm{f}} \frac{\pi}{4} \left(r_{\mathrm{o}}^4 - r_{\mathrm{i}}^4 \right) = \frac{32.2 \left(\frac{\mathrm{ft}}{\mathrm{s}^2} \right)}{32.2 \left(\frac{\mathrm{lb\,ft}}{\mathrm{lbf\,s}^2} \right)} 124.64 \left(\frac{\mathrm{lb}}{\mathrm{ft}^3} \right) \frac{\pi}{4} \left\{ \left[\frac{\frac{9.625}{2}\,(\mathrm{in})}{12 \left(\frac{\mathrm{in}}{\mathrm{ft}} \right)} \right]^4 \right.$$

$$\left. - \left[\frac{\frac{8.681}{2}\,(\mathrm{in})}{12 \left(\frac{\mathrm{in}}{\mathrm{ft}} \right)} \right]^4 \right\} = 0.86 \text{ lbf ft} \tag{D.29}$$

This is a relatively small value in oilfield calculations (0.86 lbf ft or 1.16 J), so we almost always choose to ignore it. But if we choose to assume its value to be negligible, then we must certainly acknowledge at least to ourselves that we are doing so.

D.4.7 Moment in an inclined tube

That was for a horizontal tube, but what is generalized result for an inclined tube? In this example, the inclination angle is α, h is the depth at the center of the tube end, and s is a coordinate along the axis of the inclined tube. Now the pressure varies along the length of the tube.

$$\begin{aligned}
\sum M_x \;=\; & 0 \int_{s_a}^{\ell} g\,\rho_s \pi \left(r_o^2 - r_i^2\right)(s - s_a)\sin\alpha\,\mathrm{d}s \\
& + \int_{s_a}^{\ell}\int_{0}^{2\pi} g\,\rho_f \left\{[h - (\ell - s)\cos\alpha] + r_o \sin\alpha\cos\theta\right\} r_o\,(s - s_a)\cos\theta\,\mathrm{d}\theta\,\mathrm{d}s \\
& - \int_{s_a}^{\ell} \in_0^{2\pi} g\,\rho_f \left\{[h - (\ell - s)\cos\alpha] + r_i \sin\alpha\cos\theta\right\} r_i\,(s - s_a)\cos\theta\,\mathrm{d}\theta\,\mathrm{d}s \\
& + g\,\rho_f \int_0^{2\pi}\int_{r_i}^{r_o} g\,\rho_f\,(h + r\cos\theta\sin\alpha)\,r^2\cos\theta\,\mathrm{d}r\,\mathrm{d}\theta - M_a = 0 \\
M_a \;=\; & \frac{(\ell - s_a)^2}{2} g\left[\rho_s \pi\left(r_o^2 - r_i^2\right) - \rho_f \pi r_o^2 + \rho_f \pi r_i^2\right]\sin\alpha + g\rho_f \frac{\pi}{4}\left(r_o^4 - r_i^4\right)\sin\alpha \\
M_a \;=\; & \frac{(\ell - s_a)^2}{2} g\pi\left(r_o^2 - r_i^2\right)(\rho_s - \rho_f)\sin\alpha + g\rho_f \frac{\pi}{4}\left(r_o^4 - r_i^4\right)\sin\alpha \qquad \text{(D.30)}
\end{aligned}$$

This was also a bit tedious to do, but most of the terms evaluate to zero and the results are identical to the horizontal case, except for the sine of the inclination angle. Note that, as the inclination angle goes to zero (vertical wellbore), both terms, the gravitational moment and the pressure-end moment, vanish, as one would expect. Likewise, both terms are a maximum when the tube is horizontal.

D.5 Oilfield calculations

It is important that we become familiar with routine calculations involving hydrostatics in bore-hole applications. This is particularly important, because more often than not, we do not have measured pressures down hole, and we must rely on surface pressures and known fluid densities to calculate down-hole pressures and loads. In drilling and casing applications, we typically work with gauge pressures as opposed to absolute pressures. Atmospheric pressure is negligible in the context of these types of applications, so it typically is ignored, but at least we acknowledge here that we recognize the difference between absolute pressures, which include atmospheric pressure, and gauge pressures, which do not.

D.5.1 Hydrostatic pressures in wellbores

Liquid Columns

Calculating hydrostatic pressure of a liquid column in a wellbore is probably the most frequent type of calculation made in drilling, completion, intervention, and stimulation work. It is easy to do and one of the first things a field engineer learns to do. The best way to understand it is with an example. Figure D.9 shows a simple but common wellbore situation. A tube is hanging freely in a vertical wellbore with an

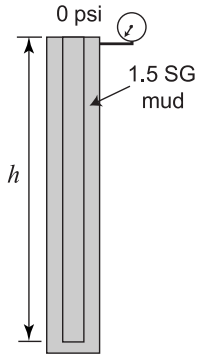

Figure D.9 An open-end tube suspended in a well.

open end. The wellbore fluid has a specific gravity of 1.5 and the depth of the tube is h. What is the hydrostatic pressure at the end of the tube?

The pressure can be calculated as

$$p = p_0 + g\rho_f h = p_0 + g\,(1.5\rho_w)\,h$$

where ρ_w is the density of water. This calculation is quite simple in SI units, because the density and depth are always in consistent units. For instance, if the depth is 3000 m, then the calculation is

$$p = 0 + \left(9.81\frac{\text{m}}{\text{s}^2}\right)(1.5)\left(998\frac{\text{kg}}{\text{m}^3}\right)(3000\,\text{m}) = 43.97 \times 10^6\frac{\text{N}}{\text{m}^2} = 43.97\,\text{MPa}$$

SI units are consistent and all these types of calculations are straight forward; however, USC units are not consistent and conversion factors are required. The fact that pressure is measured in psi (lbf/in.^{2}), depth in ft, and density in lb/gal basically means that length, area, and volume are measured in three distinct and inconsistent units. So let us derive the necessary conversion factor such that we may have it available for use in all our oilfield calculations of this type. One way to do this is as follows:

$$p = p_0 + g\,C_L\,g_c\,\rho_f\,h \tag{D.31}$$

where C_L is a conversion factor for the length, area, and volume units and g_c is a conversion factor for the mass units as previously discussed. We can calculate the value of this factor as

$$C_L = \left(\frac{\text{gal}}{231\,\text{in}^3}\right)\left(\frac{12\,\text{in}}{\text{ft}}\right)$$

$$C_L = 0.051948\,\left(\frac{\text{gal}}{\text{in}^2\,\text{ft}}\right)$$

$$\boxed{C_L \approx 0.052\,\left(\frac{\text{gal}}{\text{in}^2\,\text{ft}}\right)} \tag{D.32}$$

This is the factor commonly used in the oil field, and since any deviation of local gravity from standard gravity is usually negligible, the term $g \cdot g_c$ is assumed to be unity and generally is ignored in the USC system of units. However, this has also led to a certain amount of misunderstanding on the

part of those using these units, since the gravitational acceleration is an essential part of any equation dealing with gravitational body forces (e.g., hydrostatic pressure) and cannot be omitted. We could use the proper formula for pressure in a fluid of constant density as

$$p = p_0 + g\rho_f h \tag{D.33}$$

with the understanding that, when using USC units for calculation, it actually means

$$p = p_0 + g\, C_L\, g_c\, \rho_f\, h \tag{D.34}$$

and always keeping in mind that g_c is a conversion factor for ρ_h and not g. We take one more step to simplify that for our use. If we use specific weight instead of density, it makes the use of conversion factors somewhat easier. Specific weight is defined as

$$\gamma \equiv g\rho \tag{D.35}$$

In the English engineering system, this means

$$\gamma = g\, g_c \rho \tag{D.36}$$

The SI units of specific weight are N/m^3, and in USC units, they are lbf/gal. This makes the pressure formula slightly less cumbersome because the specific weight is a *pressure gradient*.

$$p = p_0 + \gamma\, h \tag{D.37}$$

Remember though that, in USC units, we still need the conversion factor for length, area, and volume as

$$p = p_0 + C_L \gamma\, h \tag{D.38}$$

If we take the previous example, with a depth of, say 10,000 ft, and calculate the pressure at the end of the tube it goes like this:

$$p = p_0 + C_L\, \gamma\, h$$

$$p = 0 + \left(0.052 \frac{\text{gal}}{\text{in}^2\,\text{ft}}\right)(1.5)\left(8.33 \frac{\text{lbf}}{\text{gal}}\right)(10,000\,\text{ft})$$

$$p = 6487\, \frac{\text{lbf}}{\text{in}^2}$$

And in SI units

$$p = p_0 + \gamma\, h$$

$$p = 0 + (1.5)\left(9810 \frac{\text{N}}{\text{m}^3}\right)(3048\,\text{m})$$

$$p = 44.85\ \text{MPa}$$

In the SI unit calculation, we used the specific weight of water at 4 °C to make life easier, so the results are slightly different. If you prefer, you could use the density at 20 °C and the specific weight of water would be $\gamma = g\rho = 9.81\,(998) = 9790\ N/m^3$. That type of calculation should become routine for the engineer or anyone doing hydrostatic calculations in wellbores. From now on, we do not show the conversion factor in the formula, so that the formula is not unit specific, but you must remember to include it when using USC units.

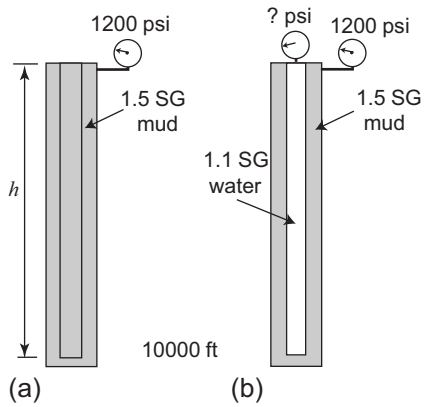

Figure D.10 (a) Same well with surface pressure and (b) same well with different fluids and surface pressure.

Figure D.10a shows another example of the same well with pressure on the surface. The formula is the same but the pressure at the surface is not zero in this case.

$$p = p_0 + \gamma_{\text{mud}}\, h$$
$$p = p_0 + (1.5\, \gamma_{\text{wtr}})\, h$$

If the surface pressure is 1200 psi, calculate the pressure at the bottom of the tube:

$$p = 1200 + 0.052\,(1.5)\,(8.33)\,(10000) = 7697 \text{ psi}$$

Figure D.10b shows different fluids in the same wellbore. In this case, the fluid in the annulus has a specific gravity of 1.5, as before, but the fluid in the tubing has a specific gravity of 1.1.

There is a pressure of 1200 psi on the annulus, and the tubing is closed at the surface. Here, our task is to calculate the pressure at the surface in the tubing. There are various ways to do this, but the easiest way is to set up an equality knowing the pressure in both the tubing and annulus are equal at the bottom of the tubing:

$$p_{0\,\text{tbg}} + \gamma_{\text{tbg}}\, h = p_{0\,\text{ann}} + \gamma_{\text{ann}}\, h$$

$$p_{0\,\text{tbg}} = p_{0\,\text{ann}} + \left(\gamma_{\text{ann}} - \gamma_{\text{tbg}}\right) h$$

$$p_{0\,\text{tbg}} = 1200 + (0.052)\,(1.5 - 1.1)\,(8.33)\,(10000)$$

$$p_{0\,\text{tbg}} = 2933 \text{ psi}$$

For a slightly different perspective, suppose we do not know the density of the fluid in the tubing, but we measure the pressure at the surface of the tubing to be 2000 psi. All other variables are the same. What is the specific gravity of the fluid in the tubing? What is the density of the fluid in the tubing? We start out exactly the same; that is, we know the pressure at the bottom of the tubing:

$$p_{0\,\text{tbg}} + \gamma_{\text{tbg}}\, h = p_{0\,\text{ann}} + \gamma_{\text{ann}}\, h$$

$$\rho_{\text{tbg}} = \frac{p_{0\,\text{ann}} + \gamma_{\text{ann}}\, h - p_{0\,\text{tbg}}}{g\, h}$$

$$\rho_{tbg} = \frac{p_{0\,ann} - p_{0\,tbg}}{g\,h} + \rho_{ann}$$

$$\frac{\rho_{tbg}}{\rho_{wtr}} = \frac{p_{0ann} - p_{0\,tbg}}{\gamma_{wtr}\,h} + \frac{\gamma_{ann}}{\gamma_{wtr}}$$

$$\hat{\rho}_{tbg} = \frac{p_{0\,ann} - p_{0\,tbg}}{\gamma_{wtr}\,h} + \hat{\rho}_{ann}$$

$$\hat{\rho}_{tbg} = \frac{1200 - 2000}{0.052\,(8.33)\,10000} + 1.5$$

$$\hat{\rho}_{tbg} = 1.32$$

And the answer to the second question is

$$\rho_{tbg} = \hat{\rho}_{tbg}\,\rho_{wtr} = 1.32\,(8.33) \approx 11.0\ \frac{\text{lb}}{\text{gal}}$$

The only difficulty with this particular problem is where to use the conversion factors, and that is just a matter of practice and familiarity with the units.

D.5.2 Buoyed weight of casing

To calculate the axial loads on casing, we have to find the weight of the casing in the fluid that surrounds it. We show the specific details of the calculations in Chapter 4, but will define some of the nomenclature here.

Weight of Casing in Air

In some casing designs, we use what we call the weight of the casing string in air. However, strictly speaking, we actually mean the weight of casing in a vacuum, since air is a gas and there is a difference in the pressure on the top and on the bottom of a casing string suspended in a borehole containing only air. However, this buoyant force is relatively small compared to the weight of the casing and usually ignored in practice. So *when we speak of the weight of casing in air, we actually ignore all buoyant forces on the casing string.* To calculate the weight of a casing string suspended vertically in air, we merely multiply the weight per unit length times the length to get the weight of the string and the axial load at the surface.

Weight of Casing in a Liquid

When the casing is hanging in a liquid, we must include the buoyant forces on the tube to determine the buoyed weight of the string and the axial loads. We already distinguished between the true axial load and something called the effective load. We saw that Archimedes' principle gave us the correct load at the surface but did not give us the true axial load at any other point within the string, but rather, what we called the effective axial load in Chapter 4. Another factor to consider is that, in most casing string designs, the wall thickness is not the same for the entire string, and that contributes further to the inaccuracy of using Archimedes' principle. To get the true axial load, we must use the actual forces attributable to the weight of the tube and the hydrostatic pressure at the points where it acts on cross-sectional areas.

The best way to understand the calculation procedure for the true axial load is to refer to a schematic of a casing string with different inside diameters. Figure D.11 shows a schematic of a casing string with

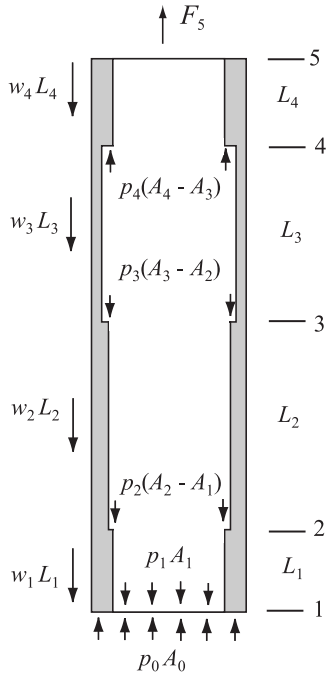

Figure D.11 Schematic of hydrostatic forces on a casing string.

four sections with three internal changes of diameter. We number the tops and bottoms of these sections as nodes starting at node 1 at the bottom and ending with node 5 at the top.[2] Wherever the cross-sectional area changes, we will have two calculations to make because there is a pressure step at that node. We calculate the axial force in the top of the joint just below the node, and then the axial load in the bottom of the joint just above the node. Please note the pressure at a cross-sectional area change has no effect on the casing below that point, *it only affects the axial load above that point*. There are a number of ways we could cast these equations, but this is an easy way to formulate them for programming. The first equation calculates the axial force at the bottom of section j just above its bottom node, j, and the second equation calculates the axial force at the top of section j just below its top node, $j + 1$.

$$\begin{aligned} F_j^{\downarrow} &= -p_0 A_0 + p_1 A_1 + \sum_{i=2}^{j} p_i \left(A_i - A_{i-1}\right) + \sum_{i=1}^{j-1} w_i L_i \\ j &= 1, \ldots, n \end{aligned} \tag{D.39}$$

$$\begin{aligned} F_j^{\uparrow} &= -p_0 A_0 + p_1 A_1 + \sum_{i=2}^{j} p_i \left(A_i - A_{i-1}\right) + \sum_{i=1}^{j} w_i L_i \\ j &= 1, \ldots, n \end{aligned} \tag{D.40}$$

[2] This numbering scheme is different from the first edition, and is a bit easier to program with most software (the earlier scheme was set for compatibility with C++).

where

$j =$ section number

$n =$ total number of sections in string

and the arrows denote the top or bottom of the sections (not the direction of the loads).

Note: Mathematically, the convention is that when a summation index, i, is initially greater than the summation limit, j or $j-1$, then the summation is zero. And in a case where $j-1<0$, then the summation is zero. This is standard in mathematics, but be cautioned that this is not always consistent in some programming languages.

While those formulas lend themselves easily to programming, they are a bit confusing if doing the calculations manually because they separate the bottom and top loads of each section and calculate them separately. When doing the calculations manually, we prefer to do them sequentially without having to repeat so many of the calculations in the summations. Here is a way to more easily visualize the process when doing the calculations sequentially and manually. The subscripts on the force, F_j , will refer to a section number. The arrow superscripts designate the bottom or top of section j. For example, $F_j^{\downarrow}$ is the load at the bottom of section j, and $F_j^{\uparrow}$ is the load at the top of section j. From the diagram, we easily see that the load at the bottom of section 1 is $F_1^{\downarrow} = -p_0A_0 + p_1A_1$. At the top of section 1 it is equal to the force at the bottom of section 1 plus the weight of section 1, $F_1^{\uparrow} = F_1^{\downarrow} + w_1L_1$. In the summation equations (D.39) and (D.40), these two quantities are calculated for each summation. For n sections of casing, both of these forces are calculated $2n$ times. The forces at the top and bottom of section 2 are calculated $2n-1$ times and so forth. If we calculate these in a sequence, $F_1^{\downarrow}, F_1^{\uparrow}, F_2^{\downarrow}, F_2^{\uparrow}, F_3^{\downarrow}, F_3^{\downarrow}$, and so on, we eliminate the repetitious calculations. We can further reduce the work of manual calculation by lumping similar types of calculations into groups.

Here is a simple procedure for manual calculation of the trues axial load:

1. Calculate the cross-sectional areas: $A_0, A_1, \ldots, A_n$.
2. Calculate the unbuoyed weight of each section: $W_i = w_iL_i$.
3. Calculate the pressure at each node: $p_0, p_1, p_2, \ldots, p_n, p_{n+1}$.
4. Starting at the bottom, calculate the force at the bottom of section 1, $F_1^{\downarrow}$, then the top of section 1, $F_1^{\uparrow}$, bottom of section 2, $F_2^{\downarrow}$, top of section 2, $F_2^{\uparrow}$, etc.

The procedure would then go in sequence as follows:

$$F_1^{\downarrow} = -p_0A_0 + p_1A_1$$

$$F_1^{\uparrow} = F_1^{\downarrow} + W_1$$

$$F_2^{\downarrow} = F_1^{\uparrow} + p_2\,(A_2 - A_1)$$

$$F_2^{\uparrow} = F_2^{\downarrow} + W_2$$

$$\vdots$$

$$F_j^{\downarrow} = F_{j-1}^{\uparrow} + p_j\left(A_j - A_{j-1}\right) \tag{D.41}$$

$$F_j^{\uparrow} = F_j^{\downarrow} + W_j \tag{D.42}$$

$$\vdots$$

$$F_n^{\downarrow} = F_{n-1}^{\uparrow} + p_n\,(A_n - A_{n-1})$$
$$F_n^{\uparrow} = F_n^{\downarrow} + W_n$$

Notice that we always start at the bottom. That is because the pressure at a node has no effect on the forces below it.

Buoyed Weight of Casing in Inclined and Curved Wellbores

Casing rarely hangs vertically in an actual wellbore. Most wells are inclined to some extent, and the wellbores are also curved. The casing is partially or sometimes totally supported by the walls of the borehole. Therefore, the axial load is that component of the gravitational body force not supported by the borehole wall. We ignore friction for now, but discuss it at length in Chapter 7. So, for our purposes here, the only force acting on the casing are the body forces of the casing attributable to gravity and the hydrostatic forces of the fluid in the wellbore.

There are two approaches we might take: (1) a trigonometric resolution of gravitational and pressure forces (as in the first edition) which is a bit tedious unless using specific software (see Figure D.12), or (2) use only true vertical depths for section lengths and pressure forces. The second is considerably easier to do and gives exactly the same result. The only caveat is that the section lengths are vertical projections and must be resolved into actual lengths for purchasing and actually running the casing. This is the method we use in this edition.

A Clarification on Buoyed Axial Loads

In Chapter 4, it is stated that the true axial load based on equilibrium forces and hydrostatics and the effective axial load based on Archimedes' principle will both give the same axial load at the surface. That is a true statement, but if you actually calculate them using the equations above and the buoyancy factors as shown in Chapter 4, you will find that the results do not agree. The difference is relatively small, but we know the results should be exactly the same except for a little numerical roundoff. Why don't they agree? It comes back to the fact that we use the nominal weight in our calculations, and the nominal weight is not the actual weight. If we used the actual weight to calculate the effective load, it would give us the exact buoyed load at the surface. But the equations above for the true load would not. The reason

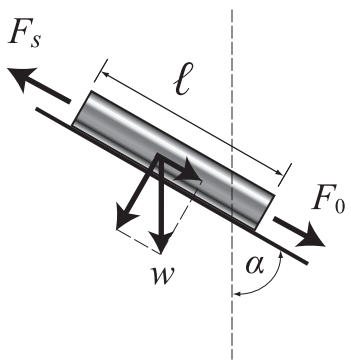

Figure D.12 A segment of casing in an inclined wellbore.

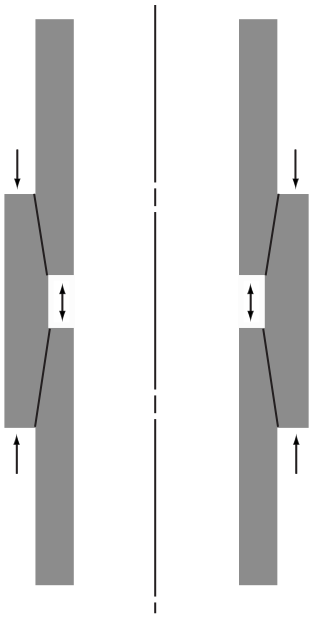

Figure D.13 Schematic of hydrostatic forces on a coupling.

the true load would not be accurate is because we did not take into account the couplings. There are buoyant forces on the couplings that are not accounted for in our casing schematic (Figure D.11). The forces acting on a coupling are shown in Figure D.13. While the difference between the pressure acting downward on the top edge and the upward pressure on the bottom edge is small, it makes a difference when you consider 200, 300, or more couplings. It is still easy to calculate the true axial load by using the actual body weight of the pipe from the pipe body formula (Equation (1.2) in Chapter 1). Then add in the weight and buoyant force on the couplings (you need calculate the magnitude of only one). If you program the procedure, all you need is ID and OD of the pipe, the OD of the coupling, and the density of the steel.

D.5.3 The ubiquitous vacuum

The foolish gaffes regarding a vacuum could be a great source of humor and professional teasing were it not for the serious costs that have often resulted. A perfect vacuum is zero absolute pressure and does not exist. In oilfield terms, that is roughly 15 psi less than atmospheric pressure. A near perfect vacuum by itself does not cause casing to collapse. It does not suspend a significant column of fluid in an annulus. I will not mention any specific instances (and I know of several) because, to this day, those involved are still embarrassed. If your design or operation procedure is close enough to a disaster that you have to consider a vacuum, then you are too close to worry about it. Revise your design or pause to think about the actual magnitude of a vacuum.

D.6 Closure

We may have spent an inordinate amount of time on basic hydrostatics, especially as the subject applies to oilfield casing in wellbores. One reason for this is that it is an important topic: a secondary reason is that there seems to exist a pervasive degree of confusion in the oil field about hydrostatics, especially in regard to buoyancy.

This page intentionally left blank

Appendix E: Borehole environment

Chapter outline head

E.1 Introduction to the borehole environment

We easily imagine a borehole as a vertical cylindrical hole drilled through a rigid medium. This is an ideal for visualization and understanding. Unfortunately, that picture is an idealization that is not true in practice. Actual boreholes are not straight except possibly over small intervals nor are they vertical except within small intervals. The rock in which the borehole is drilled is not a rigid medium, and though we may treat it as such, its mechanical behavior cannot be taken for granted in all applications. In this appendix, we examine the characteristics and mechanical behavior of this rock medium in brief. We then turn to the geometry of the borehole path and some of its consequences.

E.2 Pore pressure in rocks

Before getting into the mechanics of rock behavior, let us first explore an important property of sedimentary rocks, *porosity*. All sedimentary rocks contain voids called *pores*, the space between the

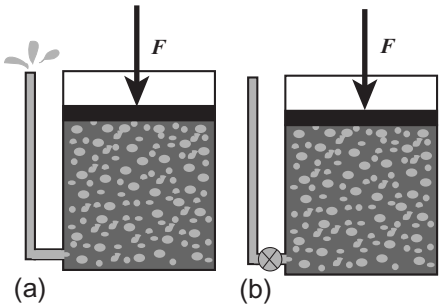

Figure E.1 Soil compaction model. (a) Free drainage and (b) restricted drainage.

solid grains of the sedimentary deposition and any other solids formed in the process. The volume fraction of the bulk rock that constitutes the pores is called *porosity*, $\phi = V_{\text{pores}}/V_{\text{bulk rock}}$. All pore spaces contain some type of fluid. The connectivity of pore spaces (if any) allows those fluids to flow through the rock. The measure of the conductivity of rock to fluid flow through the pore spaces is called *permeability*. While porosity and permeability are physically related, there is no general correlation between the two and the two terms are not interchangeable.

Pore pressure (also called formation pressure) is the pressure of the fluid that fills the pore spaces (or voids) in the rock. This pressure normally determines the lower limit of the drilling fluid density (exceptions are under-balanced drilling operations or some borehole stability problems). All sedimentary rock contains some type of fluid in the pore spaces and this fluid may be in the form of liquid or gas. In general, the pressure of the fluid is dependent on the depth of the rock and the density of the fluid, and in particular it depends on the connectivity, if any, of the pore spaces to the surface. We can illustrate the deposition process with a simple picture used by Terzaghi and Peck [72] to illustrate the nature of soil compaction as in Figure E.1a.

The cylinder, a, in the figure contains porous rock and liquid. A downward force, F, is applied to the piston representing the weight of subsequent layers of rock (called overburden) deposited above the sample. As the force (overburden weight) is increased with increasing deposition, the rock in the cylinder is compressed forcing some of the fluid into the drain tube whose length represents the depth of the rock below the earth's surface. If the fluid can flow freely into the tube and to the surface, it can be seen that no matter how deep the rock or the weight of the overburden the pressure of the fluid in the pore spaces will be equivalent to the hydrostatic pressure of the fluid column in the tube. This closely models the situation in many formations that have porosity or channels that freely connect to the surface (though the connection may be far from obvious). In this instance, the pore pressure of the formation is equal to the hydrostatic pressure of the fluid column between the formation and the surface. Typically, such a fluid contains dissolved minerals such as salt that makes the density greater than fresh water.

In general, the path through pore spaces of various formations from some depth to the surface is not quite so direct, and there may be considerable variation if the deposition, for instance, is occurring at a faster rate than the fluid can escape. This is illustrated in Figure E.1b where we have placed a valve or choke in the drain tube.

If we restrict the rate at which the fluid is allowed to escape as the formation is compacted by the increasing overburden, then the pressure of the fluid in the second cylinder will be higher than in the first cylinder because of the reduced rate at which the fluid is allowed to escape. Such a restriction could be caused by very low permeability formations between the sample and the surface for instance. If the

deposition rate slows or stops, the pore pressure might eventually equalize to the hydrostatic head of the fluid column, but such a process might require several hundred thousand years or so. In that case we might consider for all practical purposes that the escape tube is totally sealed depending upon where in the age of the process we drill into the formation. In the case where the fluid has been trapped or its escape severely restricted we consider the pore pressure to be abnormally high or *over-pressured*. It can be considerably higher than in the first model. We call such a formation an *under-compacted* formation, meaning that it has not compacted to a normal density for the given amount of overburden pressure because some of the fluid has been trapped and is also contributing to the support of the weight of the overburden. The fluid pressure could vary considerably from slightly above normal to an upper limit which would be a pressure equivalent to the weight of the overburden. We may write an expression as to the limitation of values the formation pressure can have:

$$\int_0^h g\,\rho_{\mathrm{f}}\,\mathrm{d}z \le p \le \int_0^h g\,\rho_{\mathrm{r}}\,\mathrm{d}z \tag{E.1}$$

where p is the formation pressure, g is the local acceleration of gravity, ρ_{f} and ρ_{r} are the densities of the fluid and rock, respectively, and z is a vertical coordinate axis. The limits of integration are from the surface to some depth, h. The term on the left is the hydrostatic pressure of a column of the formation fluid; the term on the right is the overburden pressure.

Since the density of the rock usually is consistent throughout a formation interval, the term on the right is generally computed incrementally as

$$p \le g \sum_{i=1}^{n} \rho_{\mathrm{r}i}\,\Delta z_i \tag{E.2}$$

where n is the number of different rock intervals and the subscript, i denotes the ith interval, and Δz_i is the ith interval thickness. This type of digital integration is a routine service of most logging companies running density logs.

Four obvious consequences of these two illustrations are that, (1) the density of an under-compacted formation will be less than that of a normally compacted formation since it contains a greater percentage of fluid; (2) if the fluid is salt water, the resistivity measurement from an electric log will be lower than the normal formation, again because it contains a greater percentage of fluid; (3) the acoustic travel time in the under-compacted formation will be less; and (4) if we are drilling through the two formations, the drilling rate will be faster through the under-compacted formation because it is less dense and the differential pressure between the drilling fluid and pore pressure will be less, hence the drilled cuttings will be more easily removed from the formation face. These four mechanisms are the primary means we have to detect the presence of abnormally high-pressured formations. While the fluid entrapment mechanism explains most of the abnormally high-pressured formations in the world, there are other causes such as a long gas column in a steeply dipped reservoir, artesian flow, a reservoir that has been pressured by a higher pressure reservoir during uncontrolled subsurface flow in a blowout, flow in an un-cemented casing annulus, and so forth. We have no means to detect these other types of situations except by direct measurements or previous knowledge of the situation.

On the other extreme, there are situations where the formation pore pressures are abnormally low, that is, less than the gradient of salt water. These cases are generally caused by depletion of the normal pore pressure by production of the fluids from the formation. This type of situation is generally known in advance of drilling (but not always).

Another point that is quite important is this. Much of what we know about formation pore pressures in a given area seems to fail miserably at shallow depths. A number of rigs have been lost because of drilling into shallow pockets of trapped gas. The uncertainty and unpredictability of the presence of these small shallow gas accumulations often require that small diameter pilot holes be drilled in some areas to ascertain their presence prior to starting a well. And in the case of low pressure there was at least one occurrence of a rig drilling into a shallow man-made mine shaft that swallowed the entire rig and all the water from a small lake. The data that one has available for casing point selection will seldom include data near the surface, and one should never assume that the absence of such data means that pore pressures near the surface are of no consequence.

There are various methods for determining or estimating the magnitude of pore pressures in a wellbore, and while we cannot go into those methods, here is a brief list of some methods and sources.

- Before drilling
  - Production data in area
  - Direct measurements in other wells
  - Log correlations
  - Paleontology correlations
  - Seismic correlations
- While drilling
  - Shale density measurements
  - Drilling rate monitoring
  - Gas monitoring
  - Full mud logging
  - Logging while drilling

For this text we will assume that we already have access to reasonable pore pressure estimates for our borehole, and after reading the above we have some fundamental understanding of what it means. Further in-depth reading may be found in the book by Fertl [12].

E.3 Basic rock mechanics

All rock under the surface is in a state of stress. This stress state is almost always a compressive state, in other words, subsurface rock is always under pressure. The source of the stress in most sedimentary environments is a gravitational load. Tectonic activity is another, but far beyond our discussion here. Simply put, the weight of the overlying rock, called the *overburden*, tends to vertically compress the rock beneath. The vertically compressed rock then tends to expand laterally because of the vertical compression. However, it cannot freely expand laterally because it is constrained by more rock also subject to the same overburden. Figure E.2a illustrates a block of subsurface rock with its typical principal *in situ* stress components. There is a vertical stress component, σ_v, a maximum horizontal component, labeled σ_H, and a minimum horizontal component, labeled σ_h. This is the normal case for most sedimentary environments, but be aware—not always. Usually, the relative magnitudes of the three principal stress components are $\sigma_v > \sigma_H > \sigma_h$ and the difference between the first two is usually significantly greater than the difference between the last two.

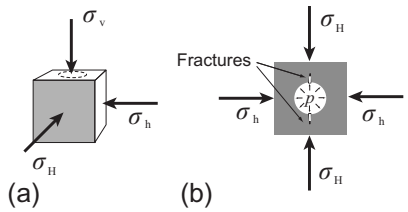

Figure E.2 *In situ* stress field. (a) General case and (b) fracture direction (top view).

It is relatively easy to determine the magnitude of the vertical stress component from density logs using

$$\sigma_{\mathrm{v}} = g \sum_{i=1}^{n} \rho_i \, \Delta z_i \tag{E.3}$$

The magnitude and direction of the minimum horizontal stress component can actually be measured with a mini-fracture test (more later), but quantifying the maximum horizontal stress component is much more difficult. Fortunately, we seldom need that value except in borehole stability analyses. What is most significant in our interest is the magnitude of the minimum horizontal stress component. In a vertical borehole, σ_{h} and the tensile strength of the rock determine the fracture pressure. A top view of a vertical borehole in Figure E.2b shows that a fracture initiates perpendicular to σ_{h} because it represents the least resistance to a fracture opening. This is a significant fact to remember: *a fracture always propagates perpendicular the least principal stress component.* Any exception usually mean flaws in the rock or a stress field that is changing because of large volumes and rates of fluids pumped during a hydraulic fracturing process. So if we know σ_{h} and the tensile strength of the rock we can calculate the fracture strength of the rock in this borehole with reasonable accuracy.[1]

We must discuss briefly one related topic. It was once common to theorize that rock was totally constrained laterally for all practical purposes because the only relief points for the constraint were often hundreds of miles distant. The consequence of such a theory is that the horizontal stress components are the same value in all directions, and that leads to the simple plane strain formula

$$\sigma_{\mathrm{h}} = \frac{\nu}{1-\nu}\sigma_{\mathrm{v}} \tag{E.4}$$

where σ_{h}, σ_{v}, and ν are the horizontal stress component, the vertical stress component, and Poisson's ratio for the rock, respectively. The vertical stress component is calculated using Equation (E.3). Equation (E.4) is then an easy formula and the reasoning makes sense. Unfortunately, the underlying assumption of total constraint is false. There are constraint reliefs such that the horizontal components are seldom equal and the formula is correct almost nowhere. It has been shown to be off by near 1000% in shallow depths and 100% in some deeper depths. The reason I even bring up this point is that this formula has historically been and still is being used to predict fracture pressures and gradients in drilling operations, *and it has been successful*. Why? It is because the Poisson's ratio value used in the formula is not the actual Poisson ratio of the rock but a "correlation" factor that has been "calibrated" to certain geographical areas and formations so that it yields a reasonable approximation of the minimum

[1] Inclined and horizontal boreholes bring added complexity that we will not address in this elementary discussion.

horizontal stress component to which is closely related to fracture pressure in a vertical well. It does not work in highly deviated and horizontal wells.

E.4 Fracture pressure

The pressure at which the matrix of a rock will physically fracture and admit the entrance of whole liquids depends upon a number of things. Here is what we normally expect when we think about that definition of fracture pressure:

- The wellbore liquid cannot enter the formation pore spaces prior to fracture (e.g., a filter cake building mud or an impermeable formation such as shale)
- The formation is in a state of compression from an *in situ* stress field (from overburden, lateral constraints, and/or tectonic activity)
- The formation matrix has some amount of cementation and hence some amount of tensile strength (may be relatively small though)

For this formation to be hydraulically fractured, the pressure of the liquid in the wellbore has to exceed both the near borehole stress field that is compressing the rock at the point of fracture and the tensile strength of the rock matrix at that point of fracture initiation. The near borehole stress field is usually not the same as the *in situ* stress field because the rock deforms slightly when some of it is removed to form the borehole, and consequently the stress field near the borehole has changed. Once the fracture is initiated, the fluid enters the fracture and the fracture will propagate at a lower pressure than the initial fracture pressure. The reason that the propagation pressure is lower than the original fracture pressure is that once the fracture is open, the fluid pressure acts similar to a wedge in the fracture. In other words, mechanical advantage is gained as the fracture length grows (up to a limit).

That definition is widely accepted. It is normally the way we interpret "fracture pressure" and that is what we usually assume when we design casing. However, the "fracture pressure" we utilize at the time of casing depth selection and casing design often comes from several different sources such as leakoff tests, integrity tests, fracture gradient curves/correlations, pilot hole mini-fracture tests, and production stimulation fracture treatments. Often the values obtained from these sources are not what we assumed from the above definition. Additionally, there are certain consequences of that definition of fracture pressure that we do not always anticipate, such as:

- Once fractured a formation as described above can never be pressured again to the original fracture pressure in that wellbore because it has no tensile strength at that point once fractured. Upon repressuring, the formation will open at the fracture closure pressure because the tensile strength, if any, is now permanently lost. The fracture closure pressure is a function of the *in situ* stress field and not the rock itself. The original tensile strength at the point of fracture is never restored. The rock is broken, and it stays broken. (*Note*: some mud systems may form plugs that can sometimes effectively divert the point of fracture to a different point in the rock matrix and cement can sometimes restore some tensile strength at a point).
- The fracture pressure also depends on the orientation and inclination of the borehole in most cases. The reason for that is that the principal *in situ* stress components are generally not equal in magnitude and their orientation in relation to the wellbore can vary. That is a complicating factor in that the fracture pressure is commonly reduced as the borehole inclination increases. The fracture pressure in an inclined wellbore will also vary with the azimuthal direction of the inclined wellbore as well as inclination angle.

Here are some other situations to consider about fracture pressure.

- Some formations have no tensile strength, e.g., unconsolidated sandstones, formations with micro fractures, faults, and so forth.
- A borehole fluid can actually enter the pore spaces under pressure prior to fracture (e.g., fracturing a porous formation with a clear fluid such as brine water).

In the case of no tensile strength, the fracture pressure depends entirely on the *in situ* stress field. It will open at the same pressure each time so that fracturing it does not reduce its strength as in the previous case. This is why in many areas it is perfectly "safe" to fracture a zone while drilling, because the "strength" of the formation has not been reduced. In actuality, the formation has no tensile strength; the compressive *in situ* stress field is what holds it together.

In the case of the pressured fluid entering the pore spaces before fracture occurs, the fracture pressure will usually be lower than in the earlier definition because there is mechanical advantage to the pressurized fluid in the pore spaces.

So we see that fracture pressure depends on orientation of the borehole to the stress field, the type of fracturing fluid we use, the permeability of the rock, and the tensile strength of the rock, if any. Awareness of those variations enable us to better understand exactly what fracture pressure means. However, fracture pressure values come from various sources, and we must understand the nature of the sources to know what the values mean.

E.5 Borehole stability

Though seldom considered in casing design, the stability of a borehole has for the most part been considered a drilling problem. With the significant increase in the number of horizontal wells being drilled, especially into shale formations that will be cased and fractured, it becomes a consideration in casing design too. When we consider that 90% of borehole stability problems occur in shales, we must have at least some rudimentary understanding of the phenomenon. We will present an overview here without going into the details of the rock mechanics involved. First, we look at an example stability curve, Figure E.3. This curve is for a specific formation at a specific depth, and shows a stable region between a collapse region on the left and a fracture region on the right as functions of mud density and inclination angle. You will notice that as the borehole is inclined more and more (toward the top) the window of stability decreases. Why is this? It has to do with the *in situ* stress field not being isotropic. The three principal *in situ* stress components are not equal, and in general we have $\sigma_{\mathrm{v}} > \sigma_{\mathrm{H}} > \sigma_{rmh}$ (vertical, maximum horizontal, minimum horizontal components). In a vertical well, the stability is governed by the two smaller stress components, σ_{H} and σ_{h}. But as the inclination angle increases the vertical stress component, σ_{v}, which is the largest of the three, begins to take on a more dominant role. The case shown here is somewhat severe, but it is from an actual well analysis.

If that were not enough, the stability curve also depends on the direction of the borehole as well as the inclination. Figure E.4 shows a case where it is not possible to select a mud density that will allow the hole to remain stable when inclined at more that about 65°. This is a curve for the same formation, same depth, and same well. The difference is that the first curve is an analysis based on drilling in the best direction and the second is based on drilling in the worst direction for stability. What is the best direction? the worst direction?

To answer that we must look at what is taking place in the rock when we drill a borehole through it. Since the rock is already in a state of compressive stress, it deforms some amount when we drill a borehole through it. In other words, we remove some of the rock and the remaining rock deforms because some amount supporting material has been removed. The local stress field changes. The question is: does

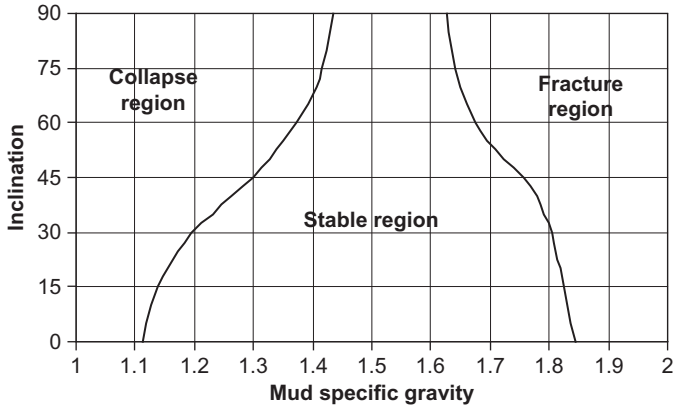

Figure E.3 A borehole stability plot in direction of σ_h.

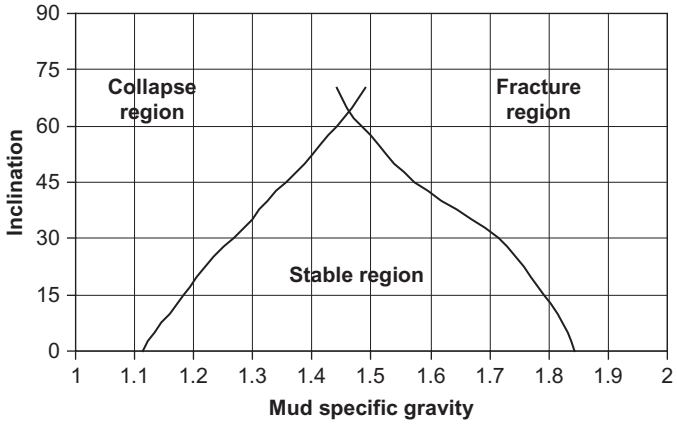

Figure E.4 A borehole stability plot, in direction of σ_H.

this change in the near-borehole stress field cause the rock to fail? That is what a stability analysis seeks to answer, as in Figures E.3 and E.4.

Figure E.5a shows a subsurface rock element with the three principal *in situ* stress components, where $\sigma_v > \sigma_H > \sigma_h$. In Figure E.5b, we have drawn the outline of two boreholes to be drilled through that rock, one vertical, and the other horizontal in the direction of the maximum horizontal stress component, σ_H.

In a thought experiment we may "drill" these two example boreholes, and if we know the original *in situ* stress components, we may calculate the resulting stress field around the borehole wall. In our case we will assume the following values: $\sigma_v = 10,000$ psi, $\sigma_H = 7500$ psi, and $\sigma_h = 7000$ psi. We can calculate all the resulting stress components at the borehole wall, but since the tangential stress component, σ_θ, is usually the most critical we will plot it (see Figure E.6). The plot shows the values of σ_θ at the borehole wall all around its circumference. (The starting point for measuring θ is immaterial in the vertical case, but in the figure it starts on the σ_H-axis.)

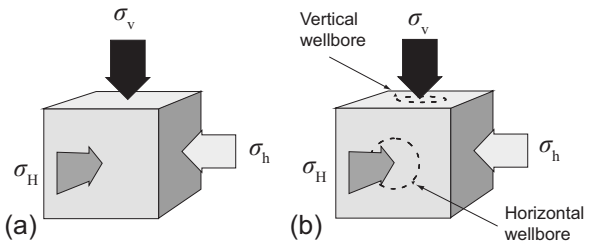

Figure E.5 *In situ* stress. (a) Typical orientation and (b) planned borehole orientations.

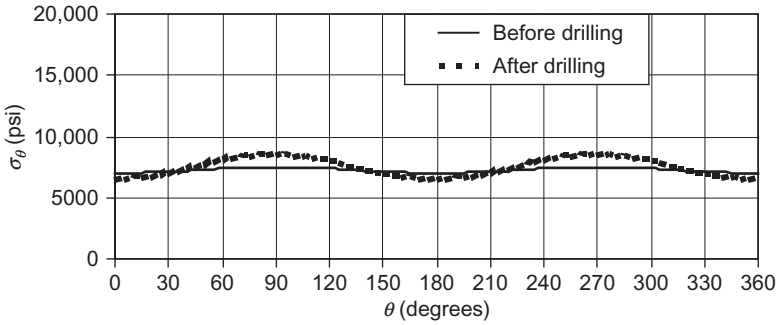

Figure E.6 Tangential stress component around borehole wall in a vertical well.

While it is hardly discernible in the graph, the tangential stress around the undrilled borehole circumference varies from 7000 to 7500 psi, the values of the horizontal *in situ* stress components. After the borehole is drilled, the resulting tangential stress around the circumference of the borehole wall varies from 6500 to 8500 psi. Such a difference tends to cause the borehole cross section to become slightly oval in shape. While this is not always obvious in most drilling situations, it is obvious in some and the hole must be reamed a little on each connection.[2] Once reamed additional deformation is usually inconsequential.

Next, we make the same plot for a horizontal borehole as shown in Figure E.5b. Again, we plot the tangential stress components in the rock where the borehole circumference will be when drilled. Then we calculate and plot the tangential stress components around the drilled borehole wall (see Figure E.7 where σ_θ is measured from the high side of the horizontal borehole). Here, we see that the predrilling stress components vary from 7000 psi on the high and low sides of the hole to 10,000 psi on the two sides, but once rock is removed to form the borehole, the rock deforms and the tangential stress component varies from about 4000 psi on the high and low points to 16,000 psi on the sides. This is a significantly more severe change in near-borehole stress field than in a vertical well in the same rock. It is this extreme difference that tends to cause excessive oval deformation and failure of the borehole in some horizontal wells.

[2] This has been quite troublesome in some coiled tubing drilling operations where there is no periodic pickup for connections. If drilling proceeds too far before reaming, it may not be possible to pull the bit back through the drilled interval.

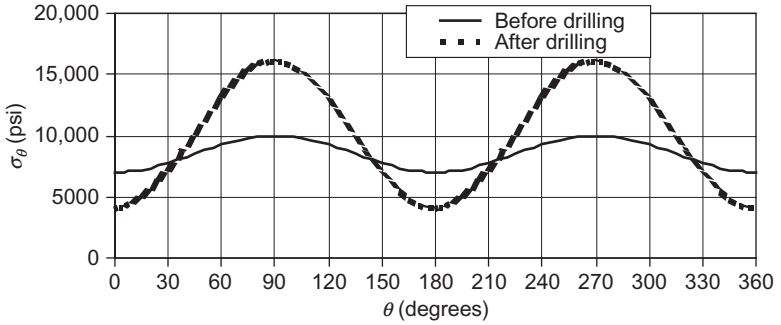

Figure E.7 Tangential stress components around borehole wall in a horizontal well.

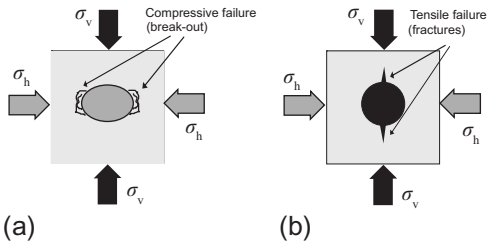

Figure E.8 Borehole instability. (a) Compressive break-out failure and (b) tensile fracture failure.

We must understand one thing about this deformation: *Unless the two in situ stress components perpendicular to the borehole axis are equal, the borehole deformation will result in an oval-shaped borehole, and there is nothing we can do to prevent it*. The degree of ovality may be insignificant or it may be sufficient to cause failure in some of the rock on the borehole wall. And in the case of rock failure, that too could be relatively insignificant or it could mean total borehole collapse. The only means we have of mitigating the effects and resulting damage of the deformation is by controlling the internal pressure (mud density), but because pressure is the same in all directions it cannot restore the near-borehole formation to its original round shape. Too little pressure and the formation may fail in compression on the two sides tangent to the maximum stress component as in Figure E.8a, and too much pressure and it may fracture the formation on the two sides where the wall is tangent to the minimum stress component (Figure E.8b).

Since the compressive and tensile failure points are at different locations on the borehole wall, it is possible that they can both occur concurrently. For example, we see that the borehole stability curve in Figure E.4 shows the two curves crossing at about 65° inclination. Had we extended those two curves beyond their intercept we would have defined an area where both collapse and fracture are possible, and that is exactly what can happen in some boreholes.

One critically important point, that must be understood when drilling horizontal wells for hydraulic fracturing, and that is that the *hydraulic fractures will always propagate perpendicular to the minimum principal in situ stress component*. Usually that is the minimum horizontal stress component, σ_h. Figure E.9 illustrates fracture propagation from boreholes drilled in the directions of the three principal *in situ* stress components. While the cylindrical borehole geometry affects the fracture orientation upon initiation at the borehole wall, once away from the wall, the fractures will always propagate and grow

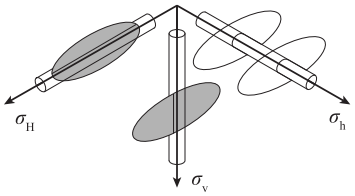

Figure E.9 Fracture propagation from boreholes oriented in the three principal *in situ* stress component directions where $\sigma_v > \sigma_H > \sigma_h$.

in a direction perpendicular to the minimum principal *in situ* component as shown. Obviously then, the borehole on the left side of the figure drilled in the direction of σ_H will have a very poor response a fracturing treatment except in cases where one is attempting to overcome vertical permeability limitations in a thin bed or one near a gas or water contact where fracture length as measured away from the wellbore is not desired.

The intent of this section is to give you a brief overview of the nature of borehole stability as it applies to highly deviated wellbores. Space here does not allow us to go into detail about obtaining data and making calculations for a stability analysis, but for your information the following are required:

- *In situ* stress components, σ_v, σ_H, σ_h (magnitudes and direction)
- Rock strength/failure properties
- Rock failure model

More information may be obtained in the book by Fjær et al. [71] and the paper by Yew and Li [73]. Also, in Chapter 2, we discussed other aspects and showed a pressure chart of a mini-frac used to obtain fracture data.

E.6 Borehole path

The basic tools for determining a borehole path are an *inclinometer* for measuring the borehole inclination (the deviation angle, α, of the borehole from vertical), a *magnetic compass* for measuring the borehole direction (azimuth angle, β, from magnetic north), and the *drill pipe measurements* for determining the length, Δs, along the borehole path between directional survey points. The resulting data defines a spatial direction vector at each survey point using α and β. The drill pipe measurement, Δs, is the distance between two of the vectors as *measured along the borehole path between them*. Contrary to what is often assumed, that is not enough information to specify the location of a second survey point even when the first of the two is known exactly. We must assume some shape of the borehole path between survey points in order to specify the location of the second survey point.

E.6.1 Minimum curvature method

The method for determining a borehole path used almost exclusively today is known as the *minimum curvature method* as proposed by Taylor and Mason [38] in 1972. They arrived at their method by minimizing a quadratic curve that will describe the minimum length quadratic path between two survey points and having the same vector directions as the survey vectors at the two ends. Their result is that the minimum quadratic borehole path between two survey points is approximated by a segment of a circle

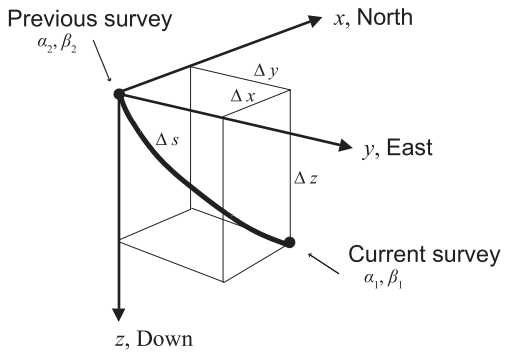

Figure E.10 Minimum curvature notation scheme.

in a plane. Their equations may be written in several forms using trigonometric identities, but here they are in the form presented in Taylor's and Mason's paper:

$$\Delta x = \frac{\Delta s}{\varphi}\left(v_x \sin\varphi + \frac{u_x - v_x\cos\varphi}{\sin\varphi} - \frac{(u_x - v_x\cos\varphi)\cos\varphi}{\sin\varphi}\right) \tag{E.5}$$

$$\Delta y = \frac{\Delta s}{\varphi}\left(v_y \sin\varphi + \frac{u_y - v_y\cos\varphi}{\sin\varphi} - \frac{\left(u_y - v_y\cos\varphi\right)\cos\varphi}{\sin\varphi}\right) \tag{E.6}$$

$$\Delta z = \frac{\Delta s}{\varphi}\left(v_z \sin\varphi + \frac{u_z - v_z\cos\varphi}{\sin\varphi} - \frac{(u_z - v_z\cos\varphi)\cos\varphi}{\sin\varphi}\right) \tag{E.7}$$

where

$v_x = \sin\alpha_1 \cos\beta_1$

$v_y = \sin\alpha_1 \sin\beta_1$

$v_z = \cos\alpha_1$

$u_x = \sin\alpha_2 \cos\beta_2$

$u_y = \sin\alpha_2 \sin\beta_2$

$u_z = \cos\alpha_2$

and

$$\varphi = \cos^{-1}\left[u_x v_x + u_y v_y + u_z v_z\right] \tag{E.8}$$

Note: φ *must be in radians in these equations*.

The numerical subscripts refer to the current survey (1) and the previous survey (2). The letter subscripts refer to the physical directions: x is North/South, y is East/West, and z is Down/Up. The quantities Δx, Δy, and Δz represent the changes in North/South, East/West, Down/Up, respectively, since the previous survey with North (+), South (−), East (+), West (−), Down (+), and Up (−). The quantity, Δs, is the measured length of the well path between the two survey points.

E.6.2 Interpolations on the borehole path

For a number of computations, such as contact force for friction calculations and casing wear, and for bending stress magnification, it is often necessary to determine the location of points along a borehole path on a finer nodal mesh than is given by the directional survey results which are typically on intervals ranging from 30 to 90 ft. where the direction is being tightly controlled and significantly longer intervals elsewhere. There are various ways to do this, the most common being a simple linear interpolation of the inclination and azimuth angles separately between survey points. While that produces sufficient accuracy for most measurements and calculations, it ignores the foundational premise of the current survey method used by the industry. Such an interpolation constitutes a radius of curvature method, whereas the well path is calculated by a minimum curvature method. Here, we show a consistent method of interpolation based on the same assumptions of the minimum curvature method.

General interpolation procedure

Given two successive survey sets, (α_a, β_a, s_a) and (α_b, β_b, s_b) at survey points a and b respectively, we want to determine the survey data for any arbitrary nodal point(s) between them using the minimum curvature method as the basis of the interpolation (refer to Figure E.10). The survey angles at points a and b describe two tangent vectors on the geodesic curve connecting the two points. That and the length of that geodesic, $\Delta s = s_b - s_a$, give us enough information to determine a tangent vector at any node on the curve between the two points. The general procedure is as follows.

1. Translate measured angles (inclination and azimuth) for the two tangent vectors into coordinate descriptions in the global coordinate system
2. Using the minimum curvature assumption that these two vectors are in the same plane, calculate the angle between them using the inner product
3. Using that angle and the arc length distance between them, determine the radius of curvature of the well path geodesic
4. Calculate the binormal vector to the arc using the vector product (cross product) of the two tangent vectors
5. Calculate the normal vector at point a using the vector product of the binormal vector and the tangent vector at point a
6. These three orthogonal vectors (tangent, normal, and binormal) form a local coordinate system at point a from which we can determine a tangent vector at any node between point a and point b
7. Determine the incremental angle along the geodesic between point a and the interpolation node
8. Calculate the tangent vector at the node in the local coordinate system
9. Calculate the projection of that tangent vector back into the global coordinate system
10. Calculate the inclination and azimuth at that node

Specific interpolation procedure

Starting at the top of the borehole, the interpolation nodes will be numbered $i = 1, 2, \ldots, n$. The node variables for inclination, azimuth, and measured depth will be noted as α_i, β_i, and s_i, respectively. The survey points will be numbered $k = 1, 2, \ldots, m$ and generally $n > m$. The survey variables for inclination, azimuth, and measured depth will be noted likewise as A_k, B_k, and S_k. In order to simplify the notation for interpolation within each survey interval we define six scalar variables α_a, β_a, and s_a as the values for A_k, B_k, and S_k, respectively, at the beginning of the interval and α_b, β_b, and s_b as the values for A_{k+1}, B_{k+1}, and S_{k+1} at the end of the interval.

Initialize the survey index, $k = 1$

1. Loop through all the nodes $i = 1, n$ incrementing the survey intervals as required:
2. Initialize α_a, β_a, s_a, α_b, β_b, and s_b.

3. Determine if the node depth, s_i, falls within the measured depth interval of surveys a and b, such that $s_a \leq s_i < s_b$. Note that the first survey depth is considered to be part of the interval and the second is not. We use the closed/open interval, $[s_a, s_b)$, where s_b defines the end of the interval but is not included in the interval. This is an arbitrary computational convenience.
4. If s_i does not fall within the interval, proceed to the next survey interval by incrementing k and repeat the first step.
5. If $s_i = s_b$ then assign that node the values of the survey at that same depth, $\alpha_i = \alpha_a$ and $\beta_i = \beta_a$, return to the first step where the node number, i, will be incremented to $i + 1$. (Usually node 1 will coincide with the first survey and in that case you would assign that survey value to node 1, return to step 1 and increment to node 2.)
6. If s_i is within the interval and $s_i \neq s_a$, determine the two unit vectors in global coordinates using the following transform.

$$\hat{\mathbf{t}} = \left(\sin\alpha_a \cos\beta_a \,\hat{\mathbf{e}}_1, \sin\alpha_a \sin\beta_a \,\hat{\mathbf{e}}_2, \cos\alpha_a \,\hat{\mathbf{e}}_3\right) \tag{E.9}$$

$$\hat{\mathbf{v}} = \left(\sin\alpha_b \cos\beta_b \,\hat{\mathbf{e}}_1, \sin\alpha_b \sin\beta_b \,\hat{\mathbf{e}}_2, \cos\alpha_b \,\hat{\mathbf{e}}_3\right) \tag{E.10}$$

In the Cartesian coordinate system that we are using, both those tangent vectors are unit vectors.

7. The scalar product (inner or dot product) of these two unit vectors is the cosine of the angle between them, so

$$\cos\varphi = \hat{\mathbf{t}} \cdot \hat{\mathbf{v}} \rightarrow \varphi = \cos^{-1}\left(\hat{\mathbf{t}} \cdot \hat{\mathbf{v}}\right)$$

and we have

$$\varphi = \cos^{-1}\left(t_1 v_1 + t_2 v_2 + t_3 v_3\right) \tag{E.11}$$

8. Since we assumed that the borehole path is a geodesic on a sphere we can now determine the radius of the sphere with the familiar arc formula, $s = r\theta$, and in our nomenclature where $s = \Delta s = s_b - s_a$ the radius is

$$r = \left|\frac{\Delta s}{\varphi}\right| \tag{E.12}$$

We use the absolute value signs here as a radius is always taken to be positive. However, in our case Δs will always be positive unless we have made a mistake because $s_b > s_a$.

9. We know that the two tangent vectors are in the same plane as the two radius vectors, and that the two radius vectors are normal to the two tangent vectors, respectively. Hence a radius vector is usually called a normal vector. A vector normal to both the tangent vectors and the radius vectors (remember they are all in the same plane) is called a binormal vector. The binormal vector is easily found using the vector product (or cross product) of the two survey tangent vectors.

$$\mathbf{b} = \hat{\mathbf{t}} \times \hat{\mathbf{v}} = \det\begin{bmatrix} \hat{\mathbf{e}}_1 & \hat{\mathbf{e}}_2 & \hat{\mathbf{e}}_3 \\ t_1 & t_2 & t_3 \\ v_1 & v_2 & v_3 \end{bmatrix}$$

$$\mathbf{b} = \left[\left(t_2 v_3 - t_3 v_2\right)\hat{\mathbf{e}}_1, \left(t_3 v_1 - t_1 v_3\right)\hat{\mathbf{e}}_2, \left(t_1 v_2 - t_2 v_3\right)\hat{\mathbf{e}}_3\right] \tag{E.13}$$

The two vertical bars denote the determinant of the matrix given by the expansion on the right. The vectors, $\hat{\mathbf{t}}$ and $\hat{\mathbf{v}}$ are unit vectors, but they are not orthogonal to each other so their product $\mathbf{b}$ is not a unit vector, so it will be convenient to unitize it now.

$$\hat{\mathbf{b}} = \frac{\mathbf{b}}{\|\mathbf{b}\|} = \frac{\left(b_1\hat{\mathbf{e}}_1, b_2\hat{\mathbf{e}}_2, b_3\hat{\mathbf{e}}_3\right)}{\sqrt{b_1^2 + b_2^2 + b_3^2}} \tag{E.14}$$

10. At the first survey point we have the unit tangent vector, $\hat{\mathbf{t}}$, and the unit binormal vector, $\hat{\mathbf{b}}$, but we do not yet have the normal vector at that survey point which we will need to form a local coordinate system aligned with the three principal direction vectors at that point. Again we use the vector product but with the unit tangent vector and binormal vectors, $\hat{\mathbf{t}}$ and $\hat{\mathbf{b}}$, at survey point a to calculate the normal vector.

$$\hat{\mathbf{n}} = \hat{\mathbf{b}} \times \hat{\mathbf{t}} = \det \begin{bmatrix} \hat{\mathbf{e}}_1 & \hat{\mathbf{e}}_2 & \hat{\mathbf{e}}_3 \\ b_1 & b_2 & b_3 \\ t_1 & t_2 & t_3 \end{bmatrix}$$

$$\hat{\mathbf{n}} = \left[(b_2\, t_3 - b_3\, t_2)\, \hat{\mathbf{e}}_1, (b_3\, t_1 - b_1\, t_3)\, \hat{\mathbf{e}}_2, (b_1\, t_2 - b_2\, t_3)\, \hat{\mathbf{e}}_3 \right] \tag{E.15}$$

In this case the unit vectors, $\hat{\mathbf{b}}$ and $\hat{\mathbf{t}}$, are orthogonal to each other and their orthogonal vector product, the normal vector, $\mathbf{n}$ is also a unit vector.

11. From this local coordinate system we will interpolate the tangent vectors at any point within the interval between point a and point b. Note that we will no longer need the tangent vector, $\mathbf{v}$, within this interval because we only needed it to establish the plane in which the tangents and radii reside. The triad of unit vectors we have just calculated form a local unit basis, $\hat{\mathbf{e}}$:

$$\hat{\mathbf{t}} = \hat{\mathbf{e}'}_1$$
$$\hat{\mathbf{b}} = \hat{\mathbf{e}'}_2$$
$$\hat{\mathbf{n}} = \hat{\mathbf{e}'}_3$$

12. Next we calculate the tangent vector at a node in the local coordinate system by first determining the distance and angle between the node and survey point a.

$$\Delta s = s_i - s_a$$

$$\Delta\varphi = \frac{\Delta s}{r} \tag{E.16}$$

13. Then we calculate the tangent vector in local coordinates

$$\tau'_1 = \cos(\Delta\varphi) \tag{E.17}$$

$$\tau'_2 = \sin(\Delta\varphi) \tag{E.18}$$

$$\tau'_3 = 0 \tag{E.19}$$

14. Then we calculate the projection of this vector into the global coordinates

$$\hat{\tau}_1 = \frac{\tau'_1\, \hat{t}_1}{|\tau'_1|} + \frac{\tau'_2\, \hat{n}_1}{|\tau'_2|} \tag{E.20}$$

$$\hat{\tau}_2 = \frac{\tau'_1\, \hat{t}_2}{|\tau'_1|} + \frac{\tau'_2\, \hat{n}_2}{|\tau'_2|} \tag{E.21}$$

$$\hat{\tau}_3 = \frac{\tau'_1\, \hat{t}_2}{|\tau'_1|} + \frac{\tau'_2\, \hat{n}_3}{|\tau'_2|} \tag{E.22}$$

15. And lastly, we convert this nodal tangent vector to an inclination angle and azimuth

$$\alpha_i = \tan^{-1}\left(\frac{\hat{\tau}_2}{\hat{\tau}_1}\right) \tag{E.23}$$

$$\beta_i = \left| \tan^{-1}\left(\frac{\sqrt{\hat{\tau}_1^2 + \hat{\tau}_2^2}}{\hat{\tau}_3}\right) \right| \tag{E.24}$$

A programmable algorithm for this procedure is listed later.

Programming borehole path calculations

The algorithm for doing directional survey calculations using Taylor and Masons method is fairly straightforward and the calculations may easily be done manually using a hand-held calculator though almost no one does that now. The serious drawback to manual calculations is that the errors are cumulative, so that an error in one calculation carries forward to all subsequent calculations. The task of programming directional survey calculations for a spreadsheet or some compiled program is easy but there are a few eccentricities involved that should be noted.

Accounting for straight sections

It is not uncommon that two consecutive surveys will be identical, and in fact this is often desirable in vertical wells and some sections of directional wells. A program designed to employ only the minimum curvature algorithm will likely crash when it encounters two consecutive and identical surveys because the radius of curvature between the two identical surveys goes to infinity, in other words, the section is not a curve but is straight. A simple logic test to compare successive surveys can avoid this totally and the straight section can be handled by a straightforward trigonometric calculation. Along this line, it has been noted that some directional service companies using spreadsheets to calculate directional surveys have gotten around this with a procedure that adds and subtracts very small amounts to the data during calculations to avoid any infinities in the minimum curvature calculations. While this reeks of programming laziness, the quantities used are usually on the order of 1.0×10^{-8} so the accuracy may not be affected beyond the accuracy of the measurements themselves.

Accounting for large azimuth changes

While one might think large azimuth changes between survey points are rare, that is not the case. In near vertical wells with small inclination it is not that unusual to see azimuth changes of up to 180° between consecutive surveys. Though the magnitude of the change of azimuth might be large, at very small inclination angles the change in the borehole path is minimal. Two problems arise in programming azimuth. One is the case of the zero inclination in which azimuth is meaningless because there is no azimuth for a vertical borehole. As common practice, the azimuth may be assigned arbitrarily to the same value as the previous survey, or especially in the case of the surface location it may be set to zero.

The other case that must be accounted for and which arises in *contact force calculations* where a net change in azimuth, $\Delta\beta = \beta_b - \beta_a$, cannot be more than 180° or less than −180°, i.e., $-180° < \Delta\beta \leq 180°$.[3] For example, if the azimuth for one survey is $\beta_a = 12°$ and the next survey azimuth is $\beta_b = 344°$, then the net change in azimuth between the two surveys is −28° not 332°. This is shown mathematically as

$$\text{if} \begin{cases} \beta_b - \beta_a < -180° \rightarrow \Delta\beta = \beta_b - \beta_a + 360° \\ \beta_b - \beta_a \geq 180° \rightarrow \Delta\beta = \beta_b - \beta_a - 360°\,. \end{cases}$$

Other considerations

It is always good to keep in mind that a drilling assembly is a relatively large physical object that does not change direction rapidly or lend itself to mathematical oddities like reversing direction between

[3] While one can consider a rotation of up to 360°, the net change in direction cannot exceed ±180°.

surveys (except as previously discussed for small inclinations). Also, the mathematical possibility exists that since the two survey vectors are assumed to be in the same plane the inner product could be zero meaning that the two survey directions are perpendicular to each other, which should not be the case in a drilled borehole where the survey points are reasonably spaced.

Interpolation algorithm

For programming purposes the interpolation procedure is given in two algorithms below where

$s_t =$ total measured depth
$s_i =$ nodal measured depth
$\alpha_i =$ nodal inclination
$\beta_i =$ nodal azimuth
$S_k =$ survey measured depth
$A_k =$ survey inclination
$B_k =$ survey azimuth

All other variables should be self explanatory. In this general algorithm, we assume the first survey is at zero depth and that the first node is also at zero depth, otherwise the algorithms should be modified to take other cases into account. The procedure consists of two algorithms. The first is the main or controlling program that sets up the survey data and calls the interpolation subroutine.

Algorithm E.1 Main Interpolation Program

```
set n equal to number of nodes
set m equal to number of surveys
calculate nodal depth interval; Δs = s_t/n
initialize first depth s_i = 0 at i = 1
for remaining node depths, i = 2,n
  {increment depth; s_i = s_i-1 + Δs}
initialize survey counter, k = 1
do while k < m
{
  for each interpolation node, i = 1,n
  {
     if (s_i = S_k)
        {set node depth to first survey depth; s_i = S_k
         set node incl. to survey incl.; α_i = A_k
         set node azimuth to survey azimuth; β_i = B_k}
     else if (S_k < s_i < S_k+1)
        {call Minimum Curvature Interpolation subroutine}
     else
        {increment survey counter; k = k+1}
  }
}
```

The algorithm for the interpolation subroutine is:

Algorithm E.2 Minimum Curvature Interpolation Subroutine

```
{
  calculate tangent vectors; t̂ and v̂, eqns.E.9 and E.10
  calculate included angle; φ, eqn. E.11
  calculate depth increment; Δs = s_b − s_a
  calculate radius of curvature; r = Δs/φ, eqn. E.12
  calculate the bi-normal vector, b, eqn. E.13
  unitize the bi-normal vector, b̂, eqn. E.14
  calculate the unit normal vector, n̂, eqn. E.15
  calculate the angle from survey to node, Δφ, eqn. E.16
  calculate the nodal local tangent vector, τ, eqns.(E.17)-(E.19)
  calculate the nodal global tangent vector, τ̂, eqns.(E.20)-(E.22)
  calculate the nodal inclination, α_i, eqn. E.23
  calculate the nodal azimuth, β_i, eqn. E.24
}
```

We now have an interpolated survey at that node using the minimum curvature method for the interpolation rather than a linear interpolation of inclination and azimuth separately which amounts to a radius of curvature interpolation.

Comments on the interpolation method

While this method is more refined than a linear interpolation, the difference in the results is not necessarily that significant in many applications, and for a two-dimensional borehole profile where there is no change in azimuth, the results are exactly the same. The algorithm is easily programmed and interpolations can be made for a mesh of one foot, a half meter, or one meter intervals if desired. The run time is very short (less than a second) on most desktop and laptop PCs using Fortran or C++, but a little longer if programmed within a spreadsheet using VBA. The interpolation method can generate a uniform mesh at much shorter intervals than is common for actual directional survey data. This does make a difference when calculating borehole friction and especially in calculating points of maximum contact force for determining the critical casing wear locations. Though the final results may not include the actual survey points except where the nodes and survey points may accidentally coincide, this is not seen as a disadvantage in this type of work.

This interpolation method is quite useful in a number of borehole applications. The run time for one foot intervals is negligible, but output for plotting purposes is excessive at those intervals. The usual procedure is a subroutine to scan larger intervals of say, 100 ft., and pick the maximum value (contact force, bending stress magnification, etc.) within that interval for output and plotting.

E.7 Closed-Form friction solutions

The full discussion of borehole friction is in Chapter 7, but here I add some additional information that may be of peripheral interest. From the three-dimensional differential equations for borehole friction derived by Sheppard et al. [41], we may specialize these into two-dimensional form by assuming there is no change in azimuth ($\beta = 0$). Further, we assume that the borehole path is a series of circular arcs as calculated by the minimum curvature method which is the standard for determining the borehole path

and location. With these assumptions we are able to obtain closed-form solutions for borehole friction in both upward and downward motions as well as in pure rotation mode.

E.7.1 Closed-Form drag solutions

In two dimensions, the governing differential equation for tension may be solved exactly if we have a closed-form expression for the curvature as a function of the axial coordinate s.

$$\frac{\mathrm{d}\hat{F}}{\mathrm{d}s} = \bar{w}\,\cos\alpha \pm \mu \left| \hat{F}\frac{\mathrm{d}\alpha}{\mathrm{d}s} + \bar{w}\,\sin\alpha \right| \tag{E.25}$$

Now for sections with constant build angle the curvature, $\mathrm{d}\alpha/\mathrm{d}s$, is given exactly by

$$\frac{\mathrm{d}\alpha}{\mathrm{d}s} = \frac{\alpha - \alpha_0}{s} \tag{E.26}$$

This is a first-order linear ordinary differential equation and is easy to solve. There is a complicating facet, though, and that is the necessity of maintaining the absolute value of the contact force even though these terms must be separated to get a solution. Without going into the details we will give the solutions, and the necessary criteria for their use.

Closed-Form solutions for upward motion

The two solutions for pulling casing out of the hole where the friction term is positive are

$$\begin{aligned}\hat{F}^{(+)} &= \mathrm{e}^{\mu(\alpha-\alpha_0)}\left\{\hat{F}_0 + \frac{\bar{w}\,s}{(\alpha-\alpha_0)\left(\mu^2+1\right)}\left[\left(\mu^2-1\right)\sin\alpha_0 + 2\mu\cos\alpha_0\right]\right\} \\ &\quad - \frac{\bar{w}\,s}{(\alpha-\alpha_0)\left(\mu^2+1\right)}\left[\left(\mu^2-1\right)\sin\alpha + 2\mu\cos\alpha\right]\end{aligned} \tag{E.27}$$

and

$$\begin{aligned}\hat{F}^{(-)} &= \mathrm{e}^{-\mu(\alpha-\alpha_0)}\left\{\hat{F}_0 + \frac{\bar{w}\,s}{(\alpha-\alpha_0)\left(\mu^2+1\right)}\left[\left(\mu^2-1\right)\sin\alpha_0 - 2\mu\cos\alpha_0\right]\right\} \\ &\quad - \frac{\bar{w}\,s}{(\alpha-\alpha_0)\left(\mu^2+1\right)}\left[\left(\mu^2-1\right)\sin\alpha - 2\mu\cos\alpha\right]\end{aligned} \tag{E.28}$$

The $(-)$ solution, Equation (E.28), is used where the following conditions exist

$$\hat{F}\frac{\mathrm{d}\alpha}{\mathrm{d}s} < \bar{w}\,\sin\alpha \quad \text{and} \quad \left|\hat{F}\frac{\mathrm{d}\alpha}{\mathrm{d}s}\right| > \bar{w}\,\sin\alpha$$

for all other cases the $(+)$ solution, Equation (E.27), is used.

Closed-Form solutions for downward motion

For running casing in the hole, the sign of the friction term is negative. This leads to solution equations identical to Equations (E.27) and (E.28). However, in this case where

$$\hat{F}\frac{\mathrm{d}\alpha}{\mathrm{d}s} < \bar{w}\,\sin\alpha \quad \text{and} \quad \left|\hat{P}\frac{\mathrm{d}\alpha}{\mathrm{d}s}\right| > \bar{w}\sin\alpha$$

we must use Equation (E.27), the (+) solution, and for all other cases we must use Equation (E.28), the (−) solution.

Remarks on the Closed-Form solution

While the closed-form solutions may appear rather complex they are quite easily set into simple computer programs. The complicating factor is the problem of dealing with two solution equations and patching them together where the magnitudes of the gravitational contact force is smaller in magnitude than the contact force from tension. In order to patch these equations together it is necessary to get the solution at incremental points along with the values of the contact force components to determine which equation to use. This would seem to defeat the purpose of having an exact solution since a numerical solution requires an incremental approach also.

E.7.2 Closed-Form torque solution

For a constant curvature in a two-dimensional wellbore, the equation for rotational torque reduces to

$$\frac{\mathrm{d}T_\mathrm{q}}{\mathrm{d}s} = r_\mathrm{o}\,\mu \left| \bar{w}\,\sin\alpha + \hat{F}\frac{\mathrm{d}\alpha}{\mathrm{d}s} \right| \tag{E.29}$$

and

$$\hat{F} = \hat{F}_0 - \int_0^s \bar{w}\,\cos\alpha\,\mathrm{d}\bar{s} \tag{E.30}$$

The constant curvature in a plane means that

$$\frac{\mathrm{d}\alpha}{\mathrm{d}s} = \pm\kappa = \mathrm{sgn}\,(\alpha_s - \alpha_0)\,\kappa \tag{E.31}$$

where sgn is the signum operator, e.g., if $(a-b) > 0$ then $\mathrm{sgn}\,(a-b) = +1$ and if $(a-b) < 0$ then $\mathrm{sgn}\,(a-b) = -1$, and κ is the curvature of the borehole path (assumed constant here) and is considered negative in a build section (remember s is measured from the bottom so that $\mathrm{d}\alpha/\mathrm{d}s$ is decreasing in a build section), and positive in a drop-off section so that we may substitute Equations (E.30) and (E.31) into Equation (E.29) and separate variables to get

$$\mathrm{d}T_\mathrm{q} = r_\mathrm{o}\,\mu \left| \bar{w}\,\sin\alpha\,\mathrm{d}s + \mathrm{sgn}\,(\alpha_s - \alpha_0)\left(\hat{F}_0 - \int_0^L \bar{w}\cos\alpha\,\mathrm{d}s_0\right)\kappa\,\mathrm{d}s \right| \tag{E.32}$$

Recalling that for a constant curvature

$$\mathrm{d}s = \frac{\mathrm{d}\alpha}{\kappa} \tag{E.33}$$

and Equation (3.8.8) becomes

$$\mathrm{d}T_\mathrm{q} = r_\mathrm{o}\mu \left| \frac{1}{\kappa}\bar{w}\sin\alpha\,\mathrm{d}\alpha + \mathrm{sgn}\,(\alpha_s - \alpha_0)\left(\hat{F}_0 - \int_{\alpha_0}^{\alpha} \frac{1}{\kappa}\,\bar{w}\cos\bar{\alpha}\,\mathrm{d}\bar{\alpha}\right)\mathrm{d}\alpha \right| \tag{E.34}$$

Assuming the weight per unit length is a constant, we now integrate this equation

$$\int_{T_{\mathrm{q}\,0}}^{T_{\mathrm{q}\,s}} \mathrm{d}T_{\mathrm{q}} = r_{\mathrm{o}}\,\mu \left| \frac{1}{\kappa}\,\bar{w} \int_{\alpha_0}^{\alpha_s} \sin\alpha\,\mathrm{d}\alpha + \mathrm{sgn}\,(\alpha_s - \alpha_0) \int_{\alpha_0}^{\alpha_s} \left(\hat{F}_0 - \frac{1}{\kappa}\,\bar{w} \int_{\alpha_0}^{\alpha} \cos\bar{\alpha}\,\mathrm{d}\bar{\alpha} \right) \mathrm{d}\alpha \right| \tag{E.35}$$

we get the closed-form solution

$$\begin{aligned} T_{\mathrm{q}\,s} \;&= T_{\mathrm{q}\,0} + r_{\mathrm{o}}\,\mu \,\Big|\, r_{\kappa}\,\bar{w}\,(\cos\alpha_0 - \cos\alpha_s) \\ &\quad + \mathrm{sgn}\,(\alpha_s - \alpha_0) \left\{ \hat{F}_0\,(\alpha_s - \alpha_0) - \frac{1}{\kappa}\,\bar{w}\,[\cos\alpha_0 - \cos\alpha_s - (\alpha_s - \alpha_0)\sin\alpha_0] \right\} \Big| \end{aligned} \tag{E.36}$$

and as before this solution is valid only for sections where the curvature and the buoyed weight are constants.

E.8 Closure

It is not within the scope of this text to detail the various methods for quantifying pore pressures or fracture pressures. The brief overview given in this appendix may at least cast a little insight into the subject for those whose backgrounds do not include any study of geology or reservoir mechanics. There are a number of reliable sources for quantifying pore pressures and fracture pressures for well planning. Unfortunately, the majority of those are local to the Louisiana and Texas Gulf Coast. Those methods will work anywhere, but the correlations are quite restricted geographically, and my reluctance to include any here is strictly motivated by a desire to keep any part of this text from being restricted to a limited geographical area. A readable source of information on rock mechanics is the book by Fjær et al. [71]. And another good source for understanding and quantifying pore pressures and fracture pressures is the book by Fertl [12]. In any event, one should be aware that the pore pressure and fracture pressure data that we use in casing design is only approximate at best.

This page intentionally left blank

Appendix F: Summary of useful formulas

Chapter outline head

Listed in this appendix for convenience and quick reference are many of the formulas and equations from the text. There is little or no qualification listed here and one should refer to the text if uncertain as to any formula's assumptions and use.

Precaution

There are no conversion factors in these formulas, so consistent units must be used.

F.1 Borehole geometry

Curvature

Borehole curvature, reference equation (7.15):

$$\kappa \equiv \frac{\mathrm{d}\theta}{\mathrm{d}s} \tag{F.1}$$

Radius of Curvature

Reference equation (7.16):

$$r_\kappa = \frac{1}{|\kappa|} \tag{F.2}$$

F.2 Directional well equations

Minimum Curvature Method

See Appendix E

$$\Delta x = \frac{\Delta s}{\varphi}\left(v_x \sin\varphi + \frac{u_x - v_x\cos\varphi}{\sin\varphi} - \frac{(u_x - v_x\cos\varphi)\cos\varphi}{\sin\varphi}\right) \tag{F.3}$$

$$\Delta y = \frac{\Delta s}{\varphi}\left(v_y \sin\varphi + \frac{u_y - v_y\cos\varphi}{\sin\varphi} - \frac{\left(u_y - v_y\cos\varphi\right)\cos\varphi}{\sin\varphi}\right) \tag{F.4}$$

$$\Delta z = \frac{\Delta s}{\varphi}\left(v_z \sin\varphi + \frac{u_z - v_z\cos\varphi}{\sin\varphi} - \frac{(u_z - v_z\cos\varphi)\cos\varphi}{\sin\varphi}\right) \tag{F.5}$$

where

$v_x = \sin\alpha_1 \cos\beta_1$

$v_y = \sin\alpha_1 \sin\beta_1$

$v_z = \cos\alpha_1$

$u_x = \sin\alpha_2 \cos\beta_2$

$u_y = \sin\alpha_2 \sin\beta_2$

$u_z = \cos\alpha_2$

and

$$\varphi = \cos^{-1}\left[u_x v_x + u_y v_y + u_z v_z\right] \tag{F.6}$$

Note: φ *must be in radians in these equations*.

Amontons-Coulomb Friction

Reference equation (7.1):

$$F \leq \mu N \tag{F.7}$$

Critical Inclination Angle

Reference equation (7.6):

$$\alpha_{\text{cr}} = \tan^{-1}\frac{1}{\mu} \tag{F.8}$$

Differential Friction Equation, Sheppard et al. [41]

Reference equation (7.7):

$$\frac{\mathrm{d}\hat{F}}{\mathrm{d}s} = \bar{w}\,\cos\alpha \pm \mu\left[\left(\hat{F}\frac{\mathrm{d}\alpha}{\mathrm{d}s} + \bar{w}\sin\alpha\right)^2 + \left(\bar{w}\,\frac{\mathrm{d}\beta}{\mathrm{d}s}\sin\alpha\right)^2\right]^{\frac{1}{2}} \tag{F.9}$$

Incremental Friction Equations, Johancsik et al. [40]

Reference Equations (7.8) and (7.9):

$$\hat{F}_n = \hat{F}_0 + \sum_{i=1}^{n} \left[(s_i - s_{i-1})\, \bar{w}_i \cos\left(\frac{\alpha_{i-1} + \alpha_i}{2} \right) \pm \mu_i N_i \right] \tag{F.10}$$

and

$$N_i = (s_{i-1} - s_i) \left\{ \left[\bar{w}_i \sin\left(\frac{\alpha_{i-1} + \alpha_i}{2} \right) + \hat{F}_{i-1} \left(\frac{\alpha_i - \alpha_{i-1}}{s_{i-1} - s_i} \right) \right]^2 \right. \tag{F.11}$$
$$\left. + \left[\hat{F}_{i-1} \left(\frac{\beta_i - \beta_{i-1}}{s_{i-1} - s_i} \right) \sin\left(\frac{\alpha_{i-1} + \alpha_i}{2} \right) \right]^2 \right\}^{\frac{1}{2}}$$

Torque Equation, Differential Form

Reference equation (7.11):

$$\frac{\mathrm{d}T_\mathrm{q}}{\mathrm{d}s} = r_\mathrm{o}\, \mu \left[\left(\bar{w} \sin\alpha + \hat{F} \frac{\mathrm{d}\alpha}{\mathrm{d}s} \right)^2 + \left(\hat{F} \frac{\mathrm{d}\beta}{\mathrm{d}s} \sin\alpha \right)^2 \right]^{\frac{1}{2}} \tag{F.12}$$

Torque Equations, Incremental Form

Reference Equations (7.12) and (7.13):

$$T_{\mathrm{q}\,n} = T_{\mathrm{q}\,0} + \sum_{i=1}^{n} r_i\, \mu_i\, N_i \tag{F.13}$$

and

$$\hat{F}_i = \hat{F}_o + \sum_{k=1}^{i} (s_{k-1} - s_k)\, \bar{w}_k \cos\left(\frac{\alpha_{k-1} + \alpha_k}{2} \right) \tag{F.14}$$

The contact force in this set is calculated with Equation (F.11).

Axial Load

To convert from effective axial load, $\hat{F}$, at a point (reference equation (7.10)):

$$F_i = \hat{F}_i - (p_\mathrm{o} A_\mathrm{o} - p_\mathrm{i} A_\mathrm{i}) \tag{F.15}$$

Bending Stress

Reference equation (7.23):

$$\sigma_\mathrm{b} = \pm E \frac{r}{r_\kappa} \tag{F.16}$$

Bending Stress Magnification

The equations for the bending stress magnification factor, λ_b, are quite lengthy and require considerable qualification. Refer to Section 7.6.2 for these equations.

F.3 Hydrostatics equations

Basic Differential Equation

Reference equation (D.3):

$$\mathrm{d}p = \rho\, g\, \mathrm{d}z \tag{F.17}$$

Basic Integral Equation

Reference equation (D.4):

$$\int_{p_0}^{p_h} \mathrm{d}p = \int_{h_0}^{h} \rho\, g\, \mathrm{d}z \tag{F.18}$$

Basic Common Form

Reference equation (D.7) where ρ and g are constants:

$$\Delta p = \rho\, g\, \Delta h \tag{F.19}$$

Gas Equation for Design

Reference equation (D.16):

$$p = p_0 \exp \frac{Mg\,(h - h_0)}{ZRT_{\mathrm{avg}}} \tag{F.20}$$

or an alternate version, reference equation (D.17):

$$p = p_0 \left(\frac{T_0 + k_{\mathrm{T}} h}{T_0 + k_{\mathrm{T}} h_0} \right)^{\frac{Mg}{ZRk_{\mathrm{T}}}} \tag{F.21}$$

Generalized Archimedes' Principle

Reference equation (D.18):

$$\hat{W} = g\left(\rho_{\mathrm{solid}} - \rho_{\mathrm{liquid}}\right) V_{\mathrm{solid}} \tag{F.22}$$

Buoyancy Factor

Reference equation (D.19):

$$k_{\mathrm{b}} \equiv \frac{\hat{W}}{W} = 1 - \frac{\rho_{\mathrm{liquid}}}{\rho_{\mathrm{solid}}} \tag{F.23}$$

Buoyed Axial Load

Bottom of a section, reference equation (39):

$$\begin{aligned} F_j^{\downarrow} &= -p_0 A_0 + p_1 A_1 + \sum_{i=2}^{j} p_i \left(A_i - A_{i-1}\right) + \sum_{i=1}^{j-1} w_i L_i \\ j &= 1, \ldots, n \end{aligned} \tag{F.24}$$

Top of a section, reference equation (D.40):

$$F_j^{\uparrow} = -p_0 A_0 + p_1 A_1 + \sum_{i=2}^{j} p_i \left(A_i - A_{i-1}\right) + \sum_{i=1}^{j} w_i L_i \tag{F.25}$$

$$j = 1, \ldots, n$$

or alternately as reference Equations (41) and (42):

$$F_j^{\downarrow} = F_{j-1}^{\uparrow} + p_j \left(A_j - A_{j-1}\right) \tag{F.26}$$

$$F_j^{\uparrow} = F_j^{\downarrow} + W_j$$

F.4 Geometric equations for tubes

Cross-sectional Area

$$A_{\mathrm{t}} = \pi \left(r_{\mathrm{o}}^2 - r_{\mathrm{i}}^2\right) = \frac{\pi}{4}\left(d_{\mathrm{o}}^2 - d_{\mathrm{i}}\right) \tag{F.27}$$

Second Area Moment, Axial

$$I_{\mathrm{a}} = \frac{\pi}{4}\left(r_{\mathrm{o}}^4 - r_{\mathrm{i}}^4\right) = \frac{\pi}{64}\left(d_{\mathrm{o}}^4 - d_{\mathrm{i}}^4\right) \tag{F.28}$$

where a is any diameter.

Radius of Gyration

$$r_{\mathrm{g}} = \sqrt{\frac{I}{A}} = \frac{1}{2}\sqrt{r_{\mathrm{o}}^2 + r_{\mathrm{i}}^2} = \frac{1}{4}\sqrt{d_{\mathrm{o}}^2 + d_{\mathrm{i}}^2} \tag{F.29}$$

Polar Area Moment

$$J_z = \frac{\pi}{2}\left(r_{\mathrm{o}}^4 - r_{\mathrm{i}}^4\right) \tag{F.30}$$

F.5 Axial stress and displacement equations

Axial Stretch at a Point

Reference Equations (C.143):

$$u_z = \frac{1}{A_{\mathrm{t}} E}\left[\left(P + \bar{w}\,\ell\right) z - \frac{\bar{w}}{2} z^2\right] \tag{F.31}$$

$$\text{for } 0 \le z \le \ell$$

Total Axial Stretch

Reference equation (C.144):

$$u = \frac{1}{A_t E}\left[P\ell + \frac{\bar{w}}{2}\,\ell^2\right] \text{ for } z = \ell \tag{F.32}$$

Load for Specified Displacement

Reference equation (C.145):

$$P = \frac{AE\,u}{L} - \frac{w\,L}{2} \tag{F.33}$$

Incremental Displacement

Reference equation (C.146):

$$\Delta u = \frac{\Delta P L}{AE} \tag{F.34}$$

Incremental Load

Reference equation (C.147):

$$\Delta P = \frac{AE\,\Delta u}{L} \tag{F.35}$$

Free Pipe

Reference equation (C.148):

$$L = \frac{AE\,\Delta u}{\Delta P} \tag{F.36}$$

Composite Bar or Tube

If the bar or tube is composed of more than one size (still prismatic in each size), then we can expand the previous formulas, reference Equations (C.149) and (C.150):

$$\Delta\, u = \frac{\Delta P}{E}\sum_{i=1}^{n}\frac{L_i}{A_i} \tag{F.37}$$

and

$$\Delta P = \Delta u\, E\left(\sum_{i=1}^{n}\frac{L_i}{A_i}\right)^{-1} \tag{F.38}$$

Axial Stress

Reference equation (6.1):

$$\sigma_z = \frac{F_z}{A_t} = \frac{F_z}{\pi\left(r_o^2 - r_i^2\right)} = \frac{F_z}{\frac{\pi}{4}\left(d_o^2 - d_i^2\right\}\right)} \tag{F.39}$$

F.6 Tube bending equations

Maximum Planar Bending Stress

Reference Equations (7.23) and (C.172):

$$\sigma_{\mathrm{b}} = \pm E \frac{r}{r_\kappa} \qquad r_{\mathrm{i}} \le r \le r_{\mathrm{o}} \tag{F.40}$$

Planar Bending Differential Equation

Reference Equation (C.166):

$$\frac{\mathrm{d}^2}{\mathrm{d}x^2}\left(EI_y \frac{\mathrm{d}^2 u_z}{\mathrm{d}x^2}\right) + f\,(x) = 0 \tag{F.41}$$

Boundary Conditions for Integrating Equation (F.41)

Reference equation (C.167):

$$\begin{aligned} u_z &= \text{transverse displacement} \\ \frac{\mathrm{d}u_z}{\mathrm{d}x} &= \text{slope} \\ \frac{\mathrm{d}^2 u_z}{\mathrm{d}x^2} &= \text{curvature (approximate)} \\ EI_y \frac{\mathrm{d}^2 u_z}{\mathrm{d}x^2} &= \text{moment} \\ EI_y \frac{\mathrm{d}^3 u_z}{\mathrm{d}x^3} &= \text{shear} \\ EI_y \frac{\mathrm{d}^4 u_z}{\mathrm{d}x^4} &= -f\,(x) = \text{the transverse load} \end{aligned} \tag{F.42}$$

F.7 Tube pressure equations

Lamé General Solution

Reference Equations (6.2), (6.3) and (6.4):

$$\sigma_r = \frac{r_{\mathrm{i}}^2 r_{\mathrm{o}}^2\,(p_{\mathrm{o}} - p_{\mathrm{i}})}{r_{\mathrm{o}}^2 - r_{\mathrm{i}}^2}\,\frac{1}{r^2} + \frac{p_{\mathrm{o}} r_{\mathrm{o}}^2 - p_{\mathrm{i}} r_{\mathrm{i}}^2}{r_{\mathrm{o}}^2 - r_{\mathrm{i}}^2} \tag{F.43}$$

$$\sigma_\theta = -\frac{r_{\mathrm{i}}^2 r_{\mathrm{o}}^2\,(p_{\mathrm{o}} - p_{\mathrm{i}})}{r_{\mathrm{o}}^2 - r_{\mathrm{i}}^2}\,\frac{1}{r^2} + \frac{p_{\mathrm{o}} r_{\mathrm{o}}^2 - p_{\mathrm{i}} r_{\mathrm{i}}^2}{r_{\mathrm{o}}^2 - r_{\mathrm{i}}^2} \tag{F.44}$$

$$\Delta\sigma_z = \begin{cases} \dfrac{p_{\mathrm{i}}\, r_{\mathrm{i}}^2 - p_{\mathrm{o}}\, r_{\mathrm{o}}^2}{r_{\mathrm{o}}^2 - r_{\mathrm{i}}^2} & \text{capped ends, both} \quad \text{free ends, one or both} \\ 0 & \text{open ends, one or both} \quad \text{free ends, one or both} \\ \nu\ (\Delta\sigma_\theta + \Delta\sigma_r) & \text{open or capped ends} \quad \text{fixed ends, both} \end{cases} \tag{F.45}$$

Lamé Inner Wall Solution, $r = r_\mathrm{i}$

Reference Equations (6.5) and (6.6):

$$\sigma_r = -p_\mathrm{i} \tag{F.46}$$

$$\sigma_\theta = \frac{p_\mathrm{i}\left(r_\mathrm{o}^2 + r_\mathrm{i}^2\right) - 2p_\mathrm{o}r_\mathrm{o}^2}{r_\mathrm{o}^2 - r_\mathrm{i}^2} \tag{F.47}$$

Lamé Outer Wall Solution, $r = r_\mathrm{o}$

Reference Equations (6.7) and (6.8):

$$\sigma_r = -p_\mathrm{o} \tag{F.48}$$

$$\sigma_\theta = \frac{-p_\mathrm{o}\left(r_\mathrm{o}^2 + r_\mathrm{i}^2\right) + 2p_\mathrm{i}r_\mathrm{i}^2}{r_\mathrm{o}^2 - r_\mathrm{i}^2} \tag{F.49}$$

Lamé Change in Axial Stress Caused by Change in Pressure

Initial axial stress is calculated from Equation (F.39). The change caused by pressure is given as:

$$\Delta\sigma_z = \begin{cases} \dfrac{p_\mathrm{i}\,r_\mathrm{i}^2 - p_\mathrm{o}\,r_\mathrm{o}^2}{r_\mathrm{o}^2 - r_\mathrm{i}^2} & \text{capped ends (both)} & \text{free (one or both)} \\ 0 & \text{open ends (one or both)} & \text{free (one or both)} \\ \nu\ (\Delta\sigma_\theta + \Delta\sigma_r) & \text{open or capped ends} & \text{fixed (both)} \end{cases} \tag{F.50}$$

F.8 Torsion equations

General Torsion Formula

Reference equation (6.9):

$$\sigma_{r\theta} = \frac{rT_\mathrm{q}}{J_z} = \frac{2\,r\,T_\mathrm{q}}{\pi\left(r_\mathrm{o}^4 - r_\mathrm{i}^4\right)} \qquad r_\mathrm{i} \le r \le r_\mathrm{o} \tag{F.51}$$

Rotational Deflection

$$\theta = \frac{T_\mathrm{q}\,L}{J_z\,G} = \frac{2T_\mathrm{q}\,L}{\pi\left(r_\mathrm{o}^4 - r_\mathrm{i}^4\right)G} \tag{F.52}$$

F.9 Lateral buckling equations

Lateral Buckling

Reference equation (6.56):

$$F_\mathrm{crit} = 2\sqrt{\frac{4EI\,g\,k_\mathrm{b}\,\rho_\ell\,\sin\alpha}{\Delta r}} \tag{F.53}$$

Stability Condition

Reference Equations (6.49), (6.50), (6.51) and (6.52):

$$\sigma_z \geq \frac{A_\mathrm{i} p_\mathrm{i} - A_\mathrm{o} p_\mathrm{o}}{A_\mathrm{o} - A_\mathrm{i}} \tag{F.54}$$

$$\sigma_z \geq \frac{ri^2 p_\mathrm{i} - r_\mathrm{o}^2 p_\mathrm{o}}{r_\mathrm{o}^2 - r_\mathrm{i}^2} \tag{F.55}$$

$$F_z \geq A_\mathrm{i} p_\mathrm{i} - A_\mathrm{o} p_\mathrm{o} \tag{F.56}$$

$$\sigma_z \geq \frac{1}{2}\left(\sigma_\theta + \sigma_r\right) \tag{F.57}$$

Neutral Stability Point

Reference equation (6.54):

$$\hat{F}_z = F_z + (A_\mathrm{o} p_\mathrm{o} - A_\mathrm{i} p_\mathrm{i}) = 0 \tag{F.58}$$

F.10 Thermal equations

Axial Stress, Thermal

One-dimensional thermoelastic Hooke's equation, reference equation (6.62):

$$\sigma = \sigma_0 + E\,\varepsilon - E\,\alpha\,\Delta T \tag{F.59}$$

F.11 General solid mechanics

The important general equations of solid mechanics in Appendix C are too numerous to include here, and you are referred to that appendix. The equations for the von Mises yield criteria are listed. Some solutions from that appendix for axial stretch and planar bending of tubes are listed in separate categories in this appendix, however.

F.11.1 Yield criteria

The von Mises Yield Criterion

Reference equation (C.104)

$$Y \geq \sqrt{3J_2} \tag{F.60}$$

Yield Measure, Principal Stress

Principal stress formulation, reference equation (C.108):

$$\Psi \equiv \sqrt{3J_2} = \left\{\frac{1}{2}\left[(\sigma_1 - \sigma_2)^2 + (\sigma_2 - \sigma_3)^2 + (\sigma_3 - \sigma_1)^2\right]\right\}^{\frac{1}{2}} \tag{F.61}$$

If torsion is the only shear stress in the tube, the principal stress components are given by reference equation (C.113):

$$\begin{aligned}\sigma_1 &= \frac{\sigma_\theta + \sigma_r}{2} + \sqrt{\left(\frac{\sigma_\theta - \sigma_r}{2}\right) + \sigma_{r\theta}^2} \\ \sigma_2 &= \frac{\sigma_\theta + \sigma_r}{2} - \sqrt{\left(\frac{\sigma_\theta - \sigma_r}{2}\right) + \sigma_{r\theta}^2} \\ \sigma_3 &= \sigma_r\end{aligned} \tag{F.62}$$

Yield Measure, Cylindrical Coordinates, No Torque

Principal stress formulation in cylindrical coordinates with not shear stress components, reference equation (C.111):

$$\Psi = \left\{\frac{1}{2}\left[(\sigma_\theta - \sigma_r)^2 + (\sigma_r - \sigma_z)^2 + (\sigma_z - \sigma_\theta)^2\right]\right\}^{\frac{1}{2}} \tag{F.63}$$

Yield Measure, General Stress Field, Cylindrical Coordinates

General stress formulation in cylindrical coordinates, reference equation (C.112):

$$\Psi = \left\{\frac{1}{2}\left[(\sigma_\theta - \sigma_r)^2 + (\sigma_r - \sigma_z)^2 + (\sigma_z - \sigma_\theta)^2\right] + 3\left(\sigma_{r\theta}^2 + \sigma_{rz}^2 + \sigma_{\theta z}^2\right)\right\}^{\frac{1}{2}} \tag{F.64}$$

F.12 API/ISO performance equations

Pipe Body Yield

Reference equation (6.11):

$$F_{\max} = Y A_{\mathrm{t}} \tag{F.65}$$

API Internal Yield, Barlow Formula

Reference equation (6.12):

$$p = 0.875\, Y \frac{d_{\mathrm{o}} - d_{\mathrm{i}}}{d_{\mathrm{o}}} \tag{F.66}$$

Lamé Internal Yield

Reference equation (6.16):

$$p_{\mathrm{i}} = Y \frac{d_{\mathrm{o}}^2 - d_{\mathrm{i}}^2}{\sqrt{3d_{\mathrm{o}}^4 + d_{\mathrm{i}}^4}} \tag{F.67}$$

Reduced API Wall Thickness for Use in Equation (F.67)

Reference equation (6.17):

$$\tilde{d}_{\mathrm{i}} \equiv d_{\mathrm{o}} - 0.875\,(d_{\mathrm{o}} - d_{\mathrm{i}}) \tag{F.68}$$

ISO Ductile Rupture

Reference equation (6.18):

$$p = 2k_1 U \frac{\tilde{t}_{\mathrm{w}} - k_2\,\delta}{d_o - \tilde{t}_{\mathrm{w}} + k_2\delta} \tag{F.69}$$

Yield Collapse Formula

Reference Equations (6.19) and (6.20):

$$p_{\mathrm{YC}} = 2Y\left[\frac{(d_{\mathrm{o}}/t_{\mathrm{w}}) - 1}{(d_{\mathrm{o}}/t_{\mathrm{w}})^2}\right] \tag{F.70}$$

Valid range:

$$(d_{\mathrm{o}}/t_{\mathrm{w}}) \leq \frac{A - 2 + \sqrt{(A-2)^2 + 8\,(B + C/Y)}}{2\,(B + C/Y)} \tag{F.71}$$

Plastic Collapse Formula

Reference Equations (6.21) and (6.22):

$$p_{\mathrm{PC}} = Y\left[\frac{A}{(d_{\mathrm{o}}/t_{\mathrm{w}})} - B\right] - C \tag{F.72}$$

Valid range:

$$\frac{A - 2 + \sqrt{(A-2)^2 + 8\,(B + C/Y)}}{2\,(B + C/Y)} < (d_{\mathrm{o}}/t_{\mathrm{w}}) \leq \frac{Y\,(A - F)}{C + Y\,(B - G)} \tag{F.73}$$

Transition Collapse Formula

Reference Equations (6.23) and (6.24):

$$p_{\mathrm{TC}} = Y\left[\frac{F}{(d_{\mathrm{o}}/t_{\mathrm{w}})} - G\right] \tag{F.74}$$

Valid range:

$$\frac{Y\,(A - F)}{C + Y\,(B - G)} < (d_{\mathrm{o}}/t_{\mathrm{w}}) \leq \frac{2 + B/A}{3B/A} \tag{F.75}$$

Elastic Collapse Formula

Reference Equations (6.25) and (6.26):

$$p_{\mathrm{EC}} = \frac{46.95 \times 10^6}{(d_{\mathrm{o}}/t_{\mathrm{w}})\,[(d_{\mathrm{o}}/t_{\mathrm{w}}) - 1]^2} \tag{F.76}$$

Valid range:

$$(d_o/t_w) > \frac{2 + B/A}{3B/A} \tag{F.77}$$

API Constants, USC

Reference equation (6.27):

$$\begin{aligned} A &= 2.8762 + 0.10679 \times 10^{-5} Y + 0.21301 \times 10^{-10} Y^2 \\ &\quad -0.53132 \times 10^{-16} Y^3 \\ B &= 0.026233 + 0.50609 \times 10^{-6} Y \\ C &= -465.93 + 0.030867 Y - 0.10483 \times 10^{-7} Y^2 \\ &\quad +0.36989 \times 10^{-13} Y^3 \\ F &= \frac{46.95 \times 10^6 \left[\frac{3B/A}{2 + (B/A)}\right]^3}{Y\left[\frac{3B/A}{2 + (B/A)} - (B/A)\right]\left[1 - \frac{3B/A}{2 + (B/A)}\right]^2} \\ G &= FB/A \end{aligned} \tag{F.78}$$

API Constants, SI

Reference equation (6.28):

$$\begin{aligned} A &= 2.8762 + 0.15489 \times 10^{-3} Y + 0.44809 \times 10^{-6} Y^2 \\ &\quad -0.16211 \times 10^{-9} Y^3 \\ B &= 0.026233 + 0.73402 \times 10^{-4} Y \\ C &= -3.2125 + 0.030867 Y - 0.15204 \times 10^{-5} Y^2 \\ &\quad +0.77810 \times 10^{-9} Y^3 \\ F &= \frac{3.237 \times 10^5 \left[\frac{3B/A}{2 + (B/A)}\right]^3}{Y\left[\frac{3B/A}{2 + (B/A)} - (B/A)\right]\left[1 - \frac{3B/A}{2 + (B/A)}\right]^2} \\ G &= FB/A \end{aligned} \tag{F.79}$$

ISO Collapse Formulas

Reference Equations (6.29), (6.30) and (6.31):

$$p_{clps} = \frac{p_{elas} + p_{yld} - \left[\left(p_{elas} - p_{yld}\right)^2 + 4 p_{elas} p_{yld} H_t\right]^{\frac{1}{2}}}{2\left(1 - H_t\right)} \tag{F.80}$$

where

$$p_{\text{elas}} = \frac{0.825\,(2E)}{\left(1-\nu^2\right)\left(\frac{d_\text{o}}{t_\text{w}}\right)\left(\frac{d_\text{o}}{t_\text{w}}-1\right)^2} \tag{F.81}$$

is the elastic collapse portion, and

$$p_{\text{yld}} = 2k_\text{y}Y\left(\frac{t_\text{w}}{d_\text{o}}\right)\left(1+\frac{t_\text{w}}{2d_\text{o}}\right) \tag{F.82}$$

is the yield collapse portion.

Simplified Reduced Collapse Strength

Reference equation (6.36):

$$k_{\text{clps}} = \sqrt{1-0.75\left(\frac{F}{A_\text{t}Y}\right)^2} - 0.5\frac{F}{A_\text{t}Y} \tag{F.83}$$

Simplified Reduced Collapse Strength, Westcott et al. [26]

Reference equation (6.37):

$$k_{\text{clps}} = \sqrt{1-0.932\left(\frac{F}{A_\text{t}Y}\right)^2} - 0.26\frac{F}{A_\text{t}Y} \tag{F.84}$$

Traditional API Reduced Yield for Collapse

Reference equation (6.45):

$$\tilde{Y} = Y\sqrt{1-\frac{3}{4}\left(\frac{\sigma_z}{Y}\right)^2} - \frac{\sigma_z}{2} \tag{F.85}$$

API Collapse Correction for Presence of External Pressure

Reference equation (6.46):

$$\tilde{p}_{\text{clps}} = p_{\text{reduced}} + p_\text{i}\left(1-\frac{2t_\text{w}}{d_\text{o}}\right) \tag{F.86}$$

Collapse Pressure from Slip-Type Casing Hanger

Not an API/ISO formula, reference equation (5.1):

$$p_{\text{hgr}} = k_\text{D}\,\frac{W}{A_{\text{slip}}\tan\phi} \tag{F.87}$$

This page intentionally left blank

Glossary

Terms Related to Mathematics

Associative $abc = (ab)c = a(bc)$
Commutative $ab = ba$

Terms Related to Borehole Applications

Azimuth The compass direction of the horizontal projection of a borehole path at a specific point on that path. Usually measured from true north, magnetic north, or grid north, but may use any arbitrary reference.

Biaxial loading Loading on two principal tube axes, usually the axial and tangential axes.

BOP Blowout preventer. A large piece of equipment on top of the casing that is essentially a valve that can be closed (manually and/or hydraulically) to prevent uncontrolled flow of formation fluids to the surface (blowout). Usually a set of three or more are installed, one closes on open hole, one closes around drill pipe, and one flexible type closes around various sizes of pipe.

Borehole A hole drilled into the earth from the surface. Usually refers to the un-cased hole, but usage is not consistent in the literature (also see wellbore).

Build section The portion of a directional well where the inclination angle is increased to a specified point.

Build rate The rate at which inclination angle is increasing in a directional well.

Burst A common and often misleading term referring to internal yield of a tube due to a positive pressure differential ($\Delta p > 0$) from the inside directed toward the outside. Usually does not refer to actual rupture or failure, but rather, to the internal pressure at initial yield.

Casing The relatively larger diameter pipe that is cemented in the borehole and becomes a permanent part of the well. It provides borehole integrity (from collapse, erosion, fracture), prevents flow of formation fluids into the borehole, and prevents flow of borehole fluids into formations. Standard sizes range from 4-1/2″ to 30″ (114 to 762 mm) though other options are available.

Casing string Casing joints that are assembled into a continuous length in a well.

Collapse Radial buckling and postbuckling collapse of a tube due to a negative pressure differential ($\Delta p < 0$) directed from the outside toward the inside. Usually, a combination of elastic instability and yielding.

Connections The means by which pipe joints are connected to each other. Typically, connections are threaded ends with the pin (male) end run at the bottom and the box (female) end at the top. The connections usually fall into one of two general categories, integral, where both the box and pin threads cut on the pipe body, and coupled where both ends of the pipe body are threaded as pins and a separate box-box coupling is installed on one end.

Coupling A threaded female-female (box-box) collar used in joining two male (pin) threaded joints of pipe together.

Directional survey A reading from a down-hole instrument consisting of an inclination angle and a directional azimuth along with a depth measurement.

Drill collars Heavy, thick-walled pipe immediately on top of the bit. Used to give weight to the bit in order to drill. Selection is based on providing enough weight to drill efficiently yet keep the drill pipe above in a state of effective tension to prevent lateral buckling of the drill pipe and its premature fatigue failure while rotating.

Drill pipe Relatively sturdy pipe extending from the surface to near the top of the drill collars which are connected to the drill bit. Relatively thick-walled because of high degree of wear from many hours of rotation in a borehole. Common diameters range from 2-7/8″ to 6-5/8″ (73 to 143 mm).

Drill string Refers to the entire drilling assembly: principally the drill pipe, drill collars, and bit but also any other tools (stabilizers, cross-over subs, etc.) that are in the down hole assembly ("string").

ERW Electric resistance welding is the process of welding metal by fusion when heated electrically and using no filler material as with conventional welding.

EU External upset. Outside diameter of pipe is increased above nominal at joint end(s) for threading. (see also IU, IEU).

Flush-joint Pipe with both box and pin end threads cut into the tube with no upset or couplings.

Inclination angle The inclination of a borehole at some point along its path, *always measured from vertical*.

IU Internal upset. Inside diameter of pipe is decreased below nominal at joint end(s) providing extra thickness for threading. Uncommon in casing (see also EU, IEU).

Joint A single length of pipe as it comes from the manufacturer, usually with a connection on each end (male on one end and female on the other). Typically lengths range from 20 ft ($\sim$ 6m) to 42 ft ($\sim$ 13m).

LT&C API 8-rd long thread and coupling (see also ST&C).

Lateral A horizontal (or near horizontal) section of a directional well.

OCTG Oil Country Tubular Goods Oilfield casing, tubing, drill pipe, and line pipe

Over-pull An amount of tension in casing over and above the suspended weight of the casing in a borehole.

Pipe Refers to one or more joints of pipe collectively, either assembled into a *string* or not. The plural, "pipes," is never used, but is expressed in terms of *strings* or *joints*. For example a well may be said to have four *stings of pipe* (casing and/or tubing) in it, or a truckload of pipe may consist of 24 *joints of pipe*.

psi units of pressure, lbf/in.^{2}.

Q&T Quenched and tempered. A hardening process in the manufacture of casing.

SG Specific gravity. Density compared to water 62.43 lb/ft^3, 8.33 ppg, or 1000 kg/m^3.

Shoe track The pipe and float equipment below the float collar that is full of cement after a primary cement job. Typically, a float collar, two joints of casing, and a float shoe.

Spherical stress A stress state in a solid (analogous to hydrostatic stress) in which all three principal stress components are equal, $\sigma_1 = \sigma_2 = \sigma_3$.

ST&C API 8-rd short thread and coupling (see also LT&C).

Stand A length of pipe (usually drill pipe) made up of two, three, or four joints (depending on the height of the derrick) that are set aside in the derrick when a string is being pulled out of the hole for some purpose, such as changing a bit, but with the intent that it will be run back in the hole. Rather than disconnect each joint, only every second, third, or fourth joint is disconnected and each stand is set aside vertically in the derrick to speed the pulling and running process.

String Refers to a completely assembled length of pipe joints such as a drill string, casing string, tubing string, etc.

Sub A short length of pipe that is typically used to change from one type of thread to another, and called a *cross-over sub*. May also serve other purposes such as adjusting the length of a specific section of a string to facilitate handling the pipe.

Tubing Smaller diameter pipe through which oil or gas flows to the surface. It is intended to be removable and replaceable should the need arise. Common sizes range from 1-1/4″ to 5″ (32 to 127 mm).

Wellbore The hole drilled in the rock and the casing in it. This usage not consistent in the literature (also see borehole).

This page intentionally left blank

References

[1] ISO 80000-2, Quantities and Units—Mathematical Signs and Symbols to be Used in the Natural Sciences and Technology, International Organization for Standardization, Geneva, 2009.

[2] ISO 90000-4, Quantities and Units—Mechanics, International Organization for Standardization, Geneva, 2006.

[3] T.G. Byrom, Casing and Liners for Drilling and Completion, Gulf Publishing Company, Houston, TX, 2007.

[4] SPE Style Guide, Society of Petroleum Engineers, Richardson, TX, 2011.

[5] API Specification 5CT, Specifications for Casing and Tubing, American Petroleum Institute, Washington, DC, 2004.

[6] ISO 11960, Petroleum and Natural Gas Industries—Steel Pipes for Use as Casing or Tubing for Wells, International Organization for Standardization, Geneva, 2004.

[7] API Recommended Practice 5B1, Threading, Gauging, and Thread Inspection of Casing, Tubing, and Line Pipe Threads, American Petroleum Institute, Washington, DC, 1999.

[8] G.A. Valigura, P. Cernocky, Shell Exploration and Production Company list of connections tested for well service pressures >8000 psi, based on standardized API/ISO qualification testing procedures, SPE 97605, 2005.

[9] API Bulletin 5C2, Bulletin of Performance Properties of Casing, Tubing, and Drill Pipe, American Petroleum Institute, Washington, DC, 1999.

[10] API Bulletin 5C3, Bulletin on Formulas and Calculations for Casing, Tubing, Drill Pipe, and Line Pipe Properties, American Petroleum Institute, Washington, DC, 1994.

[11] ISO/TR 10400, Petroleum and Natural Gas Industries—Formulae and Calculations for the Properties of Casing, Tubing, Drill Pipe, and Line Pipe Used as Casing or Tubing, International Organization for Standardization, Geneva, 2007.

[12] W.H. Fertl, Abnormal Formation Pressures, Elsevier Scientific Publishing Co., Amsterdam, Oxford, New York, 1976.

[13] C.M. Prentice, Maximum load casing design, SPE 2560, 1970.

[14] A.S. Halal, R.F. Mitchell, Casing design for trapped annulus pressure buildup, SPE/IADC 25694, 1993.

[15] EUB Directive 010: Minimum Casing Design Requirements, Alberta Energy and Utilities Board, Alberta, Canada, 2004.

[16] F.J. Klever, A.G. Tallin, The role of idealization in understanding design margins, SPE 97574, 2005.

[17] W. Ramberg, W.R. Osgood, Description of stress-strain curves by three parameters, NACA Technical Note 902, July 1943.

[18] P. Ludwick, Elemente der Technologischen Mechanik, Springer-Verlag, Berlin, 1909.

[19] T.G Byrom, D.H. Allen, Dynamic thermoviscoplastic response of a hypersonic leading edge, J. Therm. Stresses 17 (1994) 419-434.

[20] M.K. Yeh, S. Kyriakides, Collapse of inelastic thick-walled tubes under external pressure, J. Energ. Resour. Technol. Trans. ASME 108 (1986) 35-47.

[21] S. Kyriakides, C.D. Babcock, D. Elyada, Initiation of propagating buckles from local pipeline damages, J. Energ. Resour. Technol. Trans. ASME 106 (1984) 79-87.

[22] E. Chater, J.W. Hutchinson, On the propagation of bulges and buckles, J. Appl. Mech. Trans. ASME 51 (1984) 269-277.

[23] S. Kyriakides, E. Corona, Mechanics of Offshore Pipelines, Volume 1: Buckling and Collapse, Elsevier, Burlington, MA, 2007.
[24] T. Tamano, T. Mimaki, S. Yanagimoto, A new empirical formula for collapse resistance of commercial casing, Proc. 2nd Int. OMAES, (1983) 489-495.
[25] F.J. Klever, T. Tamano, A new OCTG strength equation for collapse under combined loads, SPE Drill. Compl. 21(3) (2006) 164-179.
[26] B.B. Wescott, C.A. Dunlop, E.N. Kimler, Setting depths for casing, in: API Drilling and Production Practice, American Petroleum Institute, Dallas, TX (now Washington, DC), 1940.
[27] A. Lubinski, Influence of tension and compression on straightness and buckling tubular goods in oil wells, in: API Division of Production, vol. 31(4), American Petroleum Institute, New York (now Washington, DC) (1951) 31-56.
[28] A. Klinkenberg, The neutral zone in drill pipe and casing and their significance in relation to buckling and collapse, in: API Drilling and Production Practice, American Petroleum Institute, New York (now Washington, DC), (1951) 64-76.
[29] H.B. Woods, Discussion on paper by Klinkenberg, in: API Drilling and Production Practice, American Petroleum Institute, New York (now Washington, DC), (1951) 77-79.
[30] R. Dawson, Drill pipe buckling in inclined holes, J. Petrol. Technol. 36(10) (1984) 1734-1740.
[31] X. He, A. Kyllingstad, Helical buckling and lockup conditions for coiled tubing in curved wells, SPE 25370, 1993.
[32] R.F. Mitchell, A buckling criterion for constant curvature wellbores, SPE J. 4(4) (1999) 349-352.
[33] R.F. Mitchell, Lateral buckling of pipe with connectors in curved wellbores, SPE Drill. Compl. 18(1) (2003) 22-23.
[34] S.P. Timoshenko, J.H. Goodier, Theory of Elasticity, second ed., McGraw-Hill, New York, 1970.
[35] G.H. Holliday, Calculation of allowable maximum casing temperature to prevent tension failures in thermal wells, in: ASME Petroleum Mechanical Engineering Conference, September 21-22, Tulsa, Oklahoma, 1969.
[36] M.J. Jellison, J.N. Brock, The impact of compression forces on casing-string designs and connectors, SPE Drill. Compl. 15(4) (2000) 241-248.
[37] F.J. Klever, A design strength equation for collapse of expandable OCTG, SPE Drill. Compl. 25(3) (2010) 391-408.
[38] H.L. Taylor, C.M. Mason, A systematic approach to well surveying calculations, Soc. Petrol. Eng. J. 12(6) (1972) 474-488.
[39] C.J.M. Wolff, J.P. De Wardt, Borehole position uncertainty, analysis of measuring methods and derivation of a systematic error model, SPE 9223, 1980.
[40] C.A. Johancsik, D.B. Friesen, R. Dawson, Torque and drag in directional wells—prediction and measurement, J. Petrol. Technol. 36(6) (1984) 987-982.
[41] M.C. Sheppard, C. Wick, T. Burgess, Designing well paths to reduce drag and torque, SPE Drill. Eng. 2(4) (1987) 344-350.
[42] J.H. Nestor, D.R. Jenkins, R. Simon, Resistance to failure of oil-well casing subjected to non-uniform transverse loading, in: Drilling and Production Practices, (1955) 374-378.
[43] G.E. King, The effect of high-density perforating on the mechanical crush resistance of casing, SPE 18843, 1989.
[44] C. Marx, A.H. El-Sayed, Evaluation of collapse strength of cemented pipe-in-pipe casing strings, SPE/IADC 13432, 1985.
[45] A.H. El-Sayed, F. Khalaf, Resistance of cemented concentric casing string under non-uniform loading, SPE 17927, 1989.
[46] A. Lubinski, Maximum permissible dog-legs in boreholes, J. Petrol. Technol. 13(2) (1961) 175-194.
[47] P.R. Paslay, E.P. Cernocky, Bending stress magnification in constant curvature dog-legs with impact on drillstring and casing, SPE 22547, 1991.
[48] J.F. Greenip Jr., How to design casing strings for horizontal wells, Petrol. Eng. Int. 62(12) (1989).

[49] J.G. Simmonds, A Brief on Tensor Analysis, Springer-Verlag, New York, 1982.
[50] C. Truesdale, R.A. Toupin, The classical field theories, in: S. Flügge (Ed.), Encyclopedia of Physics, vol. III(Part 1), Springer-Verlag, Berlin, (1960) 226-793.
[51] C. Truesdale, W. Noll, The non-linear field theories, in: S. Flügge (Ed.), Encyclopedia of Physics, vol. III(Part 3), Springer-Verlag, Berlin, (1965) 1-602.
[52] Y.C. Fung, Foundations of Solid Mechanics, Prentice-Hall, Englewood Cliffs, NJ, 1965.
[53] D.H. Allen, W.E. Haisler, Introduction to Aerospace Structural Analysis, John Wiley & Sons, New York, 1985.
[54] G.I. Taylor, H. Quinney, The plastic deformation of metals, Philos. Trans. R. Soc. Lond. Ser. A 230 (1931) 323-362.
[55] J.F. Bell, Experimental foundations of solid mechanics, in: C.F. Truesdale (Ed.), Mechanics of Solids, vol. 1, Springer-Verlag, Berlin, Heidelberg, New York, Tokyo, (1973) 1-813 (Originally published in Encyclopedia Phys. VIa/1-4).
[56] B. Budiansky, Comments by session chairman, in: S. Nemat-Nasser, R.J. Asaro, G. Hagemier (Eds.), Theoretical Foundations for Large-Scale Computations for Nonlinear Material Behavior, Martinus Nijhoff Publishers, Dordrecht, the Netherlands, (1982) 383-400.
[57] K.R. Newman, Finite element analysis of coiled tubing forces, SPE 89502, 2004.
[58] A.R. McSpadden, O.D. Coker III, G.C. Ruan, Advanced casing design with finite-element model of effective dogleg severity, radial displacements, and bending loads, SPE Drill. Compl. 27(3) (2012) 436-448.
[59] R.L. Burden, J.D. Faires, Numerical Analysis, fifth ed., PWS-Kent Publishing Company, Boston, 1993.
[60] O.C. Zienkiewicz, R.L. Taylor, J.Z. Zhu, The Finite Element Method: Its Basis and Fundamentals, sixth ed., Elsevier, Burlington, MA, 2005.
[61] K.H. Huebner, D.L. Dewhirst, D.E. Smith, T.G. Byrom, The Finite Element Method for Engineers, fourth ed., John Wiley & Sons, New York, 2001.
[62] L.P. Lebedev, M.J. Cloud, V.A. Eremeyev, Tensor Analysis with Applications in Mechanics, World Scientific, Singapore, 2010.
[63] L.E. Malvern, Introduction to the Mechanics of a Continuous Medium, Prentice-Hall, Englewood Cliffs, NJ, 1969.
[64] Y.C. Fung, A First Course in Continuum Mechanics, second ed., Prentice-Hall, Englewood Cliffs, NJ, 1977.
[65] F. Irgens, Continuum Mechanics, Springer-Verlag, Berlin, 2010.
[66] N. Jeevanjee, An Introduction to Tensors and Group Theory for Physicists, Springer Science + Business Media, New York, 2011.
[67] I.N. Bronshtein, K.A. Semendyayev, G. Musiol, H. Muehlig, Handbook of Mathematics, fifth ed., Springer-Verlag, Berlin, Heidelberg, 2007.
[68] B. Kolman, Elementary Linear Algebra, fourth ed., MacMillan, New York, 1986.
[69] R.M. Bowen, C.-C. Wang, Introduction to Vectors and Tensors, Vol. 1: Linear and Multilinear Algebra, Vol. 2: Vector and Tensor Analysis, Plenum Press, New York, 1976.
[70] R. Larson, D.C. Falvo, Elementary Linear Algebra, sixth ed., Houghton Mifflin Harcourt, New York, 2009.
[71] E. Fjær, R.M. Holt, P. Horsrud, A.M. Raaen, R. Risnes, Petroleum Related Rock Mechanics, Elsevier Scientific Publishing Co., Amsterdam, Oxford, New York, 1992.
[72] K. Terzaghi, R.B. Peck, Theoretical Soil Mechanics in Engineering Practice, John Wiley & Sons, New York, 1948.
[73] C.H. Yew, Y. Li, Fracturing of a deviated well, SPE Prod. Eng. 3(4) (1988) 429-437.

This page intentionally left blank

Index

Note: Page numbers followed by *f* indicate figures and *t* indicate tables.